ANALYTIC PROPERTIES AND CREMONA APPROXIMATION OF TRANSFER MAPS FOR HAMILTONIAN SYSTEMS

by

Dan Tyler Abell

Dissertation submitted to the Faculty of the Graduate School
of The University of Maryland in partial fulfillment
of the requirements for the degree of
Doctor of Philosophy
1995

DEPARTMENT OF PHYSICS
UNIVERSITY OF MARYLAND
COLLEGE PARK, MARYLAND 20742

Abstract

Title of Dissertation: Analytic Properties and Cremona Approximation of Transfer Maps for Hamiltonian Systems

Dan Tyler Abell, Doctor of Philosophy, 1995

Dissertation directed by: Alex J. Dragt
Professor
Department of Physics

The motion of a dynamical system may be approximated as a sequence of discrete steps in time described by transfer maps. In the field of accelerator physics, Taylor series maps constitute a special, heavily-used class of such maps, which, despite their wide use, have poorly understood, or little appreciated, convergence properties. In Part I we show first how one may expect a (very general) transfer map to be analytic within some, perhaps quite limited, region of phase space. We then show that the underlying singularity structure of the original map—as determined by the dynamical system itself—governs the domain of convergence of a given Taylor series map. We conclude Part I by using the quartic anharmonic oscillator as an example to illustrate not only the complicated, rich, and very subtle behavior of such domains of convergence, but also the care and understanding required when drawing conclusions about the applicability of Taylor maps.

Following a Hamiltonian flow for a finite interval of time produces a symplectic map. In Part II we describe a procedure for converting a truncated Taylor series approximation for a symplectic map into a polynomial map that is exactly symplectic—*i.e.*, a Cremona map—in such a way that the Cremona map agrees with the original Taylor map through terms of any desired order. We then introduce the concept of sensitivity vectors and show how that concept allows one to characterize optimal Cremona symplectifications. We also give explicit constructions for optimal Cremona symplectifications in two- and four- and six-dimensional phase spaces. At the end, we apply these methods to some maps of physical interest. We expect that Cremona maps may be useful for studying the long-term behavior of particles circulating in storage rings.

ANALYTIC PROPERTIES AND CREMONA APPROXIMATION OF TRANSFER MAPS FOR HAMILTONIAN SYSTEMS

by

Dan Tyler Abell

Dissertation submitted to the Faculty of the Graduate School
of The University of Maryland in partial fulfillment
of the requirements for the degree of
Doctor of Philosophy
1995

Advisory Committee:

Professor Alex J. Dragt, Chairman/Advisor
Professor Robert L. Gluckstern
Professor Steven S. Kudla
Professor William M. MacDonald
Professor John H. Maddocks

Dan T. Abell
Department of Physics
University of Maryland
College Park, MD 20742-4111
USA

E-mail address: dabell@quark.umd.edu

Dedication

To Anne A. Hunter, my beloved wife,
and to Alex J. Dragt, my adviser,
for their unwavering support.

Acknowledgements

Those familiar with bicycle road racing know that one achieves success in that sport not solely by dint of personal effort. Individual riders receive the laurels, but every rider relies on the strength and support of his team. So it is in Ph.D. research, and it gives me great pleasure to acknowledge those who have helped me accomplish this work.

First I thank my adviser, Dr. Alex J. Dragt, a great rider who paced me up the difficult climbs of theoretical physics, showed me how to navigate safely the exhilarating descents, and encouraged me in the lonely time trials. I feel privileged and honored to have had this opportunity to work and learn with him, and I am especially grateful for his role as a mentor: his wisdom, kindness, and broad and deep knowledge of physics have proved a constant source of inspiration. Without his patient guidance and generous supply of ideas, this dissertation would not exist.

Thanks, also, to Dr. Robert L. Gluckstern. He taught me "E&M", provided much needed support and encouragement, and, in addition, suggested the proof outlined in footnote 33 (on p. 135). While working with him on various projects, I have learned a tremendous amount of physics.

I am indebted to Ms. Rachel Needle: with grace and good humor—even in times of crisis—she managed to decipher my messy scrawls (with arrows going every which way), and convert them to legible form with admirable speed and accuracy. In addition, she made many travel arrangements on my behalf, and skillfully insulated me from many aspects of the University's bureaucracy.

In this last regard, I am also grateful to Ms. Dorothy Kennedy, who cut through some of the red tape associated with my trip to Italy; to Ms. Lorraine DeSalvo, who answered numerous questions and requests about matters large and small; and to Ms. Jane Hessing, without whose cheerful help I would long ago have been buried beneath a mountain of forms.

I am indebted also to Mr. Norman Reese. He answered numerous questions on the subtleties of computers—UNIX in particular; and whenever a computer problem collided with a deadline, he always found the time to help. I am especially grateful for the many times he took care of communications problems between the computers and the printers, and for the help he gave me in backing up my computer files.

Several other professors contributed in various ways from the conception to the completion of this dissertation. Dr. William MacDonald taught me much of what I know about *Mathematica*, and did so in a way that made me feel we were learning together. I highly recommend his course to others. Dr. Daniel Fivel shared with me his stimulating conversation, his remarkable insight concerning the foundations of quantum mechanics, and, of course, his infectious good-natured humor. And Dr. Richard Ellis provided wise counsel and critical support during the last eighteen months.

Besides my adviser, there were many others who contributed—sometimes on a daily basis—to the development and execution of the ideas put forth in this dissertation. Dr. Johannes van Zeijts showed me how (*i.e.*, did most of the work) to modify his code TLIE to perform map calculations for systems with just a single degree of freedom. That modified code, TLIE2, allowed us to determine the very high order truncated Taylor maps in §6.5. In addition, he answered innumerable questions about UNIX and, for the longest time, loaned me his books on POSTSCRIPT. With Dr. Ivan Gjaja I had many fruitful conversations, and his probing questions always challenged me. Dr. Étienne Forest modified his computer program IRWIN to implement some of the important ideas developed in Part II, graciously answered my many questions, and provided some of the figures in §17.2.

With my fellow graduate students, I have enjoyed a wonderful sense of camaraderie and shared purpose. In particular, I recall a number of conversations with Wen-Hao Cheng on the subject of Landau damping and, likewise, numerous discussions with Marco Venturini on the topic of Lie algebras and symplectic maps. Special thanks to Dr. Huanchun Ye for

his willingness to listen, his careful and complete explanations, and his constantly inquisitive mind. On numerous occasions he sat down with me to help puzzle out a new idea. In addition to his invaluable help in physics, I have enjoyed in his company myriad gustatory adventures, unusual cinema, and long discussions of history, economics, and philosophy. He has had a challenging and delightful influence on my ideas, and I treasure our friendship.

Several professors at other institutions kindly responded to my inquiries on various matters. Drs. Lawrence Biedenharn and James Louck pointed me towards information on $SU(3)$. Dr. J. J. Seidel answered some questions about cubature formulas on the sphere. And Dr. Ronald Cools not only sent me a long list of very useful references, but also corresponded with me concerning Conjecture 16.2.

In addition, I gratefully acknowledge the financial support received from the U. S. Department of Energy under grant DEFG05-92ER40748.

Dr. Ellen Williams guided and supported me during my early years in experimental physics, and it was under her direction that I did my Masters work. Drs. Angelo Bardasis and John Layman gave me good advice along with generous amounts of time and support during my transition from experimental to theoretical physics. And Dr. Robert Park, a fellow cycling enthusiast, also provided encouragement and wise counsel, especially during that time of transition.

I am fortunate to have the love and support of a large and wonderful extended family: My parents Bess and Tyler Abell not only instilled in me a love of learning, but also provided me with an excellent education. My great-uncle Dan T. Moore, whose own interest in physics continues to serve as an inspiration, proudly encouraged me in my pursuit of science. My grandmother Luvie Pearson, who taught me to read and often whisked me away on fascinating excursions, also encouraged and supported my work. And my brother, Lyndon, has been a staunch ally. In addition, I am deeply appreciative of and thankful for my dear friends Richard and Letel Barber and my godparents Judith and Dennis Goode—their companionship, advice, encouragement, and laughter always rejuvenated me. And, of course, I am most especially thankful for and gratefully acknowledge the love and understanding of my wife and best friend, Anne A. Hunter.

Contents

Dedication v
Acknowledgements vii
List of Tables xi
List of Figures xiii

Part I. Analytic Properties of Transfer Maps 1
1. Introduction I 3
2. The Concept of a Transfer Map 4
3. The Taylor Series Representation 7
4. Complex Variable Theory 9
4.1. The Theory of Functions of a Single Complex Variable 9
4.2. The Theory of Functions of Several Complex Variables 9
5. Estimating the Domain of Convergence of a Taylor Series Map 15
5.1. Taylor Series Maps of a Single Variable 15
5.2. Taylor Series Maps of Two Variables 16
6. Example: The Anharmonic Oscillator 18
6.1. General Description 18
6.2. Exact Solution 19
6.3. Singularity Structure 25
6.4. Domain of Convergence 28
6.5. Taylor Series Map 36
6.6. Estimated Domain of Convergence 37
6.7. Accuracy of the Taylor Series Map 40
6.8. Discussion 43
7. Summary I 45

Part II. Cremona Approximation of Transfer Maps 47
8. Introduction II 49
9. Symplectic Maps and the Factored-Product Representation 51
9.1. Lie Operators and Lie Transformations 51
9.2. Important Properties and Notational Matters 51
9.3. The Factored-Product Representation 53
10. Cremona Maps and the Jolt Representation 55
10.1. Kicks, Jolts, and their Associated Maps 55
10.2. The Vector Space of Dynamical Polynomials 55
10.3. The Jolt Representation 56
11. Jolt Decomposition of Homogeneous Polynomials 58
12. Optimizing the Decomposition 60
12.1. Jolt Strengths and Gram Eigenvalues 60
12.2. The Gram Operator 61
13. The Space of Relevant $\mathcal{L}_j$ 63
13.1. Avoiding Redundancy 63
13.2. A Factorization for Symplectic Matrices 65
13.3. The Relevant $\mathcal{L}_j$ 66
13.4. Other Possible Restrictions 68
14. The Continuum Limit 70
14.1. Transition to the Continuum Limit 70
14.2. The Continuum Limit 70

15. Gram Eigenvalues in the Continuum Limit 72
15.1. One Degree of Freedom 72
15.2. Two Degrees of Freedom 75
15.3. Three Degrees of Freedom 97
15.4. Using the Manifold $[U(1)]^n$ 118
16. Return to the Discrete Case 123
16.1. One Degree of Freedom 123
16.2. Two Degrees of Freedom 136
16.3. Three Degrees of Freedom 154
17. Applications to Maps of Physical Interest 170
17.1. Cremona Symplectification of the Anharmonic Oscillator 170
17.2. Cremona Symplectification of the Advanced Light Source 182
18. Summary II 190

Appendices 193
Appendix A. Elliptic Functions 195
A.1. General Properties of Elliptic Functions 195
A.2. The Jacobian Elliptic Functions 198
Appendix B. Converting between the Taylor Series and Factored-Product Representations 204
Appendix C. Converting between the Factored-Product and Jolt Representations 206
Appendix D. Action of $e^{:f_2:}$ for One Degree-of-Freedom Systems 208
Appendix E. Properties of the Matrix $d(W)$ 209
Appendix F. The Modified Iwasawa Factorization 212
Appendix G. The Coset Space $U(3)/SO(3)$ 213
Appendix H. *Mathematica* Packages 214
Appendix I. *Mathematica* Notebooks 252

References 291
293

List of Tables

13.1	Lower bounds on $N(P, n)$.	64
15.1	An $SU(2)$ basis for f_1's.	81
15.2	An $SU(2)$ basis for f_2's.	84
15.3	An $SU(2)$ basis for f_3's.	85
15.4	An $SU(2)$ basis for f_4's.	86
15.4	An $SU(2)$ basis for f_4's (ctd.).	87
15.5	An $SU(2)$ basis for f_5's.	88
15.5	An $SU(2)$ basis for f_5's (ctd.).	89
15.6	Gram eigenvalues for $n = 2$, $\mathcal{U} = SU(2)$.	93
15.7	Gram eigenvalues for $n = 2$, $\mathcal{U} = U(2)$.	97
15.8	An $SU(3)$ basis for the space off_l's, $l \in \{0, 1, \ldots, 5\}$.	106
15.9	Gram eigenvalues for $n = 3$.	116
15.10	Gram eigenvalues for $[U(1)]^n$.	121
16.1	Some cubature formulas for the two-sphere.	145
16.2	Values of $N_{sph}(P)$, $N(P, 2)$, and N_s for $P \in \{3, \ldots, 14\}$.	148
16.3	The number of points for product cubature formula on $\mathbb{S}^1 \otimes \mathbb{S}^2$.	149
16.4	Values of α and N_{t2} for cubature formulas on the two-torus.	152
16.5	Values of $N_{s3}(P)$ and $N(P, 3)$ for $P \in \{3, \ldots, 12\}$.	160
16.6	Results of preliminary efforts to maximize $\lambda_{min}^{(4)}$ using five of the dihedral-like sub-groups of $SU(3)$.	166
16.7	Values of α, β, and N_{t3} for cubature formulas on the three-torus.	167
A.1	Primitive periods of the twelve Jacobian elliptic functions.	199
A.2	Degenerate cases of the twelve Jacobian elliptic functions.	201

List of Figures

4.1 Example of an absolute convergence diagram. 11
4.2 Computing the domain of absolute convergence. 12
4.3 Example of a logarithmic image. 13
6.1 Potential energy of the quartic anharmonic oscillator. 19
6.2 Phase-space portrait of the quartic anharmonic oscillator. 19
6.3 Real singularities for the anharmonic oscillator's time-seven map. 29
6.4 Geometry of a small change in p^i. 32
6.5 Absolute convergence diagram for the anharmonic oscillator's time-seven map. 34
6.6 The absolute convergence diagram for the anharmonic oscillator at three different time steps. 34
6.7 Amplitude dependence of the radius of convergence for Taylor expansions in the time t. 36
6.8 "Estimated" domain of convergence for the anharmonic oscillator's time-seven map. 37
6.9 "Estimated" domain of convergence for several different time steps. 38
6.10 Comparison of conjectured and true DACs for the anharmonic oscillator's time-seven Taylor map. 39
6.11 Comparison between the conjectured DAC and the singularities of the anharmonic oscillator's time-seven map. 39
6.12 The anharmonic oscillator: tracking results for the order forty-seven Taylor map with $\tau = 1$, 7, and 15. 41
6.13 Contour levels of the phase-space error Δz for $\tau = 1$. 42
6.14 Contour levels of the phase-space error Δz for $\tau = 7$. 42
6.15 Contour levels of the phase-space error Δz for $\tau = 15$. 43
16.1 Determinant versus $\lambda_{min}^{(4)}$ for random Gram matrices. 125
16.2 Histogram of $\lambda_{min}^{(4)}$ for random Gram matrices. 125
16.3 Determinant versus $\lambda_{min}^{(4)}$ for random Gram matrices near the choice of equally spaced angles. 126
16.4 Overlay of Figures 16.1 and 16.3. 126
16.5 Determinant versus minimum eigenvalue for Gram matrices found using a genetic algorithm. 128
16.6 Angular plot of thirty-two different sets of angles found with a genetic algorithm. 128
16.7 Comparisons between unmodified $\Sigma(108)$ Gram eigenvalues and continuum-limit Gram eigenvalues. 163
16.8 Comparisons between modified $\Sigma(108)$ Gram eigenvalues and continuum-limit Gram eigenvalues. 165
17.1 A grid of initial conditions. 171
17.2 The non-linear part of the anharmonic oscillator: exact results for $\tau = 1$. 171
17.3 The non-linear part of the anharmonic oscillator: Taylor map results for $\tau = 1$. 172
17.4 The non-linear part of the anharmonic oscillator: Cremona map results for $\tau = 1$. 173
17.5 The non-linear part of the anharmonic oscillator: exact results for $\tau = 7$. 174
17.6 The non-linear part of the anharmonic oscillator: Taylor map results for $\tau = 7$. 175

17.7 The non-linear part of the anharmonic oscillator: Cremona map results for $\tau = 7$. 176
17.8 The anharmonic oscillator: Taylor tracking for time $\tau = 1$. 178
17.9 The anharmonic oscillator: Cremona tracking for time $\tau = 1$. 179
17.10 The anharmonic oscillator: Taylor tracking for time $\tau = 7$. 180
17.11 The anharmonic oscillator: Cremona tracking for time $\tau = 7$. 181
17.12 The anharmonic oscillator: high-order Cremona tracking for time $\tau = 7$. 182
17.13 The ALS: results of acting on a beam of points in phase space with a fourth-order truncated Taylor map. 183
17.14 The ALS: results of acting on a beam of points in phase space with a Cremona symplectification of the fourth-order Taylor map. 184
17.15 The ALS: tracking results using a ninth-order truncated Taylor map. 185
17.16 The ALS: tracking results using a fourth-order truncated Taylor map. 185
17.17 The ALS: tracking results using a random twelve-point Cremona symplectification of the fourth-order truncated Taylor map. 186
17.18 The ALS: tracking results using a Cremona symplectification of the fourth-order truncated Taylor map based on the twelve-point cubature formula for the two-sphere. 186
17.19 The ALS: (x, p_x) and (y, p_y) tracking results using a ninth-order Taylor map. 187
17.20 The ALS: (x, p_x) and (y, p_y) tracking results using a sixth-order Taylor map. 188
17.21 The ALS: (x, p_x) and (y, p_y) tracking results using a Cremona symplectification. 189
A.1 The absolute value of a Weierstrass function $\wp(z)$. 196
A.2 A lattice of congruent points. 196
A.3 The complete elliptic integrals $K(m)$ and $K'(m)$. 198
A.4 A lattice of points for defining the Jacobian elliptic functions. 199
A.5 The co-polar trio sn, cn, dn, with parameter $m = 0.6$. 201

Part I. Analytic Properties of Transfer Maps

1. Introduction I

The study of a physical phenomenon often involves the construction and subsequent investigation of a suitable mathematical model in the form of a dynamical system; and one of the most powerful tools for the study of such systems is the concept of a transfer map. In many dynamical systems, for example, the questions of primary interest focus on such global issues as the stability of a motion and the presence (and stability) of fixed points. Upon using transfer maps to study such aspects, we in effect translate questions about the time evolution of a system into questions about the motion of points under the action of a map on the corresponding phase space. In so doing, we hide the details of the motion and emphasize its global structure. Thus do the questions one might ask of a map subsume many of the questions one might ask of the underlying dynamical system.

In the process of analyzing a dynamical system used to model some physical phenomenon, one typically discovers that the desired map cannot be extracted and written down in a closed or finite form. Hence, even though maps come in many flavors, and may be cooked according to different recipes, almost all start with the same basic ingredient: a Taylor series map, which represents the state of a dynamical system after some finite interval as a collection of Taylor series expanded in terms of the initial conditions. In spite of the wide application of Taylor series maps, little is known about their analytic and convergence properties, and that little often goes unappreciated.

Here in Part I of this thesis we shall explore some of these analytic and convergence properties, and we shall address in particular the question "What limits the domain of validity of a Taylor series map—and how?" In §2 we describe the concept of a transfer map and quote some fundamental theorems that justify not only the existence of transfer maps, but also their advantages. Then in §3 we describe the Taylor series representation for transfer maps. Following that, in §4 we summarize some of the basic theorems from the theory of functions of several complex variables. In §5 we examine how one may by extrapolation form a conjecture about the domain of a given Taylor map based solely on a knowledge of a finite number of coefficients. All this material forms the core of our understanding of what limits the domain of convergence of Taylor series maps. Of course it is in principle well known to mathematicians, but it has not previously been applied in the field of accelerator physics, even though accelerator physicists make extensive use of Taylor series maps. Then in §6 we explore a particular dynamical system—an anharmonic oscillator. There we determine the analytic solution and describe the singularities of the anharmonic oscillator in the complex planes of the initial conditions. We use this information together with the theorems from several complex variable theory to determine the domain of convergence of a Taylor series map for three different time steps. These results, while relatively straightforward, are new and illustrate the care and understanding required when drawing conclusions about the applicability of Taylor maps. In §7 we complete Part I with a summary.

2. The Concept of a Transfer Map

In the most general terms a *transfer map* is a function, or mapping, that reveals how a system changes during a fixed interval of time. One starts by giving a mathematical description of the physical system of interest—or, more precisely, of an idealized image of the physical system. In particular, one can model a large and very general class of systems by finite sets of coupled first-order ordinary differential equations (ODEs) having the form

$$\dot{z} = f(t, z; c). \tag{2.1}$$

Here $z = (z_1, \ldots, z_m)$ is a vector describing the state of the system as a point in an abstract m-dimensional space called the *phase space* of the system; $c = (c_1, \ldots, c_k)$ is a vector of *control parameters*, generally held fixed, whose values affect the global behavior of the system; and the dot, as usual, denotes differentiation with respect to the time, or some *time-like* variable, t. Using this model, one can translate any question about the time evolution of the physical system into a question about the motion of points in the corresponding phase space.

Doing a simple analysis, we might start from some initial state z^i at time t^i and describe the time evolution of the system as a path traced in phase space by the moving point $z(t)$. On the other hand, we often wish to know how the system evolves not from a *single* initial condition, but rather from a *range* of initial conditions. We envision, for example, wanting to know the behavior of a distribution of particles, or wanting to know the sensitivity of a given trajectory with respect to its initial state. To answer such questions, we can imagine using a small set of initial conditions as markers and then taking snapshots of the phase space at a sequence of equally spaced times. By observing our markers, we can determine how the motion transforms the phase space.

Boiled down to its essence, a transfer map describes how a system changes between successive snapshots. Suppose z^i represents the initial state of our dynamical system at time t^i, and that we wish to know the final state z^f at some later time t^f. We may then express the transformation from the phase space at time t^i to the phase space at time t^f as

$$z^f = \mathcal{M}^{t^f \leftarrow t^i} z^i. \tag{2.2a}$$

Here (2.2a) describes the final state as the result of the transfer map $\mathcal{M}^{t^f \leftarrow t^i}$ acting on the initial state. In other words, $\mathcal{M}^{t^f \leftarrow t^i}$ maps any given point in phase space to a new point in phase space. If only the time interval $\tau = t^f - t^i$ is relevant, then one may write (2.2a) in the simpler form

$$z^f = \mathcal{M}^{\tau} z^i. \tag{2.2b}$$

While this form certainly applies to autonomous (*i.e.*, time-independent) systems, the reader should observe that it applies also to systems for which the right-hand side f of (2.1) is periodic in t with period τ.

The form given in (2.2b), if it applies, is especially useful because the map $\mathcal{M}^{\tau}$ contains all of the dynamical information about the system. In the case of periodic systems $\mathcal{M}^{\tau}$ may also depend on where t^i occurs within one period, but it remains true that $\mathcal{M}^{\tau}$ contains all of the dynamical information. For example, suppose the map has a fixed point z^0, so that $z^0 = \mathcal{M}^{\tau} z^0$. The existence of such a fixed point implies that the underlying dynamical system has a periodic orbit. One can then easily ascertain the stability of the system in the neighborhood of the periodic orbit by examining the linear part of the map $\mathcal{M}^{\tau}$. In particular, one may represent the linear part of the map about the point z^0 by the *Jacobian matrix* M with elements given by

$$M_{ab}(z^0) = \left. \frac{\partial z_a^f}{\partial z_b^i} \right|_{z^0}.$$

The eigenvalues of M reveal the nature of the system in the neighborhood of the periodic orbit [30]. As another example, one may follow, or "track", the motion of the system simply by iterating the map.

We now ask the natural question: "Under what circumstances can we express a solution to (2.1) in the form given in (2.2a)?" The process described above—of extracting the essence of a physical system and exhibiting it in the form shown in (2.1)—works so well that we often forget the extraordinary intellectual difficulties that hindered its conception. Since the remarkable birth of classical physics some three-hundred years ago, mathematicians have learned and then taught us a great deal about differential equations. For our purposes here, their most important teachings comprise the famous existence and uniqueness theorems concerning solutions to (2.1). We may summarize these as (*e.g.* see Brauer and Nohel [13])

Theorem 2.1. *Consider any set of m first-order ordinary differential equations given in the form of* (2.1) *with c held fixed. Assume that f and its partial derivatives $\partial f_i/\partial z_j$ all exist and are continuous and bounded on some domain $\mathcal{D}$ in the $(m+1)$-dimensional space of (t, z). Then there exists a unique solution or* integral curve *of* (2.1) *passing through each point of $\mathcal{D}$. In other words, given any point (t^i, z^i) in $\mathcal{D}$, there exists a unique*

$$z(t) = \phi(t; t^i, z^i; c) \tag{2.3}$$

satisfying (2.1) *and having the property*

$$z(t^i) = \phi(t^i; t^i, z^i; c) = z^i. \tag{2.4}$$

The solution (2.3) *can be extended both forward and backward in time as long as $(t, z) = (t, \phi(t))$ remains in $\mathcal{D}$. Furthermore, this solution is continuous in the variables t, t^i, and z^i.*[1]

On writing the equations of motion (2.1) in terms of a time derivative, we appear to give special attention to the time (or the time-like variable). Expressing the solution (2.3) as $z(t)$ further emphasizes the role time plays. But Theorem 2.1 informs us that we may equally well view the solution (2.3) as a function of the initial conditions. When we adopt this point of view, we see that Theorem 2.1 guarantees us that any system described by (2.1) and satisfying the appropriate conditions has a transfer map $\mathcal{M}^{t^f \leftarrow t^i}$; and, furthermore, that transfer map is uniquely defined.

With the existence of transfer maps established, we now address two additional questions: "How do the control parameters affect the map?" and "What can we say about the map if f is analytic?"

In any physical system that we model, there always exist parameters whose values we must measure. We then include these parameters by making them part of the vector of control parameters c in (2.1). But since errors affect all measurements, we would like some assurance that small differences between the measured and true values of the c_j will not prove too harmful. This is the subject of (*e.g.* see [13])

Theorem 2.2. *Suppose the partial derivatives of f with respect to the control parameters, $\partial f_i/\partial c_j$, all exist and are continuous and bounded on some domain $\mathcal{C}$ of the manifold defined by the set of all possible control vectors c. Then at all points $c \in \mathcal{C}$ the solution* (2.3) *will be continuous in each of the parameters c_j.*

In the language of transfer maps, Theorem 2.2 assures us that sufficiently small variations in c produce correspondingly small changes in the transfer map . Therefore, if our model contains an accurate representation of the system, then we stand a good chance of making successful predictions. The mathematician, however, offers little insight concerning the construction of

[1] Other versions of the existence-uniqueness theorem (*e.g.* see Petrovski [71]) place less stringent requirements on the function f, but this simpler rendition meets our needs.

good models, so we must always look to experiment for information about the quality of our models.

For a host of reasons, including computational convenience, researchers often use analytic functions for the right-hand side of (2.1). Since the class of analytic functions has very special properties, one might expect the corresponding solution (2.3) to have similarly special properties. The following theorem addresses just this point.

Theorem 2.3 (Poincaré)**.** *Suppose f on the right-hand side of* (2.1) *denotes a set of analytic functions on some domain $\mathcal{G}$ of the manifold defined by the variables t, z, and c. Then the solution* (2.3) *will be analytic in the variables t, t^i, z^i, and c as long as $(t, z(t), c)$ remains in $\mathcal{G}$* [71].

This theorem derives its value from the fundamental fact that one may express any analytic function as a convergent power series. (We shall say more about this later.) A common application of Theorem 2.3 is to the computation of perturbative power series expansions in terms of some control parameter c_j [62]. In this thesis we shall take advantage of Theorem 2.3 to express the final conditions z^f as a power series in the initial conditions z^i.

We close this section with the following comment: Satisfying the analyticity requirements of Theorem 2.3 often (at least in physics) proves less onerous than it appears. For example, imagine that we wish to model the motion of a charged particle in a system of static electric and magnetic fields. It can be shown that even though the charges and currents that generate the electric and magnetic fields may not be analytic distributions, the fields themselves are analytic in any region free of sources [42]. This remarkable fact derives from the mathematical properties of Maxwell's equations and allows us to apply Theorem 2.3 to many models of charged-particle dynamics.

3. The Taylor Series Representation

We now confine our attention to systems covered by Theorem 2.3. In other words, we consider only those systems described by an equation of motion having the form given in (2.1) for which the right-hand side, $f(t, z; c)$, is analytic on some domain of all its variables. With these restrictions, as we shall see in §4, one may write each component of the final state as (on some domain) a convergent power series expanded in terms of the initial conditions:

$$\begin{aligned} z_1^f &= T_1(z_1^i, \ldots, z_m^i), \\ &\vdots \\ z_m^f &= T_m(z_1^i, \ldots, z_m^i), \end{aligned} \tag{3.1a}$$

where the T_j denote a collection of Taylor series, each expanded about the same point z^i in phase space. and written in terms of the initial conditions z^i. In series form, about the origin, (3.1a) becomes

$$z_a^f = K_a + \sum_b R_{ab}\, z_b^i + \sum_{bc} T_{abc}\, z_b^i z_c^i + \sum_{bcd} U_{abcd}\, z_b^i z_c^i z_d^i + \cdots , \tag{3.1b}$$

where the indices $a, b, \ldots$, run from from 1 to m, the dimension of the phase space. The coefficients K_a denote the constant terms, while the R_{ab} define the (first-order) transfer matrix, and the T_{abc}, U_{abcd}, etc., define generalized higher-order transfer matrices. We call (3.1) a *Taylor series map*, or Taylor map, because it expresses in Taylor series form exactly the idea contained in (2.2): a Taylor map acts on an initial point in phase space and returns a final point in phase space.

The reader should note that the Taylor series coefficients in (3.1) depend not only on the the various control parameters c_j, but also on the initial and final times t^i and t^f (or, for autonomous systems, on the time interval $\tau = t^f - t^i$). Furthermore, the coefficients may not be independent. In Hamiltonian systems, for example, the coefficients are constrained by the symplectic condition [28, 30], which we shall discuss in §8.

The Taylor series representation of a map, as given in (3.1), has two principal virtues: familiarity and computational speed. After calculating a suitable number of coefficients (the hard part), we can (given sufficient attention to efficient algorithms) compute z^f from z^i with great speed. Furthermore, we can apply the Taylor series map to any number of initial conditions—a valuable feature. We may, for example, want a very finely grained image of the phase-space transformation effected by some map. We can obtain this information by applying the corresponding Taylor series map once to a large number of closely spaced initial conditions. On the other hand, we might want to track just a few initial conditions through many cycles of a periodic system. In this example we can choose to represent one cycle either as a single map or as the composition of several maps. Whether we use one or several maps does not matter: we still recycle the code. Thus in both of these examples we can use the same map or maps repeatedly.

The Taylor series representation does, however, have a significant drawback: for most systems the series (3.1b) does not terminate. This difficulty has a number of important consequences. To begin with, a *truncated* Taylor series map may differ significantly from the original map. For example, even if the original map corresponds to a conservative Hamiltonian system, the truncated Taylor series map generally violates both the symplectic condition and conservation of energy. Moreover, carrying the series to higher order can only alleviate—but never eliminate—the problem. For a system in an m-dimensional phase space, the order l terms in the Taylor series map require a total of

$$m \binom{l+m-1}{l} = m \frac{(l+m-1)!}{l!(m-1)!}$$

coefficients. The use of a high-order Taylor series map therefore requires the computation and storage of a large number of coefficients. Furthermore, and most important, the series may not converge. We shall focus our attention on illuminating the principal features of the domain of convergence: what does it look like, and what factors affect its size and shape?

As a simple example of a Taylor series map, consider the dynamical system described by the Hamiltonian

$$H_{quar} = \frac{1}{2}(p^2 + q^2) - \frac{1}{4}q^4, \tag{3.2}$$

where q is the coördinate, and p is its conjugate momentum. We shall discuss this system in considerable detail in §6; for now, however, simply note that this Hamiltonian describes a particle of unit mass in the potential of an anharmonic oscillator—a harmonic oscillator with a quartic "correction". As H_{quar} is polynomial in q and p, the corresponding equations of motion,

$$\begin{aligned} \dot{q} &= \frac{\partial H_{quar}}{\partial p} = p, \\ \dot{p} &= -\frac{\partial H_{quar}}{\partial q} = -q + q^3, \end{aligned}$$

have everywhere analytic right-hand sides, and Theorem 2.3 therefore applies. Using the techniques of Lie algebra [28, 87] or automatic differentiation [11, 12, 72], we can compute the coefficients of the Taylor series map to very high order. Here we present the first few terms of the map expanded about the origin, $z = (q, p) = (0, 0)$, using a time step $\tau = 7$:

$$\begin{aligned} q^f &= 0.7539\, q^i + 0.6570\, p^i + 1.765\, {q^i}^3 - 1.626\, {q^i}^2\, p^i + 1.603\, q^i\, {p^i}^2 - 1.768\, {p^i}^3 + \cdots, \\ p^f &= -0.6570\, q^i + 0.7539\, p^i + 2.283\, {q^i}^3 + 2.091\, {q^i}^2\, p^i + 2.052\, q^i\, {p^i}^2 + 1.603\, {p^i}^3 + \cdots. \end{aligned} \tag{3.3}$$

(See §6.5.) The coefficients of the linear terms turn out to be $\cos(\tau)$ and $\pm\sin(\tau)$ and arise from the quadratic terms in the Hamiltonian (3.2). The presence of the quartic term in H_{quar} generates the infinite series of higher order terms.

4. Complex Variable Theory

4.1. The Theory of Functions of a Single Complex Variable

As a prelude to our study of the theory of functions of several complex variables, we briefly recall a couple of the salient definitions and results from the theory of functions of a single complex variable. We shall then recognize the theorems for functions in several variables as natural extensions of more well-known results.

By a *domain* we shall mean a non-empty open connected set in the complex plane. By *connected* we mean that one may join any two points using a curve that lies entirely within the domain. We call such a domain *simply connected* if any closed curve in the domain can be deformed to a point without the curve passing out of the domain. In other words, a simply connected domain contains no interior boundaries, or "holes". A function $w = f(z)$ is called *analytic* on a domain $\mathcal{D}$ if it possesses a derivative everywhere in $\mathcal{D}$. Then we have the following two important theorems. (For proofs of these theorems, consult any moderately complete text on complex analysis, *e.g.* [4, 15].)

Theorem 4.1 (Cauchy's Integral Formula)**.** *Suppose $f(z)$ is analytic on a simply connected domain $\mathcal{D}$, and suppose also that Γ is a simple closed curve contained in $\mathcal{D}$. Then for any z_0 inside Γ*

$$f(z_0) = \frac{1}{2\pi i} \oint_\Gamma \frac{f(z)}{z - z_0}\, dz. \tag{4.1}$$

Theorem 4.2 (Taylor Series)**.** *Suppose $f(z)$ is analytic on a domain $\mathcal{D}$ containing the point z_0. Define R as the radius of the largest circle which is centered at z_0 and which has its interior entirely within $\mathcal{D}$. One may then write $f(z)$ as a power series in z:*

$$f(z) = \sum_{n=0}^{\infty} c_n (z - z_0)^n. \tag{4.2a}$$

This sum is the Taylor series for f about the point z_0, and it converges absolutely inside the circle $|z - z_0| < R$. Furthermore, the coefficients c_n are given by

$$c_n = \frac{1}{n!} f^{(n)}(z_0) = \frac{1}{2\pi i} \oint_\Gamma \frac{f(z)}{(z - z_0)^{n+1}}\, dz, \tag{4.2b}$$

where Γ has the same properties as in Theorem 4.1.

When we examine functions of several complex variables, we shall learn that Theorems 4.1 and 4.2 possess natural analogues. What will be different, and what we shall pay especial attention to, is the *shape* of the domain of convergence. Whereas the natural domain for a Taylor series in a single complex variable has a circular boundary, the natural domain for a Taylor series in several complex variables has a much more dynamic shape.

4.2. The Theory of Functions of Several Complex Variables

In this section we describe specifically the theory of functions of *two* complex variables; but, as the discerning reader will note, all the results we state have natural generalizations [52, 79]. The discussion we give here follows that of Kaplan [53, Ch. 9].

Given two complex numbers z_1 and z_2, we define $\mathbb{C}^2$ as the two-dimensional complex space of points (z_1, z_2). The natural metric for $\mathbb{C}^2$ gives the distance between points (z_1', z_2') and (z_1'', z_2'') as

$$d = \left(|z_1' - z_1''|^2 + |z_2' - z_2''|^2 \right)^{1/2}.$$

By identifying $z_k = x_k + i y_k$, we note that $\mathbb{C}^2$ is equivalent to the four-dimensional Euclidean space $\mathbb{R}^4$ having points labeled by (x_1, y_1, x_2, y_2) together with the usual metric. Then one may define a domain in $\mathbb{C}^2$ exactly as in the one-dimensional case: a non-empty open connected set in the space $\mathbb{C}^2$ (or its equivalent $\mathbb{R}^4$).

For functions in $\mathbb{C}^2$, a natural domain is the *polycylinder*, a set of points (z_1, z_2) for which

$$|z_1 - a_1| < r_1 \quad \text{and} \quad |z_2 - a_2| < r_2,$$

where both r_1 and r_2 are positive real numbers, and a_1 and a_2 are complex. (Said another way, a polycylinder is the Cartesian product of two circular domains in $\mathbb{C}^1$.) The *boundary* of such a polycylinder is the set of points (z_1, z_2) satisfying

$$|z_1 - a_1| = r_1 \quad \text{and} \quad |z_2 - a_2| \leq r_2,$$

together with those points satisfying

$$|z_1 - a_1| \leq r_1 \quad \text{and} \quad |z_2 - a_2| = r_2.$$

A *generalized polycylindrical domain* in $\mathbb{C}^2$ is the set of points (z_1, z_2) for which each z_j belongs to $\mathcal{D}_j$, where $\mathcal{D}_j$ is some domain in the complex z_j plane.

A function of two complex variables is a function $F(z_1, z_2)$ whose arguments z_1 and z_2 each vary over a complex plane. Such a function is called *holomorphic*, or *analytic*, on a domain $\mathcal{D}$ if it is analytic everywhere in $\mathcal{D}$ with respect to each of its variables separately. In particular, F is holomorphic in $\mathcal{D}$ if the partial derivatives $\partial F/\partial z_1$ and $\partial F/\partial z_2$ both exist in $\mathcal{D}$.

For functions in $\mathbb{C}^2$, the analogue to Theorem 4.1 is

Theorem 4.3. *Suppose F is holomorphic in the generalized polycylinder $\mathcal{D}$: z_1 in $\mathcal{D}_1$, z_2 in $\mathcal{D}_2$. Suppose also that Γ_1 and Γ_2 are piecewise smooth simple closed curves in $\mathcal{D}_1$ and $\mathcal{D}_2$, respectively, and that the interiors of Γ_1 and Γ_2 are contained in $\mathcal{D}_1$ and $\mathcal{D}_2$, respectively. Then, if z_1^0 lies inside Γ_1, and z_2^0 lies inside Γ_2,*

$$F(z_1^0, z_2^0) = \frac{1}{(2\pi i)^2} \oint_{\Gamma_1} \oint_{\Gamma_2} \frac{F(z_1, z_2)}{(z_1 - z_1^0)(z_2 - z_2^0)}\, dz_1\, dz_2. \tag{4.3}$$

Note the remarkably restrictive constraint this theorem places on holomorphic functions of two complex variables: the values of F on the *two*-dimensional set $\Gamma_1 \times \Gamma_2$ determine the value of F at any other point in a *four*-dimensional space. Here we are counting the number of real dimensions.

In analogy with Theorem 4.2 we also have the following two theorems for functions in $\mathbb{C}^2$.

Theorem 4.4. *Under the same hypotheses as Theorem 4.3, the function F has partial derivatives of all orders, and they are given by*

$$\frac{\partial^{m+n} F(z_1^0, z_2^0)}{\partial z_1^m\, \partial z_2^n} = \frac{m!\, n!}{(2\pi i)^2} \oint_{\Gamma_1} \oint_{\Gamma_2} \frac{F(z_1, z_2)}{(z_1 - z_1^0)^{m+1}(z_2 - z_2^0)^{n+1}}\, dz_1\, dz_2. \tag{4.4}$$

Theorem 4.5. *Suppose $F(z_1, z_2)$ is holomorphic on a domain $\mathcal{D}$ containing the point (z_1^0, z_2^0). Then in a (perhaps small) neighborhood of (z_1^0, z_2^0), one may expand $F(z_1, z_2)$ as a convergent power series in z_1 and z_2:*

$$F(z_1, z_2) = \sum_{m,n=0}^{\infty} c_{mn} (z_1 - z_1^0)^m (z_2 - z_2^0)^n. \tag{4.5a}$$

This double sum is the Taylor series for F and has coefficients given by

$$c_{mn} = \frac{1}{m!\, n!} \frac{\partial^{m+n} F(z_1^0, z_2^0)}{\partial z_1^m\, \partial z_2^n} = \frac{1}{(2\pi i)^2} \oint_{\Gamma_1} \oint_{\Gamma_2} \frac{F(z_1, z_2)}{(z_1 - z_1^0)^{m+1}(z_2 - z_2^0)^{n+1}}\, dz_1\, dz_2. \tag{4.5b}$$

Furthermore, the double sum converges absolutely in any polycylinder $\left|z_1 - z_1^0\right| < r_1$ and $\left|z_2 - z_2^0\right| < r_2$ contained in $\mathcal{D}$.

After thinking about (4.5a), one might suspect that the r_1 and r_2 of Theorem 4.5 must depend upon one another: as r_1 increases, the maximum possible value for r_2 decreases (or at least never increases). The following theorem supports this conclusion, where now we specialize to Taylor series expansions taken about the origin $(z_1^0, z_2^0) = (0, 0)$.

Theorem 4.6 (Domain of Absolute Convergence)**.** *Suppose that for some* $z_1 = a_1 \neq 0$ *and* $z_2 = a_2 \neq 0$ *the double series*

$$\sum_{m,n=0}^{\infty} c_{mn}\, z_1^m z_2^n \tag{4.6a}$$

converges for some arrangement of its terms as a simple series.[2] *Then the series converges absolutely for all points* (z_1, z_2) *in the polycylinder*

$$|z_1| < |a_1| = r_1 \quad \textit{and} \quad |z_2| < |a_2| = r_2. \tag{4.6b}$$

This theorem places certain restrictions on the shape of the domain of absolute convergence (DAC) for a two-dimensional Taylor series expanded about the origin. In particular, since only absolute values matter, we may describe the real four-dimensional DAC using a two-dimensional plot that shows all values of $|z_1|$ and $|z_2|$ for which the series converges. Such a plot is called the *absolute convergence diagram*, and we show a typical example in Figure 4.1. In addition, we recall that an absolutely convergent series will converge, and will converge to the same value, for any arrangement as a simple series [76, p. 78].

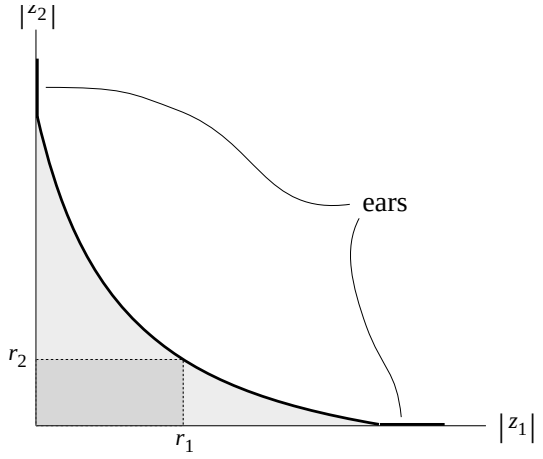

FIGURE 4.1. Example of an absolute convergence diagram. Theorem 4.6 shows that if a series converges for some point (r_1, r_2), then it converges for all pairs (z_1, z_2) having moduli $\big(|z_1|, |z_2|\big)$ inside the rectangle defined by the origin and the point (r_1, r_2).

The last theorem suggests the following recipe for determining the absolute convergence diagram of the function $F(z_1, z_2)$ (for Taylor series expansions about the origin). Begin by holding z_2 fixed at the value $r_2 e^{i\phi_2}$ and writing $f_{z_2}(z_1)$ for the resulting function of the single complex variable z_1. Then locate in the z_1-plane the singularities of f_{z_2} that lie nearest the origin $z_1 = 0$. Figure 4.2(a) shows a possible arrangement for a function whose only singularities are poles. Now alter the function f_{z_2} by varying the phase—but not the modulus—of z_2. As z_2 sweeps through a full circle of radius r_2, the singularities of f_{z_2} will trace out (possibly quite complicated) closed curves. Figure 4.2(b) illustrates a possible scenario based on the arrangement shown in Figure 4.2(a). Now measure the distance r_1 from the origin of the z_1-plane to the nearest point on any of the curves traced out by the singularities of f_{z_2}. Then according to Theorem 4.5, the point (r_1, r_2) lies on the boundary of

[2]By a *simple series* we mean that the terms $c_{mn}\, z_1^m z_2^n$ are arranged in some definite sequence $t_0, t_1, t_2, \ldots$, and we examine the convergence of the series $\sum_{j=0}^{\infty} t_j$. Of course a necessary condition for the convergence of a simple series is that the terms $t_j \to 0$ as $j \to \infty$.

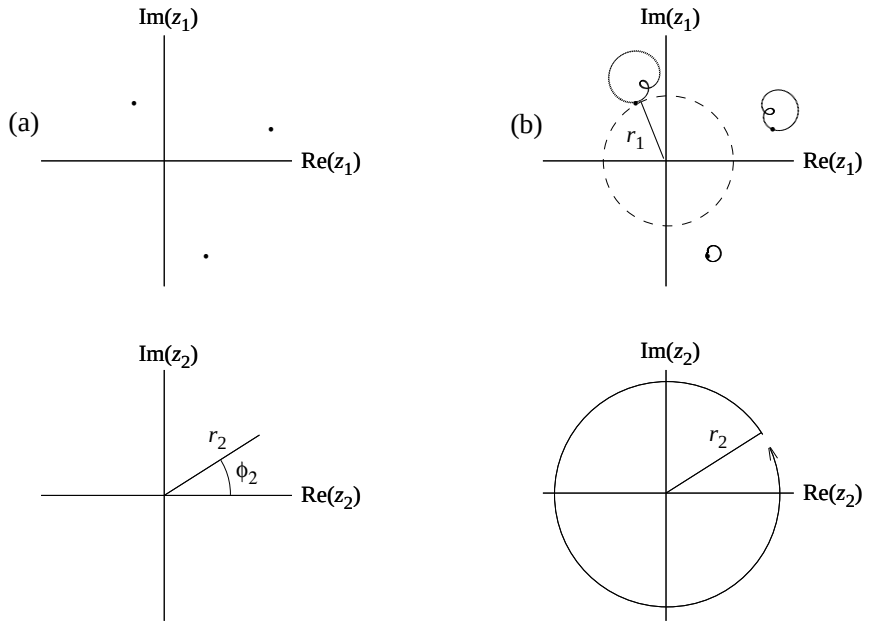

FIGURE 4.2. Computing the domain of absolute convergence. We sketch here a possible scenario for a function $F(z_1, z_2)$ whose only singularities are poles. The upper pair of graphs represents the complex z_1-plane, while the lower pair represents the complex z_2-plane. For a fixed value of $z_2 = r_2 e^{i\phi_2}$, the function $F(z_1, z_2)$ might have singularities near the origin as shown on the left in (a). As the phase ϕ_2 of z_2 sweeps through an interval of 2π, the singularities in the z_1-plane trace out closed curves, as shown on the right in (b).

the absolute convergence diagram for the Taylor series expansion of the function $F(z_1, z_2)$ in the neighborhood of the origin. By repeating the process just described for a range of values of the modulus $r_2 = |z_2|$, one can trace out the entire boundary of the absolute convergence diagram.

As the discussion of the previous paragraph implies, we shall concentrate much of our attention on the singularities of the maps we wish to Taylor expand. We therefore want to comment on how the singularity structure of functions of several complex variables differs from that of the more familiar functions of one complex variable. In the study of analytic functions of a single complex variable one frequently encounters non-removable isolated singularities such as poles and branch points. (One may also encounter an infinite number of non-isolated singularities that form a natural boundary.) Indeed, such isolated singularities play an important role in the theory. On the other hand, functions holomorphic in $\mathbb{C}^n$ for $n \geq 2$ behave very differently: non-removable singularities are *never* isolated. This fact means that by making appropriate adjustments to z_2, one may follow continuously a singularity of $F(z_1, z_2)$ in the argument z_1 as the other argument z_2 changes. Hence there exists a singularity curve of the form $z_1(z_2)$. Furthermore, there exists the possibility that "one" singularity may trace out part (or perhaps all) of the boundary of the absolute convergence diagram.

In a similar vein we note that functions holomorphic in $\mathbb{C}^n$ for $n \geq 2$ have no isolated zeroes. Unless such a holomorphic function F is identically zero, every neighborhood of a zero z^0 contains points other than z^0 at which $F = 0$ as well as points at which $F \neq 0$.

Theorem 4.6 places straightforward limitations on the possible shapes for domains of absolute convergence, but it turns out that even more restrictive conditions exist. Before we describe these, however, we must introduce the concepts of a Reinhardt domain and its logarithmic image.

A *Reinhardt domain with center* (z_1^0, z_2^0) is a domain $\mathcal{D}$ in $\mathbb{C}^2$ having the property that for each (z_1', z_2') in $\mathcal{D}$, all (z_1, z_2) for which

$$\left|z_1 - z_1^0\right| = \left|z_1' - z_1^0\right| \quad \text{and} \quad \left|z_2 - z_2^0\right| = \left|z_2' - z_2^0\right|$$

are also in $\mathcal{D}$. One may view a Reinhardt domain as a generalization to $\mathbb{C}^2$ of the annular domain in $\mathbb{C}^1$. However, a Reinhardt domain has a more dynamic structure than a simple Cartesian product between two annular domains in $\mathbb{C}^1$: the size (*i.e.*, both the radius and the width) of the annulus in the z_1 plane can vary with the size of the annulus in the z_2 plane.

A *complete Reinhardt domain with center* (z_1^0, z_2^0) is a domain $\mathcal{D}$ in $\mathbb{C}^2$ having the property that for each (z_1', z_2') in $\mathcal{D}$, all (z_1, z_2) for which

$$\left|z_1 - z_1^0\right| \leq \left|z_1' - z_1^0\right| \quad \text{and} \quad \left|z_2 - z_2^0\right| \leq \left|z_2' - z_2^0\right|$$

are also in $\mathcal{D}$. In other words, one completes a Reinhardt domain by adding the centers of the annuli to the domain. Like the Reinhardt domain, a complete Reinhardt domain represents more than a simple Cartesian product between two disks: the size of the disk in the z_1 plane can vary with the size of the disk in the z_2 plane.

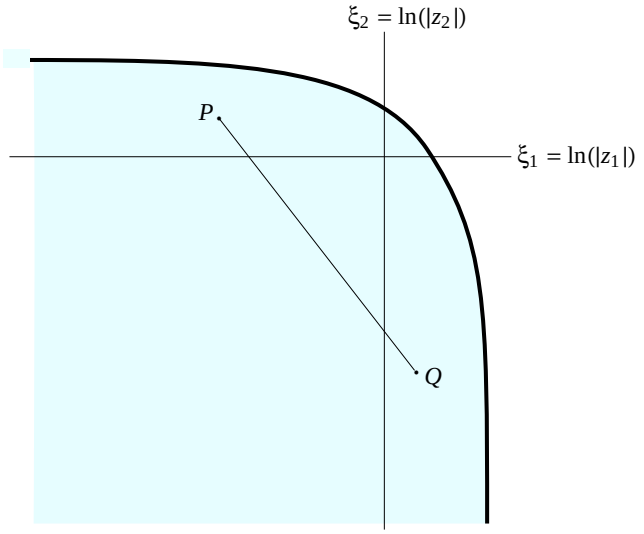

FIGURE 4.3. Example of a logarithmic image $\mathcal{D}_{log}$. We show here the logarithmic image of the domain $\mathcal{D}$ shown earlier in Figure 4.1.

Now suppose $\mathcal{D}$ is a complete Reinhardt domain with center $(0, 0)$. For each point (z_1, z_2) in $\mathcal{D}$ form the point $(\xi_1, \xi_2) = \big(\ln|z_1|, \ln|z_2|\big)$. Then the points (ξ_1, ξ_2) form a (two-dimensional) set denoted by $\mathcal{D}_{log}$ and called the *logarithmic image of* $\mathcal{D}$. We describe the domain $\mathcal{D}$ as *logarithmically convex* if $\mathcal{D}_{log}$ is convex. (The set $\mathcal{D}_{log}$ is called *convex* if one can join any two points P and Q in $\mathcal{D}_{log}$ by a straight line in $\mathcal{D}_{log}$). We illustrate this concept by showing in Figure 4.3 the logarithmic image of the domain shown earlier in Figure 4.1. The reader may note from this example that convexity of the logarithmic image does not imply convexity of the domain itself. Observe also that given the domain of convergence for the power series (4.6a), one may easily form the logarithmic image of that domain by logarithmically scaling the axes of the absolute convergence diagram.

We can now state the following

Theorem 4.7. *Suppose the series* (4.6a) *converges for all points* (z_1, z_2) *in some set* $\mathcal{A}$ *and that* $\mathcal{A}$ *has the non-empty interior* $\mathcal{A}^{int}$*. Then* $\mathcal{A}^{int}$ *is a complete Reinhardt domain with center* $(0, 0)$*. The series converges absolutely in* $\mathcal{A}^{int}$ *and uniformly in any closed polycylinder contained in* $\mathcal{A}^{int}$*. And, furthermore,* $\mathcal{A}^{int}$ *is a logarithmically convex complete Reinhardt domain.*

The last statement in this theorem—that $\mathcal{A}^{int}$ is logarithmically convex—represents a significant constraint on the shape of the DAC. Suppose, for example, that one seeks a rough picture of the DAC for a power series having the form given in (4.6a). After establishing a few points on the boundary of the DAC, one may transform to the logarithmic image, form the smallest convex set having the known locations on the boundary, and then re-transform back to the original $\left(|z_1|, |z_2|\right)$-plane. Then Theorem 4.7 guarantees us that the resulting domain belongs to the true DAC.

We note in passing that Theorems 4.6 and 4.7 do allow for the possibility that the set of points for which the power series (4.6a) converges may include sections in the coördinate planes (*i.e.*, $z_1 = 0$ or $z_2 = 0$) that extend beyond where one would expect them based on the interior of the absolute convergence diagram. This possibility explains the "ears" that stick out along the axes in Figure 4.1.

5. Estimating the Domain of Convergence of a Taylor Series Map

In §4 we learned how to determine the domain of absolute convergence (DAC) for a given Taylor map by examining the analytic properties of the map it is meant to represent. (See Theorem 4.6 and Figure 4.2.) Now suppose we know only a given Taylor map—in particular, a *truncated* Taylor map. Can we then say anything about the DAC? Strictly speaking, of course, the answer to this question is "No," because there exist an infinite number of ways to complete the series that appear in any given truncated Taylor map. In this sense then, the title of this section is something of a misnomer: we cannot *estimate* a DAC; we can only conjecture about or guess at a possible DAC. On the other hand, if the series that appear in the Taylor map are not in some sense pathological, we might hope by extrapolation to make a reasonable conjecture as to what the DAC looks like. In this section we describe a means for making just such a conjecture. Our method consists of examining the behavior of the known coefficients to conjecture a pattern and then extrapolating this pattern indefinitely. Assuming the validity of this pattern and its extrapolation, we deduce a DAC.

5.1. **Taylor Series Maps of a Single Variable**

Consider a function f of a single complex variable z such that f is analytic at the origin. Then according to Theorem 4.2, one may Taylor expand f within some neighborhood of the origin in the form

$$f(z) = \sum_n a_n z^n, \tag{5.1a}$$

with coefficients a_n given by

$$a_n = \frac{1}{2\pi i} \oint_\Gamma \frac{f(\xi)}{\xi^{n+1}}\, d\xi = \frac{1}{2\pi R^n} \int_0^{2\pi} \frac{f(Re^{i\theta})}{e^{in\theta}}\, d\theta. \tag{5.1b}$$

Here the path of integration traverses a circle of finite but sufficiently small radius $R = |\xi|$ centered on the origin. A very simple upper bound on the size of these coefficients a_n has the form

$$|a_n| \le \frac{1}{2\pi R^n} \int_0^{2\pi} \left|f(Re^{i\theta})\right|\, d\theta \equiv \frac{\tilde{f}(R)}{R^n}, \tag{5.2}$$

where $\tilde{f}(R)$ represents the average value of $|f|$ along the circular path of integration. If we fix the value of R, (5.2) tells us that for all n

$$|a_n|\, R^n \le \text{constant},$$

or, equivalently,

$$\ln\bigl(|a_n|\, R^n\bigr) \le \text{constant}. \tag{5.3}$$

Since the terms in the series (5.1a) must approach zero as $n \to \infty$ in order for the series to converge, the result (5.3) implies that for R inside the radius of absolute convergence, the values of $\ln\bigl(|a_n|\, R^n\bigr)$ will, on average, fall as n increases. Then as R approaches the radius of convergence, the values of $\ln\bigl(|a_n|\, R^n\bigr)$ will fall less rapidly. And when R reaches the radius of convergence, the values of $\ln\bigl(|a_n|\, R^n\bigr)$ will, on average, remain constant with n. We therefore concoct the following recipe for using only a finite number of coefficients a_n to make a conjecture about the radius of convergence of the Taylor series (5.1a):

1. Select a value for R and then plot $\ln\bigl(|a_n|\, R^n\bigr)$ versus n; but omit all points for which $a_n = 0$.
2. Fit a straight line through the points plotted in Step 1 and determine the slope $m(R)$ of that line.
3. Define the conjectured radius of convergence R_{cj} by the condition $m(R_{cj}) = 0$.

Of course one should not expect this recipe to work well unless the points plotted in Step 1 have at least a modest linear correlation.

Using the recipe just described in the last paragraph, we can derive a simple formula for the conjectured radius of convergence R_{cj}. First recall that standard least-squares analysis gives the slope m of the "best fit" straight line through a collection of points $\{(x_1, y_1), \dots, (x_N, y_N)\}$ as [6, p. 104]

$$m = \frac{N\sum_i x_i y_i - \sum_i x_i \cdot \sum_i y_i}{N\sum_i x_i^2 - \left(\sum_i x_i\right)^2}.$$

Then for the points given in Step 1 of the above recipe, we find for a given value of R the slope

$$m(R) = \frac{N\sum_n n\ln\bigl(|a_n|\,R^n\bigr) - \sum_n n \cdot \sum_n \ln\bigl(|a_n|\,R^n\bigr)}{N\sum_n n^2 - \left(\sum_n n\right)^2}.$$

Now applying the condition $m(R_{cj}) = 0$, we obtain

$$N\sum_n n\ln|a_n| + N\sum_n n^2 \ln R_{cj} = \sum_n n \cdot \sum_n \ln|a_n| + \sum_n n \cdot \sum_n n \ln R_{cj},$$

or, solving for $\ln R_{cj}$,

$$\ln R_{cj} = \frac{(1/N)\sum_n n \cdot \sum_n \ln|a_n| - \sum_n n\ln|a_n|}{\sum_n n^2 - (1/N)\left(\sum_n n\right)^2}.$$

For the conjectured radius of convergence we therefore obtain the result

$$R_{cj} = \exp\left(\frac{(1/N)\sum_n n \,\sum_n \ln|a_n| - \sum_n n\ln|a_n|}{\sum_n n^2 - (1/N)\left(\sum_n n\right)^2}\right). \tag{5.4}$$

Here each sum includes only those terms that correspond to non-zero coefficients in the Taylor series, and N equals the number of non-zero coefficients.

5.2. **Taylor Series Maps of Two Variables**

A Taylor map of two variables z_1 and z_2 has the form (*cf.* (3.1))

$$\begin{aligned} z_1^f &= T_1(z_1^i, z_2^i), \\ z_2^f &= T_2(z_1^i, z_2^i), \end{aligned} \tag{5.5}$$

where T_1 and T_2 denote a pair of Taylor series in two variables. We want to find for this map some way of making a reasonable conjecture about the DAC from a knowledge of only a finite number of series coefficients. One approach, the one we shall use, looks for ways to reduce each of the two-variable Taylor series T_1 and T_2 to appropriate one-variable Taylor series—to which we may then apply the formula (5.4).

To reduce a Taylor series T in the two variables z_1 and z_2, consider making the replacements

$$\begin{aligned} z_1 &\mapsto r\cos\theta, \\ z_2 &\mapsto r\sin\theta, \end{aligned} \tag{5.6}$$

for some definite value of θ, say $\frac{\pi}{6}$. Then T becomes a one-variable Taylor series in the variable r, say, $T_{\pi/6}(r)$. Applying (5.4) to $T_{\pi/6}(r)$, we then obtain a conjecture about where the line $\left(r\cos\frac{\pi}{6}, r\sin\frac{\pi}{6}\right)$—in Cartesian coördinates—crosses the boundary of the DAC.

To refine our conjecture somewhat, we should account for the fact that a single point $\left(|z_1|, |z_2|\right) = (r_1, r_2)$ in the absolute convergence diagram encompasses all points in $\mathbb{C}^2$ of the form $(r_1 e^{i\phi_1}, r_2 e^{i\phi_2})$. We might thus modify (5.6) to

$$\begin{aligned} z_1 &\mapsto e^{i\phi_1} r\cos\theta, \\ z_2 &\mapsto e^{i\phi_2} r\sin\theta, \end{aligned} \tag{5.7}$$

and thereby obtain from (5.4) a conjecture $R_{cj}(\theta, \phi_1, \phi_2)$ that depends on the phase angles ϕ_1 and ϕ_2 as well as on the angle θ. It turns out, however, that only θ and the relative phase $\alpha = \phi_1 - \phi_2$ matter. To see this, consider the generic series

$$a_{10}z_1 + a_{01}z_2 + a_{20}z_1^2 + a_{11}z_1z_2 + a_{02}z_2^2 + \cdots .$$

Making the replacements (5.7) converts this series to the form

$$\begin{aligned}
&a_{10}e^{i\phi_1}r\cos\theta + a_{01}e^{i\phi_2}r\sin\theta \\
&\qquad + a_{20}e^{i2\phi_1}r^2\cos^2\theta + a_{11}e^{i(\phi_1+\phi_2)}r^2\cos\theta\sin\theta + a_{02}e^{i2\phi_2}r^2\sin^2\theta + \cdots \\
&= (a_{10}e^{i\phi_1}\cos\theta + a_{01}e^{i\phi_2}\sin\theta)r \\
&\qquad + (a_{20}e^{i2\phi_1}\cos^2\theta + a_{11}e^{i(\phi_1+\phi_2)}\cos\theta\sin\theta + a_{02}e^{i2\phi_2}\sin^2\theta)r^2 + \cdots \\
&= (a_{10}\cos\theta + a_{01}e^{i\alpha}\sin\theta)re^{i\phi_1} \\
&\qquad + (a_{20}\cos^2\theta + a_{11}e^{i\alpha}\cos\theta\sin\theta + a_{02}e^{i2\alpha}\sin^2\theta)(re^{i\phi_1})^2 + \cdots \\
&= a_1(\theta,\alpha)re^{i\phi_1} + a_2(\theta,\alpha)(re^{i\phi_1})^2 + \cdots ,
\end{aligned}$$

where $\alpha = \phi_1 - \phi_2$. Since we wish to examine the *absolute* convergence of this series, the overall phase ϕ_1 becomes irrelevant; only the phase difference $\alpha = \phi_1 - \phi_2$ matters.[3]

Bringing together the ideas of the last two paragraphs, we can now give a recipe for using only a finite number of series coefficients a_{mn} in a two-variable Taylor series $T(z_1, z_2)$ to make a conjecture about the DAC:

(1) Make the replacements

$$\begin{aligned} z_1 &\mapsto r\cos\theta, \\ z_2 &\mapsto e^{i\alpha}r\sin\theta, \end{aligned} \tag{5.8}$$

in the Taylor series $T(z_1, z_2)$, and treat the result as a Taylor series $T'(r)$ in the single variable r.

(2) Use the formula (5.4) on the one-variable Taylor series $T'(r)$ for a given value of θ and α, and define the result as $R_{cj}(\theta, \alpha)$.

(3) Then define

$$R_{cj}(\theta) = \min_{\alpha} R_{cj}(\theta, \alpha). \tag{5.9}$$

(4) Make a polar plot, in the first quadrant, of $R_{cj}(\theta)$ versus θ. The resulting curve defines a conjecture for the DAC of the two-variable Taylor series $T(z_1, z_2)$.

To determine a corresponding conjecture for the DAC of the Taylor series map (5.5), simply overlay the domains determined separately for the Taylor series T_1 and T_2. The inner envelope of these two domains then defines a conjecture for the DAC of the full Taylor series map.

[3]One could, of course, have chosen to pull out the phase factor $e^{i\phi_2}$. Were we to do this, however, the final result, a conjectured DAC, would be the same.

6. Example: The Anharmonic Oscillator

In this section we shall use a concrete example—an anharmonic oscillator—to illustrate the theory described in §4.2 along with some of that theory's implications. In particular, we shall examine the dynamical system described by the Hamiltonian

$$H_{quar} = \frac{1}{2}(p^2 + q^2) - \frac{1}{4}q^4, \tag{6.1}$$

where q and p denote respectively the coördinate and its conjugate momentum. This Hamiltonian describes the motion of a unit mass in the potential of an anharmonic oscillator—in this case a harmonic oscillator with a quartic "correction"—and generates the equations of motion

$$\dot{q} = \frac{\partial H_{quar}}{\partial p} = p, \tag{6.2a}$$

$$\dot{p} = -\frac{\partial H_{quar}}{\partial q} = -q + q^3. \tag{6.2b}$$

We begin by discussing the general behavior of this oscillator in §6.1, giving a detailed analytic solution in §6.2, and describing the singularity structure of this system in §6.3. Using that knowledge, we then determine in §6.4 some DACs for Taylor maps with three different time steps. In addition, we go on to make some important and quite general observations concerning DACs. Then, after describing in §6.5 very briefly how to obtain Taylor map coefficients, we show in §6.6 that coefficients so obtained do indeed contain information about the DAC. In §6.7, we discuss the accuracy of Taylor maps in relation to their respective DACs. We then conclude §6 with a discussion in §6.8 of important lessons to learn from this example of an anharmonic oscillator.

6.1. **General Description**

Since H_{quar} is autonomous, the energy $E = H_{quar}$ does not vary. Then an examination of the potential energy

$$V_{quar}(q) = \frac{1}{2}q^2 - \frac{1}{4}q^4,$$

shown in Figure 6.1, makes clear the following points:

- Oscillatory motion occurs when $E < \frac{1}{4}$ and the initial coördinate q^i lies inside the well (*i.e.*, $q^i \in (-1, 1)$).
- At small amplitudes, the motion is essentially simple harmonic with period 2π. Furthermore, since the restoring force, $-dV_{quar}/dq$, weakens with amplitude, the period lengthens as amplitude increases.
- For $E = \frac{1}{4}$, the system has unstable fixed points at $p^i = 0$, $q^i = \pm 1$. There is a separatrix that separates the phase-space regions of bounded and unbounded motion, and these fixed points lie on the separatrix.
- When either $E > \frac{1}{4}$ or q^i lies outside the well, the system moves rapidly out to infinity and, as a simple calculation shows, reaches infinity in a *finite* amount of time. At the energy $E = \frac{1}{4}$, for example, the time to reach infinity from a point $q^i > 1$ is given by the relation

$$\tau_\infty = \int_{q^i}^{\infty} \frac{dq}{p} = \sqrt{2}\int_{q^i}^{\infty} \frac{dq}{q^2 - 1} = \sqrt{2}\coth^{-1}(q^i) = \sqrt{2}\tanh^{-1}\left(\frac{1}{q^i}\right).$$

The phase-space portrait shown in Figure 6.2 presents an elegant distillation of these points.

Although the non-physical nature of the Hamiltonian H_{quar} at large values of q represents an apparent difficulty, we shall turn it to our advantage. Suppose we change the sign of the quartic term in H_{quar}; then a particle having arbitrary *real* values for the initial conditions q^i and p^i will oscillate indefinitely. However, as we saw in §4.2 and as we shall make clear through our discussion of the anharmonic oscillator, the analytic structure of a system depends

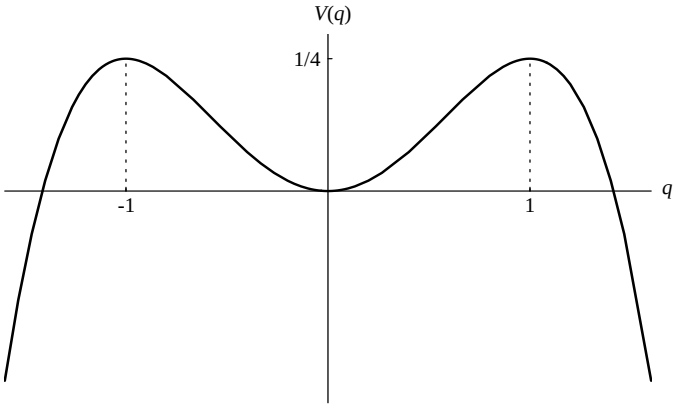

FIGURE 6.1. Potential energy of the quartic anharmonic oscillator.

equally on the behavior of the system for *complex* values of the dynamical variables. And a trajectory in the complex phase-space of the anharmonic oscillator can reach infinity in finite time—even when the quartic term has a positive sign. We shall say more in §6.8 about this case, but for now we choose the negative sign for the simple reason that then (some of) the singularities admit a simple physical interpretation.

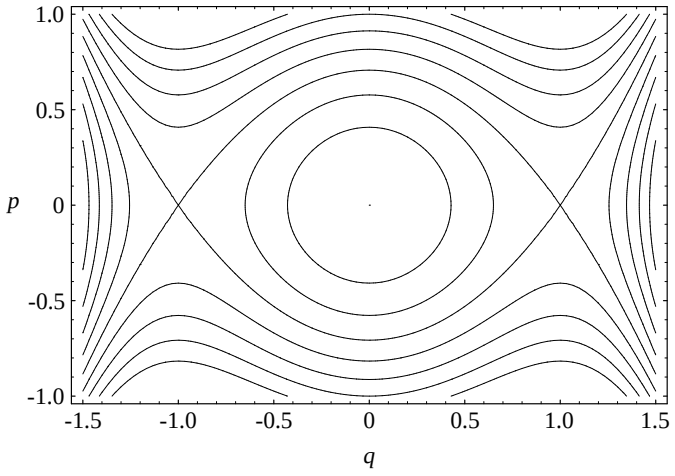

FIGURE 6.2. Phase-space portrait of the quartic anharmonic oscillator.

6.2. **Exact Solution**

6.2.1. *General Solution of the Quartic Oscillator.* Let us start not with the Hamiltonian in (6.1) but with the more general Lagrangian

$$L = \frac{1}{2}m\Big(\frac{dQ}{dt}\Big)^2 - \frac{1}{2}k\,Q^2 - \frac{\beta}{4}k'Q^4,$$

with $m, k, k' > 0$ and $\beta = \pm 1$. (Note that this means $\beta = \frac{1}{\beta}$.) By suitable scalings of the coördinate Q, the time t, and the Lagrangian itself (which has no effect on Lagrange's equations of motion), one can then obtain, without loss of generality, the equivalent Lagrangian

$$L_{quar} = \frac{1}{2}\dot{q}^2 - \frac{1}{2}q^2 - \frac{\beta}{4}q^4.$$

This Lagrangian now yields the Hamiltonian

$$H_{quar} = \frac{1}{2}(p^2 + q^2) + \frac{\beta}{4}q^4,$$

which equals our original Hamiltonian (6.1) for the choice of sign $\beta = -1$. Since this Hamiltonian is time-independent, it is itself an integral of the motion with a constant value E along any one trajectory; hence

$$H_{quar} = \frac{1}{2}(p^2 + q^2) + \frac{\beta}{4}q^4 = E. \tag{6.3}$$

The Hamiltonian (6.3) produces the equations of motion

$$\dot{q} = p, \tag{6.4a}$$

$$\dot{p} = -q - \beta q^3, \tag{6.4b}$$

where $\beta = \pm 1$. To determine the solution of these equations, solve (6.3) for the momentum p and substitute the result into (6.4a). Separating the variables t and q, and then integrating, we obtain

$$t - t^i = \int_{t^i}^{t} dt' = \int_{q^i}^{q^f} \frac{dq}{\sqrt{2E - q^2 - \frac{\beta}{2}q^4}}. \tag{6.5}$$

Our goal is to extract from this result the dependence of q^f on the time t and the initial conditions q^i and p^i. To this end we note first that the integrand contains the square-root of a quartic polynomial, so the right-hand side of (6.5) is an elliptic integral (see Appendix A). It turns out that this integral can be transformed to a rather simple standard form and then "inverted" to obtain q^f as a function of time.

To simplify and then invert the integral in (6.5), note that in the oscillatory mode the quartic oscillator has a maximum positive excursion q_m determined by setting p equal to zero in the Hamiltonian (6.3). Solving for q, and choosing signs for the square roots so as to ensure $q_m \approx +\sqrt{2E}$ for small E, we find

$$q_m = \sqrt{\beta\left(-1 + \sqrt{1 + \beta 4E}\right)}. \tag{6.6a}$$

In a similar manner for the maximum positive momentum p_m, we find

$$p_m = \sqrt{2E}. \tag{6.6b}$$

Now define the frequency

$$\omega_m = \frac{p_m}{q_m}. \tag{6.6c}$$

Using these definitions and making the substitution $x = q/q_m$, we can rewrite (6.5) in the form

$$\omega_m(t - t^i) = \int_{q^i/q_m}^{q^f/q_m} \frac{dx}{\sqrt{1 - \frac{q_m^2}{2E}x^2 - \beta\frac{q_m^4}{4E}x^4}}. \tag{6.7}$$

We also define the parameter

$$m = -\beta\frac{q_m^4}{4E} \tag{6.8}$$

and then note (after some algebra) that

$$m + 1 = \frac{q_m^2}{2E}. \tag{6.9}$$

Selecting our origin in time so that $t^i = 0$, we can now write (6.7) in the form

$$\omega_m t = \int_{q^i/q_m}^{q^f/q_m} \frac{dx}{\sqrt{(1-x^2)(1-mx^2)}}. \tag{6.10}$$

The integral in (6.10) has the form of a difference between two incomplete elliptic integrals of the first kind. Using (A.14b), we may write (6.10) in the form

$$F(\sin^{-1}(q^f/q_m)|m) = \omega_m t + F(\sin^{-1}(q^i/q_m)|m)$$

and then invert the elliptic integral to obtain

$$\frac{q^f}{q_m} = \mathrm{sn}(\omega_m t + \varphi|m). \tag{6.11a}$$

Here we have defined

$$\varphi = F(\sin^{-1}(q^i/q_m)|m). \tag{6.11b}$$

The solution (6.11a) uses the function sn, one of the twelve Jacobian elliptic functions. For the benefit of those readers not familiar with elliptic functions, we include in Appendix A a description of these functions and some of their remarkable properties. To simplify (6.11), we use the addition theorem (A.7a) for the function sn; the solution becomes

$$\frac{q^f}{q_m} = \mathrm{sn}(\omega_m t + \varphi|m) = \frac{\mathrm{sn}(\omega_m t)\,\mathrm{cn}(\varphi)\,\mathrm{dn}(\varphi) + \mathrm{sn}(\varphi)\,\mathrm{cn}(\omega_m t)\,\mathrm{dn}(\omega_m t)}{1 - m\,\mathrm{sn}^2(\omega_m t)\,\mathrm{sn}^2(\varphi)},$$

where the parameter m for the elliptic functions is given by (6.8). (From here on we shall follow the usual practice of not displaying the parameter explicitly unless its absence will cause confusion.) By using the Pythagorean identities (A.8) together with (A.14b), one can evaluate the elliptic functions at the location φ of (6.11b):

$$\begin{aligned} \mathrm{sn}\,\varphi &= q^i/q_m, \\ \mathrm{cn}\,\varphi &= \pm\sqrt{1-(q^i/q_m)^2}, \\ \mathrm{dn}\,\varphi &= \pm\sqrt{1-m(q^i/q_m)^2}. \end{aligned}$$

Then note, using (6.3), (6.6b), (6.8), and (6.9), that

$$\mathrm{cn}\,\varphi\ \mathrm{dn}\,\varphi = \pm\sqrt{(1-(q^i/q_m)^2)(1-m(q^i/q_m)^2)} = \pm p^i/p_m.$$

With these results and (6.6c), the solution for q^f then becomes

$$q^f = q_m\,\mathrm{sn}(\omega_m t + \varphi|m) = \frac{q^i\,\mathrm{cn}(\omega_m t)\,\mathrm{dn}(\omega_m t) \pm (p^i/\omega_m)\,\mathrm{sn}(\omega_m t)}{1 - m(q^i/q_m)^2\,\mathrm{sn}^2(\omega_m t)}. \tag{6.12}$$

To complete the solution for the anharmonic oscillator, we determine the correct choice of sign in (6.12) by examining its behavior for small t. Using the series expansions (A.5), we may approximate (6.12) as

$$q^f = q^i \pm p^i t + O(t^2);$$

hence we select the positive sign. We then obtain our final expression for the motion generated by the Hamiltonian H_{quar} in (6.3):

$$q(t) = \frac{q^i\,\mathrm{cn}(\omega_m t)\,\mathrm{dn}(\omega_m t) + (p^i/\omega_m)\,\mathrm{sn}(\omega_m t)}{1 - m(q^i/q_m)^2\,\mathrm{sn}^2(\omega_m t)}, \tag{6.13a}$$

where (6.8) defines the parameter m of the elliptic functions.[4] According to (6.4a), we can determine the conjugate momentum p by evaluating the time derivative of the coördinate

[4]The reader is hereby forgiven for not thinking (6.13a) simpler than our initial solution (6.11a). As we shall see, however, the form in (6.13a) proves quite useful—particularly for locating the singularities of the motion (see §6.3).

$q(t)$. Using the derivatives (A.9) and the Pythagorean identities (A.8), we obtain (after considerable algebra)

(6.13b)
$$p(t) = \frac{\left[p^i \operatorname{cn}\operatorname{dn} - (1+m)\omega_m q^i \operatorname{sn}\right]\left[1 + m(q^i/q_m)^2 \operatorname{sn}^2\right] + 2m\left[\operatorname{sn}^2 + (q^i/q_m)^2\right]\omega_m q^i \operatorname{sn}}{\left[1 - m(q^i/q_m)^2 \operatorname{sn}^2\right]^2},$$

where here all of the Jacobian elliptic functions use the same argument and parameter as in (6.13a). Note that in the solution (6.13) the choice of sign $\beta = \pm 1$ for the quartic term in the Hamiltonian (6.3) appears only via the constants q_m and ω_m defined in (6.6), and the parameter m defined in (6.8). In addition, the reader should observe that the initial conditions q^i and p^i appear in the solution (6.3) not only in the locations explicitly shown, but *also* via the energy dependence of m, q_m, and ω_m.

The alert reader will have noticed our glib treatment of the choice of branch in (6.5) and afterwards. Our solution can, in fact, be fully justified, but we shall not delve into the matter as a proper explanation requires a discussion of Riemann surfaces [74, 84].

6.2.2. *Degenerate Solutions of the Quartic Oscillator.* The results (6.13) describe the general motion of the quartic anharmonic oscillator in terms of Jacobian elliptic functions. There also exist, however, some degenerate motions.[5] Recall, for example, our original Hamiltonian (6.1), or (6.3) with $\beta = -1$. There the degenerate cases correspond to the separatrices and fixed points that occur at particular values of the energy E, or, equivalently, the parameter m. (See Figure 6.2.) For the general Hamiltonian (6.3) we begin identifying the degenerate cases by finding the fixed points. Setting $\dot{q}$ and $\dot{p}$ to zero in the equations of motion (6.4), we find three fixed points:

$$q_o = 0,\ q_\pm = \pm\sqrt{-\beta} \tag{6.14}$$

—all with $p = 0$. (Recall that $\beta = \pm 1 = \frac{1}{\beta}$.) According to (6.3), these fixed points correspond to energies $E = 0$ and $-\frac{\beta}{4}$; and according to (6.6a) and (6.8), these energies correspond to parameters $m = 0$ and $m = 1$, respectively.[6] As described in §A.2.2, these parameter values do indeed correspond to special cases of the Jacobian elliptic functions: the elliptic functions become circular or hyperbolic when the parameter equals respectively zero (at $E = 0$) or one (at $E = -\frac{\beta}{4}$).

Solution for $E = -\frac{\beta}{4}$ ($m = 1$). For $\beta = +1$ this energy necessarily entails purely complex motion. For $\beta = -1$ and real initial conditions, however, this energy corresponds to motion along one of the separatrices shown in Figure 6.2. The possible motions then comprise sitting atop one of the unstable fixed points; approaching one of the unstable fixed points, which requires an infinite amount of time; or traveling away from one unstable fixed point out to infinity in a finite amount of time and then returning from infinity to approach the other unstable fixed point in an infinite amount of time. We shall see these observations borne out in the solution below.

Using (6.6), we note that at the energy $E = -\frac{\beta}{4}$,

$$q_m^2 = -\beta,$$

and

$$\omega_m = \frac{1}{\sqrt{2}}.$$

[5]Of course these degenerate solutions can be obtained, when necessary, by taking suitable limits of the general solution. For certain numerical work, however, it proves useful to have explicit expressions.

[6]For the case $E = 0$, we must use $\lim_{E\to 0}$ to obtain the proper result.

Using these values and the degenerate cases listed in Table A.2 for the Jacobian elliptic functions, we can now reduce the general solution (6.13a) to the form

$$q(t) = \frac{q^i \operatorname{sech}^2\big(t/\sqrt{2}\big) + \sqrt{2}\, p^i \tanh\big(t/\sqrt{2}\big)}{1 + \beta {q^i}^2 \tanh^2\big(t/\sqrt{2}\big)}. \tag{6.15}$$

To simplify this expression further, we will need the relation

$$2p^2 = -\beta\big(1 + \beta q^2\big)^2. \tag{6.16}$$

This expression, obtained by setting $E = -\frac{\beta}{4}$ in (6.3), will prove most useful.

If $p^i = 0$, then (6.16) tells us that ${q^i}^2 = -\beta$, which means, according to (6.14), that q^i must be one of the fixed points $q_\pm$. We can see this directly from our solution (6.15): since here $\beta {q^i}^2 = -1$, we obtain

$$q(t) = \frac{q^i \operatorname{sech}^2\big(t/\sqrt{2}\big)}{1 - \tanh^2\big(t/\sqrt{2}\big)} = q^i. \tag{6.17}$$

If $q^i = 0$, then (6.15) becomes

$$q(t) = \sqrt{2}\, p^i \tanh\big(t/\sqrt{2}\big), \tag{6.18}$$

where now, according to (6.16), $p^i = \pm\sqrt{-\frac{\beta}{2}}$.

If neither q^i nor p^i vanishes, we can still simplify (6.15). First note from (6.16) that $\beta = -\big(1 + \beta {q^i}^2\big)^2 / 2{p^i}^2$, hence one may write the denominator of (6.15) as

$$\begin{aligned} 1 + \beta {q^i}^2 \tanh^2\big(t/\sqrt{2}\big) &= 1 - \frac{{q^i}^2}{2{p^i}^2}\big(1 + \beta {q^i}^2\big)^2 \tanh^2\big(t/\sqrt{2}\big) \\ &= (1 - \chi^2\tau^2) = (1 - \chi\tau)(1 + \chi\tau), \end{aligned} \tag{6.19}$$

where

$$\tau = \tanh\big(t/\sqrt{2}\big), \tag{6.20}$$

and, from (6.16),

$$\chi = \frac{q^i}{\sqrt{2}\, p^i}\big(1 + \beta {q^i}^2\big) = \pm\sqrt{-\beta}\, q^i. \tag{6.21}$$

Next consider the quantity

$$(1 - \chi\tau)(1 + \tau/\chi) = 1 - \tau^2 + (1/\chi - \chi)\tau = (1 - \tau^2) + \left(\frac{1 - \chi^2}{\chi}\right)\tau.$$

Since

$$\frac{1 - \chi^2}{\chi} = \frac{1 + \beta {q^i}^2}{\frac{q^i}{\sqrt{2}\, p^i}\big(1 + \beta {q^i}^2\big)} = \frac{\sqrt{2}\, p^i}{q^i},$$

and

$$1 - \tau^2 = \operatorname{sech}^2\big(t/\sqrt{2}\big),$$

we learn that

$$q^i(1 - \chi\tau)(1 + \tau/\chi) = q^i \operatorname{sech}^2\big(t/\sqrt{2}\big) + \sqrt{2}\, p^i \tanh\big(t/\sqrt{2}\big), \tag{6.22}$$

which is just the numerator of (6.15). Now using (6.19)–(6.22), we can reduce (6.15) to the form

$$q(t) = q^i \frac{1 + \tau/\chi}{1 + \chi\tau} = \frac{q^i + \frac{\sqrt{2}\, p^i}{1 + \beta {q^i}^2} \tanh\big(t/\sqrt{2}\big)}{1 + \frac{q^i}{\sqrt{2}\, p^i}\big(1 + \beta {q^i}^2\big) \tanh\big(t/\sqrt{2}\big)}. \tag{6.23}$$

When we first began discussing this case, $E = -\frac{\beta}{4}$, we commented on the real-valued motion for the system with $\beta = -1$, shown in Figure 6.2. From the result (6.23) just obtained, we can see our specific observations borne out. Consider first the case of t approaching infinity. Since $\lim_{t\to\infty} \tanh\bigl(t/\sqrt{2}\bigr) = 1$,

$$\lim_{t\to\infty} q(t) = q^i\left(\frac{1+1/\chi}{1+\chi}\right) = \frac{q^i}{\chi} = \pm\sqrt{-\beta} = q_\pm,$$

where we have used (6.20), (6.21), and (6.14). The unit mass of our quartic oscillator will therefore approach one of the fixed points as $t \to \infty$. This behavior corresponds to motion along the (possibly complex) separatrix. Now consider our other observation, the one about arriving at infinity in finite time. The particle will reach infinity when the denominator in (6.23) vanishes, *i.e.*, when $\chi\tanh\bigl(t/\sqrt{2}\bigr) = -1$, which can happen only if χ is a real number of magnitude greater than one. For the system with $\beta = -1$ (Figure 6.2), this means q^i is pure real and $\bigl|q^i\bigr| > 1$; and for the system with $\beta = +1$, this means q^i is pure imaginary and $\bigl|q^i\bigr| > 1$. In addition, if $\chi < -1$, the particle will reach infinity in finite time; if $\chi > 1$ the particle will also reach infinity in finite time, but only by traversing its orbit backwards from the initial time $t = 0$.

As with the general solution, we can determine the degenerate solutions for the conjugate momentum p by evaluating the time derivative of the coördinate $q(t)$. If $p^i = 0$, (6.17) implies

$$p(t) = 0. \tag{6.24}$$

If $q^i = 0$, (6.18) implies

$$p(t) = p^i\,\mathrm{sech}^2\bigl(t/\sqrt{2}\bigr). \tag{6.25}$$

And if neither q^i nor p^i vanishes, then (6.21) and (6.23) imply (after some algebra) that

$$p(t) = p^i\frac{\mathrm{sech}^2\bigl(t/\sqrt{2}\bigr)}{\bigl[1+\chi\tanh\bigl(t/\sqrt{2}\bigr)\bigr]^2}. \tag{6.26}$$

Solution for $E = 0$ ($m = 0$). Our work for this special case will parallel closely that just completed for the case $E = -\frac{\beta}{4}$. If energy $E = 0$, the choice of sign $\beta = +1$ means that for real initial conditions the unit mass rests on the bottom of the potential well centered at the origin; and for non-zero initial conditions the motion is necessarily purely complex. On the other hand, the choice of sign $\beta = -1$, as in the Hamiltonian (6.1), means that for real initial conditions, the possible motions comprise sitting on the stable fixed point at the origin or repeatedly circulating out to infinity and back with period 2π. We shall see these observations borne out in the solution below.

Using (6.6) and taking the limit as E vanishes, we find

$$\omega_m = 1.$$

In addition, we note from (6.8) and (6.9) that as $E \to 0$, or $m \to 0$,

$$\frac{m}{q_m^2} = -\beta\frac{q_m^2}{4E} = -\frac{\beta}{2}\frac{q_m^2}{2E} = -\frac{\beta}{2}(m+1) \to -\frac{\beta}{2}.$$

Using these two results and Table A.2, we can reduce the general solution (6.13a) for the coördinate q to the form

$$q(t) = \frac{q^i\cos t + p^i\sin t}{1+\frac{\beta}{2}{q^i}^2\sin^2 t}. \tag{6.27}$$

To simplify this expression further, we will need the relation

$$2p^2 = -\beta q^2(q^2+2\beta), \tag{6.28}$$

obtained by setting $E = 0$ in the Hamiltonian (6.3).

If $q^i = 0$, then (6.28) implies $p^i = 0$, and (6.27) therefore becomes

$$q(t) = 0. \tag{6.29}$$

If $p^i = 0$, then (6.28) tells us that $q^i = 0, \pm\sqrt{-2\beta}$. We have already disposed of the $q^i = 0$ case. For $q^i = \pm\sqrt{-2\beta}$, (6.27) reduces to

$$q(t) = \frac{q^i \cos t}{1 - \sin^2 t} = \frac{q^i}{\cos t}. \tag{6.30}$$

If neither q^i nor p^i vanishes, we can still simplify (6.27). First note from (6.28) that $\frac{\beta}{2} q^4 = -(q^2 + p^2)$; hence we may write ${q^i}^2$ times the denominator of (6.27) as

$${q^i}^2 - \left({q^i}^2 + {p^i}^2\right) \sin^2 t = {q^i}^2 \cos^2 t - {p^i}^2 \sin^2 t.$$

Using this result, we can now reduce (6.27) to the form

$$q(t) = {q^i}^2 \frac{q^i \cos t + p^i \sin t}{{q^i}^2 \cos^2 t - {p^i}^2 \sin^2 t} = \frac{{q^i}^2}{q^i \cos t - p^i \sin t}. \tag{6.31}$$

As we did for the case $E = -\frac{\beta}{4}$, we now observe how the result (6.31) just obtained for $E = 0$ bears out the observations we made earlier for the system with $\beta = -1$. The solution in (6.31) is periodic with period 2π (independent of β!). Furthermore, for non-zero but real initial conditions, the solution becomes infinite whenever $\tan(t) = q^i/p^i$. In other words, the unit mass in our quartic anharmonic oscillator repeatedly circulates out to infinity and back. The reader will note that although the overall motion has period 2π, the trips to infinity occur with period π. The motion in this case corresponds to a particular orbit which passes to the right of the $q^i = +1$ unstable fixed point (see Figure 6.2), travels out to $+\infty$, returns from $-\infty$ along an orbit that passes to the left of the $q^i = -1$ unstable fixed point, goes back out to $-\infty$, and then returns from $+\infty$ along the initial curve to the right of $q^i = +1$.

We now determine the degenerate solutions for the conjugate momentum p by taking the time derivative of the coördinate q. If $q^i = 0$, (6.29) implies

$$p(t) = 0. \tag{6.32}$$

If $p^i = 0$, (6.30) implies

$$p(t) = q^i \frac{\sin t}{\cos^2 t}. \tag{6.33}$$

And if neither q^i nor p^i vanishes, then (6.31) implies

$$p(t) = {q^i}^2 \frac{p^i \cos t + q^i \sin t}{(q^i \cos t - p^i \sin t)^2}. \tag{6.34}$$

6.3. **Singularity Structure**

According to the material discussed in §4.2 (Theorem 4.6 and Figure 4.2 in particular), one must have a thorough knowledge of a function's singularity structure in order to find the DAC for a Taylor series representation of that function. In a similar fashion, one must know the singularities of the motion of a dynamical system in order to find the DAC for any corresponding Taylor map. For our example—the anharmonic oscillator—we shall use the analytic results of §6.2 in this section to characterize and determine the singularities of the motion. Then in §6.4 we shall determine the actual DAC for several Taylor maps corresponding to different size steps in time.

6.3.1. *Characterizing the Singularities.* First examine the equations of motion (6.4) for the anharmonic oscillator. Since the right-hand sides are both polynomial in the variables q and p, they fail to be analytic only at infinity. This information and Poincaré's theorem together tell us that the general solution (6.13) for the anharmonic oscillator will be analytic with respect to q^i, p^i, and t as long as neither $q(t)$ nor $p(t)$ becomes infinite. Furthermore, because the energy remains constant along a given trajectory, the Hamiltonian (6.3) implies that q and p become infinite together.[7] It follows that the singularities of the dynamical variables $q(t)$ and $p(t)$ must occur at identical locations; hence we need to determine the singularities only of one or the other. Because the analytic expressions given in §6.2 for $q(t)$ appear simpler than those for $p(t)$, we shall examine the singularities of the coördinate $q(t)$.

According to the general solution (6.13a) for $q(t)$, singularities of the motion can occur only if the numerator becomes infinite or the denominator vanishes. Let us examine first the infinities of the numerator. Here we must treat separately the cases $q^i \neq 0$ and $q^i = 0$. To investigate the first case, recall that the co-polar trio of Jacobian elliptic functions sn, cn, and dn share exactly the same singularities, all of which are *simple* poles occurring on a regular lattice in the complex plane of the argument $\omega_m t$. (See §A.2.1.) Since the product of two simple poles yields a double pole, it follows that for $q^i \neq 0$ and a value of $\omega_m t$ near one of those common poles, the leading order behavior of the numerator in (6.13a) is $q^i \operatorname{cn}(\omega_m t) \operatorname{dn}(\omega_m t)$. But notice that the denominator in $q(t)$ *also* contains a double pole, and hence the quotient at this location can be finite. Indeed, using (A.6), we see that near a pole of the functions sn, cn, and dn, (6.13a) becomes

$$q(t) \approx -\frac{q^i \operatorname{cn}(\omega_m t) \operatorname{dn}(\omega_m t)}{m(q^i/q_m)^2 \operatorname{sn}^2(\omega_m t)} = -\frac{q_m^2}{m q^i} \operatorname{cs}(\omega_m t) \operatorname{ds}(\omega_m t).$$

Here cs and ds are two other Jacobian elliptic functions, and they also have simple poles; but never do these poles coincide with the poles of sn, cn, and dn. Therefore, in the case $q^i \neq 0$, all the singularities in the numerator of (6.13a) correspond to removable singularities of $q(t)$. For the case $q^i = 0$, (6.13a) reduces to

$$q(t) = \frac{p^i}{\omega_m} \operatorname{sn}(\omega_m t). \tag{6.35}$$

In this case $q(t)$ simply inherits all the singularities of the elliptic function sn, and these are well understood (see §A.2.1).

We turn now to the other possible source of singularities in the motion $q(t)$: the zeroes of

$$D_{quar}(q^i, p^i; t) = 1 - m \left(\frac{q^i}{q_m}\right)^2 \operatorname{sn}^2(\omega_m t), \tag{6.36}$$

the denominator in (6.13a). Such zeroes occur whenever

$$\operatorname{sn}(\omega_m t) = \pm \frac{1}{\sqrt{m}} \frac{q_m}{q^i}. \tag{6.37}$$

It turns out that the solutions of this equation yield enough information to determine the DAC for any Taylor map representation of the anharmonic oscillator. At first, however, this does not seem possible. Since the Jacobian elliptic functions are of order two, Theorem A.3 tells us that (6.37) has four solutions—two for each choice of sign—in any period parallelogram (PP); and this suggests that $q(t)$ is an elliptic function of order four. But we know from (6.35) that when $q^i = 0$, the solution $q(t)$ is an elliptic function of order two. In addition, note that even if $q^i \neq 0$, we can (at least in some cases) adjust the initial time t^i (and the initial momentum p^i) so that the oscillator will follow the same trajectory as before—but with $q^i = 0$. These observations suggest that two of the possible singularities determined by (6.37) must be removable.

[7] Of course the choice of sign $\beta = +1$ means that q and p can reach infinity only for complex values of the initial conditions q^i and p^i.

To see that two of the singularities identified by (6.37) might indeed be removable, note first that the Pythagorean relations (A.8) allow us to write the numerator of (6.13a) as

$$\begin{aligned} q^i \operatorname{cn}(\omega_m t) \operatorname{dn}(\omega_m t) + \frac{p^i}{\omega_m} \operatorname{sn}(\omega_m t) & \\ &= \pm q^i \sqrt{(1 - \operatorname{sn}^2(\omega_m t))(1 - m \operatorname{sn}^2(\omega_m t))} + \frac{p^i}{\omega_m} \operatorname{sn}(\omega_m t) \\ &= \pm q^i \sqrt{1 - (m+1) \operatorname{sn}^2(\omega_m t) + m \operatorname{sn}^4(\omega_m t)} + \frac{p^i}{\omega_m} \operatorname{sn}(\omega_m t). \end{aligned}$$

Then observe that, according to (6.8), (6.9), and (6.37),

$$(m+1) \operatorname{sn}^2(\omega_m t) = \frac{q_m^2}{2E} \frac{q_m^2}{m {q^i}^2} = -\beta \frac{q_m^4}{2E} \frac{1}{{q^i}^2} \frac{4E}{q_m^4} = -2\beta \frac{1}{{q^i}^2},$$

and

$$m \operatorname{sn}^4(\omega_m t) = \frac{1}{m} \frac{q_m^4}{{q^i}^4} = -\beta \frac{4E}{q_m^4} \frac{q_m^4}{{q^i}^4} = -\beta \frac{4E}{{q^i}^4}.$$

In addition, the use of (6.6b), (6.6c), (6.8), and (6.37) reveals that

$$\frac{p^i}{\omega_m} \operatorname{sn}(\omega_m t) = \pm \frac{p^i}{q^i} \frac{1}{\sqrt{m}} \frac{q_m}{\omega_m} = \pm \frac{p^i}{q^i} \sqrt{-\beta \frac{4E}{q_m^4}} \frac{q_m^2}{p_m} = \pm \frac{p^i}{q^i} \sqrt{-\beta \frac{4E}{p_m^2}} = \pm \sqrt{-2\beta} \frac{p^i}{q^i}.$$

Putting these results together and using the Hamiltonian (6.3), we find that the numerator of (6.13a) becomes

$$\begin{aligned} \pm q^i \sqrt{1 + 2\beta \frac{1}{{q^i}^2} - \beta \frac{4E}{{q^i}^4}} \pm \sqrt{-2\beta} \frac{p^i}{q^i} & \\ &= \pm q^i \sqrt{1 + 2\beta \frac{1}{{q^i}^2} - \beta \frac{2{p^i}^2 + 2{q^i}^2 + \beta {q^i}^4}{{q^i}^4}} \pm \sqrt{-2\beta} \frac{p^i}{q^i} \\ &= \pm q^i \sqrt{1 + 2\beta \frac{1}{{q^i}^2} - 2\beta \frac{{p^i}^2}{{q^i}^4} - 2\beta \frac{1}{{q^i}^2} - \beta^2} \pm \sqrt{-2\beta} \frac{p^i}{q^i}. \end{aligned}$$

And because $\beta^2 = 1$, the numerator now takes the form

$$q^i \operatorname{cn}(\omega_m t) \operatorname{dn}(\omega_m t) + \frac{p^i}{\omega_m} \operatorname{sn}(\omega_m t) = \pm \sqrt{-2\beta} \frac{p^i}{q^i} \pm \sqrt{-2\beta} \frac{p^i}{q^i}, \tag{6.38}$$

which may or may not vanish, depending on the relative sign of the two terms. To see what happens with these signs, consider a PP centered on the origin for the function $\operatorname{sn}(\omega_m t|m)$. Now suppose $\omega_m t_1$ and $\omega_m t_2$ denote the two points in this PP that satisfy (6.37) with the plus sign. Since the function sn is odd, it follows that the points $-\omega_m t_1$ and $-\omega_m t_2$, which belong the same PP, must be the two points that satisfy (6.37) with the minus sign. Now recall that the functions cn and dn are both even and hence do not change sign with $\omega_m t$. It therefore follows from (6.38) that of the four points in the PP that satisfy (6.37)—*i.e.*, cause the denominator of (6.13a) to vanish—exactly two also cause the numerator of (6.13a) to vanish. Then in those cases the zeroes of the denominator may indeed be removable.

The observations made in the last two paragraphs show that not all the zeroes of (6.37) need correspond to singularities of the anharmonic oscillator. On the other hand, because we want to determine the DAC, we need to know only the absolute values $\left|q^i\right|$ and $\left|p^i\right|$. Now consider what happens when we change the sign of one or both of the variables q^i and p^i. Because the Hamiltonian (6.3) is even in q and p, such a change of sign has no effect on the energy E, and therefore no effect on the values of m, q_m, p_m, or ω_m. Hence (6.38) tells us that if a particular choice of q^i, p^i, and t leads to a removable singularity of $q(t)$—*i.e.*, a zero

of both numerator and denominator—then reversing the *relative* sign of q^i and p^i will lead to a non-removable singularity, and vice versa. It therefore follows that any point (q^i, p^i) that satisfies (6.37) for a fixed time step τ yields a point $\left(\left|q^i\right|, \left|p^i\right|\right)$ that limits the DAC for the anharmonic oscillator's time-τ map.

Now observe that if $q^i = 0$ and the energy E has any finite non-zero value,[8] then the right-hand side of (6.37) becomes infinite. The solutions of (6.37) thus include the non-removable singularities found when we examined the numerator of $q(t)$ (see (6.35)). We therefore conclude that *the set of all points $z^i = (q^i, p^i)$ that satisfy* (6.37) *with the time step τ completely determines the entire DAC for a Taylor map representation of the anharmonic oscillator's time-τ map.*

6.3.2. *Symmetries of the Singularities.* From the equations of motion (6.4) for the anharmonic oscillator, we can immediately identify two useful symmetries of the motion: complex conjugation and sign reversal. If, for example, $z(t) = (q(t), p(t))$ represents one particular solution to (6.4), then $z^*(t) = (q^*(t), p^*(t))$ and $-z(t) = (-q(t), -p(t))$ represent two others. It follows that if the point (q^i, p^i) is one singularity of the time-τ map, then so are the points (q^{i^*}, p^{i^*}), $(-q^i, -p^i)$, and $(-q^{i^*}, -p^{i^*})$.[9] In addition, for our present needs we can identify a third symmetry: The observations of §6.3.1 tell us that for the purposes of determining a DAC for the anharmonic oscillator, we may change the signs of q and p independently.

The symmetries just identified offer an important means for reducing the amount of work involved in finding the DAC of a time-τ map for the anharmonic oscillator. To see this, begin by noting that since one of the points $\{q^i, q^{i^*}, -q^i, -q^{i^*}\}$ must lie in the first quadrant, we can identify all the solutions of (6.37) by looking at just the first quadrant of q^i and the (entire) plane of complex p^i. Next observe that any point in the lower-half-plane can be removed to the upper-half-plane by simple negation, and further that in determining the DAC, we may change the signs of q and p independently. It therefore follows that if we wish to determine the DAC of a time-τ map for the anharmonic oscillator, we need to examine only the first quadrant of the complex q^i plane and the upper-half-plane of complex p^i for solutions to (6.37).

6.4. **Domain of Convergence**

6.4.1. *A Real Singularity.* We turn now to the actual determination of a DAC for a given Taylor map. In particular, let us examine the dynamical system described by the Hamiltonian (6.1), or (6.3) with $\beta = -1$, and consider the map $\mathcal{M}^\tau$ that carries the point $z^i = (q^i, p^i)$ forward in time by a fixed amount τ, say $\tau = 7$.[10] One outer limit on the DAC for the time-seven map can be obtained in a fairly straightforward manner by considering only real q^i and p^i. After setting $\tau = 7$, look at what happens when $p^i = 0$—*i.e.*, when we release the anharmonic oscillator from rest. If $\left|q^i\right| < 1$, the system will oscillate indefinitely. But if, say, $q^i > 1$, the system will reach infinity in a finite time; and as q^i increases, the time to reach infinity will shrink. For some particular coördinate value q_0^i, the system will reach infinity in exactly the time step $\tau = 7$: $\mathcal{M}^{\tau=7}(q_0^i, 0) = \infty$. The point $(q_0^i, 0)$ thus represents one singularity of the time-seven map for the anharmonic oscillator. Now increase the momentum p^i to some tiny positive value p_1^i—*i.e.*, give the system a tiny push in the positive direction at the time of release. In this case the system released at q_0^i will require less than seven units of time to reach infinity. We must therefore release the system from some point $q_1^i < q_0^i$ in order to again reach infinity in exactly one time step, *i.e.*, so that $\mathcal{M}^{\tau=7}(q_1^i, p_1^i) = \infty$. If we continue to increase p^i, the corresponding q^i will continue to decrease—until we reach some value of p^i for which $\mathcal{M}^{\tau=7}(0, p^i) = \infty$. Figure 6.3 shows the locus of points $\left(\left|q^i\right|, \left|p^i\right|\right)$ thus

[8] If both q^i and E vanish, then $q(t) = p(t) = 0$; hence no singularity can arise in this case.

[9] That changing the sign of both q^i and p^i gives another singularity follows also from some of the observations in §6.3.1.

[10] Since $7 \sim 2\pi$, this choice of τ corresponds, in the language of accelerator physics, to a map for approximately one betatron oscillation.

obtained. That curve must form an outer limit for the DAC of the anharmonic oscillator's time-seven map.

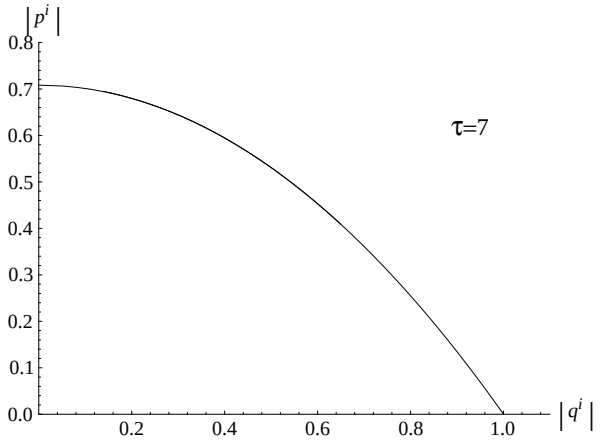

FIGURE 6.3. Real singularities for the anharmonic oscillator's time-seven map. The curve shown here represents a locus of points (q^i, p^i) for which $\mathcal{M}^{\tau=7}(q^i, p^i) = \infty$. The reader may note that this curve lies very near the separatrix. This happens because the time step $\tau = 7$ is relatively long in this example: The separatrix, by definition, contains in its neighborhood points that reach infinity for any $\tau \to \infty$; and the behavior for $\tau = 7$ is not so different from that for $\tau = \infty$.

6.4.2. *Complex Singularities.* If only real values of q^i and p^i were relevant, all of the points below the curve in Figure 6.3 would belong to the DAC for the anharmonic oscillator's time-seven map. However, according to the theorems in §4.2, we must examine our dynamical system for not only real but also complex initial conditions q^i and p^i. On doing so, we shall discover that singularities of the map $\mathcal{M}^\tau$ can exist for values of q^i and p^i whose absolute values lie inside the curve determined by the singularities on the real axes.

Figure 4.2 illustrates the basic idea behind finding the DAC of the Taylor map representation of a time-τ map for a given dynamical system. In addition, §6.3.2 describes how we may for the anharmonic oscillator take advantage of certain symmetries to reduce the amount of work required. To implement these ideas, we might fix p^i to some location in the upper-half-plane, evaluate $\left|D_{quar}(q^i, p^i; \tau)\right|$ over an appropriate region in the first quadrant of q^i,[11] and then note the location of any zeroes. Making successive changes in p^i, we can produce a sequence of pictures of $|D_{quar}|$, each time noting the locations of zeroes and thus accumulating the data required to determine the DAC for the time-τ map. This method, however, suffers from two principal drawbacks. First, evaluating $|D_{quar}|$ is a relatively slow operation. Second, and worse, some of the zeroes turn out to be extremely sharp and therefore require the evaluation of $|D_{quar}|$ to very high resolution over the first quadrant of the q^i plane.

6.4.3. *Tracking the Singularities.* A better approach to finding the DAC for the time-τ map makes just one high-resolution image of $\left|D_{quar}(q^i, p^i; \tau)\right|$ to determine accurately the locations of the half-dozen or so zeroes nearest the origin. Then, rather than making new pictures for each subsequent value of p^i, it uses Newton's method to home in on the new values of q^i after each small change in p^i. As long as we make sufficiently small changes in p^i, only a few

[11] The curve obtained in Figure 6.3 gives a connection between $\left|q^i\right|$ and $\left|p^i\right|$ that defines the "appropriate" region.

iterations will be required to determine the new values of q^i. In this manner we may track the singularities in the q^i plane as we vary p^i.

To implement the tracking of singularities, recall first that if u_k lies near a root of the function $y(u)$, then Newton's method gives the contraction map

$$u_{k+1} = u_k - \frac{y(u_k)}{y'(u_k)} \tag{6.39}$$

as an improved estimate of the nearby root [16, 50]. Furthermore, this map when iterated converges very rapidly (if at all), and it works even if y and u are complex.

Now observe that the function $D_{quar}(q^i, p^i; t)$ of (6.36), whose roots we wish to locate in the q^i plane for fixed p^i and t, has the basic structure

$$D_{quar}(q^i, p^i; t) = 1 - {q^i}^2 f(E), \tag{6.40}$$

where

$$f(E) = \frac{m}{q_m^2}\,\mathrm{sn}^2(\omega_m \tau) \tag{6.41}$$

is a function of q^i and p^i only via the energy E given by (6.1). (Here, because we shall hold the time step fixed, we have suppressed the t-dependence of f.) To apply the contraction map (6.39) to D_{quar}, note that $\partial E/\partial q^i = q^i - {q^i}^3 = q^i(1 - {q^i}^2)$, and hence

$$\begin{aligned} \frac{\partial D_{quar}}{\partial q^i}(q^i, p^i; t) &= -{q^i}^2 f'(E)\frac{\partial E}{\partial q^i} - 2q^i f(E) \\ &= -{q^i}^3\big(1 - {q^i}^2\big) f'(E) - 2q^i f(E). \end{aligned} \tag{6.42}$$

Because of the complicated dependence of f on E, it is easiest to replace $f'(E)$ by the simple estimate

$$\overline{f}(E) = \frac{f(E+\varepsilon) - f(E-\varepsilon)}{2\varepsilon} \approx f'(E), \tag{6.43}$$

where ε is an appropriately small number. In the present work we have found a useful choice in

$$\varepsilon = \max(10^{-4}, 10^{-4}E).$$

Using (6.39)–(6.43), we then obtain a contraction map for q^i in the form

$$q_{k+1} = q_k + \frac{1 - q_k^2 f(E)}{q_k^3(1 - q_k^2)\overline{f}(E) + 2q_k f(E)}. \tag{6.44}$$

Suppose we start from a point (q^i, p^i) that satisfies (6.37) and then change p^i to $p^i + dp^i$. It turns out that using the original q^i as a starting point for the contraction map (6.44) works successfully only if $\left|dp^i\right|$ is very tiny. Efficient tracking of the roots of $D_{quar}(q^i, p^i; t)$ therefore requires some means of estimating dq^i for any given dp^i. To do this, recall that we are following solutions of $D_{quar}(q^i, p^i; t) = 0$. Taking the differential of both sides yields the relation

$$\frac{\partial D_{quar}}{\partial q^i}dq^i + \frac{\partial D_{quar}}{\partial p^i}dp^i = 0,$$

which implies the estimate

$$dq^i \approx -\frac{\partial D_{quar}/\partial p^i}{\partial D_{quar}/\partial q^i}dp^i. \tag{6.45}$$

From (6.40) we find

$$\frac{\partial D_{quar}}{\partial p^i}(q^i, p^i; t) = -{q^i}^2 f'(E)\frac{\partial E}{\partial p^i} = -{q^i}^2 p^i f'(E). \tag{6.46}$$

Now using (6.42), (6.43), (6.45), and (6.46), we obtain

$$dq^i \approx \frac{-{q^i}^2 p^i \overline{f}(E) dp^i}{{q^i}^3\big(1-{q^i}^2\big)\overline{f}(E) + 2q^i f(E)} = \frac{-q^i p^i \overline{f}(E) dp^i}{{q^i}^2\big(1-{q^i}^2\big)\overline{f}(E) + 2f(E)}. \tag{6.47}$$

In summary, then, we may determine in the following manner the DAC for a Taylor map representation of the anharmonic oscillator's time-τ map:

(1) For a finite non-zero value of momentum p^i in the upper-half-plane, make a high-resolution image of $\big|D_{quar}(q^i, p^i; \tau)\big|$ in the first quadrant of the q^i plane. Then, with the aid of the contraction map (6.44), locate the zeroes of D_{quar} that appear in this image.
(2) In some systematic fashion vary p^i in the upper-half-plane—say back and forth along a sequence of semicircles of increasingly larger radii centered on the origin.
(3) For each step dp^i and for each solution (q^i, p^i) of (6.37) evaluate dq^i according to (6.47).
(4) For each solution (q^i, p^i) of (6.37), identify another nearby solution $(\bar{q^i}, \bar{p^i})$ by using the point $(q^i + dq^i, p^i + dp^i)$ as a starting point for iterating the contraction map (6.44).
(5) For each point identified in Steps 3 and 4 as a solution of (6.37), plot the point $\big(\big|q^i\big|, \big|p^i\big|\big)$ in the absolute convergence diagram. The inner envelope of these points forms the DAC for the anharmonic oscillator's time-τ map.

6.4.4. *Tracking the Nearest Singularities.* The technique just described in §6.4.3 for tracking the singularities of the anharmonic oscillator in order to determine a DAC does indeed work, and it is certainly faster than creating and examining lots of high-resolutions images of $\big|D_{quar}(q^i, p^i; \tau)\big|$; but still it requires a profligate computational effort. In this section we describe a useful refinement that eliminates much of the work.

Figure 4.2 illustrates the basic approach for computing a DAC for the anharmonic oscillator. (In that figure z_1 and z_2 play respectively the roles of q^i and p^i.) The principal idea involves changing the phase θ_p of the initial momentum

$$p^i = r_p e^{i\theta_p}, \tag{6.48}$$

watching the movement of each singularity—or root of D_{quar}—as it moves around a closed curve in the q^i plane, and then identifying on each curve the point q^i_c with minimum modulus. Repeating this process for many different values of r_p, we can determine the DAC for the time-τ map. Note that the profligacy of this method results from sampling a large range of θ_p; if we could instead identify immediately the new value of θ_p, then we could effect a considerable computational savings. Consider, for example, the closed curve traced in the q^i plane by just one of the roots (q^i, p^i) of D_{quar} as p^i rotates about the circle $\big|p^i\big| = r_p =$ constant (see Figure 4.2(b)). In addition, let (q^i_c, p^i_c) denote the point on this curve for which $\big|q^i\big|$ has a minimum. If we now increase the modulus of p^i, the curve in the q^i plane will expand, and we shall find on this expanded curve a new point $(\bar{q^i}_c, \bar{p^i}_c)$ for which $\bar{q^i}$ has minimum modulus. In general, we would like to track the roots of $D_{quar}(q^i, p^i; \tau)$ in such a way that as we vary $\big|p^i\big|$, we follow the points (q^i_c, p^i_c).

Figure 6.4 indicates the essential geometry of a small change in p^i. For a given change dr_p in $r_p = \big|p^i\big|$, we want to use first (6.47) to estimate dq^i, and then the contraction map (6.44) to home in on the new value $\bar{q^i}$ of the coördinate. We shall therefore need to know quite accurately the value of φ that places us on the path that minimizes $\big|\bar{q^i}\big|$. Using (6.48), writing

$$dp^i = \rho(\varphi) e^{i(\theta_p + \varphi)}, \tag{6.49}$$

and applying the law of cosines to the triangle with sides p^i, dp^i, and $p^i + dp^i$, we obtain

$$(r_p + dr_p)^2 = r_p^2 + \rho^2(\varphi) + 2r_p\rho(\varphi)\cos\varphi;$$

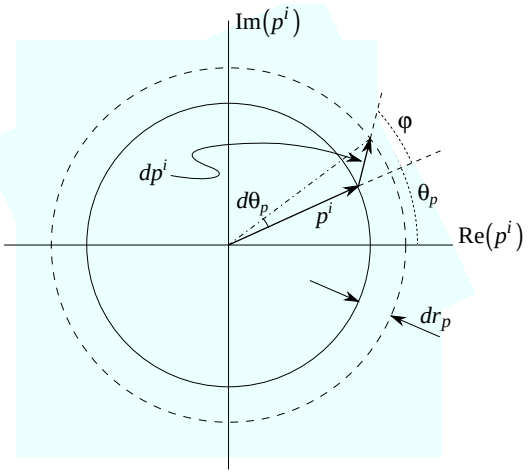

FIGURE 6.4. Geometry of a small change in p^i.

hence

$$0 = \rho^2(\varphi) + 2r_p\rho(\varphi)\cos\varphi - (2r_p + dr_p)dr_p.$$

Solving this quadratic equation for $\rho(\varphi)$ yields

$$\rho(\varphi) = -r_p\cos\varphi \pm \sqrt{r_p^2\cos^2\varphi + (2r_p + dr_p)dr_p},$$

or, since $\rho(\varphi) > 0$,

$$\rho(\varphi) = r_p\left(\sqrt{\eta + \cos^2\varphi} - \cos\varphi\right) = r_p\kappa(\varphi), \tag{6.50}$$

where

$$\eta = \left(2 + \frac{dr_p}{r_p}\right)\frac{dr_p}{r_p}, \tag{6.51}$$

$$\kappa(\varphi) = \sqrt{\eta + \cos^2\varphi} - \cos\varphi. \tag{6.52}$$

If we write (6.47) in the form

$$dq^i \approx -\xi q^i dp^i,$$

where

$$\xi = \frac{p^i\,\overline{f}(E)}{{q^i}^2\big(1 - {q^i}^2\big)\overline{f}(E) + 2f(E)}, \tag{6.53}$$

then we may use (6.47), (6.48), (6.50), and (6.53) to estimate the new value of the coördinate q^i as

$$\begin{aligned}\bar{q^i} \approx q^i + dq^i &= q^i\big(1 - \xi dp^i\big) = q^i\big(1 - \xi\rho(\varphi)e^{i\theta_p + \varphi}\big)\\ &= q^i\big(1 - \xi r_p e^{i\theta_p}\kappa(\varphi)e^{i\varphi}\big) = q^i\big(1 - \xi p^i\kappa(\varphi)e^{i\varphi}\big).\end{aligned}$$

To minimize $\big|\bar{q^i}\big|$, we therefore choose $\varphi = \bar{\varphi}$ so as to minimize $\big|1 - \xi p^i\kappa(\varphi)e^{i\varphi}\big|$.

We can now write down an improved scheme for determining the DAC for a Taylor map representation of the anharmonic oscillator's time-τ map.

(1) Using the basic procedure given at the end of §6.4.3, move p^i along a full semi-circular arc of constant modulus $r_p = \big|p^i\big|$ in the upper-half-plane and track the singularities in the q^i plane. The result will be a set of closed curves in the q^i plane. (This follows from two observations: (i) Moving p^i around an entire circle must produce closed curves in the q^i plane. (ii) The symmetries described in §6.3.2 allow us to reduce our examination of the p^i plane to just the upper-half-plane.)

(2) Along each closed curve identified in Step 1, determine the point $z_c^i = (q_c^i, p_c^i)$ for which $\left|q_c^i\right|$ is a minimum.
(3) Change $r_p = \left|p^i\right|$ by a small amount dr_p, and for each point z_c^i determine the angle $\bar{\varphi}_c$ that minimizes the quantity

$$\gamma(\varphi) = \left|1 - \xi p_c^i \kappa(\varphi) e^{i\varphi}\right|, \tag{6.54}$$

where $\kappa(\varphi)$ and ξ are given by (6.52) and (6.53), respectively.
(4) Define

$$dp_c^i = \rho(\bar{\varphi}_c) e^{i(\theta_p + \bar{\varphi}_c)},$$

and evaluate

$$dq_c^i = -\xi q_c^i dp_c^i.$$

(5) For each point z_c^i determine the point $\bar{z^i}_c = (\bar{q^i}_c, \bar{p^i}_c)$ by using $(q_c^i + dq_c^i, p_c^i + dp_c^i)$ as a starting point for iterating the contraction map (6.44). Then plot all the points $\left(\left|\bar{q^i}_c\right|, \left|\bar{p^i}_c\right|\right)$ in the absolute convergence diagram.
(6) Repeat Steps 3–5 for a range of r_p.

The inner envelope of all these points forms the DAC for the anharmonic oscillator's time-τ map.

We must issue two caveats concerning the procedure just described for finding the DAC of a given Taylor map. First, for small values of r_p one must use very small values of dr_p to ensure that $\frac{dr_p}{r_p}$ remains small. Second, wherever the curve $\left(\left|q_c^i\right|, \left|p_c^i\right|\right)$ has a slope near zero, even tiny changes dr_p can yield unacceptably large values of dq^i. The solution in this case is simply to reverse the roles of q and p in the above analysis. The procedure remains essentially the same, differing only in the following ways:

- Everywhere, except for labels on the phase-space axes, make the interchanges

$$p^i \leftrightarrow q^i, \quad r_p \leftrightarrow r_q,$$
$$p_c^i \leftrightarrow q_c^i, \quad \theta_p \leftrightarrow \theta_q.$$

- The contraction map for p is

$$p_{k+1} = p_k + \frac{1 - {q^i}^2 f(E)}{{q^i}^2 p_k \overline{f}(E)}. \tag{6.55}$$

- Replace ξ of (6.53) by

$$\zeta = \frac{{q^i}^2\left(1 - {q^i}^2\right)\overline{f}(E) + 2f(E)}{q^i {p^i}^2 \overline{f}(E)}. \tag{6.56}$$

6.4.5. *Domains of Absolute Convergence.* Using the recipe just described in §6.4.4 for determining a DAC for the anharmonic oscillator, we obtain the results shown in Figure 6.5 for the case $\tau = 7$. There we plot the paths traced in the $\left(\left|q^i\right|, \left|p^i\right|\right)$ plane by three different singularities, and the shaded region represents the DAC. The Taylor series map for the anharmonic oscillator with time $\tau = 7$ converges for any initial point $z^i = (q^i, p^i)$ inside this domain. Furthermore, the Taylor series map diverges for any initial point outside this domain. The reader should note in particular that two different complex singularities cut inside the region shown earlier in Figure 6.3.

Now consider how the DAC changes as the time step changes. If we choose a larger time step τ, then we must, in some sense, start farther from infinity in order to arrive there in exactly one time step. Hence, the singularities of the map $\mathcal{M}^\tau$ move inwards, towards the origin, as τ increases. Figure 6.6 illustrates exactly this behavior; it shows the DAC boundaries obtained by following the procedure of §6.4.4 for three different time steps: $\tau = 1$, 7, and 15. For a time step of one, the boundary of the DAC lies well *outside* the separatrix.

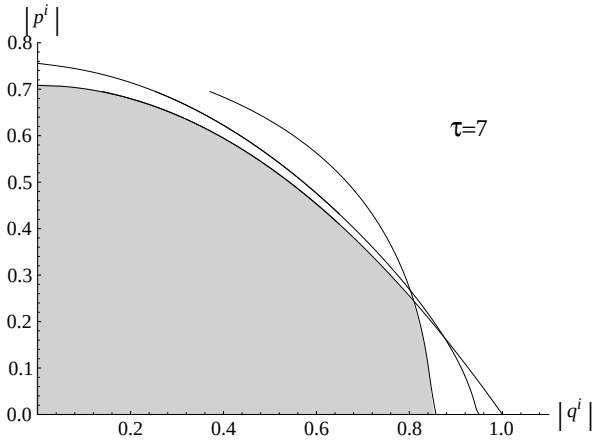

FIGURE 6.5. Absolute convergence diagram for the time-seven map. This graph shows the path in the $(|q^i|, |p^i|)$ plane of three singularities of the anharmonic oscillator's time-seven map. The inner envelope of these curves bounds the DAC (the shaded region) for the corresponding Taylor series map.

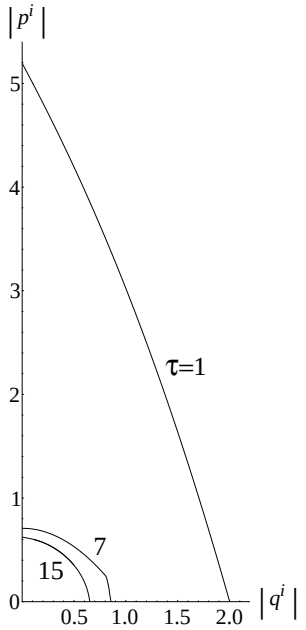

FIGURE 6.6. This graph shows the DAC boundaries for the Taylor series map at three different time steps: $\tau = 1$, 7, and 15. The boundary for $\tau = 1$ lies well outside the separatrix. For $\tau = 7$, a relatively long time step, part of the boundary lies right next to the separatrix, while the rest of the boundary cuts inside the separatrix. And for $\tau = 15$ all of the boundary lies inside the separatrix.

Then as the time step increases, the DAC shrinks. At a time step of fifteen the boundary of the DAC lies well *inside* the separatrix.

From the DACs shown in Figure 6.6, we may draw an important conclusion: there exists *no* necessary connection between, on the one hand, a DAC for a Taylor map (with the time

τ real and held fixed) expanded in terms of the initial conditions in phase space and, on the other hand, a domain of convergence for a corresponding solution (with real initial conditions) given as a Taylor series expanded in terms of the time t. To see this, recall that a Taylor series expansion in t about $t = 0$ has a domain of convergence determined by the distance from the origin to the nearest singularity in the plane of complex time. Let us therefore write the motion of the anharmonic oscillator in the form (*cf.* (6.11))

$$q^i = q_m \,\mathrm{sn}\big(\omega_m(t - t_*)|m\big) \tag{6.57}$$

and examine the temporal singularities of this solution. As described in §A.2.1, poles of $\mathrm{sn}(u|m)$ occur whenever

$$u = 2\mu K(m) + i(2\nu + 1)K'(m), \tag{6.58}$$

for any $\mu, \nu \in \mathbb{Z}$. Here $K(m)$ and $K'(m)$ denote respectively the complete elliptic integral of the first kind and its cousin $K(1 - m)$ (see (A.4) and Figure A.3). Then the complex times

$$t_{\mu\nu} = \frac{\omega_m t_* + 2\mu K(m)}{\omega_m} + i\,\frac{(2\nu + 1)K'(m)}{\omega_m} \tag{6.59}$$

represent all the temporal singularities of (6.57).

Now consider just the (real) oscillatory motion of the anharmonic oscillator. In that case the energy E and the parameter m satisfy respectively

$$0 < E < \frac{1}{4} \;\text{ and }\; 0 < m < 1.$$

In addition, the constants ω_m and t_* and the elliptic integrals $K(m)$ and $K'(m)$ are all real. Then, as expected in this case, no temporal singularity $t_{\mu\nu}$ sits on the real t axis. To determine the distance to the nearest singularity in the complex time plane, first observe from (6.57) that the constant t_* controls the phase of the oscillator. Since we might start this dynamical system with any value of the phase, only the imaginary part of $t_{\mu\nu}$ matters; hence we obtain from (6.59) the radius of convergence for a Taylor series solution (with real initial conditions) expanded in the time t:

$$t_{ns} = \frac{K'(m)}{\omega_m} = \frac{1}{\sqrt{1 - {q_m}^2/2}}\,K'\!\left(\frac{{q_m}^2/2}{1 - {q_m}^2/2}\right). \tag{6.60}$$

Here we have used (6.6) and (6.8) to express t_{ns} in terms of the maximum amplitude q_m, and Figure 6.7 shows this amplitude dependence of t_{ns}. Now observe that an amplitude of $q_m = 0.5$, for example, gives $t_{ns} \approx 2.578$. In other words, when the amplitude equals 0.5, a Taylor series expansion in t for the motion of the anharmonic oscillator will converge only for $t < 2.578$. On the other hand, Figure 6.6 shows that a Taylor series map expanded in the initial conditions $z^i = (q^i, p^i)$ will converge at an amplitude of 0.5 for a time step τ as large as, even somewhat larger than, 15—nearly an order of magnitude greater than the temporal radius of convergence! Looking at this same data from a different angle, one may note from Figure 6.7 that a Taylor series solution expanded in t will converge for $t \sim 7$ only for amplitudes $q_m \lesssim 0.005$—more than two orders of magnitude smaller than the maximum amplitude allowed by the DAC of the time-seven Taylor map! Thus do we see, in a concrete example, that *for a given dynamical system the radius of convergence for a Taylor series solution (with real initial conditions) expanded in the time has no bearing on the DAC of a Taylor map expanded in the initial conditions (with the time τ real and held fixed).*

In the above discussion we have made a distinction between two different ways of writing a Taylor series solution for the anharmonic oscillator: either as an expansion in the initial conditions, with τ real and held fixed; or as an expansion in the time, with the initial conditions real and held fixed. Furthermore, we have seen that their respective convergence domains—one in the time, and one in the initial conditions—have no bearing on one another. In one sense, however, the description given so far resembles a pair of photographs taken

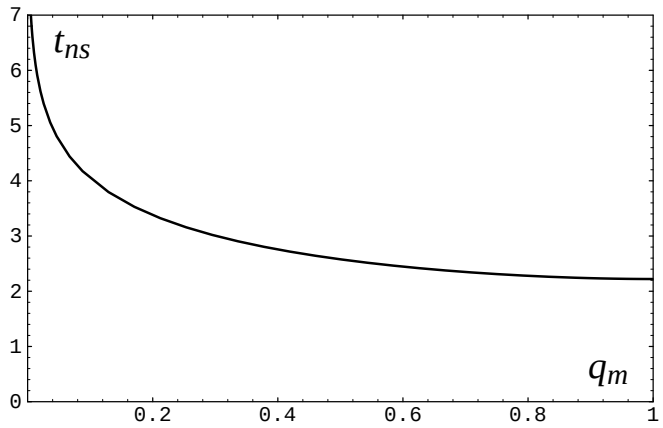

FIGURE 6.7. Amplitude dependence of the radius of convergence for Taylor expansions in the time t.

from opposite sides of a convoluted three-dimensional object:[12] Each picture gives us useful information, but we cannot necessarily reconstruct the object from either of the two pictures alone, or, in extreme cases, even from both pictures taken together. To see the whole of the anharmonic oscillator, we must look at its motion in all of $\mathbb{C}^3$, the space of complex q^i, p^i, and t. The singularities that appear there in that larger space determine the convergence domains for both types of Taylor series solutions we have examined. The differences that appear arise as consequences of fixing either t or (q^i, p^i) to real values and looking at Taylor series solutions expanded in terms of the remaining complex variables.

From Figure 6.6 we may draw a second, equally important, conclusion: there exists *no* connection between the separatrix and the DAC. The size of the DAC is determined not by the size of the region of stability in the real part of phase space, but rather by the complex dynamics of the system and the choice of time step τ. To make this same observation from a slightly different point of view, refer back to Theorem 2.3. Because the right-hand sides of the equations of motion (6.2) are analytic for all $(q, p) \in \mathbb{C}^2$, Poincaré's theorem tells us that as long as the system does not reach infinity, the motion of the anharmonic oscillator will be analytic in the elapsed time τ and the initial conditions $z^i = (q^i, p^i)$. Since the motion is analytic in τ, it follows that for arbitrary initial conditions z^i, one can always find a non-zero time step τ (possibly quite small) such that the system cannot reach infinity in the time allotted. Put another way, *one can obtain an arbitrarily large DAC—but at the cost of having to use a small (perhaps microscopic) time step* τ. Conversely, since the motion is analytic in the initial conditions z^i, it follows that for an arbitrary time step τ, one can always find an open set of non-zero initial conditions $z^i = (q^i, p^i)$ (possibly quite near the origin) such that again the system cannot reach infinity in the time allotted. In other words, *one may use an arbitrarily large time step* τ*, but at the cost of having to make do with a small (perhaps microscopic) DAC.*

6.5. **Taylor Series Map**

One very efficient method for computing the coefficients of a Taylor series map to high order employs the Lie algebraic techniques introduced in and used throughout Part II of this thesis. For an autonomous Hamiltonian system the technique boils down to series expanding the exponential operator in the expression

$$z_a^f = e^{-\tau :H:} z_a^i. \tag{6.61}$$

[12]Indeed, the matter here seems far more subtle than the difficulties faced by the Flatlander A. Square in his attempts to comprehend the sphere [1].

Here z_a denotes one of the dynamical variables—q or p in our case, τ the desired time step, and $:H:$ the Lie operator associated with the system's Hamiltonian H. (See §9, Appendix B, and any of the references [25, 28, 30, 33].) The only difficulty with this technique is that quadratic terms in H lead to an infinity of slowly converging terms of a given order. One can refine (6.61) so as to avoid this difficulty by cutting the time step τ by some power of two, say 2^n, and then successively squaring the resultant Taylor map n times. For a modest value of n, which will depend on the size of the time step τ and the Hamiltonian H, one can quickly (on a computer) evaluate to machine precision a truncated Taylor map approximation to $\exp(-\tau/2^n :H:)z_a^i$. Then, after n squarings, we obtain the desired result (6.61). This refinement is sometimes called "scaling and squaring" [29, 66].

Because the anharmonic oscillator involves just two phase-space variables, we can obtain extremely high-order coefficients with only a few minutes of computer time. Using TLIE2, a modified version of the program TLIE [87], we determined the coefficients of Taylor maps for the anharmonic oscillator at time steps $\tau = 1$, 7, and 15; and, for no particular reason, we chose to compute those maps through order forty-seven. To verify their correctness, we checked a few of the high-order coefficients against numerical evaluations of the double contour integral in (4.5b). The coefficients thus obtained—even using a crude method of numerical integration—agreed with those given by TLIE2 to better than five significant figures. Much earlier, in (3.3), we exhibited the first few coefficients of the Taylor map for time $\tau = 7$.

6.6. **Estimated Domain of Convergence**

Using the method described in §5.2, we can make a conjecture as to what a DAC looks like based on the finite number of Taylor map coefficients obtained in §6.5. Figures 6.8 and 6.9 show such conjectures for the anharmonic oscillator's Taylor maps with time steps $\tau = 1$, 7, and 15. These results should be compared with the exact DAC boundaries shown in Figures 6.5 and 6.6.

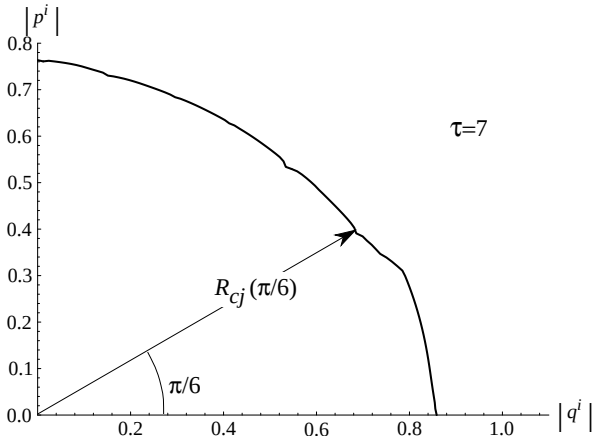

FIGURE 6.8. This figure shows a conjecture for the DAC of the anharmonic oscillator's time-seven Taylor map. This result was obtained using the method of §5.2 with the order forty-seven truncated Taylor map coefficients found in §6.5.

For time steps $\tau = 1$ and 15, the curves in Figures 6.6 and 6.9 agree extremely well with one another. In fact, for $\tau = 1$ we can see no visible difference between the two graphs. However, a small but significant discrepancy does exist for $\tau = 7$. As illustrated in Figure 6.10, the conjectured DAC for $\tau = 7$ agrees very well with the true DAC along only part of the boundary. A comparison of our conjecture with all three of the singularities we tracked indicates why this happens: Along the section where the conjectured boundary does

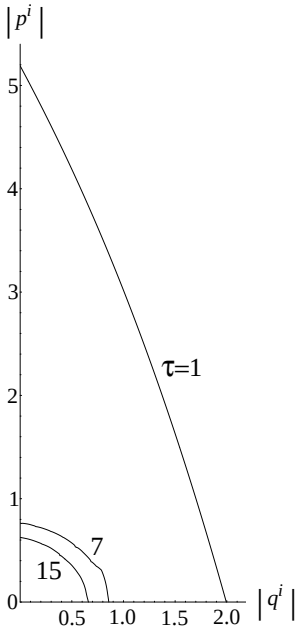

FIGURE 6.9. In this figure we show conjectures for the DACs of the anharmonic oscillator's Taylor maps for time steps $\tau = 1$, 7, and 15. As in Figure 6.8 these results are based on the Taylor map coefficients through order forty-seven.

not see the true boundary, it instead sees one of the other singularities; indeed, it follows that other singularity very closely (see Figure 6.11). We computed numerically the residues of these two singularities—the one followed by our conjecture and the one that bounds the true DAC—and found that the pole which actually bounds the DAC has a residue that is about sixty-three times smaller in magnitude than that of the pole seen by our conjectured boundary (*i.e.*, the one seen by the Taylor map coefficients through order forty-seven). From this information we can make a rough estimate of the order at which the DAC conjectured from the Taylor map coefficients will begin to notice the singularity that really bounds the true DAC. Based on a pole of residue b at a distance R from the origin, we may estimate the magnitude of the coefficients in a Taylor series as roughly $\frac{b}{R^{n+1}}$.[13] At the order where the conjectured DAC boundary begins to notice the pole with the tiny residue, coefficients based on the two different poles should be roughly comparable. Hence, since the two singularities with residues b_1 and $b_2 \approx 63 b_1$ strike the $|p^i|$ axis in Figure 6.5 at radii of about $R_1 = 0.707$ and $R_2 = 0.755$, respectively, we look for the order n which makes

$$\frac{b_1}{R_1^{n+1}} = \frac{b_2}{R_2^{n+1}}.$$

This order is given by

$$n = \frac{\ln(b_2/b_1)}{\ln(R_2/R_1)} - 1,$$

[13]Consider the function $g_1(z) = \frac{b}{z-\zeta}$, $\zeta \neq 0$, which has residue b at ζ. Its Taylor expansion about the origin has coefficients given exactly by $a_n = \frac{-b}{\zeta^{n+1}}$. Now consider a more general function $g_2(z)$, which also has a pole of residue b at $\zeta \neq 0$. If all the singularities of g_2 other than ζ are farther from the origin than ζ, one can, by a suitable choice of contour, use (5.1b) to show that the Taylor expansion of g_2 about the origin has coefficients given approximately by $a_n \approx \frac{-b}{\zeta^{n+1}}$ for sufficiently large n.

and for our present case we find $n \approx 62$. We therefore expect that the DAC conjectured for the time-seven Taylor map will not begin to reflect the presence of the pole with the smaller residue until we include Taylor map coefficients of degree at least sixty-two.

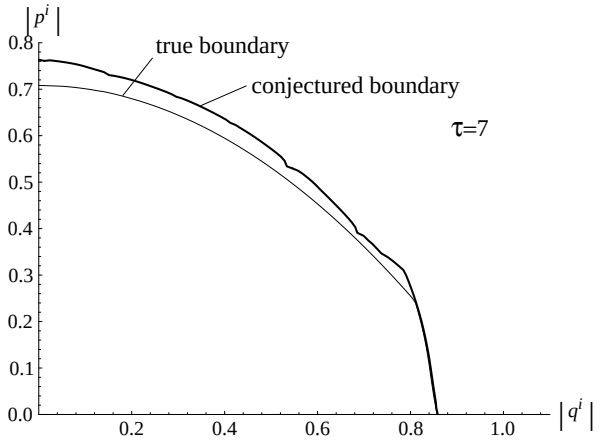

FIGURE 6.10. A comparison between the DAC for the time-seven Taylor series map and the DAC conjectured from the Taylor series coefficients through order forty-seven.

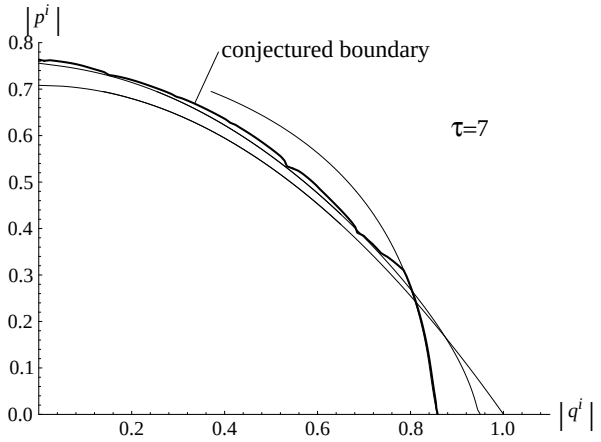

FIGURE 6.11. A comparison between the singularities of the time-seven map and the DAC conjectured from the Taylor series coefficients through order forty-seven.

That the exact and conjectured DACs agree with one another tells us that in some sense the Taylor map coefficients know about the singularities of the map. The reader should not, however, think that any mystery attends this observation. Any undergraduate course in mathematics that introduces the concept of Taylor series representations for functions of a single variable discusses the connection between singularities and convergence radii; and they also discuss how to determine convergence radii based on the series coefficients (albeit not solely on a finite number of coefficients). In the discussion of the theory of functions of several complex variables in §4.2, we learned that the DAC of a Taylor series map is determined by the singularities of the corresponding transfer map. The striking agreement between the true DACs shown in Figure 6.6 and the conjectured DACs in Figure 6.9 merely emphasizes the fact that the Taylor map coefficients do indeed see those singularities—both real and complex.

6.7. **Accuracy of the Taylor Series Map**

A finite domain of convergence of course has a very real effect on how we can use a given Taylor series map. In particular, we should not expect a *truncated* Taylor map to work well for points in phase space near the boundary of the DAC. For the anharmonic oscillator—which we have solved exactly—we shall examine the effect of the finite DAC in two different ways. Later, in Part II of this thesis, we shall examine a different aspect of truncated Taylor maps, and in that context we shall again examine the anharmonic oscillator (see especially §17.1).

To examine the effect of a finite DAC on Taylor maps for the anharmonic oscillator, the first approach we shall use compares the phase-space portraits generated by our truncated Taylor map approximations with the exact phase-space portrait shown in Figure 6.2. Using a map $\mathcal{M}^\tau$ that carries a dynamical system forward in time by an amount τ, and simply iterating the equation (*cf.* (2.2))

$$z^{n+1} = \mathcal{M}^\tau z^n, \tag{6.62}$$

with the initial condition $z^0 = z^i$, we can determine the future state of that system at any time t that equals an integer multiple of the time step τ. By using (6.62) to track a few initial conditions for many iterations, we can paint a phase-space portrait of the dynamical system described by $\mathcal{M}^\tau$.

Figure 6.12 shows, for the anharmonic oscillator, three approximate phase-space portraits obtained by applying to several initial conditions 500 iterations of the order forty-seven truncated Taylor maps for time steps $\tau = 1$, 7, and 15. The $\tau = 1$ portrait contains two initial conditions that lie outside the separatrix, but all the other initial conditions lie on the q^i axis ($p^i = 0$) with $0 < q^i < 1$. For $\tau = 15$ the phase-space orbits generated by the truncated Taylor map agree well with the true phase-space orbits up to about $q^i = 0.50$ (at least for the 500 iterations shown). Similarly, for $\tau = 7$ the orbits agree well up to about $q^i = 0.65$. And for $\tau = 1$ the truncated Taylor map generates an accurate phase-space portrait throughout the region enclosed by the separatrix; moreover, the $\tau = 1$ map renders accurately even some orbits (the large dots) that lie outside the separatrix.

Now recall the comparisons made in §6.6 between the true and conjectured DACs for the anharmonic oscillator. Those comparisons taught us that the Taylor map coefficients do indeed know about the singularities of the underlying transfer map. We can observe this same fact reflected in the tracking results of Figure 6.12. There each of the order forty-seven truncated Taylor maps—for $\tau = 1$, 7, and 15—produces orbits in phase space that agree well with the exact orbits at points significantly inside their respective Taylor DACs. Furthermore, it is obvious that the maps for $\tau = 7$ and $\tau = 15$ do not work outside their DACs; and, in fact, those maps appear to work less well at points approaching their DAC boundaries (from the inside). These last observations also hold for the $\tau = 1$ map, but to see them requires a tool more precise than the tracking results.

Our second approach to examining the effect of a finite DAC on Taylor maps for the anharmonic oscillator employs the more precise tool just referred to. Here we shall simply measure the distance in phase space between the results of applying the exact and truncated Taylor series maps once to the same initial conditions. In other words, we evaluate

$$\Delta z(q^i, p^i) = \sqrt{\left(q^f_{ex} - q^f_{tay}\right)^2 + \left(p^f_{ex} - p^f_{tay}\right)^2}, \tag{6.63}$$

where $\left(q^f_{ex}, p^f_{ex}\right)$ denotes the result of applying the exact map to the initial point (q^i, p^i) in phase space, and $\left(q^f_{tay}, p^f_{tay}\right)$ denotes the result of applying the order forty-seven truncated Taylor map to the same initial condition. Figures 6.13–6.15 show, in the first quadrant of the real (q^i, p^i) plane, four different contour levels of Δz for each of the truncated Taylor maps with time steps $\tau = 1$, 7, and 15. In all three figures the phase-space error Δz changes by

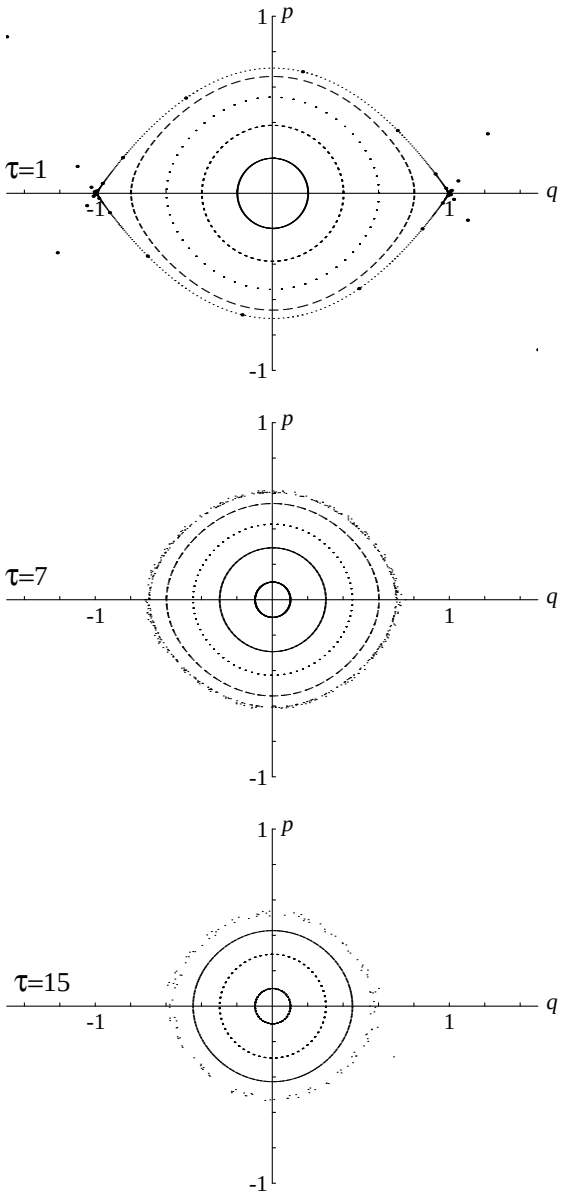

FIGURE 6.12. This figure shows the results of tracking the motion of the anharmonic oscillator using order forty-seven truncated Taylor series maps with three different time steps: $\tau = 1$ (top), 7 (middle), and 15 (bottom). The large points in the $\tau = 1$ plot indicate orbits whose initial conditions lie outside, but close to, the separatrix.

a factor of ten between adjacent contour levels, with $\Delta z = 10^{-4}$ on the inner-most contour and $\Delta z = 10^{-1}$ on the outer-most contour.

Because all the terms in the Hamiltonian (6.1) for the anharmonic oscillator are even in the dynamical variables, it follows that all the terms in the Taylor map are odd. As we truncated the Taylor series after order forty-seven, the first terms neglected in the series are therefore those of order forty-nine. Hence the phase-space error Δz should increase at a rate

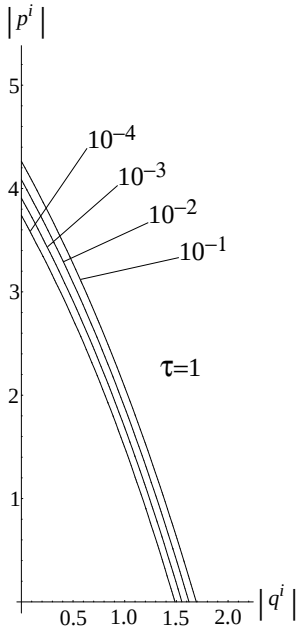

FIGURE 6.13. Contour levels of the phase-space error Δz for the anharmonic oscillator's order forty-seven truncated Taylor map with time step $\tau = 1$.

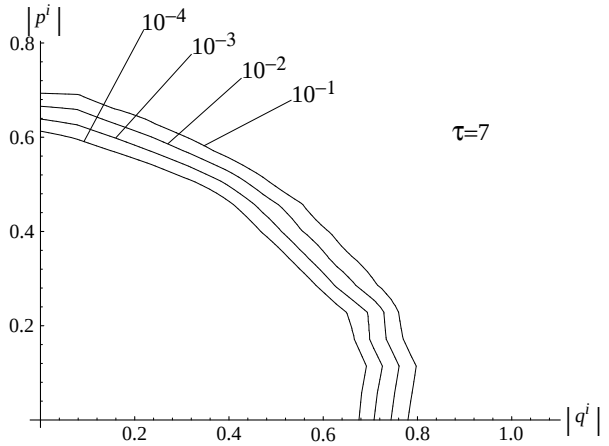

FIGURE 6.14. Contour levels of the phase-space error Δz for the anharmonic oscillator's order forty-seven truncated Taylor map with time step $\tau = 7$.

roughly proportional to r^{49}. The approximately uniform spacing between the contour levels of Δz reflects this power-law behavior, and a rough calculation confirms that the exponent is indeed about forty-nine.

Now compare Figures 6.13–6.15 with Figures 6.5 and 6.6; *i.e.*, compare the contour levels of the phase-space error Δz with the DACs for the Taylor maps. In each case—$\tau = 1$, 7, and 15—as Δz increases, the sequence of contour levels for Δz approaches the boundary of the DAC. This behavior provides further concrete evidence for the observation we made earlier in §6.4.5: the domain over which a Taylor map converges is governed by singularities in the complex phase space of the particular dynamical system.

The results in Figure 6.13 appear especially noteworthy: They show that the $\tau = 1$ truncated Taylor map gives accurate results even for a substantial region of phase space

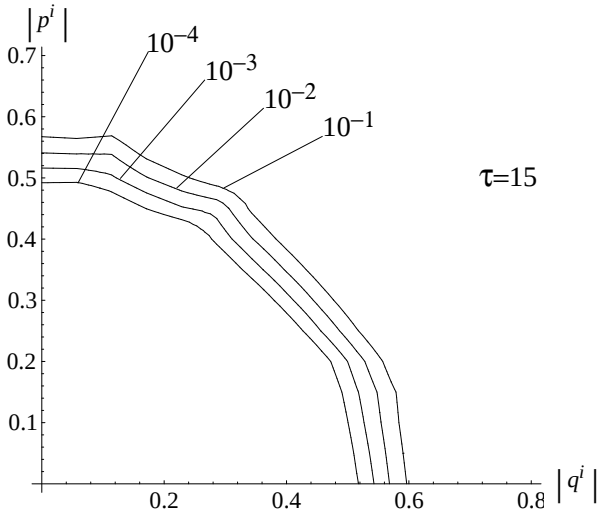

FIGURE 6.15. Contour levels of the phase-space error Δz for the anharmonic oscillator's order forty-seven truncated Taylor map with time step $\tau = 15$.

outside the separatrix. In addition, the power-law behavior of Δz indicates—and numerical tests confirm—that the map returns results close to machine precision over a substantial fraction of the stable region of phase space, inside the separatrix. For initial conditions outside the stable region bounded by the separatrix, we cannot iterate the Taylor series map more than a few times (or perhaps only once); nonetheless, as long as the result of one iteration remains well inside the DAC, we can go on to perform the next iteration. The contour levels of Δz give us a measure of what constitutes "well inside the domain of convergence".

6.8. **Discussion**

The reader who wishes to carry away just a few pieces of information about Taylor maps from our example of the anharmonic oscillator should take the knowledge that the DAC for a Taylor representation of a map depends on the singularities of the map as a function of several (at least two) complex variables, and that there exists an inverse relationship between the size of the time step and the size of the DAC. Moreover, these statements apply to many dynamical systems. While this may seem obvious to some, it has been a source of confusion to many. For example, Talman [86] investigated the suitability of truncated Taylor maps (or differential maps) for doing tracking studies. In particular, he used truncated Taylor maps of modest (seventh and ninth) order with a time step of 1.6π to track the motion of a simple pendulum and compared the results obtained with the exact solution, which is known in terms of elliptic functions. He observed that one can obtain accurate tracking results with a modest order truncated Taylor map only for a limited number of iterations, and furthermore that the number of accurate iterations decreases with increasing amplitude.

In a subsequent report that attempted to explain Talman's results, Hagel and Zotter [48] examined the motion of the simple pendulum by writing its solution as a Taylor series expanded in terms of the time t. They pointed out—quite correctly—that the exact solution for the simple pendulum has poles for complex values of t, and that therefore a solution based on a Taylor series in t will diverge for $|t|$ greater than the distance to the nearest singularity in the plane of complex time. At an amplitude of $10°$, the smallest Talman used, this distance is about 1.2π. Since Talman's step-size was roughly 30% larger, Hagel and Zotter claimed that the complex singularities in t were responsible for the limited number of iterations for which Talman obtained accurate results.

Although we may need to know the locations of the complex time singularities in order to address certain questions concerning the simple pendulum, the alert reader will recognize that such knowledge does not, in fact, answer the specific questions raised by Talman's data. Recall what we have learned from our study of the anharmonic oscillator; recall in particular the lessons learned in §6.4.5: (i) the singularities in the plane of complex time (for real initial conditions) have no bearing on the Taylor map's DAC; and (ii) we may choose any size time step we wish (by giving up, if necessary, phase-space area in the DAC). These conclusions were drawn from very general arguments based on Poincaré's theorem and hence apply not only to the anharmonic oscillator but also to a broad class of dynamical systems—including the simple pendulum.

The motion of the simple pendulum, like that for the anharmonic oscillator, has an exact solution in terms of elliptic functions. Therefore it too has singularities in the complex planes of the initial conditions. For the simple pendulum, also, it then follows that any Taylor map with a finite time step $\tau \neq 0$ contains a finite non-zero domain of phase space in its DAC. In addition, as indicated by Figures 6.13–6.15 in §6.7, the accuracy of a given truncated Taylor map degrades rapidly in the neighborhood of the DAC's boundary.[14] As a consequence, the explanation for Talman's results is not that he chose too large a time step; rather, his choice of step size determined a DAC, and his modest order truncated Taylor maps could not produce accurate results except for relatively small amplitudes.

We should note that even for very small amplitudes ($\sim 10^\circ$), Talman's truncated Taylor maps could not track the simple pendulum for more than a few thousand iterations. This difficulty arises not only from the issues raised above, concerning the boundary of the DAC, but also from the accumulation of errors that result from the truncated Taylor map's violation of the symplectic condition. We shall discuss this subject in Part II of this thesis.

The fact that purely complex singularities can affect the DAC for a Taylor series representation of the map $\mathcal{M}^\tau$ resembles the behavior of, for example, the function $1/(1+x^2)$. This function is perfectly well behaved for all real values of x; but, as everybody knows, its Taylor series expansion about the origin converges only inside the unit circle. In addition, this limited domain of convergence reflects the presence of complex singularities at $x = \pm i$.

Because of its importance, we make one last effort to underscore the fact that the observation just made holds also for Taylor maps of more than one variable—*i.e.*, that complex singularities in the domain of the initial conditions are indeed responsible for limiting the DAC. To do this, examine what happens when we choose the sign $\beta = +1$ in (6.3), the Hamiltonian for the anharmonic oscillator. In this case the system executes bounded periodic motion for all real values of the initial conditions (q^i, p^i); there is no separatrix. As a consequence, the map $\mathcal{M}^\tau$ has no singularities in the entire real (q^i, p^i) plane. We must not, however, be lulled into a false sense of security. Observe that making the replacements

$$q \to iq \quad \text{and} \quad p \to ip$$

transforms the equations of motion (6.4) for the anharmonic oscillator with $\beta = +1$ into the same equations of motion with $\beta = -1$. In other words, one can transform between these two systems—$\beta = \pm 1$—by making a simple rotation about each of the origins in the complex planes of q^i and p^i. Since the DAC records only absolute values, it follows that the DAC for the anharmonic oscillator does not depend on β—*i.e.*, it does not depend on whether the quartic term is positive or negative! Hence the same convergence diagrams—Figures 6.5 and 6.6—apply to Taylor series representations of the two different transfer maps $\mathcal{M}^\tau_{(\beta=+1)}$ and $\mathcal{M}^\tau_{(\beta=-1)}$.

[14] Note that Figures 6.13–6.15 show the phase-space errors made by truncated Taylor maps of order forty-seven. Taylor maps truncated at lower orders will not work as well.

7. Summary I

In Part I of this thesis we have examined some analytic properties of transfer maps, with a special emphasis on the convergence properties of Taylor series representations. We began by showing that for a broad class of physical systems a few standard theorems from the theory of ordinary differential equations not only justify the existence of transfer maps but also delineate some basic properties of transfer maps. Of central import to our study is Poincaré's theorem (Theorem 2.3), from which follows most of our subsequent work. Using Poincaré's theorem and the properties of analytic functions in several complex variables, we examined the convergence properties of Taylor series representations for transfer maps. In particular, we showed that if a dynamical system has singularities in the complex planes of the expansion variables, then a Taylor series representation for any corresponding transfer map has a limited domain of absolute convergence; and, furthermore, the complex singularities of the underlying dynamical system control the size and shape of that domain.

A principal lesson to learn here concerns the relationship between the dynamics of a system under study and the domain of convergence of a corresponding Taylor map. Poincaré's theorem and the theory of functions in several complex variables together tell us that the fundamental constraints on a Taylor series map for a given dynamical system arise from those locations where the right-hand side of the equations of motion (2.1) fail to be analytic. As illustrated in Figure 6.6 for the anharmonic oscillator, the presence of a separatrix poses no fundamental difficulty. Instead, suppose we choose a fixed real τ and obtain a time-τ map in the form of a Taylor series representation expanded in the initial conditions. Then a *singularity* of the time-τ map is any point z^i in the space of complex initial conditions which travels to a singularity of the right-hand side of (2.1) in exactly time τ. These are the singularities that limit the domain of convergence of a Taylor series map.

Experience teaches us to exercise caution when using large steps in time (*i.e.*, the independent variable) for a Taylor series map. In Part I of this thesis we have spelled out the principles that underlie this intuition and have used the anharmonic oscillator as a concrete example. Based on very general principles, there exists an inverse relationship between the size of a time step τ and the size of a corresponding domain of convergence. Within this constraint, however, we may choose as large a time step, or as large a region in phase space, as we please.

While this material is in principle well known to mathematicians, it has not previously been applied in the field of accelerator physics. The new material in Part I of this thesis comprises the explicit observations for a non-trivial dynamical system of the interaction between the singularities of the motion and the domain of absolute convergence for the Taylor representation of the corresponding transfer map.

Part II. Cremona Approximation of Transfer Maps

8. Introduction II

Because they illuminate a broad variety of physical phenomena, dynamical systems derived from Hamiltonians form an important class of systems upon which we focus our attention. For our purposes, the most significant characteristic of Hamiltonian systems is that they obey the *symplectic condition*. Consider a transfer map $\mathcal{M}$, as defined by (2.2), derived from some Hamiltonian system. The *Jacobian matrix* M at the point z^0, which has entries

$$M_{ab}(z^0) = \left.\frac{\partial z_a^f}{\partial z_b^i}\right|_{z^0}, \tag{8.1}$$

represents the linear part of $\mathcal{M}$ at z^0 and describes the effect on z^f of small variations in z^i about the point z^0. For a Hamiltonian system with n degrees of freedom the corresponding phase space has dimension $m = 2n$; and the points in phase space may be labeled by $z = (z_1 \dots z_n, z_{n+1} \dots z_{2n}) = (q_1 \dots q_n, p_1 \dots p_n)$, where the q_i and p_i denote respectively the coördinates and their conjugate momenta. Using this ordering of the phase-space coördinates z_a, we define the $2n \times 2n$ matrix

$$J = \begin{pmatrix} 0 & I \\ -I & 0 \end{pmatrix}, \tag{8.2}$$

where I denotes the $n \times n$ identity matrix, and 0 denotes the $n \times n$ zero matrix. Then for any Hamiltonian system, the Jacobian matrix M satisfies

$$\tilde{M}(z^0) J M(z^0) = J \quad \forall\, z^0, \tag{8.3}$$

where $\tilde{M}$ denotes the transpose of M. This requirement is called the symplectic condition. Furthermore, any map $\mathcal{M}$ whose Jacobian matrix satisfies (8.3) is called a *symplectic map* [30].

In the Taylor series representation (3.1) of a map $\mathcal{M}$, the symplectic condition comprises a set of non-linear relations between Taylor series coefficients of different orders. As a consequence, the act of truncating a Taylor series map—which amounts to setting to zero all coefficients beyond some order—generally breaks the symplectic condition. For some questions one might ask, this symplectic violation does little harm. For other questions, however, such as those that concern the stability of the motion, numerical experiments have demonstrated the importance of preserving the symplectic condition. Indeed, such experiments have shown that the serious errors which arise during iteration of a truncated Taylor map often stem from the violation of the symplectic condition rather than from the loss of information stored in the truncated higher-order terms [34]. We emphasize that the most one can hope for is that carrying a given Taylor series map to higher order will increase the number iterations for which it produces useful results—and after which trouble is encountered. In other words, computing a Taylor map to higher order may alleviate the symptoms, but it cannot cure the disease!

To address questions about the long-term stability of a dynamical system, one must use maps that obey the symplectic condition, *i.e.*, symplectic maps. However, as indicated earlier in §1, the map extracted from a dynamical system often takes the form of a (non-symplectic) truncated Taylor series map. Because the violation of the symplectic condition is far more serious than the loss of high-order terms, one may hope for a procedure that symplectifies a Taylor map by adding high-order terms that are, in some sense, as small as possible. In an ambitious moment, one might also insist that the resulting map be quick to compute. Here in Part II of this thesis we describe just such a procedure. Since the resulting map has the special form of a Cremona map, we refer to our procedure as *Cremona symplectification of Taylor maps*.

In the next two sections we describe the factored-product representation of symplectic maps and the jolt representation of Cremona maps. The conversion to Cremona maps depends on a process we call jolt decomposition and uses the concept of sensitivity vectors. We discuss

these matters in §11 but relegate to Appendices B and C the remaining particulars of how to convert between the Taylor series, factored-product, and jolt representations of symplectic maps. In §12 we show how one can compare different possible jolt decompositions by using the eigenvalues of the Gram matrix built from the sensitivity vectors. In §13 we determine which linear transformations affect the process of jolt decomposition. The search for an optimal decomposition then leads very naturally, in §§14–15, to an investigation of jolt decomposition in the continuum limit. We then show, in §16, how the use of numerical quadrature (cubature) formulas allows one to return to the discrete case while retaining an optimal decomposition. At the end, in §17, we apply the methods described to some maps of physical interest, and then, in §18, we summarize our results.

The material in §§8–10 is largely review—save for the new concept of jolts in §10.1, the inner product introduced in §10.2, and the generality of the presentation in §10.3. And save for the group-theoretical results and cubature formulas drawn from referenced literature—all the material in the remaining sections is new.

9. Symplectic Maps and the Factored-Product Representation

Because of the importance of the symplectic condition for Hamiltonian systems, we would like a convenient method for representing and working with symplectic maps. Lie transformations provide just such a method [30].

9.1. **Lie Operators and Lie Transformations**

For a Hamiltonian system with n degrees of freedom, we usually label the points in the corresponding $2n$-dimensional phase space by $z = (z_1, \ldots, z_n, z_{n+1}, \ldots, z_{2n}) = (q_1, \ldots, q_n, p_1, \ldots, p_n)$. For convenience we sometimes refer to both the coördinates q_i and their conjugate momenta p_i as dynamical coördinates. In addition, we refer to any function on phase space, $f(z)$, as a dynamical function or, occasionally, as a dynamical variable. By extension, if f is also a polynomial, we refer to it as a dynamical polynomial.

Given any dynamical function f, we define the associated *Lie operator* $:f:$ by the rule

$$:f: = \sum_i \left(\frac{\partial f}{\partial q_i} \frac{\partial}{\partial p_i} - \frac{\partial f}{\partial p_i} \frac{\partial}{\partial q_i} \right). \tag{9.1}$$

In other words, one computes the action of the Lie operator $:f:$ on any dynamical variable g by evaluating the Poisson bracket of f with g:

$$:f:g = [f, g]. \tag{9.2}$$

We then define powers of $:f:$ very naturally by the composition of operators. Thus,

$$:f:^2 g = :f:(:f:g) = [f, [f, g]].$$

For completeness we also define $:f:^0$ as the identity operator.

Given powers of $:f:$, one may then discuss power series in $:f:$. We define the *Lie transformation* associated with f as the very special power series

$$e^{:f:} = \exp(:f:) = \sum_{k=0}^{\infty} \frac{1}{k!} :f:^k . \tag{9.3}$$

Lie transformations have the wonderful feature that they provide an endless supply of symplectic maps. Thus, for *any* dynamical function f, the transformation defined by

$$z_a^f = e^{:f:} z_a^i \tag{9.4}$$

has the form (2.2) with $\mathcal{M}$ a symplectic map.

9.2. **Important Properties and Notational Matters**

Before continuing our discussion of symplectic maps, we note (without proof) some important properties of Lie operators and Lie transformations. With respect to ordinary multiplication of functions, Lie operators act as *derivations*:

$$:f:(gh) = (:f:g)h + g(:f:h). \tag{9.5}$$

It follows from (9.5) that, with respect to the same multiplication, Lie transformations act as *isomorphisms*:

$$e^{:f:}(gh) = (e^{:f:}g)(e^{:f:}h). \tag{9.6}$$

The analogous properties hold for Lie operators and Lie transformations with respect to Poisson bracket multiplication of functions:

$$:f:[g, h] = [:f:g, h] + [g, :f:h], \tag{9.7}$$

$$e^{:f:}[g, h] = [e^{:f:}g, e^{:f:}h]. \tag{9.8}$$

(That Lie transformations generate symplectic maps follows directly from (9.8).) Another property concerns the action of Lie transformations on Lie operators:

$$:e^{:f:}g: = e^{:f:} :g: e^{-:f:}. \tag{9.9}$$

Speaking most properly, we must say that Lie operators and Lie transformations act on dynamical variables. However, little confusion results if we sometimes treat them as acting directly on phase space. Thus, instead of writing (9.4) for each $a \in \{1, \dots, 2n\}$, we often abuse the notation to write more simply

$$z^f = e^{:f:} z^i. \tag{9.10}$$

It follows from (9.6) that we may, in this vein, write the action of a Lie transformation, $e^{:f(z):}$, on a dynamical function, $g(z)$, in the form

$$e^{:f:} g(z) = g(e^{:f:} z). \tag{9.11}$$

In much of our subsequent discussion, we shall place a subscript on a dynamical function to indicate that it represents a homogeneous dynamical polynomial of a certain degree. Thus, we use f_k (sometimes generically) to denote a homogeneous dynamical polynomial of degree k. Using this notation and the definition (9.2), we can easily determine that Lie operators of the form $:f_2:$ and Lie transformations of the form $e^{:f_2:}$ preserve the degree of the functions on which they act. In particular, the Lie transformation $e^{:f_2:}$ acts linearly on phase space. We shall therefore often use a matrix representation for $e^{:f_2:}$'s: thus,

$$e^{:f_2:} z_a = \sum_b R^f_{ab} z_b, \tag{9.12a}$$

or, in matrix form,

$$e^{:f_2:} z = R^f z. \tag{9.12b}$$

Notice that R^f must, of course, obey the symplectic condition (8.3). In other words, R^f must be a *symplectic matrix*.

An important consequence of our decision to put the matrix representation of an $e^{:f_2:}$ in the form (9.12) is that linear Lie transformations and their corresponding matrices act in opposite orders. To see this, note that

$$\begin{aligned} e^{:f_2:} e^{:g_2:} z_a &= e^{:f_2:} \Big(\sum_b R^g_{ab} z_b \Big) = \sum_b R^g_{ab}\, e^{:f_2:} z_b \\ &= \sum_{bc} R^g_{ab} \big(R^f_{bc} z_c \big) = \sum_c \big(R^g R^f \big)_{ac} z_c, \end{aligned} \tag{9.13a}$$

or, in matrix form,

$$e^{:f_2:} e^{:g_2:} z = \big(R^g R^f \big)\, z. \tag{9.13b}$$

Now suppose $\mathcal{L}(R)$ denotes the linear symplectic transformation corresponding to the matrix R. Then, according to (9.12b) and (9.13b),

$$\mathcal{L}(R_1 R_2) z = (R_1 R_2) z = \mathcal{L}(R_2) \mathcal{L}(R_1) z. \tag{9.14}$$

We therefore obtain the general result

$$\mathcal{L}(R_1 R_2) = \mathcal{L}(R_2) \mathcal{L}(R_1). \tag{9.15}$$

Observe carefully the change in the order of the factors. Note also another obvious consequence of (9.14):

$$\mathcal{L}(R^{-1}) = [\mathcal{L}(R)]^{-1}. \tag{9.16}$$

9.3. **The Factored-Product Representation**

Observe that when f denotes a dynamical polynomial, one can use the exponential power series (9.3) to convert a symplectic map of form (9.4) into a Taylor map of form (3.1). However, since we often have a Taylor map at hand, we would also like to "go the other way". The following theorem addresses this matter and, in the process, defines the very useful *factored-product representation*, (9.17), for symplectic maps [33].

Theorem 9.1 (Factorization Theorem)**.** *If $\mathcal{M}$ is any symplectic map having a Taylor series representation,* (3.1)*, then $\mathcal{M}$ may be written uniquely in the factored-product form*

$$\mathcal{M} = e^{:f_1:} e^{:f_2^c:} e^{:f_2^a:} e^{:f_3:} e^{:f_4:} \cdots , \tag{9.17}$$

where each f_k denotes a homogeneous polynomial of degree k in the variables z^i. Moreover, the quadratic polynomials f_2^c and f_2^a have the special form

$$f_2 = -\frac{1}{2} \sum_{ab} S_{ab}\, z_a z_b,$$

where S denotes a symmetric matrix. For f_2^c, the matrix S commutes with the matrix J of (8.2)*; and for f_2^a, S anti-commutes with J.*

As a representation for symplectic maps, (9.17) has many virtues; we list two of the most important:

- Each Lie transformation has a well-characterized content. The factors $e^{:f_1:}$ and $e^{:f_2:}$ generate respectively constant and linear terms in the Taylor series (3.1), while the remainder, $e^{:f_3:} e^{:f_4:} \cdots$, generates non-linear terms. In particular, $e^{:f_3:}$ generates terms of quadratic and higher order, $e^{:f_4:}$ generates terms of cubic and higher order, and so on.
- The various f_k's have independent coefficients; indeed, we may often label individual coefficients according to specific traits they represent in the overall map. This means, in addition, that maps in factored-product form require far less computer memory than maps in Taylor series form. Furthermore, even if we have an imprecise knowledge of the coefficients, the resulting map, (9.17), remains symplectic.

An important feature of the factored-product representation follows from these two virtues. Suppose, as is usually the case, that we know the Taylor series coefficients only through some finite order, say $P-1$; then we can determine the factorization (9.17) only through the factor $e^{:f_P:}$. (Appendix B describes an order-by-order procedure for constructing the polynomials f_k.) As each succeeding factor in (9.17) contains information of increasingly higher order, it seems reasonable, from a perturbation theory point of view, to terminate that product after the order of interest. We then write the truncated product as

$$\mathcal{M}_P = e^{:f_1:} e^{:f_2^c:} e^{:f_2^a:} e^{:f_3:} \cdots e^{:f_P:}. \tag{9.18}$$

Now note that truncating the product is equivalent to setting $f_k = 0$ for all $k > P$. Because of the virtues listed above, the map $\mathcal{M}_P$—a truncated product of Lie transformations—represents a symplectic approximation to the original map $\mathcal{M}$.

The factored-product representation, (9.17), does, however, share the same principal drawback as the Taylor series representation, (3.1): evaluating the action of most Lie transformations, (9.3), requires summing an infinite series. Even computing the result to machine precision on a computer requires excessive amounts of time for studies that demand repeated iterations of the map. Therefore, despite the many virtues of (9.17) for representing symplectic maps, we seek an alternative representation which can be computed quickly. This leads us to the subject of Cremona maps and their jolt representations.

Before going on to discuss Cremona maps, we make two final comments about the factored-product representation, (9.17). The factor $e^{:f_1:}$ generates simple translations; these can always be computed exactly. The factors $e^{:f_2^c:}$ and $e^{:f_2^a:}$ generate linear transformations; these can

always be represented by matrices and computed to machine precision. As these first factors present no difficulty, we shall devote our attention to the remaining, non-linear, part of the map, which we write as

$$\mathcal{N} = e^{:f_3:} e^{:f_4:} \cdots . \tag{9.19}$$

In actual practice, we shall devote our attention to the truncated product version of (9.19), which we write as

$$\mathcal{N}_P = e^{:f_3:} \cdots e^{:f_P:}. \tag{9.20}$$

10. Cremona Maps and the Jolt Representation

We assign the adjective *Cremona* to any map which is both symplectic and polynomial.[15] Our interest in Cremona maps stems directly from their definition: as they are symplectic, we can use them to approximate the behavior of Hamiltonian systems; as they are polynomial, we can compute them rapidly and exactly.

10.1. **Kicks, Jolts, and their Associated Maps**

Since any linear symplectic map is also a polynomial map, we know that an infinity of Cremona maps exists. That an abundance of non-linear Cremona maps exists is only slightly harder to demonstrate. First define a *jolt* as any dynamical function g that satisfies the condition

$$:g:^2 z_a = 0 \quad \forall a \in \{1, \ldots, 2n\}. \tag{10.1}$$

Then according to (9.3), the associated Lie transformation generates the map

$$z_a^f = e^{:g:} z_a^i = z_a^i + :g: z_a^i = z_a^i + [g, z_a^i], \tag{10.2}$$

which we call a *jolt map*. Next note that for any dynamical polynomial g that satisfies (10.1), the corresponding map, (10.2), will be polynomial; hence, because Lie transformations always produce symplectic maps, polynomial jolts generate Cremona maps. Now notice that any function of the coördinates alone,

$$g = g(q^i), \text{ with } q^i = (q_1^i, \ldots, q_n^i), \tag{10.3}$$

satisfies (10.1), so there do indeed exist an abundance of non-linear Cremona maps.

Observe that if a function g has the special form (10.3), then the corresponding jolt map, (10.2), affects only the momenta. Such maps are called *kick maps*, and we refer to the generators, (10.3), as *kicks*. Thus, jolt maps represent a generalization of kick maps.

To see that there exist jolts which are not kicks, employ the identity (9.9). Using $\mathcal{L}$ to denote the Lie transformation $e^{:f:}$, we obtain

$$:\mathcal{L}g:^2 = (\mathcal{L} :g: \mathcal{L}^{-1})^2 = \mathcal{L} :g: \mathcal{L}^{-1} \mathcal{L} :g: \mathcal{L}^{-1} = \mathcal{L} :g:^2 \mathcal{L}^{-1}. \tag{10.4}$$

Now notice that if $\mathcal{L}$ denotes a linear symplectic map—an $e^{:f_2:}$—then the action of $\mathcal{L}$ on z (and therefore also of $\mathcal{L}^{-1}$ on z) produces a linear combination of the z_a. We conclude from (10.1) and (10.4) that if g is a kick, then $\mathcal{L}g(q) = g(\mathcal{L}q) = g^{new}(z)$ is a jolt. The corresponding jolt map has the form

$$e^{:\mathcal{L}g:} = e^{\mathcal{L}:g:\mathcal{L}^{-1}} = \mathcal{L} e^{:g:} \mathcal{L}^{-1}. \tag{10.5}$$

Thus can one build many possible Cremona maps using only linear symplectic transformations and kick maps.

10.2. **The Vector Space of Dynamical Polynomials**

One can show, by a combinatorial calculation, that [30]

$$M(l,d) \equiv \left\{ \begin{array}{c} \text{the number of monomials} \\ \text{of degree } l \text{ in } d \text{ variables} \end{array} \right\} = \binom{l+d-1}{l} = \frac{(l+d-1)!}{(d-1)!\, l!}. \tag{10.6}$$

In the vector space of dynamical polynomials let us introduce a set of general monomials of degree l:

$$G_r^{(l)}(z) = G_r^{(l)}(q,p) = \frac{q_1^{r_1} \cdots q_n^{r_n}\, p_1^{r_{n+1}} \cdots p_n^{r_{2n}}}{\sqrt{r_1! \cdots r_{2n}!}}, \tag{10.7}$$

[15] Moser [68], Engel [36, 37], and Keller [54] have employed the eponymous term *Cremona* in their studies of polynomial maps which carry the plane into itself and have unit Jacobian determinant. Such maps are automatically symplectic [30]. We have extended the use of the term Cremona to denote symplectic polynomial maps of $\mathbb{R}^{2n}$ into $\mathbb{R}^{2n}$. The Italian mathematician Cremona [21] studied bi-rational mappings in the context of what is now part of the subject of algebraic geometry [80, 82].

where $r_1+\cdots+r_{2n}=l$. Although each monomial is determined by the collection of exponents $\{r_1,\ldots,r_{2n}\}$, we label the monomials (10.7) of degree l by a single index r that ranges from 1 to $M(l,2n)$. By $Q_k^{(l)}$ we shall denote those general monomials which contain only q's: thus,

$$Q_k^{(l)}(q)=\frac{q_1^{k_1}\cdots q_n^{k_n}}{\sqrt{k_1!\cdots k_n!}}, \tag{10.8}$$

where $k_1+\cdots+k_n=l$. As with the general monomials, we use a single index k to label the q-monomials of degree l; hence k ranges from 1 to $M(l,n)$.

Let us also introduce in the space of dynamical polynomials a (very special) inner product $\langle\,,\rangle$ defined by

$$\big\langle G_r^{(l)}, G_{r'}^{(l')}\big\rangle=\delta_{ll'}\delta_{rr'}. \tag{10.9a}$$

In words, the $G_r^{(l)}$ (and therefore also the $Q_k^{(l)}$) are orthonormal with respect to this inner product. We observe that the $G_r^{(l)}$ form an orthonormal basis for all dynamical polynomials. In a like manner, the $Q_k^{(l)}$ form an orthonormal basis for all polynomials in the q's alone. Now suppose we have two dynamical polynomials $f=\sum_{lr}f_{lr}G_r^{(l)}$ and $g=\sum_{lr}g_{lr}G_r^{(l)}$. Then we extend the inner product (10.9a), in a natural way, to the entire vector space of dynamical polynomials by defining

$$\big\langle f,g\big\rangle=\sum_{lr}f_{lr}^*g_{lr}, \tag{10.9b}$$

where the * means "take the complex conjugate".

An important feature of the scalar product defined by (10.9) is that any transformation belonging to the $U(n)$ subgroup of $Sp(2n,\mathbb{R})$ leaves this inner product unchanged [30]. In symbols this means

$$\big\langle\mathcal{L}f,\mathcal{L}g\big\rangle=\big\langle f,g\big\rangle$$

for any $\mathcal{L}$ in the $U(n)$ subgroup of $Sp(2n,\mathbb{R})$. Using $\mathcal{L}^\dagger$ to denote the Hermitian adjoint of $\mathcal{L}$ with respect to this inner product, we find

$$\big\langle f,g\big\rangle=\big\langle\mathcal{L}f,\mathcal{L}g\big\rangle=\big\langle f,\mathcal{L}^\dagger\mathcal{L}g\big\rangle \tag{10.10}$$

for any f and g. Hence

$$\mathcal{L}^\dagger=\mathcal{L}^{-1}; \tag{10.11}$$

thus any element of the $U(n)$ subgroup of $Sp(2n,\mathbb{R})$ is unitary with respect to the inner product (10.9). We shall see later the value of this feature.

For future reference we record here the Hermitian adjoints of the Lie operators associated with the quadratic basis monomials for the space of quadratic dynamical polynomials [30]:

$$\begin{aligned}
:q_jq_k:^\dagger&=-:p_jp_k:,\\
:p_jp_k:^\dagger&=-:q_jq_k:,\\
:q_jp_k:^\dagger&=:q_kp_j:.
\end{aligned} \tag{10.12}$$

10.3. **The Jolt Representation**

We turn now to a description of the *jolt representation* for approximating a given Taylor map with an appropriate Cremona map.

Suppose we obtain for some Hamiltonian system a truncated Taylor series map $\mathcal{T}_P$ with coefficients through order $P-1$. As shown by the factorization theorem, Theorem 9.1, we can obtain from $\mathcal{T}_P$ a symplectic approximation $\mathcal{M}_P$ in the form (9.18). Our goal, Cremona symplectification, is to approximate the non-linear part of this map, the $\mathcal{N}_P$ of (9.20), by a

Cremona map written as a product of N jolt maps of the form (10.5). Appendix C describes an order-by-order procedure for converting the map $\mathcal{N}_P$ into the form

$$\mathcal{J}_P = \mathcal{L}_1 e^{:g^1:} \mathcal{L}_1^{-1} \cdots \mathcal{L}_N e^{:g^N:} \mathcal{L}_N^{-1} \tag{10.13}$$

in such a way that the polynomial expansion of $\mathcal{J}_P z_a^i$ agrees with the Taylor series expansion of $\mathcal{N}_P z_a^i$ through terms of order $P-1$. We use the symbol $\simeq$ to indicate this agreement; thus,

$$\mathcal{J}_P \simeq \mathcal{N}_P.$$

Appendix C also describes how to do the conversion in the other direction, *i.e.*, how to convert a given Cremona map $\mathcal{J}_P$ into the corresponding factored-product map $\mathcal{N}_P$.

The kicks g^j in (10.13) have the special form

$$g^j = \frac{1}{N} \sum_{l=3}^{P} \frac{1}{M(l,n)} \sum_{k=1}^{M(l,n)} \beta_{jk}^{(l)} Q_k^{(l)}, \tag{10.14}$$

where N denotes the number of jolts, $M(l,n)$ is given by (10.6), and the $\beta_{jk}^{(l)}$ represent a set of *jolt strengths* that depend on the specific map $\mathcal{N}_P$ of (9.20). The procedure given in Appendix C shows in particular how to determine the $\beta_{jk}^{(l)}$ using a knowledge of the map $\mathcal{N}_P$ together with a given, appropriately chosen, set of linear symplectic transformations $\mathcal{L}_j$. The $\mathcal{L}_j$ must therefore be chosen in advance; indeed, we shall focus much of our attention in Part II of this thesis on how to choose a set of $\mathcal{L}_j$ so as to represent as closely as possible any given non-linear symplectic map $\mathcal{N}_P$ as a Cremona map using the jolt representation $\mathcal{J}_P$ of (10.13).

Before closing this section, we make a few observations about the set of all Cremona maps that can be represented as a product of simple jolt maps of the form (10.5). These maps, by design, are inherently symplectic and can be evaluated rapidly. They are also defined everywhere, so no question arises concerning a domain of convergence. In addition, as these maps have obvious inverses of the same form, they constitute a group. The jolt representation (10.13) therefore offers a number of useful features for approximating symplectic maps. However, one potential difficulty may arise. By construction, the polynomial expansion of $\mathcal{J}_P$ agrees with the Taylor map for $\mathcal{N}_P$ through terms of order $P-1$; the higher order terms, on the other hand, may have very different coefficients. Indeed, those coefficients arising from the jolt representation can be so large as to render the resulting Cremona map useless. By properly choosing the set of linear symplectic transformations $\mathcal{L}_1, \ldots, \mathcal{L}_N$, we aim to avoid such offensively large high-order coefficients.

11. Jolt Decomposition of Homogeneous Polynomials

Suppose we have a homogeneous dynamical polynomial of degree l:

$$h_l = \sum_{r=1}^{M(l,2n)} c_r^{(l)} G_r^{(l)}. \tag{11.1}$$

If we can find a set of N linear symplectic transformations, $\mathcal{L}_j$, and a set of coefficients $a_{jk}^{(l)}$ such that

$$h_l = \frac{1}{NM(l,n)} \sum_{j=1}^{N} \sum_{k=1}^{M(l,n)} a_{jk}^{(l)} \mathcal{L}_j Q_k^{(l)}, \tag{11.2}$$

then, because each term in (11.2) is a jolt, we say we have found a *jolt decomposition* of h_l. If we can use the same set of $\mathcal{L}_j$ to obtain jolt decompositions for two or more dynamical polynomials, then we say we have found a *simultaneous* jolt decomposition. The principal challenge to realizing a Cremona approximation for some symplectic map, $\mathcal{N}_P$, involves finding a simultaneous jolt decomposition for any given set of homogeneous polynomials of degree $l \in \{3, 4, \ldots, P\}$.[16] Although one could, in principle, choose a different set of $\mathcal{L}_j$ for each map or collection of h_l, that is not a useful approach. As we shall see, finding a good set of $\mathcal{L}_j$ compares to finding a needle in a haystack. We would instead like to find and announce one set of $\mathcal{L}_j$ that is in some sense optimal and works for *any* collection of h_l's with degree $l \leq P$.

To see how one can obtain a jolt decomposition of a dynamical polynomial h_l, first note that one can extract the coefficients of (11.1) by using the inner product of (10.9) and projecting h_l onto the monomials $G_r^{(l)}$: thus,

$$c_r^{(l)} = \left\langle G_r^{(l)}, h_l \right\rangle.$$

Inserting (11.2) in this expression, we obtain

$$c_r^{(l)} = \frac{1}{NM(l,n)} \sum_{j=1}^{N} \sum_{k=1}^{M(l,n)} a_{jk}^{(l)} \left\langle G_r^{(l)}, \mathcal{L}_j Q_k^{(l)} \right\rangle = \frac{1}{NM(l,n)} \sum_{jk} a_{jk}^{(l)} \sigma_{jk}^r, \tag{11.3}$$

where we have defined the quantities

$$\sigma_{jk}^r = \left\langle G_r^{(l)}, \mathcal{L}_j Q_k^{(l)} \right\rangle. \tag{11.4}$$

We shall treat the subscript, jk, as a "single index" and view the σ_{jk}^r as the entries of a vector in a vector space V^l of dimension $N \times M(l,n)$. The superscript, r, labels the different vectors, which we call *sensitivity vectors*. (Although the σ^r also depend on the order l, we have suppressed the desire to add another index. Still, this imprecision should present no difficulty to the reader.) In addition, we use $a^{(l)}$ to denote the vector in V^l having entries $a_{jk}^{(l)}$. Introducing an inner product in V^l, $\{\,,\}$, which includes a factor of $1/[NM(l,n)]$, we can now write (11.3) in the (more compact) form

$$c_r^{(l)} = \{\sigma^r, a^{(l)}\}; \quad r = 1, 2, \ldots, M(l, 2n). \tag{11.5}$$

According to (11.5), any part of $a^{(l)}$ that contributes to the $c_r^{(l)}$ must belong to the subspace of V^l spanned by the sensitivity vectors. We therefore make the ansatz

$$a^{(l)} = \sum_{s=1}^{M(l,2n)} \alpha_s^{(l)} \sigma^s, \tag{11.6}$$

[16] The essential idea here—that of finding decompositions of the form (11.2) for homogeneous polynomials and then using an order-by-order procedure to convert a given symplectic map into a polynomial symplectic map—was first developed by John Irwin [51]. Although he considered only a restricted class of $\mathcal{L}_j$'s, his ideas inspired our work. The formulation developed here is completely general.

where the $\alpha_s^{(l)}$ denote a set of as yet undetermined coefficients. Inserting (11.6) into (11.5), we obtain

$$c_r^{(l)} = \sum_s \{\sigma^r, \sigma^s\}\alpha_s^{(l)} = \sum_s \Gamma(l)_{rs}\alpha_s^{(l)}. \tag{11.7}$$

The quantities $\Gamma(l)_{rs}$, defined by

$$\Gamma(l)_{rs} = \{\sigma^r, \sigma^s\} = \frac{1}{NM(l,n)} \sum_{jk} \sigma_{jk}^r \sigma_{jk}^s, \tag{11.8}$$

denote the entries of the (real symmetric) *Gram matrix* formed from the sensitivity vectors. For future reference, we note that because the sensitivity vectors are real, we may write the Gram matrix elements explicitly as

$$\Gamma(l)_{rs} = \{\sigma^r, (\sigma^s)^*\} = \frac{1}{NM(l,n)} \sum_{jk} \left\langle G_r^{(l)}, \mathcal{L}_j Q_k^{(l)} \right\rangle \left\langle \mathcal{L}_j Q_k^{(l)}, G_s^{(l)} \right\rangle. \tag{11.9}$$

In matrix notation (11.7) reads $c^{(l)} = \Gamma(l)\alpha^{(l)}$; hence, we can solve for

$$\alpha^{(l)} = \Gamma(l)^{-1} c^{(l)} \tag{11.10}$$

if the Gram matrix $\Gamma(l)$ is invertible. We can then use (11.6) and (11.10) to obtain the jolt strengths:[17]

$$a_{jk}^{(l)} = \sum_{rs} c_r^{(l)} [\Gamma(l)^{-1}]_{rs} \sigma_{jk}^s. \tag{11.11}$$

Our solution for the jolt strengths, (11.11), depends upon the Gram matrix being invertible. As the definitions (11.4) and (11.8) show, the sensitivity vectors σ^r, and hence also the Gram matrix $\Gamma(l)$, depend only on the choice of the linear symplectic transformations $\mathcal{L}_j$. This observation provides us with the *sine qua non* for choosing the $\mathcal{L}_j$: they must produce a non-singular Gram matrix.

[17] We initially defined the jolt strengths as the coefficients $\beta_{jk}^{(l)}$ in (10.14). As there exists an intimate relationship (*cf.* Appendix C) between these $\beta_{jk}^{(l)}$ and the $a_{jk}^{(l)}$ of (11.2), we apply the name *jolt strengths* to both.

12. Optimizing the Decomposition

As we shall discuss later, in §16.1.2, we have found that even randomly chosen sets of linear symplectic transformations $\mathcal{L}_j$ stand a modest chance of producing non-singular Gram matrices. On the other hand, we have found that such random $\mathcal{L}_j$'s stand an excellent chance of producing terrible Cremona approximations. We therefore wish to know what other requirements should a set of $\mathcal{L}_j$ satisfy in order to yield good Cremona approximations?

12.1. **Jolt Strengths and Gram Eigenvalues**

To aid our query, let us examine the action on z_a of two jolt maps of the form (10.5). On using (9.3) and (10.1) to expand the exponentials, we obtain

$$\begin{aligned} e^{:\mathcal{L}_1 g^1:} e^{:\mathcal{L}_2 g^2:} z_a &= e^{:\mathcal{L}_1 g^1:}(z_a + [\mathcal{L}_2 g^2, z_a]) \\ &= z_a + [\mathcal{L}_1 g^1, z_a] + [\mathcal{L}_2 g^2, z_a] + [\mathcal{L}_1 g^1, [\mathcal{L}_2 g^2, z_a]] + \cdots . \end{aligned} \tag{12.1}$$

(This series must, of course, terminate.) Observe that if the kicks g^1 and g^2 have the form (10.14), then the first three pieces of this sum contain terms of degree $P-1$ and lower, while the next piece contains terms of degree 3 through $2P-3$. (Recall that $P \geq 3$.) If (12.1) represents a Cremona approximation to some Taylor series map whose coefficients are known through order $P-1$, then the terms in (12.1) with degree less than P must, by construction, agree with the Taylor map. However, the remaining terms, which arise from multiple Poisson brackets, generally differ from the Taylor map. In fact, as indicated at the end of §10.3, those terms may make ruinously large contributions to the Cremona approximation. By comparison, if the Taylor map we start with accurately represents some true map of interest, then those high order Taylor series terms must (in some sense) be small.

Based on the observations of the last paragraph, we formulate a further requirement for the linear symplectic transformations, $\mathcal{L}_j$: choose the set of $\mathcal{L}_j$ so as to minimize the high order terms that arise from such multiple Poisson brackets as appear in (12.1). To see how one might approach this goal, consider expanding $[\mathcal{L}_1 g^1, [\mathcal{L}_2 g^2, z_a]]$ by using the expression (10.14); the result involves products of the various jolt strengths describing g^1 and g^2. We conclude that minimizing the size of the jolt strengths constitutes one (rather crude) method for reducing the possibly damaging high order terms. We shall therefore frame our requirement for the $\mathcal{L}_j$ in the following fashion: choose the set of $\mathcal{L}_j$ so as to minimize the length of the vectors whose entries are the jolt strengths—the $a^{(l)}$ of (11.2).

In making the ansatz (11.6), we have already taken one step towards minimizing the jolt strengths $a^{(l)}$: adding to $a^{(l)}$ any component not in the space spanned by the σ^r can only make the $a^{(l)}$ longer. To reduce further the size of the $a^{(l)}$, note that in the vector space V^l we may use (11.6), (11.8), (11.10), and the symmetry of $\Gamma(l)$ to express the squared length of $a^{(l)}$ in the form

$$\begin{aligned} \{a^{(l)}, a^{(l)}\} &= \sum_{rs} \alpha_r^{(l)} \{\sigma^r, \sigma^s\} \alpha_s^{(l)} = \sum_{rs} \alpha_r^{(l)} \Gamma(l)_{rs} \alpha_s^{(l)} \\ &= \big(\Gamma(l)\alpha^{(l)}, \alpha^{(l)}\big) = \big(c^{(l)}, \Gamma(l)^{-1} c^{(l)}\big). \end{aligned} \tag{12.2}$$

Now notice that because the Gram matrix $\Gamma(l)$ is real symmetric, it can be diagonalized by a real orthogonal transformation, it has real eigenvalues, and it has a set of real orthonormal eigenvectors. In addition, the Gram matrix is positive: Consider any set of coefficients $\beta_r^{(l)}$, and define the vectors $b^{(l)}$ in analogy with (11.6); thus,

$$b^{(l)} = \sum_s \beta_s^{(l)} \sigma^s.$$

Then we obtain

$$\big(\beta^{(l)}, \Gamma(l)\beta^{(l)}\big) = \sum_{rs} \beta_r^{(l)} \Gamma(l)_{rs} \beta_s^{(l)} = \{b^{(l)}, b^{(l)}\} \geq 0.$$

Furthermore, if $\Gamma(l)$ is invertible—as we require—then $\Gamma(l)$ is positive definite; hence, the eigenvalues are all positive.

Let $\chi_r^{(l)}$, $r \in \{1, \ldots, M(l, 2n)\}$, denote a set of orthonormal eigenvectors for $\Gamma(l)$; and let $\lambda_r^{(l)}$ denote the corresponding eigenvalues. As the $\chi_r^{(l)}$ form a basis, the vector $c^{(l)}$ has an expansion of the form

$$c^{(l)} = \sum_r \xi_r^{(l)} \chi_r^{(l)}.$$

We can use this expansion to place an upper-bound on (12.2):

$$\begin{aligned} \{a^{(l)}, a^{(l)}\} &= \big(c^{(l)}, \Gamma(l)^{-1} c^{(l)}\big) = \sum_{rs} \xi_r^{(l)} \xi_s^{(l)} \big(\chi_r^{(l)}, \Gamma(l)^{-1} \chi_s^{(l)}\big) \\ &= \sum_r (\xi_r^{(l)})^2 / \lambda_r^{(l)} \leq \sum_r (\xi_r^{(l)})^2 / \lambda_{min}^{(l)} = (c^{(l)}, c^{(l)}) / \lambda_{min}^{(l)}. \end{aligned} \tag{12.3}$$

Here we use the fact that $\Gamma(l)^{-1}$ shares the eigenvectors of $\Gamma(l)$—but with reciprocal eigenvalues; and we use $\lambda_{min}^{(l)}$ to denote the smallest eigenvalue of $\Gamma(l)$. Now observe that (11.1) and (10.9b) allow us to rewrite (12.3) as

$$\{a^{(l)}, a^{(l)}\} \leq \frac{\langle h_l, h_l \rangle}{\lambda_{min}^{(l)}}. \tag{12.4}$$

Since $\langle h_l, h_l \rangle$ is fixed, (12.4) says that any jolt decomposition of the dynamical polynomial, h_l, yields jolt strengths, $a^{(l)}$, which have an upper bound proportional to the reciprocal of the smallest Gram eigenvalue. We can now express our requirement for the $\mathcal{L}_j$ in the following modified form: *choose the set of $\mathcal{L}_j$ so as to make the smallest Gram eigenvalue as large as possible.*

12.2. **The Gram Operator**

Before going on to discuss which $\mathcal{L}_j$ are relevant to our needs, we introduce an additional concept—that of the Gram operator.

Recall that the monomials $G_r^{(l)}$ are orthonormal with respect to the inner product (10.9) and form a basis for the space of f_l's, the space of dynamical polynomials of degree l. Now suppose we find another set of such functions, $\psi_\nu^{(l)}$: another basis for the space of f_l's which is also orthonormal with respect to the inner product (10.9). Then in the space of f_l's we may write the identity operator in the dyadic form

$$\sum_\nu \left|\psi_\nu^{(l)}\right\rangle\left\langle\psi_\nu^{(l)}\right|.$$

Let us insert this form of the identity into (11.9) in two places: after the $G_r^{(l)}$ and before the $G_s^{(l)}$. We obtain the expression

$$\Gamma(l)_{rs} = \frac{1}{NM(l,n)} \sum_{jk} \sum_{\nu\nu'} \langle G_r^{(l)}, \psi_\nu^{(l)} \rangle \langle \psi_\nu^{(l)}, \mathcal{L}_j Q_k^{(l)} \rangle \langle \mathcal{L}_j Q_k^{(l)}, \psi_{\nu'}^{(l)} \rangle \langle \psi_{\nu'}^{(l)}, G_s^{(l)} \rangle.$$

Because both the $G_r^{(l)}$ and the $\psi_\nu^{(l)}$ represent orthonormal bases for the same space, the matrix connecting them, which has elements $\langle G_r^{(l)}, \psi_\nu^{(l)} \rangle$, must be unitary. Denoting these matrix elements $U_{r\nu}$, we may write the Gram matrix in the form

$$\Gamma(l)_{rs} = \sum_{\nu\nu'} U_{r\nu} \left(\frac{1}{NM(l,n)} \sum_{jk} \langle \psi_\nu^{(l)}, \mathcal{L}_j Q_k^{(l)} \rangle \langle \mathcal{L}_j Q_k^{(l)}, \psi_{\nu'}^{(l)} \rangle \right) U^\dagger_{\nu' s}. \tag{12.5}$$

Now observe that the quantity inside the large parentheses of (12.5) represents the entries of a new matrix $\bar{\Gamma}(l)$ obtained from the Gram matrix $\Gamma(l)$ by a unitary similarity transformation:

$$\Gamma(l) = U \bar{\Gamma}(l) U^\dagger.$$

Also notice the resemblance between the matrix entries $\Gamma(l)_{rs}$ of (11.9) and the matrix entries $\bar{\Gamma}(l)_{\nu\nu'}$ in the expression (12.5). Because our interest in the Gram matrix will focus on its eigenvalues, and because $\Gamma(l)$ and $\bar{\Gamma}(l)$ have the same eigenvalue spectrum, the matrices $\Gamma(l)$ and $\bar{\Gamma}(l)$ are equivalent for our purposes, and we shall make no essential distinction between them. The comparison of (11.9) and (12.5) therefore suggests that we simplify matters by introducing a *Gram operator* written in the dyadic form

$$\widehat{\Gamma}(l) = \frac{1}{NM(l,n)} \sum_{jk} \left|\mathcal{L}_j Q_k^{(l)}\right\rangle\left\langle \mathcal{L}_j Q_k^{(l)}\right| = \frac{1}{NM(l,n)} \sum_{jk} \mathcal{L}_j \left|Q_k^{(l)}\right\rangle\left\langle Q_k^{(l)}\right| \mathcal{L}_j{}^{\dagger}. \tag{12.6}$$

Using this operator, we may write more simply

$$\Gamma(l)_{rs} = \left\langle G_r^{(l)}\middle|\widehat{\Gamma}(l)\middle|G_s^{(l)}\right\rangle,$$

and

$$\bar{\Gamma}(l)_{\nu\nu'} = \left\langle \psi_\nu^{(l)}\middle|\widehat{\Gamma}(l)\middle|\psi_{\nu'}^{(l)}\right\rangle.$$

In other words, as long as we apply to the Gram operator $\widehat{\Gamma}(l)$ orthonormal bases for the space of f_l's, we will obtain equivalent representations for the Gram matrix $\Gamma(l)$.

To complete this section, let us introduce one additional bit of notation. According to (12.6), we may write the Gram operator in the form

$$\widehat{\Gamma}(l) = \frac{1}{N} \sum_j \widehat{\Gamma}(j,l), \tag{12.7a}$$

where

$$\widehat{\Gamma}(j,l) = \frac{1}{M(l,n)} \sum_k \mathcal{L}_j \left|Q_k^{(l)}\right\rangle\left\langle Q_k^{(l)}\right| \mathcal{L}_j{}^{\dagger}. \tag{12.7b}$$

Note that both $\widehat{\Gamma}(l)$ and $\widehat{\Gamma}(j,l)$ are Hermitian operators. We shall describe later, in §13.3, another important property of the *partial Gram operator* $\widehat{\Gamma}(j,l)$.

13. The Space of Relevant $\mathcal{L}_j$

The space of all linear symplectic transformations that act on a $2n$-dimensional phase space constitutes an important Lie group denoted $Sp(2n, \mathbb{R})$ and called the symplectic group. In the process of searching this space for a set of N such transformations $\mathcal{L}_j$ that meet our criteria, we encounter an immediate difficulty: $Sp(2n, \mathbb{R})$ is not compact [20, 30]. To avoid searching the whole of this infinite space, we shall look at whether or not we can limit ourselves to a smaller (preferably compact) subgroup or subspace.

13.1. **Avoiding Redundancy**

In our effort to ascertain which linear symplectic transformations matter, let us look first at the requirement that the Gram matrix $\Gamma(l)$ made from the sensitivity vectors σ^r be invertible. According to standard matrix theory, a Gram matrix is invertible if and only if the vectors used to construct it, in our case the σ^r, are linearly independent. Since there are $M(l, 2n)$ such vectors, and since they belong to an $(N \times M(l, n))$-dimensional vector space, linear independence means that

$$M(l, 2n) \leq NM(l, n). \tag{13.1}$$

This relation implies a lower bound on the number of jolts needed to ensure that the jolt decomposition (11.2) holds for $l \in \{3, 4, \ldots, P\}$. For the Gram matrix $\Gamma(l)$ to be invertible for all these values of l, it follows that the number of $\mathcal{L}_j$ we need, $N = N(P, n)$, must be an integer that satisfies the inequality

$$N(P, n) \geq M(P, 2n)/M(P, n). \tag{13.2}$$

We list in Table 13.1, for various values of P and for $n = 1, 2,$ and 3, the smallest values of $N(P, n)$ consistent with (13.2). As we shall see later, in the case $n = 1$ and P even we can meet these lower bounds. In the case $n = 1$ and P odd and in the cases $n = 2$ and $n = 3$, however, we must usually exceed these lower bounds in order to increase the smallest eigenvalue λ_{min} of the Gram matrix $\Gamma(l)$.

The condition (13.1) is necessary but, of course, not by itself sufficient to guarantee the linear independence of the σ^r. Consider the $NM(l, n) \times M(l, 2n)$ matrix whose columns are the sensitivity vectors, (11.4):

$$\left(\sigma^1, \sigma^2, \ldots, \sigma^{M(l,2n)}\right) = \begin{pmatrix} \langle G_1^{(l)}, \mathcal{L}_1 Q_1^{(l)} \rangle & \cdots & \langle G_{M(l,2n)}^{(l)}, \mathcal{L}_1 Q_1^{(l)} \rangle \\ \langle G_1^{(l)}, \mathcal{L}_1 Q_2^{(l)} \rangle & \cdots & \langle G_{M(l,2n)}^{(l)}, \mathcal{L}_1 Q_2^{(l)} \rangle \\ \vdots & \ddots & \vdots \\ \langle G_1^{(l)}, \mathcal{L}_N Q_{M(l,n)}^{(l)} \rangle & \cdots & \langle G_{M(l,2n)}^{(l)}, \mathcal{L}_N Q_{M(l,n)}^{(l)} \rangle \end{pmatrix}. \tag{13.3}$$

In order for the σ^r to be linearly independent, this matrix must have maximum rank, $M(l, 2n)$. We now make the following observation: Suppose $\mathcal{L}_1$ denotes the identity transformation and $\mathcal{L}_2$ denotes a transformation that converts any q-monomial, $Q_k^{(l)}$, into a linear combination of q-monomials. Then each row of (13.3) that contains an $\mathcal{L}_2$ will be a linear combination of the rows that contain $\mathcal{L}_1$. More generally, if $\mathcal{L}_i$ and $\mathcal{L}_j$ denote any two transformations that mix the q-monomials only among themselves, then the $\mathcal{L}_i$ and $\mathcal{L}_j$ rows of (13.3) will be linearly dependent. We shall avoid such unnecessary redundancy.

We also address another, somewhat more subtle, form of redundancy. Consider again the fundamental jolt decomposition (11.2). Let us replace there the symbol $\mathcal{L}_j$ by the symbol $\mathcal{L}(R_j)$, where, as in (9.14), R_j denotes the symplectic matrix corresponding to the linear symplectic transformation $\mathcal{L}_j$. Now suppose each R_j has a factorization

$$R_j = W_j \cdot U_j, \tag{13.4}$$

TABLE 13.1. Lower bounds on $N(P,n)$ as determined by (13.2).

	$n=1$			$n=2$			$n=3$		
P	$M(P,2)$	$M(P,1)$	$N(P,1)$	$M(P,4)$	$M(P,2)$	$N(P,2)$	$M(P,6)$	$M(P,3)$	$N(P,3)$
3	4	1	4	20	4	5	56	10	6
4	5	1	5	35	5	7	126	15	9
5	6	1	6	56	6	10	252	21	12
6	7	1	7	84	7	12	462	28	17
7	8	1	8	120	8	15	792	36	22
8	9	1	9	165	9	19	1287	45	29
9	10	1	10	220	10	22	2002	55	37
10	11	1	11	286	11	26	3003	66	46
11	12	1	12	364	12	31	4368	78	56
12	13	1	13	455	13	35	6188	91	68

where W_j and U_j also denote symplectic matrices. And further suppose that each W_j has the property that $\mathcal{L}(W_j)$ maps the q_k only among themselves, so that

$$\big\langle p_i, \mathcal{L}(W_j) q_k \big\rangle = 0, \quad i,k \in \{1,2,\ldots,n\}. \tag{13.5}$$

It then follows from this expression and (9.6) that the $\mathcal{L}(W_j)$ also transform the q-monomials $Q_k^{(l)}$ of (10.8) only among themselves. In other words, the $\mathcal{L}(W_j)$ transform q-monomials into q-monomials, and we therefore write

$$\mathcal{L}(W_j) Q_k^{(l)} = \sum_{k'} d(W_j)_{k'k} Q_{k'}^{(l)}. \tag{13.6}$$

Combining the expressions (13.4) and (13.6), and making use of (9.15), we obtain the result

$$\mathcal{L}(R_j) Q_k^{(l)} = \mathcal{L}(U_j)\mathcal{L}(W_j) Q_k^{(l)} = \sum_{k'} d(W_j)_{k'k} \mathcal{L}(U_j) Q_{k'}^{(l)}. \tag{13.7}$$

Let us now apply the result (13.7) to the jolt decomposition (11.2). We find that

$$\begin{aligned} h_l &= \frac{1}{NM(l,n)} \sum_{jk} a_{jk}^{(l)} \mathcal{L}(R_j) Q_k^{(l)} = \frac{1}{NM(l,n)} \sum_{jkk'} d(W_j)_{k'k}\, a_{jk}^{(l)} \mathcal{L}(U_j) Q_{k'}^{(l)} \\ &= \frac{1}{NM(l,n)} \sum_{jk'} \Big(\sum_k d(W_j)_{k'k} a_{jk}^{(l)} \Big) \mathcal{L}(U_j) Q_{k'}^{(l)}. \end{aligned}$$

On defining the modified jolt strengths

$$\bar{a}_{jk'}^{(l)} = \sum_k d(W_j)_{k'k}\, a_{jk}^{(l)}, \tag{13.8}$$

we may then write (11.2) in the form

$$h_l = \frac{1}{NM(l,n)} \sum_{jk'} \bar{a}_{jk'}^{(l)} \mathcal{L}(U_j) Q_{k'}^{(l)}. \tag{13.9}$$

In other words, if one can obtain a jolt decomposition using the $\mathcal{L}(R_j)$, with the R_j given by (13.4), then one can obtain a jolt decomposition using the $\mathcal{L}(U_j)$. Furthermore, the converse also holds: As shown by Theorem E.1 in Appendix E, the elements $d(W_j)_{k'k}$ form an invertible matrix. Hence, one can invert (13.8) to determine the $a_{jk}^{(l)}$ in terms of the $\bar{a}_{jk'}^{(l)}$; and one may therefore obtain a jolt decomposition in terms of the $\mathcal{L}(R_j)$ from a jolt decomposition in terms of the $\mathcal{L}(U_j)$. We leave for later the important question of how the choice of R_j versus U_j affects the sizes of the jolt strengths.

13.2. **A Factorization for Symplectic Matrices**

Let us write the real symplectic matrix $M \in Sp(2n,\mathbb{R})$ in the $n \times n$ block form

$$M = \begin{pmatrix} A & B \\ C & D \end{pmatrix}. \tag{13.10}$$

One may factor this matrix into a product of other symplectic matrices having particular forms [30], and we shall present one such factorization that will prove especially useful to us in our effort to determine which parts of the space $Sp(2n,\mathbb{R})$ we need not explore.

Let u denote any $n \times n$ unitary matrix, and define

$$M(u) = \begin{pmatrix} \mathrm{Re}(u) & \mathrm{Im}(u) \\ -\mathrm{Im}(u) & \mathrm{Re}(u) \end{pmatrix}. \tag{13.11}$$

Using the fact that u is unitary, one can show by direct calculation that $M(u)$ obeys the symplectic condition (8.3). In addition, one can verify by further straightforward calculation that

$$M(u_1 u_2) = M(u_1) M(u_2), \tag{13.12a}$$

and

$$M(I_n) = I_{2n}, \tag{13.12b}$$

where I_n and I_{2n} denote respectively the $n \times n$ and $2n \times 2n$ identity matrices. In other words, the matrices $M(u)$ retain the group structure of the unitary matrices u. It follows that $M(u)$ is a symplectic matrix that belongs to $U(n)$—the largest compact subgroup of $Sp(2n, \mathbb{R})$ [30].

Now consider any real symplectic matrix M of the form (13.10). It can be shown (see Appendix F) that there exist $n \times n$ matrices F, G, and u such that F is invertible, u is unitary, and

$$M = \begin{pmatrix} F & 0 \\ G & F^{-1} \end{pmatrix} M(u). \tag{13.13}$$

Moreover, both factors in (13.13) are symplectic matrices. We shall call this factorization a *modified Iwasawa factorization*.

13.3. **The Relevant $\mathcal{L}_j$**

As in §13.1 let us use $\mathcal{L}(R_j)$ to denote $\mathcal{L}_j$. Applying the modified Iwasawa factorization to each symplectic matrix R_j, we obtain

$$R_j = \begin{pmatrix} F_j & 0 \\ G_j & F_j^{-1} \end{pmatrix} M(u_j). \tag{13.14}$$

Now notice that, by our convention (9.12) for representing linear symplectic transformations as matrices, the matrix

$$W_j = \begin{pmatrix} F_j & 0 \\ G_j & F_j^{-1} \end{pmatrix}$$

has the property that $\mathcal{L}(W_j)$ maps the q_k, and hence also the $Q_k^{(l)}$, only among themselves. (*Cf.*, Appendix E.) It follows that with $U_j = M(u_j)$ the factorization (13.14) has exactly the form described in (13.4). Therefore, according to the argument of §13.1, given *any* jolt decomposition of the form (11.2), there exists a corresponding decomposition of the form (13.9) with the $U_j = M(u_j)$ drawn from the $U(n)$ subgroup of $Sp(2n, \mathbb{R})$.

To streamline the notation, let us write $\mathcal{L}(U_j) = \mathcal{L}(M(u_j))$ more simply as $\mathcal{L}(u_j)$. For future reference we note that (9.15) and (13.12a) imply that in this notation

$$\mathcal{L}(u_1 u_2) = \mathcal{L}(u_2)\mathcal{L}(u_1), \tag{13.15}$$

which looks precisely like (9.15). Now the jolt decomposition (13.9) becomes (here dropping the bar from over the a)

$$h_l = \frac{1}{NM(l,n)} \sum_{jk'} a_{jk'}^{(l)} \mathcal{L}(u_j) Q_{k'}^{(l)}. \tag{13.16}$$

In other words, we may restrict our search for the $\mathcal{L}_j$ to the compact subspace $U(n)$ contained within $Sp(2n, \mathbb{R})$.

It turns out that we can, in fact, restrict our search to an even smaller subspace. To see this, we begin by noting, as Gantmacher shows, that one may write any unitary matrix u in the form

$$u = re^{is}, \tag{13.17}$$

where r and s denote respectively real orthogonal and real symmetric matrices. As the elements r belong to the subgroup $O(n)$, the factorization (13.17) decomposes $U(n)$ into the coset space $U(n)/O(n)$. To emphasize this fact, we shall write (13.17) in the form

$$u = r \cdot c, \tag{13.18}$$

where the matrix

$$c = e^{is} \tag{13.19}$$

labels elements of the (right) coset space $U(n)/O(n)$.

Recall the Gram operator $\widehat{\Gamma}(l)$ introduced in §12.2. Since we shall choose our $\mathcal{L}_j$ from the $U(n)$ subgroup of $Sp(2n,\mathbb{R})$, we slightly modify the formulas (12.7), writing instead

$$\widehat{\Gamma}(l) = \frac{1}{N}\sum_j \widehat{\Gamma}(u_j, l), \tag{13.20a}$$

and

$$\widehat{\Gamma}(u_j, l) = \frac{1}{M(l,n)}\sum_k \mathcal{L}(u_j)\,\big|Q_k^{(l)}\big\rangle\big\langle Q_k^{(l)}\big|\,\mathcal{L}(u_j)^\dagger. \tag{13.20b}$$

We now prove

Theorem 13.1. *The partial Gram operator $\widehat{\Gamma}(u,l)$ has the property*

$$\widehat{\Gamma}(u,l) = \widehat{\Gamma}(c,l), \tag{13.21}$$

where u has the factorization (13.18)*. In other words, $\widehat{\Gamma}(u,l)$ is a* class function*: it depends only on the $U(n)/O(n)$ coset c to which u belongs.*[18]

Proof. Using (13.15) and (13.18), factor the linear symplectic transformation $\mathcal{L}(u)$ into the form

$$\mathcal{L}(u) = \mathcal{L}(r\cdot c) = \mathcal{L}(c)\mathcal{L}(r),$$

and then insert this expression into (13.20b) to obtain

$$\widehat{\Gamma}(u,l) = \frac{1}{M(l,n)}\sum_k \mathcal{L}(c)\mathcal{L}(r)\,\big|Q_k^{(l)}\big\rangle\big\langle Q_k^{(l)}\big|\,\mathcal{L}(r)^\dagger\mathcal{L}(c)^\dagger.$$

Since r denotes a real orthogonal matrix, (13.11) gives

$$M(r) = \begin{pmatrix} r & 0 \\ 0 & r \end{pmatrix}. \tag{13.22}$$

As we argued earlier concerning the W_j, the corresponding transformation $\mathcal{L}(r)$ maps the q-monomials only among themselves, and hence (*cf.* (13.6))

$$\mathcal{L}(r)\,\big|Q_k^{(l)}\big\rangle = \sum_{k'} d(r)_{k'k}\,\big|Q_{k'}^{(l)}\big\rangle.$$

Because $d(r)$ is a real matrix, we also have the expression

$$\big\langle Q_k^{(l)}\big|\,\mathcal{L}(r)^\dagger = \sum_{k''} d(r)_{k''k}\,\big\langle Q_{k''}^{(l)}\big|.$$

Using these last two expressions, we may now write $\widehat{\Gamma}(u,l)$ in the form

$$\widehat{\Gamma}(u,l) = \frac{1}{M(l,n)}\sum_{kk'k''} d(r)_{k'k}d(r)_{k''k}\,\mathcal{L}(c)\,\big|Q_{k'}^{(l)}\big\rangle\big\langle Q_{k''}^{(l)}\big|\,\mathcal{L}(c)^\dagger.$$

To simplify this expression, note that according to Theorems E.2 and E.3 in Appendix E,

$$\begin{aligned}\sum_k d(r)_{k'k}d(r)_{k''k} &= \sum_k d(r)_{k'k}\big(\widetilde{d(r)}\big)_{kk''} = \sum_k d(r)_{k'k}d(r^{-1})_{kk''}\\ &= \big(d(r)d(r^{-1})\big)_{k'k''} = \big(d(r\,r^{-1})\big)_{k'k''} = \delta_{k'k''}.\end{aligned}$$

[18] A function f defined on a group $\mathcal{G}$ is a *class function* if $f(g_1) = f(g_2)$ for any two elements $g_1, g_2 \in \mathcal{G}$ that belong to the same equivalence class. In the parlance of group theory the term "class" usually refers to conjugacy class. Cosets, however, define another type of equivalence class and hence another equivalence relation $\sim$: $g_1 \sim g_2$ if g_1 and g_2 belong to the same coset. One may therefore use the term "class function" as we have in Theorem 13.1.

The expression for $\widehat{\Gamma}(u,l)$ therefore simplifies to

$$\widehat{\Gamma}(u,l) = \frac{1}{M(l,n)} \sum_{k'} \mathcal{L}(c) \left|Q_{k'}^{(l)}\right\rangle \left\langle Q_{k'}^{(l)}\right| \mathcal{L}(c)^{\dagger} = \widehat{\Gamma}(c,l),$$

which proves the theorem. ∎

From Theorem 13.1 we conclude that *it suffices to limit our search for a set of N linear symplectic transformations $\mathcal{L}(u_j)$ to the (right) coset space $U(n)/O(n)$ contained within $Sp(2n,\mathbb{R})$.*

13.4. **Other Possible Restrictions**

Let us review briefly what we have learned so far: We seek a set of N linear symplectic transformations $\mathcal{L}_j$. According to §11, we must choose them in such a way that the Gram matrix $\Gamma(l)$ of (11.9) is invertible. Moreover, as we learned in §12, it behooves us to choose the $\mathcal{L}_j$ so as to make the smallest eigenvalue of $\Gamma(l)$ as large as possible. And now, in §13.3, we have learned that it suffices to restrict our search for the $\mathcal{L}_j$ to the (compact) coset space $U(n)/O(n)$ contained within $Sp(2n,\mathbb{R})$.

Although the coset space $U(n)/O(n)$ is dramatically smaller than $Sp(2n,\mathbb{R})$, one may still wonder whether there exist still smaller or simpler search spaces that are also worth exploring. In other words, might some other subspaces of $U(n)$ have topological (or other) characteristics that make them either quicker or easier to search? Consider for a moment the $U(n)$ subspace $[U(1)]^n \equiv U(1) \otimes \cdots \otimes U(1)$, an n-fold direct product of $U(1)$'s. This subspace has the topological structure of an n-torus (or a Cartesian product of n circles), and we might find our geometrical image of this subspace useful in searching it for an optimal set of $\mathcal{L}_j$. Of course the set of $\mathcal{L}_j$ found in this manner may differ from—and perform more poorly than—an optimal set of $\mathcal{L}_j$ chosen from $U(n)/O(n)$; but that is another matter. We may hope in the meantime to gain some insight by studying smaller or simpler subspaces.

Pursuing the idea in the last paragraph, we shall consider several $U(n)$ subspaces in our effort to gain an understanding of $U(n)/O(n)$; and we shall study in detail the cases for $n = 1, 2,$ and 3. Of particular interest to us for $n = 2$ and $n = 3$ will be the $U(n)$ subspaces $U(n)/SO(n)$ and $SU(n)/SO(n)$. Also of interest, for n arbitrary, will be the the subspace $[U(1)]^n$. To conclude this section, we touch briefly upon what lies ahead with regard to these various subspaces.

When $n = 1$, the space $U(n) = U(1)$ is topologically equivalent to the circle, or the one-dimensional sphere, $\mathbb{S}^1$. As the treatment of the full $U(1)$ presents no difficulty, we shall not restrict ourselves to $U(1)/O(1)$. Indeed, as $O(1)$ is just the discrete group comprising the numbers 1 and -1, the discussion surrounding equations (13.4)–(13.9) shows that such transformations simply multiply each $Q_k^{(l)}$ by $(-1)^l$ and therefore change at most the signs of various jolt strengths.

In the case $n = 2$ we first examine the smaller coset space $SU(2)/SO(2)$ and then proceed to study the larger space $U(2)/SO(2)$. We note that $U(2)/SO(2)$ is covered by $U(1) \otimes SU(2)/SO(2)$, and we can do these two pieces separately. The coset space $SU(2)/SO(2)$ is topologically equivalent to the two-dimensional surface of a sphere in three-space, $\mathbb{S}^2$, and we shall be able to investigate this space without too much difficulty. In particular, we shall see that we can indeed obtain invertible Gram matrices using a set of $\mathcal{L}_j$ chosen only from $SU(2)/SO(2)$. Afterwards, we shall include the effects of the $U(1)$ piece and will see that its inclusion can improve the minimum Gram eigenvalue by a modest amount. Again, as for n=1, taking the elements W_j of (13.4) from $O(2)$ rather than $SO(2)$ amounts to changing the signs of some of the $Q_k^{(l)}$ and hence changing at most the signs of various jolt strengths.

Our approach for the case $n = 3$ will parallel that for $n = 2$: we shall study first the smaller coset space $SU(3)/SO(3)$ and then afterwards the larger space $U(3)/SO(3)$. The principal difference is that in this case we shall discover that the space $SU(3)/SO(3)$ suffices.

In other words, the $U(1)$ part of $U(3)$ has no effect on the Gram eigenvalues. In this case too, as for $n = 1$ and 2, the choice of $O(3)$ versus $SO(3)$ changes only the signs of some of the $Q_k^{(l)}$ and hence at most the signs of various jolt strengths.

As we have mentioned already, we shall also investigate the subspace $[U(1)]^n$. In this subspace the analysis can be carried out for arbitrary n, but we shall concentrate on those cases of special interest to us: $n = 2$ and $n = 3$.

14. The Continuum Limit

In our attempt to maximize the smallest Gram eigenvalue, it seems natural to try to answer the question, "How high can we aim?" In the course of answering this question, we shall find it instructive to examine the limiting case where we allow the number N of linear symplectic transformations $\mathcal{L}_j$ to approach infinity.

14.1. **Transition to the Continuum Limit**

Recall from §12, in particular the relation (12.4), that our motivation for maximizing λ_{min} sprang from our desire to minimize the size of the jolt strengths $a^{(l)}$. Let us take another look at the role of the jolt strengths in (11.2):

$$h_l = \frac{1}{NM(l,n)} \sum_{jk} a^{(l)}_{jk} \mathcal{L}_j Q^{(l)}_k .$$

According to this equation, we ought to choose the $\mathcal{L}_j$ so that the elements $\mathcal{L}_j Q^{(l)}_k$ sample the space of dynamical polynomials in a sufficiently democratic manner. To see this, suppose, for example, that a particular "direction" $\mathcal{L}Q^{(l)}$ were not easily resolved by the given set of $\mathcal{L}_j Q^{(l)}_k$. Then an h_l having a significant component in that "direction" would require some very large but somewhat self-cancelling $a^{(l)}_{jk}$'s in nearby directions in order to build the $\mathcal{L}Q^{(l)}$ component.

Although we wish to choose as few $\mathcal{L}_j$ as possible—because that will minimize the work of computing our resulting map (10.13)—let us briefly consider allowing the number of jolts N to become very large. In the vector space V^l, the squared length of the vector of jolt strengths $a^{(l)}$ is

$$\{a^{(l)}, a^{(l)}\} = \frac{1}{NM(l,n)} \sum_{jk} \left(a^{(l)}_{jk}\right)^2 .$$

If the jolt strengths were roughly comparable in size, say a, this sum would be of order

$$\frac{1}{NM(l,n)}\, NM(l,n)\, a^2 = a^2,$$

independent of N. This suggests that once we have enough $\mathcal{L}_j$ chosen in a sufficiently democratic manner, the size of the jolt strengths will not vary a great deal. We reach a similar conclusion on examining the elements of the Gram matrix, (11.9):

$$\Gamma(l)_{rs} = \frac{1}{NM(l,n)} \sum_{jk} \left\langle G^{(l)}_r, \mathcal{L}_j Q^{(l)}_k \right\rangle \left\langle \mathcal{L}_j Q^{(l)}_k, G^{(l)}_s \right\rangle .$$

Again, once we have enough appropriately chosen $\mathcal{L}_j$, the elements $\mathcal{L}_j Q^{(l)}_k$ will sample the space of dynamical polynomials in a manner sufficiently democratic as to ensure that increasing N will have relatively little effect on $\Gamma(l)$, and hence relatively little effect on the Gram eigenvalues $\lambda^{(l)}_r$. This suggests that the Gram eigenvalues are bounded above by their values in the continuum limit, where $N \to \infty$. Indeed, our numerical evidence suggests that this is, in fact, the case. We shall therefore explore the continuum limit as a means of determining "how high we can aim".

14.2. **The Continuum Limit**

In going over to the continuum limit, we sum over the N linear symplectic transformations $\mathcal{L}_j$ and then allow N to approach infinity. Hence we make the correspondences

$$\mathcal{L}_j = \mathcal{L}(u_j) \longleftrightarrow \mathcal{L}(u),$$

and

$$\frac{1}{N}\sum_{j=1}^{N} \longleftrightarrow \int_{\mathcal{U}} du,$$

where $\mathcal{U}$ denotes the appropriate range of integration, and, as in §13.3, $\mathcal{L}(u)$ stands for $\mathcal{L}(M(u))$. In typical cases $\mathcal{U}$ will denote one of the groups $U(n)$ or $SU(n)$, or, sometimes, the coset space $SU(n)/SO(n)$. We can now revise a number of the important formulas in §§11 and 13.3. In particular, we can rewrite (11.2), or (13.16), in the form

$$h_l = \frac{1}{M(l,n)} \sum_{k=1}^{M(l,n)} \int_{\mathcal{U}} du\, a_k^{(l)}(u)\, \mathcal{L}(u) Q_k^{(l)}. \tag{14.1}$$

This is the continuum limit version of the jolt decomposition of the homogeneous polynomial h_l of (11.1). The coefficients $c_r^{(l)}$ of that polynomial are now given by the continuum limit version of (11.3):

$$c_r^{(l)} = \left\langle G_r^{(l)}, h_l \right\rangle = \{a^{(l)}, \sigma^r\} = \frac{1}{M(l,n)} \sum_k \int_{\mathcal{U}} du\, a_k^{(l)}(u)\, \sigma_k^r(u), \tag{14.2}$$

where $\sigma_k^r(u)$ denotes the *sensitivity function* defined by

$$\sigma_k^r(u) = \left\langle G_r^{(l)}, \mathcal{L}(u) Q_k^{(l)} \right\rangle. \tag{14.3}$$

We can now write down the Gram matrix (11.9) in the continuum limit:

$$\Gamma(l)_{rs} = \{\sigma^r, (\sigma^s)^*\} = \frac{1}{M(l,n)} \sum_k \int_{\mathcal{U}} du \left\langle G_r^{(l)}, \mathcal{L}(u) Q_k^{(l)} \right\rangle \left\langle \mathcal{L}(u) Q_k^{(l)}, G_s^{(l)} \right\rangle. \tag{14.4}$$

Similar expressions obtain for the Gram operator (13.20) in the continuum limit; thus

$$\widehat{\Gamma}(l) = \int_{\mathcal{U}} du\, \widehat{\Gamma}(u,l), \tag{14.5a}$$

where

$$\widehat{\Gamma}(u,l) = \frac{1}{M(l,n)} \sum_k \mathcal{L}(u) \left|Q_k^{(l)}\right\rangle \left\langle Q_k^{(l)}\right| \mathcal{L}(u)^\dagger. \tag{14.5b}$$

Two important consequences will follow from our study of the continuum limit. The first, and most obvious, is that computations of the Gram matrix $\Gamma(l)$ of (14.4) or the Gram operator $\widehat{\Gamma}(l)$ of (14.5) will teach us the best possible Gram eigenvalues we can hope for by *any* choice of $\mathcal{L}_j$. The second, and less obvious, consequence is that we might hope actually to achieve the best possible eigenvalues by searching for numerical quadrature and cubature formulas to replace the appropriate group integration, $\int_{\mathcal{U}} du$. In the following sections we shall investigate each of these two topics.

15. Gram Eigenvalues in the Continuum Limit

We have constructed the expression (14.4) for the Gram matrix $\Gamma(l)$ in the continuum limit. This matrix will not, in general, be diagonal; but, as we observed in §12.1, $\Gamma(l)$ can be diagonalized by a real orthogonal transformation—and the diagonal entries will be the eigenvalues we seek. We would therefore like to find a method for achieving such a diagonalization.

In §12.2 we introduced the concept of a Gram operator, and in (14.5) we defined its continuum limit version. As we observed in §12.2, the application to the Gram operator $\widehat{\Gamma}(l)$ of any orthonormal basis for the space of f_l's will yield a representation for the Gram matrix equivalent to the $\Gamma(l)$ of (14.4). We then face the challenge of finding a set of orthonormal basis functions for which $\widehat{\Gamma}(l)$ is diagonal. We shall address this challenge for phase spaces of two, four, and six dimensions, *i.e.*, for the cases $n = 1, 2,$ and 3.

15.1. **One Degree of Freedom**

In the case of one degree of freedom, $n = 1$, we begin our study by noting that according to (10.6)

$$M(l, n) = M(l, 1) = \binom{l}{l} = 1.$$

Hence the sum over k in (14.5b) contains only one term, and the single q-monomial of degree l is

$$Q_1^{(l)} = q^l/\sqrt{l!}. \tag{15.1}$$

In addition, as we indicated in §13.4, we shall integrate over the space $\mathcal{U} = U(1)$, which is more than sufficient to cover all of the relevant linear symplectic transformations. Since we may represent any element u of $U(1)$ in the form $u = e^{i\theta}$, $\theta \in [0, 2\pi)$, we shall define

$$\mathcal{R}(\theta) = \mathcal{L}(u) = \mathcal{L}(e^{i\theta}).$$

Thus we write the Gram operator (14.5) in the form

$$\widehat{\Gamma}(l) = \frac{1}{2\pi}\int_0^{2\pi} d\theta \left|\mathcal{R}(\theta)Q_1^{(l)}\right\rangle\left\langle\mathcal{R}(\theta)Q_1^{(l)}\right|. \tag{15.2}$$

To make further progress, we must study the operator $\mathcal{R}(\theta)$.

Recall from §13.3 that we use $\mathcal{L}(u)$ as an abbreviation for $\mathcal{L}(M(u))$. Then from (13.11) we find that in our present case

$$M(u) = M(e^{i\theta}) = \begin{pmatrix} \cos\theta & \sin\theta \\ -\sin\theta & \cos\theta \end{pmatrix}. \tag{15.3}$$

Using the results of Appendix D, we may write the operator $\mathcal{R}(\theta) = \mathcal{L}(e^{i\theta})$, whose matrix representation is given by (15.3), as the Lie transformation

$$\mathcal{R}(\theta) = \exp\Big(-\frac{\theta}{2}:q^2 + p^2:\Big). \tag{15.4}$$

Note that $\mathcal{R}(\theta)$ denotes a rotation operator that effects a clock-wise rotation of phase space through an angle θ.

15.1.1. *The Eigenfunctions of* $\mathcal{R}(\theta)$. We shall find it very useful to determine the eigenfunctions of the rotation operator, the Lie transformation $\mathcal{R}(\theta)$. To begin, let us hunt for the eigenfunctions of its generator, the Lie operator $:q^2 + p^2:$. Consider the action of this Lie operator on the quantity $\xi q + \eta p$:

$$:q^2 + p^2:(\xi q + \eta p) = 2\eta q - 2\xi p.$$

Hence if $\xi q + \eta p$ denotes an eigenfunction of $:q^2 + p^2:$ with eigenvalue λ, it follows that

$$\lambda\xi = 2\eta, \text{ and } \lambda\eta = -2\xi.$$

The ratio of these two expressions implies

$$\eta^2 = -\xi^2.$$

If, say, we choose $\xi = 1$, then $\eta = \pm i$, and $\lambda = \pm 2i$. Therefore

$$z = \frac{1}{\sqrt{2}}(q + ip) \text{ and } z^* = \frac{1}{\sqrt{2}}(q - ip) \tag{15.5}$$

denote two eigenfunctions of $:q^2 + p^2:$ which are orthonormal with respect to the inner product (10.9) and have eigenvalues $2i$ and $-2i$, respectively. It follows immediately that z and z^* also denote eigenfunctions of the rotation operator (15.4) with eigenvalues $e^{-i\theta}$ and $e^{i\theta}$, respectively:

$$\mathcal{R}(\theta)z = e^{-i\theta}z, \text{ and } \mathcal{R}(\theta)z^* = e^{i\theta}z^*. \tag{15.6}$$

We now introduce a small trick. Consider the complex linear Lie transformation

$$\mathcal{T} = \exp\Big(\frac{i\pi}{8} :q^2 - p^2:\Big). \tag{15.7}$$

Using the results of Appendix D, we can easily determine that $\mathcal{T}$ acts on phase space according to the rule

$$\mathcal{T}\begin{pmatrix} q \\ p \end{pmatrix} = \frac{1}{\sqrt{2}}\begin{pmatrix} q + ip \\ i(q - ip) \end{pmatrix} = \begin{pmatrix} z \\ iz^* \end{pmatrix}. \tag{15.8}$$

Now note an important feature of $\mathcal{T}$. By making use of (10.12), we can evaluate the Hermitian adjoint of $\mathcal{T}$ with respect to the inner product (10.9):

$$\mathcal{T}^\dagger = \exp\Big(\frac{-i\pi}{8}:q^2 - p^2:^\dagger\Big) = \exp\Big(\frac{-i\pi}{8}(-:p^2: + :q^2:)\Big) = \exp\Big(\frac{-i\pi}{8} :q^2 - p^2:\Big) = \mathcal{T}^{-1}.$$

In other words, the Lie transformation $\mathcal{T}$ is unitary with respect to the inner product (10.9).

We can now complete the construction of the eigenfunctions of the rotation operator $\mathcal{R}(\theta)$. Let us first note that in the present case, $n = 1$, we may write the general monomials $G_r^{(l)}$ of (10.7) in the form

$$G_r^{(l)} = \frac{q^{l-r}p^r}{\sqrt{(l-r)!\,r!}}, \quad r \in \{0, 1, \ldots, l\}. \tag{15.9}$$

Then the dynamical polynomial

$$\psi_r^{(l)} = \mathcal{T}G_r^{(l)} = \frac{z^{l-r}(iz^*)^r}{\sqrt{(l-r)!\,r!}} \tag{15.10}$$

represents an eigenfunction of $\mathcal{R}(\theta)$. To see this, we simply compute. Using (9.6) and (15.6), we find

$$\mathcal{R}(\theta)\frac{z^{l-r}(iz^*)^r}{\sqrt{(l-r)!\,r!}} = \frac{(e^{-i\theta}z)^{l-r}(ie^{i\theta}z^*)^r}{\sqrt{(l-r)!\,r!}} = e^{-i(l-2r)\theta}\,\frac{z^{l-r}(iz^*)^r}{\sqrt{(l-r)!\,r!}}.$$

Hence the dynamical polynomial $\psi_r^{(l)}$ denotes an eigenfunction of the rotation operator with eigenvalue $e^{-i(l-2r)\theta}$:

$$\mathcal{R}(\theta)\psi_r^{(l)} = e^{-i(l-2r)\theta}\psi_r^{(l)}. \tag{15.11}$$

Note that because of the unitarity of $\mathcal{T}$, these eigenfunctions form an orthonormal basis:

$$\big\langle \psi_r^{(l)}, \psi_{r'}^{(l')} \big\rangle = \big\langle \mathcal{T}G_r^{(l)}, \mathcal{T}G_{r'}^{(l')} \big\rangle = \big\langle G_r^{(l)}, \mathcal{T}^\dagger\mathcal{T}G_{r'}^{(l')} \big\rangle = \big\langle G_r^{(l)}, G_{r'}^{(l')} \big\rangle = \delta_{ll'}\delta_{rr'}.$$

In particular note that the eigenfunctions $\psi_r^{(l)}$ with l fixed form an orthonormal basis for the space of dynamical polynomials of degree l.

15.1.2. *The Gram Matrix and its Eigenvalues.* Let us now evaluate the Gram operator $\widehat{\Gamma}(l)$ of (15.2) with respect to the orthonormal basis of eigenfunctions of $\mathcal{R}(\theta)$. In other words, let us evaluate

$$\langle \psi_r^{(l)} | \widehat{\Gamma}(l) | \psi_{r'}^{(l)} \rangle = \frac{1}{2\pi} \int_0^{2\pi} d\theta \, \langle \psi_r^{(l)}, \mathcal{R}(\theta) Q_1^{(l)} \rangle \langle \mathcal{R}(\theta) Q_1^{(l)}, \psi_{r'}^{(l)} \rangle \, . \tag{15.12}$$

Consider first the inner product $\langle \psi_r^{(l)}, \mathcal{R}(\theta) Q_1^{(l)} \rangle$. Because the operator $\mathcal{R}(\theta)$ belongs to the $U(1)$ subgroup of $Sp(2,\mathbb{R})$, it is unitary with respect to the inner product (10.9) (*cf.* §10.2). As a consequence,

$$\mathcal{R}(\theta)^\dagger = \mathcal{R}(\theta)^{-1} = \mathcal{R}(-\theta).$$

Hence, according to (15.11) and (10.9),

$$\begin{aligned} \langle \psi_r^{(l)}, \mathcal{R}(\theta) Q_1^{(l)} \rangle &= \langle \mathcal{R}(-\theta) \psi_r^{(l)}, Q_1^{(l)} \rangle \\ &= \langle e^{i(l-2r)\theta} \psi_r^{(l)}, Q_1^{(l)} \rangle = e^{-i(l-2r)\theta} \langle \psi_r^{(l)}, Q_1^{(l)} \rangle \, . \end{aligned}$$

In a similar fashion we obtain

$$\langle \mathcal{R}(\theta) Q_1^{(l)}, \psi_{r'}^{(l)} \rangle = e^{i(l-2r')\theta} \, \langle Q_1^{(l)}, \psi_{r'}^{(l)} \rangle \, .$$

Using these last two results, we may write (15.12) in the form

$$\langle \psi_r^{(l)} | \widehat{\Gamma}(l) | \psi_{r'}^{(l)} \rangle = \frac{1}{2\pi} \int_0^{2\pi} d\theta \, e^{i2(r-r')\theta} \, \langle \psi_r^{(l)}, Q_1^{(l)} \rangle \langle Q_1^{(l)}, \psi_{r'}^{(l)} \rangle \, .$$

Performing the integration over θ, we obtain the Kronecker delta $\delta_{rr'}$. Hence

$$\langle \psi_r^{(l)} | \widehat{\Gamma}(l) | \psi_{r'}^{(l)} \rangle = \delta_{rr'} \big| \langle \psi_r^{(l)}, Q_1^{(l)} \rangle \big|^2 . \tag{15.13}$$

As these elements form a diagonal matrix, they represent the eigenvalues of the Gram matrix $\Gamma(l)$:

$$\lambda_r^{(l)} = \big| \langle \psi_r^{(l)}, Q_1^{(l)} \rangle \big|^2 . \tag{15.14}$$

We can evaluate the Gram eigenvalues (15.14) by expanding $Q_1^{(l)}$ in terms of the rotation operator eigenfunctions $\psi_r^{(l)}$. Note from (15.5) that

$$q = \frac{1}{\sqrt{2}}(z + z^*), \text{ and } p = \frac{1}{i\sqrt{2}}(z - z^*). \tag{15.15}$$

It then follows from (15.15) and (15.10) that we may write the q-monomial of (15.1) in the form

$$\begin{aligned} Q_1^{(l)} &= \frac{1}{\sqrt{l!}} \left(\frac{1}{\sqrt{2}} (z + z^*) \right)^l = \frac{1}{\sqrt{l!}} \left(\frac{1}{2} \right)^{l/2} \sum_{r=0}^{l} \binom{l}{r} z^{l-r} (z^*)^r \\ &= \frac{1}{\sqrt{l!}} \left(\frac{1}{2} \right)^{l/2} \sum_r \binom{l}{r} \sqrt{(l-r)!\, r!} \, \frac{1}{i^r} \frac{z^{l-r} (iz^*)^r}{\sqrt{(l-r)!\, r!}} \\ &= \left(\frac{1}{2} \right)^{l/2} \sum_r \frac{1}{i^r} \binom{l}{r} \sqrt{\frac{(l-r)!\, r!}{l!}} \, \psi_r^{(l)} = \left(\frac{1}{2} \right)^{l/2} \sum_r \frac{1}{i^r} \binom{l}{r}^{1/2} \psi_r^{(l)} . \end{aligned}$$

Because the $\psi_r^{(l)}$ form an orthonormal basis, we obtain

$$\langle \psi_r^{(l)}, Q_1^{(l)} \rangle = \frac{1}{i^r} \left(\frac{1}{2} \right)^{l/2} \binom{l}{r}^{1/2} .$$

We therefore obtain for the Gram eigenvalues (15.14) the result

$$\lambda_r^{(l)} = \frac{1}{2^l} \binom{l}{r} ; \tag{15.16}$$

and the minimum Gram eigenvalue for the case $n = 1$ is then simply

$$\lambda_{min}^{(l)} = \frac{1}{2^l}. \tag{15.17}$$

15.2. **Two Degrees of Freedom**

In the case of two degrees of freedom, $n = 2$, we begin by noting that according to (10.6)

$$M(l, n) = M(l, 2) = \binom{l+1}{l} = l + 1.$$

Hence the sum over k in (14.5b) covers $l + 1$ q-monomials, which we denote

$$Q_k^{(l)} = \frac{q_1^{l-k} q_2^k}{\sqrt{(l-k)!\, k!}}, \quad k \in \{0, 1, \ldots, l\}. \tag{15.18}$$

As indicated in §13.4, we shall begin by integrating over just the coset space $SU(2)/SO(2)$. Later we shall include an integral over $U(1)$ so as to cover the whole of the space $U(2)/SO(2)$.

15.2.1. *A Representation for the Coset Space $SU(2)/SO(2)$.* Before we can find a representation for the coset space $SU(2)/SO(2)$, we first need an appropriate representation for the group $SU(2)$. We have found a useful choice in a variant of the standard Euler angle parameterization, which writes any element $u \in SU(2)$ as [8]

$$u(\psi, \theta, \phi) = e^{-i\psi\sigma_3/2}\, e^{-i\theta\sigma_2/2}\, e^{-i\phi\sigma_3/2}, \tag{15.19}$$

where the σ_j denote the well-known Pauli spin matrices, and the Euler angles ψ, θ, and ϕ span the intervals

$$\psi \in [0, 4\pi), \quad \theta \in [0, \pi), \quad \phi \in [0, 2\pi). \tag{15.20}$$

Recall that in general

$$e^{-i\omega\hat{\boldsymbol{n}}\cdot\boldsymbol{\sigma}/2} = \mathbf{1}\cos(\omega/2) - i(\hat{\boldsymbol{n}}\cdot\boldsymbol{\sigma})\sin(\omega/2), \tag{15.21}$$

where here $\mathbf{1}$ denotes the 2×2 identity matrix, $\hat{\boldsymbol{n}}$ denotes a three-component unit vector, and $\boldsymbol{\sigma}$ denotes the three-component "vector" of Pauli matrices, $(\sigma_1, \sigma_2, \sigma_3)$.

According to (13.18), we should construct the coset space $SU(2)/SO(2)$ by extracting out the $SO(2)$ part to the left. Now observe that, according to (15.21),

$$e^{i\alpha\sigma_2/2} = \mathbf{1}\cos(\alpha/2) + i\sigma_2\sin(\alpha/2) = \begin{pmatrix} \cos(\alpha/2) & \sin(\alpha/2) \\ -\sin(\alpha/2) & \cos(\alpha/2) \end{pmatrix} \tag{15.22}$$

belongs to $SO(2)$. We therefore choose to use not the standard Euler angle parameterization (15.19) but rather a variant thereof. Let us write an arbitrary element $u \in SU(2)$ in the form

$$u(\psi, \theta, \phi) = \tau\, e^{-i\psi\sigma_3/2}\, e^{-i\theta\sigma_2/2}\, e^{-i\phi\sigma_3/2}\, \tau^{-1}, \tag{15.23}$$

where the matrix τ denotes some particular fixed element of $SU(2)$ which remains at our disposal. Note that by a judicious insertion of identity matrices in the form $\tau^{-1}\tau$, we may write the right-hand side of (15.23) as

$$(\tau\, e^{-i\psi\sigma_3/2}\, \tau^{-1})(\tau\, e^{-i\theta\sigma_2/2}\, \tau^{-1})(\tau\, e^{-i\phi\sigma_3/2}\, \tau^{-1}).$$

We shall then select τ so as to make the left-hand factor in parentheses take the form (15.22).

From a well-known result in the quantum mechanical theory of angular momentum, we have the general formula [64]

$$e^{i\beta\sigma_j/2}\, \sigma_k\, e^{-i\beta\sigma_j/2} = \sigma_k\big(\cos\beta + \delta_{jk}(1 - \cos\beta)\big) + \frac{i}{2}[\sigma_j, \sigma_k]\sin\beta, \tag{15.24}$$

where $[\sigma_j, \sigma_k]$ denotes the familiar commutator of the matrices σ_j and σ_k. If we denote (15.24) by the symbol $\sigma_k(\beta, j)$, it follows from (15.24) that

$$e^{i\beta\sigma_j/2}\, e^{i\theta\sigma_k/2}\, e^{-i\beta\sigma_j/2} = e^{i\theta\sigma_k(\beta,j)/2}. \tag{15.25}$$

This result suggests that we set $\tau = e^{i\beta\sigma_1/2}$ with $\beta = -\pi/2$. Then

$$\sigma_3(-\pi/2, 1) = -\frac{i}{2}[\sigma_1, \sigma_3] = -\sigma_2,$$
$$\text{and} \quad \sigma_2(-\pi/2, 1) = -\frac{i}{2}[\sigma_1, \sigma_2] = \sigma_3.$$

Hence

$$\tau\, e^{-i\psi\sigma_3/2}\, \tau^{-1} = e^{i\psi\sigma_2/2},$$
$$\tau\, e^{-i\theta\sigma_2/2}\, \tau^{-1} = e^{-i\theta\sigma_3/2},$$
$$\text{and} \quad \tau\, e^{-i\phi\sigma_3/2}\, \tau^{-1} = e^{i\phi\sigma_2/2}.$$

Taking the product of these last three expressions, we obtain an alternate Euler angle parameterization for the general element $u \in SU(2)$:

$$u(\psi, \theta, \phi) = e^{i\psi\sigma_2/2}\, e^{-i\theta\sigma_3/2}\, e^{i\phi\sigma_2/2}, \tag{15.26}$$

where the Euler angles ψ, θ, and ϕ still cover the ranges given in (15.20). We shall sometimes refer to the three factors in (15.26) as u_ψ, u_θ, and u_ϕ, respectively.

Because $u_\psi = e^{i\psi\sigma_2/2}$ belongs to $SO(2)$ (*cf.* (15.22)), we have obtained in (15.26) a parameterization for $SU(2)$ of the form (13.18). This leads directly to a parameterization for arbitrary elements c in the (right) coset space $SU(2)/SO(2)$:

$$c(\theta, \phi) = u_\theta \cdot u_\phi = e^{-i\theta\sigma_3/2}\, e^{i\phi\sigma_2/2}, \tag{15.27}$$

where, from (15.20), the angles θ and ϕ span the intervals $[0, \pi)$ and $[0, 2\pi)$, respectively.

15.2.2. *Integrating Over the Coset Space $SU(2)/SO(2)$.* Before we can integrate over the coset space $SU(2)/SO(2)$, we need to know the measure dc appropriate to the representation given in (15.27). To this end we shall first integrate over the whole of $SU(2)$, using the representation given in (15.26), and then show how to eliminate the integral over ψ. From what remains, we shall be able to determine the measure dc.

For the standard Euler angle parameterization (15.19) of $SU(2)$ the appropriate measure is [8]

$$du = \frac{1}{16\pi^2} \sin\theta\, d\theta\, d\phi\, d\psi. \tag{15.28}$$

Since this measure is both left and right invariant [20], the introduction of the matrices τ and τ^{-1} in (15.23) do not alter it. Therefore, on integrating over the group $\mathcal{U} = SU(2)$, we may write the Gram operator (14.5) in the form

$$\widehat{\Gamma}(l) = \frac{1}{16\pi^2} \int_0^{2\pi} d\phi \int_0^{\pi} d\theta \sin\theta \int_0^{4\pi} d\psi\, \widehat{\Gamma}(u, l),$$

where we use (15.26) for $u = u(\psi, \theta, \phi)$. But according to Theorem 13.1, the partial Gram operator $\widehat{\Gamma}(u, l)$ depends only on the coset c to which u belongs, and hence we may perform the ψ integration immediately. It contributes a simple factor of 4π, and we find

$$\widehat{\Gamma}(l) = \frac{1}{4\pi} \int_0^{2\pi} d\phi \int_0^{\pi} d\theta \sin\theta\, \widehat{\Gamma}(c, l).$$

The two integrals, over θ and ϕ, then combine to form an integral over the spherical surface $\mathbb{S}^2$. Writing $d\Omega$ for $\sin\theta\, d\theta\, d\phi$, c_Ω for $c(\theta, \phi)$, and using (14.5b), we obtain the Gram operator in the form

$$\widehat{\Gamma}(l) = \int_{\mathbb{S}^2} \frac{d\Omega}{4\pi}\, \widehat{\Gamma}(c_\Omega, l) = \frac{1}{l+1} \sum_{k=0}^{l} \int_{\mathbb{S}^2} \frac{d\Omega}{4\pi}\, \mathcal{L}(c_\Omega)\, \big|Q_k^{(l)}\big\rangle\big\langle Q_k^{(l)}\big|\, \mathcal{L}(c_\Omega)^\dagger. \tag{15.29}$$

From this expression it follows that the $SU(2)/SO(2)$ measure $dc = d\Omega/(4\pi)$.

15.2.3. *Basis Functions for Irreducible Representations of $SU(2)$.* To find a set of orthonormal basis functions which diagonalize the Gram operator of (15.29), we have found it useful to look for basis functions that transform according to irreducible representations of $SU(2)$. In this section we show how to construct such a set of functions; then, in the following section, we show how to use them for determining the Gram eigenvalues.

Recall from our introduction to §15 that diagonalizing the Gram matrix $\Gamma(l)$ requires finding an appropriate orthonormal basis for the space of dynamical polynomials of degree l. In the present case—$n = 2$, $\mathcal{U}$=$SU(2)$—it seems reasonable to suspect that such a basis has special properties under the action of $SU(2)$; we therefore look for an orthonormal basis that transforms according to irreducible representations of $SU(2)$. We begin with a small digression to introduce the Lie algebra $sp(4,\mathbb{R})$ and, in particular, its unitary subalgebra $u(2)$. (Here $4 = 2n$.) Recall from §9.2 that Lie transformations of the form $e^{:f_2:}$ generate linear symplectic transformations, hence elements of $Sp(2n,\mathbb{R})$. A statement resembling the converse also holds: one may write any element of the Lie group $Sp(2n,\mathbb{R})$ as a finite product of Lie transformations of the generic form $e^{:f_2:}$. As the objects that appear upstairs in the exponential representation of a Lie group form the elements of the corresponding Lie algebra, we see that the real vector space of Lie operators of the form $:f_2:$ compose the Lie algebra $sp(2n,\mathbb{R})$. In this case the Lie product is the usual "commutator" defined by [30]

$$[:f:,:g:] = :f:\,:g: - :g:\,:f:\,. \tag{15.30}$$

At this point we remark that there exists another (isomorphic) representation for the Lie algebra $sp(2n,\mathbb{R})$. In this alternative, $sp(2n,\mathbb{R})$ comprises the real vector space of quadratic dynamical polynomials together with the Poisson bracket as the Lie product. The isomorphism between these two representations of $sp(2n,\mathbb{R})$ is given by the correspondence $f \longleftrightarrow :f:$ and is guaranteed by the relation [30]

$$[:f:,:g:] = :[f,g]:, \tag{15.31}$$

which follows from Jacobi's identity for Poisson brackets. (This relation shows that the commutator (15.30) does indeed produce another Lie operator.) On the left-hand side of (15.31) the square brackets denote the commutator Lie product, while on the right-hand side the square brackets denote the Poisson bracket Lie product. The notation here should engender no confusion as the contents of the square brackets indicate which operation to perform.

Let us now consider the Lie algebra $sp(4,\mathbb{R})$ as represented by the Poisson bracket Lie algebra of quadratic dynamical polynomials. As we know, one choice of basis for this Lie algebra comprises the dynamical polynomials $G_r^{(2)}$ defined in (10.7) with $n = 2$. However, a better choice takes into account the subgroup structure of $Sp(4,\mathbb{R})$. In particular, because the Lie group $Sp(4,\mathbb{R})$ contains $U(2)$ as a subgroup, it follows that the Lie algebra $sp(4,\mathbb{R})$ contains $u(2)$ as a subalgebra. The following four dynamical polynomials—$b^0,\ldots,b^3$—form a basis for this subalgebra:

$$\begin{aligned} b^0 &= \frac{1}{2}(q_1^2 + p_1^2 + q_2^2 + p_2^2),\\ b^1 &= q_1q_2 + p_1p_2,\\ b^2 &= -q_1p_2 + q_2p_1,\\ b^3 &= \frac{1}{2}(q_1^2 + p_1^2 - q_2^2 - p_2^2). \end{aligned} \tag{15.32}$$

We make several observations concerning these functions, (15.32) [30]:

(1) They form a linearly independent set.

(2) They satisfy the following Poisson bracket relations:

$$[b^0, b^j] = 0, \qquad j \in \{0, \ldots, 3\}; \tag{15.33a}$$

$$[b^j, b^k] = -2\sum_{l=1}^{3} \varepsilon_{jkl} b^l, \qquad j, k \in \{1, \ldots, 3\}. \tag{15.33b}$$

Here ε_{jkl} denotes the completely anti-symmetric Levi-Civita tensor.

(3) The first two points confirm that the functions b^j do indeed form a basis for the four-dimensional $u(2)$ Lie algebra contained within $sp(4, \mathbb{R})$.

(4) The relations (15.33) show, in addition, that the functions b^1, b^2, and b^3 form a basis for the $su(2)$ subalgebra, while b^0 forms a basis for the $u(1)$ subalgebra.

(5) As the functions b^j form a basis for $u(2)$ under the Poisson bracket Lie algebra, so the Lie operators $:b^j:$ form a basis for $u(2)$ under the commutator product Lie algebra. By using (10.12), one can easily see that the Lie operators $:b^j:$ are anti-Hermitian (*i.e.*, $:b^j:^\dagger = -:b^j:$); hence the associated Lie transformations $\exp(:b^j:)$ are unitary with respect to the inner product (10.9). This observation illustrates the connection between the $u(2)$ subalgebra of $sp(4, \mathbb{R})$ and the $U(2)$ subgroup of $Sp(4, \mathbb{R})$.

Returning to our purpose, we recall our desire to find a basis for the space of dynamical polynomials in such a way that it transforms according to irreducible representations of $SU(2)$. To achieve this goal, we follow a procedure familiar to any student of the theory of angular momentum in quantum mechanics. First we create a slightly modified basis for the $su(2)$ Lie algebra by rearranging and rescaling our Lie operator basis $\{:b^1:, :b^2:, :b^3:\}$. We define

$$\begin{aligned} :a^1: &= -(i/2)\, :b^3:, \\ :a^2: &= -(i/2)\, :b^1:, \\ :a^3: &= -(i/2)\, :b^2:. \end{aligned} \tag{15.34}$$

Observe that as the $:b^j:$ denote anti-Hermitian operators, so the $:a^j:$ denote Hermitian operators. From (15.31), (15.33b), and (15.34) it follows that

$$[:a^j:, :a^k:] = i\sum_l \varepsilon_{jkl}\, :a^l:. \tag{15.35}$$

In other words, the Lie operators $:a^j:$ satisfy the same commutation relations as do the usual angular momentum operators—J_x, J_y, and J_z—of quantum mechanics.

The reader may recall that essentially all the characteristics of angular momentum in quantum mechanics—the eigenvalue spectrum in particular—follow from the commutation relations (15.35) [7, 77]. We shall take immediate advantage of this fact. For example, the eigenstates representing a particle of spin j transform as a $(2j+1)$-dimensional irreducible representation of $SU(2)$. Furthermore, the allowed values of spin, integral and half-integral values of j, label *all* of the irreducible representations of $SU(2)$. In looking for an appropriate basis for the dynamical polynomials of degree l, we therefore seek linear combinations of the $G_r^{(l)}$ that transform as spin-j eigenstates.

Continuing our angular momentum analogy, we define the Hermitian operator (*not* a Lie operator)

$$A^2 = :a^1:^2 + :a^2:^2 + :a^3:^2, \tag{15.36}$$

which plays the role of J^2. In addition, we define the so-called "ladder" operators

$$:a^+: = :a^1 + ia^2:, \tag{15.37a}$$

$$:a^-: = :a^1 - ia^2: = :a^+:^\dagger. \tag{15.37b}$$

These operators—(15.36), (15.37a), and (15.37b)—behave exactly as do their quantum mechanical counterparts. They satisfy the important identity

$$A^2 = \frac{1}{2}(:a^+::a^-: + :a^-::a^+:) + :a^3:^2, \tag{15.38}$$

and they obey the useful commutation relations

$$[:a^+:, :a^-:] = 2\,:a^3:, \tag{15.39a}$$

$$[:a^3:, :a^\pm:] = \pm\,:a^\pm:\,. \tag{15.39b}$$

It follows that we can construct simultaneous eigenfunctions of the operators A^2 and $:a^3:$ with an eigenvalue spectrum identical to that for spin-j particles in quantum mechanics. Furthermore, the application of $:a^+:$ or $:a^-:$ will raise or lower the $:a^3:$ eigenvalue by 1, in exact analogy with the usual quantum mechanical rules

$$J_\pm \left|j, m\right\rangle = \sqrt{(j \mp m)(j \pm m + 1)}\, \left|j, m \pm 1\right\rangle. \tag{15.40}$$

Now begins the actual construction of basis functions that transform according to irreducible representations of $SU(2)$. We examine first the dynamical polynomials of degree one. In the present case, $n = 2$, there are four such functions: q_1, q_2, p_1, p_2. A straightforward computation yields the relations

$$:a^1: \begin{pmatrix} q_1 \\ q_2 \\ p_1 \\ p_2 \end{pmatrix} = \frac{i}{2} \begin{pmatrix} p_1 \\ -p_2 \\ -q_1 \\ q_2 \end{pmatrix}, \quad :a^2: \begin{pmatrix} q_1 \\ q_2 \\ p_1 \\ p_2 \end{pmatrix} = \frac{i}{2} \begin{pmatrix} p_2 \\ p_1 \\ -q_2 \\ -q_1 \end{pmatrix}, \quad \text{and} \quad :a^3: \begin{pmatrix} q_1 \\ q_2 \\ p_1 \\ p_2 \end{pmatrix} = \frac{i}{2} \begin{pmatrix} q_2 \\ -q_1 \\ p_2 \\ -p_1 \end{pmatrix}. \tag{15.41}$$

It then follows that

$$A^2 \begin{pmatrix} q_1 \\ q_2 \\ p_1 \\ p_2 \end{pmatrix} = \frac{3}{4} \begin{pmatrix} q_1 \\ q_2 \\ p_1 \\ p_2 \end{pmatrix} = \frac{1}{2}\left(\frac{1}{2} + 1\right) \begin{pmatrix} q_1 \\ q_2 \\ p_1 \\ p_2 \end{pmatrix}. \tag{15.42}$$

We conclude from (15.42) and its quantum mechanical analogue,

$$J^2 \left|j, m\right\rangle = j(j+1) \left|j, m\right\rangle, \tag{15.43}$$

that all four of the $G_r^{(1)}$ behave as spin-$\frac{1}{2}$ objects. On the other hand, spin-$\frac{1}{2}$ objects generate two-dimensional representations of $SU(2)$ [64, 77]. This implies, and we shall soon see, that two copies of spin-$\frac{1}{2}$ occur within the space of dynamical polynomials of degree one.

A close examination of the last of the relations (15.41) suggests that we build eigenfunctions of $:a^3:$ by taking appropriate linear combinations of either q_1 and q_2 or p_1 and p_2. If $\xi q_1 + \eta q_2$ denotes an eigenfunction of $:a^3:$ with eigenvalue $1/2$, then

$$\frac{1}{2}(\xi q_1 + \eta q_2) = :a^3:(\xi q_1 + \eta q_2) = -\frac{i\eta}{2} q_1 + \frac{i\xi}{2} q_2,$$

and hence $\eta = i\xi$. It follows that the dynamical variable

$$y_1 = \frac{1}{\sqrt{2}}(q_1 + i q_2) \tag{15.44a}$$

denotes a function with eigenvalue $1/2$ under both the operators A^2 and $:a^3:$. The factor of $1/\sqrt{2}$ normalizes this eigenfunction with respect to the inner product (10.9). Applying the lowering operator $:a^-:$ to y_1, and using (15.41) along with the analogue of (15.40), we

obtain[19]

$$y_2 = :a^-: y_1 = \frac{1}{\sqrt{2}}(p_2 + ip_1). \tag{15.44b}$$

One may easily verify that this function has eigenvalue $1/2$ under A^2, eigenvalue $-1/2$ under $:a^3:$, and unit norm. The functions y_1 and y_2 therefore compose an orthonormal basis for a spin-$\frac{1}{2}$ (*i.e.*, two-dimensional) representation of $SU(2)$.

We now look for the other spin-$\frac{1}{2}$ representation of $SU(2)$. If $\xi p_1 + \eta p_2$ denotes another eigenfunction of $:a^3:$ with eigenvalue $1/2$, then

$$\frac{1}{2}(\xi p_1 + \eta p_2) = :a^3:(\xi p_1 + \eta p_2) = -\frac{i\eta}{2}p_1 + \frac{i\xi}{2}p_2.$$

Again $\eta = i\xi$, and it follows that

$$y_3 = \frac{1}{\sqrt{2}}(p_1 + ip_2) = iy_2^* \tag{15.44c}$$

denotes another, independent, normalized function with eigenvalue $1/2$ under both the operators A^2 and $:a^3:$. In addition, because y_3 contains only the p_j, it is not only independent of, but also orthogonal to y_1. Application of the lowering operator to y_3 yields

$$y_4 = :a^-: y_3 = -\frac{1}{\sqrt{2}}(q_2 + iq_1) = -iy_1^*. \tag{15.44d}$$

After verifying that y_4 has eigenvalues $1/2$ and $-1/2$ under the operators A^2 and $:a^3:$, respectively, we see that the functions y_3 and y_4 compose a second orthonormal basis for a spin-$\frac{1}{2}$ representation of $SU(2)$.

Let us summarize the results of the last two paragraphs. We have found a set of orthonormal functions $\{y_1, \ldots, y_4\}$ that span the space of f_1's, the dynamical polynomials of degree one; moreover, they transform as two identical copies of a spin-$\frac{1}{2}$ representation of $SU(2)$. To emphasize the latter point, we show the action of the $:a^j:$ on the y's:

$$:a^1: \begin{pmatrix} y_1 \\ y_2 \\ y_3 \\ y_4 \end{pmatrix} = \frac{1}{2}\begin{pmatrix} y_2 \\ y_1 \\ y_4 \\ y_3 \end{pmatrix}, \quad :a^2: \begin{pmatrix} y_1 \\ y_2 \\ y_3 \\ y_4 \end{pmatrix} = \frac{i}{2}\begin{pmatrix} y_2 \\ -y_1 \\ y_4 \\ -y_3 \end{pmatrix}, \quad \text{and} \quad :a^3: \begin{pmatrix} y_1 \\ y_2 \\ y_3 \\ y_4 \end{pmatrix} = \frac{1}{2}\begin{pmatrix} y_1 \\ -y_2 \\ y_3 \\ -y_4 \end{pmatrix}. \tag{15.45}$$

Observe that no mixing occurs between the (y_1, y_2) subspace and the (y_3, y_4) subspace. Furthermore, the $:a^j:$ have the exact same action on each of the two subspaces. In other words, the separate spin-$\frac{1}{2}$ representations carried by the two subspaces are not merely equivalent, they are *identical*. By this we mean that the corresponding matrices for these two representations look identical to one another.

Having constructed an f_1 basis that transforms according to irreducible representations of $SU(2)$, we would now like to do the same for f_2's, f_3's, and so on. We can build an f_2 basis by forming direct products of various pairs of the two spin-$\frac{1}{2}$ representations that compose the f_1 basis. In a similar fashion, we can build corresponding bases for the higher-order f_l's by forming multiple direct products. In the quantum mechanical theory of angular momenta, one finds this same program under the rubric "addition of angular momenta". Indeed, we may directly apply the usual Clebsch-Gordan technology [7] to the process of building higher-order bases with the appropriate transformation properties under $SU(2)$.

Anticipating our construction of eigenfunctions of higher degree, we introduce a useful notation for the basis polynomials that carry irreducible representations of $SU(2)$. We denote them

$$\varphi(j, m; l, \mu). \tag{15.46}$$

[19]For the y's we make an exception to our customary practice of using subscripts to denote homogeneous functions of a given degree. As the reader will soon see, we shall use the y_j as we do the q_j and p_j—as a set of coördinate variables, or dynamical coördinates.

TABLE 15.1. Basis polynomials for the space of f_1's, arranged to carry irreducible representations of $SU(2)$.

$$\boxed{\begin{array}{ll} \Phi_{11}^{1/2} & \begin{cases} \varphi(\frac{1}{2}, \quad \frac{1}{2}; 1, 1) = y_1 = \quad (q_1 + iq_2)/\sqrt{2} \\ \varphi(\frac{1}{2}, -\frac{1}{2}; 1, 1) = y_2 = \quad (p_2 + ip_1)/\sqrt{2} \end{cases} \\ \Phi_{10}^{1/2} & \begin{cases} \varphi(\frac{1}{2}, \quad \frac{1}{2}; 1, 0) = y_3 = \quad (p_1 + ip_2)/\sqrt{2} \\ \varphi(\frac{1}{2}, -\frac{1}{2}; 1, 0) = y_4 = -(q_2 + iq_1)/\sqrt{2} \end{cases} \end{array}}$$

Here j and m label respectively the A^2 and $:a^3:$ eigenvalues. In addition, l denotes the degree of the polynomial—whether written in terms of the q's and p's or in terms of the y's. And the last label, μ, indicates the degree of φ in the (y_1, y_2) subspace. Using this notation, we write our new basis polynomials (15.44) for the space of f_1's in the form

$$\begin{aligned} &\varphi(\tfrac{1}{2}, \quad \tfrac{1}{2}; 1, 1) = y_1, \\ &\varphi(\tfrac{1}{2}, -\tfrac{1}{2}; 1, 1) = y_2; \end{aligned} \tag{15.47a}$$

$$\begin{aligned} &\varphi(\tfrac{1}{2}, \quad \tfrac{1}{2}; 1, 0) = y_3, \\ &\varphi(\tfrac{1}{2}, -\tfrac{1}{2}; 1, 0) = y_4. \end{aligned} \tag{15.47b}$$

We comment that the index j of (15.46) labels the "spin" of the associated representation, while the index m, essentially the z component of the spin, labels the basis polynomials within the representation. Since for any (allowed) value of j we shall find an infinity of spin-j representations, the indices l and μ serve to label the particular copy of spin-j to which the given polynomial belongs. To denote these different representations, we shall use the symbol

$$\Phi_{l\mu}^{j}. \tag{15.48}$$

By this we mean that for each $u \in SU(2)$ the linear Lie transformation $\mathcal{L}(u)$ acts on the basis polynomials (15.46) according to

$$\mathcal{L}(u)\varphi(j, m; l, \mu) = \sum_{m'=-j}^{j} \left[\Phi_{l\mu}^{j}(u)\right]_{mm'} \varphi(j, m'; l, \mu). \tag{15.49}$$

Thus (15.48) stands for the spin-j representation carried by polynomials of degree l which are of degree μ in the variables y_1 and y_2. Hence we denote the representations carried by (15.47a) and (15.47b) as $\Phi_{11}^{1/2}$ and $\Phi_{10}^{1/2}$, respectively. Our choice of notations in (15.46) and (15.48) is justified by the fact that we shall build the higher-order basis elements using various direct products of the representations $\Phi_{11}^{1/2}$ and $\Phi_{10}^{1/2}$.

Before continuing, we make three observations concerning the higher-order basis polynomials we are about to construct, the $\varphi(j, m; l, \mu)$ with $l \geq 2$. Our first observation concerns the allowed values of the spin, j. Because an arbitrary f_l has degree l, it follows that our l^{th}-degree basis polynomials will arise from l-fold direct products of the spin-$\frac{1}{2}$ representations, $\Phi_{11}^{1/2}$ and $\Phi_{10}^{1/2}$. Hence each of the representations carried by the f_l's must have integer or half-integer spin j, according as l is even or odd, with $j \leq \frac{l}{2}$.

Our second observation concerns the eigenvalues possible for the various monomials. Consider an arbitrary term in one of the basis polynomials, say the monomial

$$y_1^{r_1} y_2^{r_2} y_3^{r_3} y_4^{r_4} \tag{15.50}$$

of total degree $l = r_1 + r_2 + r_3 + r_4$ and (y_1, y_2) degree $\mu = r_1 + r_2$. By using (9.5) and (15.45), one can as follows easily evaluate its $:a^3:$ eigenvalue m:

$$\begin{aligned}
:a^3:\big(y_1^{r_1}y_2^{r_2}y_3^{r_3}y_4^{r_4}\big) &= :a^3:\Big(\prod_{i=1}^4 y_i^{r_i}\Big) = \sum_{j=1}^4\Big(\big(:a^3: y_j^{r_j}\big)\prod_{i\neq j} y_i^{r_i}\Big)\\
&= \sum_j\Big(\big(:a^3: y_j\big)\, r_j\, y_j^{r_j-1}\prod_{i\neq j} y_i^{r_i}\Big) = \sum_j\Big(\big(:a^3: y_j\big)\frac{r_j}{y_j}\Big)\prod_i y_i^{r_i}\\
&= \frac{1}{2}(r_1 - r_2 + r_3 - r_4)\prod_i y_i^{r_i} = m\big(y_1^{r_1}y_2^{r_2}y_3^{r_3}y_4^{r_4}\big).
\end{aligned}$$

Hence

$$m = \frac{1}{2}(r_1 - r_2 + r_3 - r_4) = \frac{l}{2} - (r_2 + r_4) = (r_1 + r_3) - \frac{l}{2}. \tag{15.51}$$

In other words, every y-monomial (15.50) is an eigenfunction of $:a^3:$ with eigenvalue (15.51). It follows that the monomials within any given one of the basis elements we seek—all simultaneous eigenfunctions of A^2 and $:a^3:$—must have the same $:a^3:$ eigenvalue m. Note that because the r_j denote integers, the result (15.51) confirms our first observation about the allowed spin values j carried by the f_l's. Further note that any basis element of degree l with z-component $m = l/2$, the highest possible m value, must have $r_2 = r_4 = 0$. This fact suggests that $y_1^{r_1}y_3^{r_3}$ is an eigenfunction of A^2, even though in general the monomials (15.50) are not eigenfunction of A^2. Indeed, a calculation similar to, but somewhat more tedious than, that given above demonstrates that

$$A^2 y_1^\mu y_3^{l-\mu} = \frac{l}{2}\Big(\frac{l}{2} + 1\Big) y_1^\mu y_3^{l-\mu}. \tag{15.52}$$

Hence $y_1^\mu y_3^{l-\mu}$ denotes a simultaneous eigenfunction of A^2 and $:a^3:$ and corresponds to an object of spin $j = l/2$ with z-component $m = j$ (*cf.* (15.43)).

Our third observation concerns an efficient means for normalizing polynomials in the y's under the inner product of (10.9). Consider the complex linear Lie transformation

$$\mathcal{T} = \exp\Big(-\frac{i\pi}{4}:q_1p_2 + q_2p_1:\Big) = \exp\Big(-\frac{i\pi}{4}:g:\Big), \tag{15.53}$$

where $g = q_1p_2 + q_2p_1$. The transformation $\mathcal{T}$ will play a role here, in the $n = 2$ case, similar to that played by the Lie transformation (15.7) of the same name in the $n = 1$ case. To begin, notice from (10.12) that this $\mathcal{T}$, (15.53), like its namesake (15.7), is unitary with respect to the inner product (10.9). Now evaluate the action of $\mathcal{T}$ on phase space by straightforwardly applying the definition (9.3). First note that

$$:g:\begin{pmatrix} q_1\\ q_2\\ p_1\\ p_2\end{pmatrix} = \begin{pmatrix} -q_2\\ -q_1\\ p_2\\ p_1\end{pmatrix}, \text{ and } :g:^2\begin{pmatrix} q_1\\ q_2\\ p_1\\ p_2\end{pmatrix} = \begin{pmatrix} q_1\\ q_2\\ p_1\\ p_2\end{pmatrix}.$$

Hence all even powers of $:g:$ act as identity operators, and all odd powers of $:g:$ have the same action as $:g:^1$. It follows that

$$\begin{aligned}
\exp\Big(-\frac{i\pi}{4}:g:\Big)z &= \cosh\Big(-\frac{i\pi}{4}:g:\Big)z + \sinh\Big(-\frac{i\pi}{4}:g:\Big)z\\
&= \cos\Big(\frac{\pi}{4}\Big)z - i\sin\Big(\frac{\pi}{4}\Big):g:z = \frac{1}{\sqrt{2}}(z - i:g:z).
\end{aligned}$$

The Lie transformation $\mathcal{T}$ therefore has the action

$$\mathcal{T}\, z = \exp\Big(-\frac{i\pi}{4}:g:\Big)\begin{pmatrix} q_1 \\ q_2 \\ p_1 \\ p_2 \end{pmatrix} = \frac{1}{\sqrt{2}}\begin{pmatrix} q_1 + ip_2 \\ q_2 + ip_1 \\ p_1 - iq_2 \\ p_2 - iq_1 \end{pmatrix} = \begin{pmatrix} y_1 \\ -y_4 \\ -iy_2 \\ -iy_3 \end{pmatrix}; \tag{15.54}$$

and its inverse, $\mathcal{T}^{-1} = \mathcal{T}^\dagger$, has the action

$$\mathcal{T}^\dagger y = \exp\Big(-\frac{i\pi}{4}:g:\Big)\begin{pmatrix} y_1 \\ y_2 \\ y_3 \\ y_4 \end{pmatrix} = \begin{pmatrix} q_1 \\ ip_1 \\ ip_2 \\ -q_2 \end{pmatrix}. \tag{15.55}$$

We are now prepared to evaluate inner products between polynomials in the y_k. Using (9.5), (10.7), (10.9), (15.55), and the fact that $\mathcal{T}$ is unitary, we compute the inner product of two y-monomials as follows:

$$\begin{aligned}
\big\langle y_1^{r_1} y_2^{r_2} y_3^{r_3} y_4^{r_4},\, y_1^{r_1'} y_2^{r_2'} y_3^{r_3'} y_4^{r_4'} \big\rangle &= \big\langle y_1^{r_1} y_2^{r_2} y_3^{r_3} y_4^{r_4}, \mathcal{T}\mathcal{T}^\dagger y_1^{r_1'} y_2^{r_2'} y_3^{r_3'} y_4^{r_4'} \big\rangle \\
&= \big\langle \mathcal{T}^\dagger y_1^{r_1} y_2^{r_2} y_3^{r_3} y_4^{r_4}, \mathcal{T}^\dagger y_1^{r_1'} y_2^{r_2'} y_3^{r_3'} y_4^{r_4'} \big\rangle \\
&= (-1)^{r_4'+r_4}\, i^{r_2'-r_2+r_3'-r_3}\, \big\langle q_1^{r_1} p_1^{r_2} p_2^{r_3} q_2^{r_4}, q_1^{r_1'} p_1^{r_2'} p_2^{r_3'} q_2^{r_4'} \big\rangle \\
&= (-1)^{r_4'+r_4}\, i^{r_2'-r_2+r_3'-r_3}\, r_1!\, r_2!\, r_3!\, r_4!\, \delta_{r_1 r_1'} \delta_{r_2 r_2'} \delta_{r_3 r_3'} \delta_{r_4 r_4'}.
\end{aligned}$$

Hence

$$\big\langle y_1^{r_1} y_2^{r_2} y_3^{r_3} y_4^{r_4},\, y_1^{r_1'} y_2^{r_2'} y_3^{r_3'} y_4^{r_4'} \big\rangle = r_1!\, r_2!\, r_3!\, r_4!\, \delta_{r_1 r_1'} \delta_{r_2 r_2'} \delta_{r_3 r_3'} \delta_{r_4 r_4'}. \tag{15.56}$$

In other words, inner products between polynomials in the y's behave in essentially the same way as do inner products between polynomials in the q's and p's. For example, the monomials

$$\frac{y_1^{r_1} y_2^{r_2} y_3^{r_3} y_4^{r_4}}{\sqrt{r_1!\, r_2!\, r_3!\, r_4!}}$$

form a set of orthonormal y-monomials analogous to the general monomials we defined in (10.7).

We have now assembled all the machinery necessary to construct higher-order basis functions that transform according to irreducible representations of $SU(2)$. To build these eigenfunctions, one may use either of two essentially equivalent methods. The first starts by taking advantage of (15.51) and (15.52) to write down that basis element for the representation $\Phi_{l\mu}^{l/2}$ which has the highest value of m:

$$\varphi(\tfrac{l}{2}, \tfrac{l}{2}; l, \mu) = \frac{y_1^{\mu}\, y_3^{l-\mu}}{\sqrt{\mu!\,(l-\mu)!}}. \tag{15.57}$$

Repeated application of the the ladder operator $:a^-:$ to this eigenfunction, taking into account the analogue of (15.40), yields the remaining basis elements that carry the representation $\Phi_{l\mu}^{l/2}$. One can do this for each $\mu \in \{0, 1, \ldots, l\}$. Then one builds the rest of the basis polynomials for the space of f_l's by insisting that the basis elements be orthonormal and further applying the operator $:a^-:$.

The second method for constructing higher-order basis polynomials simply uses the well-known Clebsch-Gordan technology for $SU(2)$. Recall from the standard theory of group representations the Clebsch-Gordan series for a direct product of two irreducible representations of $SU(2)$. In our language, using the symbols (15.48), the Clebsch-Gordan series is

$$\Phi_{l_1\mu_1}^{j_1} \otimes \Phi_{l_2\mu_2}^{j_2} \approx \Phi_{l\mu}^{j_1+j_2} \oplus \Phi_{l\mu}^{j_1+j_2-1} \oplus \ldots \oplus \Phi_{l\mu}^{|j_1-j_2|}, \tag{15.58}$$

TABLE 15.2. Basis polynomials for the space of f_2's, arranged to carry irreducible representations of $SU(2)$.

$$\begin{array}{|l|}\hline
\Phi^1_{22}\begin{cases}\varphi(1,\quad 1;2,2)=y_1^2/\sqrt{2}\\ \varphi(1,\quad 0;2,2)=y_1y_2\\ \varphi(1,-1;2,2)=y_2^2/\sqrt{2}\end{cases}\\
\Phi^1_{21}\begin{cases}\varphi(1,\quad 1;2,1)=y_1y_3\\ \varphi(1,\quad 0;2,1)=(y_1y_4+y_2y_3)/\sqrt{2}\\ \varphi(1,-1;2,1)=y_2y_4\end{cases}\\
\Phi^1_{20}\begin{cases}\varphi(1,\quad 1;2,0)=y_3^2/\sqrt{2}\\ \varphi(1,\quad 0;2,0)=y_3y_4\\ \varphi(1,-1;2,0)=y_4^2/\sqrt{2}\end{cases}\\
\Phi^0_{21}\begin{cases}\varphi(0,\quad 0;2,1)=(y_1y_4-y_2y_3)/\sqrt{2}\end{cases}\\ \hline
\end{array}$$

where $l=l_1+l_2$, $\mu=\mu_1+\mu_2$, and $\approx$ denotes the equality of representations. One may then assemble the basis polynomials (15.46) according to the rule [7, 20]

$$\varphi(j,m;l,\mu)=\sum_{m_2=-j_2}^{j_2}\left(\begin{array}{cc|c}j_1 & j_2 & j\\ m-m_2 & m_2 & m\end{array}\right)\varphi(j_1,m-m_2;l_1,\mu_1)\varphi(j_2,m_2;l_2,\mu_2), \tag{15.59}$$

where $j\in\{j_1+j_2,\ldots,|j_1-j_2|\}$, and the symbols $\left(\begin{smallmatrix}j_1 & j_2\\ m_1 & m_2\end{smallmatrix}\middle|\begin{smallmatrix}j\\ m\end{smallmatrix}\right)$ denote the usual Clebsch-Gordan coefficients connecting spin j with spins j_1 and j_2.[20] This formula, however, must be used with some care. In particular, tabulated Clebsch-Gordan coefficients assume that the direct product elements $\varphi(j_1,m_1;l_1,\mu_1)\otimes\varphi(j_2,m_2;l_2,\mu_2)$ form an orthonormal set. But under our choice of norm the assumption on normalization does not always hold for the φ's. (For example, $\varphi(\frac{1}{2},\frac{1}{2};1,1)\otimes\varphi(\frac{1}{2},\frac{1}{2};1,0)=y_1y_3$ has norm 1, while $\varphi(\frac{1}{2},\frac{1}{2};1,1)\otimes\varphi(\frac{1}{2},\frac{1}{2};1,1)=y_1^2$ has norm 2.) To use a standard table of Clebsch-Gordan coefficients, one must first build all the basis polynomials of interest, using (15.59), and *then* normalize them.

To illustrate the first method, we show explicitly how to construct the basis polynomials for the space of f_2's by forming all possible direct products of the first-order representations, $\Phi^{1/2}_{11}$ and $\Phi^{1/2}_{10}$. From standard angular momentum theory we know that such direct products produce direct sums of spin-1 and spin-0 representations (*cf.* (15.58)). Consider first $\Phi^{1/2}_{11}\otimes\Phi^{1/2}_{11}$. According to (15.57) the normalized basis element for Φ^1_{22} with the highest value of m is

$$\varphi(1,\quad 1;2,2)=y_1^2/\sqrt{2}.$$

After twice applying the lowering operator $:a^-:$ to this basis element, taking into account (15.40), we obtain the remaining spin-1 basis polynomials for the representation Φ^1_{22}:

$$\begin{aligned}\varphi(1,\quad 0;2,2)&=y_1y_2;\\ \varphi(1,-1;2,2)&=y_2^2/\sqrt{2}.\end{aligned}$$

These three eigenfunctions are constructed from symmetric products of elements that carry the spin-$\frac{1}{2}$ representation $\Phi^{1/2}_{11}$. The corresponding spin-0 eigenfunction, on the other hand,

[20] We remark that in the present case the restriction on the Clebsch-Gordan coefficients that the m values add algebraically, *i.e.*, that $m=m_1+m_2$, follows directly from (15.51).

TABLE 15.3. Basis polynomials for the space of f_3's, arranged to carry irreducible representations of $SU(2)$.

$$
\begin{array}{|l|}
\hline
\Phi_{33}^{3/2}\begin{cases}\varphi(\frac{3}{2},\ \ \frac{3}{2};3,3)=y_1^3/\sqrt{3!}\\ \varphi(\frac{3}{2},\ \ \frac{1}{2};3,3)=y_1^2y_2/\sqrt{2}\\ \varphi(\frac{3}{2},-\frac{1}{2};3,3)=y_1y_2^2/\sqrt{2}\\ \varphi(\frac{3}{2},-\frac{3}{2};3,3)=y_2^3/\sqrt{3!}\end{cases}\\
\Phi_{32}^{3/2}\begin{cases}\varphi(\frac{3}{2},\ \ \frac{3}{2};3,2)=y_1^2y_3/\sqrt{2}\\ \varphi(\frac{3}{2},\ \ \frac{1}{2};3,2)=(2y_1y_2y_3+y_1^2y_4)/\sqrt{3!}\\ \varphi(\frac{3}{2},-\frac{1}{2};3,2)=(2y_1y_2y_4+y_2^2y_3)/\sqrt{3!}\\ \varphi(\frac{3}{2},-\frac{3}{2};3,2)=y_2^2y_4/\sqrt{2}\end{cases}\\
\Phi_{31}^{3/2}\begin{cases}\varphi(\frac{3}{2},\ \ \frac{3}{2};3,1)=y_1y_3^2/\sqrt{2}\\ \varphi(\frac{3}{2},\ \ \frac{1}{2};3,1)=(2y_1y_3y_4+y_2y_3^2)/\sqrt{3!}\\ \varphi(\frac{3}{2},-\frac{1}{2};3,1)=(2y_2y_3y_4+y_1y_4^2)/\sqrt{3!}\\ \varphi(\frac{3}{2},-\frac{3}{2};3,1)=y_2y_4^2/\sqrt{2}\end{cases}\\
\Phi_{30}^{3/2}\begin{cases}\varphi(\frac{3}{2},\ \ \frac{3}{2};3,0)=y_3^3/\sqrt{3!}\\ \varphi(\frac{3}{2},\ \ \frac{1}{2};3,0)=y_3^2y_4/\sqrt{2}\\ \varphi(\frac{3}{2},-\frac{1}{2};3,0)=y_3y_4^2/\sqrt{2}\\ \varphi(\frac{3}{2},-\frac{3}{2};3,0)=y_4^3/\sqrt{3!}\end{cases}\\
\Phi_{32}^{1/2}\begin{cases}\varphi(\frac{1}{2},\ \ \frac{1}{2};3,2)=(y_1^2y_4-y_1y_2y_3)/\sqrt{3}\\ \varphi(\frac{1}{2},-\frac{1}{2};3,2)=(y_1y_2y_4-y_2^2y_3)/\sqrt{3}\end{cases}\\
\Phi_{31}^{1/2}\begin{cases}\varphi(\frac{1}{2},\ \ \frac{1}{2};3,1)=(y_2y_3^2-y_1y_3y_4)/\sqrt{3}\\ \varphi(\frac{1}{2},-\frac{1}{2};3,1)=(y_2y_3y_4-y_1y_4^2)/\sqrt{3}\end{cases}\\
\hline
\end{array}
$$

is constructed from anti-symmetric combinations; it therefore vanishes. Hence we may write $\Phi_{11}^{1/2}\otimes\Phi_{11}^{1/2}\approx\Phi_{22}^{1}$.

Now consider the direct product $\Phi_{11}^{1/2}\otimes\Phi_{10}^{1/2}$. In this case (15.57) tells us that

$$\varphi(1,\ \ 1;2,1)=y_1y_3.$$

And applying $:a^-:$ twice to this basis polynomial produces

$$\begin{aligned}\varphi(1,\ \ 0;2,1)&=(y_1y_4+y_2y_3)/\sqrt{2};\\ \varphi(1,-1;2,1)&=y_2y_4.\end{aligned}$$

These three polynomials carry the representation Φ_{21}^{1}. Because the component representations, $\Phi_{11}^{1/2}$ and $\Phi_{10}^{1/2}$, differ, we can also construct the corresponding anti-symmetric spin-0 basis polynomial for Φ_{21}^{0}. Since its (only) basis element must be both orthogonal to $\varphi(1,0;2,1)$ and normalized, it follows that (to within a sign)

$$\varphi(0,0;2,1)=(y_1y_4-y_2y_3)/\sqrt{2}.$$

Hence $\Phi_{11}^{1/2}\otimes\Phi_{10}^{1/2}\approx\Phi_{21}^{1}\oplus\Phi_{21}^{0}$.

TABLE 15.4.A. Basis polynomials for the space of f_4's, arranged to carry irreducible representations of $SU(2)$. (Continued in Table 15.4.B.)

$$
\Phi^2_{44}\begin{cases}
\varphi(2,\ \ 2;4,4) = y_1^4/\sqrt{4!}\\
\varphi(2,\ \ 1;4,4) = y_1^3y_2/\sqrt{3!}\\
\varphi(2,\ \ 0;4,4) = y_1^2y_2^2/2\\
\varphi(2,-1;4,4) = y_1y_2^3/\sqrt{3!}\\
\varphi(2,-2;4,4) = y_2^4/\sqrt{4!}
\end{cases}
$$

$$
\Phi^2_{43}\begin{cases}
\varphi(2,\ \ 2;4,3) = y_1^3y_3/\sqrt{3!}\\
\varphi(2,\ \ 1;4,3) = (3y_1^2y_2y_3 + y_1^3y_4)/\sqrt{4!}\\
\varphi(2,\ \ 0;4,3) = (y_1y_2^2y_3 + y_1^2y_2y_4)/2\\
\varphi(2,-1;4,3) = (3y_1y_2^2y_4 + y_2^3y_3)/\sqrt{4!}\\
\varphi(2,-2;4,3) = y_2^3y_4/\sqrt{3!}
\end{cases}
$$

$$
\Phi^2_{42}\begin{cases}
\varphi(2,\ \ 2;4,2) = y_1^2y_3^2/2\\
\varphi(2,\ \ 1;4,2) = (y_1y_2y_3^2 + y_1^2y_3y_4)/2\\
\varphi(2,\ \ 0;4,2) = (y_1^2y_4^2 + 4y_1y_2y_3y_4 + y_2^2y_3^2)/\sqrt{4!}\\
\varphi(2,-1;4,2) = (y_1y_2y_4^2 + y_2^2y_3y_4)/2\\
\varphi(2,-2;4,2) = y_2^2y_4^2/2
\end{cases}
$$

$$
\Phi^2_{41}\begin{cases}
\varphi(2,\ \ 2;4,1) = y_1y_3^3/\sqrt{3!}\\
\varphi(2,\ \ 1;4,1) = (3y_1y_3^2y_4 + y_2y_3^3)/\sqrt{4!}\\
\varphi(2,\ \ 0;4,1) = (y_1y_3y_4^2 + y_2y_3^2y_4)/2\\
\varphi(2,-1;4,1) = (3y_2y_3y_4^2 + y_1y_4^3)/\sqrt{4!}\\
\varphi(2,-2;4,1) = y_2y_4^3/\sqrt{3!}
\end{cases}
$$

$$
\Phi^2_{40}\begin{cases}
\varphi(2,\ \ 2;4,0) = y_3^4/\sqrt{4!}\\
\varphi(2,\ \ 1;4,0) = y_3^3y_4/\sqrt{3!}\\
\varphi(2,\ \ 0;4,0) = y_3^2y_4^2/2\\
\varphi(2,-1;4,0) = y_3y_4^3/\sqrt{3!}\\
\varphi(2,-2;4,0) = y_4^4/\sqrt{4!}
\end{cases}
$$

The remaining direct product, $\Phi^{1/2}_{10} \otimes \Phi^{1/2}_{10}$, produces a result entirely analogous to the case of $\Phi^{1/2}_{11} \otimes \Phi^{1/2}_{11}$:

$$
\begin{aligned}
\varphi(1,\ \ 1;2,0) &= y_3^2/\sqrt{2};\\
\varphi(1,\ \ 0;2,0) &= y_3y_4;\\
\varphi(1,-1;2,0) &= y_4^2/\sqrt{2}.
\end{aligned}
$$

And, of course, $\Phi^{1/2}_{10} \otimes \Phi^{1/2}_{10} \approx \Phi^1_{20}$.

The sets of basis polynomials thus obtained using either of the methods outlined will be the same because the first method corresponds to computing the Clebsch-Gordan coefficients "on the fly". Appendix H contains several *Mathematica* packages that allow one to do the required calculations using *Mathematica*. And Appendix I contains a *Mathematica* "notebook" that uses some of the packages in Appendix H to determine all of the basis polynomials through order five. Using the functions defined in that notebook, one may easily generate basis polynomials through any order desired. Tables 15.1–15.5 contain for f_1 through f_5

TABLE 15.4.B. Basis polynomials for the space of f_4's, arranged to carry irreducible representations of $SU(2)$. (Continued from Table 15.4.A.)

$$\Phi^1_{43}\begin{cases}\varphi(1,\ \ 1;4,3)=(y_1^3y_4-y_1^2y_2y_3)/\sqrt{8}\\ \varphi(1,\ \ 0;4,3)=(y_1^2y_2y_4-y_1y_2^2y_3)/2\\ \varphi(1,-1;4,3)=(y_1y_2^2y_4-y_2^3y_3)/\sqrt{8}\end{cases}$$

$$\Phi^1_{42}\begin{cases}\varphi(1,\ \ 1;4,2)=(y_1^2y_3y_4-y_1y_2y_3^2)/2\\ \varphi(1,\ \ 0;4,2)=(y_1^2y_4^2-y_2^2y_3^2)/\sqrt{8}\\ \varphi(1,-1;4,2)=(y_1y_2y_4^2-y_2^2y_3y_4)/2\end{cases}$$

$$\Phi^1_{41}\begin{cases}\varphi(1,\ \ 1;4,1)=(y_2y_3^3-y_1y_3^2y_4)/\sqrt{8}\\ \varphi(1,\ \ 0;4,1)=(y_2y_3^2y_4-y_1y_3y_4^2)/2\\ \varphi(1,-1;4,1)=(y_2y_3y_4^2-y_1y_4^3)/\sqrt{8}\end{cases}$$

$$\Phi^0_{42}\begin{cases}\varphi(0,\ \ 0;4,2)=(y_1^2y_4^2-2y_1y_2y_3y_4+y_2^2y_3^2)/\sqrt{12}\end{cases}$$

spaces, respectively, the complete set of orthonormal basis polynomials that carry irreducible representations of $SU(2)$.

We conclude this section (at last!) with two final observations concerning the f_l bases just constructed. First of all, an examination of Tables 15.1–15.5 reveals a definite pattern: The f_1's carry two two-dimensional representations of $SU(2)$; the f_2's carry three three-dimensional representations and one one-dimensional representation; the f_3's carry four four-dimensional representations and two two-dimensional representations; and so on. In general, in concert with one of our earlier observations, the space of f_l's carries representations of $SU(2)$ which behave as spin-j objects for each value of $j \in \left\{\frac{l}{2}, \frac{l}{2}-1, \ldots, j_{min}\right\}$, where j_{min} equals 0 or $\frac{1}{2}$ for even or odd l, respectively. Furthermore, if the space of f_l's carries a spin-j representation—*i.e.*, a $(2j+1)$-dimensional representation of $SU(2)$—then it carries $(2j+1)$ copies of that representation. It can be shown that this fact follows as a consequence of the *Frobenius reciprocity theorem* [27].

Our last observation generalizes the remarks we made in connection with the results (15.45). Recall that the symbol $\Phi^j_{l\mu}$ denotes a spin-j representation carried by certain polynomials of degree l; and, in particular, the index $\mu \in \left\{\frac{l}{2}-j, \frac{l}{2}-j+1, \ldots, \frac{l}{2}+j\right\}$ amounts to a label for distinguishing the different copies of spin-j carried by l^{th}-degree polynomials. Because $\Phi^{1/2}_{11}$ and $\Phi^{1/2}_{10}$ denote *identical* spin-$\frac{1}{2}$ representations of $SU(2)$, and because we have built each higher-order representation using direct products of these two fundamental representations, we may draw the following important conclusion: *with respect to the basis polynomials we have just constructed, the matrix representations $\Phi^j_{l\mu}$ for the group $SU(2)$ depend on j and l but not on μ.*

As a consequence of our last observation, we shall sometimes choose (*e.g.* in (15.49)) to denote the representation $\Phi^j_{l\mu}$ more simply as D^j, the symbol commonly used in the representation theory of $SU(2)$; but where we use this notation, the value of l should be clear from the context. On the other hand, where we wish to emphasize the basis polynomials which carry the particular representation, we shall revert to the notation $\Phi^j_{l\mu}$.

15.2.4. *The Gram Matrix and its Eigenvalues for the Case $\mathcal{U} = SU(2)/SO(2)$.* Let us now evaluate the Gram operator $\widehat{\Gamma}(l)$ of (15.29) with respect to the orthonormal basis polynomials (15.46) constructed in §15.2.3. Although it suffices in the Gram operator to integrate over the coset space $SU(2)/SO(2)$, as (15.29) indicates, we can determine the Gram eigenvalues more easily by integrating over the whole of $SU(2)$. For this section, then, we write the Gram

TABLE 15.5.A. Basis polynomials for the space of f_5's, arranged to carry irreducible representations of $SU(2)$. (Continued in Table 15.5.B.)

$$
\begin{aligned}
\Phi^{5/2}_{55} &\begin{cases}
\varphi(\tfrac{5}{2}, \quad \tfrac{5}{2}; 5, 5) = y_1^5/\sqrt{5!} \\
\varphi(\tfrac{5}{2}, \quad \tfrac{3}{2}; 5, 5) = y_1^4 y_2/\sqrt{4!} \\
\varphi(\tfrac{5}{2}, \quad \tfrac{1}{2}; 5, 5) = y_1^3 y_2^2/\sqrt{12} \\
\varphi(\tfrac{5}{2}, -\tfrac{1}{2}; 5, 5) = y_1^2 y_2^3/\sqrt{12} \\
\varphi(\tfrac{5}{2}, -\tfrac{3}{2}; 5, 5) = y_1 y_2^4/\sqrt{4!} \\
\varphi(\tfrac{5}{2}, -\tfrac{5}{2}; 5, 5) = y_2^5/\sqrt{5!}
\end{cases} \\
\Phi^{5/2}_{54} &\begin{cases}
\varphi(\tfrac{5}{2}, \quad \tfrac{5}{2}; 5, 4) = y_1^4 y_3/\sqrt{4!} \\
\varphi(\tfrac{5}{2}, \quad \tfrac{3}{2}; 5, 4) = (4y_1^3 y_2 y_3 + y_1^4 y_4)/\sqrt{5!} \\
\varphi(\tfrac{5}{2}, \quad \tfrac{1}{2}; 5, 4) = (3y_1^2 y_2^2 y_3 + 2y_1^3 y_2 y_4)/\sqrt{60} \\
\varphi(\tfrac{5}{2}, -\tfrac{1}{2}; 5, 4) = (3y_1^2 y_2^2 y_4 + 2y_1 y_2^3 y_3)/\sqrt{60} \\
\varphi(\tfrac{5}{2}, -\tfrac{3}{2}; 5, 4) = (4y_1 y_2^3 y_4 + y_2^4 y_3)/\sqrt{5!} \\
\varphi(\tfrac{5}{2}, -\tfrac{5}{2}; 5, 4) = y_2^4 y_4/\sqrt{4!}
\end{cases} \\
\Phi^{5/2}_{53} &\begin{cases}
\varphi(\tfrac{5}{2}, \quad \tfrac{5}{2}; 5, 3) = y_1^3 y_3^2/\sqrt{12} \\
\varphi(\tfrac{5}{2}, \quad \tfrac{3}{2}; 5, 3) = (2y_1^3 y_3 y_4 + 3y_1^2 y_2 y_3^2)/\sqrt{60} \\
\varphi(\tfrac{5}{2}, \quad \tfrac{1}{2}; 5, 3) = (y_1^3 y_4^2 + 6y_1^2 y_2 y_3 y_4 + 3y_1 y_2^2 y_3^2)/\sqrt{5!} \\
\varphi(\tfrac{5}{2}, -\tfrac{5}{2}; 5, 3) = (y_2^3 y_3^2 + 6y_1 y_2^2 y_3 y_4 + 3y_1^2 y_2 y_4^2)/\sqrt{5!} \\
\varphi(\tfrac{5}{2}, -\tfrac{3}{2}; 5, 3) = (2y_2^3 y_3 y_4 + 3y_1 y_2^2 y_4^2)/\sqrt{60} \\
\varphi(\tfrac{5}{2}, -\tfrac{1}{2}; 5, 3) = y_2^3 y_4^2/\sqrt{12}
\end{cases} \\
\Phi^{5/2}_{52} &\begin{cases}
\varphi(\tfrac{5}{2}, \quad \tfrac{5}{2}; 5, 2) = y_1^2 y_3^3/\sqrt{12} \\
\varphi(\tfrac{5}{2}, \quad \tfrac{3}{2}; 5, 2) = (2y_1 y_2 y_3^3 + 3y_1^2 y_3^2 y_4)/\sqrt{60} \\
\varphi(\tfrac{5}{2}, \quad \tfrac{1}{2}; 5, 2) = (y_2^2 y_3^3 + 6y_1 y_2 y_3^2 y_4 + 3y_1^2 y_3 y_4^2)/\sqrt{5!} \\
\varphi(\tfrac{5}{2}, -\tfrac{1}{2}; 5, 2) = (y_1^2 y_4^3 + 6y_1 y_2 y_3 y_4^2 + 3y_2^2 y_3^2 y_4)/\sqrt{5!} \\
\varphi(\tfrac{5}{2}, -\tfrac{3}{2}; 5, 2) = (2y_1 y_2 y_4^3 + 3y_2^2 y_3 y_4^2)/\sqrt{60} \\
\varphi(\tfrac{5}{2}, -\tfrac{5}{2}; 5, 2) = y_2^2 y_4^3/\sqrt{12}
\end{cases} \\
\Phi^{5/2}_{51} &\begin{cases}
\varphi(\tfrac{5}{2}, \quad \tfrac{5}{2}; 5, 1) = y_1 y_3^4/\sqrt{4!} \\
\varphi(\tfrac{5}{2}, \quad \tfrac{3}{2}; 5, 1) = (4y_1 y_3^3 y_4 + y_2 y_3^4)/\sqrt{5!} \\
\varphi(\tfrac{5}{2}, \quad \tfrac{1}{2}; 5, 1) = (3y_1 y_3^2 y_4^2 + 2y_2 y_3^3 y_4)/\sqrt{60} \\
\varphi(\tfrac{5}{2}, -\tfrac{1}{2}; 5, 1) = (3y_2 y_3^2 y_4^2 + 2y_1 y_3 y_4^3)/\sqrt{60} \\
\varphi(\tfrac{5}{2}, -\tfrac{3}{2}; 5, 1) = (4y_2 y_3 y_4^3 + y_1 y_4^4)/\sqrt{5!} \\
\varphi(\tfrac{5}{2}, -\tfrac{5}{2}; 5, 1) = y_2 y_4^4/\sqrt{4!}
\end{cases}
\end{aligned}
$$

operator in the form

$$\widehat{\Gamma}(l) = \frac{1}{l+1} \sum_{k=0}^{l} \int_{SU(2)} du\, \mathcal{L}(u) \left|Q_k^{(l)}\right\rangle \left\langle Q_k^{(l)}\right| \mathcal{L}(u)^\dagger. \tag{15.60}$$

TABLE 15.5.B. Basis polynomials for the space of f_5's, arranged to carry irreducible representations of $SU(2)$. (Continued from Table 15.5.A.)

$$
\Phi^{5/2}_{50}\begin{cases}
\varphi(\frac{5}{2},\ \frac{5}{2};5,0)=y_3^5/\sqrt{5!}\\
\varphi(\frac{5}{2},\ \frac{3}{2};5,0)=y_3^4y_4/\sqrt{4!}\\
\varphi(\frac{5}{2},\ \frac{1}{2};5,0)=y_3^3y_4^2/\sqrt{12}\\
\varphi(\frac{5}{2},-\frac{1}{2};5,0)=y_3^2y_4^3/\sqrt{12}\\
\varphi(\frac{5}{2},-\frac{3}{2};5,0)=y_3y_4^4/\sqrt{4!}\\
\varphi(\frac{5}{2},-\frac{5}{2};5,0)=y_4^5/\sqrt{5!}
\end{cases}
$$

$$
\Phi^{3/2}_{54}\begin{cases}
\varphi(\frac{3}{2},\ \frac{3}{2};5,4)=(y_1^4y_4-y_1^3y_2y_3)/\sqrt{30}\\
\varphi(\frac{3}{2},\ \frac{1}{2};5,4)=(y_1^3y_2y_4-y_1^2y_2^2y_3)/\sqrt{10}\\
\varphi(\frac{3}{2},-\frac{1}{2};5,4)=(y_1^2y_2^2y_4-y_1y_2^3y_3)/\sqrt{10}\\
\varphi(\frac{3}{2},-\frac{3}{2};5,4)=(y_1y_2^3y_4-y_2^4y_3)/\sqrt{30}
\end{cases}
$$

$$
\Phi^{3/2}_{53}\begin{cases}
\varphi(\frac{3}{2},\ \frac{3}{2};5,3)=(y_1^3y_3y_4-y_1^2y_2y_3^2)/\sqrt{10}\\
\varphi(\frac{3}{2},\ \frac{1}{2};5,3)=(y_1^3y_4^2+y_1^2y_2y_3y_4-2y_1y_2^2y_3^2)/\sqrt{30}\\
\varphi(\frac{3}{2},-\frac{1}{2};5,3)=(2y_1^2y_2y_4^2-y_1y_2^2y_3y_4-y_2^3y_3^2)/\sqrt{30}\\
\varphi(\frac{3}{2},-\frac{3}{2};5,3)=(y_1y_2^2y_4^2-y_2^3y_3y_4)/\sqrt{10}
\end{cases}
$$

$$
\Phi^{3/2}_{52}\begin{cases}
\varphi(\frac{3}{2},\ \frac{3}{2};5,2)=(y_1y_2y_3^3-y_1^2y_3^2y_4)/\sqrt{10}\\
\varphi(\frac{3}{2},\ \frac{1}{2};5,2)=(y_2^2y_3^3+y_1y_2y_3^2y_4-2y_1^2y_3y_4^2)/\sqrt{30}\\
\varphi(\frac{3}{2},-\frac{1}{2};5,2)=(2y_2^2y_3^2y_4-y_1y_2y_3y_4^2-y_1^2y_4^3)/\sqrt{30}\\
\varphi(\frac{3}{2},-\frac{3}{2};5,2)=(y_2^2y_3y_4^2-y_1y_2y_4^3)/\sqrt{10}
\end{cases}
$$

$$
\Phi^{3/2}_{51}\begin{cases}
\varphi(\frac{3}{2},\ \frac{3}{2};5,1)=(y_2y_3^4-y_1y_3^3y_4)/\sqrt{30}\\
\varphi(\frac{3}{2},\ \frac{1}{2};5,1)=(y_2y_3^3y_4-y_1y_3^2y_4^2)/\sqrt{10}\\
\varphi(\frac{3}{2},-\frac{1}{2};5,1)=(y_2y_3^2y_4^2-y_1y_3y_4^3)/\sqrt{10}\\
\varphi(\frac{3}{2},-\frac{3}{2};5,1)=(y_2y_3y_4^3-y_1y_4^4)/\sqrt{30}
\end{cases}
$$

$$
\Phi^{1/2}_{53}\begin{cases}
\varphi(\frac{1}{2},\ \frac{1}{2};5,3)=(-y_1y_2^2y_3^2+2y_1^2y_2y_3y_4-y_1^3y_4^2)/\sqrt{4!}\\
\varphi(\frac{1}{2},-\frac{1}{2};5,3)=(-y_1^2y_2y_4^2+2y_1y_2^2y_3y_4-y_2^3y_3^2)/\sqrt{4!}
\end{cases}
$$

$$
\Phi^{1/2}_{52}\begin{cases}
\varphi(\frac{1}{2},\ \frac{1}{2};5,2)=(-y_1^2y_3y_4^2+2y_1y_2y_3^2y_4-y_2^2y_3^3)/\sqrt{4!}\\
\varphi(\frac{1}{2},-\frac{1}{2};5,2)=(-y_2^2y_3^2y_4+2y_1y_2y_3y_4^2-y_1^2y_4^3)/\sqrt{4!}
\end{cases}
$$

According to (E.6), $\mathcal{L}(u)^\dagger=\mathcal{L}(u^{-1})$. Hence, with respect to the basis polynomials φ, we obtain the Gram matrix elements

$$
\begin{aligned}
&\Gamma(l)_{jm\mu,j'm'\mu'}=\big\langle\varphi(j,m;l,\mu)\big|\widehat{\Gamma}(l)\big|\varphi(j',m';l,\mu')\big\rangle=\\
&\qquad\frac{1}{l+1}\sum_k\int_{SU(2)}du\,\Big\langle\mathcal{L}(u^{-1})\varphi(j,m;l,\mu),Q_k^{(l)}\Big\rangle\Big\langle Q_k^{(l)},\mathcal{L}(u^{-1})\varphi(j',m';l,\mu')\Big\rangle\,.
\end{aligned}
\tag{15.61}
$$

Recall here that $j\in\big\{j_{min},\dots,\frac{l}{2}\big\}$, where j_{min} equals 0 or $\frac{1}{2}$ for even or odd l, respectively; $m\in\{-j,\dots,j\}$; and $\mu\in\big\{\frac{l}{2}-j,\dots,\frac{l}{2}+j\big\}$. Using (15.49), we may write

$$
\Big\langle\mathcal{L}(u^{-1})\varphi(j,m;l,\mu),Q_k^{(l)}\Big\rangle=\sum_\nu\big[D^j(u^{-1})\big]^*_{m\nu}\big\langle\varphi(j,\nu;l,\mu),Q_k^{(l)}\big\rangle\,,
$$

where here, pursuant to our discussion at the end of §15.2.3, we have substituted the symbol D^j for $\Phi^j_{l\mu}$. In a similar fashion we obtain

$$\left\langle Q_k^{(l)}, \mathcal{L}(u^{-1})\varphi(j',m';l,\mu')\right\rangle = \sum_{\nu'} D^{j'}(u^{-1})_{m'\nu'} \left\langle Q_k^{(l)}, \varphi(j',\nu';l,\mu')\right\rangle.$$

Inserting these last two results into (15.61), we obtain

$$\Gamma(l)_{jm\mu,j'm'\mu'} = \sum_{\nu\nu'}\Bigg[\left(\int_{SU(2)} du\ \left[D^j(u^{-1})\right]^*_{m\nu} D^{j'}(u^{-1})_{m'\nu'}\right)\times \frac{1}{l+1}\sum_k \left\langle \varphi(j,\nu;l,\mu), Q_k^{(l)}\right\rangle\left\langle Q_k^{(l)}, \varphi(j',\nu';l,\mu')\right\rangle\Bigg]. \tag{15.62}$$

By the orthogonality theorem for matrix representations of compact Lie groups, the integral over $SU(2)$ equals $\delta_{jj'}\delta_{mm'}\delta_{\nu\nu'}/d_j$, where $d_j = 2j+1$ denotes the dimensionality of a spin-j representation. The Gram matrix elements (15.62) then become

$$\Gamma(l)_{jm\mu,j'm'\mu'} = \frac{\delta_{jj'}\delta_{mm'}}{(l+1)(2j+1)}\sum_{k\nu}\left\langle \varphi(j,\nu;l,\mu), Q_k^{(l)}\right\rangle\left\langle Q_k^{(l)}, \varphi(j,\nu;l,\mu')\right\rangle. \tag{15.63}$$

In words the result (15.63) says that our basis polynomials, the φ's, reduce the Gram matrix $\Gamma(l)$ to block-diagonal form.

In fact, the φ's completely diagonalize $\Gamma(l)$. To verify this, examine the φ content of the $Q_k^{(l)}$'s. Note from Table 15.1 that

$$q_1 = \frac{1}{\sqrt{2}}(y_1 + iy_4), \quad \text{and} \quad q_2 = \frac{1}{i\sqrt{2}}(y_1 - iy_4).$$

Then using these expressions in (15.18), we obtain

$$\begin{aligned} Q_k^{(l)} &= \frac{q_1^{l-k}q_2^k}{\sqrt{(l-k)!\,k!}} = \left(\frac{1}{2}\right)^{l/2}\frac{i^{-k}}{\sqrt{(l-k)!\,k!}}(y_1+iy_4)^{l-k}(y_1-iy_4)^k \\ &= \left(\frac{1}{2}\right)^{l/2}\frac{i^{-k}}{\sqrt{(l-k)!\,k!}}\sum_{r_1=0}^{l-k}\sum_{r_2=0}^{k}\binom{l-k}{r_1}\binom{k}{r_2}y_1^{r_1}(iy_4)^{l-k-r_1}y_1^{r_2}(-iy_4)^{k-r_2} \\ &= \left(\frac{1}{2}\right)^{l/2}\frac{i^{l-3k}}{\sqrt{(l-k)!\,k!}}\sum_{r_1r_2}\binom{l-k}{r_1}\binom{k}{r_2}i^{r_2-r_1}y_1^{r_1+r_2}y_4^{l-(r_1+r_2)}. \end{aligned}$$

This means (*cf.* (15.51)) that $Q_k^{(l)}$ has a decomposition of the form

$$Q_k^{(l)} = \sum_{j\mu}\vartheta^{lk}_{j\mu}\,\varphi(j,\mu-\tfrac{l}{2};l,\mu), \tag{15.64}$$

where the $\vartheta^{lk}_{j\mu}$ denote a set of complex coefficients. Note in each term of this expansion the interconnection between the values of the z spin component, $\mu - \frac{l}{2}$, and the index μ, which labels the different copies of spin-j. Now look at how this connection affects the Gram matrix elements (15.63). In particular, look at just the sum over ν:

$$\sum_{\nu}\left\langle \varphi(j,\nu;l,\mu), Q_k^{(l)}\right\rangle\left\langle Q_k^{(l)}, \varphi(j,\nu;l,\mu')\right\rangle.$$

Because of (15.64) each term in this summation contains a factor $\delta_{\nu,\mu-l/2}\delta_{\nu,\mu'-l/2}$. As a consequence, μ and μ' must equal one another, and hence the φ's do indeed diagonalize the

Gram matrix:

$$\begin{aligned}\Gamma(l)_{jm\mu,j'm'\mu'} &= \frac{\delta_{jj'}\delta_{mm'}\delta_{\mu\mu'}}{(l+1)(2j+1)}\sum_{k\nu}\delta_{\nu,\mu-l/2}\big|\langle\varphi(j,\nu;l,\mu),Q_k^{(l)}\rangle\big|^2 \\ &= \frac{\delta_{jj'}\delta_{mm'}\delta_{\mu\mu'}}{(l+1)(2j+1)}\sum_{k}\big|\langle\varphi(j,\mu-\tfrac{l}{2};l,\mu),Q_k^{(l)}\rangle\big|^2.\end{aligned} \tag{15.65}$$

We obtain directly the Gram eigenvalues we seek:

$$\lambda^{(l)}_{jm\mu} = \frac{1}{(l+1)(2j+1)}\sum_{k}\big|\langle\varphi(j,\mu-\tfrac{l}{2};l,\mu),Q_k^{(l)}\rangle\big|^2, \tag{15.66}$$

where $j\in\{j_{min},\ldots,\frac{l}{2}\}$; $m\in\{-j,\ldots,j\}$; and $\mu\in\{\frac{l}{2}-j,\ldots,\frac{l}{2}+j\}$. Since these eigenvalues do not depend on m, each has an associated degeneracy of $2j+1$. Other degeneracies, of course, may also occur; and we shall, in a moment, discuss one such degeneracy.

At this point is seems easiest to ask a computer to evaluate the Gram eigenvalues (15.66). Before doing that, however, we shall make two observations. The first will concern an additional degeneracy in the eigenvalue spectrum that approximately halves the number of eigenvalues we need to compute. And the second shows that it suffices to sum over roughly half the $Q_k^{(l)}$. Together these two observations lead to a substantial computational savings, and we treat each in turn.

The Gram eigenvalues (15.66) have a degeneracy associated with the different values of μ. It turns out that

$$\lambda^{(l)}_{jm\mu} = \lambda^{(l)}_{jm(l-\mu)}, \tag{15.67}$$

and hence eigenvalues with $\mu\neq l/2$ have a degeneracy of $2(2j+1)$, while eigenvalues with $\mu=l/2$ have a degeneracy of just $(2j+1)$. To verify this extra two-fold degeneracy, we introduce another complex linear Lie transformation:

$$\mathcal{S} = \exp\Big(\frac{i\pi}{2}:q_1p_2+q_2p_1:\Big) = \exp\Big(\frac{i\pi}{2}:g:\Big), \tag{15.68}$$

(*cf.* the operator $\mathcal{T}$ in (15.53)). Like $\mathcal{T}$, the operator $\mathcal{S}$ is unitary with respect to the inner product (10.9). In addition, because $\mathcal{T}$ and $\mathcal{S}$ differ only in the factor multiplying $:g:$, a very slight modification of our calculation for $\mathcal{T}$ yields the result

$$\mathcal{S}\begin{pmatrix}q_1\\q_2\\p_1\\p_2\end{pmatrix} = \begin{pmatrix}-iq_2\\-iq_1\\ip_2\\ip_1\end{pmatrix}. \tag{15.69}$$

From this result one can show that $\mathcal{S}$ commutes with A^2. To see this, use (9.9) and (15.36) to obtain

$$\mathcal{S}A^2\mathcal{S}^{-1} = \mathcal{S}\Big(\sum_{j=1}^{3}:a^j:^2\Big)\mathcal{S}^{-1} = \sum_j\big(\mathcal{S}:a^j:\mathcal{S}^{-1}\big)^2 = \sum_j\big(:\mathcal{S}a^j:\big)^2.$$

But using (9.6), (15.32), (15.34), and (15.69), one may show by straightforward computation that

$$\mathcal{S}a^1 = a^1,\quad \mathcal{S}a^2 = -a^2, \text{ and } \mathcal{S}a^3 = -a^3.$$

It follows that $\mathcal{S}^{-1}A^2\mathcal{S}=A^2$, and hence $\mathcal{S}$ commutes with A^2. The significance of this fact, of course, is that $\mathcal{S}$ acting on a $\varphi(j,m;l,\mu)$ cannot change the A^2 eigenvalue j.

In order to use the transformation $\mathcal{S}$ to verify (15.67), we must determine how $\mathcal{S}$ acts on the q-monomials $Q_k^{(l)}$ and the basis polynomials φ. From the result (15.69) we can immediately determine how $\mathcal{S}$ affects the q-monomials $Q_k^{(l)}$ of (15.18):

$$\mathcal{S}Q_k^{(l)} = \mathcal{S}\frac{q_1^{l-k}q_2^k}{\sqrt{(l-k)!\,k!}} = \frac{(-iq_2)^{l-k}(-iq_1)^k}{\sqrt{(l-k)!\,k!}} = (-i)^l\frac{q_1^kq_2^{l-k}}{\sqrt{k!\,(l-k)!}} = (-i)^lQ_{l-k}^{(l)}. \tag{15.70}$$

And we can also determine how $\mathcal{S}$ affects the y's:

$$\mathcal{S}\begin{pmatrix} y_1 \\ y_2 \\ y_3 \\ y_4 \end{pmatrix} = \mathcal{S}\frac{1}{\sqrt{2}}\begin{pmatrix} q_1 + iq_2 \\ p_2 + ip_1 \\ p_1 + ip_2 \\ -(q_2 + iq_1) \end{pmatrix} = \frac{1}{\sqrt{2}}\begin{pmatrix} -iq_2 + q_1 \\ ip_1 - p_2 \\ ip_2 - p_1 \\ iq_1 - q_2 \end{pmatrix} = i\begin{pmatrix} y_4 \\ y_3 \\ y_2 \\ y_1 \end{pmatrix}. \tag{15.71}$$

Now examine the action of $\mathcal{S}$ on the basis polynomials $\varphi(j, m; l, \mu)$ of (15.46). As noted above, $\mathcal{S}$ cannot affect the value of j. In addition, because $\mathcal{S}$ is linear, it cannot change the degree l. To determine how $\mathcal{S}$ affects m and μ, consider a typical term in φ of the form (15.50), and use (15.71) to obtain

$$\mathcal{S}\, y_1^{r_1} y_2^{r_2} y_3^{r_3} y_4^{r_4} = i^{r_1+r_2+r_3+r_4} y_4^{r_1} y_3^{r_2} y_2^{r_3} y_1^{r_4} = i^l y_1^{r_4} y_2^{r_3} y_3^{r_2} y_4^{r_1}.$$

According to (15.51) and our notation for the φ's of (15.46), the initial monomial on the left-hand side belongs to a $\varphi(j, m; l, \mu)$ with $m = \frac{l}{2} - (r_2 + r_4)$ and $\mu = r_1 + r_2$, while the monomial on the right-hand side belongs to a $\varphi(j, m'; l, \mu')$ with $m' = (r_4 + r_2) - \frac{l}{2} = -m$ and $\mu' = r_4 + r_3 = l - \mu$. In other words, the linear Lie transformation $\mathcal{S}$ acting on a φ does the following: (i) it leaves alone the A^2 eigenvalue j; (ii) it negates the z spin component; and (iii) it changes each monomial in the representation labeled by l and μ to a monomial in the representation labeled by l and $l - \mu$. As a consequence, the linear Lie transformation $\mathcal{S}$ must act (to within at least a sign) according to the rule

$$\mathcal{S}\varphi(j, m; l, \mu) = \pm i^l \varphi(j, -m; l, l - \mu). \tag{15.72}$$

We can now verify our claim (15.67) about the degeneracy associated with the index μ. Using the unitarity of $\mathcal{S}$ together with (15.66), (15.70), and (15.72), we find that

$$\begin{aligned} \lambda^{(l)}_{jm\mu} &= \frac{1}{(l+1)(2j+1)} \sum_{k=0}^{l} \left| \left\langle \mathcal{S}\varphi(j, \mu - \tfrac{l}{2}; l, \mu), \mathcal{S}Q^{(l)}_k \right\rangle \right|^2, \\ &= \frac{1}{(l+1)(2j+1)} \sum_{k=0}^{l} \left| \left\langle i^l \varphi(j, \tfrac{l}{2} - \mu; l, l - \mu), (-i)^l Q^{(l)}_{l-k} \right\rangle \right|^2, \\ &= \frac{1}{(l+1)(2j+1)} \sum_{k=l}^{0} \left| \left\langle \varphi\big(j, (l - \mu) - \tfrac{l}{2}; l, (l - \mu)\big), Q^{(l)}_k \right\rangle \right|^2. \end{aligned}$$

Hence

$$\lambda^{(l)}_{jm\mu} = \lambda^{(l)}_{jm(l-\mu)},$$

as claimed. We therefore need not compute (15.66) for values of μ greater than $l/2$.

We now show that one need not sum over all the $Q^{(l)}_k$ in order to compute the Gram eigenvalues (15.66). To verify this, consider the linear Lie transformation

$$\mathcal{P} = \exp\Big(\frac{\pi}{2} :q_1 p_2 - q_2 p_1:\Big) = \exp\Big(-\frac{\pi}{2} :b^2:\Big), \tag{15.73}$$

which belongs to the unitary subgroup $U(2)$ of $Sp(4, \mathbb{R})$, and evaluate its action on the q-monomials $Q^{(l)}_k$ and the basis polynomials φ. Repeating for $\mathcal{P}$ the steps that led to (15.70) and (15.72) yields the results

$$\mathcal{P}Q^{(l)}_k = (-1)^k Q^{(l)}_{l-k}, \tag{15.74a}$$

$$\mathcal{P}\varphi(j, m; l, \mu) = \pm(-1)^{m+l/2} i^l \varphi(j, m; l, \mu). \tag{15.74b}$$

Now consider one of the terms in (15.66). Using (15.74), and the unitarity of $\mathcal{P}$, we find

$$\begin{aligned} \left| \left\langle \varphi(j, \mu - \tfrac{l}{2}; l, \mu), Q^{(l)}_k \right\rangle \right|^2 &= \left| \left\langle \mathcal{P}\varphi(j, \mu - \tfrac{l}{2}; l, \mu), \mathcal{P}Q^{(l)}_k \right\rangle \right|^2 \\ &= \left| \left\langle \varphi(j, \mu - \tfrac{l}{2}; l, \mu), Q^{(l)}_{l-k} \right\rangle \right|^2. \end{aligned}$$

TABLE 15.6. The continuum limit Gram eigenvalues $\lambda^{(l)}_{jm\mu}$ for two degrees of freedom when $\mathcal{U} = SU(2)$. The last column lists the degeneracy of each eigenvalue.

l	j	μ	$\lambda^{(l)}_{jm\mu}$	degen.
1	1/2	0	1/4	4
2	1	1	1/18	3
		0	1/9	6
	0	1	1/6	1
3	3/2	1	1/48	8
		0	1/16	8
	1/2	1	1/12	4
4	2	2	1/150	5
		1	1/100	10
		0	1/25	10
	1	2	1/30	3
		1	1/20	6
	0	2	1/15	1
5	5/2	2	1/360	12
		1	1/180	12
		0	1/36	12
	3/2	2	1/60	8
		1	1/30	8
	1/2	2	1/24	4

In other words, we can reduce the work involved in computing the Gram eigenvalues by roughly a factor of two:

$$\lambda^{(l)}_{jm\mu} = \frac{1}{(l+1)(2j+1)} \sum_{c=0}^{\lfloor l/2 \rfloor} N_c \left| \langle \varphi(j, \mu - \tfrac{l}{2}; l, \mu), Q^{(l)}_c \rangle \right|^2, \tag{15.75}$$

where $\lfloor l/2 \rfloor$ denotes the largest integer less than or equal to $l/2$, and

$$N_c = \begin{cases} 1, & \text{if } c = l/2; \\ 2, & \text{otherwise.} \end{cases} \tag{15.76}$$

Appendix I includes the *Mathematica* notebook used to compute the Gram eigenvalues according to (15.75) for $l \in \{1, \ldots, 5\}$, and Table 15.6 summarizes the results.

15.2.5. *The Gram Matrix and its Eigenvalues for the Case* $\mathcal{U} = U(2)/SO(2)$. In the last section, §15.2.4, we found the Gram matrix and its eigenvalues for the restricted case in which $\mathcal{L}(u)$ belongs to the coset space $SU(2)/SO(2)$. Let us now extend our results to the larger space $U(2)/SO(2)$, which, according to §13.3, contains all of the relevant $\mathcal{L}(u)$. Because $U(1) \otimes SU(2)/SO(2)$ covers $U(2)/SO(2)$, we can perform this extension by reusing most of the work in the previous section and simply overlaying an integration over the $U(1)$ subspace.

Although it suffices in the Gram operator to integrate over just the coset space $U(2)/SO(2)$, we can determine the Gram eigenvalues more easily by integrating over the whole of $U(2)$. Theorem 13.1 assures us that the added integration over the $SO(2)$ subspace will not affect our results. For this section, then, we write the Gram operator exactly as in (15.60), but with the integral over $SU(2)$ replaced by an integral over $U(2)$.

Given any unitary matrix $u \in U(2)$, one can always write it in the form

$$u = v\, e^{i\theta/2}, \tag{15.77}$$

where $v \in SU(2)$, $\theta \in [0, 2\pi]$, and $\det(u) = e^{i\theta}$. As a consequence, the integral over $U(2)$ factors into two pieces:

$$\int\limits_{U(2)} du \;=\; \int\limits_{SU(2)} dv \int\limits_0^{2\pi} \frac{d\theta}{2\pi};$$

and likewise the linear symplectic transformation $\mathcal{L}(u)$ factors into two pieces:

$$\mathcal{L}(u) = \mathcal{L}(e^{i\theta/2}\mathbf{1})\mathcal{L}(v) = \mathcal{R}(\theta)\mathcal{L}(v),$$

where $\mathcal{R}(\theta) = \mathcal{L}(e^{i\theta/2}\mathbf{1})$. We can therefore write the Gram operator as

$$\widehat{\Gamma}(l) = \frac{1}{l+1} \sum_{k=0}^{l} \int\limits_{SU(2)} dv \int\limits_0^{2\pi} \frac{d\theta}{2\pi}\, \mathcal{R}(\theta)\mathcal{L}(v)\, \big|Q_k^{(l)}\big\rangle\big\langle Q_k^{(l)}\big|\, \mathcal{L}(v)^\dagger \mathcal{R}(\theta)^\dagger. \tag{15.78}$$

Note that this Gram operator differs from that of (15.60) only with regard to the $U(1)$ subspace parameterized by the variable θ.

Before we can make further progress, we need to know a great deal about the operator $\mathcal{R}(\theta)$. Recall from §13.3 that we write $\mathcal{L}(u)$ for $\mathcal{L}(M(u))$. Then using (13.11), we find that $\mathcal{R}(\theta) = \mathcal{L}(e^{i\theta/2}\mathbf{1})$ acts on phase space according to the rule

$$\begin{aligned}
\mathcal{R}(\theta) \begin{pmatrix} q_1 \\ q_2 \\ p_1 \\ p_2 \end{pmatrix} &= M(e^{i\theta/2}\mathbf{1}) \begin{pmatrix} q_1 \\ q_2 \\ p_1 \\ p_2 \end{pmatrix} = M \begin{pmatrix} e^{i\theta/2} & 0 \\ 0 & e^{i\theta/2} \end{pmatrix} \begin{pmatrix} q_1 \\ q_2 \\ p_1 \\ p_2 \end{pmatrix} \\
&= \begin{pmatrix} \cos(\theta/2) & 0 & \sin(\theta/2) & 0 \\ 0 & \cos(\theta/2) & 0 & \sin(\theta/2) \\ -\sin(\theta/2) & 0 & \cos(\theta/2) & 0 \\ 0 & -\sin(\theta/2) & 0 & \cos(\theta/2) \end{pmatrix} \begin{pmatrix} q_1 \\ q_2 \\ p_1 \\ p_2 \end{pmatrix}.
\end{aligned} \tag{15.79a}$$

Observe that $\mathcal{R}(\theta)$ does not mix the (q_1, p_1) subspace with the (q_2, p_2) subspace. Indeed, we may express the action of $\mathcal{R}(\theta)$ on each subspace as

$$\mathcal{R}(\theta) \begin{pmatrix} q_j \\ p_j \end{pmatrix} = \begin{pmatrix} \cos(\theta/2) & \sin(\theta/2) \\ -\sin(\theta/2) & \cos(\theta/2) \end{pmatrix} \begin{pmatrix} q_j \\ p_j \end{pmatrix}. \tag{15.79b}$$

Compare this result with (15.3) and (15.4); and note that the Lie operator associated with any function of one subspace, say $:f(q_1, p_1):$, always commutes with the Lie operator associated with any other function of the other subspace, say $:g(q_2, p_2):$. Therefore, using (15.32), we may write $\mathcal{R}(\theta)$ in the form

$$\mathcal{R}(\theta) = \exp\Big(-\frac{\theta}{2} :\frac{1}{2}(q_1^2 + p_1^2 + q_2^2 + p_2^2):\Big) = \exp\Big(-\frac{\theta}{2} :b^0:\Big). \tag{15.80}$$

In other words, this $\mathcal{R}(\theta) = \mathcal{L}(e^{i\theta/2}\mathbf{1})$ is a generalization of the operator $\mathcal{R}(\theta)$ defined in §15.1; hence we shall refer to (15.80) also as a *rotation operator*. Now recall that the dynamical polynomials b^j of (15.32), $j \in \{1, 2, 3\}$, form a basis for the $su(2)$ Lie subalgebra contained within $sp(4, \mathbb{R})$; and further recall (*cf.* (15.33a)) that b^0 commutes with b^j and generates the corresponding $u(1)$ subalgebra. It follows—as the alert reader has already noticed—that the rotation operator $\mathcal{R}(\theta)$ commutes with $\mathcal{L}(v)$. In addition, it also follows that $\mathcal{R}(\theta)$ commutes with the angular momentum-like operators $:a^j:$ of (15.34), A^2 of (15.36), and $:a^\pm:$ of (15.37).

Let us note a few more properties of the rotation operator $\mathcal{R}(\theta)$. First, it follows from (10.12) and (15.80) that this operator is unitary:

$$\mathcal{R}(\theta)^\dagger = \mathcal{R}(-\theta) = \mathcal{R}(\theta)^{-1}. \tag{15.81}$$

Now study how the rotation operator $\mathcal{R}(\theta)$ acts on the y's and how it affects the $SU(2)$ basis polynomials φ of (15.46). By straightforward computation using (15.79) and Table 15.1, one finds that

$$\mathcal{R}(\theta)\begin{pmatrix} y_1 \\ y_2 \\ y_3 \\ y_4 \end{pmatrix} = \begin{pmatrix} y_1 \\ y_2 \\ y_3 \\ y_4 \end{pmatrix} \cos\Big(\frac{\theta}{2}\Big) + \begin{pmatrix} y_3 \\ y_4 \\ -y_1 \\ -y_2 \end{pmatrix} \sin\Big(\frac{\theta}{2}\Big). \tag{15.82}$$

Now examine how $\mathcal{R}(\theta)$ affects the basis polynomial $\varphi(j,m;l,\mu)$. Because it commutes with A^2 and $:a^3:$, it cannot alter the values of j and m. It does, however, affect the value of μ. In general, therefore, $\mathcal{R}(\theta)$ produces a linear combination of φ's with the same values of j, m, and l:

$$\mathcal{R}(\theta)\varphi(j,m;l,\mu) = \sum_{\nu=\frac{l}{2}-j}^{\frac{l}{2}+j} R^{jm}(\theta)_{\nu\mu}\varphi(j,m;l,\nu). \tag{15.83}$$

The expansion coefficients $R^{jm}(\theta)_{\nu\mu}$ that appear in (15.83) have several properties worth noting. First observe that we can use the orthonormality of the φ with respect to the inner product (10.9) to write the coefficients explicitly as

$$R^{jm}(\theta)_{\nu\mu} = \big\langle \varphi(j,m;l,\nu), \mathcal{R}(\theta)\varphi(j,m;l,\mu)\big\rangle\,. \tag{15.84}$$

Then further observe that because the φ's are all real linear combinations of y-monomials, and because $\mathcal{R}(\theta)$ acting on the y's produces only real linear combinations of y's, *the expansion coefficients* (15.84) *must be real.*

It also turns out that the expansion coefficients (15.84) do not depend on the index m. To verify this claim, observe that, by relations analogous to (15.40),

$$:a^+::a^-:\varphi(j,m;l,\mu) = (j+m)(j-m+1)\varphi(j,m;l,\mu),$$

and recall that the rotation operator commutes with $:a^\pm:$. As a consequence, since $:a^+:^\dagger = :a^-:$, we obtain

$$\begin{aligned} R^{jm}(\theta)_{\nu\mu} &= \Big\langle \varphi(j,m;l,\nu),\, \mathcal{R}(\theta)\frac{:a^+::a^-:}{(j+m)(j-m+1)}\varphi(j,m;l,\mu)\Big\rangle \\ &= \frac{1}{(j+m)(j-m+1)}\,\big\langle :a^-:\varphi(j,m;l,\nu), \mathcal{R}(\theta)\,:a^-:\varphi(j,m;l,\mu)\big\rangle \\ &= \big\langle \varphi(j,m-1;l,\nu), \mathcal{R}(\theta)\varphi(j,m-1;l,\mu)\big\rangle \\ &= R^{j,m-1}(\theta)_{\nu\mu}. \end{aligned}$$

We may therefore write the expansion coefficients more simply as

$$R^j(\theta)_{\nu\mu} = R^{jj}(\theta)_{\nu\mu} = \big\langle \varphi(j,j;l,\nu), \mathcal{R}(\theta)\varphi(j,j;l,\mu)\big\rangle\,. \tag{15.85}$$

One may view the expansion coefficients $R^j(\theta)_{\nu\mu}$ of (15.85) as the entries of a $(2j+1)\times(2j+1)$ matrix $R^j(\theta)$. Now note that because the coefficients $R^j(\theta)_{\nu\mu}$ are real matrix elements of a unitary operator with respect to an orthonormal basis, it follows that the matrix $R^j(\theta)$ is orthogonal. Therefore, in terms of its matrix elements, we obtain the symmetry

$$R^j(\theta)_{\nu\mu} = R^j(-\theta)_{\mu\nu}. \tag{15.86}$$

Let us now apply what we have learned about the rotation operator $\mathcal{R}(\theta)$ to the task of evaluating the matrix elements of the Gram operator (15.78) with respect to the basis polynomials φ of (15.46). Using (15.78), (15.81), (15.83), (15.85), and the reality of $R^j(\theta)$,

we obtain

$$\begin{aligned}
\Gamma(l)_{jm\mu,j'm'\mu'} &= \big\langle \varphi(j,m;l,\mu)\big|\widehat{\Gamma}(l)\big|\varphi(j',m';l,\mu')\big\rangle \\
&= \frac{1}{l+1}\sum_{k=0}^{l}\int\limits_{SU(2)} dv \int\limits_0^{2\pi}\frac{d\theta}{2\pi}\,\Big\langle \mathcal{L}(v)^\dagger\mathcal{R}(\theta)^\dagger\varphi(j,m;l,\mu), Q_k^{(l)}\Big\rangle \times \\
&\qquad\qquad \Big\langle Q_k^{(l)}, \mathcal{L}(v)^\dagger\mathcal{R}(\theta)^\dagger\varphi(j',m';l,\mu')\Big\rangle \\
&= \frac{1}{l+1}\sum_{k=0}^{l}\int\limits_{SU(2)} dv \int\limits_0^{2\pi}\frac{d\theta}{2\pi}\sum_{\nu\nu'}\Big(R^j(-\theta)_{\nu\mu}R^{j'}(-\theta)_{\nu'\mu'}\,\Big\langle \mathcal{L}(v)^\dagger\varphi(j,m;l,\nu), Q_k^{(l)}\Big\rangle \times \\
&\qquad\qquad \Big\langle Q_k^{(l)}, \mathcal{L}(v)^\dagger\varphi(j',m';l,\nu')\Big\rangle\Big) \\
&= \sum_{\nu\nu'}\left[\left(\int\limits_0^{2\pi}\frac{d\theta}{2\pi}\,R^j(-\theta)_{\nu\mu}R^{j'}(-\theta)_{\nu'\mu'}\right)\times \right. \\
&\qquad\qquad \left.\left(\frac{1}{l+1}\sum_{k=0}^{l}\int\limits_{SU(2)} dv\,\Big\langle \mathcal{L}(v)^\dagger\varphi(j,m;l,\nu), Q_k^{(l)}\Big\rangle\Big\langle Q_k^{(l)}, \mathcal{L}(v)^\dagger\varphi(j',m';l,\nu')\Big\rangle\right)\right].
\end{aligned}$$

Comparing this last expression with (15.61), we observe that the second factor in parentheses is just one of the Gram matrix elements evaluated using the smaller space $\mathcal{U} = SU(2)$. According to (15.65), these elements are diagonal, and hence we now write the Gram matrix elements in the form

$$\Gamma(l)_{jm\mu,j'm'\mu'} = \delta_{jj'}\delta_{mm'}\int\limits_0^{2\pi}\frac{d\theta}{2\pi}\,K^j(\theta)_{\mu\mu'}, \tag{15.87}$$

where

$$K^j(\theta)_{\mu\mu'} = \sum_{\nu=\frac{l}{2}-j}^{\frac{l}{2}+j}\lambda^{(l)}_{jm\nu}R^j(-\theta)_{\nu\mu}R^j(-\theta)_{\nu\mu'}, \tag{15.88}$$

and the $\lambda^{(l)}_{jm\nu}$ denote the $SU(2)$ Gram eigenvalues given by (15.75). Recall that the eigenvalues $\lambda^{(l)}_{jm\nu}$ do not depend on the index m. It follows that the $U(2)$ Gram matrix—and hence also its eigenvalues—also does not depend on m. Each eigenvalue for the $U(2)$ Gram matrix therefore also has an associated degeneracy of $(2j+1)$.

The Gram matrix as given by the elements (15.87) is not completely diagonal—only block diagonal. To complete the determination of the Gram eigenvalues, then, we must evaluate the matrix elements of each block and then the corresponding eigenvalues. To reduce the amount of computation required, we note that from the definition (15.88) it follows directly that $K^j(\theta)$, and hence also $\Gamma(l)$, is symmetric. (This should not surprise the reader.)

Appendix I includes the *Mathematica* notebook used to compute the Gram matrix $\Gamma(l)$ and thence the corresponding eigenvalues, which we shall denote $\bar{\lambda}^{(l)}_j$, according to the formula (15.87) for $l \in \{1,\ldots,5\}$. Table 15.7 summarizes the results. On comparing the eigenvalues listed in Tables 15.6 and 15.7, the reader will notice that restricting oneself from $U(2)$ (or $U(2)/SO(2)$) to the smaller space $SU(2)$ (or $SU(2)/SO(2)$) causes a reduction in the minimum Gram eigenvalues by a factor of $\frac{2}{3}$ for $l = 2$ and 3, and by a factor of $\frac{8}{15}$ $(=\frac{2}{3}\cdot\frac{4}{5})$ for $l = 4$ and 5.

Now recall that, according to (12.4), the size of the minimum Gram eigenvalues governs one bound on the size of the jolt strengths, which we wish to minimize. And further recall that

TABLE 15.7. The continuum limit Gram eigenvalues $\bar{\lambda}_j^{(l)}$ for two degrees of freedom when $\mathcal{U} = U(2)$. The last column lists the degeneracy of each eigenvalue.

l	j	$\bar{\lambda}_j^{(l)}$	degen.
1	1/2	1/4	4
2	1	1/9	3
		1/12	6
	0	1/6	1
3	3/2	1/32	8
		5/96	8
	1/2	1/12	4
4	2	19/600	5
		1/80	10
		1/40	10
	1	1/20	3
		1/24	6
	0	1/15	1
5	5/2	1/192	12
		7/576	12
		3/160	12
	3/2	1/48	8
		7/240	8
	1/2	1/24	4

our motivation for calculating the Gram eigenvalues in the continuum limit was to determine upper bounds on the Gram eigenvalues for the discrete case. The results shown in Tables 15.6 and 15.7 suggest that a jolt map based on the jolt decomposition (11.2) with the linear symplectic transformations $\mathcal{L}_j$ chosen from the space $SU(2)/SO(2)$ may perform somewhat less well than a similar jolt map with the $\mathcal{L}_j$ chosen from the larger space $U(2)/SO(2)$. Determining just how serious the difference in performance is will require numerical experiments with real maps.

15.3. **Three Degrees of Freedom**

The reader may very naturally approach the analysis for three degrees of freedom with some trepidation, but this case in some ways lends itself to a more straightforward analysis than the case of two degrees of freedom. Recall from §15.2.3 that (for $n = 2$) if the dynamical polynomials of degree l carry a spin-j representation, then they carry $2j + 1$ copies of spin-j. This simple fact presented the principal complication to diagonalizing the Gram matrix $\Gamma(l)$ when we integrated over the space $\mathcal{U} = SU(2)$. Indeed, the prime motivation for our method of constructing the $SU(2)$ basis polynomials given in Tables 15.1–15.5 came from our desire to ensure that the different copies of spin-j were not simply equivalent but in fact *identical*. As we shall describe, this complication does not arise for the case of three degrees of freedom.

In the present case, $n = 3$, we note that according to (10.6)

$$M(l, n) = M(l, 3) = \binom{l+2}{l} = \frac{(l+1)(l+2)}{2}$$

Hence the sum over k in (14.5b) covers $(l+1)(l+2)/2$ q-monomials, which we denote as

$$Q^{(l)}_{k_2k_3} = \frac{q_1^{l-k_2-k_3} q_2^{k_2} q_3^{k_3}}{\sqrt{(l-k_2-k_3)!\,k_2!\,k_3!}}, \tag{15.89}$$

where $k_2 \in \{0,1,\ldots,l\}$, and $k_3 \in \{0,1,\ldots,l-k_2\}$. We shall sometimes—as in (15.90) below—abbreviate (15.89) more simply as $Q^{(l)}_k$, with the single index $k \in \{1,\ldots,\frac{1}{2}(l+1)(l+2)\}$ subsuming the two separate indices k_2 and k_3. Thus we write the Gram operator (14.5) in the form

$$\widehat{\Gamma}(l) = \frac{2}{(l+1)(l+2)} \sum_k \int_{\mathcal{U}} du\, \mathcal{L}(u) \left|Q^{(l)}_k\right\rangle\!\left\langle Q^{(l)}_k\right| \mathcal{L}(u)^\dagger. \tag{15.90}$$

As indicated in §13.4, we shall integrate first over $\mathcal{U} = SU(3)$—which, by Theorem 13.1, we know gives the same results as integrating over $\mathcal{U} = SU(3)/SO(3)$. Afterwards we shall extend our results to include all of $U(3)$ in our integration.

15.3.1. *Basis Functions for Irreducible Representations of $SU(3)$.* We want a basis set of orthonormal dynamical polynomials that diagonalizes the Gram matrix $\Gamma(l)$. To this end, in parallel with the case $n = 2$, we look for basis functions that transform according to irreducible representations of the group $SU(3)$. Since the basis we shall use has been constructed by others, we restrict ourselves to introducing and describing that basis.

In the parlance of group theory, $SU(3)$ has a "rank two Lie algebra", $su(3)$. This means, among other things, that two indices, say j_1 and j_2, suffice to label all the irreducible representations of $SU(3)$, or $su(3)$. We shall therefore use the pair "(j_1, j_2)" to denote these different representations. The indices j_1 and j_2 take all non-negative integer values, and the corresponding representation has dimension [20, 30]

$$d(j_1,j_2) = (j_1+1)(j_2+1)(\tfrac{1}{2}(j_1+j_2)+1). \tag{15.91}$$

Another common notation for the irreducible representations of $SU(3)$ uses simply the dimension as a label. To distinguish the representations (j_1,j_2) and (j_2,j_1), which obviously have the same dimension, one uses a diacritical mark of some sort (along with a convention as to which one is which). Thus we may call the $(2,0)$ representation simply 6, and the $(0,2)$ representation $\bar{6}$. This notation, however, does not distinguish all the irreducible representations. The $(2,1)$ and $(4,0)$ representations, for example, both have dimension fifteen. For these cases, then, one must give j_1 and j_2 explicitly.

Bég and Ruegg in [9] constructed a basis set of angular functions,

$$\psi^{j_1j_2}_{II_3Y}(\theta,\xi,\phi_1,\phi_2,\phi_3),$$

on the five-sphere[21] $\mathbb{S}^5$ and showed that they transform according to irreducible representations of $SU(3)$.[22] These functions are given by

$$\psi^{j_1j_2}_{II_3Y} = \frac{1}{\sin\theta}\, d^{\frac{1}{2}(j_1+j_2+1)}_{\frac{1}{6}(j_1-j_2-3Y+6I+3),\frac{1}{6}(j_1-j_2-3Y-6I-3)}(2\theta)\, d^I_{\frac{1}{3}(j_1-j_2)+\frac{1}{2}Y,I_3}(2\xi) \times e^{i\frac{1}{3}(j_1-j_2)(\phi_1+\phi_2+\phi_3)} e^{iI_3(\phi_2-\phi_3)} e^{i\frac{1}{2}Y(-2\phi_1+\phi_2+\phi_3)}, \tag{15.92}$$

[21] The five-sphere $\mathbb{S}^5$ is the five-dimensional surface of a sphere in six-dimensional space.

[22] Bég and Ruegg call the functions $\psi^{j_1j_2}_{II_3Y}$ *harmonic*, by which they mean that the $\psi^{j_1j_2}_{II_3Y}$ are eigenfunctions of the Laplace operator on the manifold $\mathbb{S}^5$. In the usual parlance, however, a harmonic function on a given differentiable manifold is one that satisfies Laplace's equation $\nabla^2\psi = 0$, where ∇^2 denotes the Laplacian on the manifold of interest. In other words, harmonic functions vanish under the action of the Laplace operator and thus correspond to eigenvalue zero. We shall therefore refer to the $\psi^{j_1j_2}_{II_3Y}$ merely as *angular* functions.

where the angles θ, ξ, and ϕ_j in $\mathbb{S}^5$ span the intervals

$$\begin{aligned} \theta &\in [0, \pi/2); \\ \xi &\in [0, \pi/2); \\ \phi_j &\in [0, 2\pi), \quad j \in \{1, 2, 3\}. \end{aligned} \tag{15.93}$$

The functions $d^j_{m'm}(\beta)$ are the well-known matrix elements of the quantum mechanical rotation operator[23] $\exp(-i\beta J_y)$:

$$d^j_{m'm}(\beta) = \left\langle jm' \middle| e^{-i\beta J_y} \middle| jm \right\rangle .$$

They are given by Wigner's formula[24] [75],

$$d^j_{m'm}(\beta) = \sqrt{(j+m')!\,(j-m')!\,(j+m)!\,(j-m)!}\times \sum_k (-1)^{k+m'-m} \frac{(\cos\beta/2)^{2j-2k-m'+m}(\sin\beta/2)^{2k+m'-m}}{(j-m'-k)!\,(j+m-k)!\,(k+m'-m)!\,k!}, \tag{15.94a}$$

or by the equivalent, but useful, alternative formula

$$d^j_{m'm}(\beta) = \sqrt{(j+m')!\,(j-m')!\,(j+m)!\,(j-m)!}\times \sum_k (-1)^{j-k-m} \frac{(\cos\beta/2)^{2k+m'+m}(\sin\beta/2)^{2j-2k-m'-m}}{(j-m'-k)!\,(j-m-k)!\,(k+m'+m)!\,k!}. \tag{15.94b}$$

In either of formulas (15.94) the summation spans all integer values of k for which none of the factorials has a negative argument.

As their notation suggests, the functions $\psi^{j_1 j_2}_{I I_3 Y}$ in (15.92) carry the irreducible representation (j_1, j_2) of $SU(3)$, or $su(3)$. The additional indices—I, I_3, and Y—label the individual basis functions carrying that representation. In Bég and Ruegg's language (which was motivated by the theory of strongly interacting particles) these indices denote respectively eigenvalues of the operators for total isotopic spin, z-component of isotopic spin, and hypercharge. The isotopic spin I and its z-component I_3 take the following values:

$$I \in \left\{0, \tfrac{1}{2}, 1, \ldots, \tfrac{1}{2}(j_1 + j_2)\right\}, \tag{15.95a}$$

$$I_3 \in \{I, I-1, \ldots, -I\}. \tag{15.95b}$$

One cannot so simply state the possible values of Y, but one *can* say that

$$Y_h = \frac{1}{3}(j_1 - j_2) \tag{15.96}$$

is one of the Y values, and all other values of Y differ from Y_h by an integer.

In a given representation, say (j_1, j_2), for a fixed value of Y only certain values of I_3, or I, can occur: the allowed values of the pair (I_3, Y) define the so-called *weight vectors* of the representation (j_1, j_2) of $su(3)$.[25] Not all of these weight vectors are necessarily unique in a given representation, but the value of total isotopic spin I distinguishes the basis functions corresponding to such degenerate weight vectors. There exists a beautiful and elegant theory—developed by Cartan—which describes not only the relations amongst the weight vectors but also how to find them using generalizations of the raising and lowering operators of $su(2)$ [10]. We shall not discuss that theory but only hint at it from time to time.

By now the reader has begun to wonder how the functions $\psi^{j_1 j_2}_{I I_3 Y}$ on $\mathbb{S}^5$ relate to our stated needs: a basis set of dynamical polynomials in six-dimensional phase space. To make the

[23] Note that we use Rose's convention [75] of a $-i$ in the exponential rather than a $+i$, as in Edmonds [35].

[24] One can also write these matrix elements more succinctly in terms of Jacobi polynomials. For technical reasons, however, that form proves less useful for our purposes.

[25] The weight vectors are given by a simple rescaling: $(I_3/\sqrt{3}, Y/2)$ [10].

connection, we shall as in §15.2 use a set of complex dynamical variables. Let us define (*cf.* (15.5))

$$z_j = \frac{1}{\sqrt{2}}(q_j + ip_j) \tag{15.97a}$$

and its complex conjugate

$$z_j^* = \frac{1}{\sqrt{2}}(q_j - ip_j) \tag{15.97b}$$

for each $j \in \{1, 2, 3\}$. Inverting these formulas, we obtain the relations

$$q_j = \frac{1}{\sqrt{2}}(z_j + z_j^*), \tag{15.98a}$$

$$p_j = \frac{-i}{\sqrt{2}}(z_j - z_j^*). \tag{15.98b}$$

In a moment we shall describe the relationship between the z's and the five-sphere. First, however, note that the complex linear Lie transformation

$$\mathcal{T} = \exp\Big(\frac{i\pi}{8} :q_1^2 - p_1^2 + q_2^2 - p_2^2 + q_3^2 - p_3^2:\Big) \tag{15.99}$$

converts the q's and p's into z's. In fact, since the different degrees of freedom—labeled 1, 2, and 3—commute with each other, the operator (15.99) is a simple generalization of the operator (15.7) of the same name in §15.1.1. Hence (*cf.* (15.8))

$$\mathcal{T}\begin{pmatrix} q_j \\ p_j \end{pmatrix} = \begin{pmatrix} z_j \\ iz_j^* \end{pmatrix}. \tag{15.100}$$

It follows also that the operator $\mathcal{T}$ of (15.99) is unitary with respect to the inner product (10.9). This means that inner products between polynomials in the z's behave in essentially the same way as do inner products between polynomials in the q's and p's (*cf.* (15.56)). In particular, the monomials

$$\frac{{z_1}^{r_1} {z_2}^{r_2} {z_3}^{r_3} {z_1^*}^{r_4} {z_2^*}^{r_5} {z_3^*}^{r_6}}{\sqrt{r_1!\, r_2!\, r_3!\, r_4!\, r_5!\, r_6!}}$$

form a set of orthonormal z-monomials analogous to the general monomials we defined in (10.7).

We can now fill in the connection between the dynamical polynomials we need and the angular functions on the five-sphere $\mathbb{S}^5$. To do this, we begin by making the definitions

$$r^2 = z_1 z_1^* + z_2 z_2^* + z_3 z_3^* = \frac{1}{2}(q_1^2 + q_2^2 + q_3^2 + p_1^2 + p_2^2 + p_3^2) \tag{15.101}$$

(the second equality follows from (15.97)) and

$$\begin{aligned} z_1 &= re^{i\phi_1} \cos\theta, \\ z_2 &= re^{i\phi_2} \sin\theta\, \cos\xi, \\ z_3 &= re^{i\phi_3} \sin\theta\, \sin\xi, \end{aligned} \tag{15.102}$$

which determine a one-to-one relationship between the complex coördinates z_j and the "polar" coördinates given by a radius r (scaled by a factor of $\frac{1}{\sqrt{2}}$) and five angles on $\mathbb{S}^5$. (Here we have tacitly assumed that the radius r and the angles on $\mathbb{S}^5$, as well as the q's and p's, are real.) The z_j^*, of course, are determined by complex conjugation. Though it is not obvious, it turns out that each angular function $\psi_{II_3Y}^{j_1 j_2}$ defined in (15.92) can be written entirely as a polynomial in terms of the variables $\zeta_j = z_j/r$ and $\zeta_j^* = z_j^*/r$. (We must divide out the radius r because the $\psi_{II_3Y}^{j_1 j_2}$ are functions of the angles alone.) Furthermore, each term in a given $\psi_{II_3Y}^{j_1 j_2}$ is of degree j_1 in the variables ζ_j and of degree j_2 in the complex conjugate variables

ζ_j^*; hence with respect to the ζ's the $\psi_{II_3Y}^{j_1 j_2}$ are polynomials of total degree $j_1 + j_2$. Said another way, each function $\psi_{II_3Y}^{j_1 j_2}$ is a quotient which contains in the numerator a polynomial in the z's of degree $j_1 + j_2$ and in the denominator the quantity $r^{j_1+j_2}$. These polynomials, however, are not yet the dynamical polynomials we seek. To complete the connection between the dynamical basis polynomials and the angular functions, we must add a bit more detail.

The most important piece of additional information we need is the following [26]

Theorem 15.1. *The space of f_l's,* i.e.*, the space of homogeneous polynomials of degree l in six-dimensional phase space, carries the following irreducible representations of su*(3)*:*

$$\begin{gathered}(0,l),(1,l-1),(2,l-2),\ldots,(l-2,2),(l-1,1),(l,0),\\ (0,l-2),(1,l-3),\ldots,(l-3,1),(l-2,0),\end{gathered}$$

$$\vdots \tag{15.103a}$$

$$\begin{cases}(0,1),(1,0) & \textit{for } l \textit{ odd},\\ (0,0) & \textit{for } l \textit{ even}.\end{cases}$$

One may express this list of representations more concisely (though less symmetrically) as the irreducible representations (j_1, j_2) where

$$\begin{aligned}&j_1 \in \{0,1,\ldots,l\},\\ &j_2 \in \{(l-j_1) \bmod 2, ((l-j_1) \bmod 2)+2,\ldots,l-j_1\}.\end{aligned} \tag{15.103b}$$

The (j_1, j_2) given by (15.103) *compose the* complete *list of irreducible representations carried by the space of f_l's. Furthermore, each representation (j_1, j_2) given by* (15.103) *occurs once—and only once—in the space of f_l's.*

Example. The f_2's carry the representations $(0,0)$, $(0,2)$, $(1,1)$, and $(2,0)$. The f_3's, on the other hand, carry the representations $(0,1)$, $(0,3)$, $(1,0)$, $(1,2)$, $(2,1)$, and $(3,0)$.

At this point we note that the angular functions $\psi_{II_3Y}^{j_1 j_2}$ cannot without modification serve as the dynamical basis polynomials we seek. One objection, of course, is that the $\psi_{II_3Y}^{j_1 j_2}$ depend on the ζ's rather than the z's. For this reason we define the modified angular functions

$$\psi_{II_3Y}^{\bar{j_1} j_2} = r^{j_1+j_2} \psi_{II_3Y}^{j_1 j_2}, \tag{15.104}$$

which are strictly polynomials in the z's. Indeed, a given $\psi_{II_3Y}^{\bar{j_1} j_2}$ is of degree j_1 in the variables z_j and of degree j_2 in the complex conjugate variables z_j^*. Although (15.104) defines polynomials in the z's—and hence polynomials in the q's and p's—we must still modify the $\psi_{II_3Y}^{\bar{j_1} j_2}$ in order to obtain the desired basis polynomials. Consider, for example, the f_3's: as just noted in the above example, they carry the $(0,1)$ representation, but the $\bar{\psi}_{II_3Y}^{01}$ have degree one. To overcome this discrepancy, however, it suffices to multiply the given $\psi_{II_3Y}^{j_1 j_2}$ by the appropriate power of r. Thus an f_l basis that transforms according to irreducible representations of $SU(3)$ is given by the dynamical polynomials

$$\psi(j_1, j_2, I, I_3, Y; l) \equiv N \cdot r^l \psi_{II_3Y}^{j_1 j_2} = N \cdot (r^2)^{\frac{1}{2}(l-j_1-j_2)} \psi_{II_3Y}^{\bar{j_1} j_2}, \tag{15.105}$$

where we have used the definition (15.104) to obtain the second equality. Here j_1 and j_2 label the irreducible representations of $SU(3)$ listed in Theorem 15.1, and the indices I, I_3, and Y label the individual basis elements within the representation (j_1, j_2). Of course r^2 is given by (15.101), and the $\psi_{II_3Y}^{j_1 j_2}$, originally given by (15.92), must be written in terms of the z's using (15.102). The factor N denotes a normalization constant which we shall determine by normalizing the dynamical polynomials with respect to the inner product (10.9). It depends on the labels l, j_1, j_2, I, and Y.

The trick we have just used—obtaining the dynamical basis polynomials we seek by multiplying the $\psi_{II_3Y}^{j_1 j_2}$ by an integer power of r—works because of the following two facts:

(1) Theorem 15.1 shows that for each representation carried by the f_l's the sum $j_1 + j_2$ differs from l always by an *even* integer (possibly zero). Hence, making up the difference in degree between a modified angular function $\psi^{\bar{j}_1 j_2}_{II_3Y}$ and the f_l's requires a polynomial of even degree. As a consequence, the $\psi(j_1, j_2, I, I_3, Y; l)$ of (15.105) are indeed polynomials in z.
(2) Multiplying $\psi^{j_1 j_2}_{II_3Y}$ by r^l does not alter the eigenvalues I, I_3, or Y.

To demonstrate the second point, we shall use the Lie algebra of $su(3)$.

One choice of basis for the eight-dimensional $su(3)$ Lie algebra comprises the generators [9, 10]

$$\begin{aligned} H_1 &= \frac{-i}{2\sqrt{3}} :z_2 z_2^* - z_3 z_3^*:, \\ H_2 &= \frac{-i}{6} :-2z_1 z_1^* + z_2 z_2^* + z_3 z_3^*:, \end{aligned} \tag{15.106a}$$

$$\begin{aligned} E_1 &= \frac{-i}{\sqrt{6}} :z_2 z_3^*:, & E_{-1} &= \frac{-i}{\sqrt{6}} :z_2^* z_3:, \\ E_2 &= \frac{-i}{\sqrt{6}} :z_2 z_1^*:, & E_{-2} &= \frac{-i}{\sqrt{6}} :z_2^* z_1:, \\ E_3 &= \frac{-i}{\sqrt{6}} :z_3 z_1^*:, & E_{-3} &= \frac{-i}{\sqrt{6}} :z_3^* z_1:, \end{aligned} \tag{15.106b}$$

Using the relations (15.97) or (15.102), one may rewrite these generators in terms of either the q's and p's or the angles in $\mathbb{S}^5$. When written in terms of q's and p's, the basis elements (15.106) represent a Lie subalgebra of the full Lie algebra of $sp(6, \mathbb{R})$.

To simplify computations in the $su(3)$ Lie algebra, we rewrite the action of a Lie operator (*cf.* (9.1)) in terms of the z's. First note, using (9.8) and (15.100), that

$$\begin{aligned} [z_j, z_k] &= [\mathcal{T} q_j, \mathcal{T} q_k] = \mathcal{T}[q_j, q_k] = 0, \\ [z_j^*, z_k^*] &= [-i\mathcal{T} p_j, -i\mathcal{T} p_k] = -\mathcal{T}[p_j, p_k] = 0, \\ [z_j, z_k^*] &= [\mathcal{T} q_j, -i\mathcal{T} p_k] = -i\mathcal{T}[q_j, p_k] = -i\delta_{jk}. \end{aligned}$$

It follows then [73, p. 167] that

$$:f:g = [f, g] = -i \sum_j \left(\frac{\partial f}{\partial z_j} \frac{\partial g}{\partial z_j^*} - \frac{\partial f}{\partial z_j^*} \frac{\partial g}{\partial z_j} \right). \tag{15.107}$$

Hence the z_j and z_j^* behave essentially the same as the q_j and p_j; we need only insert an extra factor of $-i$.

In a similar fashion one may convert the formulas (10.12) for the Hermitian adjoints of quadratic monomials into analogous formulas in terms of the z's. To do this, we first prove the following simple

Theorem 15.2. *If $\mathcal{U}$ denotes any unitary Lie transformation, then*

$$\mathcal{U}:f:^\dagger \mathcal{U}^{-1} = :\mathcal{U} f:^\dagger.$$

Proof. Since $\mathcal{U}$ is unitary, $\mathcal{U}^\dagger = \mathcal{U}^{-1}$. Then because $\mathcal{U}$ is a Lie transformation, we can use (9.9) to obtain

$$\langle \psi, \mathcal{U}:f:^\dagger \mathcal{U}^\dagger \varphi \rangle = \langle \mathcal{U} :f: \mathcal{U}^\dagger \psi, \varphi \rangle = \langle :\mathcal{U} f: \psi, \varphi \rangle = \langle \psi, :\mathcal{U} f:^\dagger \varphi \rangle .$$

As this result holds for arbitrary functions ψ and φ, the theorem follows. ∎

Now apply (9.9) and Theorem 15.2 to the adjoint relations (10.12) using the unitary Lie transformation $\mathcal{T}$ of (15.99). We obtain

$$\begin{aligned} :z_j z_k:^\dagger &= :z_j^* z_k^*:, \\ :z_j^* z_k^*:^\dagger &= :z_j z_k:, \\ :z_j z_k^*:^\dagger &= -:z_j^* z_k:. \end{aligned} \tag{15.108}$$

(One may also prove these relations by using (10.12) and (15.97) and doing a somewhat tedious calculation.)

From the adjoint relations (15.108) one may see that the $su(3)$ basis elements H_1 and H_2 of (15.106a) are Hermitian with respect to the inner product (10.9). In addition, the basis elements E_α of (15.106b) satisfy the relation

$${E_\alpha}^\dagger = E_{-\alpha}. \tag{15.109}$$

The eigenvalues I, I_3, and Y of the $SU(3)$ basis functions must correspond to a set of mutually commuting operators. The fact that the $su(3)$ basis elements H_1 and H_2 commute, as one can verify using (15.31) and (15.107), suggests a connection. Indeed, the operators for z-component of isotopic spin and hypercharge have the representations [9]

$$\begin{aligned} \widehat{I}_3 &= \sqrt{3}H_1 = \frac{-i}{2}:z_2 z_2^* - z_3 z_3^*:, \\ \widehat{Y} &= 2H_2 = \frac{-i}{3}:-2z_1 z_1^* + z_2 z_2^* + z_3 z_3^*:. \end{aligned} \tag{15.110}$$

Before discussing the operator for total isotopic spin, which we shall denote $\widehat{I^2}$, we pause to observe that every z-monomial is an eigenfunction of the operators $\widehat{I}_3$ and $\widehat{Y}$. On denoting the general z-monomial by[26]

$$\mathfrak{z}_r = {z_1}^{r_1} {z_2}^{r_2} {z_3}^{r_3} {z_1^*}^{r_4} {z_2^*}^{r_5} {z_3^*}^{r_6},$$

one can, by straightforward computation using (15.107), demonstrate that

$$:z_j z_j^*:\mathfrak{z}_r = i(r_j - r_{j+3})\,\mathfrak{z}_r. \tag{15.111}$$

From this result and (15.110) follow the relations

$$\begin{aligned} \widehat{I}_3\,\mathfrak{z}_r &= \frac{1}{2}(r_2 - r_3 - r_5 + r_6)\,\mathfrak{z}_r, \\ \widehat{Y}\,\mathfrak{z}_r &= \frac{1}{3}(-2r_1 + r_2 + r_3 + 2r_4 - r_5 - r_6)\,\mathfrak{z}_r. \end{aligned} \tag{15.112}$$

Together with our earlier claim that the modified angular functions $\psi^{\bar{j}_1 j_2}_{I I_3 Y}$ are of degrees j_1 and j_2 in terms of the z_j and z_j^* respectively, the relations (15.112) place stringent constraints on the possible forms of the dynamical basis polynomials that transform as irreducible representations of $SU(3)$.

There exist amongst the basis elements (15.106) of $su(3)$ important commutation relations that determine the properties of the basis functions[27] $\psi(j_1, j_2, I, I_3, Y; l)$. These relations include three that give the embedding of $su(2)$ within $su(3)$ as represented by isotopic spin. If we use $\widehat{I}_3$ instead of H_1 and define

$$\widehat{I}_\pm = \sqrt{6}E_{\pm 1}, \tag{15.113}$$

[26]Note that in $\mathfrak{z}_r$ we use the subscript r to stand for the set of exponents $\{r_1, \ldots, r_6\}$. The reader should not confuse this r with the radius r defined in (15.101).

[27]Here the reader might recall how the $su(2)$ commutation relations determine essentially all important properties in the quantum theory of angular momentum [7, 77].

then these relations may be written

$$\big[\widehat{I}_3, \widehat{I}_\pm\big] = \pm\, \widehat{I}_\pm, \tag{15.114a}$$

$$\big[\widehat{I}_+, \widehat{I}_-\big] = 2\, \widehat{I}_3\,. \tag{15.114b}$$

(One can prove these relations using (15.31), (15.107), (15.106b), and (15.110).) It follows that the operators $\widehat{I}_\pm$ play the roles of raising and lowering operators for the eigenvalue I_3. And indeed a restriction to the $su(2)$ part of $su(3)$ will appear very familiar to anyone who has studied angular momentum in quantum mechanics. The operator for total isotopic spin, $\widehat{I^2}$, turns out to be a *Casimir operator* [20, p. 592] constructed from the basis elements $\widehat{I}_+$, $\widehat{I}_-$, and $\widehat{I}_3$:

$$\widehat{I^2} = \widehat{I}_3{}^2 + \frac{1}{2}\big(\widehat{I}_+\,\widehat{I}_- + \widehat{I}_-\,\widehat{I}_+\big). \tag{15.115a}$$

Though not a Lie operator, this operator *is* Hermitian. Using the commutation relation (15.114b), we may also write $\widehat{I^2}$ in the alternative forms

$$\begin{aligned}\widehat{I^2} &= \widehat{I}_3{}^2 - \widehat{I}_3 + \widehat{I}_+\,\widehat{I}_- \\ &= \widehat{I}_3{}^2 + \widehat{I}_3 + \widehat{I}_-\,\widehat{I}_+\,.\end{aligned} \tag{15.115b}$$

Then the raising and lowering operators act on the basis polynomials ψ of (15.105) according to the rules

$$\begin{aligned}\widehat{I}_+\,\psi(j_1, j_2, I, I_3, Y; l) &= -\sqrt{(I - I_3)(I + I_3 + 1)}\;\psi(j_1, j_2, I, I_3 + 1, Y; l), \\ \widehat{I}_-\,\psi(j_1, j_2, I, I_3, Y; l) &= -\sqrt{(I + I_3)(I - I_3 + 1)}\;\psi(j_1, j_2, I, I_3 - 1, Y; l).\end{aligned} \tag{15.116}$$

Except for the choice of phase, these rules follow from (15.115b) using the well-known arguments borrowed from the theory of angular momentum in quantum mechanics. The remaining basis elements of (15.106b), $E_{\pm 2}$ and $E_{\pm 3}$, behave like generalized raising and lowering operators that affect the eigenvalues of both $\widehat{I}_3$ and $\widehat{Y}$ simultaneously.

Let us return now to the question of why multiplying the angular functions $\psi^{j_1 j_2}_{I I_3 Y}$ by r^l delivers us the dynamical basis polynomials we want. Using (15.101), (15.106b), (15.107), (15.112), and (15.113), we find that

$$\begin{aligned}\widehat{I}_+\, r^2 &= -i\,[z_2 z_3^*, z_1 z_1^* + z_2 z_2^* + z_3 z_3^*] = -(z_3^* z_2 - z_2 z_3^*) = 0, \\ \widehat{I}_-\, r^2 &= -i\,[z_2^* z_3, z_1 z_1^* + z_2 z_2^* + z_3 z_3^*] = -(-z_3 z_2^* + z_2^* z_3) = 0, \\ \widehat{I}_3\, r^2 &= \widehat{I}_3(z_1 z_1^* + z_2 z_2^* + z_3 z_3^*) = \frac{1}{2}(0 + 0 + 0) r^2 = 0,\end{aligned}$$

and

$$\widehat{Y}\, r^2 = \widehat{Y}(z_1 z_1^* + z_2 z_2^* + z_3 z_3^*) = \frac{1}{3}(0 + 0 + 0) r^2 = 0.$$

In other words, r^2 denotes a dynamical polynomial of isotopic spin zero and hypercharge zero. Because any Lie operator $\widehat{L}$ acts as a derivation (*cf.* (9.5)), we have the general relation

$$\widehat{L}\, r^k = k r^{k-1}\big(\widehat{L}\, r\big).$$

Then from the above relations it follows that

$$\widehat{I}_+\, r^l = \widehat{I}_-\, r^l = \widehat{I}_3\, r^l = \widehat{Y}\, r^l = 0;$$

hence, using the first form in (15.115b),

$$\widehat{I^2}\, r^l = \big(\widehat{I}_3{}^2 - \widehat{I}_3 + 6\,\widehat{I}_+\,\widehat{I}_-\big) r^l = 0.$$

We now conclude that

$$\widehat{I}_3\big(r^l \psi^{j_1 j_2}_{I I_3 Y}\big) = \big(\widehat{I}_3\, r^l\big)\psi^{j_1 j_2}_{I I_3 Y} + r^l\big(\widehat{I}_3\, \psi^{j_1 j_2}_{I I_3 Y}\big) = I_3\big(r^l \psi^{j_1 j_2}_{I I_3 Y}\big).$$

In a similar fashion we conclude that

$$\widehat{Y}\big(r^l\psi^{j_1j_2}_{II_3Y}\big) = Y\big(r^l\psi^{j_1j_2}_{II_3Y}\big),$$

and

$$\widehat{I^2}\big(r^l\psi^{j_1j_2}_{II_3Y}\big) = I(I+1)\big(r^l\psi^{j_1j_2}_{II_3Y}\big).$$

These last three relations prove that multiplying the angular functions $\psi^{j_1j_2}_{II_3Y}$ by r^l has no effect on the eigenvalues I, I_3, and Y. It then follows that the polynomials $\psi(j_1, j_2, I, I_3, Y; l)$ defined by (15.105) do indeed compose an f_l basis that transforms according to irreducible representations of $SU(3)$.

An alternative to the proof just given relies on the (straightforward to prove) fact that all of the generators (15.106) of the $su(3)$ Lie algebra return zero when acting on the r^2 of (15.101). It follows that any element of $SU(3)$ acting on $r^l\psi^{j_1j_2}_{II_3Y}$ returns r^l times the result of that same $SU(3)$ element acting on $\psi^{j_1j_2}_{II_3Y}$; hence *the polynomials* $\psi(j_1, j_2, I, I_3, Y; l)$ *inherit the same transformation properties as* $\psi^{j_1j_2}_{II_3Y}$ *under irreducible representations of* $SU(3)$.

The alert reader will recall (*cf.* §12.2) that we want an *orthogonal* basis of dynamical polynomials. The orthogonality of the $\psi(j_1, j_2, I, I_3, Y; l)$ follows automatically from the fact that they have distinct eigenvalues with respect to the mutually commuting Hermitian operators $\widehat{I^2}$, $\widehat{I}_3$, and $\widehat{Y}$ [41, p. 163].

The angular functions $\psi^{j_1j_2}_{II_3Y}$ —and likewise the modified angular functions $\psi^{\bar{j}_1j_2}_{II_3Y}$—possess certain symmetries that arise from well-known symmetries of the matrix elements $d^j_{m'm}(\beta)$. In particular, the symmetries

$$d^j_{m'm}(\beta) = d^j_{mm'}(-\beta) = (-1)^{m-m'}d^j_{mm'}(\beta) = (-1)^{m-m'}d^j_{-m',-m}(\beta) \tag{15.117a}$$

and

$$d^j_{m'm}(\beta+\pi) = (-1)^{j-m}d^j_{m',-m}(\beta) = (-1)^{j+m'}d^j_{-m',m}(\beta) \tag{15.117b}$$

follow directly from the formulas (15.94). (We might also add that the first equality of (15.117a) expresses the unitarity of the matrices $d^j_{m'm}$.) From the symmetries (15.117) one may obtain the following important symmetry for the modified angular functions written in terms of the z's:

$$\bar{\psi}^{j_2j_1}_{I,I_3,-Y}(z_1, z_1^*, z_2, z_2^*, z_3, z_3^*) = (-1)^{I-I_3}\psi^{\bar{j}_1j_2}_{II_3Y}(z_1^*, z_1, z_3^*, z_3, z_2^*, z_2). \tag{15.118}$$

In words, performing the exchange $j_1 \leftrightarrow j_2$ and reversing the sign of Y gives the same result as performing the exchange $z_2 \leftrightarrow z_3$, complex conjugating all of the z's, and multiplying by the phase factor[28] $(-1)^{I-I_3}$. This symmetry applies equally well to the dynamical basis polynomials $\psi(j_1, j_2, I, I_3, Y; l)$ of (15.105).

The reader will find in Appendix H the *Mathematica* package `sp6tools.m` which defines the operators and functions necessary to perform all of the calculations in this section. In particular, the function `psi[]` returns the orthonormal dynamical basis polynomials $\psi(j_1, j_2, I, I_3, Y; l)$ of (15.105). Table 15.8 lists those basis elements with $l \in \{0, \ldots, 5\}$ which carry the representations (j_1, j_2) having $j_1 \geq j_2$. The symmetry relation (15.118) determines all of the other basis polynomials which have $l \leq 5$.

[28] If one uses Edmond's convention for the $d^j_{m'm}$, then the phase factor is $(-1)^{I+I_3}$. The statement of the symmetry relation (15.118) as given in [73] omits this factor.

Table 15.8: Orthonormal basis polynomials $\psi(j_1, j_2, I, I_3, Y; l)$ for the space of f_l's ($l \in \{1, \ldots, 5\}$) arranged to carry irreducible representations of $SU(3)$. This table includes only those basis functions which carry representations (j_1, j_2) having $j_1 \geq j_2$. Use the symmetry relation (15.118) to obtain the remaining basis elements.

I	I_3	Y	ψ
$\boxed{l=0}$			
$(j_1,j_2)=(0,0)$			
0	0	0	-1
$\boxed{l=1}$			
$(j_1,j_2)=(1,0)$			
1/2	1/2	1/3	z_2
1/2	−1/2	1/3	$-z_3$
0	0	−2/3	$-z_1$
$\boxed{l=2}$			
$(j_1,j_2)=(2,0)$			
1	1	2/3	$-{z_2}^2/\sqrt{2}$
1	0	2/3	$z_2 z_3$
1	−1	2/3	$-{z_3}^2/\sqrt{2}$
1/2	1/2	−1/3	$z_1 z_2$
1/2	−1/2	−1/3	$-z_1 z_3$
0	0	−4/3	$-{z_1}^2/\sqrt{2}$
$(j_1,j_2)=(1,1)$			
1/2	1/2	1	$z_2 z_1^*$
1/2	−1/2	1	$-z_3 z_1^*$
1	1	0	$-z_2 z_3^*$
1	0	0	$-(z_2 z_2^* - z_3 z_3^*)/\sqrt{2}$
1	−1	0	$z_3 z_2^*$
0	0	0	$-(2z_1 z_1^* - z_2 z_2^* - z_3 z_3^*)/\sqrt{6}$
1/2	1/2	−1	$z_1 z_3^*$
1/2	−1/2	−1	$z_1 z_2^*$
$(j_1,j_2)=(0,0)$			
0	0	0	$-r^2/\sqrt{3}$
$\boxed{l=3}$			
$(j_1,j_2)=(3,0)$			
3/2	3/2	1	${z_2}^3/\sqrt{6}$
3/2	1/2	1	$-{z_2}^2 z_3/\sqrt{2}$
3/2	−1/2	1	$z_2 {z_3}^2/\sqrt{2}$
3/2	−3/2	1	$-{z_3}^3/\sqrt{6}$
1	1	0	$-z_1 {z_2}^2/\sqrt{2}$
1	0	0	$z_1 z_2 z_3$
1	−1	0	$-z_1 {z_3}^2/\sqrt{2}$
1/2	1/2	−1	${z_1}^2 z_2/\sqrt{2}$

$SU(3)$ basis polynomials for the space of f_l's (ctd.)

I	I_3	Y	ψ
$1/2$	$-1/2$	-1	$-{z_1}^2 z_3/\sqrt{2}$
0	0	-2	$-{z_1}^3/\sqrt{6}$
$(j_1,j_2)=(2,1)$			
1	1	$4/3$	$-{z_2}^2 z_1^*/\sqrt{2}$
1	0	$4/3$	$z_2 z_3 z_1^*$
1	-1	$4/3$	$-{z_3}^2 z_1^*/\sqrt{2}$
$3/2$	$3/2$	$1/3$	$z_2{}^2 z_3^*/\sqrt{2}$
$3/2$	$1/2$	$1/3$	$z_2(z_2 z_2^* - 2z_3 z_3^*)/\sqrt{6}$
$3/2$	$-1/2$	$1/3$	$-z_3(2z_2 z_2^* - z_3 z_3^*)/\sqrt{6}$
$3/2$	$-3/2$	$1/3$	$z_3{}^2 z_2^*/\sqrt{2}$
$1/2$	$1/2$	$1/3$	$z_2(3z_1 z_1^* - z_2 z_2^* - z_3 z_3^*)/\sqrt{12}$
$1/2$	$-1/2$	$1/3$	$-z_3(3z_1 z_1^* - z_2 z_2^* - z_3 z_3^*)/\sqrt{12}$
1	1	$-2/3$	$-z_1 z_2 z_3^*$
1	0	$-2/3$	$-z_1(z_2 z_2^* - z_3 z_3^*)/\sqrt{2}$
1	-1	$-2/3$	$z_1 z_3 z_2^*$
0	0	$-2/3$	$-z_1(z_1 z_1^* - z_2 z_2^* - z_3 z_3^*)/\sqrt{4}$
$1/2$	$1/2$	$-5/3$	${z_1}^2 z_3^*/\sqrt{2}$
$1/2$	$-1/2$	$-5/3$	${z_1}^2 z_2^*/\sqrt{2}$
$(j_1,j_2)=(1,0)$			
$1/2$	$1/2$	$1/3$	$r^2 z_2/2$
$1/2$	$-1/2$	$1/3$	$-r^2 z_3/2$
0	0	$-2/3$	$-r^2 z_1/2$
$\boxed{l=4}$			
$(j_1,j_2)=(4,0)$			
2	2	$4/3$	$-{z_2}^4/\sqrt{24}$
2	1	$4/3$	$z_2{}^3 z_3/\sqrt{6}$
2	0	$4/3$	$-{z_2}^2 {z_3}^2/2$
2	-1	$4/3$	$z_2 {z_3}^3/\sqrt{6}$
2	-2	$4/3$	$-{z_3}^4/\sqrt{24}$
$3/2$	$3/2$	$1/3$	$z_1 {z_2}^3/\sqrt{6}$
$3/2$	$1/2$	$1/3$	$-z_1 {z_2}^2 z_3/\sqrt{2}$
$3/2$	$-1/2$	$1/3$	$z_1 z_2 {z_3}^2/\sqrt{2}$
$3/2$	$-3/2$	$1/3$	$-z_1 {z_3}^3/\sqrt{6}$
1	1	$-2/3$	$-{z_1}^2 {z_2}^2/2$
1	0	$-2/3$	${z_1}^2 z_2 z_3/\sqrt{2}$
1	-1	$-2/3$	$-{z_1}^2 {z_3}^2/2$
$1/2$	$1/2$	$-5/3$	${z_1}^3 z_2/\sqrt{6}$
$1/2$	$-1/2$	$-5/3$	$-{z_1}^3 z_3/\sqrt{6}$
0	0	$-8/3$	$-{z_1}^4/\sqrt{24}$
$(j_1,j_2)=(3,1)$			
$3/2$	$3/2$	$5/3$	$z_2{}^3 z_1^*/\sqrt{6}$
$3/2$	$1/2$	$5/3$	$-{z_2}^2 z_3 z_1^*/\sqrt{2}$

$SU(3)$ basis polynomials for the space of f_l's (ctd.)

I	I_3	Y	ψ
$3/2$	$-1/2$	$5/3$	$z_2{z_3}^2{z_1}^*/\sqrt{2}$
$3/2$	$-3/2$	$5/3$	$-{z_3}^3{z_1}^*/\sqrt{6}$
2	2	$2/3$	$-{z_2}^3{z_3}^*/\sqrt{6}$
2	1	$2/3$	$-{z_2}^2(z_2{z_2}^* - 3z_3{z_3}^*)/\sqrt{24}$
2	0	$2/3$	$z_2z_3(z_2{z_2}^* - z_3{z_3}^*)/\sqrt{4}$
2	-1	$2/3$	$-{z_3}^2(3z_2{z_2}^* - z_3{z_3}^*)/\sqrt{24}$
2	-2	$2/3$	${z_3}^3{z_2}^*/\sqrt{6}$
1	1	$2/3$	$-{z_2}^2(4z_1{z_1}^* - z_2{z_2}^* - z_3{z_3}^*)/\sqrt{40}$
1	0	$2/3$	$z_2z_3(4z_1{z_1}^* - z_2{z_2}^* - z_3{z_3}^*)/\sqrt{20}$
1	-1	$2/3$	$-{z_3}^2(4z_1{z_1}^* - z_2{z_2}^* - z_3{z_3}^*)/\sqrt{40}$
$3/2$	$3/2$	$-1/3$	$z_1{z_2}^2{z_3}^*/\sqrt{2}$
$3/2$	$1/2$	$-1/3$	$z_1z_2(z_2{z_2}^* - 2z_3{z_3}^*)/\sqrt{6}$
$3/2$	$-1/2$	$-1/3$	$-z_1z_3(2z_2{z_2}^* - z_3{z_3}^*)/\sqrt{6}$
$3/2$	$-3/2$	$-1/3$	$z_1{z_3}^2{z_2}^*/\sqrt{2}$
$1/2$	$1/2$	$-1/3$	$z_1z_2(3z_1{z_1}^* - 2(z_2{z_2}^* + z_3{z_3}^*))/\sqrt{30}$
$1/2$	$-1/2$	$-1/3$	$-z_1z_3(3z_1{z_1}^* - 2(z_2{z_2}^* + z_3{z_3}^*))/\sqrt{30}$
1	1	$-4/3$	$-{z_1}^2z_2{z_3}^*/\sqrt{2}$
1	0	$-4/3$	$-{z_1}^2(z_2{z_2}^* - z_3{z_3}^*)/\sqrt{4}$
1	-1	$-4/3$	${z_1}^2z_3{z_2}^*/\sqrt{2}$
0	0	$-4/3$	$-{z_1}^2(2z_1{z_1}^* - 3(z_2{z_2}^* + z_3z_3*))/\sqrt{60}$
$1/2$	$1/2$	$-7/3$	${z_1}^3{z_3}^*/\sqrt{6}$
$1/2$	$-1/2$	$-7/3$	${z_1}^3{z_2}^*/\sqrt{6}$
$(j_1, j_2) = (2, 2)$			
1	1	2	$-{z_2}^2{{z_1}^*}^2/2$
1	0	2	$z_2z_3{{z_1}^*}^2/\sqrt{2}$
1	-1	2	$-{z_3}^2{{z_1}^*}^2/2$
$3/2$	$3/2$	1	${z_2}^2z_1^*{z_3}^*/\sqrt{2}$
$3/2$	$1/2$	1	$z_2z_1^*(z_2{z_2}^* - 2z_3{z_3}^*)/\sqrt{6}$
$3/2$	$-1/2$	1	$-z_3z_1^*(2z_2{z_2}^* - z_3{z_3}^*)/\sqrt{6}$
$3/2$	$-3/2$	1	${z_3}^2z_1^*{z_2}^*/\sqrt{2}$
$1/2$	$1/2$	1	$z_2z_1^*(3z_1{z_1}^* - 2(z_2{z_2}^* + z_3{z_3}^*))/\sqrt{30}$
$1/2$	$-1/2$	1	$-z_3z_1^*(3z_1{z_1}^* - 2(z_2{z_2}^* + z_3{z_3}^*))/\sqrt{30}$
2	2	0	$-{z_2}^2{{z_3}^*}^2/2$
2	1	0	$-z_2{z_3}^*(z_2{z_2}^* - z_3{z_3}^*)/\sqrt{4}$
2	0	0	$-({z_2}^2{{z_2}^*}^2 - 4z_2z_3{z_2}^*{z_3}^* + {z_3}^2{{z_3}^*}^2)/\sqrt{24}$
2	-1	0	$z_3{z_2}^*(z_2{z_2}^* - z_3{z_3}^*)/\sqrt{4}$
2	-2	0	$-{z_3}^2{{z_2}^*}^2/2$
1	1	0	$-z_2{z_3}^*(4z_1{z_1}^* - z_2{z_2}^* - z_3{z_3}^*)/\sqrt{20}$
1	0	0	$-(z_2{z_2}^* - z_3{z_3}^*)(4z_1{z_1}^* - z_2{z_2}^* - z_3{z_3}^*)/\sqrt{40}$
1	-1	0	$z_3{z_2}^*(4z_1{z_1}^* - z_2{z_2}^* - z_3{z_3}^*)/\sqrt{20}$
0	0	0	$-(3{z_1}^2{{z_1}^*}^2 - 6z_1z_1^*(z_2{z_2}^* + z_3{z_3}^*) + (z_2{z_2}^* + z_3{z_3}^*)^2)/\sqrt{120}$
$3/2$	$3/2$	-1	$z_1z_2{{z_3}^*}^2/\sqrt{2}$

$SU(3)$ basis polynomials for the space of f_l's (ctd.)

I	I_3	Y	ψ
$3/2$	$1/2$	-1	$z_1 z_3^*(2z_2 z_2^* - z_3 z_3^*)/\sqrt{6}$
$3/2$	$-1/2$	-1	$z_1 z_2^*(z_2 z_2^* - 2z_3 z_3^*)/\sqrt{6}$
$3/2$	$-3/2$	-1	$-z_1 z_3 {z_2^*}^2/\sqrt{2}$
$1/2$	$1/2$	-1	$z_1 z_3^*(3z_1 z_1^* - 2(z_2 z_2^* + z_3 z_3^*))/\sqrt{30}$
$1/2$	$-1/2$	-1	$z_1 z_2^*(3z_1 z_1^* - 2(z_2 z_2^* + z_3 z_3^*))/\sqrt{30}$
1	1	-2	$-{z_1}^2 {z_3^*}^2/2$
1	0	-2	$-{z_1}^2 z_2^* z_3^*/\sqrt{2}$
1	-1	-2	$-{z_1}^2 {z_2^*}^2/2$
$(j_1, j_2) = (2, 0)$			
1	1	$2/3$	$-r^2 {z_2}^2/\sqrt{10}$
1	0	$2/3$	$r^2 z_2 z_3/\sqrt{5}$
1	-1	$2/3$	$-r^2 {z_3}^2/\sqrt{10}$
$1/2$	$1/2$	$-1/3$	$r^2 z_1 z_2/\sqrt{5}$
$1/2$	$-1/2$	$-1/3$	$-r^2 z_1 z_3/\sqrt{5}$
0	0	$-4/3$	$-r^2 {z_1}^2/\sqrt{10}$
$(j_1, j_2) = (1, 1)$			
$1/2$	$1/2$	1	$r^2 z_2 z_1^*/\sqrt{5}$
$1/2$	$-1/2$	1	$-r^2 z_3 z_1^*/\sqrt{5}$
1	1	0	$-r^2 z_2 z_3^*/\sqrt{5}$
1	0	0	$-r^2(z_2 z_2^* - z_3 z_3^*)/\sqrt{10}$
1	-1	0	$r^2 z_3 z_2^*/\sqrt{5}$
0	0	0	$-r^2(2z_1 z_1^* - z_2 z_2^* - z_3 z_3^*)/\sqrt{30}$
$1/2$	$1/2$	-1	$r^2 z_1 z_3^*/\sqrt{5}$
$1/2$	$-1/2$	-1	$r^2 z_1 z_2^*/\sqrt{5}$
$(j_1, j_2) = (0, 0)$			
0	0	0	$-r^4/\sqrt{24}$
$\boxed{l = 5}$			
$(j_1, j_2) = (5, 0)$			
$5/2$	$5/2$	$5/3$	${z_2}^5/\sqrt{120}$
$5/2$	$3/2$	$5/3$	$-{z_2}^4 z_3/\sqrt{24}$
$5/2$	$1/2$	$5/3$	${z_2}^3 {z_3}^2/\sqrt{12}$
$5/2$	$-1/2$	$5/3$	$-{z_2}^2 {z_3}^3/\sqrt{12}$
$5/2$	$-3/2$	$5/3$	$z_2 {z_3}^4/\sqrt{24}$
$5/2$	$-5/2$	$5/3$	$-{z_3}^5/\sqrt{120}$
2	2	$2/3$	$-z_1 {z_2}^4/\sqrt{24}$
2	1	$2/3$	${z_1 z_2}^3 z_3/\sqrt{6}$
2	0	$2/3$	$-z_1 {z_2}^2 {z_3}^2/2$
2	-1	$2/3$	$z_1 z_2 {z_3}^3/\sqrt{6}$
2	-2	$2/3$	$-z_1 {z_3}^4/\sqrt{24}$
$3/2$	$3/2$	$-1/3$	${z_1}^2 {z_2}^3/\sqrt{12}$
$3/2$	$1/2$	$-1/3$	$-{z_1}^2 {z_2}^2 z_3/2$
$3/2$	$-1/2$	$-1/3$	${z_1}^2 z_2 {z_3}^2/2$

$SU(3)$ basis polynomials for the space of f_l's (ctd.)

I	I_3	Y	ψ
$3/2$	$-3/2$	$-1/3$	$-{z_1}^2{z_3}^3/\sqrt{12}$
1	1	$-4/3$	$-{z_1}^3{z_2}^2/\sqrt{12}$
1	0	$-4/3$	${z_1}^3z_2z_3/\sqrt{6}$
1	-1	$-4/3$	$-{z_1}^3{z_3}^2/\sqrt{12}$
$1/2$	$1/2$	$-7/3$	${z_1}^4z_2/\sqrt{24}$
$1/2$	$-1/2$	$-7/3$	$-{z_1}^4z_3/\sqrt{24}$
0	0	$-10/3$	$-{z_1}^5/\sqrt{120}$
$(j_1, j_2) = (4, 1)$			
2	2	2	$-{z_2}^4z_1^*/\sqrt{24}$
2	1	2	${z_2}^3z_3z_1^*/\sqrt{6}$
2	0	2	$-{z_2}^2{z_3}^2z_1^*/2$
2	-1	2	$z_2{z_3}^3z_1^*/\sqrt{6}$
2	-2	2	$-{z_3}^4z_1^*/\sqrt{24}$
$5/2$	$5/2$	1	${z_2}^4z_3^*/\sqrt{24}$
$5/2$	$3/2$	1	${z_2}^3(z_2z_2^* - 4z_3z_3^*)/\sqrt{120}$
$5/2$	$1/2$	1	$-{z_2}^2z_3(2z_2z_2^* - 3z_3z_3^*)/\sqrt{60}$
$5/2$	$-1/2$	1	$z_2{z_3}^2(3z_2z_2^* - 2z_3z_3^*)/\sqrt{60}$
$5/2$	$-3/2$	1	$-{z_3}^3(4z_2z_2^* - z_3z_3^*)/\sqrt{120}$
$5/2$	$-5/2$	1	${z_3}^4z_2^*/\sqrt{24}$
$3/2$	$3/2$	1	${z_2}^3(5z_1z_1^* - z_2z_2^* - z_3z_3^*)/\sqrt{180}$
$3/2$	$1/2$	1	$-{z_2}^2z_3(5z_1z_1^* - z_2z_2^* - z_3z_3^*)/\sqrt{60}$
$3/2$	$-1/2$	1	$z_2{z_3}^2(5z_1z_1^* - z_2z_2^* - z_3z_3^*)/\sqrt{60}$
$3/2$	$-3/2$	1	$-{z_3}^3(5z_1z_1^* - z_2z_2^* - z_3z_3^*)/\sqrt{180}$
2	2	0	$-z_1{z_2}^3z_3^*/\sqrt{6}$
2	1	0	$-z_1{z_2}^2(z_2z_2^* - 3z_3z_3^*)/\sqrt{24}$
2	0	0	$z_1z_2z_3(z_2z_2^* - z_3z_3^*)/2$
2	-1	0	$-z_1z_3{}^2(3z_2z_2^* - z_3z_3^*)/\sqrt{24}$
2	-2	0	$z_1{z_3}^3z_2^*/\sqrt{6}$
1	1	0	$-z_1{z_2}^2(2z_1z_1^* - z_2z_2^* - z_3z_3^*)/\sqrt{24}$
1	0	0	$z_1z_2z_3(2z_1z_1^* - z_2z_2^* - z_3z_3^*)/\sqrt{12}$
1	-1	0	$-z_1z_3{}^2(2z_1z_1^* - z_2z_2^* - z_3z_3^*)/\sqrt{24}$
$3/2$	$3/2$	-1	${z_1}^2{z_2}^2z_3^*/2$
$3/2$	$1/2$	-1	${z_1}^2z_2(z_2z_2^* - 2z_3z_3^*)/\sqrt{12}$
$3/2$	$-1/2$	-1	$-{z_1}^2z_3(2z_2z_2^* - z_3z_3^*)/\sqrt{12}$
$3/2$	$-3/2$	-1	${z_1}^2{z_3}^2z_2^*/2$
$1/2$	$1/2$	-1	${z_1}^2z_2(z_1z_1^* - z_2z_2^* - z_3z_3^*)/\sqrt{12}$
$1/2$	$-1/2$	-1	$-{z_1}^2z_3(z_1z_1^* - z_2z_2^* - z_3z_3^*)/\sqrt{12}$
1	1	-2	$-{z_1}^3z_2z_3^*/\sqrt{6}$
1	0	-2	$-{z_1}^3(z_2z_2^* - z_3z_3^*)/\sqrt{12}$
1	-1	-2	${z_1}^3z_3z_2^*/\sqrt{6}$
0	0	-2	$-{z_1}^3(z_1z_1^* - 2(z_2z_2^* + z_3z_3^*))/\sqrt{72}$
$1/2$	$1/2$	-3	${z_1}^4z_3^*/\sqrt{24}$
$1/2$	$-1/2$	-3	${z_1}^4z_2^*/\sqrt{24}$

$SU(3)$ basis polynomials for the space of f_l's (ctd.)

I	I_3	Y	ψ
$(j_1, j_2) = (3, 2)$			
3/2	3/2	7/3	$z_2{}^3 z_1^{*2}/\sqrt{12}$
3/2	1/2	7/3	$-z_2{}^2 z_3 z_1^{*2}/2$
3/2	−1/2	7/3	$z_2 z_3{}^2 z_1^{*2}/2$
3/2	−3/2	7/3	$-z_3{}^3 z_1^{*2}/\sqrt{12}$
2	2	4/3	$-z_2{}^3 z_1^* z_3^*/\sqrt{6}$
2	1	4/3	$-z_2{}^2 z_1^*(z_2 z_2^* - 3 z_3 z_3^*)/\sqrt{24}$
2	0	4/3	$z_2 z_3 z_1^*(z_2 z_2^* - z_3 z_3^*)/2$
2	−1	4/3	$-z_3{}^2 z_1^*(3 z_2 z_2^* - z_3 z_3^*)/\sqrt{24}$
2	−2	4/3	$z_3{}^3 z_1^* z_2^*/\sqrt{6}$
1	1	4/3	$-z_2{}^2 z_1^*(2 z_1 z_1^* - z_2 z_2^* - z_3 z_3^*)/\sqrt{24}$
1	0	4/3	$z_2 z_3 z_1^*(2 z_1 z_1^* - z_2 z_2^* - z_3 z_3^*)/\sqrt{12}$
1	−1	4/3	$-z_3{}^2 z_1^*(2 z_1 z_1^* - z_2 z_2^* - z_3 z_3^*)/\sqrt{24}$
5/2	5/2	1/3	$z_2{}^3 z_3^{*2}/\sqrt{12}$
5/2	3/2	1/3	$z_2{}^2 z_3^*(2 z_2 z_2^* - 3 z_3 z_3^*)/\sqrt{60}$
5/2	1/2	1/3	$z_2(z_2{}^2 z_2^{*2} - 6 z_2 z_3 z_2^* z_3^* + 3 z_3{}^2 z_3^{*2})/\sqrt{120}$
5/2	−1/2	1/3	$-z_3(3 z_2{}^2 z_2^{*2} - 6 z_2 z_3 z_2^* z_3^* + z_3{}^2 z_3^{*2})/\sqrt{120}$
5/2	−3/2	1/3	$z_3{}^2 z_2^*(3 z_2 z_2^* - 2 z_3 z_3^*)/\sqrt{60}$
5/2	−5/2	1/3	$-z_3{}^3 z_2^{*2}/\sqrt{12}$
3/2	3/2	1/3	$z_2{}^2 z_3^*(5 z_1 z_1^* - z_2 z_2^* - z_3 z_3^*)/\sqrt{60}$
3/2	1/2	1/3	$z_2(z_2 z_2^* - 2 z_3 z_3^*)(5 z_1 z_1^* - z_2 z_2^* - z_3 z_3^*)/\sqrt{180}$
3/2	−1/2	1/3	$-z_3(2 z_2 z_2^* - z_3 z_3^*)(5 z_1 z_1^* - z_2 z_2^* - z_3 z_3^*)/\sqrt{180}$
3/2	−3/2	1/3	$z_3{}^2 z_2^*(5 z_1 z_1^* - z_2 z_2^* - z_3 z_3^*)/\sqrt{60}$
1/2	1/2	1/3	$z_2(6 z_1{}^2 z_1^{*2} - 8 z_1 z_1^*(z_2 z_2^* + z_3 z_3^*) + (z_2 z_2^* + z_3 z_3^*)^2)/\sqrt{360}$
1/2	−1/2	1/3	$-z_3(6 z_1{}^2 z_1^{*2} - 8 z_1 z_1^*(z_2 z_2^* + z_3 z_3^*) + (z_2 z_2^* + z_3 z_3^*)^2)/\sqrt{360}$
2	2	−2/3	$-z_1 z_2{}^2 z_3^{*2}/2$
2	1	−2/3	$-z_1 z_2 z_3^*(z_2 z_2^* - z_3 z_3^*)/2$
2	0	−2/3	$-z_1(z_2{}^2 z_2^{*2} - 4 z_2 z_3 z_2^* z_3^* + z_3{}^2 z_3^{*2})/\sqrt{24}$
2	−1	−2/3	$z_1 z_3 z_2^*(z_2 z_2^* - z_3 z_3^*)/2$
2	−2	−2/3	$-z_1 z_3{}^2 z_2^{*2}/2$
1	1	−2/3	$-z_1 z_2 z_3^*(2 z_1 z_1^* - z_2 z_2^* - z_3 z_3^*)/\sqrt{12}$
1	0	−2/3	$-z_1(z_2 z_2^* - z_3 z_3^*)(2 z_1 z_1^* - z_2 z_2^* - z_3 z_3^*)/\sqrt{24}$
1	−1	−2/3	$z_1 z_3 z_2^*(2 z_1 z_1^* - z_2 z_2^* - z_3 z_3^*)/\sqrt{12}$
0	0	−2/3	$-z_1(z_1{}^2 z_1^{*2} - 3 z_1 z_1^*(z_2 z_2^* + z_3 z_3^*) + (z_2 z_2^* + z_3 z_3^*)^2)/\sqrt{60}$
3/2	3/2	−5/3	$z_1{}^2 z_2 z_3^{*2}/2$
3/2	1/2	−5/3	$z_1{}^2 z_3^*(2 z_2 z_2^* - z_3 z_3^*)/\sqrt{12}$
3/2	−1/2	−5/3	$z_1{}^2 z_2^*(z_2 z_2^* - 2 z_3 z_3^*)/\sqrt{12}$
3/2	−3/2	−5/3	$-z_1{}^2 z_3 z_2^{*2}/2$
1/2	1/2	−5/3	$z_1{}^2 z_3^*(z_1 z_1^* - z_2 z_2^* - z_3 z_3^*)/\sqrt{12}$
1/2	−1/2	−5/3	$z_1{}^2 z_2^*(z_1 z_1^* - z_2 z_2^* - z_3 z_3^*)/\sqrt{12}$
1	1	−8/3	$-z_1{}^3 z_3^{*2}/\sqrt{12}$

$SU(3)$ basis polynomials for the space of f_l's (ctd.)

I	I_3	Y	ψ
1	0	$-8/3$	$-{z_1}^3 z_2^* z_3^*/\sqrt{6}$
1	-1	$-8/3$	$-{z_1}^3 {z_2^*}^2/\sqrt{12}$
$(j_1, j_2) = (3, 0)$			
3/2	3/2	1	$r^2 {z_2}^3/6$
3/2	1/2	1	$-r^2 {z_2}^2 z_3/\sqrt{12}$
3/2	$-1/2$	1	$r^2 z_2 {z_3}^2/\sqrt{12}$
3/2	$-3/2$	1	$-r^2 {z_3}^3/6$
1	1	0	$-r^2 z_1 {z_2}^2/\sqrt{12}$
1	0	0	$r^2 z_1 z_2 z_3/\sqrt{6}$
1	-1	0	$-r^2 z_1 {z_3}^2/\sqrt{12}$
1/2	1/2	-1	$r^2 {z_1}^2 z_2/\sqrt{12}$
1/2	$-1/2$	-1	$-r^2 {z_1}^2 z_3/\sqrt{12}$
0	0	-2	$-r^2 {z_1}^3/6$
$(j_1, j_2) = (2, 1)$			
1	1	4/3	$-r^2 {z_2}^2 z_1^*/\sqrt{12}$
1	0	4/3	$r^2 z_2 z_3 z_1^*/\sqrt{6}$
1	-1	4/3	$-r^2 {z_3}^2 z_1^*/\sqrt{12}$
3/2	3/2	1/3	$r^2 {z_2}^2 z_3^*/\sqrt{12}$
3/2	1/2	1/3	$r^2 z_2 (z_2 z_2^* - 2 z_3 z_3^*)/6$
3/2	$-1/2$	1/3	$-r^2 z_3 (2 z_2 z_2^* - z_3 z_3^*)/6$
3/2	$-3/2$	1/3	$r^2 {z_3}^2 z_2^*/\sqrt{12}$
1/2	1/2	1/3	$r^2 z_2 (3 z_1 z_1^* - z_2 z_2^* - z_3 z_3^*)/\sqrt{72}$
1/2	$-1/2$	1/3	$-r^2 z_3 (3 z_1 z_1^* - z_2 z_2^* - z_3 z_3^*)/\sqrt{72}$
1	1	$-2/3$	$-r^2 z_1 z_2 z_3^*/\sqrt{6}$
1	0	$-2/3$	$-r^2 z_1 (z_2 z_2^* - z_3 z_3^*)/\sqrt{12}$
1	-1	$-2/3$	$r^2 z_1 z_3 z_2^*/\sqrt{6}$
0	0	$-2/3$	$-r^2 z_1 (z_1 z_1^* - z_2 z_2^* - z_3 z_3^*)/\sqrt{24}$
1/2	1/2	$-5/3$	$r^2 {z_1}^2 z_3^*/\sqrt{12}$
1/2	$-1/2$	$-5/3$	$r^2 {z_1}^2 z_2^*/\sqrt{12}$
$(j_1, j_2) = (1, 0)$			
1/2	1/2	1/3	$r^4 z_2/\sqrt{40}$
1/2	$-1/2$	1/3	$-r^4 z_3/\sqrt{40}$
0	0	$-2/3$	$-r^4 z_1/\sqrt{40}$

15.3.2. *The Gram Matrix and its Eigenvalues for the Case* $\mathcal{U} = SU(3)/SO(3)$. Let us now evaluate the Gram operator $\widehat{\Gamma}(l)$ of (15.90) with respect to the orthonormal basis polynomials (15.105) described in §15.3.1. As mentioned earlier, we shall integrate over the whole of $\mathcal{U} = SU(3)$, but Theorem 13.1 assures us that setting $\mathcal{U} = SU(3)/SO(3)$ will produce the same results.

For the sake of brevity, let us agree temporarily to abbreviate the basis polynomials $\psi(j_1, j_2, I, I_3, Y; l)$ by ψ^j_μ. Here j labels the representation and stands for the pair (j_1, j_2); likewise, μ labels the the basis elements within the representation and stands for the trio (I, I_3, Y). The degree l we shall make clear from the context. In the same manner we shall abbreviate $\psi(j_1', j_2', I', I_3', Y')$ by $\psi^{j'}_{\mu'}$. Using these abbreviations and the fact that the ψ's

carry irreducible representations of $SU(3)$, we may write the action on ψ^j_μ by the linear Lie transformation $\mathcal{L}(u)$ in the form (*cf.* (15.49))

$$\mathcal{L}(u)\psi^j_\mu = \sum_\nu D^j(u)_{\mu\nu}\psi^j_\nu. \tag{15.119}$$

Here we abbreviate the matrix representation of $SU(3)$ in a fashion similar to the ψ's: The symbol $D^j(u)$ thus stands for the (unitary) matrix corresponding to the element u in the $SU(3)$ representation (j_1, j_2); and the subscripts μ and ν label the different triplets of (I, I_3, Y) that index the matrix entries in $D^j(u)$.

Using (15.90), (E.6), and the abbreviations described above, we obtain the Gram matrix elements with respect to the basis polynomials ψ of (15.105):

$$\begin{aligned}\Gamma(l)_{j\mu,j'\mu'} &= \langle\psi^j_\mu|\widehat{\Gamma}(l)|\psi^{j'}_{\mu'}\rangle \\ &= \frac{2}{(l+1)(l+2)}\sum_k \int_{SU(3)} du \left\langle \mathcal{L}(u^{-1})\psi^j_\mu, Q^{(l)}_k\right\rangle\left\langle Q^{(l)}_k, \mathcal{L}(u^{-1})\psi^{j'}_{\mu'}\right\rangle.\end{aligned} \tag{15.120}$$

We can apply to (15.120) essentially the exact same argument as was given in the case $n = 2$ between equations (15.61) and (15.63). The present argument will differ on only the following two points: (i) the $n = 3$ case does *not* have an extra label to distinguish different copies of a given representation (see Theorem 15.1); (ii) we must use the formula (15.91) for the dimensionality $d(j_1, j_2)$ of the representation labeled by $j\,(\equiv (j_1, j_2))$. Therefore, after performing the integration over $SU(3)$, we obtain the result

$$\Gamma(l)_{j\mu,j'\mu'} = \frac{\delta_{jj'}\delta_{\mu\mu'}2}{(l+1)(l+2)d(j_1,j_2)}\sum_{k\nu}\left|\langle\psi^j_\nu, Q^{(l)}_k\rangle\right|^2. \tag{15.121}$$

Note that the ψ^j_μ basis diagonalizes the Gram operator. Hence we obtain immediately the Gram eigenvalues:

$$\lambda^{(l)}_{j_1j_2} = \frac{2}{(l+1)(l+2)d(j_1,j_2)}\sum_{k\nu}\left|\langle\psi^j_\nu, Q^{(l)}_k\rangle\right|^2. \tag{15.122}$$

Since the eigenvalues do not depend on $\mu\,(\equiv (I, I_3, Y))$, each has an associated degeneracy of $d(j_1, j_2)$.

Before computing the Gram eigenvalues, we make three observations about the formula (15.122). The first concerns an additional degeneracy in the eigenvalue spectrum that approximately halves the number of eigenvalues we need to compute. The second shows that we need not sum over all the $Q^{(l)}_k$. And the third shows that we need not sum over all the $\nu\,(\equiv (I, I_3, Y))$. Together these three observations lead to a considerable computational savings, and we demonstrate each in turn.

To prove the first observation, simply apply the symmetry relation (15.118) to our formula for the eigenvalues, and use the fact that $d(j_1, j_2) = d(j_2, j_1)$:

$$\begin{aligned}\lambda^{(l)}_{j_2j_1} &= \frac{2}{(l+1)(l+2)d(j_2,j_1)}\sum_{k_2k_3}\sum_{II_3Y}\left|\langle\psi(j_2,j_1,I,I_3,Y;l), Q^{(l)}_{k_2k_3}\rangle\right|^2 \\ &= \frac{2}{(l+1)(l+2)d(j_1,j_2)}\sum_{k_2k_3}\sum_{II_3Y}\left|\langle(-1)^{I-I_3}\psi(j_1,j_2,I,I_3,-Y;l), Q^{(l)}_{k_2k_3}\rangle\right|^2 \\ &= \lambda^{(l)}_{j_1j_2}.\end{aligned} \tag{15.123}$$

We conclude that eigenvalues with $j_1 \neq j_2$ have a degeneracy of $2d(j_1, j_2)$, while eigenvalues with $j_1 = j_2$ have a degeneracy of just $d(j_1, j_2)$. One therefore need not compute (15.122) for, say, $j_1 < j_2$.

We now show that one need not sum over all the $Q_k^{(l)}$ in order to obtain the Gram eigenvalues (15.122). To verify this, consider the linear symplectic Lie transformation $\mathcal{P}_c = \mathcal{L}(u_c)$ determined by the orthogonal matrix

$$u_c = \begin{pmatrix} 0 & 1 & 0 \\ 0 & 0 & 1 \\ 1 & 0 & 0 \end{pmatrix}.$$

By definition $\mathcal{P}_c$ belongs to the $SO(3)$ subgroup of $Sp(6,\mathbb{R})$. Because $\mathcal{L}(u)$ stands for $\mathcal{L}(M(u))$, we can use (13.11) to determine the action of $\mathcal{P}_c$ on the q's and p's:

$$\mathcal{P}_c \begin{pmatrix} q_1 \\ q_2 \\ q_3 \\ p_1 \\ p_2 \\ p_3 \end{pmatrix} = M(u_c) \begin{pmatrix} q_1 \\ q_2 \\ q_3 \\ p_1 \\ p_2 \\ p_3 \end{pmatrix} = \begin{pmatrix} q_2 \\ q_3 \\ q_1 \\ p_2 \\ p_3 \\ p_1 \end{pmatrix}.$$

In words, $\mathcal{P}_c$ effects a cyclic permutation on the indices for the q's and, separately, also for the p's. It can be shown that $\mathcal{P}_c$ is indeed a Lie transformation and that in fact

$$\mathcal{P}_c = \exp\Big(\frac{2\pi}{3\sqrt{3}} :q_1(p_2 - p_3) + q_2(p_3 - p_1) + q_3(p_1 - p_2):\Big). \tag{15.124}$$

Since $\mathcal{P}_c$ simply permutes indices, $\mathcal{P}_c Q_k^{(l)}$ must be another one of the $Q^{(l)}$'s—call it $Q_{k'}^{(l)}$. Now consider just the sum over ν in (15.122). Because $\mathcal{P}_c$ belongs to $SO(3)$, hence also to $SU(3)$, we can use (10.10), (15.119), and the unitarity of the the representation $D^j(u)$ to obtain

$$\begin{aligned} \sum_\nu \big|\langle \psi_\nu^j, Q_k^{(l)}\rangle\big|^2 &= \sum_\nu \big|\langle \mathcal{P}_c\psi_\nu^j, \mathcal{P}_c Q_k^{(l)}\rangle\big|^2 = \sum_\nu \Big|\Big\langle \sum_{\nu'} D^j(u_c)_{\nu\nu'}\psi_{\nu'}^j, Q_{k'}^{(l)}\Big\rangle\Big|^2 \\ &= \sum_{\nu'}\sum_\nu \big|D^j(u_c)_{\nu\nu'}\big|^2 \big|\langle \psi_{\nu'}^j, Q_{k'}^{(l)}\rangle\big|^2 = \sum_{\nu'} \big|\langle \psi_{\nu'}^j, Q_{k'}^{(l)}\rangle\big|^2 = \sum_\nu \big|\langle \psi_\nu^j, \mathcal{P}_c Q_k^{(l)}\rangle\big|^2. \end{aligned}$$

This result tells us that if $Q_k^{(l)}$ and $Q_{k'}^{(l)}$ differ only by a cyclic permutation of q-indices, then they contribute equal amounts to the Gram eigenvalues (15.122).

Now consider three other Linear symplectic transformations:

$$\begin{aligned} \mathcal{P}_1 &= e^{\pi/2 :q_2p_3 - q_3p_2:}, \\ \mathcal{P}_2 &= e^{\pi/2 :q_3p_1 - q_1p_3:}, \\ \mathcal{P}_3 &= e^{\pi/2 :q_1p_2 - q_2p_1:}. \end{aligned} \tag{15.125}$$

For each of these $\mathcal{P}_a$ the Hermiticity of the Lie polynomial in the exponent (*cf.* (10.12)) guarantees that $\mathcal{P}_a$ belongs to the $SU(3)$ subgroup of $Sp(6,\mathbb{R})$. (In fact each belongs to the $SO(3)$ subgroup.) Using an argument similar to that in Appendix D, one can sum the exponential series (9.3) for each of the $\mathcal{P}_a$ to determine their action on the q's and p's:

$$\mathcal{P}_1 \begin{pmatrix} q_1 \\ q_2 \\ q_3 \\ p_1 \\ p_2 \\ p_3 \end{pmatrix} = \begin{pmatrix} q_1 \\ q_3 \\ -q_2 \\ p_1 \\ p_3 \\ -p_2 \end{pmatrix}, \quad \mathcal{P}_2 \begin{pmatrix} q_1 \\ q_2 \\ q_3 \\ p_1 \\ p_2 \\ p_3 \end{pmatrix} = \begin{pmatrix} -q_3 \\ q_2 \\ q_1 \\ -p_3 \\ p_2 \\ p_1 \end{pmatrix}, \quad \mathcal{P}_3 \begin{pmatrix} q_1 \\ q_2 \\ q_3 \\ p_1 \\ p_2 \\ p_3 \end{pmatrix} = \begin{pmatrix} q_2 \\ -q_1 \\ q_3 \\ p_2 \\ -p_1 \\ p_3 \end{pmatrix}.$$

Note that $\mathcal{P}_a$ leaves q_a alone and, modulo a sign, swaps the other two q's; it acts similarly on the p's. It follows that each $\mathcal{P}_a$ converts $Q_k^{(l)}$ into another one of the $Q^{(l)}$'s (modulo a sign).

Applying to the $\mathcal{P}_a$ in the last paragraph the argument used for $\mathcal{P}_c$, we now conclude that if $Q_k^{(l)}$ and $Q_{k'}^{(l)}$ differ by *any* permutation of their q-indices, then they contribute the

same amount to the Gram eigenvalues (15.122). We may therefore group the $Q_k^{(l)}$ into classes according to the equivalence relation $Q_k^{(l)} \sim Q_{k'}^{(l)}$ if one can be obtained from the other by permuting the indices on the q's. Now suppose that class c contains N_c elements and that $Q_c^{(l)}$ denotes a representative element. We may then write the Gram eigenvalues (15.122) in the form

$$\lambda_{j_1 j_2}^{(l)} = \frac{2}{(l+1)(l+2)d(j_1,j_2)} \sum_c N_c \sum_\nu \left|\langle \psi_\nu^j, Q_c^{(l)} \rangle\right|^2. \tag{15.126}$$

To prove our last observation—that one need not sum over all the ψ_ν^j in order to compute the Gram eigenvalues—use (15.97a) to expand the $Q_k^{(l)}$ of (15.89) in terms of the z's. One obtains the result

$$\begin{aligned} Q_{k_2 k_3}^{(l)} &= \frac{(1/\sqrt{2})^l}{\sqrt{(l-k_2-k_3)!\,k_2!\,k_3!}} (z_1 + z_1^*)^{l-k_2-k_3} (z_2 + z_2^*)^{k_2} (z_3 + z_3^*)^{k_3} \\ &= \frac{(1/2)^{l/2}}{\sqrt{(l-k_2-k_3)!\,k_2!\,k_3!}} \sum_{r_1 r_2 r_3} \binom{l-k_2-k_3}{r_1} \binom{k_2}{r_2} \binom{k_3}{r_3} \times \\ &\qquad\qquad z_1^{\,l-k_2-k_3-r_1} z_2^{\,k_2-r_2} z_3^{\,k_3-r_3} z_1^{*r_1} z_2^{*r_2} z_3^{*r_3} \end{aligned}$$

Using (15.112), we can determine the $\widehat{I}_3$ eigenvalues for each term in this sum:

$$I_3 = \frac{1}{2}(k_2 - r_2 - k_3 + r_3 - r_2 + r_3) = \frac{1}{2}(k_2 - k_3) - (r_2 - r_3).$$

Therefore as $(r_2 - r_3)$ ranges from $-k_3$ to $+k_2$, I_3 covers the values

$$I_3 \in \left\{-\tfrac{1}{2}(k_2+k_3), \ldots, \tfrac{1}{2}(k_2+k_3)\right\} \tag{15.127}$$

in unit increments. In other words, we need not include in the sum over ν in (15.126) any ψ_ν^j whose I_3 value does not belong to the range given in (15.127).[29]

One may perform for the eigenvalues Y an analysis identical to that just given for the eigenvalues I_3. Using (15.112), we find

$$\begin{aligned} Y &= \frac{1}{3}(-2l + 2k_2 + 2k_3 + 2r_1 + k_2 - r_2 + k_3 - r_3 + 2r_1 - r_2 - r_3) \\ &= -\frac{2}{3}l + (k_2 + k_3) + \frac{2}{3}(2r_1 - r_2 - r_3). \end{aligned}$$

As $(2r_1 - r_2 - r_3)$ ranges from $-(k_2+k_3)$ to $2(l-k_2-k_3)$, Y covers the values

$$Y \in \left\{-\tfrac{1}{3}(2l-k_2-k_3), \ldots, \tfrac{1}{3}(2l-k_2-k_3)\right\} \tag{15.128}$$

in increments of $\frac{4}{3}$ if $k_2 = k_3 = 0$ and in increments of $\frac{2}{3}$ otherwise. We therefore need not include in the sum over ν in (15.126) any ψ_ν^j whose Y value does not belong to the range given in (15.128).

Putting our observations together, we may now write the Gram eigenvalues in the form

$$\lambda_{j_1 j_2}^{(l)} = \lambda_{j_2 j_1}^{(l)} = \frac{2}{(l+1)(l+2)d(j_1,j_2)} \sum_c N_c \sum_{I I_3 Y} \left|\langle \psi(j_1, j_2, I, I_3, Y; l), Q_c^{(l)} \rangle\right|^2, \tag{15.129}$$

where N_c denotes the number of distinct $Q_{k_2 k_3}^{(l)}$ which are equivalent under permutation of q-indices, and $Q_c^{(l)}$ denotes a representative element from each equivalence class. In addition, the sums over I_3 and Y are constrained by (15.127) and (15.128), which of course depend on the particular $Q_c^{(l)}$; and the sum over I must be consistent with the possible values of I_3.

[29]The form of the interval in (15.127) strongly suggests that the possible values of I are constrained to lie in the set $\{I_{min}, \ldots, \frac{1}{2}(k_2+k_3)\}$, where I_{min} equals 0 or $\frac{1}{2}$ for even or odd values of (k_2+k_3), respectively. Although computations seem to bear this out, this conjecture has so far resisted proof.

TABLE 15.9. The continuum limit Gram eigenvalues $\lambda^{(l)}_{j_1 j_2}$ for three degrees of freedom when $\mathcal{U} = SU(3)$. The last column lists the degeneracy of each eigenvalue.

l	(j_1, j_2)	$\lambda^{(l)}_{j_1 j_2}$	degen.
1	$(1,0)$	$1/6$	6
2	$(2,0)$	$1/24$	12
	$(1,1)$	$5/96$	8
	$(0,0)$	$1/12$	1
3	$(3,0)$	$1/80$	20
	$(2,1)$	$3/160$	30
	$(1,0)$	$1/32$	6
4	$(4,0)$	$1/240$	30
	$(3,1)$	$7/960$	48
	$(2,2)$	$19/2160$	27
	$(2,0)$	$1/80$	12
	$(1,1)$	$7/480$	8
	$(0,0)$	$1/48$	1
5	$(5,0)$	$1/672$	42
	$(4,1)$	$1/336$	70
	$(3,2)$	$17/4032$	84
	$(3,0)$	$1/192$	20
	$(2,1)$	$1/144$	30
	$(1,0)$	$1/96$	6
6	$(6,0)$	$1/1792$	56
	$(5,1)$	$9/7168$	96
	$(4,2)$	$11/5376$	120
	$(3,3)$	$69/28672$	64
	$(4,0)$	$1/448$	30
	$(3,1)$	$3/896$	48
	$(2,2)$	$31/8064$	27
	$(2,0)$	$1/192$	12
	$(1,1)$	$3/512$	8
	$(0,0)$	$1/128$	1
7	$(7,0)$	$1/4608$	72
	$(6,1)$	$5/9216$	126
	$(5,2)$	$83/82944$	162
	$(4,3)$	$25/18432$	180
	$(5,0)$	$1/1024$	42
	$(4,1)$	$5/3072$	70
	$(3,2)$	$13/6144$	84
	$(3,0)$	$1/384$	20
	$(2,1)$	$5/1536$	30
	$(1,0)$	$7/1536$	6

Appendix I includes the *Mathematica* notebook used to compute the Gram eigenvalues according to (15.129) for $l \in \{1, \ldots, 5\}$, and Table 15.9 summarizes the results.

15.3.3. *The Gram Matrix and its Eigenvalues for the Case* $\mathcal{U} = U(3)/SO(3)$. In the last section we listed in Table 15.9 the continuum-limit Gram eigenvalues for the restricted case in which $\mathcal{L}(u)$ belongs to the coset space $SU(3)/SO(3)$. Upon extending our results to cover the whole of $U(3)$—which, according to Theorem 13.1, will yield the same results as $U(3)/SO(3)$—we shall find, as claimed in §13.4, that the $U(1)$ part of $U(3)$ has no effect on the Gram eigenvalues. In other words, the eigenvalues listed in Table 15.9 for $\mathcal{U} = SU(3)/SO(3)$ apply also to the case $\mathcal{U} = U(3)/SO(3)$, or $\mathcal{U} = U(3)$.

To prove the claim made in the last paragraph, we begin by recalling the argument given in §15.2.5 for $\mathcal{U} = U(2)/SO(2)$ in the case $n = 2$. With only minor modification, that argument applies also for the present case. In particular, (15.78) becomes

$$\widehat{\Gamma}(l) = \frac{2}{(l+1)(l+2)} \sum_k \int_{SU(3)} dv \int_0^{2\pi} \frac{d\theta}{2\pi}\, \mathcal{R}(\theta)\mathcal{L}(v)\, \big|Q_k^{(l)}\big\rangle\big\langle Q_k^{(l)}\big|\, \mathcal{L}(v)^\dagger \mathcal{R}(\theta)^\dagger, \tag{15.130}$$

where, similar to (15.80),

$$\mathcal{R}(\theta) = \exp\Big(-\frac{\theta}{3} :\frac{1}{2}(q_1^2 + p_1^2 + q_2^2 + p_2^2 + q_3^2 + p_3^2):\Big) \tag{15.131a}$$

denotes a rotation operator that obeys (15.81). Now observe that we may use (15.101) to write (15.131a) in the form

$$\mathcal{R}(\theta) = \exp\Big(-\frac{\theta}{3} :(z_1 z_1^* + z_2 z_2^* + z_3 z_3^*):\Big) = \exp\Big(-\frac{\theta}{3} :r^2:\Big). \tag{15.131b}$$

It follows from this expression and (15.111) that

$$\begin{aligned} \mathcal{R}(\theta) z_j &= e^{-i\theta/3} z_j, \\ \mathcal{R}(\theta) z_j^* &= e^{i\theta/3} z_j^*, \end{aligned} \tag{15.132}$$

and

$$\mathcal{R}(\theta) {z_1}^{r_1} {z_2}^{r_2} {z_3}^{r_3} {z_1^*}^{r_4} {z_2^*}^{r_5} {z_3^*}^{r_6} = e^{-i(r_1+r_2+r_3)\theta/3} e^{i(r_4+r_5+r_6)\theta/3} {z_1}^{r_1} {z_2}^{r_2} {z_3}^{r_3} {z_1^*}^{r_4} {z_2^*}^{r_5} {z_3^*}^{r_6}. \tag{15.133}$$

To determine how $\mathcal{R}(\theta)$ acts on the $SU(3)$ basis polynomials $\psi(j_1, j_2, I, I_3, Y; l)$, use this last expression together with (9.6), (15.105), and the fact that the modified angular functions $\psi_{II_3Y}^{\bar{j}_1 j_2}$ are of degree j_1 in the variables z_j and of degree j_2 in the variables z_j^*. We conclude that

$$\mathcal{R}(\theta)\psi(j_1, j_2, I, I_3, Y; l) = e^{-i(j_1 - j_2)\theta/3} \psi(j_1, j_2, I, I_3, Y; l). \tag{15.134}$$

Let us now evaluate the Gram operator $\widehat{\Gamma}(l)$ of (15.130) with respect to the orthonormal basis polynomials (15.105). Using (15.81), the results of §15.3.2, and the same abbreviations

used in (15.120), we find

$$\begin{aligned}\Gamma(l)_{j\mu,j'\mu'} &= \big\langle \psi_\mu^j \big| \widehat{\Gamma}(l) \big| \psi_{\mu'}^{j'} \big\rangle \\ &= \frac{2}{(l+1)(l+2)} \sum_k \int\limits_{SU(3)} dv \int\limits_0^{2\pi} \frac{d\theta}{2\pi} \, \Big\langle \mathcal{L}(v^{-1}) \mathcal{R}(-\theta) \psi_\mu^j, Q_k^{(l)} \Big\rangle \times \\ &\qquad\qquad \Big\langle Q_k^{(l)}, \mathcal{L}(v^{-1}) \mathcal{R}(-\theta) \psi_{\mu'}^{j'} \Big\rangle \\ &= \frac{2}{(l+1)(l+2)} \Big(\int\limits_0^{2\pi} \frac{d\theta}{2\pi} \, e^{-i(j_1-j_2)\theta/3} e^{i(j_1'-j_2')\theta/3} \Big) \times \\ &\qquad\qquad \sum_k \int\limits_{SU(3)} dv \, \Big\langle \mathcal{L}(v^{-1}) \psi_\mu^j, Q_k^{(l)} \Big\rangle \Big\langle Q_k^{(l)}, \mathcal{L}(v^{-1}) \psi_{\mu'}^{j'} \Big\rangle \\ &= \Big(\int\limits_0^{2\pi} \frac{d\theta}{2\pi} \, e^{-i(j_1-j_1'-j_2+j_2')\theta/3} \Big) \delta_{jj'} \delta_{\mu\mu'} \lambda_{j_1 j_2}^{(l)} = \delta_{jj'} \delta_{\mu\mu'} \lambda_{j_1 j_2}^{(l)},\end{aligned}$$

where the $\lambda_{j_1 j_2}^{(l)}$ denote exactly the Gram eigenvalues found in the previous section using $SU(3)$. (In the last step we have used the fact that $\delta_{jj'}$ means $\delta_{j_1 j_1'} \delta_{j_2 j_2'}$.) It follows that the $SU(3)$ basis polynomials $\psi(j_1, j_2, I, I_3, Y; l)$ diagonalize the Gram operator also for the case $\mathcal{U} = U(3)/SO(3)$, and the Gram eigenvalues remain *unchanged* from those given in Table 15.9.

15.4. **Using the Manifold** $[U(1)]^n$

In this section we compute for n degrees of freedom the continuum-limit Gram eigenvalues for the case in which the linear symplectic transformations $\mathcal{L}(u)$ belong to the space $\mathcal{U} = [U(1)]^n = U(1) \otimes \cdots \otimes U(1)$ (n times). The analysis given here amounts to a straightforward generalization of that given for $n = 1$ in §15.1.

Linear symplectic transformations $\mathcal{L}(u)$ chosen from the space $\mathcal{U} = [U(1)]^n$ have the form

$$\mathcal{L}(u) = \mathcal{R}(\theta_1, \ldots, \theta_n) = \mathcal{R}_1(\theta_1) \ldots \mathcal{R}_n(\theta_n), \tag{15.135a}$$

where (*cf.* (15.4))

$$\mathcal{R}_j(\theta_j) = \exp\Big(-\frac{\theta_j}{2} :q_j^2 + p_j^2: \Big). \tag{15.135b}$$

Observe that each $\mathcal{R}_j(\theta_j)$ obeys (15.81). Also, because they act independently on different degrees of freedom, the $\mathcal{R}_j$ all commute with one another. One may therefore construct eigenfunctions of $\mathcal{R}(\theta_1, \ldots, \theta_n)$ simply by taking products of eigenfunctions of the constituent $\mathcal{R}_j(\theta_j)$.

In (10.7) of §10.2 we defined the general monomials $G_r^{(l)}(q, p)$. For the present purposes we shall find it convenient to give the same definition in a somewhat different notation:

$$G_r^{(l)}(q, p) = G_{1r_1}^{(l_1)} \ldots G_{nr_n}^{(l_n)}, \tag{15.136a}$$

where

$$G_{jr_j}^{(l_j)} = \frac{q_j^{l_j - r_j} p_j^{r_j}}{\sqrt{(l_j - r_j)!\, r_j!}}. \tag{15.136b}$$

These monomials must, of course, obey the homogeneity relation $l_1 + \cdots + l_n = l$ and have $r_j \in \{0, 1, \ldots, l_j\}$ for each $j \in \{1, \ldots, n\}$.

Now define a complex linear symplectic Lie transformation $\mathcal{T}$ analogous to (15.7):

$$\mathcal{T} = \mathcal{T}_1 \ldots \mathcal{T}_n,$$

where

$$\mathcal{T}_j = \exp\Big(\frac{i\pi}{8} :q_j^2 - p_j^2:\Big).$$

The $\mathcal{T}_j$, like the $\mathcal{R}_j$, all commute with one another. As a consequence $\mathcal{T}$ acts on phase space according to the rule (*cf.* (15.8))

$$\mathcal{T}\begin{pmatrix} q_j \\ p_j \end{pmatrix} = \begin{pmatrix} z_j \\ iz_j^* \end{pmatrix}, \tag{15.137}$$

where z_j and z_j^* denote the generalizations of (15.5) given in (15.97). Note also that $\mathcal{T}$, like its namesake (15.7), is unitary with respect to the inner product (10.9).

We can now write down the eigenfunctions of $\mathcal{R}(\theta_1, \dots, \theta_n)$. By analogy with (15.10) and (15.11), the dynamical polynomial

$$\psi_{jr_j}^{(l_j)} = \mathcal{T}_j G_{jr_j}^{(l_j)} = \frac{z_j^{l_j - r_j} (iz_j^*)^{r_j}}{\sqrt{(l_j - r_j)!\, r_j!}} \tag{15.138a}$$

is an eigenfunction of the operator $\mathcal{R}_j(\theta_j)$ with eigenvalue $e^{-i(l_j - 2r_j)\theta_j}$. Hence the dynamical polynomial

$$\psi_r^{(l)} = \mathcal{T} G_r^{(l)} = \mathcal{T}_1 G_{1r_1}^{(l_1)} \dots \mathcal{T}_n G_{nr_n}^{(l_n)} = \psi_{1r_1}^{(l_1)} \dots \psi_{nr_n}^{(l_n)} \tag{15.138b}$$

obeys the eigenvalue equation

$$\mathcal{R}(\theta_1, \dots, \theta_n)\psi_r^{(l)} = e^{-i(l_1 - 2r_1)\theta_1} \cdots e^{-i(l_n - 2r_n)\theta_n} \psi_r^{(l)}. \tag{15.139}$$

As with our original $\psi_r^{(l)}$, the unitarity of the Lie transformation $\mathcal{T}$ guarantees that these $\psi_r^{(l)}$ form an orthonormal basis for the space of dynamical polynomials of degree l.

Let us now evaluate the Gram operator $\widehat{\Gamma}(l)$ with respect to the orthonormal basis of eigenfunctions of $\mathcal{R}(\theta_1, \dots, \theta_n)$. Using (14.5), (15.81), and (15.139), we obtain the Gram matrix elements

$$\begin{aligned} \Gamma(l)_{rr'} &= \big\langle \psi_r^{(l)} \big| \widehat{\Gamma}(l) \big| \psi_{r'}^{(l)} \big\rangle \\ &= \frac{1}{M(l,n)} \sum_k \int_0^{2\pi} \cdots \int_0^{2\pi} \frac{d\theta_1}{2\pi} \cdots \frac{d\theta_n}{2\pi} \big\langle \mathcal{R}(\theta_1, \dots, \theta_n)^\dagger \psi_r^{(l)}, Q_k^{(l)} \big\rangle \times \\ &\qquad\qquad \big\langle Q_k^{(l)}, \mathcal{R}(\theta_1, \dots, \theta_n)^\dagger \psi_{r'}^{(l)} \big\rangle \\ &= \frac{1}{M(l,n)} \sum_k \int_0^{2\pi} \cdots \int_0^{2\pi} \frac{d\theta_1}{2\pi} \cdots \frac{d\theta_n}{2\pi}\, e^{-i(l_1 - 2r_1 - l_1' + 2r_1')\theta_1} \cdots \times \\ &\qquad\qquad e^{-i(l_n - 2r_n - l_n' + 2r_n')\theta_n} \big\langle \psi_r^{(l)}, Q_k^{(l)} \big\rangle \big\langle Q_k^{(l)}, \psi_{r'}^{(l)} \big\rangle. \end{aligned} \tag{15.140}$$

To make further progress, we must examine the inner product $\langle \psi_r^{(l)}, Q_k^{(l)} \rangle$, and we can do this by expanding the $Q_k^{(l)}$ in terms of the $\psi_r^{(l)}$. Using (10.8), (15.98a), and (15.138a), we obtain

$$\begin{aligned} Q_k^{(l)} &= \frac{q_1^{k_1} \cdots q_n^{k_n}}{\sqrt{k_1! \cdots k_n!}} = \prod_j \frac{1}{\sqrt{k_j!}} \biggl(\frac{1}{\sqrt{2}} \biggr)^{k_j} (z_j + z_j^*)^{k_j} \\ &= \prod_j \biggl(\frac{1}{\sqrt{2}} \biggr)^{k_j} \cdot \prod_j \frac{1}{\sqrt{k_j!}} \sum_{r_j} \binom{k_j}{r_j} z_j^{k_j - r_j} z_j^{*r_j} \\ &= \biggl(\frac{1}{2} \biggr)^{l/2} \prod_j \sum_{r_j} \sqrt{\frac{k_j!}{(k_j - r_j)!\, r_j!}} \, (-i)^{r_j} \frac{z_j^{k_j - r_j} (i z_j^*)^{r_j}}{\sqrt{(k_j - r_j)!\, r_j!}} \\ &= \biggl(\frac{1}{2} \biggr)^{l/2} \prod_j \sum_{r_j} (-i)^{r_j} \sqrt{\binom{k_j}{r_j}} \, \psi_{j r_j}^{(k_j)} \\ &= \biggl(\frac{1}{2} \biggr)^{l/2} \sum_{r_1 \ldots r_n} (-i)^{r_1 + \cdots + r_n} \sqrt{\binom{k_1}{r_1} \cdots \binom{k_n}{r_n}} \, \psi_{1 r_1}^{(k_1)} \cdots \psi_{n r_n}^{(k_n)}. \end{aligned} \tag{15.141}$$

Now use this result to compute the inner product of $\psi_r^{(l)}$ with $Q_k^{(l)}$:

$$\begin{aligned} \langle \psi_r^{(l)}, Q_k^{(l)} \rangle &= \biggl(\frac{1}{2} \biggr)^{l/2} \sum_{\bar{r}_1 \cdots \bar{r}_n} (-i)^{\bar{r}_1 + \cdots + \bar{r}_n} \sqrt{\binom{k_1}{\bar{r}_1} \cdots \binom{k_n}{\bar{r}_n}} \, \langle \psi_{1 r_1}^{(l_1)} \cdots \psi_{n r_n}^{(l_n)}, \psi_{1 \bar{r}_1}^{(k_1)} \cdots \psi_{n \bar{r}_n}^{(k_n)} \rangle \\ &= \delta_{l_1 k_1} \cdots \delta_{l_n k_n} (-i)^{r_1 + \cdots + r_n} \biggl(\frac{1}{2} \biggr)^{l/2} \sqrt{\binom{k_1}{r_1} \cdots \binom{k_n}{r_n}}. \end{aligned}$$

In a similar manner

$$\langle Q_k^{(l)}, \psi_{r'}^{(l)} \rangle = \delta_{k_1 l_1'} \cdots \delta_{k_n l_n'} (+i)^{r_1' + \cdots + r_n'} \biggl(\frac{1}{2} \biggr)^{l/2} \sqrt{\binom{k_1}{r_1'} \cdots \binom{k_n}{r_n'}}.$$

Now take the product of these last two results and sum over k:

$$\begin{aligned} &\sum_k \langle \psi_r^{(l)}, Q_k^{(l)} \rangle \langle Q_k^{(l)}, \psi_{r'}^{(l)} \rangle \\ &\quad = \sum_{k_1 \ldots k_n} \delta_{l_1 k_1} \delta_{k_1 l_1'} \cdots \delta_{l_n k_n} \delta_{k_n l_n'} i^{r_1' - r_1 + \cdots + r_n' - r_n} \biggl(\frac{1}{2} \biggr)^{l} \sqrt{\binom{k_1}{r_1} \binom{k_1}{r_1'} \cdots \binom{k_n}{r_n} \binom{k_n}{r_n'}} \\ &\quad = \delta_{l_1 l_1'} \cdots \delta_{l_n l_n'} \biggl(\frac{1}{2} \biggr)^{l} \sqrt{\binom{l_1}{r_1} \binom{l_1}{r_1'} \cdots \binom{l_n}{r_n} \binom{l_n}{r_n'}}. \end{aligned}$$

On inserting this result into our calculation for the Gram matrix elements and integrating over θ_j, we obtain a $\delta_{r_j r_j'}$ for each $j \in \{1, \ldots, n\}$. Hence

$$\Gamma(l)_{rr'} = \langle \psi_r^{(l)} | \widehat{\Gamma}(l) | \psi_{r'}^{(l)} \rangle = \frac{1}{M(l,n) 2^l} \prod_j \delta_{l_j l_j'} \delta_{r_j r_j'} \binom{l_j}{r_j} = \frac{\delta_{rr'}}{M(l,n) 2^l} \prod_j \binom{l_j}{r_j}.$$

As these elements form a diagonal matrix, they represent the eigenvalues of the Gram matrix for the case in which $\mathcal{U} = [U(1)]^n$:

$$\lambda_r^{(l)} = \frac{1}{M(l,n) 2^l} \prod_{j=1}^n \binom{l_j}{r_j}. \tag{15.142}$$

Note that these eigenvalues depend on all of the indices $\{r_1, \ldots, r_n, l_1, \ldots, l_n\}$ that define the $\psi_r^{(l)}$. In addition, observe that for $n = 1$ we recover from (15.142) the result originally obtained in (15.16).

For the cases of especial interest—two and three degrees of freedom—we may put (15.142) in the following particular forms: For $n = 2$,

$$\lambda_{jrs}^{(l)} = \frac{1}{(l+1)2^l} \binom{l-j}{r} \binom{j}{s}, \tag{15.143}$$

where $j \in \{0, \ldots, l\}$, $r \in \{0, \ldots, l-j\}$, and $s \in \{0, \ldots, j\}$. And for $n = 3$,

$$\lambda_{jkrst}^{(l)} = \frac{1}{(l+1)(l+2)2^{l-1}} \binom{l-j-k}{r} \binom{j}{s} \binom{k}{t}, \tag{15.144}$$

where $j \in \{0, \ldots, l\}$, $k \in \{0, \ldots, l-j\}$, $r \in \{0, \ldots, l-j-k\}$, $s \in \{0, \ldots, j\}$, and $t \in \{0, \ldots, k\}$. Appendix I includes the *Mathematica* notebook used to compute the Gram eigenvalues according to (15.143) and (15.144) for $l \in \{1, \ldots, 5\}$. Table 15.10 summarizes the results. On comparing Tables 15.7, 15.9, and 15.10, we note that, at least for the cases calculated, the minimum Gram eigenvalues for $U(n)/SO(n)$ and $[U(1)]^n$ are the same.

Table 15.10: The continuum limit Gram eigenvalues for two and three degrees of freedom when $\mathcal{U} = [U(1)]^n$.

l	$\lambda^{(l)}(n=2)$	degen.	$\lambda^{(l)}(n=3)$	degen.
1	1/4	4	1/6	6
2	1/12	8	1/24	18
	1/6	2	1/12	3
3	1/32	12	1/80	38
	1/16	4	1/40	12
	3/32	4	3/80	6
4	1/80	16	1/240	66
	1/40	4	1/120	24
	3/80	8	1/80	24
	1/20	5	1/60	9
	3/40	2	1/40	3
5	1/192	20	1/672	102
	1/96	4	1/336	36
	1/64	8	1/224	48
	1/48	8	1/168	30
	5/192	4	5/672	6
	1/32	8	1/112	24
	5/96	4	5/336	6
6	1/448	24	1/1792	146
	1/224	4	1/896	48
	3/448	8	3/1792	72
	1/112	8	1/448	54
	5/448	8	5/1792	24
	3/224	8	3/896	54
	1/56	4	1/224	13
	9/448	4	9/1792	12
	5/224	8	5/896	24
	3/112	2	3/448	6

Gram eigenvalues for $[U(1)]^n$ (ctd.)

l	$\lambda^{(l)}(n=2)$	degen.	$\lambda^{(l)}(n=3)$	degen.
	15/448	4	15/1792	6
	5/112	2	5/448	3
7	1/1024	28	1/4608	198
	1/512	4	1/2304	60
	3/1024	8	1/1536	96
	1/256	8	1/1152	78
	5/1024	8	5/4608	48
	3/512	12	1/768	84
	7/1024	4	7/4608	6
	5/512	12	1/576	24
	3/256	8	1/512	24
	15/1024	8	5/2304	60
	9/512	4	1/384	42
	5/256	8	5/1536	24
	21/1024	4	1/256	12
	35/1024	4	5/1152	24
			7/1536	6
			35/4608	6

16. Return to the Discrete Case

In the last section we determined the Gram eigenvalues in the continuum limit as a means of characterizing the quality of different sets of linear symplectic transformations $\mathcal{L}_j$ for use in jolt decompositions of the form (11.2). To implement jolt decomposition on a computer, we now return to the discrete case asking, "Do there exist sets of $\mathcal{L}_j$ which yield the optimal Gram eigenvalues found in (15.16) and Tables 15.6, 15.7, 15.9, and 15.10?" This question leads very naturally to a study of minimal formulas for numerical quadrature and cubature[30] on the various group manifolds studied in §15.

16.1. **One Degree of Freedom**

In the case of one degree of freedom, $n = 1$, let us begin our study by examining the Gram matrix elements. Taking matrix elements of the Gram operator (15.2) with respect to the (real) general monomials $G_r^{(l)}$, we obtain

$$\Gamma(l)_{rs} = \frac{1}{2\pi}\int_0^{2\pi} d\theta \left\langle G_r^{(l)}, \mathcal{R}(\theta)Q_1^{(l)}\right\rangle\left\langle \mathcal{R}(\theta)Q_1^{(l)}, G_s^{(l)}\right\rangle. \tag{16.1}$$

One rather obvious method for returning to the discrete case replaces the above integral by a suitable quadrature formula [50]. Hence we rewrite (16.1) in the form (*cf.* (11.9))

$$\Gamma(l)_{rs} = \sum_{j=1}^{N} w_j \left\langle G_r^{(l)}, \mathcal{R}_j Q_1^{(l)}\right\rangle\left\langle \mathcal{R}_j Q_1^{(l)}, G_s^{(l)}\right\rangle, \tag{16.2}$$

where $\mathcal{R}_j$ denotes $\mathcal{R}(\theta_j)$, and where the quadrature formula chosen determines the angles θ_j and the weights w_j. (Note that here the weights w_j play the role of the factor $1/N$ in (11.9); henceforth, where appropriate, we shall make this replacement.) The reader might guess that a sufficient number of θ_j's spaced evenly about a circle with equal weights would give the best results, and indeed such a choice leads to the optimal Gram eigenvalues given by (15.16). To put this choice in perspective, however, we shall study the full range of possibilities that (16.2) allows.

16.1.1. *The Gram Matrix Elements.* We can obtain a formula for the Gram matrix elements (16.2) by straightforward computation. First note from (15.1), (15.3), (15.4), and (15.9) that

$$\begin{aligned}\mathcal{R}_j Q_1^{(l)} = \mathcal{R}(\theta_j)\frac{q^l}{\sqrt{l!}} &= \frac{1}{\sqrt{l!}}(q\cos\theta_j + p\sin\theta_j)^l = \frac{1}{\sqrt{l!}}\sum_{r=0}^{l}\binom{l}{r}(q\cos\theta_j)^{l-r}(p\sin\theta_j)^r \\ &= \sum_r \sqrt{\frac{l!}{(l-r)!\,r!}}\,(\cos\theta_j)^{l-r}(\sin\theta_j)^r\frac{q^{l-r}p^r}{\sqrt{(l-r)!\,r!}} = \sum_r \binom{l}{r}^{1/2} c_j^{l-r}s_j^r G_r^{(l)},\end{aligned}$$

where here, in the last step, we have abbreviated $\cos\theta_j$ by c_j and $\sin\theta_j$ by s_j. We therefore obtain for the sensitivity vectors (recall (11.4)) the result

$$\sigma_j^r = \left\langle G_r^{(l)}, \mathcal{R}_j Q_1^{(l)}\right\rangle = \binom{l}{r}^{1/2} c_j^{l-r}s_j^r. \tag{16.3}$$

On defining the (not necessarily square) matrix $S(l)$ having elements

$$S(l)_{rj} = \sqrt{w_j}\,\sigma_j^r = \sqrt{w_j}\binom{l}{r}^{1/2} c_j^{l-r}s_j^r, \tag{16.4}$$

[30] The multi-dimensional generalizations of quadrature formulas are called *cubature* formulas [18].

we may, since the sensitivity vectors are real, compute the Gram matrix according to $\Gamma(l) = S(l) \cdot \widetilde{S(l)}$. In other words, the Gram matrix elements are

$$\Gamma(l)_{rs} = \sum_j S(l)_{rj} S(l)_{sj} = \left[\binom{l}{r} \binom{l}{s} \right]^{1/2} \sum_j w_j c_j^{2l-(r+s)} s_j^{r+s}. \tag{16.5}$$

16.1.2. *Choosing Angles Randomly.* If we could not find a good quadrature formula to use in (16.2), we might, for lack of a better alternative, try making random choices for the angles θ_j and weights w_j. To gauge how well or poorly such an approach might work—especially for the higher-dimensional cases having no obvious cubature formulas—let us examine the particular example of $l = 4$ in one degree of freedom. For this example (15.16) gives the continuum-limit Gram eigenvalues,

$$\frac{1}{16}, \quad \frac{1}{4}, \quad \frac{3}{8}, \quad \frac{1}{4}, \quad \frac{1}{16},$$

and hence the best possible minimum Gram eigenvalue is

$$\frac{1}{16} = 0.0625.$$

In addition, the continuum-limit Gram determinant is

$$\frac{3}{2^{15}} = \frac{3}{32768} \approx 9.155 \times 10^{-5}.$$

According to Table 13.1, we shall, for $l = 4$, need at least $N = 5$ angles and their corresponding weights. (We shall soon see that in fact $N = 5$ suffices.) The angles may be chosen randomly from the interval $[0, 2\pi]$, but the weights require a little more consideration: At a bare minimum the quadrature formula should work for a constant function, and this requirement implies that the weights w_j should satisfy the constraint

$$\sum_{j=1}^{N} w_j = 1. \tag{16.6}$$

Using (16.5) with 1000 sets of five positive random weights constrained to have unit sum and five random angles chosen from the interval $[0, 2\pi]$, Figure 16.1 shows a plot of the Gram determinant versus the minimum Gram eigenvalue. Using the same angles and weights, Figure 16.2 shows a histogram of the minimum Gram eigenvalues. As the reader will note, almost all of the sets of $\mathcal{R}_j$ (determined by the θ_j) and their corresponding weights lead to very small minimum Gram eigenvalues and Gram determinants. Indeed, roughly $\frac{2}{3}$ of the sets lead to values at least two orders of magnitude smaller than optimal, and all but a few dozen lead to values at least one order of magnitude smaller than optimal. If one does not choose the weights w_j randomly, but instead defines either equal weights, $w_j = 1/N$, or proportional weights, $w_j \propto \theta_{j+1} - \theta_{j-1}$ (again with the constraint (16.6)), then the resulting Gram matrices yield results very similar to those shown in Figures 16.1 and 16.2 for random weights.

As suggested earlier, and as we prove later in §16.1.6, choosing five angles θ_j spaced equally about a circle together with five equal weights $w_j = \frac{1}{5}$ yields, for $l = 4$, a Gram matrix having eigenvalues identical to those for the continuum-limit. To gauge the sensitivity of this "equal-angle formula", let us briefly examine how small random deviations from equally spaced angles affect the resulting Gram eigenvalues and determinant. Figure 16.3 shows the determinant versus the minimum eigenvalue for 1000 different Gram matrices built using random angular variations of not more than $\pm 2\pi/50$ ($\approx \pm 7.2°$) about the choice of equally spaced angles, $\theta_j = 2\pi j/5$ for $j \in \{0, 1, \ldots, 4\}$. For direct comparison Figure 16.4 shows the result of combining Figures 16.1 and 16.3.

The reader will note that the upper-right-hand-most point in Figure 16.4—the point corresponding to equally spaced angles or, equivalently, to the optimum values found in the

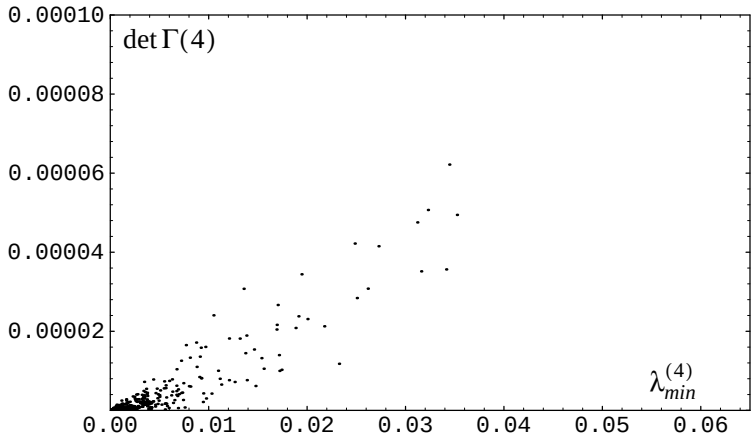

FIGURE 16.1. This plot shows the Gram determinant $\det \Gamma(4)$ versus the minimum Gram eigenvalue $\lambda_{min}^{(4)}$ for 1000 different randomly chosen sets of five angles θ_j and five weights w_j, subject to the constraint (16.6). The Gram matrices were evaluated using (16.5) with $l = 4$. The continuum-limit values would produce a point near the upper-right-hand corner of this plot.

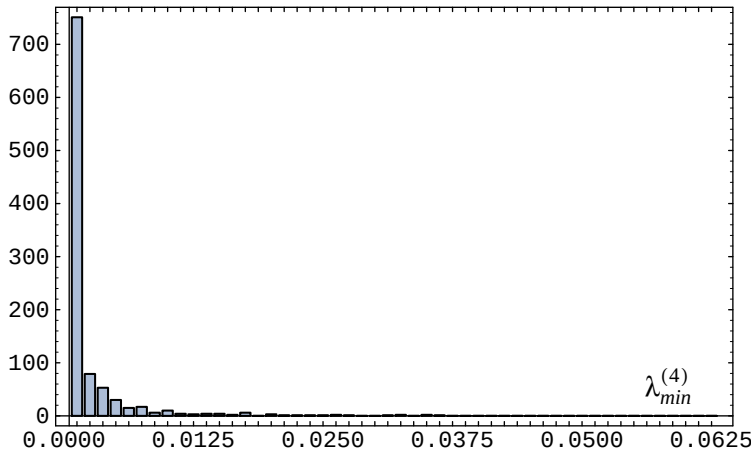

FIGURE 16.2. This histogram shows for the same Gram matrices as used in Figure 16.1 the number of occurrences of a minimum Gram eigenvalue in a given range of values.

continuum limit—appears to represent a maximum for not only the smallest Gram eigenvalue $\lambda_{min}^{(4)}$ but also for the Gram determinant $\det \Gamma(4)$. This pattern also holds for values of l besides $l = 4$. That the maxima of these two functions should coincide seems rather remarkable, indeed hard to understand: if one chooses a different normalization for the general monomials $G_r^{(l)}$, then the maxima of $\lambda_{min}^{(l)}$ and $\det \Gamma(l)$ may no longer coincide. If, for example, one omits the denominator from the definition of the $G_r^{(l)}$ in (10.7), then the choice of equally spaced angles leads to a maximum only for $\det \Gamma(l)$. Recall, however, that we have chosen to maximize the eigenvalue $\lambda_{min}^{(l)}$ based on the role it plays in our upper bound (12.4) for the jolt strengths $a^{(l)}$. But the calculation given in (12.3) suggests that having large values for all of the Gram eigenvalues should also prove useful, and hence maximizing $\det \Gamma(l)$ is probably also a worthy goal. That the maxima of $\lambda_{min}^{(l)}$ and $\det \Gamma(l)$ should coincide (see

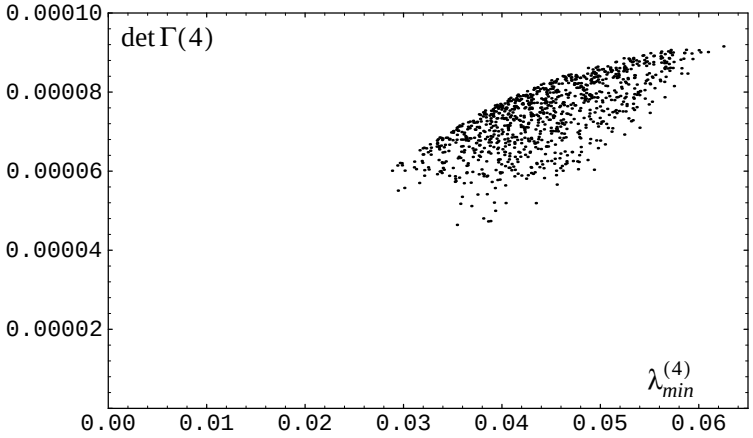

FIGURE 16.3. This plot shows the Gram determinant $\det\Gamma(4)$ versus the minimum Gram eigenvalue $\lambda^{(4)}_{min}$ for 1000 different Gram matrices obtained using (16.5) with equal weights $w_j = \frac{1}{5}$ and angles $\theta_j = 2\pi j/5 + r_j$ where r_j denotes random numbers chosen from the interval $[-2\pi/50, 2\pi/50]$. The upper-right-hand-most point in the plot corresponds to the "equal-angle" case of $r_j = 0$ or, equivalently, to the optimum values found in the continuum limit.

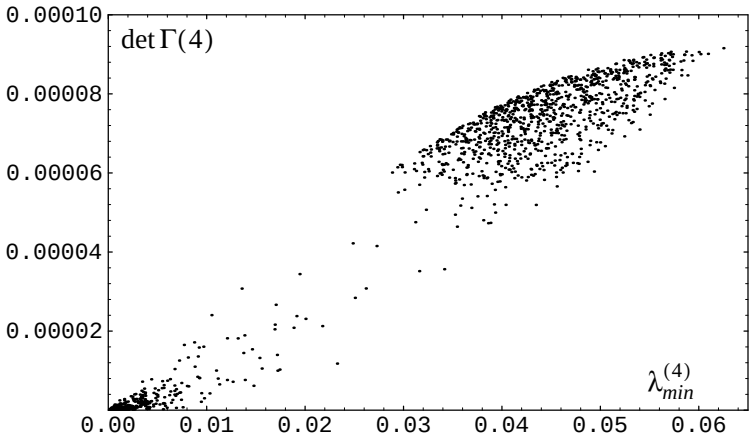

FIGURE 16.4. This plot combines the results shown in Figures 16.1 and 16.3.

the end of §16.1.4 for further discussion) when we use the normalization in (10.7) and (10.9) suggests that that choice of normalization is a particularly good one.

16.1.3. *Searching for Good Sets of Angles.* The results shown in Figures 16.1 and 16.2 suggest that random choice does not work well for producing sets of angles and weights that make the minimum Gram eigenvalue as large as possible. As an alternative to random choice we may use some kind of search (optimization) procedure to hunt for good sets of angles and weights. We have tried several such procedures, but with limited success. Only genetic algorithms—often called GAs—seem particularly promising.

A proper description of how GAs work is outside the scope of this thesis, but, very briefly, they work as follows.[31] The parameters to be varied (in our case the angles and weights) are

[31]Genetic algorithms come in a variety of flavors; here we describe a "plain vanilla" GA.

stored in a long string, or *chromosome*, using a binary encoding or some other similar format. The quantity to be optimized (in our case the smallest Gram eigenvalue) is then defined as a function that determines the *fitness* of a given chromosome. Starting with an initial population of individuals—each individual defined by a single chromosome—a GA evolves successive generations using the principles of natural selection and genetic recombination. Starting with an initial population of size $2p$, a GA randomly selects individuals—with a probability weighted according to their fitness—to form p pairs that serve as "parents" for the succeeding generation. This means, of course, that individuals, *i.e.*, chromosomes, with a high relative fitness will very likely "mate" several times (with different individuals), and individuals with a low relative fitness may not mate at all. Thus do GAs incorporate the principle of natural selection. After selecting the p sets of parents, a GA then produces two "children" from each set of parents (hence every generation contains $2p$ individuals) by using various *genetic operators* modeled on processes found in real biological systems. Most common are the *crossover* and *mutation* operators. One version of the crossover operator places the parent chromosomes side by side, chooses some point at random along the pair, and then interchanges all of the genetic information to the right of that point. Thus the parents

```
xxxxxxx
yyyyyyy
```

may produce the children

```
xxxxyyy
yyyyxxx.
```

Using a variation called *two-point crossover*, the same parents might produce the children

```
xxyyxxx
yyxxyyy.
```

The mutation operator, as its name suggests, simply alters, with some appropriately low probability, a single bit in an individual chromosome. Thus

```
xxxxxxx
```

may become

```
xyxxxxx.
```

After determining the fitness of each child in the new generation, the GA repeats the process with those children as parents of the next generation. In typical applications the GA terminates after either the current generation's genetic diversity (defined by some appropriate measure) drops below a predetermined minimum or the number of generations exceeds a predetermined maximum.

Genetic algorithms have proved adept at tackling a variety of computationally difficult tasks, including the well-known Traveling Salesman Problem [22]. Although they do not work well for determining exact answers, GAs excel at finding approximate answers near global optima: they are not easily fooled into settling on local optima. From the above description, GAs may sound rather *ad hoc*. There does, however, exist a body of mathematical work that gives some justification for why GAs appear to work so well [45]; and there exists an expanding literature on both the theory and the applications of genetic algorithms. The interested reader may consult the review article by Forrest [40] or the new journal *Evolutionary Computation* [23].

Figure 16.5 shows the Gram determinant $\det \Gamma(4)$ versus the minimum Gram eigenvalue $\lambda^{(4)}_{min}$ for the best individual found in each of sixty-four different runs of a genetic algorithm. Each run of the GA evolved for at most fifty generations using a population of size sixteen in an attempt to maximize $\lambda^{(4)}_{min}$. In the case shown here, only the angles were varied; all the weights w_j were held fixed at the value $\frac{1}{5}$. Shown in Figure 16.6 are the angles for the best thirty-two of the individuals shown in Figure 16.5. The reader will note in that figure

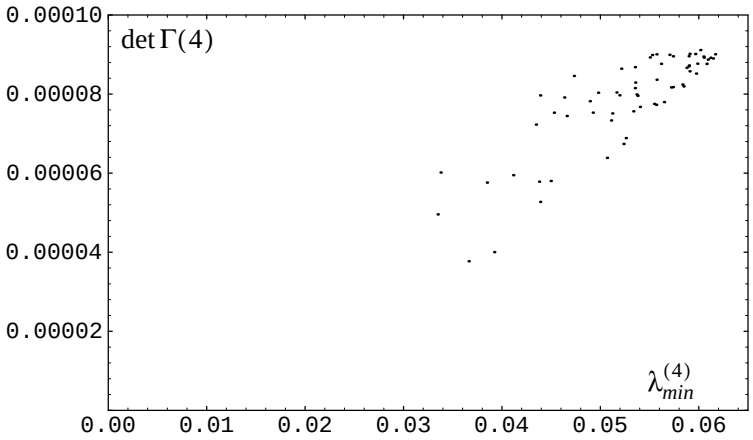

FIGURE 16.5. This plot shows the determinant $\det \Gamma(4)$ versus the minimum eigenvalue $\lambda^{(4)}_{min}$ for sixty-four different Gram matrices obtained using a genetic algorithm with a fitness function given by $\lambda^{(4)}_{min}$. (See the text for more details.)

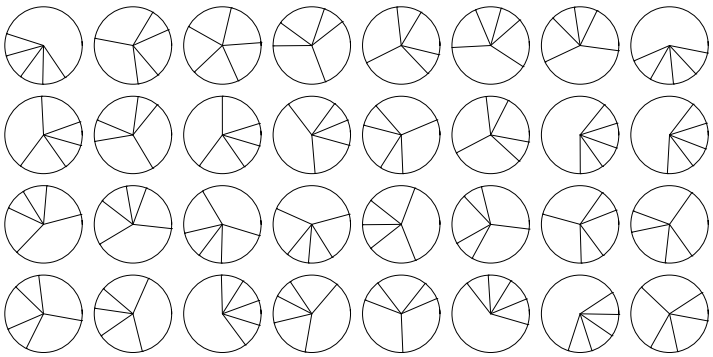

FIGURE 16.6. This graphic shows on separate circles the sets of five angles corresponding to each of the best thirty-two individuals shown in Figure 16.5. Here θ increases in the counter-clockwise direction from an origin, $\theta = 0$, at "three'o'clock". The sets of angles are displayed so that as one "reads" from left to right and down the page the value of $\lambda^{(4)}_{min}$ decreases monotonically.

that only one of the sets of angles looks clearly like the case of equal spacing (top row, third from the left). The reader may also notice certain patterns amongst the various sets of angles illustrated in Figure 16.6. In particular, those sets comprise just four arrangements of angles,

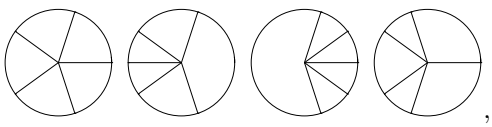

rotated by varying amounts. Furthermore, one may transform any of these arrangements into any other simply by adding π to one or more of the angles. We shall during the next two sections examine the origins and implications of these patterns.

16.1.4. *The Gram Determinant.* For a certain subset of Gram matrices $\Gamma(l)$, namely those obtained using $N = l + 1$ angles, we can evaluate the determinant analytically. The result we find will illuminate some of the patterns seen in Figure 16.6.

Using $N = l + 1$ angles makes the matrix $S(l)$ defined by (16.4) a square matrix. Since $\Gamma(l) = S(l) \cdot \widetilde{S(l)}$, it follows (in this case) that

$$\det \Gamma(l) = \big(\det S(l)\big)^2,$$

and hence it suffices to compute $\det S(l)$. First note that

$$\begin{aligned}
\det S(l) &= \begin{vmatrix} \sqrt{w_1}\binom{l}{0}^{1/2} c_1^l & \sqrt{w_2}\binom{l}{0}^{1/2} c_2^l & \cdots & \sqrt{w_{l+1}}\binom{l}{0}^{1/2} c_{l+1}^l \\ \sqrt{w_1}\binom{l}{1}^{1/2} c_1^{l-1}s_1^1 & \sqrt{w_2}\binom{l}{1}^{1/2} c_2^{l-1}s_2^1 & \cdots & \sqrt{w_{l+1}}\binom{l}{1}^{1/2} c_{l+1}^{l-1}s_{l+1}^1 \\ \vdots & \vdots & \ddots & \vdots \\ \sqrt{w_1}\binom{l}{l}^{1/2} s_1^l & \sqrt{w_2}\binom{l}{l}^{1/2} s_2^l & \cdots & \sqrt{w_{l+1}}\binom{l}{l}^{1/2} s_{l+1}^l \end{vmatrix} \\
&= \prod_{j=1}^{l+1} \sqrt{w_j} \cdot \prod_{r=0}^{l} \binom{l}{r}^{1/2} \cdot \begin{vmatrix} c_1^l & c_2^l & \cdots & c_{l+1}^l \\ c_1^{l-1}s_1^1 & c_2^{l-1}s_2^1 & \cdots & c_{l+1}^{l-1}s_{l+1}^1 \\ \vdots & \vdots & \ddots & \vdots \\ s_1^l & s_2^l & \cdots & s_{l+1}^l \end{vmatrix} \\
&= \sqrt{\prod_j w_j \cdot \prod_r \binom{l}{r}} \cdot \prod_{i=1}^{l+1} c_i^l \cdot \begin{vmatrix} 1 & 1 & \cdots & 1 \\ t_1^1 & t_2^1 & \cdots & t_{l+1}^1 \\ \vdots & \vdots & \ddots & \vdots \\ t_1^l & t_2^l & \cdots & t_{l+1}^l \end{vmatrix},
\end{aligned}$$

where t_k denotes $s_k/c_k = \tan\theta_k$. The determinant that remains in this expression is a *Vandermonde determinant* and has the value

$$\begin{vmatrix} 1 & 1 & \cdots & 1 \\ t_1^1 & t_2^1 & \cdots & t_{l+1}^1 \\ \vdots & \vdots & \ddots & \vdots \\ t_1^l & t_2^l & \cdots & t_{l+1}^l \end{vmatrix} = \prod_{1\le j<k\le l+1} (t_k - t_j).$$

Now observe that this product has l factors that contain a t_1, l factors that contain a t_2, and so on. We may therefore write

$$\begin{aligned}
\prod_i c_i^l \cdot \prod_{1\le j<k\le l+1} (t_k - t_j) &= \prod_{1\le j<k\le l+1} c_j c_k\,(t_k - t_j) \\
&= \prod_{j<k} (\sin\theta_k \cos\theta_j - \sin\theta_j \cos\theta_k) = \prod_{j<k} \sin(\theta_k - \theta_j),
\end{aligned}$$

and hence

$$\det S(l) = \sqrt{\prod_i w_i \cdot \prod_r \binom{l}{r}} \cdot \prod_{j<k} \sin(\theta_k - \theta_j). \tag{16.7}$$

We conclude that

$$\det \Gamma(l) = \big(\det S(l)\big)^2 = \prod_i w_i \cdot \prod_r \binom{l}{r} \cdot \prod_{j<k} \sin^2(\theta_k - \theta_j) \tag{16.8}$$

for Gram matrices obtained using $N = l + 1$ angles.

Because our result (16.8) says that the Gram determinant depends only on the differences between the various angles, at least when $N = l + 1$, we may immediately deduce that changing all $l + 1$ angles by some fixed amount ϕ does not alter the Gram determinant. This conclusion conforms with our earlier observation that the various arrangements of angles seen

in Figure 16.6 appear in many different orientations. We shall see in the next section that this conclusion holds for arbitrary Gram matrices $\Gamma(l)$.

Because $\sin(\alpha+\pi) = -\sin\alpha$, we may also deduce from our result (16.8) that adding π to one or more of the $l+1$ angles does not alter the Gram determinant. This conclusion conforms with our observation that one can transform between the various arrangements of angles seen in Figure 16.6 simply by adding π to one or more of the angles. In the next section we shall learn that adding π to one or more of the angles θ_j has in fact no effect at all on the general Gram matrix $\Gamma(l)$. It follows, of course, that adding π to one or more of the angles can have no effect on the determinant of arbitrary Gram matrices.

One may also deduce from our result (16.8) that if any two angles θ_k and θ_j differ by an integer multiple of π, then the Gram determinant will vanish. Note that for odd degree l this means that $l+1$ equally spaced angles cannot work, for then the determinant of $\Gamma(l)$ will equal zero, and hence the Gram matrix will not satisfy the invertibility requirement. We shall see more clearly why this happens when we study minimal quadrature formulas in §16.1.6.

We conclude this section by demonstrating that when l is even the choice of equally spaced angles and equal weights leads to an extremum for the Gram determinant in (16.8). To test for an extremum with respect to the angles, we check that

$$\frac{\partial}{\partial\theta_i}\det S(l) = 0$$

for each of the $l+1$ angles θ_i. First note that $\partial_{\theta_i}\sin(\theta_i-\theta_j) = \cos(\theta_i-\theta_j) = \sin(\theta_i-\theta_j)\cot(\theta_i-\theta_j)$, and, similarly, $\partial_{\theta_i}\sin(\theta_k-\theta_i) = -\sin(\theta_k-\theta_i)\cot(\theta_k-\theta_i)$. Therefore, using (16.7) and writing $A(l,w)$ for $\sqrt{\prod_i w_i\cdot\prod_r\binom{l}{r}}$, we obtain

$$\begin{aligned}\frac{\partial}{\partial\theta_i}\det S(l) &= A(l,w)\,\frac{\partial}{\partial\theta_i}\prod_{j<k}\sin(\theta_k-\theta_j)\\ &= A(l,w)\prod_{j<k}\sin(\theta_k-\theta_j)\cdot\Bigl(\sum_{\nu<i}\cot(\theta_i-\theta_\nu)-\sum_{\nu>i}\cot(\theta_\nu-\theta_i)\Bigr)\\ &= \det S(l)\cdot\sum_{\nu\neq i}\cot(\theta_i-\theta_\nu).\end{aligned}$$

Assuming that $\det S(l)\neq 0$—since we require an invertible Gram matrix —we need check only that

$$\sum_{\nu\neq i}\cot(\theta_i-\theta_\nu) = 0.$$

For $N = l+1$ equally spaced angles let us write $\theta_\nu = \frac{2\pi\nu}{l+1}$ for $\nu\in\{0,1,\dots,l\}$. (We could, of course, use instead $\theta'_\nu = \theta_\nu+\phi$ for any fixed ϕ.) Then, as one may confirm by drawing a picture or doing some algebra, we find

$$\sum_{\nu\neq i}\cot(\theta_i-\theta_\nu) = \sum_{\nu\neq i}\cot\Bigl(\frac{2\pi}{l+1}(i-\nu)\Bigr) = \sum_{\nu=1}^{l}\cot\Bigl(\frac{2\pi\nu}{l+1}\Bigr).$$

By using the same picture or doing a little more algebra, one may also confirm that

$$\sum_{\nu=1}^{l}\cot\Bigl(\frac{2\pi\nu}{l+1}\Bigr) = 0$$

for *even* values of l. Hence the Gram determinant of (16.8) has an extremum when l is even and the angles are equally spaced. In addition, because $\cot(\theta+\pi) = \cot\theta$, this conclusion holds also for any of the four arrangements of angles seen in Figure 16.6.

To test for an extremum with respect to the weights, we check that

$$\frac{\partial}{\partial w_j} \det \Gamma(l) = 0$$

for each of the $N = l+1$ weights w_j—subject to the constraint (16.6). From (16.8) it follows that we must have

$$\frac{\partial}{\partial w_j} \prod_i w_i = 0,$$

again subject to the constraint (16.6). A straightforward application of the method of Lagrange multipliers yields the solution

$$w_j = \frac{1}{N} = \frac{1}{l+1},$$

independent of j. Putting this result together with that of the last paragraph, we now see that for even degree l the Gram determinant (16.8) has an extremum when the weights w_j are all equal and the angles θ_j form any of the four arrangements of angles seen in Figure 16.6.

16.1.5. *Properties of the Gram Matrix.* In the last section we learned that, at least in certain cases, the Gram determinant does not change when we add a fixed amount ϕ to all of the angles. This fact suggests that perhaps in general the entire spectrum of Gram eigenvalues does not change. This is indeed true, and is in fact a simple consequence of the following theorem and its corollary, which, for future reference, we state and prove for any number of degrees of freedom.

Theorem 16.1. *Let us use the partial Gram operator of* (13.20b) *or* (14.5b) *to define a* partial Gram matrix $\Gamma(u,l)$ *with elements*

$$\Gamma(u,l)_{rs} = \frac{1}{M(l,n)} \sum_k \left\langle G_r^{(l)}, \mathcal{L}(u) Q_k^{(l)} \right\rangle \left\langle \mathcal{L}(u) Q_k^{(l)}, G_s^{(l)} \right\rangle . \tag{16.9}$$

In addition, let $\mathcal{L}(v)$ denote any fixed linear symplectic transformation in the $U(n)$ subgroup of $Sp(2n,\mathbb{R})$. Now suppose we replace $\mathcal{L}(u)$ with $\mathcal{L}(v)\mathcal{L}(u) = \mathcal{L}(uv) \equiv \mathcal{L}(u')$. Then

$$\Gamma(u',l) = V \Gamma(u,l) V^\dagger, \tag{16.10}$$

where V denotes the unitary matrix with elements

$$V_{ab} = \left\langle G_a^{(l)}, \mathcal{L}(v) G_b^{(l)} \right\rangle . \tag{16.11}$$

In other words, the partial Gram matrices $\Gamma(u',l)$ and $\Gamma(u,l)$ are related by a unitary similarity transformation.

Proof. First recall that the monomials $G_r^{(l)}$ are orthonormal with respect to the inner product (10.9) and form a basis for the space of f_l's; hence we may write the identity operator in the dyadic form

$$\sum_a \left| G_a^{(l)} \right\rangle \left\langle G_a^{(l)} \right| .$$

Now observe that we may write the partial Gram matrix elements $\Gamma(u',l)_{rs}$ in the form

$$\Gamma(u',l)_{rs} = \frac{1}{M(l,n)} \sum_k \left\langle G_r^{(l)}, \mathcal{L}(v)\mathcal{L}(u) Q_k^{(l)} \right\rangle \left\langle \mathcal{L}(u) Q_k^{(l)}, \mathcal{L}(v)^\dagger G_s^{(l)} \right\rangle .$$

Inserting the above form of the identity operator into $\Gamma(u',l)$ in two places—after the $\mathcal{L}(v)$ and before the $\mathcal{L}(v)^\dagger$—we obtain

$$\Gamma(u',l)_{rs} = \frac{1}{M(l,n)} \sum_k \sum_{aa'} \left\langle G_r^{(l)}, \mathcal{L}(v) G_a^{(l)} \right\rangle \left\langle G_a^{(l)}, \mathcal{L}(u) Q_k^{(l)} \right\rangle \times \\ \left\langle \mathcal{L}(u) Q_k^{(l)}, G_{a'}^{(l)} \right\rangle \left\langle G_{a'}^{(l)}, \mathcal{L}(v)^\dagger G_s^{(l)} \right\rangle .$$

Because the operator $\mathcal{L}(v)$ is unitary with respect to the inner product (10.9), the quantities V_{ab} defined in (16.11) must constitute the elements of a unitary matrix V. Hence we may now write

$$\Gamma(u',l)_{rs} = \sum_{aa'} V_{ra} \left(\frac{1}{M(l,n)} \sum_k \langle G_a^{(l)}, \mathcal{L}(u) Q_k^{(l)} \rangle \langle \mathcal{L}(u) Q_k^{(l)}, G_{a'}^{(l)} \rangle \right) V_{a's}^\dagger.$$

In matrix form this expression becomes (16.10) and therefore completes the proof. ■

Corollary 16.1. *Define $\mathcal{L}(v)$ for fixed v as in Theorem 16.1. Then, in either the discrete or continuum-limit cases, replacing every $\mathcal{L}(u)$ by $\mathcal{L}(v)\mathcal{L}(u)$ in the Gram matrix $\Gamma(l)$ simply effects on $\Gamma(l)$ the unitary similarity transformation generated by the matrix V of* (16.11).

Proof. According to (13.20) and (16.9), we may in the discrete case write the Gram matrix as

$$\Gamma(l) = \sum_j w_j \Gamma(u_j, l), \tag{16.12}$$

where here, as in (16.2), we use weights w_j in place of the factor $1/N$. By Theorem 16.1, replacing every $\mathcal{L}(u)$ by $\mathcal{L}(v)\mathcal{L}(u) \equiv \mathcal{L}(u')$ produces the new Gram matrix

$$\Gamma(l)' = \sum_j w_j \Gamma(u_j', l) = \sum_j w_j V \Gamma(u_j, l) V^\dagger = V \left(\sum_j w_j \Gamma(u_j, l) \right) V^\dagger = V \Gamma(l) V^\dagger,$$

where V denotes the unitary matrix with elements (16.11). This proves the corollary in the discrete case. In the continuum-limit case the proof is essentially identical, but it starts with (14.5) rather than (13.20). ■

The alert reader will have noted that both Theorem 16.1 and Corollary 16.1 remain true if we replace the basis monomials $G_r^{(l)}$ by a different set of orthonormal basis functions, say $\psi_\nu^{(l)}$.

Let us now reconsider the matter of adding a fixed amount ϕ to each of the angles θ_j that define the linear symplectic transformations $\mathcal{R}_j = \mathcal{R}(\theta_j)$ in (16.2). Since $\mathcal{R}(\theta_j + \phi) = \mathcal{R}(\phi)\mathcal{R}(\theta_j)$ where $\mathcal{R}$ denotes the unitary operator defined in (15.4), Corollary 16.1 implies that rotating all the θ_j by ϕ will change the Gram matrix only by a unitary similarity transformation. But since the application of any similarity transformation to any matrix cannot change the eigenvalues of that matrix, we conclude that the eigenvalue spectrum—and hence also the determinant—of the Gram matrix is invariant under a rotation of all the angles θ_j by an arbitrary amount ϕ.

Let us now turn to our observation that, at least in certain cases, the Gram determinant does not change when we add π to one or more of the angles θ_j. Since

$$\begin{aligned} [\cos(\theta_j + \pi)]^{2l-(r+s)} [\sin(\theta_j + \pi)]^{r+s} &= (-\cos\theta_j)^{2l-(r+s)} (-\sin\theta_j)^{r+s} \\ &= (\cos\theta_j)^{2l-(r+s)} (\sin\theta_j)^{r+s}, \end{aligned}$$

we conclude that in fact adding π to one or more of the angles θ_j has no effect even on the general Gram matrix elements $\Gamma(l)_{rs}$ given by (16.5). One may reach this same conclusion in a more general fashion by noting from (15.3) and (15.4) that

$$\mathcal{R}(\pi) \begin{pmatrix} q \\ p \end{pmatrix} = - \begin{pmatrix} q \\ p \end{pmatrix}, \tag{16.13}$$

and hence, because $\mathcal{R}_j Q_1^{(l)}$ is a homogeneous polynomial in q and p of degree l,

$$\mathcal{R}(\pi) \mathcal{R}_j Q_1^{(l)} = (-1)^l \mathcal{R}_j Q_1^{(l)}. \tag{16.14}$$

Then, because adding π to θ_j converts $\mathcal{R}_j$ to $\mathcal{R}(\pi)\mathcal{R}_j$, we conclude that adding π to θ_j modifies the summation (16.2) for the gram matrix element $\Gamma(l)_{rs}$ by simply multiplying the j-th term by $(-1)^{2l} = 1$, which means no modification at all.

We note here that the property derived in the last paragraph is really a reflection of the fact that adding π to some of the angles θ_j changes at most the signs of the corresponding jolt strengths in the jolt decomposition (11.2). To see this, first observe that in one degree of freedom the jolt decomposition (11.2) takes the form

$$h_l = \sum_{j=1}^{N} w_j a_j^{(l)} \mathcal{R}_j Q_1^{(l)}, \tag{16.15}$$

where $Q_1^{(l)}$ is given by (15.1). Then, using (16.14), we see that adding π to θ_j simply changes the jolt strength $a_j^{(l)}$ by the factor $(-1)^l$.

Before going on to the next section, we mention one further property of the Gram matrix $\Gamma(l)$. First observe that the continuum-limit Gram matrix elements $\Gamma(l)_{rs}$ given in (16.1) do not change if we add to the integration variable θ some fixed angle ϕ or if, equivalently, we replace $\mathcal{R}(\theta)$ by $\mathcal{R}(\phi)\mathcal{R}(\theta)$ (again for some fixed ϕ). Now suppose that the discrete form (16.2) of the Gram matrix elements derives from some quadrature formula for the circle which yields exact results for all functions in some important set $\mathcal{F}$. (In our case the functions of interest are the products of sensitivity functions for all degrees l up to and including some maximum degree P.) Then because that quadrature formula is exact on $\mathcal{F}$, we will obtain the same results if we replace all the $\mathcal{R}_j$ in (16.2) by $\mathcal{R}(\phi)\mathcal{R}_j$. Put another way, if the quadrature formula we choose is exact for the functions appearing in our Gram matrix elements (16.2), then replacing $\mathcal{R}_j$ by $\mathcal{R}(\phi)\mathcal{R}_j$ will not change $\Gamma(l)$. On the other hand, according to one of our earlier arguments, if the quadrature formula we choose is not exact, then replacing $\mathcal{R}_j$ by $\mathcal{R}(\phi)\mathcal{R}_j$ will change $\Gamma(l)$ but not its eigenvalue spectrum.

16.1.6. *The Minimum Number of Angles.* To perform jolt decomposition on a computer, we would like to replace the integral in (16.1) with the summation in (16.2) using an appropriate quadrature formula whose angles and weights we will then insert into (16.15). To perform jolt decomposition while retaining the optimal Gram eigenvalues found in the continuum limit, we would like that quadrature formula to be exact for all products of sensitivity functions that appear in the Gram matrix elements (16.1) up through some maximum degree $l_{max} = P$. And to perform jolt decomposition quickly, we would like to use a *minimal* quadrature formula, *i.e.*, a quadrature formula that needs as few angles as possible while still returning exact results through degree P. In this section we shall determine just such a quadrature formula.

To proceed, we must first determine which functions appear in the Gram matrix elements $\Gamma(l)_{rs}$ in (16.1) for degrees $l \le P$. Using (16.1) and (16.3), we see that the functions of interest are

$$(\cos\theta)^{2l-(r+s)}(\sin\theta)^{r+s}$$

for $l \in \{1, \ldots, P\}$ and $r, s \in \{0, \ldots, l\}$. Putting these functions in exponential form,

$$\Big(\frac{e^{i\theta}+e^{-i\theta}}{2}\Big)^{2l-(r+s)}\Big(\frac{e^{i\theta}-e^{-i\theta}}{2i}\Big)^{r+s} = \frac{(-i)^{r+s}}{2^{2l}}\sum_{ab}(-1)^b\binom{2l-(r+s)}{a}\binom{r+s}{b}(e^{i\theta})^{2(l-(a+b))},$$

yields a linear combination of exponential functions of the form $(e^{i\theta})^{2(l-\mu)}$ with $\mu \in \{0, 1, \ldots, 2l\}$. We therefore seek a quadrature formula on the circle $\mathbb{S}^1$ which returns exact results for all functions of the form

$$e^{i2\theta k}, \quad k \in \{P, P-1, \ldots, -P\}. \tag{16.16}$$

Recall that

$$\frac{1}{2\pi}\int_0^{2\pi} d\theta\, e^{im\theta} = \delta_{m0}. \tag{16.17}$$

Now consider the following N-point quadrature formula for the circle $\mathbb{S}^1$:

$$Q_N[f(\theta)] \equiv \frac{1}{N}\sum_{j=0}^{N-1} f\big(\tfrac{2\pi j}{N}\big). \tag{16.18}$$

Inserting the exponential functions (16.16) into the quadrature formula (16.18), we find

$$Q_N\big[e^{i2\theta k}\big] = \frac{1}{N}\sum_{j=0}^{N-1} e^{i2k2\pi j/N} = \frac{1}{N}\sum_{j=0}^{N-1}\big(e^{i2\pi 2k/N}\big)^j.$$

For $k = 0$, this sum returns the value 1, in agreement with the exact answer in (16.17). For $k \neq 0$, we obtain

$$Q_N\big[e^{i2\theta k}\big] = \frac{1}{N}\cdot\frac{1-e^{i2\pi 2k}}{1-e^{i2\pi 2k/N}},$$

which will return the correct answer 0 as long as the denominator does not vanish. This means we must select N so as to ensure that $2k/N$ is not an integer for any $k \in \{P, P-1, \ldots, -P\}$. It follows that choosing $N > 2P$ will certainly work; but observe that choosing any *odd* N greater than P will also work because such an N cannot divide any of the integers $2k \in \{2P, 2P-2, \ldots, -2P\}$. Hence we find the smallest value of N that makes the quadrature formula (16.18) return the exact results (16.17) for all of the exponential functions in (16.16) is given by

$$N_{min} = 2\,\lceil P/2\rceil + 1 = \begin{cases} P+1, & P \text{ even;} \\ P+2, & P \text{ odd.} \end{cases} \tag{16.19}$$

(Here $\lceil P/2\rceil$ denotes the smallest integer greater than or equal to $P/2$.) Put another way, N_{min} equals the first odd integer larger than $P = l_{max}$, the highest degree of interest (*cf.* (9.20)).

We have in (16.18) an N-point quadrature formula which, for N equal to the N_{min} of (16.19), is exact for all degrees $l \leq P$. Now recall from Table 13.1 that for one degree of freedom, $n = 1$, the lower bound on N is $P + 1$. Comparing this lower bound with (16.19) proves that our quadrature formula is minimal for even values of P. It seems reasonable to believe—but we offer no proof—that the formula is minimal also for odd values of P.[32]

As a simple check on our work, let us compute the Gram determinant $\det\Gamma(l)$ from (16.8) using the angles and weights defined by the quadrature formula (16.18). The result should agree with the product of the continuum-limit Gram eigenvalues given in (15.16): in other words, we should find

$$\det\Gamma(l) = \left(\frac{1}{2^l}\right)^{l+1}\prod_{r=0}^{l}\binom{l}{r}. \tag{16.20}$$

Before continuing, observe that because (16.8) requires exactly $N = l + 1$ angles, (16.19) implies that this check will work only for *even* values of l.

[32]If we restrict ourselves to equal weights only, then it follows that our quadrature formula is minimal also for odd P.

Setting $N = l + 1$ and using the angles and weights defined by the quadrature formula (16.18), we obtain

$$\begin{aligned}\det\Gamma(l) &= \prod_{i=1}^{l+1}\frac{1}{l+1}\cdot\prod_{r=0}^{l}\binom{l}{r}\cdot\prod_{1\le j<k\le l+1}\sin^2\left(\frac{2\pi}{l+1}(k-j)\right)\\ &= \left(\frac{1}{l+1}\right)^{l+1}\cdot\prod_{r}\binom{l}{r}\cdot\left[\sin^2\Big(\frac{2\pi}{l+1}\Big)\right]^{l}\left[\sin^2\Big(\frac{2\pi 2}{l+1}\Big)\right]^{l-1}\cdots\left[\sin^2\Big(\frac{2\pi l}{l+1}\Big)\right]^{1},\end{aligned}$$

because the set of j and k such that $1 \le j < k \le l+1$ includes l pairs whose difference equals one, $l-1$ pairs whose difference equals two, and so on. Then, because $-\sin\big(\frac{2\pi}{l+1}(l+1-j)\big) = \sin\big(\frac{2\pi j}{l+1}\big)$, the above result becomes

$$\begin{aligned}\det\Gamma(l) &= \left(\frac{1}{l+1}\right)^{l+1}\cdot\prod_{r}\binom{l}{r}\cdot\prod_{j=1}^{l/2}\left[\sin^2\Big(\frac{2\pi j}{l+1}\Big)\right]^{l+1}\\ &= \prod_{r}\binom{l}{r}\cdot\left[\frac{1}{l+1}\prod_{j=1}^{l/2}\sin^2\Big(\frac{2\pi j}{l+1}\Big)\right]^{l+1}\\ &= \prod_{r}\binom{l}{r}\cdot\left[\frac{1}{l+1}\prod_{j=1}^{l/2}\sin\Big(\frac{2\pi j}{l+1}\Big)(-1)\sin\Big(\frac{2\pi}{l+1}(l+1-j)\Big)\right]^{l+1}\\ &= \prod_{r}\binom{l}{r}\cdot\left[\frac{(-1)^{l/2}}{l+1}\prod_{j=1}^{l}\sin\Big(\frac{2\pi j}{l+1}\Big)\right]^{l+1}.\end{aligned}$$

Gradshteyn and Ryzhik [47, 1.393.2] report the product trigonometric identity

$$\prod_{j=0}^{l}\sin\Big(\frac{2\pi j}{l+1}+x\Big) = \frac{(-1)^{l/2}}{2^l}\sin(l+1)x \tag{16.21}$$

for even values of l.[33] Dividing both sides of this expression by the $j = 0$ term and taking the limit $x \to 0$ yields the identity

$$\prod_{j=1}^{l}\sin\Big(\frac{2\pi j}{l+1}\Big) = (-1)^{l/2}\frac{l+1}{2^l}.$$

Using this result, we may now write the Gram determinant in the form (recall that l is even)

$$\det\Gamma(l) = \prod_{r}\binom{l}{r}\cdot\left[\frac{(-1)^{l/2}}{l+1}(-1)^{l/2}\frac{l+1}{2^l}\right]^{l+1} = \left(\frac{1}{2^l}\right)^{l+1}\prod_{r}\binom{l}{r},$$

which agrees precisely with our expectation (16.20).

[33] One can prove this identity by the following line of reasoning: Define $U(x)$ to be the product on the left-hand-side and compute the logarithmic derivative $V(x) = U'(x)/U(x) = \sum_j 1/\tan\big(\frac{2\pi j}{l+1}+x\big)$. Then, using arguments from complex analysis, show that $V = W$, where $W(x) = (l+1)/\tan(l+1)x$. (To do this, first show that for *even* l the functions V and W have the same principal parts and hence differ by at most an entire function. Then show that V and W agree at infinity and are bounded there. It follows that $V - W$ must be a constant equal to zero.) To complete the proof, integrate both sides of $V = W$ to obtain $U(x) = C_l\sin(l+1)x$, where C_l denotes the integration constant. Then determine C_l by examining $U(iy)$ at large y and thus confirm (16.21).

16.1.7. *Optimal Jolt Decompositions in One Degree of Freedom.* Let us summarize what we have learned so far. In one degree of freedom using the quadrature formula (16.18), one can obtain optimal jolt decompositions for all homogeneous dynamical polynomials

$$h_l = \sum_{r=1}^{M(l,2)} c_r^{(l)} G_r^{(l)}$$

of degree $l \leq P$ by writing (*cf.* (16.15))

$$h_l = \frac{1}{N_{min}} \sum_{j=1}^{N_{min}} a_j^{(l)} \mathcal{R}(\theta_j) Q_1^{(l)}, \tag{16.22}$$

with the angles

$$\theta_j = \frac{2\pi j}{N_{min}}. \tag{16.23}$$

Here N_{min} is given by (16.19), $\mathcal{R}(\theta)$ denotes the Lie operator in (15.4) whose matrix representation on the dynamical variables q and p is given by (15.3), and $Q_1^{(l)}$ is given by (15.1). To obtain the jolt strengths $a_j^{(l)}$, we use (11.11) written for $n = 1$:

$$a_j^{(l)} = \sum_{rs} c_r^{(l)} [\Gamma(l)^{-1}]_{rs} \sigma_j^s. \tag{16.24}$$

Here the sensitivity vector σ^r has elements σ_j^r given by (16.3), and the Gram matrix $\Gamma(l)$ has elements $\Gamma(l)_{rs}$ given by (16.5) with $w_j = 1/N_{min}$. In both (16.3) and (16.5) $c_j = \cos\theta_j$ and $s_j = \sin\theta_j$ with θ_j as in (16.23). As described at the end of §16.1.5, however, we do have the freedom to increment all of the angles θ_j by an arbitrary amount ϕ (independent of j).

16.2. **Two Degrees of Freedom**

Before we tackle the question of how to implement an optimal jolt decomposition in two degrees of freedom, let us review how we addressed the matter in the last section when we studied one degree of freedom. There our approach really comprised three steps:

(1) Determine what set of functions appears inside the integral that defines the elements of the Gram matrix $\Gamma(l)$ in the continuum limit—and do this for all degrees l up through the maximum degree of interest, $l_{max} = P$.
(2) Replace the integral in the Gram matrix elements with a minimal quadrature (cubature) formula that works exactly for all members of the set of functions determined in the first step.
(3) Translate the chosen cubature formula into a corresponding formula for performing jolt decomposition.

We can tackle the case of two degrees of freedom using this same sequence of steps. At first we shall do so using just the coset space $\mathcal{U} = SU(2)/SO(2)$ as the manifold from which to choose our linear symplectic transformations $\mathcal{L}_j = \mathcal{L}(u_j)$. Later we shall look at using instead two other spaces: $\mathcal{U} = U(1) \otimes SU(2)/SO(2)$ (which covers $U(2)/SO(2)$) and $\mathcal{U} = [U(1)]^2 = U(1) \otimes U(1)$.

16.2.1. *The Functions Inside the Gram Matrix Elements.* To determine which functions appear inside the integral that defines the Gram matrix elements for the case $\mathcal{U} = SU(2)/SO(2)$, let us examine the expression (15.62). In particular, let us remove the integral over $SU(2)$ and thus examine matrix elements of the partial Gram operator (14.5b) (*cf.* (16.9)) with respect

to the dynamical basis polynomials $\varphi(j,m;l,\mu)$ constructed in §15.2.3:

$$\Gamma(u,l)_{jm\mu,j'm'\mu'} = \sum_{\nu\nu'}\Big[\Big(\big[D^j(u^{-1})\big]^*_{m\nu}\, D^{j'}(u^{-1})_{m'\nu'}\Big)\times \frac{1}{l+1}\sum_k \Big\langle \varphi(j,\nu;l,\mu), Q_k^{(l)}\Big\rangle\Big\langle Q_k^{(l)}, \varphi(j',\nu';l,\mu')\Big\rangle\Big]. \tag{16.25}$$

To determine from this expression the functions of interest to us, we need to extract the u dependence of these matrix elements; hence we examine the product $\big[D^j(u^{-1})\big]^*_{m\nu}\, D^{j'}(u^{-1})_{m'\nu'}$. The matrices $D^j(u)$ were described earlier as spin-j representations of $SU(2)$. Let us make this statement more explicit so that we may take advantage of some results well known in the quantum mechanical theory of angular momentum.

To obtain an explicit formula for the matrix elements $D^j(u)_{mm'}$, use (15.49) together with the orthonormality of the $\varphi(j,m;l,\mu)$. Substituting the symbol D^j for $\Phi^j_{l\mu}$ (pursuant to our discussion at the end of §15.2.3), we find

$$D^j(u)_{mm'} = \big\langle \varphi(j,m';l,\mu), \mathcal{L}(u)\varphi(j,m;l,\mu)\big\rangle\,. \tag{16.26}$$

The reader may notice that the relative order of the indices m and m' on the two sides of this expression differs from the usual ordering. The choice made here takes into account the property (13.15), or (9.15), of Lie operators and ensures that the matrices $D^j(u)$ do indeed form a representation of $SU(2)$; *i.e.*,

$$D^j(u_1)D^j(u_2) = D^j(u_1u_2).$$

Now recall that we want to use the alternate Euler angle parameterization (15.26) for matrices $u \in SU(2)$; hence, with (13.15), we shall write

$$\mathcal{L}(u) = \mathcal{L}(u_\psi u_\theta u_\phi) = \mathcal{L}(u_\phi)\mathcal{L}(u_\theta)\mathcal{L}(u_\psi) = \mathcal{L}(e^{i\phi\sigma_2/2})\mathcal{L}(e^{-i\theta\sigma_3/2})\mathcal{L}(e^{i\psi\sigma_2/2}).$$

Using the Lie operators (15.34), one can write the above operator product as a sequence of Lie transformations:

$$\mathcal{L}(u) = e^{-i\phi:a^3:}e^{i\theta:a^1:}e^{-i\psi:a^3:}. \tag{16.27}$$

To see this, first note, using (15.22) and (13.11), that the linear Lie operator

$$\mathcal{L}(u_\phi) = \mathcal{L}(e^{i\phi\sigma_2/2}) = \mathcal{L}\begin{pmatrix} \cos(\phi/2) & \sin(\phi/2)\\ -\sin(\phi/2) & \cos(\phi/2)\end{pmatrix}$$

has the matrix representation

$$M(u_\phi) = \begin{pmatrix} \cos(\phi/2) & \sin(\phi/2) & 0 & 0\\ -\sin(\phi/2) & \cos(\phi/2) & 0 & 0\\ 0 & 0 & \cos(\phi/2) & \sin(\phi/2)\\ 0 & 0 & -\sin(\phi/2) & \cos(\phi/2)\end{pmatrix} \tag{16.28}$$

with respect to the q's and p's. Now consider the Lie transformation $e^{-i\phi:a^3:}$. One can see from (15.41) that $:2a^3:^2$, and hence also all even powers of $:2a^3:$, acts as an identity operator on the q's and p's. We may therefore write

$$e^{-i\phi:a^3:}z = \exp\Big(-\frac{i\phi}{2}:2a^3:\Big)z = \cos\Big(\frac{\phi}{2}\Big)z - i\sin\Big(\frac{\phi}{2}\Big):2a^3:z.$$

Using (15.41) and (16.28), we find

$$e^{-i\phi:a^3:}\begin{pmatrix}q_1\\q_2\\p_1\\p_2\end{pmatrix} = \begin{pmatrix}q_1\\q_2\\p_1\\p_2\end{pmatrix}\cos\Big(\frac{\phi}{2}\Big) + \begin{pmatrix}q_2\\-q_1\\p_2\\-p_1\end{pmatrix}\sin\Big(\frac{\phi}{2}\Big) = M(u_\phi)\begin{pmatrix}q_1\\q_2\\p_1\\p_2\end{pmatrix}.$$

It follows thus that

$$\mathcal{L}(u_\phi) = \mathcal{L}(e^{i\phi\sigma_2/2}) = e^{-i\phi:a^3:}. \tag{16.29}$$

Also, of course,

$$\mathcal{L}(u_\psi) = \mathcal{L}(e^{i\psi\sigma_2/2}) = e^{-i\psi:a^3:}. \tag{16.30}$$

Except for some minor alterations, an identical argument applies to $\mathcal{L}(u_\theta)$: The linear Lie operator

$$\mathcal{L}(u_\theta) = \mathcal{L}(e^{-i\theta\sigma_3/2}) = \mathcal{L}\begin{pmatrix} \exp(-i\theta/2) & 0 \\ 0 & \exp(i\theta/2) \end{pmatrix}$$

has the matrix representation

$$M(u_\theta) = \begin{pmatrix} \cos(\theta/2) & 0 & -\sin(\theta/2) & 0 \\ 0 & \cos(\theta/2) & 0 & \sin(\theta/2) \\ \sin(\theta/2) & 0 & \cos(\theta/2) & 0 \\ 0 & -\sin(\theta/2) & 0 & \cos(\theta/2) \end{pmatrix} \tag{16.31}$$

with respect to the q's and p's. And since $:2a^1:$ acts as an identity operator on the q's and p's (see (15.41)), we may write the action of the Lie transformation $e^{i\theta:a^1:}$ in the form

$$e^{i\theta:a^1:}z = \exp\Big(\frac{i\theta}{2}:2a^1:\Big)z = \cos\Big(\frac{\theta}{2}\Big)z + i\sin\Big(\frac{\theta}{2}\Big):2a^1:z.$$

Using (15.41) and (16.31), we find

$$e^{i\theta:a^1:}\begin{pmatrix} q_1 \\ q_2 \\ p_1 \\ p_2 \end{pmatrix} = \begin{pmatrix} q_1 \\ q_2 \\ p_1 \\ p_2 \end{pmatrix}\cos\Big(\frac{\theta}{2}\Big) + \begin{pmatrix} -p_1 \\ p_2 \\ q_1 \\ -q_2 \end{pmatrix}\sin\Big(\frac{\theta}{2}\Big) = M(u_\theta)\begin{pmatrix} q_1 \\ q_2 \\ p_1 \\ p_2 \end{pmatrix}.$$

Hence

$$\mathcal{L}(u_\theta) = \mathcal{L}(e^{-i\theta\sigma_3/2}) = e^{i\theta:a^1:}. \tag{16.32}$$

The result (16.27) follows from (16.29), (16.30), and (16.32).

With the expression (16.27) for the linear symplectic transformations $\mathcal{L}(u)$ we may now write the matrix elements (16.26) of $D^j(u)$ in the form

$$D^j\big(u(\psi,\theta,\phi)\big)_{mm'} = \big\langle \varphi(j,m';l,\mu), e^{-i\phi:a^3:}e^{i\theta:a^1:}e^{-i\psi:a^3:}\varphi(j,m;l,\mu)\big\rangle\,. \tag{16.33a}$$

Since these matrix elements are determined solely by the commutation relations among the Lie operators $:a^k:$ [20, p. 441], and since we arranged the commutation relations (15.35) to agree precisely with those of the quantum mechanical angular momentum operators J_k, we reach the delightful conclusion that the matrix elements (16.33a) are *exactly* those found in any reasonably complete text on quantum mechanics [7, 64, 75, 77]:

$$D^j\big(u(\psi,\theta,\phi)\big)_{mm'} = \big\langle jm'\big|e^{-i\phi J_z}e^{i\theta J_x}e^{-i\psi J_z}\big|jm\big\rangle\,. \tag{16.33b}$$

Recall, for example, that we defined the basis polynomials $\varphi(j,m;l,\mu)$ to have $:a^3:$ eigenvalue m; we therefore obtain from (16.33a) and the unitarity of the Lie transformations $e^{i\alpha:a^k:}$ a familiar result:

$$\begin{aligned} D^j\big(u(\psi,\theta,\phi)\big)_{mm'} &= \big\langle e^{i\phi:a^3:}\varphi(j,m';l,\mu), e^{i\theta:a^1:}e^{-im\psi}\varphi(j,m;l,\mu)\big\rangle \\ &= e^{-i(m'\phi+m\psi)}\big\langle \varphi(j,m';l,\mu), e^{i\theta:a^1:}\varphi(j,m;l,\mu)\big\rangle \\ &= e^{-i(m'\phi+m\psi)}D^j(u_\theta)_{mm'}. \end{aligned} \tag{16.33c}$$

Note that in terms of the $SU(2)/SO(2)$ coset space $c(\theta,\phi)$—see (15.26) and (15.27)—we may rewrite this expression in the form

$$D^j\big(u(\psi,\theta,\phi)\big)_{mm'} = e^{-im\psi}D^j\big(c(\theta,\phi)\big)_{mm'}. \tag{16.33d}$$

We should, however, address the fact that the (nearly universal) convention in quantum mechanics writes the matrix elements of the rotation operator in the form

$$D^j_{\mathrm{QM}}(\phi,\theta,\psi)_{m'm} = \big\langle jm'\big|e^{-i\phi J_z}e^{-i\theta J_y}e^{-i\psi J_z}\big|jm\big\rangle = e^{-i(m'\phi+m\psi)}d^j_{m'm}(\theta), \tag{16.34}$$

where the (real) matrix elements $d^j_{m'm}(\theta)$ are given by Wigner's formula (15.94). Note that here—as flagged by the subscript "QM"—the indices m' and m occur in the usual order, and the rotation operator in the middle effects rotations about the y-axis. To express (16.33b) in this form, we use the fact that (*cf.* (15.25))

$$e^{i\theta J_x} = e^{-i(\pi/2)J_z}e^{-i\theta J_y}e^{i(\pi/2)J_z}.$$

With this substitution we obtain the desired result for the matrix elements (16.33b):

$$\begin{aligned} D^j\big(u(\psi,\theta,\phi)\big)_{mm'} &= \big\langle jm'\big|e^{-i\phi J_z}e^{-i(\pi/2)J_z}e^{-i\theta J_y}e^{i(\pi/2)J_z}e^{-i\psi J_z}\big|jm\big\rangle \\ &= e^{-i(\pi/2)m'}e^{i(\pi/2)m}\big\langle jm'\big|e^{-i\phi J_z}e^{-i\theta J_y}e^{-i\psi J_z}\big|jm\big\rangle \\ &= i^{m-m'}D^j_{\mathrm{QM}}(\phi,\theta,\psi)_{m'm}. \end{aligned} \tag{16.35}$$

Now that we have in hand the connection (16.35) between our spin-j representations D^j and the conventional representations D^j_{QM}, we can proceed with extracting from the Gram matrix elements (16.25) the functions of interest to us. First recall that one can expand the product of two spin-j representations in a linear combination of other spin-j representations using the *Clebsch-Gordan series* [7, 75],

$$\begin{aligned} D^{j_1}_{\mathrm{QM}}(\phi,\theta,\psi)_{m_1'm_1}D^{j_2}_{\mathrm{QM}}(\phi,\theta,\psi)_{m_2'm_2} = \\ \sum_{j=|j_1-j_2|}^{j_1+j_2}\sum_{m',m=-j}^{j}\left(\begin{matrix}j_1 & j_2\\ m_1' & m_2'\end{matrix}\middle|\begin{matrix}j\\ m'\end{matrix}\right)\left(\begin{matrix}j_1 & j_2\\ m_1 & m_2\end{matrix}\middle|\begin{matrix}j\\ m\end{matrix}\right)D^j_{\mathrm{QM}}(\phi,\theta,\psi)_{m'm}. \end{aligned} \tag{16.36}$$

(Here, as in (15.59), the symbols $\left(\begin{smallmatrix}j_1 & j_2\\ m_1 & m_2\end{smallmatrix}\middle|\begin{smallmatrix}j\\ m\end{smallmatrix}\right)$ denote the usual Clebsch-Gordan coefficients.) By making use of the unitarity of the representations D^j, the relations (16.34) and (16.35), the symmetry relation (15.117a) for the elements $d^j_{m'm}(\theta)$, and the Clebsch-Gordan series (16.36), we may (after some algebra) write

$$\begin{aligned} \big[D^j(u^{-1})\big]^*_{m\nu}D^{j'}(u^{-1})_{m'\nu'} &= i^{(\nu+\nu')-(m+m')}D^j_{\mathrm{QM}}(\phi,\theta,\psi)_{m\nu}D^{j'}_{\mathrm{QM}}(\phi,\theta,\psi)_{-m',-\nu'} \\ &= i^{(\nu+\nu')-(m+m')}\sum_{j''}\sum_{\nu''m''}\left(\begin{matrix}j & j'\\ m & -m'\end{matrix}\middle|\begin{matrix}j''\\ m''\end{matrix}\right)\left(\begin{matrix}j & j'\\ \nu & -\nu'\end{matrix}\middle|\begin{matrix}j''\\ \nu''\end{matrix}\right)i^{m''-\nu''}D^{j''}(u)_{\nu''m''}. \end{aligned}$$

Inserting this expression into (16.25) and collecting into a single coefficient the sums over ν, ν', and k (together with anything else that doesn't look like $D^{j''}(u)_{\nu''m''}$), we find that the partial Gram matrix elements have the general form

$$\Gamma(u,l)_{jm\mu,j'm'\mu'} = \sum_{j''=|j-j'|}^{j+j'}\sum_{\nu''m''}a^{j''}_{\nu''m''}D^{j''}(u)_{\nu''m''}. \tag{16.37}$$

Here the coefficients $a^{j''}_{\nu''m''}$ depend on not only the summation variables j'', ν'', and m'', but also the degree l and the matrix element labels $jm\mu$ and $j'm'\mu'$. For the current discussion, however, we need not make explicit these latter dependences.

Recall now Theorem 13.1, which states that the partial Gram operator $\widehat{\Gamma}(u,l)$ is a class function with respect to the $O(n)$ subgroup of $U(n)$. This theorem implies that our partial Gram matrix elements (16.37) must satisfy the relation

$$\Gamma(u,l)_{jm\mu,j'm'\mu'} = \Gamma(r\cdot c,l)_{jm\mu,j'm'\mu'} = \Gamma(c,l)_{jm\mu,j'm'\mu'}, \tag{16.38}$$

where here $u \in SU(2)$, $r \in SO(2)$, and c labels the coset space $SU(2)/SO(2)$. To see the consequences of this relation, suppose f is any function defined on $SU(2)$. Then, by the completeness of the $D^j(u)$ [7, 8], f has an expansion of the form

$$f(u) = \sum_{jmm'} a^j_{mm'} D^j(u)_{mm'}.$$

Using (16.35) and the orthogonality condition for the $D^j(u)$,[34] we may extract the expansion coefficients $a^j_{mm'}$ in the form

$$a^j_{mm'} = (2j+1) \int_{SU(2)} du\, f(u)\, D^j(u)^*_{mm'}.$$

Next assume that f satisfies the class relation

$$f(u) = f(c).$$

With this assumption we can use (16.33d) and the measure du described in §15.2.2 to carry out the $SO(2)$ part of the above integration. Writing c_Ω for $c(\theta, \phi)$, we find

$$a^j_{mm'} = (2j+1) \int_{\mathbb{S}^2} \frac{d\Omega}{4\pi} \int_0^{4\pi} \frac{d\psi}{4\pi} f(c_\Omega) e^{im\psi} D^j(c_\Omega)^*_{mm'} = \delta_{m0}(2j+1) \int_{\mathbb{S}^2} \frac{d\Omega}{4\pi} f(c_\Omega) D^j(c_\Omega)^*_{0m'}.$$

In other words, the expansion coefficients $a^j_{mm'}$ vanish unless $m = 0$. As a consequence, we can always write

$$f(u) = \sum_{jm} a^j_{0m} D^j(u)_{0m}$$

for any class function $f(u)$. Observe here that the subscript zero on the $D^j(u)$ implies that only integer values of j can occur in this summation. To simplify further our expansion for f, let us recall that [7]

$$D^j_{\text{QM}}(\phi, \theta, \psi)_{m0} = \sqrt{\frac{4\pi}{2j+1}}\, Y_{jm}(\theta, \phi)^*, \tag{16.39}$$

where the symbol Y_{jm} denotes a spherical harmonic. Using this fact and (16.35), we can now see that any class function $f(u)$—and hence also our partial Gram matrix elements (16.37), or (16.25)—must have an expansion in terms of spherical harmonics:

$$f(u) = \sum_{jm} b^j_m Y_{jm}(\theta, \phi)$$

(with j taking integer values only).

With the results of the last paragraph one may now write the partial Gram matrix elements (16.37) in the form[35]

$$\Gamma(u, l)_{jm\mu, j'm'\mu'} = \Gamma(c_\Omega, l)_{jm\mu, j'm'\mu'} = \sum_{\substack{j''=|j-j'| \\ j'' \in \mathbb{Z}}}^{j+j'} \sum_{m''} b^{j''}_{m''} Y_{j''m''}(\Omega). \tag{16.40}$$

Since the basis polynomials $\varphi(j, m; l, \mu)$ for a given l have $j \leq \frac{l}{2}$ (recall the first observation made following (15.49)), and since the upper limit on the sum here equals $j + j'$, it follows from (16.25) that all the Y_{jm}'s appearing in (16.40) must have $j \leq l$. We therefore conclude that *when we choose the linear symplectic transformations $\mathcal{L}(u)$ from the coset space $\mathfrak{U} =$*

[34] Using the connection (16.35), one may show by a simple substitution that the orthogonality condition for spin-j representations of $SU(2)$ takes the same form whether expressed in terms of the D^j or the D^j_{QM}.

[35] Here $\mathbb{Z}$ denotes the set of all integers.

$SU(2)/SO(2)$, the functions of interest to us are the spherical harmonics Y_{jm} for all $j \leq l_{max} = P$.

At this point the reader may object that our identification of the spherical harmonics Y_{jm} as the functions of interest depends on our constructing matrix elements of the partial Gram operator $\widehat{\Gamma}(u,l)$ with respect to the particular basis polynomials $\varphi(j,m;l,\mu)$. To see that this choice of basis does not, in fact, make a difference, simply expand the chosen basis—the monomials $G_r^{(l)}$, say—in terms of the $\varphi(j,m;l,\mu)$. (*Cf.* the discussion leading to (12.5).) Since the coefficients in the expansions will not interfere with the required integration over $\mathbb{S}^2$ (see the next section), it follows that one's choice of basis cannot affect the identification of the functions of interest.

Let us now determine the functions of interest when we choose the linear symplectic transformations $\mathcal{L}(u)$ from the coset space $\mathcal{U} = U(1) \otimes SU(2)/SO(2)$ (which covers $U(2)/SO(2)$). In this case, using (15.77), the partial Gram operator takes the form (*cf.* (15.78))

$$\widehat{\Gamma}(u,l) = \widehat{\Gamma}(ve^{i\omega/2},l) = \frac{1}{l+1}\sum_{k=0}^{l} \mathcal{R}(\omega)\mathcal{L}(v)\left|Q_k^{(l)}\right\rangle\!\left\langle Q_k^{(l)}\right| \mathcal{L}(v)^\dagger \mathcal{R}(\omega)^\dagger,$$

where (15.80) defines the Lie operator $\mathcal{R}(\omega)$, $\omega \in [0,2\pi]$, and $v \in SU(2)$. If we form matrix elements of this operator with respect to the basis polynomials $\varphi(j,m;l,\mu)$, use the fact that $\mathcal{R}(\omega)$ and $\mathcal{L}(v)$ commute (recall the remarks made following (15.80)), and employ the same reasoning that led from (15.61) to (15.62), we obtain

$$\Gamma(ve^{i\omega/2},l)_{jm\mu,j'm'\mu'} = \sum_{\nu\nu'}\Bigg[\Big(\big[D^j(v^{-1})\big]^*_{m\nu}\, D^{j'}(v^{-1})_{m'\nu'}\Big)\times \frac{1}{l+1}\sum_k \Big\langle \varphi(j,\nu;l,\mu), \mathcal{R}(\omega)Q_k^{(l)}\Big\rangle\Big\langle \mathcal{R}(\omega)Q_k^{(l)}, \varphi(j',\nu';l,\mu')\Big\rangle\Bigg], \tag{16.41}$$

which differs in essence from (16.25) only in the presence of the rotation operator $\mathcal{R}(\omega)$ acting on the $Q_k^{(l)}$'s. Note that we may, according to Theorem 13.1, factor the $SO(2)$ subgroup out of the above matrix elements, just as in (16.38). In other words,

$$\Gamma(ve^{i\omega/2},l)_{jm\mu,j'm'\mu'} = \Gamma(c_\Omega\, e^{i\omega/2},l)_{jm\mu,j'm'\mu'}, \tag{16.42}$$

where, as in (16.40), c_Ω labels the coset space $SU(2)/SO(2)$. Because of the class relation (16.42), and because the matrix elements (16.41) are separable in the $U(1)$ and $SU(2)/SO(2)$ subspaces,[36] one can use arguments identical to those employed earlier; we deduce that the spin-j representations D^j and $D^{j'}$ appearing in (16.41) lead to the presence of spherical harmonics Y_{jm} for $j \leq P$—exactly as in (16.40) for the case $\mathcal{U} = SU(2)/SO(2)$.

Now examine the dependence of the partial Gram matrix elements (16.41) on the $U(1)$ subspace—*i.e.*, on the variable ω. To do this, first note that we can write $\mathcal{R}(\omega)$ as given by (15.80) in the form

$$\mathcal{R}(\omega) = \mathcal{R}_1(\omega/2)\mathcal{R}_2(\omega/2),$$

where the rotation operator $\mathcal{R}_j$, given by (15.135b), effects rotations only in the (q_j,p_j) plane. Second, use (15.18) and (15.141) to express $Q_k^{(l)}$ as a linear combination of the eigenfunctions of $\mathcal{R}(\omega)$:

$$\begin{aligned} Q_k^{(l)} &= \frac{q_1^{l-k}q_2^k}{\sqrt{(l-k)!\,k!}} = \left(\frac{1}{2}\right)^{l/2}\sum_{r_1=0}^{l-k}\sum_{r_2=0}^{k}(-i)^{r_1+r_2}\sqrt{\binom{l-k}{r_1}\binom{k}{r_2}}\,\psi_{1r_1}^{(l-k)}\psi_{2r_2}^{(k)} \\ &= \sum_{r_1r_2} a_{kr_1r_2}^{(l)}\psi_{1r_1}^{(l-k)}\psi_{2r_2}^{(k)}, \end{aligned}$$

[36] A more precise statement here should say that each matrix element (16.41) comprises a linear combination of terms—each of which is separable in the subspaces $U(1)$ and $SU(2)/SO(2)$.

where the symbol $a^{(l)}_{kr_1r_2}$ denotes a set of complex coefficients. Using this expansion and (15.139), we find that

$$\begin{aligned}\mathcal{R}(\omega)Q^{(l)}_k &= \sum_{r_1r_2} a^{(l)}_{kr_1r_2}\mathcal{R}_1(\omega/2)\mathcal{R}_2(\omega/2)\psi^{(l-k)}_{1r_1}\psi^{(k)}_{2r_2}\\ &= \sum_{r_1r_2} a^{(l)}_{kr_1r_2}e^{-i(l-k-2r_1)\omega/2}e^{-i(k-2r_2)\omega/2}\psi^{(l-k)}_{1r_1}\psi^{(k)}_{2r_2}\\ &= \sum_{r_1r_2} a^{(l)}_{kr_1r_2}e^{-i(l-2(r_1+r_2))\omega/2}\psi^{(l-k)}_{1r_1}\psi^{(k)}_{2r_2}.\end{aligned}$$

Observe that in this double sum the total r_1+r_2 ranges over the set $\{0,1,\ldots,l\}$. Next, insert the above expansion into both places where $\mathcal{R}(\omega)Q^{(l)}_k$ appears in the matrix elements (16.41). One obtains

$$\begin{aligned}\Gamma(ve^{i\omega/2},l)_{jm\mu,j'm'\mu'} = \sum_{\nu\nu'}\Bigg[\Big(\big[D^j(v^{-1})\big]^*_{m\nu}\,D^{j'}(v^{-1})_{m'\nu'}\Big)\times\\ \frac{1}{l+1}\sum_k\sum_{r_1r_2}\sum_{r_1'r_2'}\Big(e^{-i(l-2(r_1+r_2))\omega/2}a^{(l)}_{kr_1r_2}\,e^{i(l-2(r_1'+r_2'))\omega/2}a^{(l)}_{kr_1'r_2'}\times\\ \Big\langle\varphi(j,\nu;l,\mu),\psi^{(l-k)}_{1r_1}\psi^{(k)}_{2r_2}\Big\rangle\Big\langle\psi^{(l-k)}_{1r_1'}\psi^{(k)}_{2r_2'},\varphi(j',\nu';l,\mu')\Big\rangle\Big)\Bigg].\end{aligned}$$

Since $r_1+r_2\in\{0,1,\ldots,l\}$, and similarly for $r_1'+r_2'$, it follows that the exponential functions

$$e^{i\kappa\omega},\quad \kappa\in\{l,l-1,\ldots,-l\},$$

govern the ω-dependence of the partial Gram matrix elements (16.41).

Putting together the results of the last two paragraphs, we conclude that *when we choose the linear symplectic transformations $\mathcal{L}(u)$ from the space $\mathcal{U}=U(1)\otimes SU(2)/SO(2)$, the functions of interest to us are the product functions $e^{i\kappa\omega}Y_{jm}(\Omega)$ for all $j\le l_{max}=P$ and all $\kappa\in\{P,P-1,\ldots,-P\}$.*

We turn now to the last manifold from which we shall consider selecting the linear symplectic transformations $\mathcal{L}(u)$: the space $\mathcal{U}=U(1)\otimes U(1)$, which was discussed in §15.4. To determine the functions of interest in this case, we first obtain the partial Gram matrix elements from the Gram matrix elements (15.140) by removing the integrals over θ_j and setting $n=2$. Thus

$$\Gamma(\theta_1,\theta_2,l)_{rr'} = \frac{1}{l+1}\sum_k\left\langle\mathcal{R}(\theta_1,\theta_2)^\dagger\psi^{(l)}_r,Q^{(l)}_k\right\rangle\left\langle Q^{(l)}_k,\mathcal{R}(\theta_1,\theta_2)^\dagger\psi^{(l)}_{r'}\right\rangle.$$

Using (15.138) and the homogeneity relation $l_1+l_2=l$, we may write the rotation operator eigenfunctions $\psi^{(l)}_r$ in the form

$$\psi^{(l)}_r = \psi^{(l_1)}_{1r_1}\psi^{(l_2)}_{2r_2} = \psi^{(l-\nu)}_{1r_1}\psi^{(\nu)}_{2r_2}\equiv\psi^{(l)}_{\nu r_1r_2},\tag{16.43}$$

where the indices $\nu\in\{0,\ldots,l\}$, $r_1\in\{0,\ldots,l-\nu\}$, and $r_2\in\{0,\ldots,\nu\}$ constitute an alternate scheme for labeling these functions. From the unitarity of the rotation operator (*cf.* (15.81)) and the eigenvalue equation (15.139) we find that

$$\mathcal{R}(\theta_1,\theta_2)^\dagger\psi^{(l)}_{\nu r_1r_2} = e^{i(l-\nu-2r_1)\theta_1}e^{i(\nu-2r_2)\theta_2}\psi^{(l)}_{\nu r_1r_2}.$$

Employing this result together with the alternate labeling scheme, we can put the partial Gram matrix elements in the form

$$\begin{aligned}
&\Gamma(\theta_1,\theta_2,l)_{\nu r_1 r_2,\nu' r_1' r_2'} \\
&\quad= \frac{1}{l+1}\sum_k e^{-i(l-\nu-2r_1)\theta_1} e^{-i(\nu-2r_2)\theta_2} e^{i(l-\nu'-2r_1')\theta_1} e^{i(\nu'-2r_2')\theta_2} \\
&\qquad\qquad \left\langle \psi^{(l)}_{\nu r_1 r_2}, Q^{(l)}_k \right\rangle \left\langle Q^{(l)}_k, \psi^{(l)}_{\nu' r_1' r_2'} \right\rangle \\
&\quad= \frac{1}{l+1}\sum_k e^{i(\nu-\nu'+2(r_1-r_1'))\theta_1} e^{-i(\nu-\nu'-2(r_2-r_2'))\theta_2} \left\langle \psi^{(l)}_{\nu r_1 r_2}, Q^{(l)}_k \right\rangle \left\langle Q^{(l)}_k, \psi^{(l)}_{\nu' r_1' r_2'} \right\rangle .
\end{aligned} \tag{16.44}$$

Next consider the k-th term in this summation and observe from (15.18) that $Q^{(l)}_k$ is of degree $l-k$ in the variable q_1 and of degree k in the variable q_2. Likewise, observe from (16.43) and (15.138a) that the eigenfunction $\psi^{(l)}_{\nu r_1 r_2}$ is of degree $l-\nu$ in the variables z_1 and z_1^*, and of degree ν in the variables z_2 and z_2^*; hence, from (15.97), $\psi^{(l)}_{\nu r_1 r_2}$ is of degree $l-\nu$ in the variables q_1 and p_1, and of degree ν in the variables q_2 and p_2. It follows from these two observations that the inner product $\left\langle \psi^{(l)}_{\nu r_1 r_2}, Q^{(l)}_k \right\rangle$ must vanish whenever $k \neq \nu$.[37] With a similar result for the inner product $\left\langle Q^{(l)}_k, \psi^{(l)}_{\nu' r_1' r_2'} \right\rangle$ we see that together the two inner products appearing in (16.44) contribute a factor $\delta_{k\nu}\delta_{k\nu'} = \delta_{k\nu}\delta_{\nu\nu'}$ to each term in the summation. We may therefore express the partial Gram matrix elements in the form

$$\Gamma(\theta_1,\theta_2,l)_{\nu r_1 r_2,\nu' r_1' r_2'} = \frac{\delta_{\nu\nu'}}{l+1} e^{i2(r_1-r_1')\theta_1} e^{i2(r_2-r_2')\theta_2} \left\langle \psi^{(l)}_{\nu r_1 r_2}, Q^{(l)}_\nu \right\rangle \left\langle Q^{(l)}_\nu, \psi^{(l)}_{\nu r_1' r_2'} \right\rangle . \tag{16.45}$$

Since $r_1, r_1' \in \{0,\ldots,l-\nu\}$, it follows that $r_1 - r_1' \in \{l-\nu,\ldots,-(l-\nu)\}$; likewise, $r_2 - r_2' \in \{\nu,\ldots,-\nu\}$. Because $\nu \in \{0,\ldots,l\}$ and $l \leq l_{max} < P$, we might conclude that the functions of interest to us are product exponentials of the form $e^{i2k_1\theta_1} e^{i2k_2\theta_2}$ for all $k_1, k_2 \in \{P, P-1,\ldots,-P\}$. We can, however, place somewhat stronger constraints on k_1 and k_2. To see this, suppose k_1 is given. Then because $|k_1| = |r_1 - r_1'| \leq l-\nu$, it follows that

$$|k_2| = |r_2 - r_2'| \leq \nu \leq l - |k_1| ,$$

or, put another way,

$$|k_1| + |k_2| \leq l.$$

We therefore conclude that *when we choose the linear symplectic transformations $\mathcal{L}(u)$ from the space $\mathcal{U} = U(1) \otimes U(1)$, the functions of interest to us are the product exponentials $e^{i2k_1\theta_1} e^{i2k_2\theta_2}$ for all $k_1, k_2 \in \{P, P-1,\ldots,-P\}$ such that $|k_1| + |k_2| \leq P$.*

16.2.2. *Cubature Formulas for the Two-Sphere.* Let us now address the second of the three steps outlined at the beginning of §16.2: that of replacing the integral in the Gram matrix elements with an appropriate cubature formula. Recall from (15.29) that when we choose the linear symplectic transformations $\mathcal{L}(u)$ from the coset space $\mathcal{U} = SU(2)/SO(2)$, the required integral covers $\mathbb{S}^2$, the surface of the unit two-sphere. Based on the results of the last section, we now seek minimal cubature formulas on $\mathbb{S}^2$ that yield exact results for all spherical harmonics Y_{jm} having $j \leq P$. In other words, we want to find cubature formulas of the form

$$Q_N[f(\Omega)] \equiv \sum_{i=1}^N w_i f(\Omega_i), \tag{16.46}$$

with N as small as possible, such that for all $j \leq P$

$$Q_N\big[Y_{jm}(\Omega)\big] = \frac{\delta_{j0}\delta_{m0}}{\sqrt{4\pi}}. \tag{16.47}$$

[37] We employed the same sort of reasoning earlier, in symbols, for the argument that led from (15.140) to (15.142).

Before listing the best of the known cubature formulas for the two-sphere, we describe a simple counting argument that provides a means for estimating how close a given formula is to being minimal. First observe that (16.47) constitutes a set of

$$\sum_{j=0}^{P}(2j+1) = (P+1)^2$$

conditions that the cubature formula (16.46) must satisfy. Next note that one may specify N weights and N points so as to satisfy these constraints. The symmetry of the sphere, however, means that one point may always be fixed at, say, the "North pole", and a second point may be rotated about the polar axis to the "prime meridian". Thus, one point may be placed at the North pole, and a second may be placed on the prime meridian—with only its latitude requiring specification, and the other $N-2$ points remain free. Since two angles define each point, the total number of free variables equals N weights $+\, 2(N-2)$ variables for the free points $+$ 1 latitude for the point on the prime meridian $= 3N-3$. This suggests (but does *not* prove) that the number of points N in the cubature formula (16.46) must, for our needs, satisfy

$$3N - 3 \geq (P+1)^2,$$

or

$$N \geq N_{sph}(P) \equiv \left\lceil \frac{(P+1)^2+3}{3} \right\rceil = \left\lceil \frac{(P+1)^2}{3} \right\rceil + 1, \tag{16.48}$$

where $\lceil x \rceil$ denotes the ceiling function described earlier, after (16.19). We may thus use the number $N_{sph}(P)$ as a rough guide for judging whether or not a given cubature formula is close to minimal.[38]

Table 16.1 lists the best (in the sense of requiring as few points as possible) of the known cubature formulas on the spherical surface $\mathbb{S}^2$ for seven different values of P between three and fourteen inclusive. All of these formulas were taken from Stroud [85], published in 1971. Although other cubature formulas for the two-sphere have been published more recently [5, 24, 46, 57, 56, 58, 60, 59, 61, 78], none use as few points as those compiled in Stroud's book.[39]

Each cubature formula listed in Table 16.1 begins by stating the *degree* P (sometimes also called the *order* or the *strength*) and the number of cubature points N. For some values of P the listing also includes a brief description of the geometric nature of the set of points. Then, each triplet of the form (x, y, z) labels a point—or a set of points—on $\mathbb{S}^2$ in standard Euclidean coördinates; the W, or W_i, next to a given triplet denotes the corresponding weight for that point, or set of points. The subscript "FS" on some triplets stands for "fully symmetric" and indicates that one should include all possible distinct permutations of the three coördinates x, y, and z together with all possible distinct choices of '$+$' and '$-$' signs on the three coördinates. The triplet $(s, s, 0)_{FS}$ thus represents a total of twelve distinct points: three permutations times four choices of signs. In addition, one should treat as independent the '$\pm$' signs that appear in some of the points. The triplet $(\pm r, \pm s, 0)$ thus represents a total of four distinct points.

The reader will note that most of the cubature formulas given in Table 16.1 are for odd values of P. This fact simply reflects the underlying symmetry of the set of cubature points in relation to the symmetry of the spherical harmonics. Recall that if $\mathbf{r}$ and $-\mathbf{r}$ denote antipodal

[38]The estimate (16.48) is closely related to the concept of *efficiency* for cubature formulas; see [63] for a description. The true minimum number of cubature points might, by luck, be smaller than $N_{sph}(P)$, or it may, in fact, be larger. The latter case may be required in order to ensure real—rather than complex—solutions for the weights and points determined by (16.46) and (16.47).

[39]This may seem surprising, but most of the research on cubature formulas for $\mathbb{S}^2$ appears to have concentrated on formulas that obey certain restrictions. The so-called *spherical t-designs*, for example, have equal weights for all points, a constraint that seems to conflict with our desire to have as few cubature points as possible for a given degree P.

points on the two-sphere, then $Y_{jm}(-\mathbf{r}) = (-1)^j Y_{jm}(\mathbf{r})$. Now consider a cubature formula which uses a set of points on $\mathbb{S}^2$ which has the property that for any given point in the set, its antipodal point also belongs to the set. (In other words, the set of points is invariant under inversion through the origin.) If the given cubature formula assigns equal weights to antipodal pairs of points, then it follows from the symmetry of the spherical harmonics that that cubature formula will work exactly for all Y_{jm} for which j is odd.

Table 16.1: Some cubature formulas for $\mathbb{S}^2$, the two-dimensional surface of a three-dimensional sphere. This table lists for each $P \in \{3, 5, 7, 8, 9, 11, 14\}$ a set of points and weights such that the cubature formula (16.46) yields exact results for all spherical harmonics Y_{jm} having $j \le P$.

$\underline{P = 3,\ N = 6}$

These points are the vertices of a regular octahedron.

$$\begin{array}{cc} (r,0,0)_{FS} & W \\ r = 1 & W = \dfrac{1}{6} \end{array}$$

$\underline{P = 5,\ N = 12}$

These points are the vertices of a regular icosahedron.

$$\begin{array}{cc} (\pm r, \pm s, 0) & W \\ (0, \pm r, \pm s) & W \\ (\pm s, 0, \pm r) & W \end{array}$$

$$r^2 = \frac{5+\sqrt{5}}{10} \qquad s^2 = \frac{5-\sqrt{5}}{10} \qquad W = \frac{1}{12}$$

$\underline{P = 7,\ N = 24}$

These points are invariant under any rotation that maps a cube onto itself.

$$\begin{array}{cc} (u_i, v_i, w_i) & W \\ (u_i, -v_i, -w_i) & W \\ (u_i, w_i, -v_i) & W \\ (u_i, -w_i, v_i) & W \\ i \in \{1, \ldots, 6\} & W = \dfrac{1}{24} \end{array}$$

$$\begin{array}{ll} (u_1, v_1, w_1) = (r, s, t) & (u_4, v_4, w_4) = (-s, r, t) \\ (u_2, v_2, w_2) = (-r, t, s) & (u_5, v_5, w_5) = (t, r, s) \\ (u_3, v_3, w_3) = (s, t, r) & (u_6, v_6, w_6) = (-t, s, r) \end{array}$$

Here r, s, and t denote the positive roots of the equation

$$z^6 - z^4 + \frac{1}{5} z^2 - \frac{1}{105} = 0,$$

and have the approximate values

$$\begin{aligned} r &= 0.86624\,68181\,07821, \\ s &= 0.42251\,86537\,61111, \\ t &= 0.26663\,54015\,16705. \end{aligned}$$

Cubature Formulas for $\mathbb{S}^2$ (ctd.)

$\underline{P = 8,\ N = 30}$

$$\begin{array}{ll} (1,0,0)_{FS} & W_1 \\ (u_i, v_i, w_i) & W_2 \\ (u_i, -v_i, -w_i) & W_2 \\ (u_i, w_i, -v_i) & W_2 \\ (u_i, -w_i, v_i) & W_2 \end{array}$$

$$i \in \{1, \ldots, 6\} \qquad W_1 = \frac{16}{600} \qquad W_2 = \frac{21}{600}$$

The 24 points with weight W_2 are determined as in the $P = 7$ formula—except that here r, s, and t denote the positive roots of the equation

$$z^6 - z^4 + \frac{5}{21}z^2 - \frac{5}{441} = 0,$$

and have the approximate values

$$\begin{aligned} r &= 0.81841\,30426\,59383, \\ s &= 0.51646\,92453\,06672, \\ t &= 0.25191\,19097\,17204. \end{aligned}$$

$\underline{P = 9,\ N = 32}$

The twelve points with weight W_1 are the vertices of a regular icosahedron; and the twenty points with weight W_2 are the vertices of a regular dodecahedron (the dual of the icosahedron).

$$\begin{array}{ll} (\pm r, \pm s, 0) & W_1 \\ (0, \pm r, \pm s) & W_1 \\ (\pm s, 0, \pm r) & W_1 \\ (\pm u, \pm v, 0) & W_2 \\ (0, \pm u, \pm v) & W_2 \\ (\pm v, 0, \pm u) & W_2 \\ (\pm t, \pm t, \pm t) & W_2 \end{array}$$

$$r^2 = \frac{5+\sqrt{5}}{10} \qquad s^2 = \frac{5-\sqrt{5}}{10} \qquad W_1 = \frac{25}{840}$$

$$u^2 = \frac{3-\sqrt{5}}{6} \qquad v^2 = \frac{3+\sqrt{5}}{6} \qquad t^2 = \frac{1}{3} \qquad W_2 = \frac{27}{840}$$

$\underline{P = 11,\ N = 50}$

$$\begin{array}{ll} (r, 0, 0)_{FS} & W_1 \\ (s, s, 0)_{FS} & W_2 \\ (\pm t, \pm t, \pm t) & W_3 \\ (u, u, v)_{FS} & W_4 \end{array}$$

$$r = 1 \qquad s^2 = \frac{1}{2} \qquad t^2 = \frac{1}{3} \qquad u^2 = \frac{1}{11} \qquad v^2 = \frac{9}{11}$$

$$W_1 = \frac{9216}{725760} \qquad W_2 = \frac{16384}{725760} \qquad W_3 = \frac{15309}{725760} \qquad W_4 = \frac{14641}{725760}$$

Cubature Formulas for $\mathbb{S}^2$ (ctd.)

$\underline{P = 14,\ N = 72}$

$(\pm r, \pm s, 0)$	W_1
$(0, \pm r, \pm s)$	W_1
$(\pm s, 0, \pm r)$	W_1
(u_i, v_i, w_i)	W_2
$(u_i, -v_i, -w_i)$	W_2
$(-u_i, -v_i, w_i)$	W_2
$(-u_i, v_i, -w_i)$	W_2
(v_i, w_i, u_i)	W_2
$(v_i, -w_i, -u_i)$	W_2
$(-v_i, -w_i, u_i)$	W_2
$(-v_i, w_i, -u_i)$	W_2
(w_i, u_i, v_i)	W_2
$(w_i, -u_i, -v_i)$	W_2
$(-w_i, -u_i, v_i)$	W_2
$(-w_i, u_i, -v_i)$	W_2

$i \in \{1, \ldots, 5\}$

$$r^2 = \frac{5 - \sqrt{5}}{10} \qquad s^2 = \frac{5 + \sqrt{5}}{10} \qquad W_1 = \frac{125}{10080} \qquad W_1 = \frac{143}{10080}$$

Let y_k, $k \in \{1, \ldots, 6\}$, denote the roots of the equation

$$0 = 2556125y^6 - 5112250y^5 + 3578575y^4 - 1043900y^3 + 115115y^2 - 3562y + 9,$$

and define $z_k = \sqrt{y_k}$. Then

$$\begin{aligned}
u_1 &= \frac{-z_3 + z_4}{2s} & v_1 &= \frac{z_5 + z_6}{2s} & w_1 &= \frac{z_1 + z_2}{2s} \\
u_2 &= \frac{-z_5 + z_2}{2s} & v_2 &= \frac{z_6 + z_4}{2s} & w_2 &= \frac{z_1 + z_3}{2s} \\
u_3 &= \frac{-z_2 + z_6}{2s} & v_3 &= \frac{z_3 + z_5}{2s} & w_3 &= \frac{z_1 + z_4}{2s} \\
u_4 &= \frac{-z_6 + z_3}{2s} & v_4 &= \frac{z_4 + z_2}{2s} & w_4 &= \frac{z_1 + z_5}{2s} \\
u_5 &= \frac{-z_4 + z_5}{2s} & v_5 &= \frac{z_2 + z_3}{2s} & w_5 &= \frac{z_1 + z_6}{2s}
\end{aligned}$$

Table 16.2 lists the values of $N_{sph}(P)$ as given by (16.48), our rough estimate of N_{min}, for $P \in \{3, \ldots, 14\}$. It compares these values with the lower bounds $N(P, 2)$ from Table 13.1 as well as with the number N_s of cubature points required by the formulas listed in Table 16.1. The dashes in the column for N_s indicate that no solution to (16.46) and (16.47) is known that uses fewer points than the next entry in the table. In these cases we conjecture that the solution lies on the complexified two-sphere.

The nearness of corresponding values for $N_{sph}(P)$ and N_s given in Table 16.2 suggests that the cubature formulas given in Table 16.1 work quite well and that they may, in fact, be minimal [63]. Indeed, four of the formulas have $N_s < N_{sph}(P)$—*i.e.*, they appear to work better than we have any right to expect! These exceptional formulas are marked in Table 16.2 with an asterisk on the value of N_s.

TABLE 16.2. A comparison between the rough estimate $N_{sph}(P)$ for N_{min} (see (16.48)), the lower bound $N(P,2)$ from Table 13.1, and the number of cubature points N_s used by the formulas described in Table 16.1.

P	$N_{sph}(P)$	$N(P,2)$	N_s
3	7	5	6^*
4	10	7	–
5	13	10	12^*
6	18	12	–
7	23	15	24
8	28	19	30
9	35	22	32^*
10	42	26	–
11	49	31	50
12	58	35	–
13	67	40	–
14	76	46	72^*

16.2.3. *Cubature Formulas for the Manifold of $U(1) \otimes SU(2)/SO(2)$: a Circle crossed with a Two-Sphere.* Recall from (15.78) and the results of §15.2.2 that when we choose the linear symplectic transformations $\mathcal{L}(u)$ from the space $\mathcal{U} = U(1) \otimes SU(2)/SO(2)$, the required integral covers separately the circle $\mathbb{S}^1$ and the two-sphere $\mathbb{S}^2$—*i.e.*, the integral covers $\mathbb{S}^1 \otimes \mathbb{S}^2$. Also recall from page 142, near the end of §16.2.1, that in this case the functions of interest to us are the product functions $e^{i\kappa\omega}Y_{jm}(\Omega)$ with $j \leq P$ and $\kappa \in \{P, P-1, \ldots, -P\}$. We therefore seek minimal cubature formulas on the manifold $\mathbb{S}^1 \otimes \mathbb{S}^2$ that yield exact results for all of these functions. In other words, we want to find cubature formulas of the form

$$Q_N[f(\omega,\Omega)] \equiv \sum_{i=1}^{N} w_i f(\omega_i, \Omega_i), \tag{16.49}$$

with N as small as possible, such that for all $j \leq P$ and all $\kappa \in \{P, \ldots, -P\}$

$$Q_N\left[e^{i\kappa\omega}Y_{jm}(\Omega)\right] = \frac{\delta_{\kappa 0}\delta_{j0}\delta_{m0}}{\sqrt{4\pi}}. \tag{16.50}$$

The simplest solution to the problem just posed in the last paragraph uses a so-called *product cubature formula*—essentially a Cartesian product of two or more quadrature or cubature formulas. Suppose, for example, that

$$Q_{N_a}[f(x)] = \sum_{i=1}^{N_a} a_i f(x_i)$$

and

$$Q_{N_b}[g(y)] = \sum_{j=1}^{N_b} b_j g(y_j)$$

are two quadrature formulas that give exact results for respectively functions f in a set $\mathcal{F}$ over a domain $\mathcal{D}_{\mathcal{F}}$, and functions g in a set $\mathcal{G}$ over a domain $\mathcal{D}_{\mathcal{G}}$. Then

$$Q_{N_a N_b}[h(x,y)] = \sum_{ij} a_i b_j h(x_i, y_j) \tag{16.51}$$

is a product cubature formula that gives exact results on the domain $\mathcal{D}_{\mathcal{F}} \otimes \mathcal{D}_{\mathcal{G}}$ for any function $h(x,y)$ that can be separated into the form $f(x)g(y)$, where $f \in \mathcal{F}$ and $g \in \mathcal{G}$ [85].

Because there exist many good quadrature formulas, product cubature formulas have the great virtue of being easy to construct. Their principal drawback is that the number of points required equals the *product* of the number of points required by their component quadrature formulas. To gain a useful perspective on why this happens, suppose $\mathcal{F}$ is the set of all polynomials in x of degree at most d, while, similarly, $\mathcal{G}$ is the set of all polynomials in y of degree at most d. And further suppose that we have an appropriate N-point quadrature formula that gives exact results on both sets $\mathcal{F}$ and $\mathcal{G}$. Then the corresponding product cubature formula (16.51), which will require N^2 points, will yield exact results for all polynomials in $\mathcal{F} \otimes \mathcal{G}$. This space includes not only all polynomials in x and y of degree at most d, but also some such polynomials of degree larger than d (*e.g.*, $x^d y^d$). In essence, to purchase these additional polynomials, we must pay the price of N^2 cubature points. If we do not want these expensive (*i.e.*, higher-order) polynomials, we may shop around for less costly non-product cubature formulas.

For a cubature formula in the present case—functions of the form $e^{i\kappa\omega} Y_{jm}(\Omega)$ over the domain $\mathbb{S}^1 \otimes \mathbb{S}^2$—we can use a product of the quadrature formula (16.18) given in §16.1.6 for the circle with an appropriate cubature formula from Table 16.1 for the two-sphere. In other words, we may use the formula

$$Q_{N_c N_s}[f(\omega, \Omega)] \equiv \sum_{j=0}^{N_c-1} \sum_{i=1}^{N_s} \frac{w_i}{N_c} f(\omega_j, \Omega_i), \tag{16.52}$$

where $\omega_j = \frac{2\pi j}{N_c}$, N_c denotes the number of points on the circle, and N_s denotes the number of points on the sphere. Since the integral over the circle $\mathbb{S}^1$ should give exact results for the exponential functions $e^{i\kappa\omega}$ with $\kappa \in \{P, \ldots, -P\}$, we can use essentially the same argument as given in §16.1.6 (simply replace $2k$ by κ everywhere) to conclude that we must set $N_c > P$. Hence we choose

$$N_c = P + 1. \tag{16.53}$$

Table 16.3 lists the number of points required by the product cubature formula (16.52) when N_c is given by (16.53) and N_s is given by the appropriate value in Table 16.2.

TABLE 16.3. The number of points $N_c N_s$ required by the product cubature formula (16.52) on the manifold $\mathbb{S}^1 \otimes \mathbb{S}^2$. This table lists $N_c N_s$, for those values of P for which cubature formulas were given in Table 16.1 for the two-sphere $\mathbb{S}^2$.

P	$N_c N_s$
3	24
5	72
7	192
8	270
9	320
11	600
14	1080

Although we can certainly use the product cubature formula just described to construct corresponding jolt decompositions, we would prefer to have cubature formulas that use fewer than the (uncomfortably large) number of points $N_c N_s$ listed in Table 16.3. As the reader has probably observed, there is a correlation between, on the one hand, the maximum degree P of the polynomials to which we wish to apply jolt decomposition and, on the other hand, the strength required of our cubature formulas. In the light of this observation, we may make the following

Conjecture 16.1. *The functions of interest to us when we choose the linear symplectic transformations $\mathcal{L}(u)$ from the space $\mathcal{U} = U(1) \otimes SU(2)/SO(2)$ are the product functions $e^{i\kappa\omega}Y_{jm}(\Omega)$ for all $j \leq l_{max} = P$ and all $\kappa \in \{P-j, \ldots, -(P-j)\}$.*

If this conjecture holds, then it should be possible to construct non-product cubature formulas that use fewer than $N_c N_s$ points and yet still yield exact results for all the functions of interest to us on the manifold $\mathbb{S}^1 \otimes \mathbb{S}^2$.

16.2.4. *Cubature Formulas for the Manifold of $U(1) \otimes U(1)$: a Two-Torus.* Recall from (15.140) that when we choose the linear symplectic transformations $\mathcal{L}(u)$ from the space $\mathcal{U} = U(1) \otimes U(1)$, the required integral covers two separate circles $\mathbb{S}^1$. In other words, the integral in this case covers the two-torus $\mathbb{T}^2 = \mathbb{S}^1 \otimes \mathbb{S}^1$. Also recall, from the end of §16.2.1, that the functions of interest to us here are the product exponentials $e^{i2k_1\theta_1}e^{i2k_2\theta_2}$ with $k_1, k_2 \in \{P, P-1, \ldots, -P\}$ such that $|k_1| + |k_2| \leq P$. To simplify later discussion, we shall use the symbol $\mathcal{K}_P$ to denote the set of all such pairs (k_1, k_2) for a given value of P. Thus we define

$$\mathcal{K}_P = \big\{(k_1, k_2) \;\big|\; k_1, k_2 \in \{P, P-1, \ldots, -P\} \text{ and } |k_1| + |k_2| \leq P\big\}. \tag{16.54}$$

For convenience, let us also define $\mathcal{K}'_P$ as the set $\mathcal{K}_P$ with the pair $(0,0)$ removed: thus

$$\mathcal{K}'_P = \mathcal{K}_P - \{(0,0)\}. \tag{16.55}$$

We now want to find minimal cubature formulas that yield exact results on the manifold $\mathbb{T}^2$ for all of our product exponentials $e^{i2k_1\theta_1}e^{i2k_2\theta_2}$; hence we seek cubature formulas of the form

$$Q_N[f(\theta_1, \theta_2)] \equiv \sum_{i=1}^{N} w_i f(\theta_{1i}, \theta_{2i}), \tag{16.56}$$

with N as small as possible, such that

$$Q_N\big[e^{i2k_1\theta_1}e^{i2k_2\theta_2}\big] = \delta_{0k_1}\delta_{0k_2} \tag{16.57}$$

for all pairs $(k_1, k_2) \in \mathcal{K}_P$.

For the functions of interest to us on $\mathbb{T}^2$, we could use two copies of the quadrature rule (16.18) to build a product cubature formula of the form (16.51). Such a formula, however, would require (see (16.19))

$$N_{prod} = (2\lceil P/2 \rceil + 1)^2 \tag{16.58}$$

points. We can develop a more efficient cubature formula by using what are called *lattice rules* [81]. For our purposes, such a rule has the structure[40]

$$Q_N[f(\theta_1, \theta_2)] \equiv \frac{1}{N} \sum_{j=0}^{N-1} f\big(\tfrac{2\pi j}{N}, \alpha\tfrac{2\pi j}{N}\big), \tag{16.59}$$

where N and α are a pair of judiciously chosen positive integer constants. To see what constraints these constants must satisfy, let us apply to this lattice rule a straightforward generalization of the argument given in §16.1.6: Insert the function $e^{i2k_1\theta_1}e^{i2k_2\theta_2}$ into the quadrature formula (16.59) to obtain

$$Q_N\big[e^{i2k_1\theta_1}e^{i2k_2\theta_2}\big] = \frac{1}{N}\sum_{j=0}^{N-1} e^{i2k_1 2\pi j/N}e^{i2k_2\alpha 2\pi j/N} = \frac{1}{N}\sum_{j=0}^{N-1}\big(e^{i2\pi 2(k_1+\alpha k_2)/N}\big)^j.$$

[40] One may also, of course, choose to attach the coefficient α to the first angle rather than the second; thus

$$Q_N[f(\theta_1, \theta_2)] \equiv \frac{1}{N} \sum_{j=0}^{N-1} f\big(\alpha\tfrac{2\pi j}{N}, \tfrac{2\pi j}{N}\big).$$

For $k_1 = k_2 = 0$, this sum returns the value 1 and hence agrees with the requirement (16.57). For the cases k_1 and k_2 not both zero, the summation yields

$$Q_N\big[e^{i2k_1\theta_1}e^{i2k_2\theta_2}\big] = \frac{1}{N}\cdot\frac{1-e^{i2\pi 2(k_1+\alpha k_2)}}{1-e^{i2\pi 2(k_1+\alpha k_2)/N}},$$

which, for integer α, will return the correct answer 0 as long as the denominator does not vanish. This means we must select N and α so as to ensure

$$\frac{2(k_1+\alpha k_2)}{N} \notin \mathbb{Z} \quad \text{for all pairs } (k_1,k_2)\in\mathcal{K}'_P. \tag{16.60}$$

We may easily identify one constraint on the constant α by making two observations: First, in order to satisfy (16.60), we cannot allow $k_1+\alpha k_2$ to vanish for any pair $(k_1,k_2)\in\mathcal{K}'_P$. Second, observe that $(k_1,-1)\in\mathcal{K}'_P$ for all $k_1\in\{0,1,\ldots,P-1\}$. It follows that α cannot belong to the set $\{0,\ldots,P-1\}$, and hence

$$\alpha \geq P.$$

Cools and Sloan [19] have found minimal cubature formulas for the broader problem of all product exponentials $e^{im_1\theta_1}e^{im_2\theta_2}$ for which $m_1,m_2\in\{M,\ldots,-M\}$ and $|m_1|+|m_2|\leq M$.[41] They proved that choosing

$$\alpha = 2\lceil M/2\rceil + 1$$

and

$$N = \left\lceil \frac{(M+1)^2}{2} \right\rceil$$

makes (16.59) a minimal cubature formula for their somewhat broader class of functions. If we wish to apply these results to our more restricted problem, we must set $M=2P$; as a consequence, we find

$$\alpha = 2\lceil 2P/2\rceil + 1 = 2P+1,$$
$$N = \left\lceil \frac{(2P+1)^2}{2} \right\rceil = 2P(P+1)+1.$$

For all $P>1$, the number of cubature points here is greater than or equal to the number N_{prod} (see (16.58)) required by our product cubature formula. (Note that one might have predicted this larger number of points because Cools and Sloan's cubature formulas work for many more functions than we require.) On the other hand, it seems reasonable to guess that the best choice for α lies somewhere in the range defined by our lower bound P and the value $2P+1$ determined by Cools and Sloan's results. Let us make this guess our working hypothesis.

Testing all $\alpha\in\{P,P+1,\ldots,2P+1\}$ and searching for the smallest N (which we shall denote N_{t2}) that satisfies (16.60), we obtain the results listed in Table 16.4. For comparison, this table also lists the values of N_{prod} as given by (16.58). A close examination reveals that the values of N and α obey a definite pattern, and we therefore make the following

Conjecture 16.2. *If we choose*

$$\alpha = P+1, \tag{16.61a}$$

and

$$N = N_{t2} = 2\left\lceil \frac{P(\lceil P/2\rceil+1)}{2} \right\rceil + 1, \tag{16.61b}$$

[41] Note carefully that here, in contrast to our more restricted problem, m_1 and m_2 may be odd as well as even.

TABLE 16.4. This table lists for $P \in \{3, \ldots, 14\}$ values for α and $N = N_{t2}$ that appear to make (16.59) a minimal cubature formula on the two-torus $\mathbb{T}^2$.

P	α	N_{t2}	N_{prod}
3	4	11	25
4	5	13	25
5	6	21	49
6	7	25	49
7	8	37	81
8	9	41	81
9	10	55	121
10	11	61	121
11	12	79	169
12	13	85	169
13	14	105	225
14	15	113	225

then the lattice rule (16.59) *is a minimal cubature formula for the product exponentials* $e^{i2k_1\theta_1}e^{i2k_2\theta_2}$ *on* $\mathbb{T}^2$ *for all pairs* $(k_1, k_2) \in \mathcal{K}_P$.[42]

A somewhat more transparent way to express (16.61b) says that N_{t2} equals the first odd integer larger than $P(\lceil P/2 \rceil + 1)$.

16.2.5. *Jolt Decomposition in Two Degrees of Freedom.* Let us now summarize the process of jolt decomposition in two degrees of freedom. We begin with a set of homogeneous polynomials,

$$h_l = \sum_{r=1}^{M(l,4)} c^{(l)} G_r^{(l)},$$

of degree $l \leq P$ and want to decompose them into a linear combination of jolts. In other words, we wish to write these polynomials in the form (*cf.* (11.2))

$$h_l = \frac{1}{M(l,2)} \sum_{j=1}^{N} \sum_{k=1}^{M(l,2)} w_j a_{jk}^{(l)} \mathcal{L}_j Q_k^{(l)}, \tag{16.62}$$

where here, as described in the introduction to §16.1, we have replaced the factor $1/N$ by the weights w_j. This replacement has no effect on the logic of the derivation given in §11 for the jolt strengths $a_{jk}^{(l)}$. The only essential change occurs in the definition of the inner product $\{\,,\}$, which is now defined by (*cf.* (11.3) and (11.5))[43]

$$\{\zeta, \eta\} = \frac{1}{M(l,n)} \sum_{j=1}^{N} \sum_{k=1}^{M(l,n)} w_j \zeta_{jk} \eta_{jk}. \tag{16.63}$$

We may therefore compute $a_{jk}^{(l)}$ exactly as in (11.11):

$$a_{jk}^{(l)} = \sum_{r,s=1}^{M(l,4)} c_r^{(l)} [\Gamma(l)^{-1}]_{rs} \sigma_{jk}^s, \tag{16.64}$$

[42]Dr. Ronald Cools has since communicated to me a proof of this conjecture [17].

[43]Here we are assuming that all the weights w_j are positive. This assumption ensures that the introduction of possibly unequal weights will not radically alter the geometry of the inner product $\{\,,\}$. For example, the inner product remains positive definite. Note that, in general, numerical analysts consider positive weights a desirable property for cubature formulas.

where (see (11.4))

$$\sigma_{jk}^s = \left\langle G_s^{(l)}, \mathcal{L}_j Q_k^{(l)} \right\rangle , \tag{16.65}$$

and (*cf.* (11.8))

$$\Gamma(l)_{rs} = \frac{1}{M(l,2)} \sum_{j=1}^{N} \sum_{k=1}^{M(l,2)} w_j \sigma_{jk}^r \sigma_{jk}^s . \tag{16.66}$$

To complete the description, we need only specify the weights w_j and the linear symplectic transformations $\mathcal{L}_j$. These quantities are based on the cubature formulas described in §§16.2.2–16.2.4, and we treat each possibility in turn.

Examine first the case of using cubature formulas for the two-sphere $\mathbb{S}^2$. Recall from Theorem 13.1 and the definition (15.27) that when we choose the linear symplectic transformations $\mathcal{L}(u)$ from the coset space $SU(2)/SO(2)$, we may express them in the form

$$\mathcal{L}(c_\Omega) = \mathcal{L}\big(c(\theta,\phi)\big) = \mathcal{L}(u_\theta \cdot u_\phi).$$

Since $\mathcal{L}(u)$ stands for $\mathcal{L}(M(u))$ (see §13.3), we may use (13.12) and our convention (9.12) for representing linear Lie transformations as matrices to obtain the matrix representation of $\mathcal{L}(c_\Omega)$:

$$M(\theta,\phi) = M(u_\theta \cdot u_\phi) = M(u_\theta) M(u_\phi),$$

where $M(u_\theta)$ and $M(u_\phi)$ are given by (16.31) and (16.28), respectively. Carrying out the matrix multiplication, we obtain the result

$$M(\theta,\phi) = \begin{pmatrix} c_p c_a & c_p s_a & -s_p c_a & -s_p s_a \\ -c_p s_a & c_p c_a & -s_p s_a & s_p c_a \\ s_p c_a & s_p s_a & c_p c_a & c_p s_a \\ s_p s_a & -s_p c_a & -c_p s_a & c_p c_a \end{pmatrix}, \tag{16.67}$$

where

$$\begin{aligned} c_p &= \cos(\theta/2), \\ s_p &= \sin(\theta/2), \end{aligned} \quad \text{and} \quad \begin{aligned} c_a &= \cos(\phi/2), \\ s_a &= \sin(\phi/2). \end{aligned} \tag{16.68}$$

Here the polar angle θ and the azimuthal angle ϕ are determined by the points of an appropriate cubature formula for the two-sphere $\mathbb{S}^2$. Likewise, the weights w_j—needed by (16.62) and (16.66)—are determined by corresponding weights from the same cubature formula.

Since the $\mathcal{L}_j$'s in (16.65) act exclusively on q-monomials, we need compute their action only on the q's. Applying (16.67) to the phase-space variables z, we find

$$\mathcal{L}\big(c(\theta,\phi)\big) \begin{pmatrix} q_1 \\ q_2 \end{pmatrix} = \begin{pmatrix} q_1 c_p c_a + q_2 c_p s_a - p_1 s_p c_a - p_2 s_p s_a \\ -q_1 c_p s_a + q_2 c_p c_a - p_1 s_p s_a + p_2 s_p c_a \end{pmatrix}. \tag{16.69}$$

Next examine the case of using cubature formulas for the manifold $\mathbb{S}^1 \otimes \mathbb{S}^2$. In this case Theorem 13.1, together with (15.27) and (15.77), allows us to express the relevant linear symplectic transformations in the form

$$\mathcal{L}\big(c_\Omega\, e^{i\omega/2}\big)$$

(*cf.* also (16.42)). By the same method as above we find for this linear Lie transformation the matrix representation

$$M(\theta,\phi,\omega) = M(c_\Omega) M(e^{i\omega/2}\mathbf{1}) = M(\theta,\phi) M(e^{i\omega/2}\mathbf{1}).$$

Using (16.67) and (15.79a), and carrying out the matrix multiplication, we find

$$M(\theta,\phi,\omega) = \begin{pmatrix} c_a c_\delta & s_a c_\delta & -c_a s_\delta & -s_a s_\delta \\ -s_a c_\sigma & c_a c_\sigma & -s_a s_\sigma & c_a s_\sigma \\ c_a s_\delta & s_a s_\delta & c_a c_\delta & s_a c_\delta \\ s_a s_\sigma & -c_a s_\sigma & -s_a c_\sigma & c_a c_\sigma \end{pmatrix}, \tag{16.70}$$

where

$$\begin{aligned} c_\delta &= \cos((\theta-\omega)/2), & c_\sigma &= \cos((\theta+\omega)/2), \\ s_\delta &= \sin((\theta-\omega)/2), & s_\sigma &= \sin((\theta+\omega)/2), \end{aligned} \tag{16.71}$$

and c_a and s_a remain as given in (16.68). Also as before, the angles θ, ϕ, and ω are determined by the points of whatever cubature formula we use for the manifold $\mathbb{S}^1 \otimes \mathbb{S}^2$; and likewise for corresponding weights w_j.

In this case, for the manifold $\mathbb{S}^1 \otimes \mathbb{S}^2$, we find that the action of the linear symplectic transformations $\mathcal{L}(u)$ on the q's is given by

$$\mathcal{L}\big(c_\Omega\, e^{i\omega/2}\big)\begin{pmatrix} q_1 \\ q_2 \end{pmatrix} = \begin{pmatrix} q_1 c_a c_\delta + q_2 s_a c_\delta - p_1 c_a s_\delta - p_2 s_a s_\delta \\ -q_1 s_a c_\sigma + q_2 c_a c_\sigma - p_1 s_a s_\sigma + p_2 c_a s_\sigma \end{pmatrix}. \tag{16.72}$$

Now examine the last case—that of using cubature formulas for the two-torus $\mathbb{T}^2$. In this case the linear symplectic transformations come from the space $U(1) \otimes U(1) = [U(1)]^2$. They have the form given in (15.135) (with $n = 2$),

$$\mathcal{R}(\theta_1, \theta_2) = \mathcal{R}_1(\theta_1)\mathcal{R}_2(\theta_2),$$

and the corresponding matrix representation

$$M(\theta_1, \theta_2) = M\begin{pmatrix} e^{i\theta_1} & 0 \\ 0 & e^{i\theta_2} \end{pmatrix}.$$

Using (13.11) and the angles defined in the lattice rule (16.59), we can express this representation in the specific form

$$M(\theta_{1j}, \theta_{2j}) = \begin{pmatrix} \cos\big(\frac{2\pi j}{N_{t2}}\big) & 0 & \sin\big(\frac{2\pi j}{N_{t2}}\big) & 0 \\ 0 & \cos\big(\alpha\frac{2\pi j}{N_{t2}}\big) & 0 & \sin\big(\alpha\frac{2\pi j}{N_{t2}}\big) \\ -\sin\big(\frac{2\pi j}{N_{t2}}\big) & 0 & \cos\big(\frac{2\pi j}{N_{t2}}\big) & 0 \\ 0 & -\sin\big(\alpha\frac{2\pi j}{N_{t2}}\big) & 0 & \cos\big(\alpha\frac{2\pi j}{N_{t2}}\big) \end{pmatrix}, \tag{16.73}$$

where $j \in \{0, 1, \ldots, N_{t2} - 1\}$, and N_{t2} and α are determined by the appropriate lattice rule. If one uses values of N_{t2} and α from Table 16.4, then the corresponding weights are constant: $w_j = 1/N_{t2}$.

In this last case, for the manifold $\mathbb{T}^2$, we find that the action of the linear symplectic transformations $\mathcal{R}(\theta_{1j}, \theta_{2j})$ on the q's is given by

$$\begin{aligned} \mathcal{R}(\theta_{1j}, \theta_{2j})\begin{pmatrix} q_1 \\ q_2 \end{pmatrix} &= \begin{pmatrix} q_1 \cos(\theta_{1j}) + p_1 \sin(\theta_{1j}) \\ q_2 \cos(\theta_{2j}) + p_2 \sin(\theta_{2j}) \end{pmatrix} \\ &= \begin{pmatrix} q_1 \cos\big(\frac{2\pi j}{N_{t2}}\big) + p_1 \sin\big(\frac{2\pi j}{N_{t2}}\big) \\ q_2 \cos\big(\alpha\frac{2\pi j}{N_{t2}}\big) + p_2 \sin\big(\alpha\frac{2\pi j}{N_{t2}}\big) \end{pmatrix}. \end{aligned} \tag{16.74}$$

16.3. **Three Degrees of Freedom**

At the beginning of §16.2 we outlined a sequence of three steps leading from the continuous version of jolt decomposition back to the discrete version. The steps were those followed when we analyzed the cases of one and two degrees of freedom. In three degrees of freedom the program remains the same; its execution, however, requires rather more work. In this section we shall investigate how to construct discrete jolt decompositions in three degrees of freedom when we choose the linear symplectic transformations $\mathcal{L}_j = \mathcal{L}(u_j)$ from either of two possible manifolds: the coset space $\mathcal{U} = SU(3)/SO(3)$ or the space $\mathcal{U} = [U(1)]^3 = U(1) \otimes U(1) \otimes U(1)$. As we shall see, there exist close analogies with the corresponding manifolds $\mathcal{U} = SU(2)/SO(2)$ and $\mathcal{U} = [U(1)]^2 = U(1) \otimes U(1)$, and they will serve as very useful guides. Still, for neither manifold is our knowledge quite as complete as it is in one and two degrees of freedom, and we shall point out work that remains and possible avenues of approach.

16.3.1. *The Functions Inside the Gram Matrix Elements.* To determine the functions that appear inside the integral that defines the Gram matrix elements for the case $\mathcal{U} = SU(3)/SO(3)$, let us start from (15.120) and apply arguments analogous to those used in §16.2.1. Removing the integral over $SU(3)$ from (15.120), we write down the partial Gram matrix elements

$$\Gamma(u,l)_{j\mu,j'\mu'} = \frac{2}{(l+1)(l+2)} \sum_k \Big\langle \mathcal{L}(u^{-1})\psi^j_\mu, Q^{(l)}_k \Big\rangle \Big\langle Q^{(l)}_k, \mathcal{L}(u^{-1})\psi^{j'}_{\mu'} \Big\rangle , \tag{16.75}$$

where the ψ^j_μ, as in §15.3.2, denote a set of basis polynomials that transform according to the irreducible $SU(3)$ representation $j = (j_1, j_2)$. Here recall that the subscript μ labels distinct basis elements within a representation. In §15.3.2 we let μ stand for the trio (I, I_3, Y), which forms one possible scheme for labeling the basis functions within a representation. This labeling scheme, however, is not unique, and for the moment we leave it unspecified. (We shall return to this point later.) Now use (15.119) to expand $\mathcal{L}(u^{-1})\psi^j_\mu$ in terms of the unitary representation $D^j(u^{-1})$; then (16.75) becomes (*cf.* (15.62))

$$\Gamma(u,l)_{j\mu,j'\mu'} = \sum_{\nu\nu'} \Bigg[\Big(\big[D^j(u^{-1})\big]^*_{\mu\nu} D^{j'}(u^{-1})_{\mu'\nu'} \Big) \times \frac{2}{(l+1)(l+2)} \sum_k \Big\langle \psi^j_\nu, Q^{(l)}_k \Big\rangle \Big\langle Q^{(l)}_k, \psi^{j'}_{\nu'} \Big\rangle \Bigg]. \tag{16.76}$$

Before simplifying this expression, we take a brief detour to describe the Clebsch-Gordan series for $SU(3)$.

All the classical Lie groups have Clebsch-Gordan series that express a direct product of irreducible representations in terms of a direct sum of irreducible representations. The Clebsch-Gordan series for $SU(3)$ is [30][44]

$$D^{(j_1,j_2)} \otimes D^{(j'_1,j'_2)} \approx \bigoplus_{i=0}^{\min(j_1,j'_2)} \bigoplus_{k=0}^{\min(j_2,j'_1)} (j_1 - i, j'_1 - k; j_2 - k, j'_2 - i), \tag{16.77a}$$

where $\approx$ denotes equality of representations, and the symbol $(s, s'; t, t')$ is defined by

$$(s,s';t,t') = D^{(s+s',t+t')} \oplus \bigoplus_{i=0}^{\min(s,s')} D^{(s+s'-2i,t+t'+i)} \oplus \bigoplus_{k=0}^{\min(t,t')} D^{(s+s'+k,t+t'-2k)}. \tag{16.77b}$$

This result tells us that we may rewrite the two D's that appear inside (16.76) in the form

$$\big[D^j(u^{-1})\big]^*_{\mu\nu} D^{j'}(u^{-1})_{\mu'\nu'} = \sum_\kappa \sum_{\sigma\tau} c^{\kappa\sigma\tau}_{j\mu\nu,j'\mu'\nu'} D^\kappa(u)_{\sigma\tau}, \tag{16.78}$$

where the summation over κ includes only those representations that appear in the Clebsch-Gordan series (16.77).

We can now simplify the partial Gram matrix elements using the same argument as led from (16.25) to (16.37). Applying (16.78) to (16.76), and collecting the sums over ν, ν', and k into a single coefficient, we obtain a result of the form

$$\Gamma(u,l)_{j\mu,j'\mu'} = \sum_\kappa \sum_{\sigma\tau} a^\kappa_{\sigma\tau} D^\kappa(u)_{\sigma\tau}, \tag{16.79}$$

a form exactly analogous to that of (16.37). As with that earlier result we have suppressed the dependence of the coefficients $a^\kappa_{\sigma\tau}$ on the matrix element labels $j\mu$ and $j'\mu'$. The principal difference occurs in the summations: here the sum over κ is constrained by the $SU(3)$ Clebsch-Gordan series (16.77).

[44] See also the *Mathematica* package `SU3.m` in Appendix H. It contains the function `SU3DirectProduct[]` which performs this computation.

As we did for the two degree of freedom case in §16.2.1, we may further simplify the partial Gram matrix elements (16.79) by noting that, according to Theorem 13.1, these matrix elements are class functions with respect to the $O(3)$ subgroup of $U(3)$. Appendix G shows that one may write any element $u \in U(3)$ as a product $r \cdot c$ of a real orthogonal element $r \in SO(3)$ and a symmetric element $c \in U(3)$. It follows that we may write any element $u \in SU(3)$ in the form

$$u = r \cdot c$$

where $r \in SO(3)$, and $c \in SU(3)$ labels the coset space $SU(3)/SO(3)$. Using this fact together with the fact that $\Gamma(u, l)$ is a class function, we may write down the relation

$$\Gamma(u, l)_{j\mu, j'\mu'} = \Gamma(c, l)_{j\mu, j'\mu'} = \Gamma(\tilde{r}u, l)_{j\mu, j'\mu'}. \tag{16.80}$$

Now observe that because c may be *any* element in the same coset, this relation must hold for *every* $r \in SO(3)$. It follows that (16.80) places very strong constraints on the expansion coefficients $a^{\kappa}_{\sigma\tau}$ in (16.79).

Before we address the implications of the class relation (16.80) on the expansion of the partial Gram matrix elements (16.79), we take a brief detour to discuss states with angular momentum zero. Consider the function

$$\chi^j_\mu = \int\limits_{SO(3)} dr\, \mathcal{L}(r)\psi^j_\mu. \tag{16.81}$$

This function is left unchanged under the action of any operator $\mathcal{L}(r)$ taken from $SO(3)$. To see this, simply compute. Using (13.15), we find that

$$\mathcal{L}(r')\chi^j_\mu = \int\limits_{SO(3)} dr\, \mathcal{L}(r')\mathcal{L}(r)\psi^j_\mu = \int\limits_{SO(3)} dr\, \mathcal{L}(rr')\psi^j_\mu.$$

As $SO(3)$ is a compact Lie group, it has a left and right invariant measure, and we may therefore change the variable of integration to $r'' = rr'$ with $dr'' = dr$. On doing so, we obtain the result

$$\mathcal{L}(r')\chi^j_\mu = \int\limits_{SO(3)} dr''\, \mathcal{L}(r'')\psi^j_\mu = \chi^j_\mu, \tag{16.82}$$

which verifies the claim. In the parlance of group theory one says that the function χ^j_μ transforms according to an identity representation of $SO(3)$ contained within the representation j of $SU(3)$. To make the same statement in the language of physics, one says that the state χ^j_μ has total angular momentum zero.

Not all representations of $SU(3)$ carry an identity representation of $SO(3)$—*i.e.*, contain a state of total angular momentum J equal to zero. Indeed, it turns out that a representation (j_1, j_2) of $SU(3)$ contains a state with angular momentum zero if and only if j_1 and j_2 are both even [26]. Moreover, the state with $J = 0$ is unique (*i.e.*, has multiplicity one) in the given representation.[45] Let us agree to label the (unique) $J = 0$ state in the representation (j_1, j_2) by the symbols

$$\psi^{(j_1,j_2)}_{\text{“0”}} \quad \text{or} \quad \psi^{j}_{\text{“0”}},$$

where, as earlier, we sometimes abbreviate the pair (j_1, j_2) simply as j. If j_1 and j_2 are not both zero, then the $SU(3)$ representation (j_1, j_2) is carried by a set of dynamical polynomials which forms a vector space of dimension greater than one. In these cases we may choose an orthonormal basis for the vector space in an infinite number of ways. In §15.3.1 we made

[45] To understand these relationships better, it may help to consider the corresponding situation in the more familiar context of the group $SU(2)$. For that group the representation labeled j is carried by a set of $2j + 1$ basis functions, and one may label those functions by an index m according to the representations they carry of the subgroup $SO(2) \subset SU(2)$. Only functions with $m = 0$ carry an identity representation of $SO(2)$, and the only representations of $SU(2)$ that contain such functions are those of integer spin j.

one such choice based on the possible values of isotopic spin I, its third component I_3, and hypercharge Y. It is also possible—though not as easy—to choose a basis in such a way as to emphasize the angular momentum [26]. Were we to do so, we could immediately identify (if it exists) the vector corresponding to $J = 0$ as one of the basis elements within the given representation. On the other hand, if we choose our basis as in §15.3.1 or Table 15.8, then in general we must form a linear combination of basis elements in order to construct a function having total angular momentum zero.

Based on the observations in the last paragraph and the result (16.82), we may write the function χ^j_μ defined in (16.81) in the form

$$\chi^j_\mu = \int\limits_{SO(3)} dr\, \mathcal{L}(r)\psi^j_\mu = \alpha(j,\mu)\psi^j_{\text{“0”}}, \tag{16.83}$$

where $\alpha(j,\mu)$ denotes a proportionality constant. (Of course $\alpha(j,\mu)$ will certainly vanish whenever j_1 and j_2 are not both even.)

Let us now address the implications of the class relation (16.80) on the expansion (16.79) for the partial Gram matrix elements. We begin by applying an integral over all of $SO(3)$ to both the left- and right-hand sides of the class relation. Since the left-hand side does not depend on r, the integration leaves it unchanged. (Here we assume that the measure dr is appropriately normalized.) Since $\tilde{r}$ on the right-hand side of (16.80) may be any element in $SO(3)$, we denote it simply as r. Thus, using (16.79), we obtain

$$\Gamma(u,l)_{j\mu,j'\mu'} = \int\limits_{SO(3)} dr\, \Gamma(ru,l)_{j\mu,j'\mu'} = \int\limits_{SO(3)} dr \sum_\kappa \sum_{\sigma\tau} a^\kappa_{\sigma\tau} D^\kappa(ru)_{\sigma\tau}. \tag{16.84}$$

Now note that because the $D^j(u)$'s form a representation of $SU(3)$, one may write

$$D^j(u_1u_2)_{\sigma\tau} = \sum_\upsilon D^j(u_1)_{\sigma\upsilon} D^j(u_2)_{\upsilon\tau}. \tag{16.85}$$

Inserting this factorization into (16.84), and using the $SU(3)$ analog of (16.26), we find

$$\begin{aligned}\Gamma(u,l)_{j\mu,j'\mu'} &= \int\limits_{SO(3)} dr \sum_\kappa \sum_{\sigma\tau} \sum_\upsilon a^\kappa_{\sigma\tau} D^\kappa(r)_{\sigma\upsilon} D^\kappa(u)_{\upsilon\tau} \\ &= \sum_\kappa \sum_{\sigma\tau\upsilon} a^\kappa_{\sigma\tau} D^\kappa(u)_{\upsilon\tau} \int\limits_{SO(3)} dr \left\langle \psi^\kappa_\upsilon, \mathcal{L}(r)\psi^\kappa_\sigma \right\rangle .\end{aligned}$$

Using (16.83), we then reduce this result to the form

$$\begin{aligned}\Gamma(u,l)_{j\mu,j'\mu'} &= \sum_\kappa \sum_{\sigma\tau\upsilon} a^\kappa_{\sigma\tau} D^\kappa(u)_{\upsilon\tau} \left\langle \psi^\kappa_\upsilon, \alpha(\kappa,\sigma)\psi^\kappa_{\text{“0”}} \right\rangle \\ &= \sum_\kappa \sum_{\sigma\tau\upsilon} a^\kappa_{\sigma\tau} D^\kappa(u)_{\upsilon\tau} \alpha(\kappa,\sigma)\delta_{\upsilon\,\text{“0”}} \\ &= \sum_\kappa \sum_{\sigma\tau} \alpha(\kappa,\sigma) a^\kappa_{\sigma\tau} D^\kappa(u)_{\text{“0”}\tau} = \sum_\kappa \sum_\tau b^\kappa_\tau D^\kappa(u)_{\text{“0”}\tau}.\end{aligned} \tag{16.86}$$

Before we continue, let us pause to make some remarks about the functions

$$D^\kappa(u)_{\text{“0”}\tau} = \left\langle \psi^\kappa_\tau, \mathcal{L}(u)\psi^\kappa_{\text{“0”}} \right\rangle . \tag{16.87}$$

First observe that they are class functions—as they must be—because

$$D^\kappa(u)_{\text{“0”}\tau} = D^\kappa(r\cdot c)_{\text{“0”}\tau} = \left\langle \psi^\kappa_\tau, \mathcal{L}(c)\mathcal{L}(r)\psi^\kappa_{\text{“0”}} \right\rangle = D^\kappa(c)_{\text{“0”}\tau}.$$

(Here we have used (13.15) and (16.82).) Then recall that in two degrees of freedom, see §16.2.1, the functions $D^j(u)_{0m}$ that arose during the derivation of (16.40) were just the well-known spherical harmonics Y_{jm} (modulo complex conjugation and a proportionality

constant). Indeed, the Y_{jm}'s have a structure that corresponds exactly to that given in (16.87) (*cf.* (16.39)). To emphasize this facet of their structure, let us define the functions $\mathrm{Y}^{\kappa}_{\tau}(u)$ by

$$\begin{aligned}\mathrm{Y}^{\kappa}_{\tau}(u) &= \mathrm{Y}^{(\kappa_1,\kappa_2)}_{\tau}(u) = \mathrm{Y}^{(\kappa_1,\kappa_2)}_{\tau}(c)\\ &= \sqrt{d(\kappa_1,\kappa_2)}\,\langle \psi^{(\kappa_1,\kappa_2)}_{\tau}, \mathcal{L}(u)\psi^{(\kappa_1,\kappa_2)}_{\text{“0”}}\rangle\\ &= \sqrt{d(\kappa_1,\kappa_2)}\,D^{(\kappa_1,\kappa_2)}(u)_{\text{“0”}\tau}.\end{aligned} \tag{16.88}$$

Now further recall that the $D^{\kappa}(u)$ form a collection of non-equivalent unitary irreducible representations of the compact Lie group $SU(3)$ and hence satisfy the orthogonality relations [20, p. 81]

$$\int_{SU(3)} du\,\big[D^{j}(u)\big]^{*}_{\mu\nu} D^{j'}(u)_{\mu'\nu'} = \frac{1}{d_j}\delta_{jj'}\delta_{\mu\mu'}\delta_{\nu\nu'}, \tag{16.89}$$

where $d_j = d(j_1, j_2)$, the dimensionality of the representation $j = (j_1, j_2)$ of $SU(3)$ (see (15.91)). It follows that the functions $\mathrm{Y}^{(\kappa_1,\kappa_2)}_{\tau}(u)$ defined by (16.88) obey the corresponding orthogonality relations

$$\int_{SU(3)} du\,\Big[\mathrm{Y}^{(\kappa_1,\kappa_2)}_{\tau}(u)\Big]^{*}\,\mathrm{Y}^{(\kappa'_1,\kappa'_2)}_{\tau'}(u) = \delta_{\kappa_1\kappa'_1}\delta_{\kappa_2\kappa'_2}\delta_{\tau\tau'}. \tag{16.90a}$$

Because the $\mathrm{Y}^{(\kappa_1,\kappa_2)}_{\tau}(u)$ are class functions with respect to $SO(3)$, we may reëxpress these orthogonality relations in the form

$$\int_{SU(3)/SO(3)} dc\,\Big[\mathrm{Y}^{(\kappa_1,\kappa_2)}_{\tau}(c)\Big]^{*}\,\mathrm{Y}^{(\kappa'_1,\kappa'_2)}_{\tau'}(c) = \delta_{\kappa_1\kappa'_1}\delta_{\kappa_2\kappa'_2}\delta_{\tau\tau'}, \tag{16.90b}$$

where here, in going from (16.90a) to (16.90b), we have assumed that the integral over the subgroup $SO(3)$ is appropriately normalized. Thus may we generalize the spherical harmonics $Y_{jm}(\Omega)$ to form a set of orthonormal functions $\mathrm{Y}^{(\kappa_1,\kappa_2)}_{\tau}(c)$ defined on the coset space $SU(3)/SO(3)$.

We now return to the implications of the class relation (16.80) on the expansion of the partial Gram matrix elements. Using (16.86) and the orthonormal class functions $\mathrm{Y}^{\kappa}_{\tau}(c)$ defined in (16.88), we see that one may write the partial Gram matrix elements in the form[46]

$$\Gamma(u,l)_{j\mu,j'\mu'} = \Gamma(c,l)_{j\mu,j'\mu'} = \sum_{\kappa}\sum_{\tau} b^{\kappa}_{\tau}\,\mathrm{Y}^{\kappa}_{\tau}(c), \tag{16.91}$$

where c denotes the $SU(3)/SO(3)$ coset to which u belongs. Furthermore, the summation over $\kappa = (\kappa_1, \kappa_2)$ in (16.91) must obey the following constraints:

(1) The representations $D^{\kappa} = D^{(\kappa_1,\kappa_2)}$ must appear on the right-hand side of the Clebsch-Gordan series (16.77) for $D^{j} \otimes D^{j'}$.
(2) Only even values of κ_1 and κ_2 can occur, because for all other values of κ_1 and κ_2 the functions $\mathrm{Y}^{\kappa}_{\tau}(c)$ do not exist.

To give a more explicit description of the functions of interest, let us examine more closely the constraints 1 and 2 enumerated above. Theorem 15.1, concerning the $SU(3)$ representations (j_1, j_2) carried by homogeneous dynamical polynomials of degree l in six variables, shows that $j_1 + j_2 \leq l$. Taking into account this restriction, we can use the Clebsch-Gordan series (16.77) to determine which $SU(3)$ representations $\kappa = (\kappa_1, \kappa_2)$ appear on the right-hand side of (16.91). If one stares at the Clebsch-Gordan series long enough, it becomes “obvious” that the $SU(3)$ representations which occur are *all* (κ_1, κ_2) such that $\kappa_1 + \kappa_2 \leq 2l$. One

[46]The coefficients b^{κ}_{τ} in this expansion are not the same as those in (16.86).

may confirm this by exercising the functions `SU3reps[]` and `SU3DirectProduct[]` defined in the *Mathematica* package `SU3.m` (see Appendix H). We therefore conclude that *when we choose the linear symplectic transformations* $\mathcal{L}(u)$ *from the coset space* $\mathcal{U} = SU(3)/SO(3)$*, the functions of interest to us are those class functions* $\mathrm{Y}_\tau^{(\kappa_1,\kappa_2)}$ *defined in* (16.88) *for which* $\kappa_1 + \kappa_2 \leq 2l_{max} \leq 2P$*. (As before, this implies that* κ_1 *and* κ_2 *are both even.)*

We turn now to the other manifold from which we shall consider selecting the linear symplectic transformations $\mathcal{L}(u)$: the space $\mathcal{U} = [U(1)]^3 = U(1) \otimes U(1) \otimes U(1)$, which was discussed in §15.4. To determine the functions of interest in this case, we may, as the astute reader has already observed, employ a straightforward generalization of the argument given at the end of §16.2.1 for the manifold $\mathcal{U} = [U(1)]^2 = U(1) \otimes U(1)$. All of the arguments carry over as before; after the smoke clears, we conclude that *when we choose the linear symplectic transformations* $\mathcal{L}(u)$ *from the space* $\mathcal{U} = U(1) \otimes U(1) \otimes U(1)$*, the functions of interest to us are the product exponentials* $e^{i2k_1\theta_1}e^{i2k_2\theta_2}e^{i2k_3\theta_3}$ *for all* $k_1, k_2, k_3 \in \{P, P-1, \ldots, -P\}$ *such that* $|k_1| + |k_2| + |k_3| \leq P$*.*

16.3.2. *Cubature Formulas for the Manifold* $SU(3)/SO(3)$*.* The second step in our program for constructing discrete but optimal jolt decompositions in three degrees of freedom requires us to find on the appropriate manifolds cubature formulas that work exactly for the functions just identified in §16.3.1. When we choose the linear symplectic transformations $\mathcal{L}(u)$ from the coset space $\mathcal{U} = SU(3)/SO(3)$, we want to find cubature formulas of the form

$$Q_N[f(c)] \equiv \sum_{i=1}^{N} w_i f(c_i), \tag{16.92}$$

with N as small as possible, such that

$$Q_N\left[\mathrm{Y}_\tau^{(\kappa_1,\kappa_2)}(c)\right] = \delta_{\kappa_1 0}\delta_{\kappa_2 0}\delta_{\tau\text{“0”}} \tag{16.93}$$

for all κ_1 and κ_2 such that $\kappa_1 + \kappa_2 \leq 2P$ (with κ_1 and κ_2 both even). These conditions (16.93) follow from the orthogonality relations (16.90b) together with the fact that, by the first entry in Table 15.8, $\mathrm{Y}_{\text{“0”}}^{(0,0)}(c) = \left\langle \psi_{\text{“0”}}^{(0,0)}, \mathcal{L}(c)\psi_{\text{“0”}}^{(0,0)} \right\rangle = 1$.

The group $SU(3)$ has dimension eight, and its subgroup $SO(3)$ has dimension three; the coset space $SU(3)/SO(3)$ therefore has dimension five. Though we do not yet know the geometry of this five-dimensional manifold—let alone the appropriate measure dc for integration—we can still discover cubature formulas by various empirical means. Before we discuss one such method for discovering cubature formulas for this manifold, let us make an estimate similar to (16.48) of the number of points N required by formulas of the form (16.92). To do this, we first count how many conditions the requirement (16.93) imposes on our cubature formula (16.92). Taking into account the representations that occur, and using (15.91) for the dimensionality of a given representation, we find (after considerable algebra) that the number of conditions equals

$$\begin{aligned}\sum_{k_1=0}^{P}\sum_{k_2=0}^{P-k_1} d(2k_1, 2k_2) &= \sum_{k_1=0}^{P}\sum_{k_2=0}^{P-k_1} (2k_1+1)(2k_2+1)(k_1+k_2+1) \\ &= \frac{1}{30}(P+1)(P+2)(2P+3)(2P^2+6P+5).\end{aligned}$$

Now count how many variables we have available for constructing an N-point cubature formula on the manifold $SU(3)/SO(3)$. The fact that the manifold is five-dimensional suggests we have N weights + $5N$ variables for the cubature points = $6N$ variables. Recall, however, that in the case of two degrees of freedom we counted $3N - 3$ free variables: we subtracted three based on the symmetries of the two-sphere $\mathbb{S}^2$, symmetries related to the action of the three-dimensional group $SU(2)$ on $\mathbb{S}^2$. (Recall that $SU(2)$ and $SO(3)$ are homomorphic.) It therefore seems reasonable in the present case, $n = 3$, to subtract eight—the dimensionality of $SU(3)$—from $6N$: thus, an N-point cubature formula on the manifold $SU(3)/SO(3)$ appears

to have $6N - 8$ free variables. A comparison of this reckoning with our above count of the number of conditions suggests that

$$6N - 8 \geq \frac{1}{30}(P+1)(P+2)(2P+3)(2P^2+6P+5).$$

Hence we obtain the estimate

$$N \geq N_{s3}(P) \equiv \left\lceil \frac{1}{180}(P+1)(P+2)(2P+3)(2P^2+6P+5) + \frac{4}{3} \right\rceil \tag{16.94}$$

for the number of points required by a cubature formula of degree P on the manifold $SU(3)/SO(3)$.

TABLE 16.5. A comparison between the rough estimate $N_{s3}(P)$ for N_{min} (see (16.94)) and the lower bound $N(P,3)$ from Table 13.1.

P	$N_{s3}(P)$	$N(P,3)$
3	43	3
4	114	9
5	260	12
6	529	17
7	988	22
8	1721	29
9	2838	37
10	4479	46
11	6783	56
12	9966	68

Table 16.5 lists the values of $N_{s3}(P)$ as given by (16.94) for $P \in \{3, \ldots, 12\}$, and it compares these values with the lower bounds $N(P,3)$ from Table 13.1. Although the comparison appears wildly unfavorable, we shall see later that there is reason to be more optimistic.

The reader may recall—and a glance at Table 16.1 will confirm—that each of the cubature formulas we listed for the two-sphere $\mathbb{S}^2$ obeyed certain symmetries. Indeed, many of the cubature formulas used sets of points which were invariant under the action of some discrete subgroup of $SU(2)$. This suggests, by analogy, that we might be able to construct cubature formulas for the manifold $SU(3)/SO(3)$ based on finite discrete subgroups of $SU(3)$. To see how one might do this, observe that the elements of a discrete subgroup of $SU(3)$ constitute a set of points on the group manifold. We might therefore define the necessary linear symplectic transformations by $\mathcal{L}_j = \mathcal{L}(u_j)$, where the matrices u_j are either the elements of a finite discrete subgroup of $SU(3)$, or some appropriate modification thereof. We shall discuss just such an approach.

To build cubature formulas in the fashion just described, we must know the discrete subgroups of $SU(3)$, and we shall discuss these presently. In addition, however, we must have some method for gauging the effectiveness of whatever formulas we construct. One obvious yardstick computes the left-hand side of (16.93) for all values of κ_1, κ_2, and τ of interest and compares the results with the right-hand side of (16.93)—perhaps by looking at how much the sum of the squares of the left-hand side differs from the desired result 1. An alternate yardstick (or meterstick, if you like), the one we shall use, constructs the Gram matrices $\Gamma(l)$ for all $l \leq l_{max} = P$ and compares their eigenvalue spectra with the continuum-limit spectra determined in §15. We seek formulas that yield Gram eigenvalue spectra as close as possible to the continuum limit.

The Lie group $SU(3)$ contains a variety of distinct subgroups, both continuous and discrete. These subgroups include such Lie groups as $U(2)$, $SU(2)$, and the like, which themselves contain subgroups. Thus, for example, the discrete subgroups of $SU(3)$ include the discrete

subgroups of $SU(2)$. Subgroups that arise in this fashion will not interest us here because they correspond to leaving one or more degrees of freedom unchanged. (We have studied these possibilities in §§16.1 and 16.2.) We shall therefore focus on those finite discrete subgroups of $SU(3)$ which are not also subgroups of some Lie group smaller than $SU(3)$. These subgroups are described in several references [38, 65, 73], and two of those references [38, 73] list in detail the corresponding generators.[47]

The subgroups of $SU(3)$ of interest for our purposes—*i.e.*, those subgroups which are both finite and discrete—fall into two classes: the crystal-like groups,

$$\Sigma(60),\ \Sigma(108),\ \Sigma(168),\ \Sigma(216),\ \Sigma(648),\ \Sigma(1080),$$

and the dihedral-like groups,

$$\Delta(3n^2),\ \Delta(6n^2),$$

where $n \in \mathbb{Z}^+$. (In all cases the value in parentheses is the order of the subgroup.[48])

Though we shall look at results based on several of the subgroups just mentioned, we shall examine most closely the particular $SU(3)$ subgroup $\Sigma(108)$. One may generate this group $\Sigma(108)$ by forming all possible distinct products of the three matrices

$$A = \begin{pmatrix} 1 & 0 & 0 \\ 0 & \omega & 0 \\ 0 & 0 & \omega^2 \end{pmatrix}, \tag{16.95a}$$

$$E = \begin{pmatrix} 0 & 1 & 0 \\ 0 & 0 & 1 \\ 1 & 0 & 0 \end{pmatrix}, \tag{16.95b}$$

and

$$V = \frac{1}{i\sqrt{3}} \begin{pmatrix} 1 & 1 & 1 \\ 1 & \omega & \omega^2 \\ 1 & \omega^2 & \omega \end{pmatrix}, \tag{16.95c}$$

where $\omega = e^{i2\pi/3}$. We may give a succinct prescription for constructing all 108 distinct elements as follows: First define I to be the 3×3 identity matrix; then the set of matrices

$$\mathcal{S}_6 = \{I, E, E^2, V^2, EV^2, E^2V^2\} \tag{16.96a}$$

forms a real subgroup of order six contained within $\Sigma(108)$. According to a standard result in group theory, this subgroup $\mathcal{S}_6$ decomposes the group $\Sigma(108)$ into a set of eighteen ($= \frac{108}{6}$) distinct cosets. One may therefore write the elements of $\Sigma(108)$ in the form $\mathcal{S}_6 T_j$. Here $j \in \{1, \ldots, 18\}$, T_j denotes a representative element from each of the different cosets, and the notation $\mathcal{S}_6 T_j$ means multiply each element of $\mathcal{S}_6$ on the right by T_j. Before enumerating a set of representative coset elements, we first introduce the concept of a group center [20, p. 427]:

Definition. The *center* of a group $\mathcal{G}$ consists of those elements of $\mathcal{G}$ which commute with every element of $\mathcal{G}$.

---

[47] *Cautionary note*: Both of these references incorrectly state the generator Z, one of the elements used to construct the $SU(3)$ subgroup $\Sigma(168)$. The correct generator is

$$Z = \frac{i}{\sqrt{7}} \begin{pmatrix} a & b & c \\ b & c & a \\ c & a & b \end{pmatrix}, \quad \text{where} \quad \begin{array}{c} a = \xi^4 - \xi^3, \\ b = \xi^2 - \xi^5, \\ c = \xi - \xi^6 \end{array} \quad \text{and } \xi^7 = 1$$

[48] *N.B.* Reference [38] labels the corresponding crystal-like groups slightly differently:

$$\Sigma(60),\ \Sigma(36),\ \Sigma(168),\ \Sigma(72),\ \Sigma(216),\ \Sigma(360).$$

Except in the cases of $\Sigma(60)$ and $\Sigma(168)$ the numbers in parentheses for this choice of labeling are a factor of three smaller than the order of the corresponding subgroup given above.

For the groups $SU(3)$ and $\Sigma(108)$ the center is given by the set of three elements

$$\mathcal{C} = \{I, \omega I, \omega^2 I\}. \tag{16.96b}$$

If we now define $\mathcal{T}$ as the set of six elements

$$\mathcal{T} = \{I, A, A^2, V, AV, A^2V\}, \tag{16.96c}$$

it turns out that one may write representative elements for each of the eighteen ($= 3 \times 6$) cosets in the form $\mathcal{CT}$. We may therefore denote all 108 ($= 3 \times 6 \times 6$) elements of the $SU(3)$ subgroup $\Sigma(108)$ in the concise form

$$\mathcal{S}_6\mathcal{CT}, \tag{16.96d}$$

where $\mathcal{S}_6$, $\mathcal{C}$, and $\mathcal{T}$ are the three sets of matrices defined in (16.96a)–(16.96c).

How well do these subgroups work as raw material for building cubature formulas? To answer this question, we proceed, as described earlier, to build various Gram matrices and compare their eigenvalue spectra with those in the continuum limit. If we use an equal-weight cubature formula, then the elements of the Gram matrix $\Gamma(l)$ are given by (see (11.9))

$$\Gamma(l)_{rs} = \frac{1}{NM(l,3)} \sum_{j=1}^{N} \sum_{k=1}^{M(l,3)} \left\langle G_r^{(l)}, \mathcal{L}(u_j) Q_k^{(l)} \right\rangle \left\langle \mathcal{L}(u_j) Q_k^{(l)}, G_s^{(l)} \right\rangle, \tag{16.97}$$

where the unitary matrices u_j are the elements of whatever discrete subgroup (or modification thereof) we wish to test, and N equals the number of such matrices.

How well does the particular subgroup $\Sigma(108)$ work? Figure 16.7 shows the Gram eigenvalues for orders three (top) and four (bottom) obtained using the equal-weight formula (16.97) with the matrices u_j given by the elements (16.96) of $\Sigma(108)$; and it compares these results with the continuum-limit values given in Table 15.9 (dashed lines). The results shown here do not appear terribly promising—indeed, one of the eigenvalues for order four equals *zero*! It turns out that we can do much better.

One may easily identify why plain, unvarnished $\Sigma(108)$ does not work well: Recall that the $\Sigma(108)$ subgroup $\mathcal{S}_6$ defined in (16.96a) contains only real elements, hence only elements of $SO(3)$. It follows that the eighteen (right) cosets $\mathcal{CT}$ of $\Sigma(108)$ with respect to $\mathcal{S}_6$ (see (16.96d)) belong to the manifold $SU(3)/SO(3)$. In other words, the 108 points defined on the $SU(3)$ group manifold by the elements of $\Sigma(108)$ comprise just eighteen distinct points on the manifold of the coset space $SU(3)/SO(3)$. As a consequence, if we use just the eighteen coset representatives $\mathcal{CT}$ to compute the Gram matrices (16.97), we should obtain the exact same results as shown in Figure 16.7. This is indeed the case. Now recall that $N_{s3}(3) = 43 > 18$ (see Table 16.5). This implies that we should not expect plain $\Sigma(108)$ to yield the continuum-limit eigenvalues for any value of l that interests us ($l \geq 3$).[49]

We must add a caveat to the argument just given in the last paragraph. As we shall soon see, a modification of the elements in $\Sigma(108)$ works much better than plain $\Sigma(108)$. Indeed, the modified elements work so well as to render quite suspect the argument we gave leading to the estimate $N_{s3}(P)$ for the minimum number of points required by a cubature formula of degree P on the manifold $SU(3)/SO(3)$. In other words, we have perhaps been somewhat glib in our derivation of (16.94) and in the argument of the last paragraph.

To see how we might modify the elements of $\Sigma(108)$ so as to obtain an improved cubature formula, recall what we have learned about $\Sigma(108)$'s group structure: it contains only eighteen distinct cosets of $SU(3)/SO(3)$. We would like to correct this shortcoming by modifying the elements of $\Sigma(108)$ in such a way as to remove this coset degeneracy. One method for doing this simply applies to each element of $\Sigma(108)$ a similarity transformation generated by some fixed element $v \in SU(3)$. The set of elements so generated—$v\Sigma(108)v^{-1}$—constitutes

[49] On the other hand, because the lower bound $N(6,3) = 17 < 18$ (see Table 16.5), we might hope that $\Sigma(108)$ would yield, at the very least, invertible Gram matrices for $l \leq 6$. The bottom graphic in Figure 16.7, however, dashes even this hope.

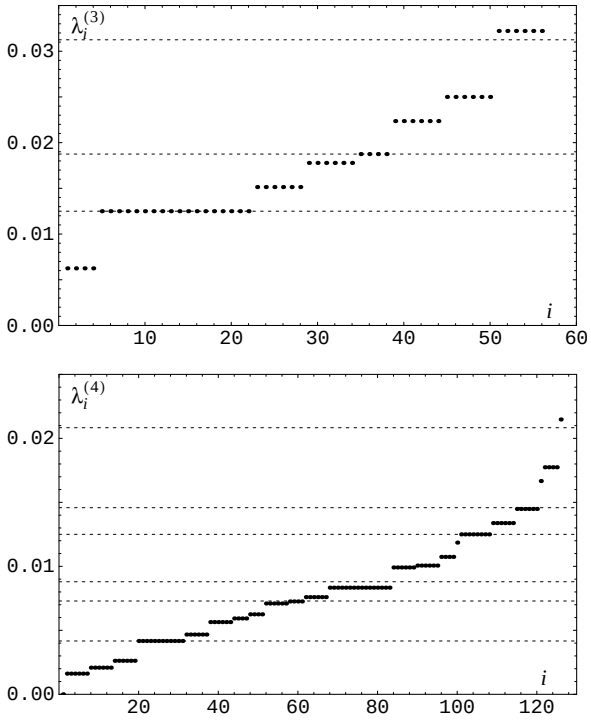

FIGURE 16.7. These two graphics compare the $\Sigma(108)$ Gram eigenvalues with those found in the continuum limit (dashed lines) for the cases $l = 3$ (top) and $l = 4$ (bottom). In the figure for the $l = 4$ case, there is one point in the lower left-hand corner, barely visible, which corresponds to a zero eigenvalue. The Gram matrix elements (16.97) were computed using MARYLIE's computational engine [32].

another, possibly different, discrete subgroup of $SU(3)$. This new subgroup, a modified $\Sigma(108)$, can have a different coset structure and may therefore work better than the original $\Sigma(108)$ for constructing a cubature formula. (The difficulty, of course, lies in choosing an appropriate v.) It turns out that we need not perform the entire similarity transformation. To see this, first observe that, by (13.15),

$$\mathcal{L}(vu_jv^{-1}) = \mathcal{L}(v^{-1})\mathcal{L}(vu_j).$$

Because v is a fixed element in $SU(3)$, it follows from this relation and Corollary 16.1 (on page 132) that the Gram matrices constructed using either the elements vu_jv^{-1} or the elements vu_j differ by at most a unitary similarity transformation. Since similar matrices have identical eigenvalue spectra, and since we focus on the eigenvalues, we may conclude that the elements vu_j will, for our purposes, work as well as the elements vu_jv^{-1}. Now also recall, from the discussion in §13.3, that we may extract from the left of vu_j any element of $SO(3)$; in other words, if $v = rt$, where $r \in SO(3)$, then it suffices to use $t \in SU(3)/SO(3)$ rather than $v \in SU(3)$. We shall therefore search for a $t \in SU(3)/SO(3)$ such that the correspondingly modified $\Sigma(108)$—*i.e.*, $t\Sigma(108)$—yields Gram eigenvalue spectra as close as possible to the continuum-limit spectra.

The search just described for the desired $t \in SU(3)/SO(3)$ requires an appropriate parameterization for elements in $SU(3)/SO(3)$. To write down one such parameterization, first note that we may use (13.15) to write

$$\mathcal{L}(tu_j) = \mathcal{L}(u_j)\mathcal{L}(t) = \mathcal{L}_j\mathcal{T} \tag{16.98}$$

for the Lie transformations based on modified elements of $\Sigma(108)$. Here $\mathcal{L}_j = \mathcal{L}(u_j)$ and $\mathcal{T} = \mathcal{L}(t)$. A complete parameterization for the most general linear symplectic transformation in $Sp(6,\mathbb{R})$ is given in [30]. Restricting this parameterization to the $SU(3)/SO(3)$ coset space contained within $Sp(6,\mathbb{R})$ yields one possible parameterization for $\mathcal{T} = \mathcal{L}(t)$:

$$\mathcal{T} = \exp(:\theta_1 b^1 + \theta_3 b^3 + \theta_4 b^4 + \theta_6 b^6 + \theta_8 b^8:), \tag{16.99a}$$

where

$$\begin{aligned} b^1 &= q_1 q_2 + p_1 p_2, \\ b^3 &= \frac{1}{2}(q_1^2 + p_1^2 - q_2^2 - p_2^2), \\ b^4 &= q_1 q_3 + p_1 p_3, \\ b^6 &= q_2 q_3 + p_2 p_3, \\ b^8 &= \frac{1}{\sqrt{12}}(q_1^2 + p_1^2 + q_2^2 + p_2^2 - 2q_3^2 - 2p_3^2). \end{aligned} \tag{16.99b}$$

Then, with the modified linear symplectic transformations defined in (16.98), the corresponding matrix elements (16.97) become

$$\Gamma(l)_{rs} = \frac{1}{NM(l,3)} \sum_{jk} \left\langle G_r^{(l)}, \mathcal{L}_j \mathcal{T} Q_k^{(l)} \right\rangle \left\langle \mathcal{L}_j \mathcal{T} Q_k^{(l)}, G_s^{(l)} \right\rangle, \tag{16.100}$$

where $\mathcal{T}$ is parameterized by the five angles $\{\theta_1, \theta_3, \theta_4, \theta_6, \theta_8\}$.

To search for a useful cubature formula based on $\Sigma(108)$, we use (16.100) with $\mathcal{L}_j = \mathcal{L}(u_j)$, $u_j \in \Sigma(108)$, to compute the Gram matrices, and adjust the five angles θ_i so as to maximize the minimum Gram eigenvalue $\lambda_{min}^{(l)}$. One particularly good choice of angles is

$$\begin{aligned} \theta_1 &= 5.37151879339066, & \theta_6 &= 0.0901220988903537, \\ \theta_3 &= -0.996058839052193, & \theta_8 &= 5.85468162906558, \\ \theta_4 &= 3.67552887308850, \end{aligned} \tag{16.101}$$

found after much searching and tweaking in an attempt to maximize the particular eigenvalue $\lambda_{min}^{(4)}$. Figure 16.8 shows the Gram eigenvalues for orders three (top) through six (bottom) as given by (16.100) using the angles (16.101). It also compares these results with the continuum-limit values given in Table 15.9 (dashed lines). Observe that the eigenvalue spectrum for $l = 3$ is very close to the continuum limit, and most of the eigenvalues for $l = 4$ are also close to the continuum-limit values. Even for the cases $l = 5$ and $l = 6$ the agreement appears so remarkable as to suggest that just a little more tweaking would bring these eigenvalues into line—that this cubature formula is otherwise exact up through $l = 6$!

After discussing why plain $\Sigma(108)$ might not work very well, we offered a caveat concerning our estimate $N_{s3}(P)$ (see Table 16.5) of the number of points required by exact cubature formulas of given degree. The motivation for that caveat should now be clear: Table 16.5 suggests that a cubature formula that gives exact results up through order 6 would need roughly 529 points, and yet a 108-point cubature formula produces the results shown in Figure 16.8. Why this happens remains a puzzle.

In principle, one may apply the search procedure just described to improve on any cubature formula constructed from a given set of unitary matrices. Attempts to do just this with some of the dihedral-like groups, however, have not (yet) met with the same success as obtained with the crystal-like group $\Sigma(108)$. See Table 16.6, which lists the results of some preliminary efforts to maximize $\lambda_{min}^{(4)}$ using five of the dihedral-like groups.

16.3.3. *Cubature Formulas for the Three-Torus.* When we choose the linear symplectic transformations $\mathcal{L}(u)$ from the space $\mathcal{U} = U(1) \otimes U(1) \otimes U(1)$, the required integral (15.140) covers three separate circles $\mathbb{S}^1$. In other words, the integral covers the three-torus $\mathbb{T}^3 = \mathbb{S}^1 \otimes \mathbb{S}^1 \otimes \mathbb{S}^1$.

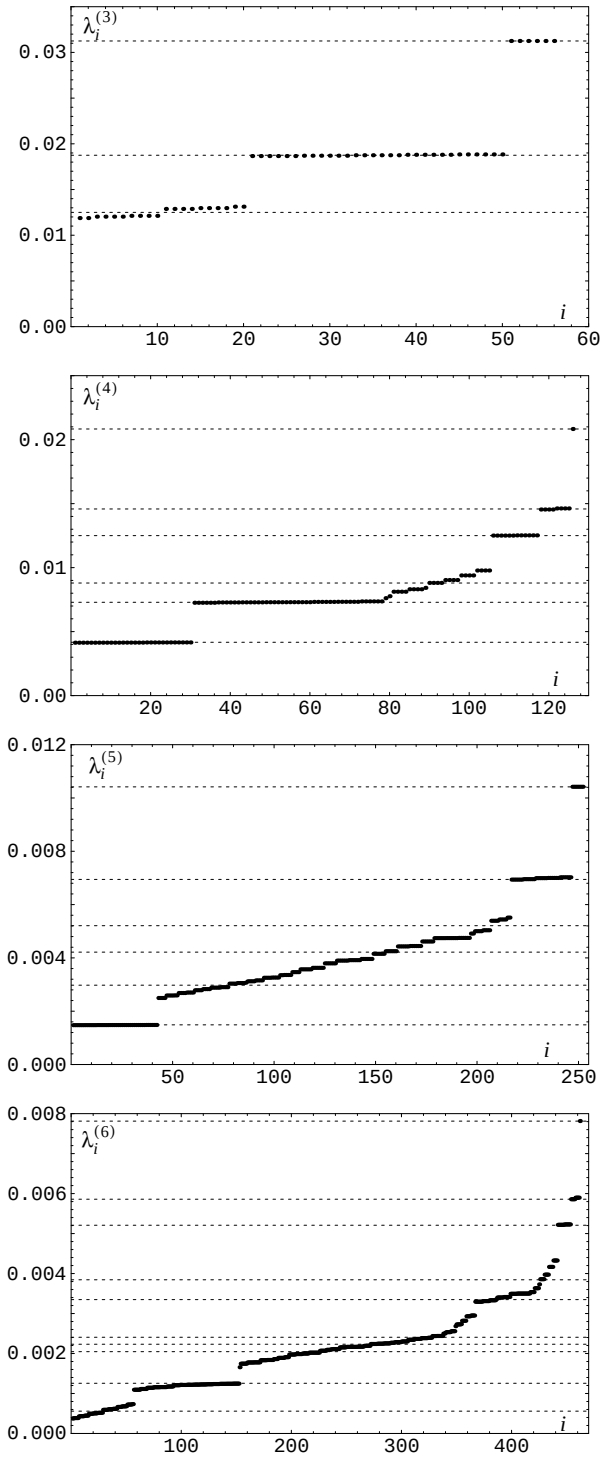

FIGURE 16.8. These four graphics compare the modified $\Sigma(108)$ Gram eigenvalues with those found in the continuum limit (dashed lines) for the cases (reading from top to bottom) $l = 3$ through $l = 6$.

TABLE 16.6. This table lists the best results so far of efforts to maximize $\lambda^{(4)}_{min}$ using five of the dihedral-like groups. For comparison, recall that the continuum-limit value of $\lambda^{(4)}_{min}$ equals $\frac{1}{240} \simeq 0.004166\cdots$.

group	n	order	$\max \lambda^{(4)}_{min}$
$\Delta(3n^2)$	2	12	0.000247
	3	27	0.00284
	4	48	0.00342
$\Delta(6n^2)$	2	24	0.00176
	3	54	0.00366

We can find cubature formulas in this case by making suitable generalizations of the arguments given in §16.2.4.

Recall from the end of §16.3.1 that the functions of interest to us here are the product exponentials $e^{i2k_1\theta_1}e^{i2k_2\theta_2}e^{i2k_3\theta_3}$ with $k_1, k_2, k_3 \in \{P, P-1, \ldots, -P\}$ such that $|k_1| + |k_2| + |k_3| \le P$. To simplify later discussion, we generalize the definition of the symbol $\mathcal{K}_P$ (*cf.* (16.54)) by writing

$$\mathcal{K}_P = \Big\{(k_1,k_2,k_3) \;\Big|\; k_1,k_2,k_3 \in \{P,P-1,\ldots,-P\} \text{ and } |k_1|+|k_2|+|k_3| \le P\Big\}. \tag{16.102}$$

As before we define $\mathcal{K}'_P$ by (16.55): it denotes the set $\mathcal{K}_P$ with the pair $(0,0)$ removed. We now want to find minimal cubature formulas that yield exact results on the manifold $\mathbb{T}^3$ for all of our product exponentials $e^{i2k_1\theta_1}e^{i2k_2\theta_2}e^{i2k_3\theta_3}$; hence we seek cubature formulas of the form

$$Q_N[f(\theta_1,\theta_2,\theta_3)] \equiv \sum_{i=1}^{N} w_i f(\theta_{1i},\theta_{2i},\theta_{3i}), \tag{16.103}$$

with N as small as possible, such that

$$Q_N\big[e^{i2k_1\theta_1}e^{i2k_2\theta_2}e^{i2k_2\theta_3}\big] = \delta_{0k_1}\delta_{0k_2}\delta_{0k_3} \tag{16.104}$$

for all triplets $(k_1,k_2,k_3) \in \mathcal{K}_P$.

By analogy with (16.59) we shall look for cubature formulas in the form of lattice rules that satisfy (16.104). In particular, we shall try

$$Q_N[f(\theta_1,\theta_2,\theta_3)] \equiv \frac{1}{N}\sum_{j=0}^{N-1} f\big(\tfrac{2\pi j}{N}, \alpha\tfrac{2\pi j}{N}, \beta\tfrac{2\pi j}{N}\big), \tag{16.105}$$

where N, α, and β are a set of judiciously chosen positive integer constants. Then, by a straightforward generalization of the argument leading from (16.59) to (16.60), we deduce that one must select N, α, and β so as to ensure

$$\frac{2(k_1+\alpha k_2+\beta k_3)}{N} \notin \mathbb{Z} \quad \text{for all triplets } (k_1,k_2,k_3) \in \mathcal{K}'_P. \tag{16.106}$$

We may easily identify several constraints on the constants α and β by making use of the observation that in order to satisfy (16.106), we cannot allow $k_1 + \alpha k_2 + \beta k_3$ to vanish for any triplet $(k_1,k_2,k_3) \in \mathcal{K}'_P$. First, since $(k_1,-1,0) \in \mathcal{K}'_P$ for all $k_1 \in \{0,1,\ldots,P-1\}$, it follows that α cannot belong to the set $\{0,\ldots,P-1\}$; hence

$$\alpha \ge P.$$

By a similar argument it also follows that

$$\beta \ge P.$$

Second, since $(0, 1, -1) \in \mathcal{K}'_P$ whenever $P > 1$, it follows that

$$\alpha \neq \beta$$

unless $P = 1$. And third, the symmetry between k_2 and k_3 in (16.106) implies that we may always select α and β such that $\alpha \leq \beta$. Testing a wide range of α's and β's that satisfy these constraints, and searching for the smallest N (which we shall denote N_{t3}) that satisfies (16.106), we obtain the values listed in Table 16.7 for α, β, and N_{t3}.

TABLE 16.7. This table lists for $P \in \{3, \ldots, 12\}$ values for α, β, and $N = N_{t2}$ that appear to make (16.105) a minimal cubature formula on the three-torus $\mathbb{T}^3$.

P	α	β	N_{t3}
3	4	6	15
4	5	8	27
5	7	11	49
6	10	16	71
7	14	23	109
8	19	26	145
9	22	36	207
10	24	39	263
11	33	46	359
12	36	50	427

16.3.4. *Jolt Decomposition in Three Degrees of Freedom.* Let us now summarize what we know about the process of jolt decomposition in three degrees of freedom. We begin with a set of homogeneous polynomials,

$$h_l = \sum_{r=1}^{M(l,6)} c^{(l)} G_r^{(l)},$$

of degree $l \leq P$ and want to decompose them into a linear combination of jolts. In other words, we wish to write these polynomials in the form (*cf.* (16.62))

$$h_l = \frac{1}{M(l,3)} \sum_{j=1}^{N} \sum_{k=1}^{M(l,3)} w_j a_{jk}^{(l)} \mathcal{L}_j Q_k^{(l)}. \tag{16.107}$$

The jolt strengths $a_{jk}^{(l)}$, the sensitivity vectors σ_{jk}^s, and the Gram matrix elements $\Gamma(l)_{rs}$ are given by (*cf.* (16.64)–(16.66))

$$a_{jk}^{(l)} = \sum_{r,s=1}^{M(l,6)} c_r^{(l)} [\Gamma(l)^{-1}]_{rs} \sigma_{jk}^s, \tag{16.108}$$

$$\sigma_{jk}^s = \left\langle G_s^{(l)}, \mathcal{L}_j Q_k^{(l)} \right\rangle, \tag{16.109}$$

and

$$\Gamma(l)_{rs} = \frac{1}{M(l,3)} \sum_{j=1}^{N} \sum_{k=1}^{M(l,3)} w_j \sigma_{jk}^r \sigma_{jk}^s. \tag{16.110}$$

To complete the description, of course, we must specify the weights w_j and the linear symplectic transformations $\mathcal{L}_j$. These quantities are based on various cubature formulas, and we have examined, in §§16.3.2 and 16.3.3, two different possibilities.

The first possibility we discussed requires the use of cubature formulas for the manifold $SU(3)/SO(3)$. To our knowledge, however, the subject of $SU(3)/SO(3)$ cubature formulas has never been studied before, and no results are available in the literature. We have partially explored, as an initial approach to the problem, the possibility of constructing suitable cubature formulas based on the use of optimally oriented discrete subgroups of $SU(3)$. To do so, we have employed linear symplectic transformations of the form given in (16.98),

$$\mathcal{L}(tu_j) = \mathcal{L}_j\mathcal{T}.$$

Here $\mathcal{L}_j = \mathcal{L}(u_j)$ has the matrix representation $M(u_j)$ given by (13.11), where the u_j belong to some appropriate finite subgroup S of $SU(3)$; and $\mathcal{T} = \mathcal{L}(t)$ is given by (16.99), where, as discussed on p. 162, the 3×3 matrix $t \in SU(3)/SO(3)$ serves to rotate the subgroup S into some optimal orientation within the full group $SU(3)$. (Here we mean optimal in the sense that the resulting cubature formula, when used in (16.110), produces Gram matrices with the same eigenvalue spectra as in the continuum limit for as high a degree l as possible.) In certain special cases one can determine the action of $\mathcal{T}$ analytically, but for arbitrary values of the five angles $\{\theta_1, \theta_3, \theta_4, \theta_6, \theta_8\}$ one must use numerical techniques [30, 66]. For the particular subgroup $\Sigma(108)$ we have found, as Figure 16.8 suggests, that the angles given by (16.101) appear very nearly optimal. We emphasize that the optimum values of those five angles will depend on the particular choice of subgroup S, and that the differences between the computed and continuum-limit eigenvalue spectra will in all likelihood depend quite sensitively on those values.

The second possibility—that of using cubature formulas for the three-torus $\mathbb{T}^3$—means that the linear symplectic transformations have the form given in (15.135) (with $n = 3$),

$$\mathcal{R}(\theta_1, \theta_2, \theta_3) = \mathcal{R}_1(\theta_1)\mathcal{R}_2(\theta_2)\mathcal{R}_3(\theta_3),$$

which has the corresponding matrix representation

$$M(\theta_1, \theta_2, \theta_3) = M\begin{pmatrix} e^{i\theta_1} & 0 & 0 \\ 0 & e^{i\theta_2} & 0 \\ 0 & 0 & e^{i\theta_3} \end{pmatrix}.$$

Using (13.11) and the angles defined in the lattice rule (16.105), we can express this representation in the specific form

$$M(\theta_{1j}, \theta_{2j}, \theta_{3j}) = \tag{16.111}$$
$$\begin{pmatrix} \cos\left(\frac{2\pi j}{N_{t3}}\right) & 0 & 0 & \sin\left(\frac{2\pi j}{N_{t3}}\right) & 0 & 0 \\ 0 & \cos\left(\alpha\frac{2\pi j}{N_{t3}}\right) & 0 & 0 & \sin\left(\alpha\frac{2\pi j}{N_{t3}}\right) & 0 \\ 0 & 0 & \cos\left(\beta\frac{2\pi j}{N_{t3}}\right) & 0 & 0 & \sin\left(\beta\frac{2\pi j}{N_{t3}}\right) \\ -\sin\left(\frac{2\pi j}{N_{t3}}\right) & 0 & 0 & \cos\left(\frac{2\pi j}{N_{t3}}\right) & 0 & 0 \\ 0 & -\sin\left(\alpha\frac{2\pi j}{N_{t3}}\right) & 0 & 0 & \cos\left(\alpha\frac{2\pi j}{N_{t3}}\right) & 0 \\ 0 & 0 & -\sin\left(\beta\frac{2\pi j}{N_{t3}}\right) & 0 & 0 & \cos\left(\beta\frac{2\pi j}{N_{t3}}\right) \end{pmatrix},$$

where $j \in \{0, 1, \ldots, N_{t3} - 1\}$, and N_{t3}, α, and β are determined by the appropriate lattice rule. If one uses values of N_{t3}, α, and β from Table 16.7, then the corresponding weights are constant: $w_j = 1/N_{t3}$.

Thus for the manifold $\mathbb{T}^3$ we find that the action of the linear symplectic transformations $\mathcal{R}(\theta_{1j}, \theta_{2j}, \theta_{3j})$ on the q's is given by

$$\mathcal{R}(\theta_{1j}, \theta_{2j}, \theta_{3j}) \begin{pmatrix} q_1 \\ q_2 \\ q_3 \end{pmatrix} = \begin{pmatrix} q_1\cos(\theta_{1j}) + p_1\sin(\theta_{1j}) \\ q_2\cos(\theta_{2j}) + p_2\sin(\theta_{2j}) \\ q_3\cos(\theta_{3j}) + p_3\sin(\theta_{3j}) \end{pmatrix}$$
$$= \begin{pmatrix} q_1\cos\left(\frac{2\pi j}{N_{t3}}\right) + p_1\sin\left(\frac{2\pi j}{N_{t3}}\right) \\ q_2\cos\left(\alpha\frac{2\pi j}{N_{t3}}\right) + p_2\sin\left(\alpha\frac{2\pi j}{N_{t3}}\right) \\ q_3\cos\left(\beta\frac{2\pi j}{N_{t3}}\right) + p_3\sin\left(\beta\frac{2\pi j}{N_{t3}}\right) \end{pmatrix}, \tag{16.112}$$

where the second equality results from the use of a lattice rule of the form (16.105).

17. Applications to Maps of Physical Interest

Using the jolt decompositions described in §16 together with the procedures detailed in Appendices B and C, we can now convert any truncated Taylor series map $\mathcal{T}_P$ of order $P-1$ into a Cremona map $\mathcal{C}_P$—*i.e.*, a polynomial symplectic map—in such a way that $\mathcal{T}_P$ and $\mathcal{C}_P$ agree through terms of order $P-1$. In other words, given any truncated Taylor map $\mathcal{T}_P$, we can obtain a *Cremona symplectification* $\mathcal{C}_P$. There then arises the natural question "How well does this work?" To answer this question (at least partially), we shall look at two particular physical systems: (i) the anharmonic oscillator described in §6, and (ii) the transverse motion of electrons in the Berkeley Advanced Light Source (ALS) storage ring.

17.1. **Cremona Symplectification of the Anharmonic Oscillator**

For one degree of freedom we may use the particular jolt decomposition given in §16.1.7, along with the procedures described in Appendices B and C, to effect a Cremona symplectification of any truncated Taylor map—of arbitrary order—that arises from a Hamiltonian dynamical system. Because the one-degree-of-freedom code Tlie2, mentioned earlier in §6.5, works to arbitrary order, it is a straightforward matter (well, almost ...) to write a Tlie2 function that automates Cremona symplectification, also to arbitrary order. This having been done, we can now experiment with how well Cremona symplectification works in one degree of freedom.

To test Cremona symplectification in one degree of freedom, we shall examine how well it works for the anharmonic oscillator illustrated in Figure 6.2 and described by the Hamiltonian (6.1). In particular, we shall look at two different measures of how well Cremona symplectification works: The first compares a truncated Taylor map and its symplectification to see how well they reproduce the non-linear part of the map. The second compares their performances for long-term tracking.

17.1.1. *Results for the Non-Linear Part of the Map.* Using a Lie algebraic formalism, one can determine a straightforward procedure for extracting the non-linear part of a map for any Hamiltonian system. First suppose we write the map under consideration in the factored-product form (see (9.17))

$$\mathcal{M} = e^{:f_1:} e^{:f_2:} e^{:f_3:} e^{:f_4:} \cdots = e^{:f_1:} e^{:f_2:} \mathcal{N},$$

where, of course, $\mathcal{N}$ denotes the non-linear part of $\mathcal{M}$. If the map of interest already exists in factored-product form, then we simply ignore the $e^{:f_1:}$ and $e^{:f_2:}$ factors to obtain $\mathcal{N}$; otherwise, we write

$$\mathcal{N} = e^{-:f_2:} e^{-:f_1:} \mathcal{M}. \tag{17.1a}$$

To take this prescription another step forward, let this map $\mathcal{N}$ act on phase space. Now observe that the translational and linear parts of $\mathcal{M}$ act according to the rules

$$e^{:f_1:} z = z + z^c,$$

and

$$e^{:f_2:} z = Rz,$$

respectively, where z^c denotes a constant vector in phase space, and R denotes the matrix representation of $e^{:f_2:}$ (*cf.* (9.12)). Hence if we write

$$z^f = \mathcal{M} z^i = z^f(z^i),$$

then we obtain the non-linear part of the map in the form

$$\begin{aligned} z^f_{NL} = \mathcal{N} z^i &= e^{-:f_2:} e^{-:f_1:} z^f(z^i) = e^{-:f_2:} z^f(z^i - z^c) \\ &= z^f\big(e^{-:f_2:}(z^i - z^c)\big) = z^f(R^{-1} z^i - z^c). \end{aligned} \tag{17.1b}$$

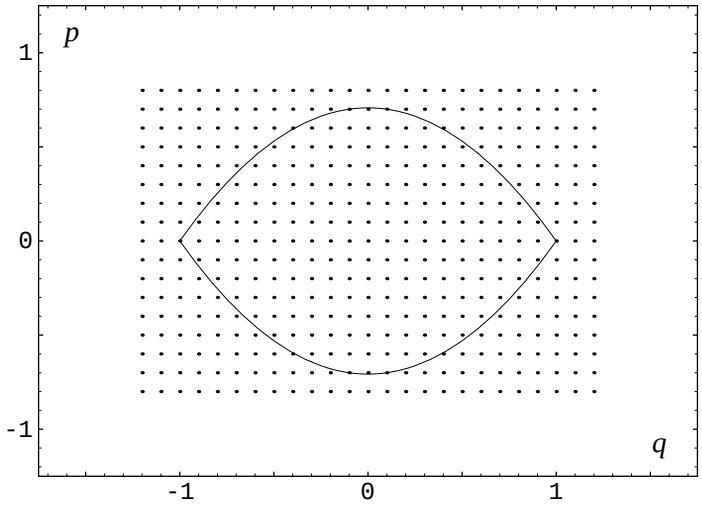

FIGURE 17.1. A grid of initial conditions. The football-shaped outline shows the boundary of the stable region in phase space for the anharmonic oscillator.

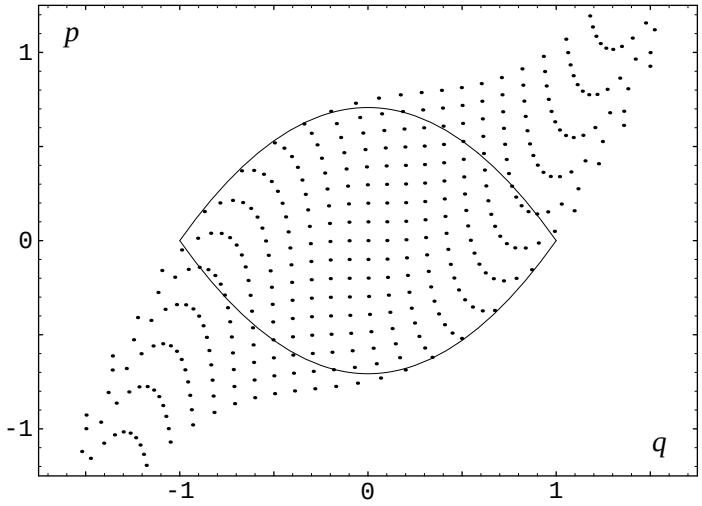

FIGURE 17.2. This graphic shows the result of applying once to the initial conditions shown in Figure 17.1 the non-linear part $\mathcal{N}$ of the exact time-one map for the anharmonic oscillator.

The reader will note that this rule is quite general: it is independent of any particular map representation, and it does not depend on the number of degrees of freedom.

Figure 17.1 shows a grid of initial conditions in phase space superimposed on an outline (the football-shaped boundary) of the part of the separatrix that bounds the stable region around the origin of the anharmonic oscillator (*cf.* Figure 6.2). Figure 17.2 then shows what happens to the grid of initial conditions after one application of the non-linear part $\mathcal{N}$ of the time-one map for the anharmonic oscillator. To make sense of this picture, recall that near the origin, the motion is essentially linear; hence the non-linear part of the map will have little effect in this region. In addition, because the period of the motion increases as one approaches the separatrix, the fact that the linear part of the map gives a simple clockwise rotation of the whole of phase space means that points near the separatrix will appear skewed *counter*clockwise. One can see both these effects by comparing Figures 17.1 and 17.2.

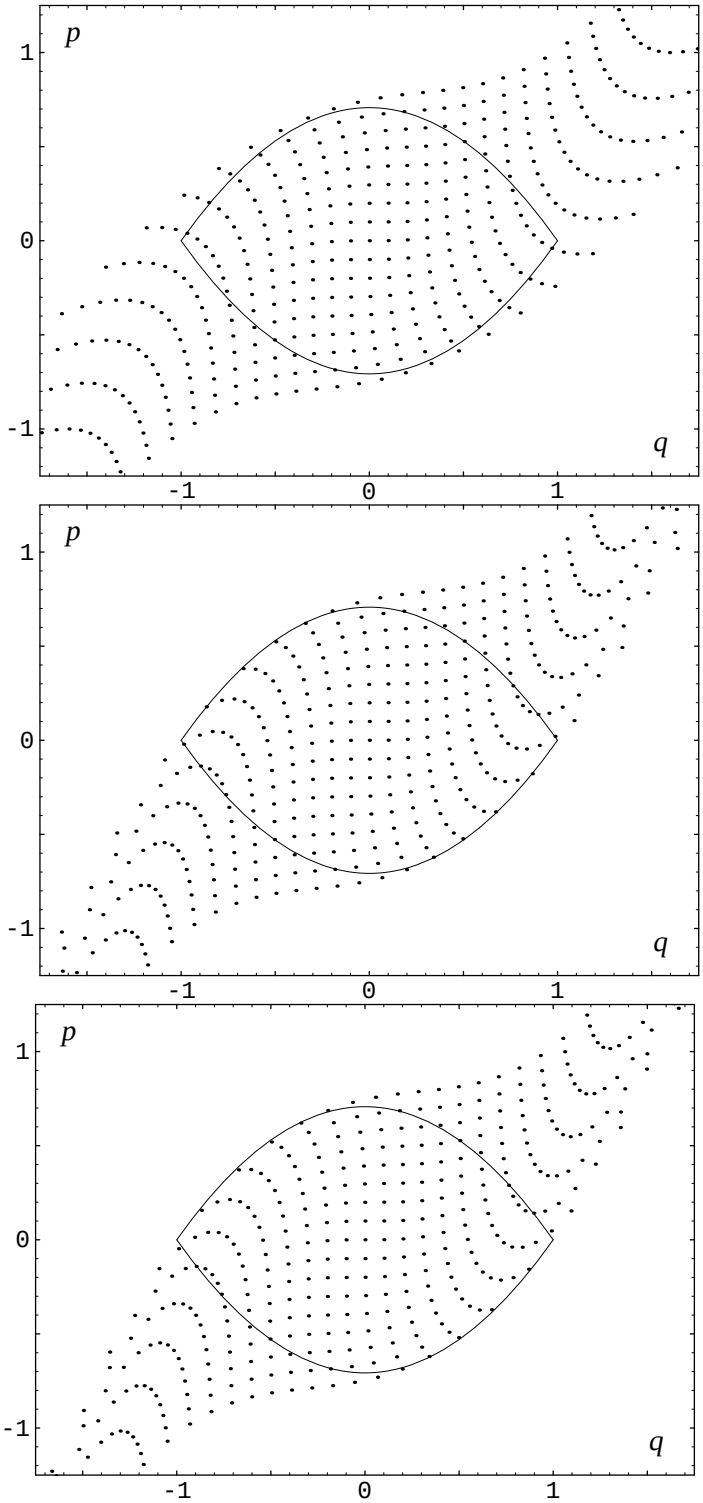

FIGURE 17.3. These graphics show for the anharmonic oscillator the results of applying once to the initial conditions shown in Figure 17.1 the non-linear part of the truncated Taylor maps $\mathcal{T}_4$ (top), $\mathcal{T}_8$ (middle), and $\mathcal{T}_{12}$ (bottom) for time $\tau = 1$.

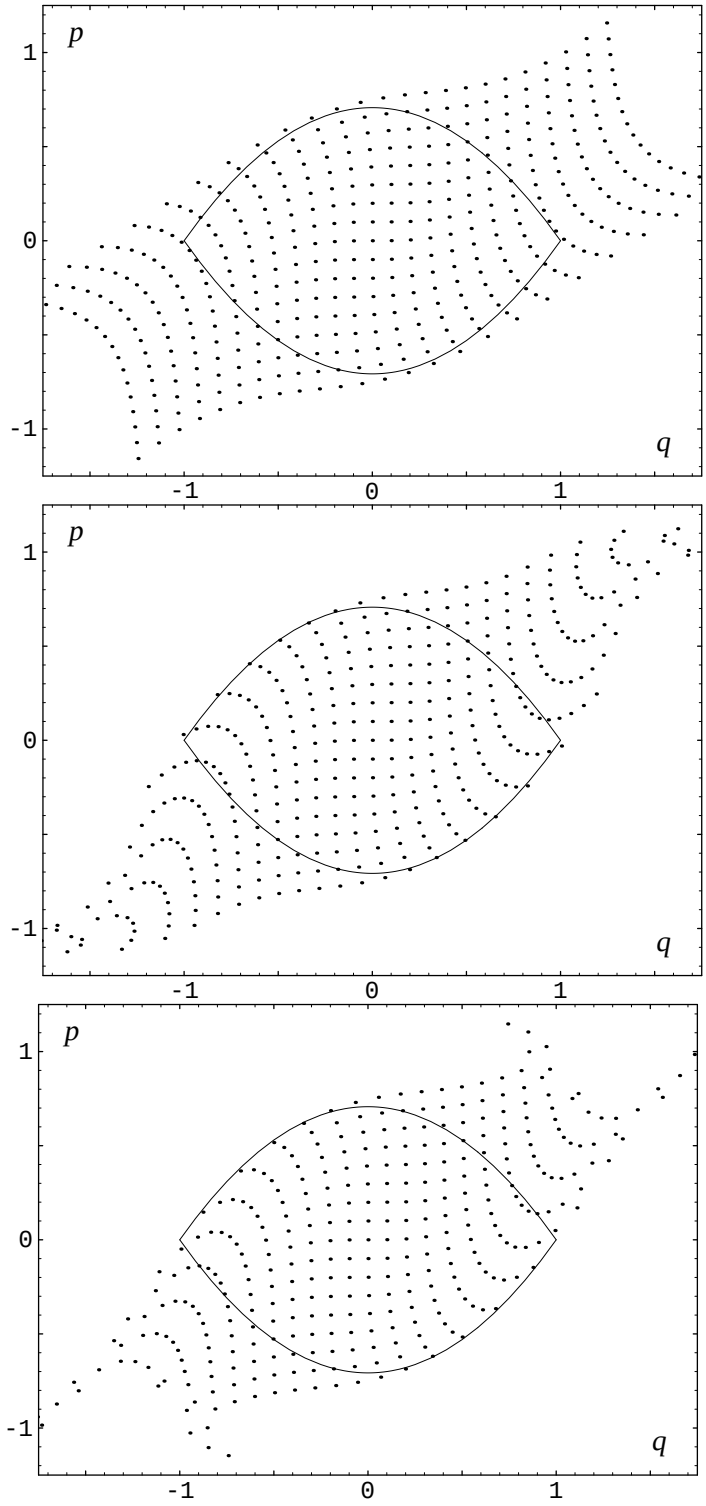

FIGURE 17.4. Theses graphics show for the anharmonic oscillator the results of applying once to the initial conditions shown in Figure 17.1 the non-linear part of the Cremona maps $\mathcal{C}_4$ (top), $\mathcal{C}_8$ (middle), and $\mathcal{C}_{12}$ (bottom) obtained by Cremona symplectification of the corresponding truncated Taylor maps $\mathcal{T}_4$, $\mathcal{T}_8$, and $\mathcal{T}_{12}$ for time $\tau = 1$.

Figure 17.3 shows the results of applying to the grid of initial conditions in Figure 17.1 a series of successively higher order truncated Taylor maps for the non-linear part $\mathcal{N}$ of the time-one map for the anharmonic oscillator. These truncated Taylor maps contain terms through order three (top), seven (middle), and eleven (bottom). A comparison of these results with the exact result in Figure 17.2 shows that the third-order truncated Taylor map $\mathcal{T}_4$ performs well over a substantial part of the stable region, inside the separatrix, and also for small regions towards the upper-right and lower-left, just outside the separatrix. The seventh-order truncated Taylor map $\mathcal{T}_8$ performs well for most of the initial conditions; indeed, it gives poor results only for those initial conditions near the upper-left and lower-right edges of the grid of initial conditions shown in Figure 17.1. And the eleventh-order truncated Taylor map $\mathcal{T}_{12}$ works well for very nearly all of the initial conditions. These results should not surprise the reader: as a comparison with Figure 6.6 shows, all of the initial conditions in Figure 17.1 fall well inside the domain of convergence for the anharmonic oscillator time-one map.

Figure 17.4 shows results comparable to those in Figure 17.3, but using instead Cremona symplectifications of the corresponding truncated Taylor maps. The Cremona symplectification of the third-order truncated Taylor map—*i.e.*, $\mathcal{C}_4$—performs well over essentially the same region of phase space as did $\mathcal{T}_4$. The other two Cremona symplectifications, $\mathcal{C}_8$ and $\mathcal{C}_{12}$, however, do not appear to work as well as their corresponding truncated Taylor series maps. Indeed a superficial comparison might even lead one to think that $\mathcal{C}_8$ is better than $\mathcal{C}_{12}$; but a more careful comparison shows that $\mathcal{C}_{12}$ does in fact perform better than $\mathcal{C}_8$ inside the separatrix and in the region just outside the separatrix.

Figures 17.5, 17.6, and 17.7 show results similar to those in Figures 17.2, 17.3, and 17.4, but for the anharmonic oscillator time-seven map. The comparisons are not so obvious as in the time-one case, but it remains true that the truncated Taylor maps become more accurate at higher order; and similarly for the corresponding Cremona symplectifications shown here. That the truncated Taylor series maps do not do well near the edge of the stable region is, of course, consistent with Figure 6.5, which shows that for the time-seven map the boundary of the domain of convergence cuts inside the separatrix.

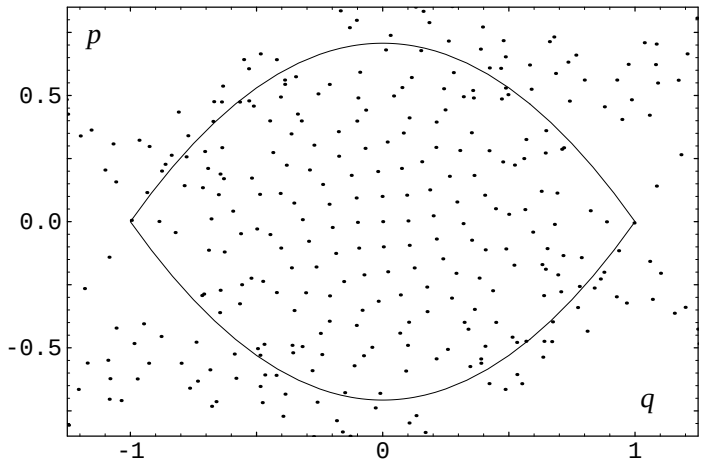

FIGURE 17.5. This graphic shows the result of applying once to the initial conditions shown in Figure 17.1 the non-linear part $\mathcal{N}$ of the exact time-seven map for the anharmonic oscillator.

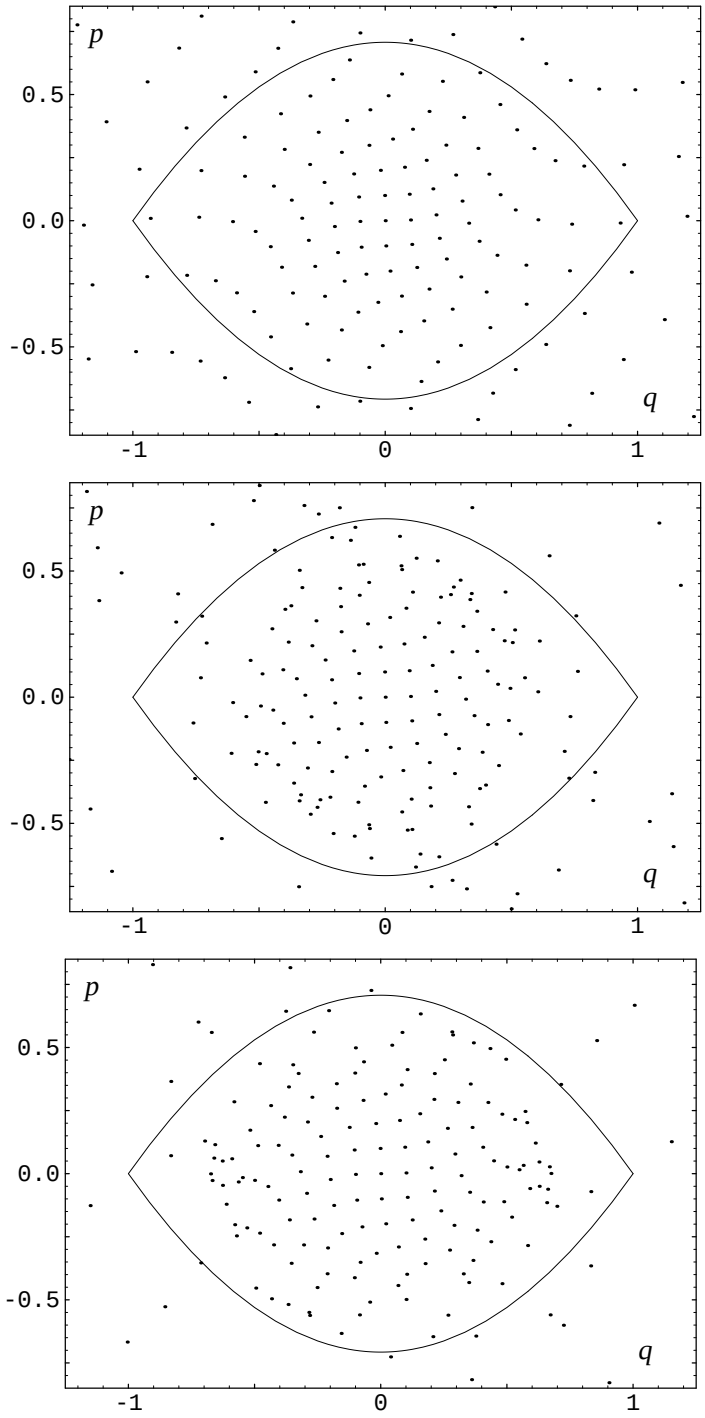

FIGURE 17.6. These graphics show for the anharmonic oscillator the results of applying once to the initial conditions shown in Figure 17.1 the non-linear part of the truncated Taylor maps $\mathcal{T}_4$ (top), $\mathcal{T}_8$ (middle), and $\mathcal{T}_{12}$ (bottom) for time $\tau = 7$.

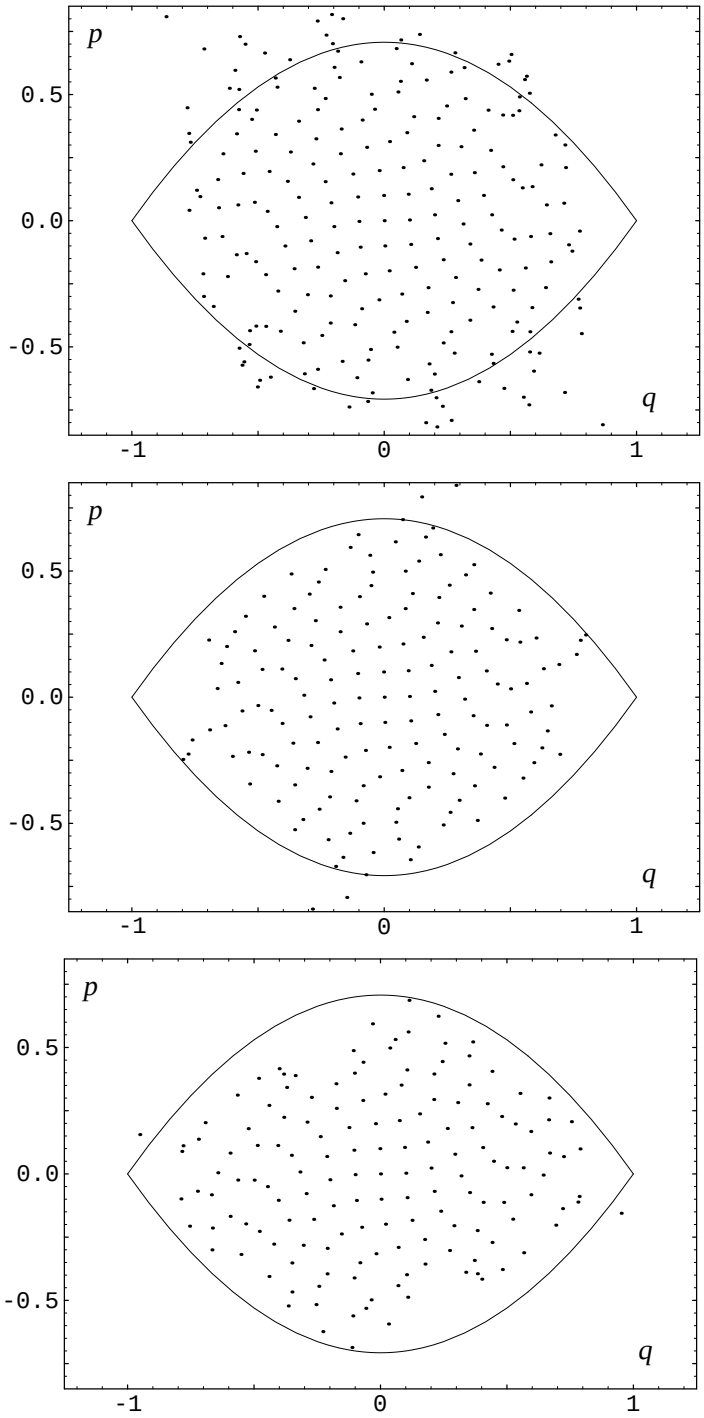

FIGURE 17.7. These graphics show for the anharmonic oscillator the results of applying once to the initial conditions shown in Figure 17.1 the non-linear part of the Cremona maps $\mathcal{C}_4$ (top), $\mathcal{C}_8$ (middle), and $\mathcal{C}_{12}$ (bottom) obtained by Cremona symplectification of the corresponding truncated Taylor maps $\mathcal{T}_4$, $\mathcal{T}_8$, and $\mathcal{T}_{12}$ for time $\tau = 7$.

17.1.2. *Results of Long-Term Tracking.* Recall from §8 that our principal motivation for developing Cremona symplectification was to find a better method for doing long-term tracking of Hamiltonian dynamical systems. Figures 17.8–17.11 address just this issue. Each graphic in these figures shows the result of applying one thousand iterations of either a truncated Taylor map or its Cremona symplectification to a small set of initial conditions. Figure 17.8 shows the results obtained using time-one truncated Taylor maps of (from top to bottom) orders three, seven and eleven; and Figure 17.9 shows the results obtained using the corresponding Cremona symplectifications. Figures 17.10 and 17.11 show similar results, but for the time-seven maps for the anharmonic oscillator. All of these pictures should be compared to the exact phase-space portrait shown in Figure 6.2.

Comparisons between the various truncated Taylor maps and their corresponding Cremona symplectifications suggest that for the purposes of long-term tracking a Cremona symplectification represents a significant improvement over its underlying truncated Taylor series map,. Indeed, even the lowest-order Cremona symplectifications appear to work remarkably well. In the uppermost graphic of Figure 17.9, for example, the inner three orbits deviate from the exact result by no more than the width of the curve; and the fourth orbit (counting from the origin) differs only slightly from the exact result. On the other hand, the underlying truncated Taylor series map—used in the uppermost graphic of Figure 17.8—works well only for much smaller amplitudes. Putting the matter slightly differently, we can say that one must use a relatively high order truncated Taylor map in order to achieve results comparable to those given by $\mathcal{C}_4$. And if the number of iterations is very large, say 10^6 rather than 10^3, then even a high-order Taylor map gives unsatisfactory results. In general, violations of the symplectic condition entailed by the use of truncated Taylor maps add up over successive iterations and thereby make it impossible to draw conclusions about long-term stability. Cremona maps, by contrast, can be iterated infinitely often. Figures 17.10 and 17.11 tell much the same story for the time-seven map.

In the bottom graphic of Figure 17.9—the Cremona symplectification of $\mathcal{T}_{12}$—we have omitted the football-shaped outline of the stable region of phase space. In its place we have added a pair of initial conditions very near the hyperbolic fixed points at $(q^i, p^i) = (\pm 1, 0)$. The large dots trace the result of iterating the Cremona symplectification $\mathcal{C}_{12}$ with these two initial conditions, and one can see that $\mathcal{C}_{12}$ for $\tau = 1$ renders accurately all of the phase-space portrait for the anharmonic oscillator on and within the separatrix.

Let us pause for a moment to remind ourselves that the process of Cremona symplectification begins with a truncated Taylor series map and adds higher-order terms solely for the purpose of satisfying the symplectic condition. All of the information about the particular dynamical system therefore comes just from a finite set of Taylor series coefficients. In other words, *the striking improvement that a Cremona symplectification appears to make on a truncated Taylor map derives solely from imposing the symplectic condition.*

The reader should not, however, become overly excited by the prospect of higher-order Cremona symplectification. Figure 17.12 shows results similar to those in Figure 17.11 using $\mathcal{C}_{26}$, a Cremona symplectification of the order-25 truncated Taylor map $\mathcal{T}_{26}$ for time $\tau = 7$. This figure makes it clear that we have much to learn about Cremona symplectification—even for one degree of freedom. On the other hand, as Figure 17.5 makes clear, the non-linear part $\mathcal{N}$ of the time-seven map is *very* non-linear. It should therefore not surprise us that Cremona symplectification performs less well in this case.

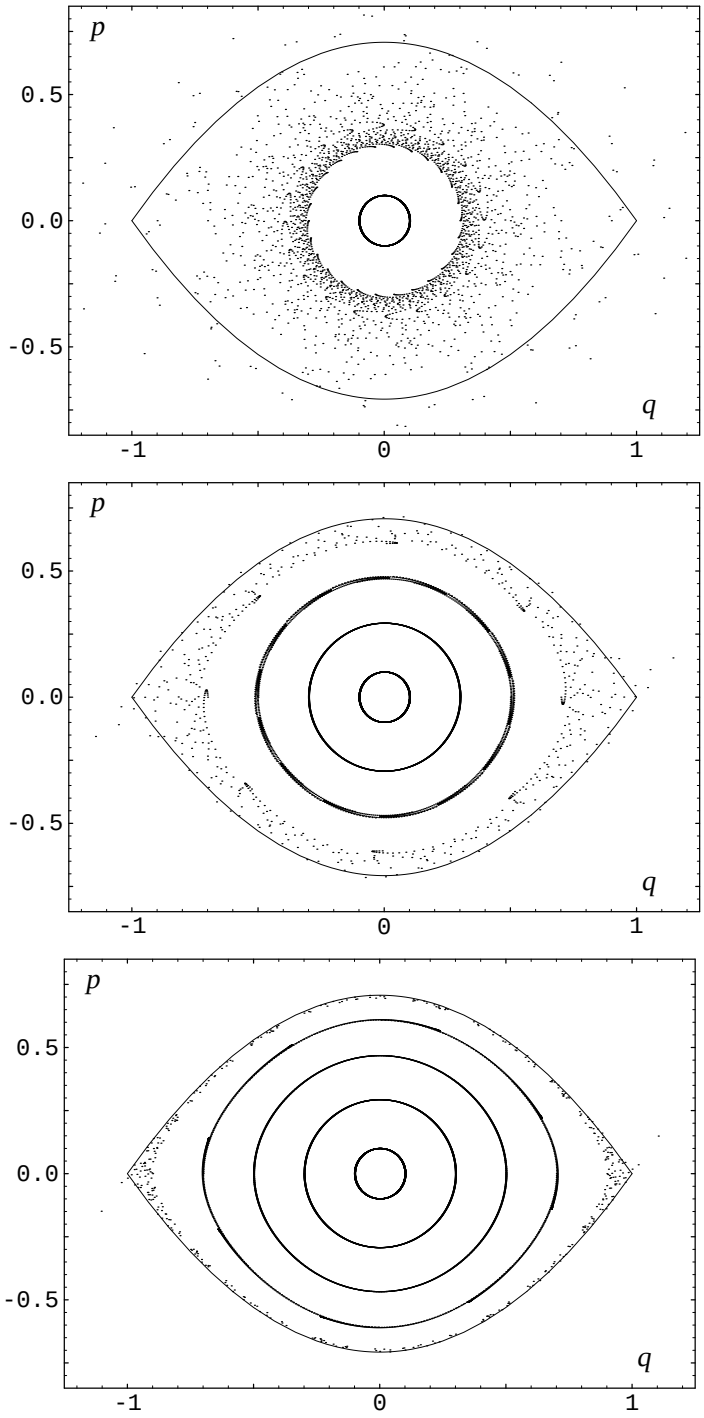

FIGURE 17.8. These graphics show for the anharmonic oscillator tracking results obtained from 1000 iterations of the truncated Taylor maps $\mathcal{T}_4$ (top), $\mathcal{T}_8$ (middle), and $\mathcal{T}_{12}$ (bottom) for time $\tau = 1$ using the initial conditions $p^i = 0$, $q^i \in \{\pm 0.1, \pm 0.3, \pm 0.5, \pm 0.7, \pm 0.9\}$.

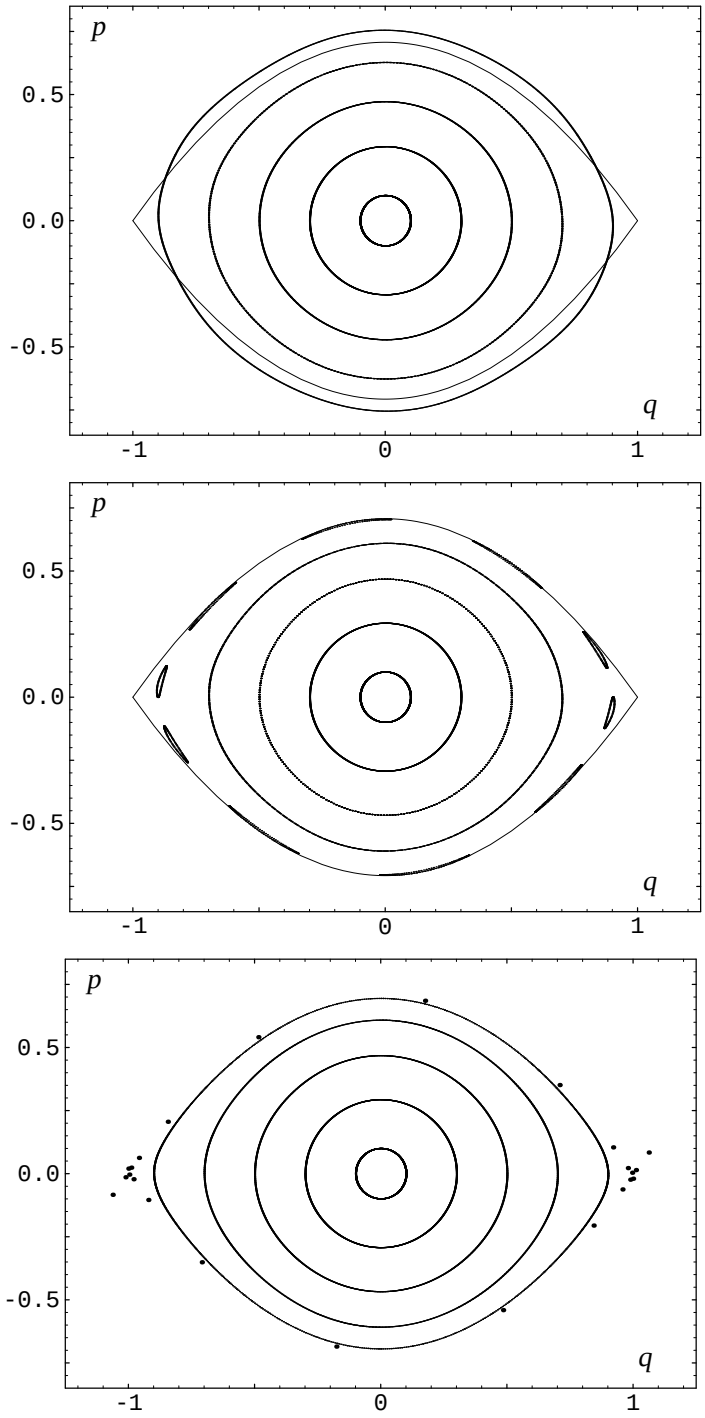

FIGURE 17.9. These graphics show for the anharmonic oscillator tracking results obtained from 1000 iterations of the Cremona maps $\mathcal{C}_4$ (top), $\mathcal{C}_8$ (middle), and $\mathcal{C}_{12}$ (bottom) for time $\tau = 1$ using the initial conditions $p^i = 0$, $q^i \in \{\pm 0.1, \pm 0.3, \pm 0.5, \pm 0.7, \pm 0.9\}$. The bottom figure also uses the initial conditions $(q^i, p^i) = (1.0, -0.2)$ and $(q^i, p^i) = (-1.0, 0.2)$.

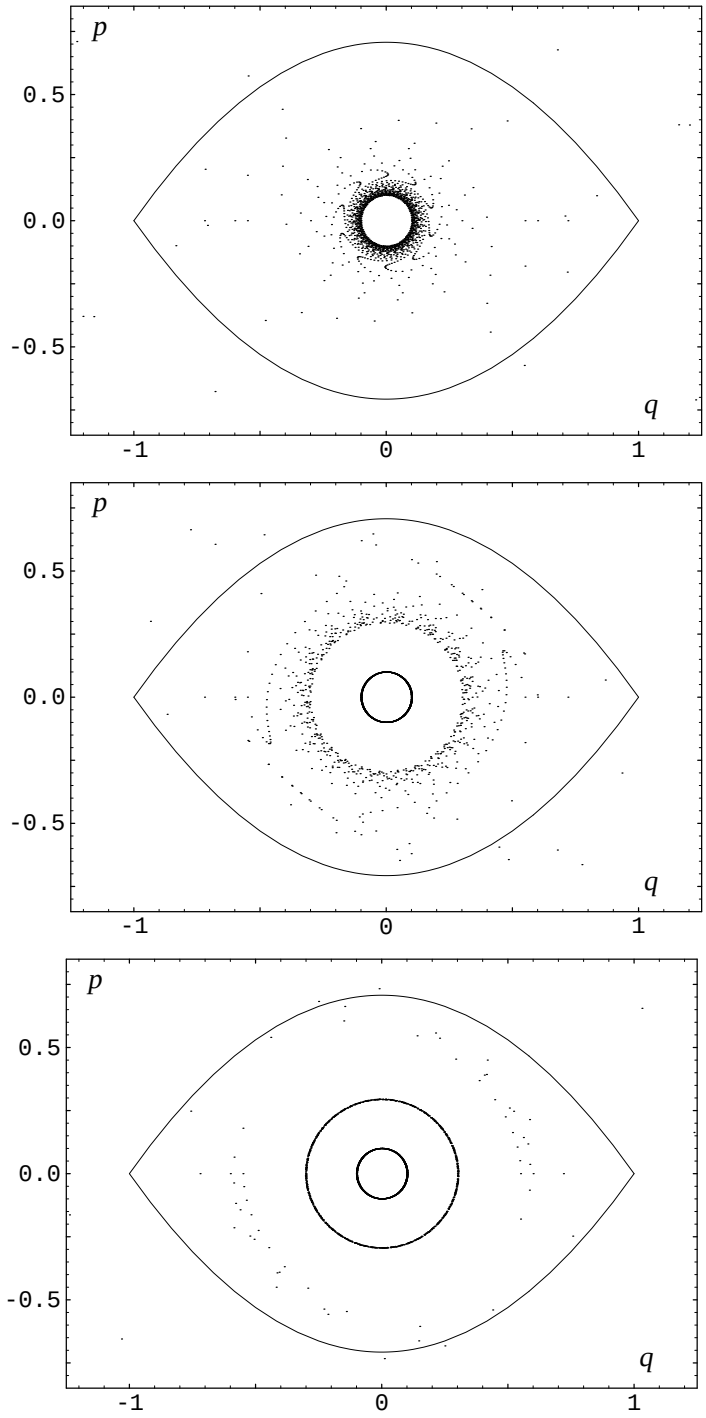

FIGURE 17.10. These graphics show for the anharmonic oscillator tracking results obtained from 1000 iterations of the truncated Taylor maps $\mathcal{T}_4$ (top), $\mathcal{T}_8$ (middle), and $\mathcal{T}_{12}$ (bottom) for time $\tau = 7$ using the initial conditions $p^i = 0$, $q^i \in \{\pm 0.1, \pm 0.3, \pm 0.55, \pm 0.6, \pm 0.72\}$.

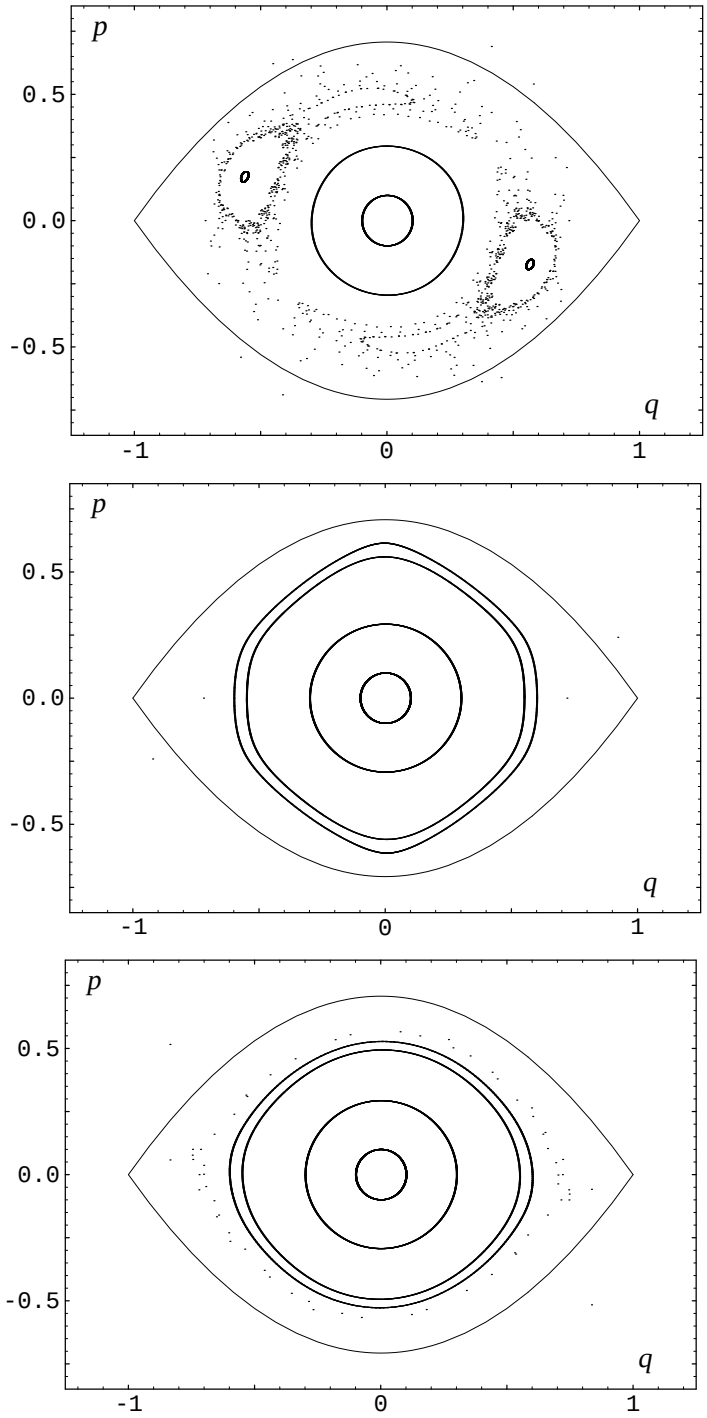

FIGURE 17.11. These graphics show for the anharmonic oscillator tracking results obtained from 1000 iterations of the Cremona maps $\mathcal{C}_4$ (top), $\mathcal{C}_8$ (middle), and $\mathcal{C}_{12}$ (bottom) for time $\tau = 7$ using the initial conditions $p^i = 0$, $q^i \in \{\pm 0.1, \pm 0.3, \pm 0.55, \pm 0.6, \pm 0.72\}$. The top figure also uses the initial conditions $(q^i, p^i) = (0.55, -0.18)$ and $(q^i, p^i) = (-0.55, 0.18)$. The stable fixed points near those last two initial conditions are period-one fixed points.

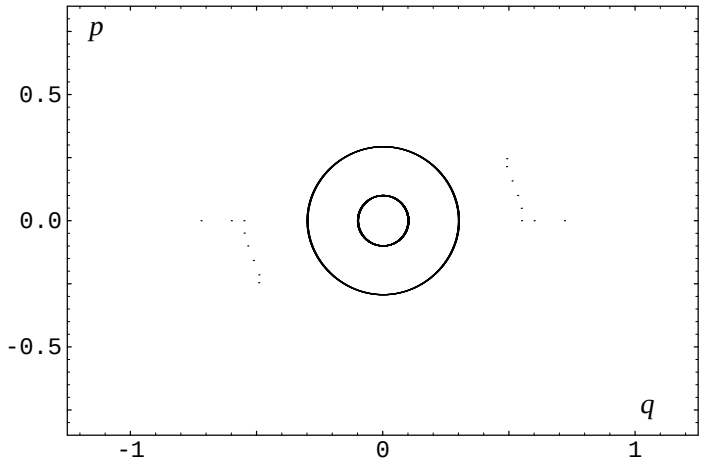

FIGURE 17.12. This figure shows for the anharmonic oscillator tracking results obtained from 1000 iterations of $\mathcal{C}_{26}$, a Cremona symplectification of the order-25 truncated Taylor map $\mathcal{T}_{26}$ for time $\tau = 7$ using the same initial conditions as in the last two figures: $p^i = 0$, $q^i \in \{\pm 0.1, \pm 0.3, \pm 0.55, \pm 0.6, \pm 0.72\}$.

17.2. **Cremona Symplectification of the Advanced Light Source**

In analogy with the discussion just given in §17.1, we may use any of the jolt decompositions described in §16.2.5 to effect a Cremona symplectification of truncated Taylor maps that arise from Hamiltonian dynamical systems in two degrees of freedom. Automating this process in two degrees of freedom is only slightly more difficult than in one degree of freedom, and this has been done by Étienne Forest in his computer code IRWIN,[50] built on top of LIELIB, his library of Lie algebraic routines.

To test Cremona symplectification in two degrees of freedom, we shall look at how well it works for modeling the transverse motion of electrons in the Lawrence Berkeley Laboratory Advanced Light Source (ALS) storage ring. As its name implies, the ALS produces light and hence the electrons in the storage ring steadily lose energy in the form of synchrotron radiation. It follows that one cannot model all aspects of this dynamical system within a Hamiltonian framework, and our treatment of the ALS will ignore the effects of synchrotron radiation. For our purposes, we shall study only the symplectic part of the motion.

Figures 17.13–17.21 show the results of some computer experiments that test Cremona symplectification using the particular jolt decomposition based on cubature formulas for the two-sphere $\mathbb{S}^2$. Underlying each of these figures is a truncated one-turn Taylor series map (which is computed ignoring synchrotron radiation) for the transverse motion of electrons in the ALS.

Figure 17.13 shows in the (x, p_x) and (y, p_y) planes the result of applying both the linear and non-linear parts of a fourth-order truncated Taylor map $\mathcal{T}_5$ once to a beam of initial conditions. Those initial conditions fill a four-dimensional sphere of radius 0.001 and have a uniform spacing of 0.0002 in the transverse phase space (x, p_x, y, p_y). Figure 17.14 shows results comparable to those in Figure 17.13, but using a Cremona symplectification $\mathcal{C}_5$ of the truncated Taylor map $\mathcal{T}_5$ based on the twelve-point cubature formula for the two-sphere

[50] This code was named after John Irwin, whose ideas [51], were very important to the early considerations of jolt maps and Cremona symplectification (see footnote 16). At our request, it was modified to implement Cremona maps in the form (10.13) (with (10.14)) using the jolt decomposition (11.2) based on any given set of $\mathcal{L}_j$. Prior to the work of thesis, however, no good sets of $\mathcal{L}_j$ were known, and the method was largely abandoned.

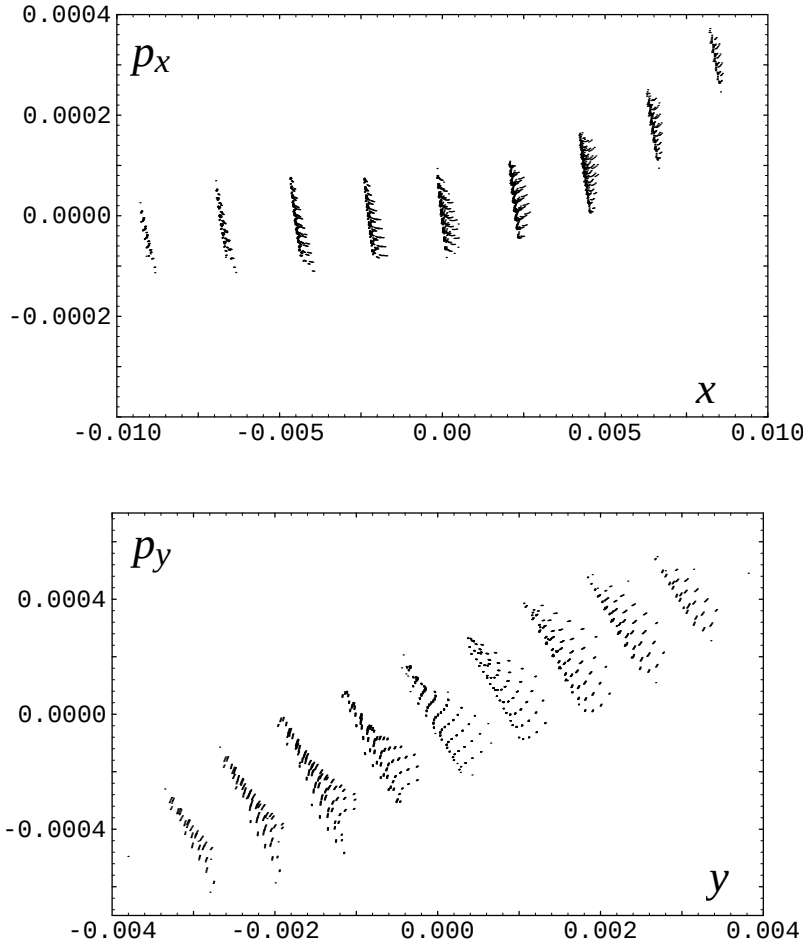

FIGURE 17.13. These graphics show, in the (x, p_x) and (y, p_y) planes, the result of applying once to a set of initial conditions a fourth-order truncated Taylor map $\mathcal{T}_5$ for the ALS.

$\mathbb{S}^2$. The agreement between these figures shows that the two maps—$\mathcal{T}_5$ and its Cremona symplectification $\mathcal{T}_5$—agree very well with one another for a single application of the map.

Figures 17.15–17.21 show some studies of long-term tracking in the ALS. Figure 17.15 shows tracking results in the (x, p_x) plane for 1000 iterations with a ninth-order truncated Taylor map using ten different initial conditions. Those initial conditions were spaced equally along a line in the (x, y) plane with $p_x = p_y = 0$. These results are very close to the "exact" result for the 1000 iterations shown [39]. Although Figure 17.15 shows results only in the (x, p_x) plane, the tracking was done using the full four-dimensional phase space. The coupling between the horizontal and vertical (*i.e.*, x and y) planes accounts for the wiggles and separations seen in some of the orbits. Figure 17.16 then shows the results obtained using 1000 iterations with a fourth-order truncated Taylor map $\mathcal{T}_5$ on the same initial conditions as in Figure 17.15. The next two figures show the corresponding results obtained using two different $\mathcal{C}_5$ Cremona symplectifications of $\mathcal{T}_5$. The first, $\mathcal{C}_5^{rand}$, uses a set of twelve randomly chosen $\mathcal{L}_j$ and gives the tracking results shown in Figure 17.17. The second, $\mathcal{C}_5^{cub}$, uses twelve $\mathcal{L}_j$ based on (16.67) and the fifth-order, twelve-point cubature formula for the two-sphere (see Table 16.1). It gives the tracking results shown in Figure 17.18.

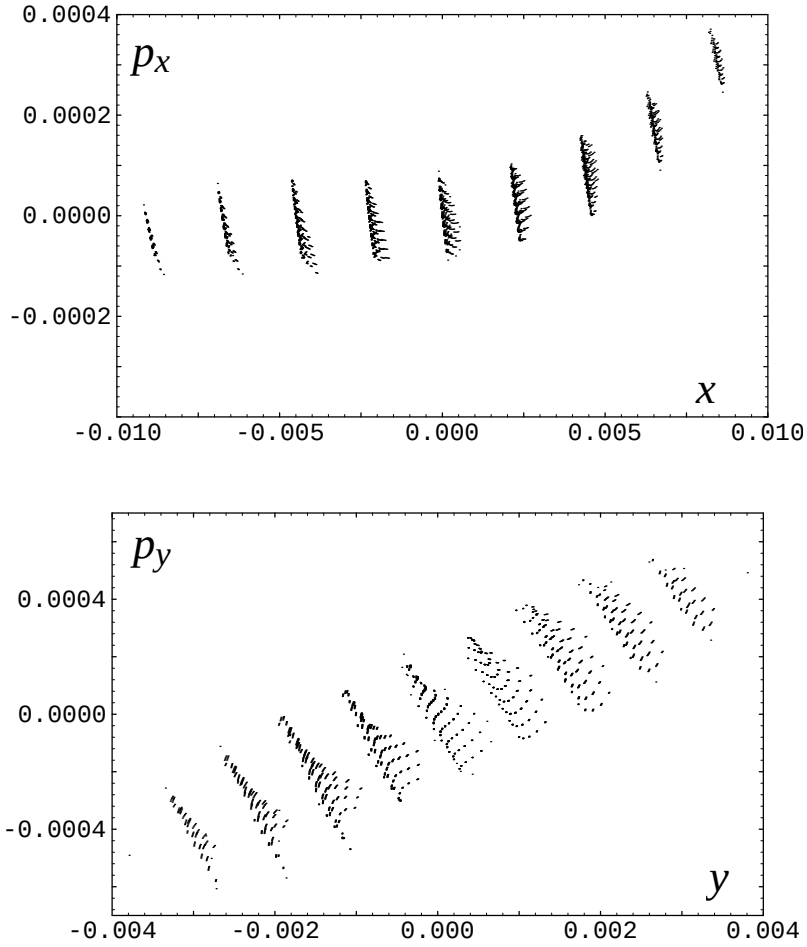

FIGURE 17.14. These graphics show, in the (x, p_x) and (y, p_y) planes, the result of applying once to a set of initial conditions a Cremona symplectification $\mathcal{C}_5$ of the truncated Taylor map $\mathcal{T}_5$ for the ALS.

From Figures 17.15 and 17.16 we see that compared to the "exact" map (*i.e.*, the ninth-order truncated Taylor map), the fourth-order truncated Taylor map $\mathcal{T}_5$ gives good results only for the first three orbits (counting from the origin). The Cremona symplectification $\mathcal{C}_5^{rand}$ based on randomly chosen $\mathcal{L}_j$ gives slightly better results, see Figure 17.17: the first four orbits agree well with one another, and the fifth is debatable. On the other hand, the Cremona symplectification $\mathcal{C}_5^{cub}$ based on the twelve-point cubature formula for the two-sphere, see Figure 17.18, gives results that seem to agree very well with the "exact" results for all ten of the orbits shown! As in one degree of freedom, the improvement that Cremona symplectification makes to a truncated Taylor map derives solely from imposing the symplectic condition; converting from a truncated Taylor map to a Cremona map adds no other information about the dynamical system. However, as shown by a comparison of $\mathcal{C}_5^{rand}$ and $\mathcal{C}_5^{cub}$, how one performs that symplectification matters a great deal. At this point the reader should look again at the histogram in Figure 16.2. That figure shows for one degree of freedom the distribution of minimum Gram eigenvalues computed from Gram matrices built using 1000 different randomly chosen sets of $\mathcal{L}_j$; and it shows that very nearly all sets of $\mathcal{L}_j$ are terrible—only a few are even mediocre. On comparing Figures 17.17 and 17.18, we

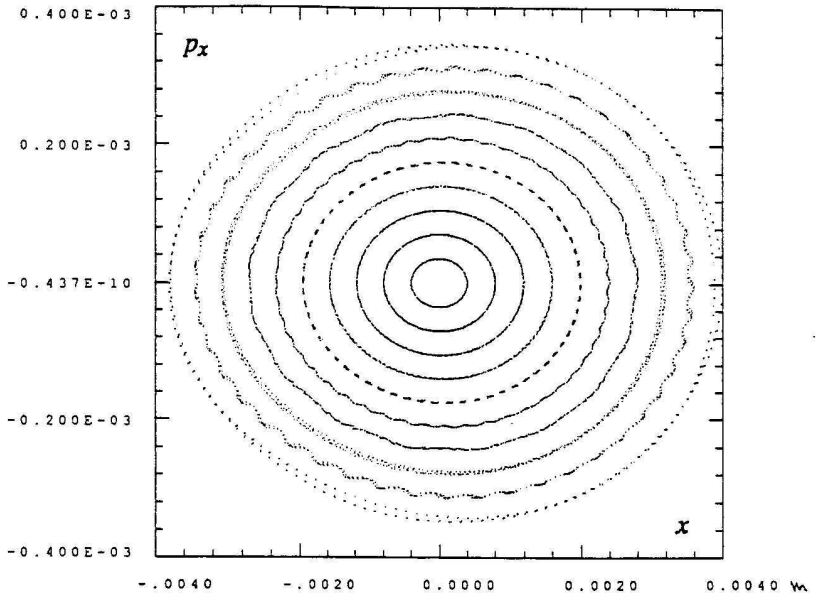

FIGURE 17.15. This figure shows, for the ALS, tracking results in the (x, p_x) plane for 1000 iterations of a ninth-order truncated Taylor map using ten different initial conditions spaced equally along a line in the (x, y) plane. The y degree of freedom is similarly excited, but not shown.

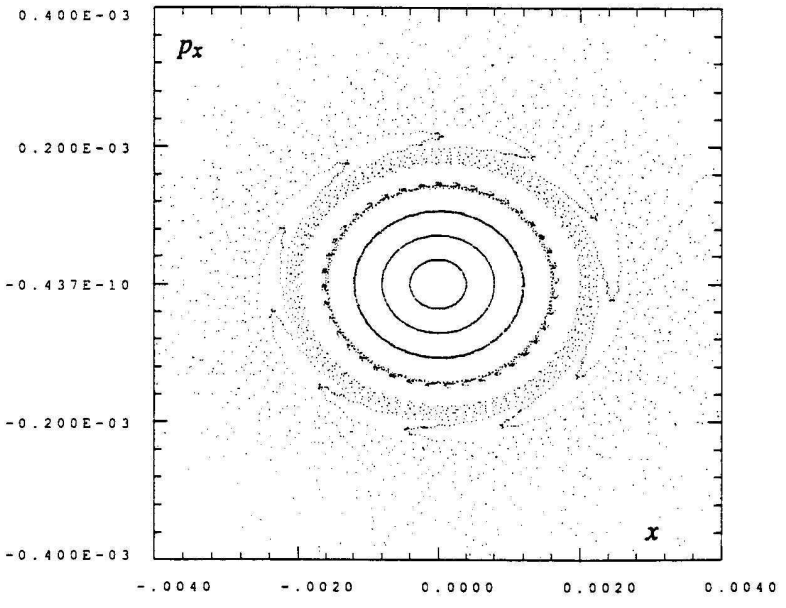

FIGURE 17.16. This figure shows, for the ALS, tracking results in the (x, p_x) plane for 1000 iterations of a fourth-order truncated Taylor map $\mathcal{T}_5$ using the same initial conditions employed in Figure 17.15.

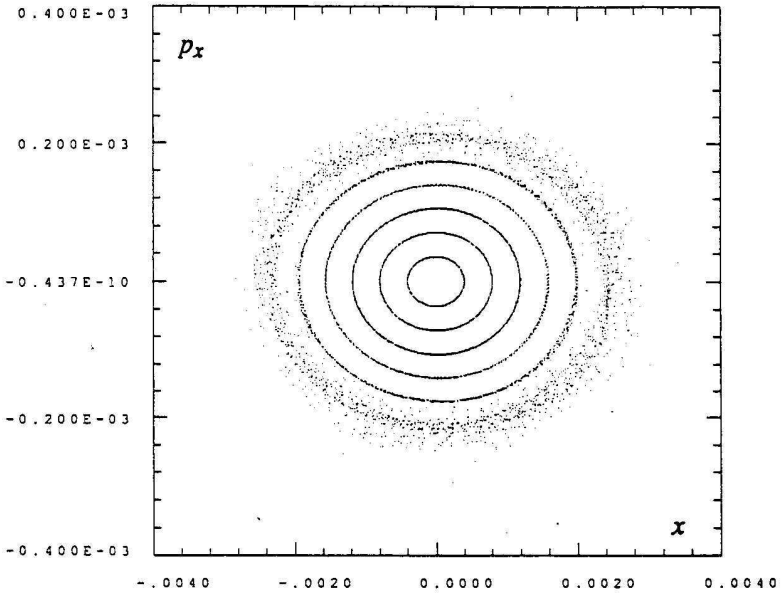

FIGURE 17.17. This figure shows, for the ALS, tracking results in the (x, p_x) plane for 1000 iterations of a Cremona symplectification $\mathcal{C}_5^{rand}$ of the fourth-order truncated Taylor map $\mathcal{T}_5$ using the same initial conditions employed in Figure 17.15. In this case the $\mathcal{L}_j$ were chosen randomly.

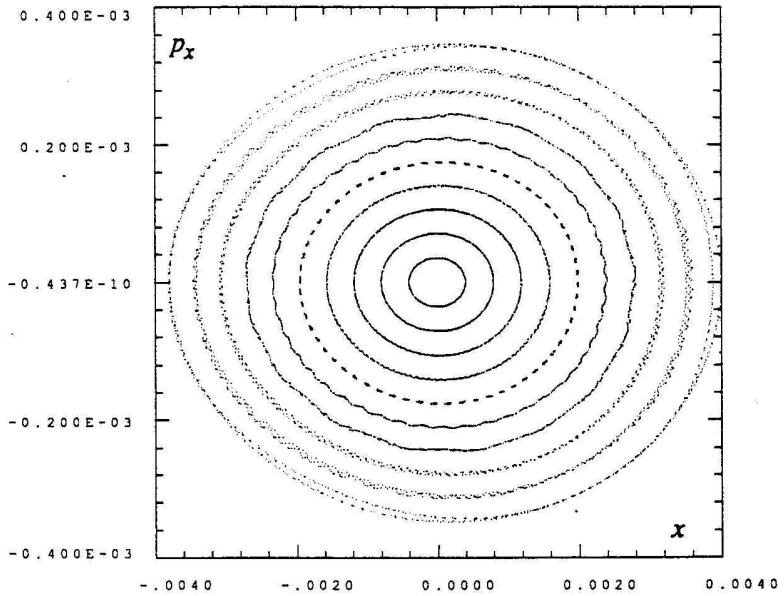

FIGURE 17.18. This figure shows, for the ALS, tracking results in the (x, p_x) plane for 1000 iterations of a Cremona symplectification $\mathcal{C}_5^{cub}$ of the fourth-order truncated Taylor map $\mathcal{T}_5$ using the same initial conditions employed in Figure 17.15. In this case the $\mathcal{L}_j$ were based on the fifth-order, twelve-point cubature formula for the two-sphere.

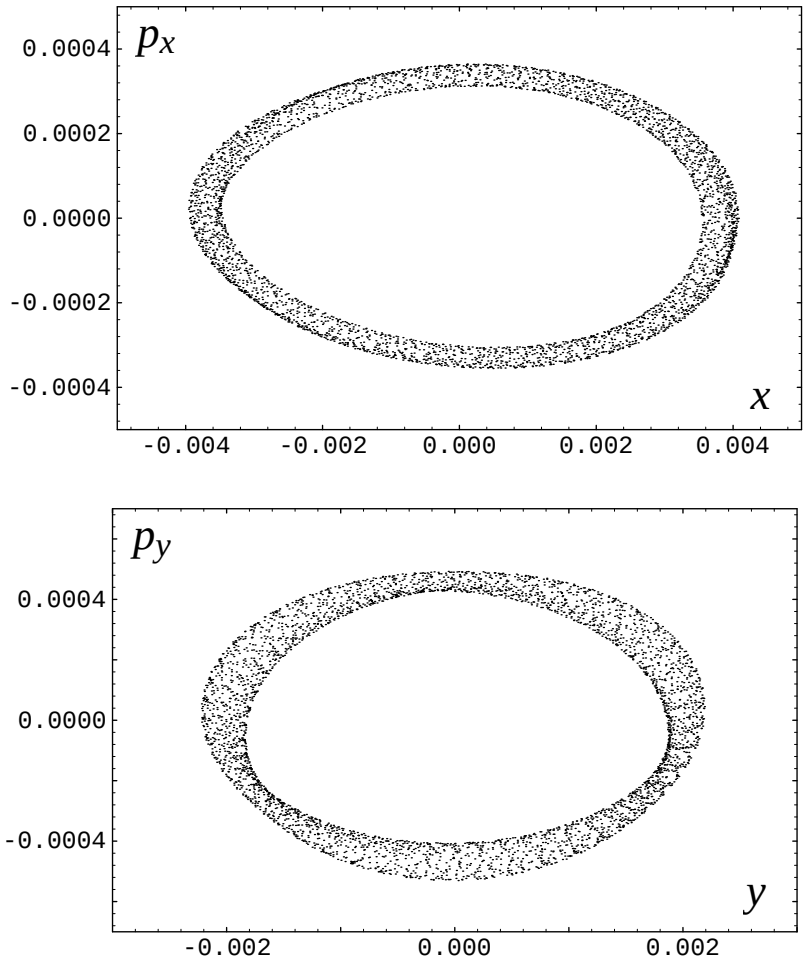

FIGURE 17.19. This figure shows, for the ALS, tracking results in the (x, p_x) and (y, p_y) planes for 4000 iterations by a ninth-order truncated Taylor map $\mathcal{T}_{10}$ using a single initial condition. (For this and the following two figures, the ALS lattice used contains extensive skew coupling not present in the lattice used for the earlier figures.)

see that same idea again in two degrees of freedom: randomly chosen $\mathcal{L}_j$ do not work well (see footnote 50), and the techniques developed in this thesis for finding optimal[51] Cremona symplectifications can indeed make a substantial difference.

Figures 17.19–17.21 show tracking results in the (x, p_x) and (y, p_y) planes (upper and lower graphics, respectively) using an ALS lattice with extensive skew-coupling (not present in the lattice used for the previous figures). Those three figures show the result of 4000 iterations applied to the single initial condition $(x, p_x, y, p_y) = (0.004, 0, 0.002, 0)$ using respectively a ninth-order one-turn truncated Taylor map $\mathcal{T}_{10}$, a sixth-order one-turn truncated Taylor map $\mathcal{T}_7$, and a Cremona symplectification $\mathcal{C}_7$ of the truncated one-turn Taylor map $\mathcal{T}_7$. The Cremona symplectification used here was based on the seventh-order, twenty-four-point cubature formula for the two-sphere (see Table 16.1). As in Figure 17.15, we may assume the results from the ninth-order truncated Taylor map, shown in Figure 17.19, to be exact—for the limited number of iterations shown.

[51] Here we mean optimal in the sense described in §12.1

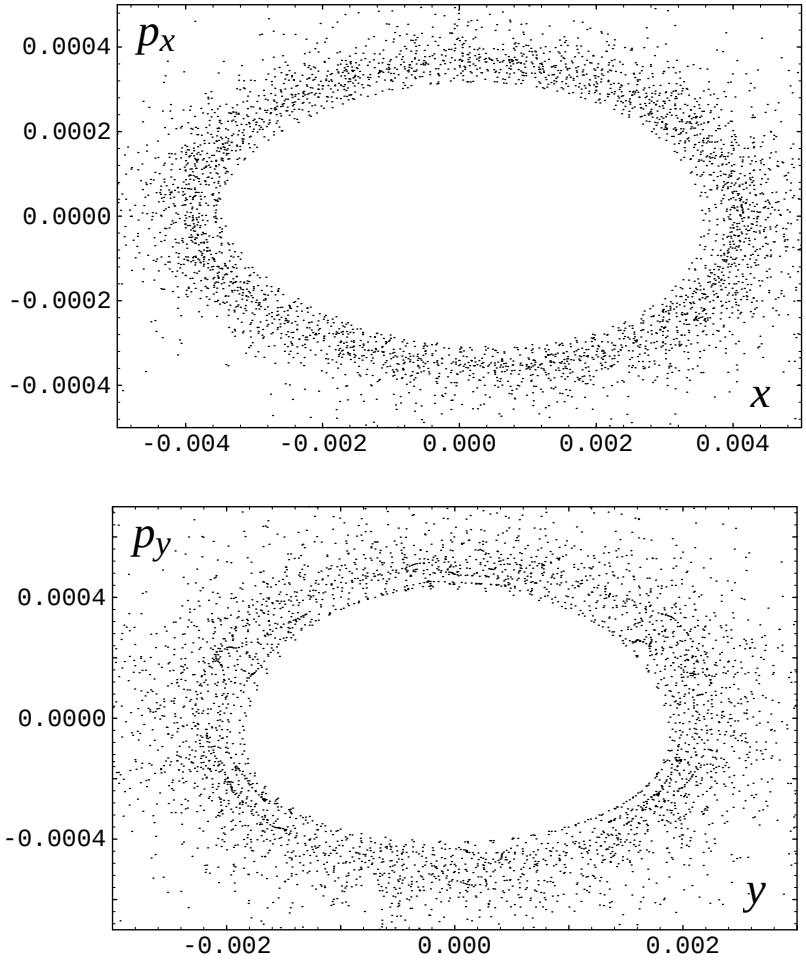

FIGURE 17.20. This figure shows, for the ALS, tracking results in the (x, p_x) and (y, p_y) planes for 4000 iterations by a sixth-order truncated Taylor map $\mathcal{T}_7$ using the same single initial condition employed in Figure 17.19.

Because of the additional skew-coupling present in the ALS lattice used for Figures 17.19–17.21, one cannot easily identify an orbit along which a particle travels. But it is immediately obvious that the sixth-order truncated Taylor map will not do the job. On the other hand, the Cremona symplectification $\mathcal{C}_7$ produces a result that agrees remarkably well with the ninth-order truncated Taylor map (*i.e.*, the "exact" map). Indeed, if we look just at the envelopes of the regions occupied by the orbits in the phase space planes of (x, p_x) and (y, p_y), we find that they appear indistinguishable from one another. At the risk of of being repetitive, we say again that the improvements we see in the results come from just two sources: imposing the symplectic condition, and performing that symplectification in an optimal fashion. We also remark that if we track more turns (*i.e.*, make more iterations) with $\mathcal{T}_{10}$, it also will exhibit the non-symplectic disease already apparent for $\mathcal{T}_7$ at 4000 turns. By contrast, the Cremona symplectification $\mathcal{C}_7$ can be iterated for an arbitrarily large number of turns.

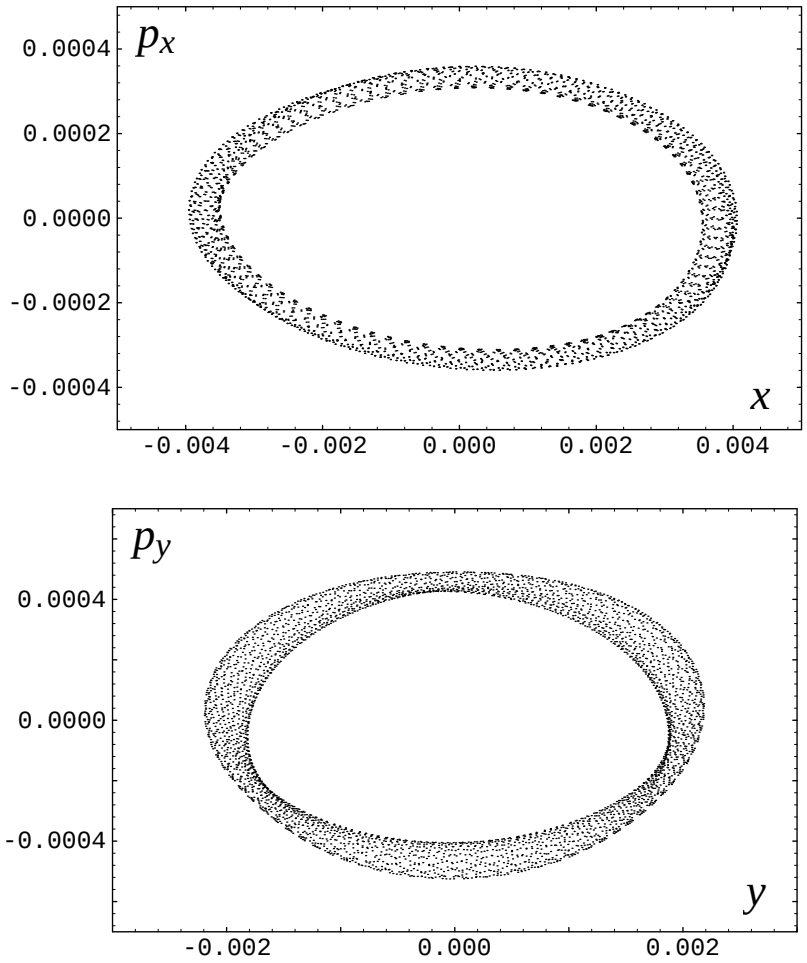

FIGURE 17.21. This figure shows, for the ALS, tracking results in the (x, p_x) and (y, p_y) planes for 4000 iterations using a single initial condition (that of Figure 17.19) by a Cremona symplectification $\mathcal{C}_7$ of the sixth-order truncated Taylor map $\mathcal{T}_7$. Here the Cremona symplectification uses the jolt decomposition based on the seventh-order, twenty-four-point cubature formula for the two-sphere.

18. Summary II

The set of all Hamiltonian systems provides useful models for a broad range of natural phenomena and, as such, constitutes a distinctive class of dynamical systems. An important focus in this thesis concerns the symplectic condition, a characteristic property of all Hamiltonian systems. Numerical experiments demonstrate—and the figures in §17 confirm—that whenever we use a transfer map to model a Hamiltonian system for long periods of time, it behooves us to use a map that respects the symplectic condition. For the complicated dynamical systems of research interest, we usually know only a truncated Taylor map that approximates the true transfer map. Therefore, at the principal focus in Part II of this thesis lies the question of how best to symplectify a given truncated Taylor map that approximates the behavior of a Hamiltonian system.

In essence, Cremona symplectification—the method developed here—adds to each of the series that appear in a truncated Taylor map a *finite* number of terms in such a way that the resultant map (which will still be a polynomial map) satisfies the symplectic condition. In practice the method uses the procedure described in §11 to obtain *jolt decompositions* of homogeneous polynomials, together with the procedures in Appendices B and C to convert a given truncated Taylor map (for a Hamiltonian system) into a corresponding Cremona map written as a product of N jolts. Here, each jolt is a polynomial symplectic map of the form

$$e^{:\mathcal{L}_j g^j:},$$

where $j \in \{1, \ldots, N\}$, the $\mathcal{L}_j$, are a set of linear symplectic transformations, and the corresponding g^j are polynomials in the q's alone. (See §10.)

In broad outline, the Cremona symplectification just described is the same as that first given by Irwin [51]. There are, however, some significant differences in the details: First, we choose our linear symplectic transformations from a larger space than did Irwin; this makes what we call *jolts* rather more general than the maps used by Irwin. Second, we have introduced in (10.9) a very useful scalar product $\langle\,,\rangle$ which is invariant under the $U(n)$ subgroup of $Sp(2n,\mathbb{R})$. Third, we have used that scalar product to define *sensitivity vectors*, *Gram matrices*, and *Gram operators*—all useful concepts, not just for computing the coefficients of the monomials that appear in the jolt polynomials g^j, but, most important, for characterizing the quality of the jolt decompositions one can obtain. This last holds the key that opens the door to *optimal* Cremona symplectification. Note here that the adjective "optimal" is essential: symplectifying a map is not enough—one must do so in an optimal fashion.

In §12.1 we developed a criterion for identifying optimal jolt decompositions, and hence optimal Cremona symplectifications: choose a set of N linear symplectic transformations $\mathcal{L}_j$ so as to make the smallest Gram eigenvalue as large as possible. In §13 we examined which were the relevant $\mathcal{L}_j$ for our purposes. We showed that one need not examine the whole of $Sp(2n,\mathbb{R})$ in looking for good sets of $\mathcal{L}_j$: it suffices to restrict our search to the right coset space $U(n)/O(n)$ contained within $Sp(2n,\mathbb{R})$. Finding optimal Cremona symplectifications then requires some means for determining the maximum possible values for the minimum Gram eigenvalues. Using some very general arguments in §14, we then identified the continuum limit as the place to find those optimal Gram eigenvalues.

In §15 we used a variety of group-theoretical arguments and a great deal of paper to calculate the Gram eigenvalues in the continuum limit. These are given in (15.16) for one degree of freedom; in Tables 15.6 and 15.7 for two degrees of freedom; and in Table 15.9 for three degrees of freedom. We also looked at the possibility of using the group manifold $[U(1)]^n$ contained within $Sp(2n,\mathbb{R})$ as the space from which to choose the $\mathcal{L}_j$. For this manifold Table 15.10 contains the continuum-limit Gram eigenvalues for both two and three degrees of freedom.

Having identified the optimal Gram eigenvalues, we then addressed in §16 the question of how to uncover finite discrete sets of $\mathcal{L}_j$ which yield Gram matrices with eigenvalue spectra

identical to those obtained in the continuum limit. We first showed that in one degree of freedom randomly chosen $\mathcal{L}_j$ are wholly unsatisfactory (see Figures 16.1 and 16.2). Moreover, Figure 16.3 suggests that even if one has a very good idea of where to look in the space of $\mathcal{L}_j$, randomly chosen $\mathcal{L}_j$ in the right neighborhood are still unsatisfactory. In general these two statements hold even more so for two and three degrees of freedom. With these difficulties in mind, we showed how one may use various quadrature and cubature formulas to determine sets of $\mathcal{L}_j$ which yield Gram matrices with eigenvalue spectra identical to those obtained in the continuum limit. In §16.1.7 for one degree of freedom we identified such sets of $\mathcal{L}_j$ for arbitrary order. In §16.2.5 for two degrees of freedom we identified nearly optimal sets of $\mathcal{L}_j$ for various orders as high as 14. And in §16.3.4 for three degrees of freedom we have identified one set of 108 $\mathcal{L}_j$ that yield Gram eigenvalues identical to those in the continuum limit up through at least order six. In addition, we have identified two potentially useful paths that may lead to other good, possibly optimal, sets of $\mathcal{L}_j$.

Using some of the good sets of $\mathcal{L}_j$ identified in §16, we then compared various Cremona symplectifications in one and two degrees of freedom with corresponding exact and truncated Taylor map results. We saw that in general one application of either a truncated Taylor map or its Cremona symplectification to a beam of initial conditions gave comparable results. On the other hand, for long-term tracking, the Cremona symplectifications performed substantially better. Indeed, Cremona symplectifications of low-order truncated Taylor maps often did as well as or better than truncated Taylor maps of significantly higher order.

Perhaps we should not be too surprised that for long-term tracking a Cremona symplectified Taylor map works much better than its underlying truncated Taylor map—after all, the symplectic condition does constitute a significant constraint on Hamiltonian dynamical systems. The more remarkable aspect of these observations is that—at least for the ALS—a Cremona symplectification of a fourth- or sixth-order truncated Taylor map works as well as the ninth-order truncated Taylor map! Now recall that, as remarked upon earlier, using a ninth-order truncated Taylor map to track electrons in the ALS for relatively short periods of time yields results that are essentially identical to those of the exact map [39]. The agreement between this ninth-order truncated Taylor map and the Cremona symplectified maps indicates that we may use either of the above Cremona symplectifications to study the long-term dynamics of the ALS.

Prior to building an expensive new storage ring or particle accelerator, such as the proposed and approved Large Hadron Collider (LHC)[52] at CERN, we would like to have some assurance that it will perform as desired. At present, the long-term stability of particle orbits in such machines is tested by doing long-term tracking studies using element-by-element tracking codes.

In element-by-element tracking, one uses kick maps to step particles through individual elements or parts of individual elements in the ring lattice. A typical lattice requires $10,000$ or more kick map applications *per turn*, and one tries to follow in this fashion the results of as many as 10^7 or 10^8 turns [31]. Such calculations therefore demand extensive amounts of computer time; indeed each truly long-term tracking calculation may require as much as several days on a supercomputer or a fast workstation. Hence the current process of accelerator design is not only expensive, but also tedious and slow.

Now consider the same process using Cremona maps. If a one-turn Cremona map can be used, then we have seen that a relatively few jolt map applications will suffice to compute the effect of each turn. Indeed the number of required jolt maps equals the number of points in the cubature formula associated with the Cremona map—typically 12 to 100—and this contrasts sharply with the $10,000$ or more kick map applications required to achieve the same

[52]The LHC will consist of two proton storage rings, each thirty kilometers in circumference, and will use superconducting magnets cooled to $1.8\,K$.

result with element-by-element tracking. We therefore expect that Cremona maps will run two to three orders of magnitude faster than current methods.

The use of Cremona maps also confers benefits other than improved computational speed. The current choice of using one or a few kick maps to model the effect of individual elements in a lattice is often a crude expedient made to minimize the use of computer time. In principle, however, it is possible to compute a one-turn truncated Taylor map using more accurate models for all elements in the lattice. From this truncated Taylor map one can construct a one-turn Cremona map that models the one-turn effects equally well. And this Cremona map can then be used for long-term tracking studies.

It follows from the above observations that for long-term tracking studies, Cremona maps have the potential to be not only 100 to 1000 times faster than current methods, but also more accurate. We therefore expect that the use of Cremona maps will come to play a large role in future accelerator design and operation.

Appendices

Appendix A. Elliptic Functions

Elliptic functions first arose in the problem of inverting a class of integrals called elliptic integrals—so-called because the integral giving the arc length of an ellipse belongs to this class. These integrals have the generic form

$$\int R(u, w)du,$$

where w^2 represents either a cubic or a quartic polynomial in u—without repeated roots—and $R(u, w)$ represents *any* rational function of u and w. The inversion of such integrals is entirely analogous [67, 74] to the problem of inverting the integral

$$z(s) = \int_0^s \frac{du}{\sqrt{1-u^2}}. \tag{A.1}$$

Any student of calculus recognizes that here $z(s) = \sin^{-1} s$ and that therefore $s = \sin z$ represents the *inverse* of the integral in (A.1). Similar integrals lead to the other circular functions. In the same manner, the inverses of elliptic integrals lead to elliptic functions, which are therefore, in a sense, generalizations of the circular functions. However, as with the circular functions there exists no need to mention integrals when introducing elliptic functions.

In this appendix we review some general properties of elliptic functions and then describe in particular the Jacobian elliptic functions.

A.1. General Properties of Elliptic Functions

Mathematicians apply the adjective *elliptic* to any function $f(z)$ defined on the complex plane which is both *meromorphic* and *doubly-periodic* [2, 55, 88]. The meromorphic property means that at each point in the domain at least one of either the function f or its reciprocal $1/f$ is analytic. In other words, an elliptic function is analytic everywhere in the finite plane except for possible poles. The doubly-periodic property means that there exist complex numbers Ω_1 and Ω_2 whose ratio Ω_1/Ω_2 is not purely real such that

$$f(z + m\Omega_1 + n\Omega_2) = f(z) \tag{A.2}$$

for all integer values of m and n. Any number Ω for which $f(z + \Omega) = f(z)$ is called a *period* of f; and if *any* such period of f can be written in the form $m\Omega_1 + n\Omega_2$, for some choice of integers m and n, then Ω_1 and Ω_2 are called *primitive periods* of f. The restriction to non-real values of the ratio Ω_1/Ω_2 means that an elliptic function is periodic in two different directions in the complex plane.

To illustrate the general nature of elliptic functions, Figure A.1 shows a three-dimensional graph over part of the complex plane of the absolute value of the particular Weierstrass function $\wp(z)$ which has primitive periods $\Omega_1 = 6$ and $\Omega_2 = i4$.[53] Notice the presence of both a doubly-periodic structure and singularities. Observe also that evaluating this specific $\wp(z)$ at any point in the complex plane is equivalent to evaluating it at the corresponding point in the rectangle defined by the four vertices $\{0, 6, 6 + i4, i4\}$. In general, a pair of primitive periods for an elliptic function need not lie on the real and imaginary axes, respectively—indeed, the choice of primitive periods is not even unique. In a typical case the four vertices $\{0, \Omega_1, \Omega_1 + \Omega_2, \Omega_2\}$ define a parallelogram called a *fundamental period parallelogram* (FPP). In addition, any simple translation of this parallelogram is called a period parallelogram (PP), with the adjective "fundamental" reserved for those PPs having one vertex at the origin. Such PPs tile the plane, and, as with the example shown in Figure A.1, evaluating an elliptic function f at any point in the complex plane is equivalent to evaluating it at the corresponding point in any PP. Such corresponding points in two different PPs (see

[53] Given any two complex numbers Ω_1 and Ω_2 such that $\Omega_1/\Omega_2 \notin \mathbb{R}$, one can always construct a Weierstrass elliptic function $\wp(z)$ which has Ω_1 and Ω_2 as primitive periods.

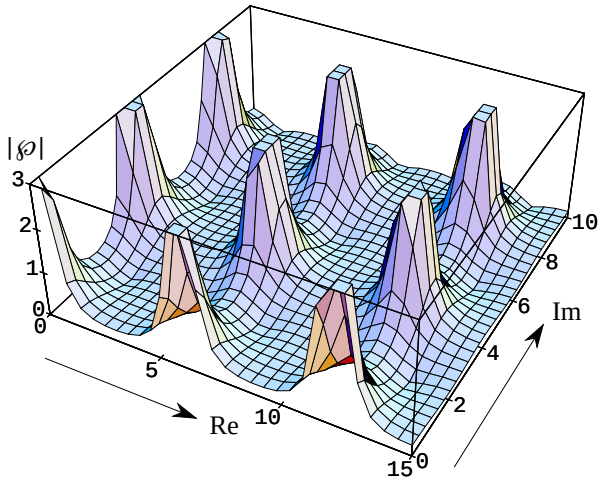

FIGURE A.1. The absolute value of a Weierstrass function $\wp(z)$ having primitives periods $\Omega_1 = 6$ and $\Omega_2 = i4$.

Figure A.2) are called *congruent*. Using more precise language, we call two points z and z' congruent if there exist integers m and n such that

$$z' = z + m\Omega_1 + n\Omega_2,$$

a relationship which is sometimes expressed by writing

$$z' \equiv z \pmod{(\Omega_1, \Omega_2)}.$$

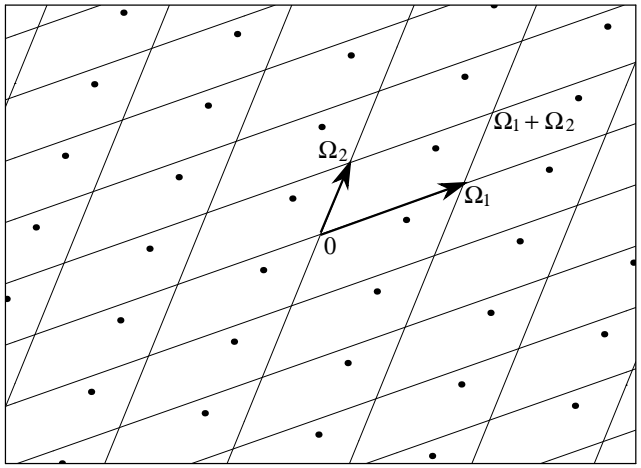

FIGURE A.2. A lattice of points (•) congruent with respect to the periods Ω_1 and Ω_2.

The following set of four theorems, known collectively as Liouville's theorems, state some of the remarkable properties of elliptic functions. They rest upon some well-known theorems in complex variable theory and derive simply from the fact that elliptic functions are meromorphic and doubly-periodic [3, 55, 70, 88].[54]

[54]At this point the reader may wish to recall some of the terminology used in the theory of functions of a complex variable. In particular, suppose a function $f(z)$ has a singularity of some finite order m at the

Theorem A.1. *In a given PP the sum of the residues of an elliptic function at all of its poles equals zero.*

Theorem A.2. *If the elliptic function $f(z)$ has no poles in a PP, then $f(z)$ is a constant. If $f(z)$ is a non-constant elliptic function, then the number of poles in a given PP—taking multiplicity into account—is finite and at least two. This number is called the* order *of f.*

Note that the order of an elliptic function equals the sum of the orders of each of its poles in a PP.

Theorem A.3. *If $f(z)$ is an elliptic function, then for any complex number w the number of roots in a PP of the equation $f(z) = w$—again taking multiplicity into account—equals the order of f. In other words, an elliptic function of order n takes a given complex value n times in any PP.*

Theorem A.4. *Suppose $f(z)$ is an elliptic function of order n having primitive periods Ω_1 and Ω_2. Suppose further that in a given PP the n roots of the equation $f(z) = w$ for arbitrary w are denoted $\{z_1, \ldots, z_n\}$ and the n poles of $f(z)$ are denoted $\{p_1, \ldots, p_n\}$. Then*

$$\sum_i z_i \equiv \sum_i p_i \pmod{(\Omega_1, \Omega_2)}. \tag{A.3}$$

According to Theorem A.2, the simplest (*i.e.*, lowest-order) non-constant elliptic functions are those of order two. These functions comprise two classes: those having one double pole—with zero residue—in each PP, and those having two simple poles—with residues that cancel—in each PP [3, 88]. The Weierstrass elliptic function $\wp$ belongs to the first class and is the subject of most theoretical investigations on elliptic functions. The Jacobian elliptic functions, of which there are twelve, belong to the second class and are of primary interest to us. We shall describe them in the following section.

A simple connection exists between elliptic functions and the more well-known circular and hyperbolic functions. If one of the periods of an elliptic function approaches infinity, then the function becomes periodic in just one direction (*i.e.*, simply-periodic), and such a function must be composed of circular or hyperbolic functions. Note that the circular functions have a single finite period along the real axis and an infinite period along the imaginary axis, while the reverse is true for the hyperbolic functions. Because of this limiting behavior, one may view elliptic functions as interpolating between, or connecting, the circular and hyperbolic functions.

Before going on to describe in more detail the Jacobian elliptic functions, we state three more of the many basic and elegant theorems about elliptic functions. The first, Theorem A.5, follows immediately from the corresponding theorem for simply periodic functions. And the closely related Theorems A.6 and A.7 follow from Theorems A.2 and A.5 [55, 70].

Theorem A.5. *Given any two elliptic functions $f(z)$ and $g(z)$ with identical primitive periods Ω_1 and Ω_2, the following functions also are elliptic functions with (not necessarily primitive) periods Ω_1 and Ω_2:*

$$f(z + C), \quad f(z) \pm g(z), \quad f(z)g(z), \quad f(z)/g(z), \quad f'(z),$$

---

location $z = a$ but is otherwise analytic in some domain that contains a. Then we may write f as a *Laurent series* in the form

$$f(z) = \frac{b_m}{(z-a)^m} + \cdots + \frac{b_1}{(z-a)} + a_0 + a_1(z-a) + \ldots.$$

The series

$$\sum_{k=1}^{m} b_k (z-a)^{-k}$$

containing just the negative powers of $z - a$ is called the *principal part* of f at a; and, similarly, the series containing just the zero and positive powers of $z - a$ is called the *regular part*. In addition, the coefficient b_1 is called the *residue* of f at a.

where C denotes a fixed constant, and the prime denotes differentiation with respect to the argument z.

Theorem A.6. *Any two elliptic functions which have the same primitive periods and the same poles with identical corresponding principal parts must differ by at most an additive constant.*

Theorem A.7. *Consider any two elliptic functions which have the same primitive periods, the same poles, and the same zeroes. If corresponding poles in the two functions have the same order and, similarly, corresponding zeroes have the same order, then the two elliptic functions must differ by at most a multiplicative constant.*

A.2. **The Jacobian Elliptic Functions**

A.2.1. *Notation and Defining Properties.* As mentioned in the previous section, the Jacobian elliptic functions have two simple poles with equal but opposite residues in each PP [2]. For these functions a single number m, called the parameter, determines the primitive periods Ω_1 and Ω_2; hence the periods cannot be independent. Indeed, they are both related to the *complete elliptic integral of the first kind* $K = K(m)$ defined by

$$K(m) = \int_0^1 \frac{dt}{\sqrt{(1-t^2)(1-m\,t^2)}} = \int_0^{\pi/2} \frac{d\theta}{\sqrt{(1-m\sin^2\theta)}} \tag{A.4}$$

and its close cousin $K' = K'(m) = K(1-m)$. Figure A.3 shows a graph of these two functions K and K' on the interval $m = [0, 1]$; in general, however, m may take any value in the complex plane $\mathbb{C}$.

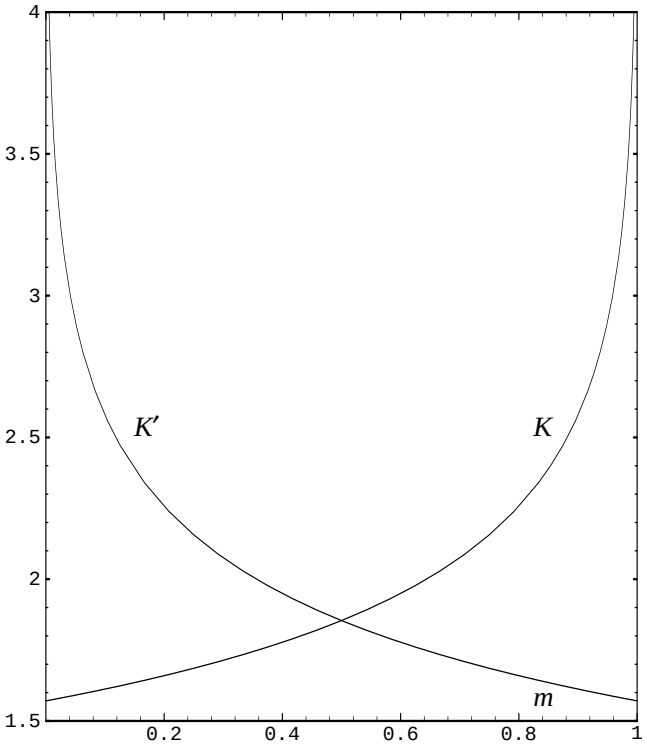

FIGURE A.3. The complete elliptic integrals K and K' as functions of the parameter m.

Over the years, various notations have been used for the Jacobian elliptic functions. The modern notation, invented by Glaisher [44], serves as a clever mnemonic device not only for

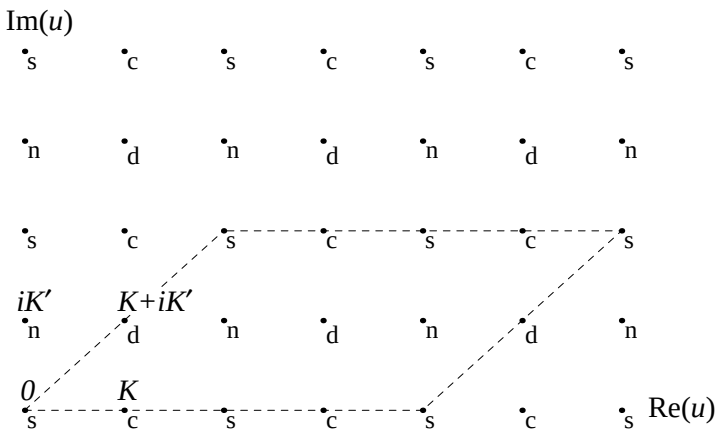

FIGURE A.4. A lattice of points for defining the Jacobian elliptic functions. The dashed outline shows a PP for the function $\mathrm{sd}\,u$.

defining and remembering the Jacobian elliptic functions, but also for computing with them. Starting with a fixed value of the parameter m, and therefore fixed values of the complete elliptic integrals $K = K(m)$ and $K' = K'(m)$, Glaisher's notation identifies the letters 's', 'c', 'd', and 'n' with respectively the points 0, K, $K + iK'$, and iK' in the complex plane. This set of points (see Figure A.4) defines a parallelogram (or a rectangle if $m \in (0, 1)$) in the complex plane. Translating this parallelogram by *even* multiples of K and iK' generates a regular lattice of points which then acts as a reference frame for defining the Jacobian elliptic functions. Each function is denoted by a pair of (distinct) letters chosen from the set $\mathcal{J} = \{\mathrm{s}, \mathrm{c}, \mathrm{d}, \mathrm{n}\}$, where the first and second letters chosen represent respectively the locations of simple zeroes and simple poles in the complex plane. (The twelve possible choices of distinct two-letter combinations chosen from $\mathcal{J}$ lead to the twelve Jacobian elliptic functions.) Furthermore, the step between two nearby points labeled by the function name is a half-period, while the step between all other pairs of nearby points is a quarter-period. The function sd, for example, has simple zeroes at all points labeled 's', simple poles at all points labeled 'd', and a PP given by the dashed outline shown in Figure A.4. Table A.1 lists primitive periods for each of the twelve Jacobian elliptic functions.

TABLE A.1. Primitive periods of the twelve Jacobian elliptic functions.

function				periods	
sn	cd	dc	ns	$4K$	$2iK'$
cn	sd	nc	ds	$4K$	$2(K + iK')$
dn	nd	sc	cs	$2K$	$4iK'$

Now notice something wonderful: According to the definition given so far, each Jacobian elliptic function has a definite order and prescribed primitive periods, poles, and zeroes. Therefore, according to Theorem A.7, these functions are fully defined to within a multiplicative constant! This constant is fixed by assigning the coefficient unity to the leading term in the expansion of the function about the origin in ascending powers of the argument [2]. Thus, for example, $\mathrm{sn}\,u$ has a zero at the origin, so its leading term is u; $\mathrm{ds}\,u$ has a pole at the origin, so its leading term is $1/u$; and $\mathrm{cn}\,u$ has neither a pole nor a zero at the origin, so its leading term is simply 1. About the origin the functions sn, cn, and dn have the following

Taylor series expansions [2]:

$$\operatorname{sn}(u|m) = u - (1+m)u^3/3! + (1+14m+m^2)u^5/5! - \cdots , \tag{A.5a}$$

$$\operatorname{cn}(u|m) = 1 - u^2/2! + (1+4m)u^4/4! - \cdots , \tag{A.5b}$$

$$\operatorname{dn}(u|m) = 1 - m\,u^2/2! + m(4+m)u^4/4! - \cdots . \tag{A.5c}$$

One further aspect of Glaisher's notation deserves mention. Note that because the functions sn and cn share the same poles *of the same order*, their poles can be neither poles nor zeroes of the ratio sn/cn. Therefore, the zeroes of the ratio must coincide with the zeroes of sn, and the poles of the ratio must coincide with the zeroes of cn. Hence it seems plausible that $\operatorname{sn} u/\operatorname{cn} u = \operatorname{sc} u$. Though a proof requires more work, this relation is indeed true; furthermore, it can be generalized. Any three functions having the same second letter—*e.g.* sn, cn, and dn—share the same set of poles and are therefore called a *co-polar trio*. Using any of the four co-polar trios, one can generate the remaining nine Jacobian elliptic functions by using the following simple rule: if 'p', 'q', and 'r' represent letters chosen from the set $\mathcal{J}$, then

$$\operatorname{pq} u \equiv \frac{\operatorname{pr} u}{\operatorname{qr} u}, \tag{A.6}$$

provided we define $\operatorname{rr} u = 1$. For example, $\operatorname{sd} u = \operatorname{sn} u/\operatorname{dn} u$, and $\operatorname{ns} u = \operatorname{nn} u/\operatorname{sn} u = 1/\operatorname{sn} u$. In a similar fashion one may define the remaining nine Jacobian elliptic functions by starting with any three functions that share the same set of zeroes—*e.g.* sc, sd, and sn.

Since the Jacobian elliptic functions really depend on two numbers, an argument and a parameter, we ought to exhibit both when writing down a function value. However, the usual practice in the literature displays only the argument, with the parameter implied and assumed constant. When necessary, the argument and parameter are listed—in that order—and separated by a vertical stroke: thus $\operatorname{sn}(u|m)$ represents $\operatorname{sn} u$ evaluated with parameter m.

Another common notation for the Jacobian elliptic functions uses not the parameter but its square-root, often denoted k and called the *modulus*. The distinction is usually made by replacing the vertical stroke with a comma, thus $\operatorname{sn}(u,k)$. One sometimes sees the modulus and argument reversed and separated by a semi-colon, thus $\operatorname{sn}(k;u)$. We shall stick with the parameter, $m = k^2$, and write $\operatorname{sn}(u|m)$ or, when no confusion can arise, simply $\operatorname{sn}(u)$ or $\operatorname{sn} u$.

A.2.2. *Degenerate Cases.* When the parameter m takes the values zero or one, the Jacobian elliptic functions degenerate into simply-periodic (sometimes constant) functions [2, 70]. To see this, note from Figure A.3 that when $m \in (0,1)$ both K and K' are real, and hence all of the Jacobian elliptic functions have periods (not necessarily primitive) that align parallel to the real and imaginary axes (as in Figure A.4). Then note that $\lim_{m\to 0} K(m) = \pi/2$ and $\lim_{m\to 0} K'(m) = \infty$, and hence as $m \to 0$ all the periods parallel to the real axis shrink to some finite value, while all the periods parallel to the imaginary axis grow to infinity: the functions become simply-periodic along the real axis. In a similar fashion as $m \to 1$ the functions become simply-periodic along the imaginary axis. The description just given suggests that as $m \to 0$ the Jacobian elliptic functions become circular functions, and as $m \to 1$ they become hyperbolic functions. This is indeed the case, and thus do the Jacobian elliptic functions form a connection between the circular and hyperbolic functions.

When the parameter m lies in the interval $(0,1)$, all the Jacobian elliptic functions take real values (except for possible poles) along the real axis. Figure A.5 shows a graph along the real axis (with $m = 0.6$) for each member of the co-polar trio sn, cn, dn. There one sees a resemblance between the elliptic functions sn and cn and the functions sin and cos. Indeed, as $m \to 0$ the functions sn and cn approach respectively the circular functions sin and cos. And as $m \to 1$ the functions sn and cn approach respectively the hyperbolic functions tanh and sech. Table A.2 lists the degenerate cases for all twelve of the Jacobian elliptic functions.

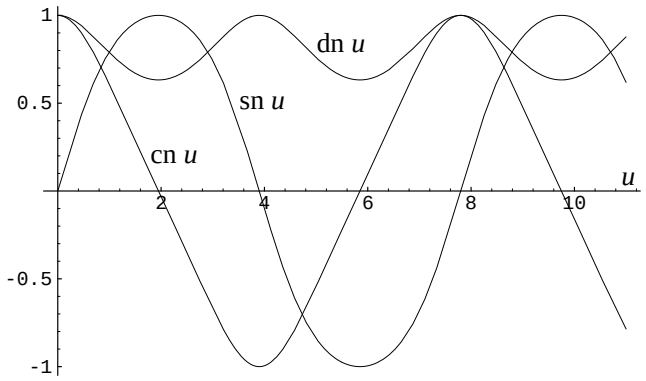

FIGURE A.5. The co-polar trio sn, cn, dn, with parameter $m = 0.6$.

TABLE A.2. Degenerate cases of the twelve Jacobian elliptic functions.

function	$m = 0$	$m = 1$
$\mathrm{sn}(u\|m)$	$\sin u$	$\tanh u$
$\mathrm{cn}(u\|m)$	$\cos u$	$\operatorname{sech} u$
$\mathrm{dn}(u\|m)$	1	$\operatorname{sech} u$
$\mathrm{sd}(u\|m)$	$\sin u$	$\sinh u$
$\mathrm{cd}(u\|m)$	$\cos u$	1
$\mathrm{nd}(u\|m)$	1	$\cosh u$
$\mathrm{sc}(u\|m)$	$\tan u$	$\sinh u$
$\mathrm{nc}(u\|m)$	$\sec u$	$\cosh u$
$\mathrm{dc}(u\|m)$	$\sec u$	1
$\mathrm{cs}(u\|m)$	$\cot u$	$\operatorname{csch} u$
$\mathrm{ns}(u\|m)$	$\csc u$	$\coth u$
$\mathrm{ds}(u\|m)$	$\csc u$	$\operatorname{csch} u$

A.2.3. *Symmetries, Addition Theorems, and Pythagorean Identities.* The Jacobian elliptic functions satisfy a number of properties familiar to the student of circular and hyperbolic functions. We list a few of the important ones for the fundamental co-polar trio sn, cn, dn [2, 69, 70]. First, each Jacobian elliptic function has the same symmetry as its circular or hyperbolic sibling. Put another way, those Jacobian elliptic functions with an 's' in their names are odd with respect to their argument, while all the rest are even. Second, every elliptic function (Jacobian or otherwise) obeys an algebraic addition theorem [3]. The following three apply to our co-polar trio:

$$\mathrm{sn}(u+v|m) = \frac{\mathrm{sn}\,u\cdot\mathrm{cn}\,v\cdot\mathrm{dn}\,v + \mathrm{sn}\,v\cdot\mathrm{cn}\,u\cdot\mathrm{dn}\,u}{1 - m\,\mathrm{sn}^2\,u\cdot\mathrm{sn}^2\,v}, \tag{A.7a}$$

$$\mathrm{cn}(u+v|m) = \frac{\mathrm{cn}\,u\cdot\mathrm{cn}\,v - \mathrm{sn}\,u\cdot\mathrm{dn}\,u\cdot\mathrm{sn}\,v\cdot\mathrm{dn}\,v}{1 - m\,\mathrm{sn}^2\,u\cdot\mathrm{sn}^2\,v}, \tag{A.7b}$$

$$\mathrm{dn}(u+v|m) = \frac{\mathrm{dn}\,u\cdot\mathrm{dn}\,v - m\,\mathrm{sn}\,u\cdot\mathrm{cn}\,u\cdot\mathrm{sn}\,v\cdot\mathrm{cn}\,v}{1 - m\,\mathrm{sn}^2\,u\cdot\mathrm{sn}^2\,v}. \tag{A.7c}$$

And last, there exist a number of Pythagorean identities relating the different Jacobian elliptic functions. These include

$$\mathrm{sn}^2\,u + \mathrm{cn}^2\,u = 1, \tag{A.8a}$$

$$\mathrm{dn}^2\,u + m\,\mathrm{sn}^2\,u = 1. \tag{A.8b}$$

In both (A.7) and (A.8) all of the Jacobian elliptic functions use the same value of the parameter m.

A.2.4. *Differentiation Formulas.* We list in this section several kinds of differentiation formulas for the Jacobian elliptic functions: derivatives with respect to the argument, derivatives with respect to the parameter, and algebraic relations between a given function and its derivative (*i.e.*, a differential equation).

To find the derivative of a Jacobian elliptic function with respect to its argument, one might take as given the appropriate addition theorem in (A.7) and then use it together with the known leading-order behavior of the Jacobian elliptic functions. A more fundamental analysis proceeds by examining the structure of the derivative [70]. For example, the (simple) poles of the function $\operatorname{sn} u$ become double poles of its derivative $\operatorname{sn}' u$. In addition, Theorem A.4 severely constrains—indeed fixes—the locations of the zeroes of $\operatorname{sn}' u$. And the known leading-order behavior of $\operatorname{sn} u$ determines the leading-order behavior of $\operatorname{sn}' u$. Theorem A.7 together with the result of this very sketchy argument leads to the conclusion that $\operatorname{sn}' u = \operatorname{cn} u \cdot \operatorname{dn} u$. The above indicated line of reasoning should convey some of the real power of Liouville's theorems. We list here the derivatives with respect the argument for the fundamental co-polar trio:

$$\operatorname{sn}' u = \operatorname{cn} u \cdot \operatorname{dn} u, \tag{A.9a}$$

$$\operatorname{cn}' u = -\operatorname{sn} u \cdot \operatorname{dn} u, \tag{A.9b}$$

$$\operatorname{dn}' u = -m \operatorname{sn} u \cdot \operatorname{cn} u. \tag{A.9c}$$

Equations (A.6) and (A.8) together with a straightforward application of the chain rule lead to similarly simple formulas for the remaining nine Jacobian elliptic functions.

One can also differentiate the Jacobian elliptic functions with respect to the parameter [69]. We list here the results for the fundamental co-polar trio:

$$\frac{\partial}{\partial m} \operatorname{sn}(u|m) = -\frac{1}{2} \operatorname{cn} u \cdot \operatorname{dn} u \int_0^u \operatorname{sd}^2 v \, dv, \tag{A.10a}$$

$$\frac{\partial}{\partial m} \operatorname{cn}(u|m) = \frac{1}{2} \operatorname{sn} u \cdot \operatorname{dn} u \int_0^u \operatorname{sd}^2 v \, dv, \tag{A.10b}$$

$$\frac{\partial}{\partial m} \operatorname{dn}(u|m) = -\frac{1}{2} \operatorname{sn} u \cdot \operatorname{cn} u \int_0^u \operatorname{nc}^2 v \, dv. \tag{A.10c}$$

(The integrals here are well-defined—*i.e.*, path-independent—because, as can be shown, the principal part of the square of a Jacobian elliptic function at any singular point has zero residue [69, p. 181].) When we speak of the derivative of an elliptic function, we shall usually mean the derivative with respect to its argument. When we mean the derivative with respect to the parameter, we so indicate explicitly.

It turns out that any elliptic function f and its derivative f' satisfy an algebraic equation. In other words, there exists some polynomial F in two variables for which $F(f, f') = 0$. Using the derivatives in (A.9) and the Pythagorean identities in (A.8), one can write down the algebraic relations between the Jacobian elliptic functions and their derivatives. The following three apply to our co-polar trio:

$$(\operatorname{sn}' u)^2 = (1 - \operatorname{sn}^2 u)(1 - m \operatorname{sn}^2 u), \tag{A.11a}$$

$$(\operatorname{cn}' u)^2 = (1 - \operatorname{cn}^2 u)(m_1 + m \operatorname{cn}^2 u), \tag{A.11b}$$

$$(\operatorname{dn}' u)^2 = (1 - \operatorname{dn}^2 u)(\operatorname{dn}^2 u - m_1). \tag{A.11c}$$

Here the parameter m and its *complement* m_1 satisfy the relation

$$m + m_1 = 1. \tag{A.12}$$

A.2.5. *Representations in Terms of Integrals.* As we mentioned in the introduction to this appendix, one may also represent the Jacobian elliptic functions as the inverses of certain elliptic integrals. A simple approach first defines the function sn in this manner and then uses the Pythagorean identities in (A.8) together with the rule (A.6) to define the remaining functions.

According to (A.11a), the function sn satisfies the first-order differential equation

$$(x')^2 = \left(\frac{dx}{du}\right)^2 = (1 - x^2)(1 - m\,x^2).$$

Since $\operatorname{sn}(0) = 0$, we may write

$$\int_0^x \frac{dt}{\sqrt{(1 - t^2)(1 - m\,t^2)}} = u, \tag{A.13a}$$

with $x = \operatorname{sn}(u|m)$. This representation of the elliptic function $\operatorname{sn} u$—as the inverse of the above integral—often serves as its definition [2, 67], but to treat the matter properly requires a discussion of Riemann surfaces [74, 84].

By making the substitution $t = \sin\theta$ in (A.13a), one can obtain another important representation for the function sn:

$$\int_0^\phi \frac{d\theta}{\sqrt{(1 - m\sin^2\theta)}} = u, \tag{A.13b}$$

with $\sin\phi = \operatorname{sn}(u|m)$. Very naturally, based on the Pythagorean identities, we then identify $\operatorname{cn}(u|m)$ with $\cos\phi$, and $\operatorname{dn}(u|m)$ with $\sqrt{1 - m\sin^2\phi}$.

The alert reader will have already noticed the connection between the two integrals in (A.13) that define the elliptic function $\operatorname{sn} u$ and the complete elliptic integral in (A.4). The integral in (A.13b), denoted $F(\phi|m)$, is called the *incomplete* elliptic integral of the first kind; and (for obvious reasons) this name is given also to the integral in (A.13a). To summarize, we may express the relationships in (A.13) in the forms

$$u = \int_0^\phi \frac{d\theta}{\sqrt{(1 - m\sin^2\theta)}} = F(\phi|m) \Longleftrightarrow \sin\phi = \operatorname{sn}(u|m), \tag{A.14a}$$

or

$$u = \int_0^x \frac{dt}{\sqrt{(1 - t^2)(1 - m\,t^2)}} = F(\sin^{-1}x|m) \Longleftrightarrow x = \operatorname{sn}(u|m). \tag{A.14b}$$

Using either of the representations in (A.14), one can see the connection between the Jacobian elliptic functions and their degenerate cases listed in Table A.2: Setting $m = 0$ transforms the integral in (A.14b) to the form in (A.1), thus confirming that $\operatorname{sn}(u|0) = \sin u$. (Setting $m = 0$ in (A.14a) produces the same result in a trivial fashion.) Likewise, setting $m = 1$ in either (A.14a) or (A.14b), with a bit more algebra, shows that $\operatorname{sn}(u|1) = \tanh u$. Using (A.5), (A.6), and (A.8), one can then confirm the remainder of Table A.2.

For more information on elliptic functions and elliptic integrals, the interested reader will find an extensive literature. In addition to the references already cited, we mention two more: The handbook by Byrd and Friedman [14] contains a large table of integrals solved in terms of elliptic functions. And the book by Spanier and Oldham [83], like Abramowitz and Stegun, lists many properties of the Jacobian elliptic functions (but their notation differs from that used here).

Appendix B. Converting between the Taylor Series and Factored-Product Representations

Suppose we know through terms of degree $P-1$ the Taylor series representation $\mathcal{T}_P$ for some mapping that describes a discrete step along the flow of a Hamiltonian dynamical system. Using a straightforward procedure, we can convert this map $\mathcal{T}_P$ to a new map $\mathcal{M}_P$ in the factored-product form (9.17) in such a way that the series expansion of $\mathcal{M}_P z$ agrees with $\mathcal{T}_P z$ through terms of degree $P-1$ (*i.e.*, so that $\mathcal{M}_P \simeq \mathcal{T}_P$, in the notation introduced in §10.3). This procedure comes directly from the proof of the factorization theorem, Theorem 9.1, and has been described in some detail elsewhere [30, 33, 49]. For the sake of completeness, however, we include here (without proof) a brief description of the procedure for those maps that have the origin as a fixed point. The restriction to this (only somewhat special) class of maps means simply that the factored-product representation (9.17) contains no factors of the form $e^{:f_1:}$.

In the Taylor series representation (3.1), a truncated Taylor map $\mathcal{T}_P$ which has the origin as a fixed point (*i.e.*, which carries the origin onto itself) must have the form

$$z_a^{(1)} = \sum_b R_{ab}\, z_b + \sum_{bc} T_{abc}\, z_b z_c + \sum_{bcd} U_{abcd}\, z_b z_c z_d + \cdots . \tag{B.1}$$

where the terms included go up through degree $P-1$. Assuming this map arises from the flow of some Hamiltonian system, we can find the corresponding map $\mathcal{M}_P$ in the factored-product form

$$\mathcal{M}_P = \mathcal{R} e^{:f_3:} e^{:f_4:} \cdots e^{:f_P:}, \tag{B.2}$$

by the following sequence of steps:

(1) The first factor $\mathcal{R}$ is the linear Lie transformation whose matrix representation has as elements the coefficients R_{ab} that appear in the linear terms of (B.1).

(2) Define $z^{(2)}$ by applying $\mathcal{R}^{-1}$ to the right-hand side of (B.1). The result will have the form

$$\begin{aligned} z_a^{(2)} &= z_a + \sum_{bc} \sum_{b'c'} T_{abc}\, (R^{-1})_{bb'} z_{b'}\, (R^{-1})_{cc'} z_{c'} + \cdots \\ &= z_a + g_a(2; z) + O(>2). \end{aligned}$$

Here, and later, we use $g_a(l; z)$ to denote a homogeneous polynomial of degree l in the variables z; and we use the notation $O(>l)$ to represent terms of degree higher than l.

(3) Given the Taylor map

$$z_a^{(l)} = z_a + g_a(l; z) + O(>l),$$

extract the homogeneous Lie polynomial f_{l+1} of degree $l+1$ by the rule

$$f_{l+1} = \frac{-1}{l+1} \sum_{ab} g_a(l; z) J_{ab} z_b,$$

where the J_{ab} denote elements of the fundamental symplectic matrix J defined in (8.2).

(4) Given the Lie polynomial f_{l+1} defined in Step 3, determine $z_a^{(l+1)}$ by the rule

$$z_a^{(l+1)} = e^{-:f_{l+1}:} z_a^{(l)} = \cdots = z_a + g_a(l+1; z) + O(>l+1).$$

The ellipsis here denotes some algebra that must be done in order to obtain the polynomials $g_a(l+1; z)$.

(5) Repeat Steps 3 and 4 until f_P has been determined.

Doing the conversion the other way—*i.e.*, determining the Taylor map $\mathcal{T}_P$ in (B.1) from a given factored-product map $\mathcal{M}_P$ of the form (B.2)—requires a straightforward application of the exponential series (9.3) with the definition (9.1) of the Lie operator $:f:$. First expand

$$e^{:f_P:} z$$

through terms of degree $P-1$. Then apply and expand in succession the operators $e^{:f_{P-1}:}$, $\ldots$, $e^{:f_3:}$. At the end, apply the linear Lie transformation $\mathcal{R}$ to obtain the final result $\mathcal{T}_P$. We must warn the casual reader, however, that other operations, such as tracking with the map in (B.2), pose considerable subtleties concerning the order in which to apply the different Lie transformations. See [30, Ch. 6] for a thorough discussion.

Appendix C. Converting between the Factored-Product and Jolt Representations

This appendix describes the procedures mentioned in §10.3 for converting the non-linear part of a symplectic map back and forth between the factored-product representation

$$\mathcal{N}_P = e^{:f_3:} \cdots e^{:f_P:} \tag{9.20}$$

and the jolt representation

$$\mathcal{J}_P = \mathcal{L}_1 e^{:g^1:} \mathcal{L}_1^{-1} \cdots \mathcal{L}_N e^{:g^N:} \mathcal{L}_N^{-1}. \tag{10.13}$$

These procedures have been described elsewhere in some detail [31, 51]; we therefore give here simply a description and refer the reader to the cited references for more complete discussions and proofs.

Converting a Cremona map $\mathcal{J}_P$ in the jolt representation (10.13) to an equivalent map $\mathcal{N}_P$ in the factored-product representation (9.20)[55] can be done in at least two different ways. One method makes use of (10.5) and the Baker-Campbell-Hausdorff theorem[56] [20, 28, 30] to combine, separate, and rearrange the factors in $\mathcal{J}_P$ in order to obtain the equivalent map $\mathcal{N}_P$. A second method (which is less efficient but easier to program to high order) uses first (9.1) and (9.3) to expand $\mathcal{J}_P z$ into a Taylor map, and then the method given in Appendix B to convert the result to the desired form $\mathcal{N}_P$.

Given a map $\mathcal{N}_P$ in the factored-product representation (9.20) and an appropriate set of N linear symplectic transformations $\mathcal{L}_j$, we can find the corresponding map $\mathcal{J}_P$ in the jolt representation (10.13) by the following sequence of steps:

(1) Define $h_3 = f_3$, and obtain its jolt decomposition (11.2), using (11.11) to determine the jolt strengths $a_{jk}^{(3)}$.

(2) Define the kicks $g^j(3)$, $j \in \{1, 2, \ldots, N\}$, by (*cf.* (10.14))

$$g^j(3) = \frac{1}{NM(3,n)} \sum_{k=1}^{M(3,n)} a_{jk}^{(3)} Q_k^{(3)}.$$

Then the non-linear Cremona map $\mathcal{J}_3$ given by

$$\mathcal{J}_3 = \prod_{j=1}^{N} \mathcal{L}_j e^{:g^j(3):} {\mathcal{L}_j}^{-1}$$

agrees with $\mathcal{N}_P$ at least for the factor $e^{:f_3:}$.

(3) In general, we shall obtain a Cremona map

$$\mathcal{J}_L = \prod_{j=1}^{N} \mathcal{L}_j e^{:g^j(L):} {\mathcal{L}_j}^{-1}$$

which agrees with $\mathcal{N}_P$ for all factors up through $e^{:f_L:}$. Convert this map $\mathcal{J}_L$ to factored-product form to obtain

$$\mathcal{J}_L = e^{:f_3:} e^{:f_4:} \cdots e^{:f_L:} e^{:\tilde{f}_{L+1}:}.$$

In other words, carry out the conversion far enough to determine the Lie polynomial $\tilde{f}_{L+1}$, which will generally differ from the Lie polynomial f_{L+1} that appears in the initial map $\mathcal{N}_P$.

(4) Define the homogeneous dynamical polynomial

$$h_{L+1} = f_{L+1} - \tilde{f}_{L+1},$$

and obtain its jolt decomposition to determine the jolt strengths $a_{jk}^{(l+1)}$.

[55] Here we mean equivalent in the sense that $\mathcal{J}_P \simeq \mathcal{N}_P$, *cf.* §10.3.

[56] The names regularly appear in other orders: *e.g.* Campbell-Baker-Hausdorff.

(5) Define the kicks $g^j(L+1)$ by (*cf.* (10.14))

$$g^j(L+1) = \frac{1}{N} \sum_{l=3}^{L+1} \frac{1}{M(l,n)} \sum_{k=1}^{M(l,n)} a_{jk}^{(l)} Q_k^{(l)},$$

(6) Repeat Steps 3–6 until the kicks $g^j = g^j(P)$ have been determined.

If the $\mathcal{L}_j$ come from a cubature formula with unequal weights w_j, then replace all occurrences of $\frac{1}{N}$ by w_j—not only in the formulas above, but also in the formula for the Gram matrix elements $\Gamma(l)_{rs}$, which are needed for computing the jolt strengths $a_{jk}^{(l)}$. (See the introduction to §16.1 and the first paragraph of §16.2.5 or §16.3.4.)

Appendix D. Action of $e^{:f_2:}$ for One Degree-of-Freedom Systems

Consider the most general f_2 for a dynamical system having one degree of freedom:

$$f_2 = -\frac{1}{2}(\gamma q^2 + 2\alpha qp + \beta p^2), \tag{D.1}$$

where α, β, and γ denote arbitrary coefficients. Evaluating the action of $e^{:f_2:}$ on any point in phase space is a straightforward exercise. First note that

$$:f_2: q = -\frac{1}{2}[2\alpha qp + \beta p^2, q] = \alpha q + \beta p,$$

and

$$:f_2: p = -\frac{1}{2}[\gamma q^2 + 2\alpha qp, p] = -\gamma q - \alpha p,$$

from which follows

$$:f_2:^2 q = :f_2:(\alpha q + \beta p) = \alpha(\alpha q + \beta p) + \beta(-\gamma q - \alpha p) = -(\beta\gamma - \alpha^2)q,$$

and

$$:f_2:^2 p = :f_2:(-\gamma q - \alpha p) = -\gamma(\alpha q + \beta p) - \alpha(-\gamma q - \alpha p) = -(\beta\gamma - \alpha^2)p.$$

Let us define the quantity

$$\omega^2 = \beta\gamma - \alpha^2. \tag{D.2}$$

Then we obtain

$$:f_2:^{2k} \begin{pmatrix} q \\ p \end{pmatrix} = (-1)^k \omega^{2k} \begin{pmatrix} q \\ p \end{pmatrix},$$

and

$$:f_2:^{2k+1} \begin{pmatrix} q \\ p \end{pmatrix} = (-1)^k \omega^{2k} \begin{pmatrix} \alpha q + \beta p \\ -\gamma q - \alpha p \end{pmatrix}.$$

Using these last two results, we may sum the exponential series:

$$\begin{aligned} e^{:f_2:} \begin{pmatrix} q \\ p \end{pmatrix} &= \sum_{k=0}^{\infty} \frac{1}{(2k)!} :f_2:^{2k} \begin{pmatrix} q \\ p \end{pmatrix} + \sum_{k=0}^{\infty} \frac{1}{(2k+1)!} :f_2:^{2k+1} \begin{pmatrix} q \\ p \end{pmatrix} \\ &= \sum_{k=0}^{\infty} (-1)^k \frac{\omega^{2k}}{(2k)!} \begin{pmatrix} q \\ p \end{pmatrix} + \sum_{k=0}^{\infty} (-1)^k \frac{\omega^{2k+1}}{(2k+1)!} \frac{1}{\omega} \begin{pmatrix} \alpha q + \beta p \\ -\gamma q - \alpha p \end{pmatrix} \\ &= \cos\omega \begin{pmatrix} q \\ p \end{pmatrix} + \frac{\sin\omega}{\omega} \begin{pmatrix} \alpha & \beta \\ -\gamma & -\alpha \end{pmatrix} \begin{pmatrix} q \\ p \end{pmatrix}. \end{aligned}$$

Therefore, based on our convention (9.12) for representing linear Lie transformations as matrices, we obtain the following matrix representation for the action of $e^{:f_2:}$:

$$e^{:f_2:} \begin{pmatrix} q \\ p \end{pmatrix} = \begin{pmatrix} \cos\omega + \alpha\frac{\sin\omega}{\omega} & \beta\frac{\sin\omega}{\omega} \\ -\gamma\frac{\sin\omega}{\omega} & \cos\omega - \alpha\frac{\sin\omega}{\omega} \end{pmatrix} \begin{pmatrix} q \\ p \end{pmatrix}. \tag{D.3}$$

Note that ω appears only as the argument of even functions: $\cos\omega$ and $\frac{\sin\omega}{\omega}$. As a consequence, the ambiguity in the sign of ω as given by (D.2) has no effect.

Appendix E. Properties of the Matrix $d(W)$

In §13.1 we considered symplectic matrices W having the special property that their corresponding linear symplectic transformations $\mathcal{L}(W)$ mapped the q_k, and hence also the $Q_k^{(l)}$, only among themselves. Thus we wrote (here dropping the subscript j on the W)

$$\mathcal{L}(W)Q_k^{(l)} = \sum_{k'} d(W)_{k'k} Q_{k'}^{(l)}. \tag{13.6}$$

This equation defines a real $M(l,n) \times M(l,n)$ matrix $d(W)$, and in this section we derive several of its properties.

We first prove a lemma about $\mathcal{L}(W)$ and then prove that $d(W)$ is invertible.

Lemma E.1. *If the linear symplectic transformation $\mathcal{L}(W)$ maps the q_k only among themselves, then so also does $\mathcal{L}(W)^{-1}$.*

Proof. As in §9 we use coördinates $(z_1, \ldots, z_n, z_{n+1}, \ldots, z_{2n}) = (q_1, \ldots, q_n, p_1, \ldots, p_n)$ to label points in phase space. With this ordering of coördinates, our convention (9.12) for representing Lie transformations as matrices implies that the linear symplectic matrix W must have the $n \times n$ block form

$$W = \begin{pmatrix} A & 0 \\ C & D \end{pmatrix}, \tag{E.1}$$

where the upper-right-hand block is an $n \times n$ zero matrix. Because W is symplectic, and hence non-singular, it follows that the diagonal blocks, both A and D, are also non-singular. (If, for example, D were not invertible, then it would necessarily have linearly dependent columns. But then W also would have linearly dependent columns, and hence W would not be invertible.) One may then easily verify that the inverse of W is

$$W^{-1} = \begin{pmatrix} A^{-1} & 0 \\ -D^{-1}CA^{-1} & D^{-1} \end{pmatrix},$$

which has the same form as (E.1). It therefore follows from this result and (9.16) that $\mathcal{L}(W)^{-1} = \mathcal{L}(W^{-1})$ maps the q_k only among themselves. ∎

Theorem E.1. *The matrix $d(W)$ defined by* (13.6) *has the inverse $d(W^{-1})$.*

Proof. Since $\mathcal{L}(W)$ maps the q_k only among themselves, it follows from Lemma E.1 that $\mathcal{L}(W^{-1})$ also maps the q_k, and hence also the $Q_k^{(l)}$, only among themselves. Expanding $\mathcal{L}(W^{-1})Q_k^{(l)}$ as in (13.6), we write

$$\mathcal{L}(W^{-1})Q_{k'}^{(l)} = \sum_{k''} d(W^{-1})_{k''k'} Q_{k''}^{(l)}. \tag{E.2}$$

Putting together (9.16), (13.6), and (E.2), we find that

$$\begin{aligned} Q_k^{(l)} &= \mathcal{L}(W)^{-1}\mathcal{L}(W)Q_k^{(l)} = \mathcal{L}(W^{-1})\mathcal{L}(W)Q_k^{(l)} = \mathcal{L}(W^{-1})\sum_{k'} d(W)_{k'k} Q_{k'}^{(l)} \\ &= \sum_{k'k''} d(W)_{k'k} d(W^{-1})_{k''k'} Q_{k''}^{(l)} = \sum_{k''} \left(\sum_{k'} d(W^{-1})_{k''k'} d(W)_{k'k} \right) Q_{k''}^{(l)} \\ &= \sum_{k''} \big(d(W^{-1})d(W) \big)_{k''k} Q_{k''}^{(l)}. \end{aligned}$$

As the $Q_k^{(l)}$ form an orthonormal basis for the subspace of functions of the q's alone, it follows from this result that

$$\big(d(W^{-1})d(W) \big)_{k''k} = \sum_{k'} d(W^{-1})_{k''k'} d(W)_{k'k} = \delta_{k''k}.$$

In other words,

$$[d(W)]^{-1} = d(W^{-1}). \tag{E.3}$$

■

Note that we may use (13.6) together with the inner product (10.9) to write the matrix elements of $d(W)$ as

$$d(W)_{k'k} = \left\langle Q^{(l)}_{k'}, \mathcal{L}(W) Q^{(l)}_k \right\rangle. \tag{E.4}$$

Let us now examine what happens when we consider transformations taken from the $U(n)$ subgroup of $Sp(2n, \mathbb{R})$. We prove another lemma and then two more theorems.

Lemma E.2. *Let $\mathcal{L}(M(u))$ denote the linear symplectic transformation corresponding to the matrix $M(u)$ defined in* (13.11)*. Then*

$$\mathcal{L}(M(u))^\dagger = \mathcal{L}(M(u))^{-1} = \mathcal{L}(M(u^\dagger)). \tag{E.5}$$

Proof. According to §13.2, $M(u)$ belongs to the $U(n)$ subgroup of $Sp(2n, \mathbb{R})$, and hence, by (10.11) and (9.16),

$$\mathcal{L}(M(u))^\dagger = \mathcal{L}(M(u))^{-1} = \mathcal{L}(M(u)^{-1}).$$

But from (13.12) and the fact that $u \in U(n)$ we obtain

$$M(u)^{-1} = M(u^{-1}) = M(u^\dagger).$$

The result (E.5) then follows. ■

Note that if we abbreviate $\mathcal{L}(M(u))$ by $\mathcal{L}(u)$, as in §13.3, (E.5) becomes

$$\mathcal{L}(u)^\dagger = \mathcal{L}(u)^{-1} = \mathcal{L}(u^\dagger) = \mathcal{L}(u^{-1}). \tag{E.6}$$

We shall use this notation in proving the following two theorems.

Theorem E.2. *Consider a matrix $M(u)$ defined by* (13.11)*, and suppose that $u = r$ denotes a real orthogonal matrix. Let us agree in this case to denote $d(M(r))$ by $d(r)$. Then*

$$d(r_1)d(r_2) = d(r_2 r_1). \tag{E.7}$$

Proof. Note that because the matrix $M(r)$ has the form given in (13.22), the transformation $\mathcal{L}(r)$ does indeed map the q_k only among themselves. It therefore makes sense to write $d(M(r))$ in the first place. Now consider the matrix element in row k'', column k'. Using (E.4) and (E.6), we find that

$$\begin{aligned}
\big(d(r_1)d(r_2)\big)_{k''k'} &= \sum_k d(r_1)_{k''k} d(r_2)_{kk'} = \sum_k \left\langle Q^{(l)}_{k''}, \mathcal{L}(r_1) Q^{(l)}_k \right\rangle \left\langle Q^{(l)}_k, \mathcal{L}(r_2) Q^{(l)}_{k'} \right\rangle \\
&= \sum_k \left\langle \mathcal{L}(r_1)^\dagger Q^{(l)}_{k''}, Q^{(l)}_k \right\rangle \left\langle Q^{(l)}_k, \mathcal{L}(r_2) Q^{(l)}_{k'} \right\rangle \\
&= \sum_k \left\langle \mathcal{L}(r_1^{-1}) Q^{(l)}_{k''}, Q^{(l)}_k \right\rangle \left\langle Q^{(l)}_k, \mathcal{L}(r_2) Q^{(l)}_{k'} \right\rangle \\
&= \left\langle \mathcal{L}(r_1^{-1}) Q^{(l)}_{k''} \right| \left(\sum_k \left| Q^{(l)}_k \right\rangle \left\langle Q^{(l)}_k \right| \right) \left| \mathcal{L}(r_2) Q^{(l)}_{k'} \right\rangle.
\end{aligned}$$

Since both $\mathcal{L}(r_1^{-1}) Q^{(l)}_{k''}$ and $\mathcal{L}(r_2) Q^{(l)}_{k'}$ are linear combinations of the $Q^{(l)}_k$ (*cf.* Lemma E.1), it follows that *for this purpose* the quantity

$$\sum_k \left| Q^{(l)}_k \right\rangle \left\langle Q^{(l)}_k \right|$$

is equivalent to the identity operator. Using (E.6), (9.15), and (E.4), we conclude that

$$\begin{aligned}\big(d(r_1)d(r_2)\big)_{k''k'} &= \big\langle \mathcal{L}(r_1^{-1})Q^{(l)}_{k''}, \mathcal{L}(r_2)Q^{(l)}_{k'}\big\rangle = \big\langle Q^{(l)}_{k''}, \mathcal{L}(r_1)\mathcal{L}(r_2)Q^{(l)}_{k'}\big\rangle \\ &= \big\langle Q^{(l)}_{k''}, \mathcal{L}(r_2r_1)Q^{(l)}_{k'}\big\rangle = d(r_2r_1)_{k''k'}.\end{aligned}$$

The result (E.7) then follows. ■

Theorem E.3. *In the notation of the previous theorem*

$$d(\tilde{r}) = d(r^{-1}) = \widetilde{d(r)}. \tag{E.8}$$

Proof. As r denotes an orthogonal matrix, $\tilde{r} = r^{-1}$. Using (E.4) and (E.6), we find that

$$d(\tilde{r})_{k'k} = d(r^{-1})_{k'k} = \big\langle Q^{(l)}_{k'}, \mathcal{L}(r^{-1})Q^{(l)}_{k}\big\rangle = \big\langle \mathcal{L}(r)Q^{(l)}_{k'}, Q^{(l)}_{k}\big\rangle .$$

Since $d(r)$ is a real matrix, we may go on to write

$$\big\langle \mathcal{L}(r)Q^{(l)}_{k'}, Q^{(l)}_{k}\big\rangle = \big\langle Q^{(l)}_{k}, \mathcal{L}(r)Q^{(l)}_{k'}\big\rangle = d(r)_{kk'} = \big(\widetilde{d(r)}\big)_{k'k}.$$

The result (E.8) then follows. ■

Appendix F. The Modified Iwasawa Factorization

Suppose M denotes a real symplectic matrix written in the $n \times n$ block form of (13.10): $M = \left(\begin{smallmatrix} A & B \\ C & D \end{smallmatrix}\right)$. Then consider the modified matrix $\bar{M} = JMJ^{-1}$, where J denotes the matrix of (8.2). As J is symplectic, so then is $\bar{M}$. It can be shown that for any symplectic matrix $\bar{M} \in Sp(2n, \mathbb{R})$ one may write a *partial Iwasawa factorization* [30]:

$$\begin{aligned} \bar{M} &= \begin{pmatrix} Y^{1/2} & 0 \\ 0 & Y^{-1/2} \end{pmatrix} \begin{pmatrix} I & Y^{-1/2}XY^{-1/2} \\ 0 & I \end{pmatrix} M(u) \\ &= \begin{pmatrix} Y^{1/2} & XY^{-1/2} \\ 0 & Y^{-1/2} \end{pmatrix} M(u). \end{aligned} \tag{F.1}$$

Here $M(u)$ denotes a matrix of the form (13.11), and X and Y denote respectively the real and imaginary parts of the complex matrix

$$Z = X + iY = -(C - iD)(A - iB)^{-1}.$$

We note (without proof) that the matrices X, Y, and Z are symmetric; the matrix Y is positive definite; and, hence, both $Y^{1/2}$ and $Y^{-1/2}$ are well-defined.

Let us now recover the matrix M from $\bar{M}$:

$$M = J^{-1}\bar{M}J = J^{-1} \begin{pmatrix} Y^{1/2} & XY^{-1/2} \\ 0 & Y^{-1/2} \end{pmatrix} JJ^{-1}M(u)J. \tag{F.2}$$

As one may easily verify, $J^{-1} = \tilde{J}$. Hence the first three factors of (F.2) become

$$\begin{aligned} &\begin{pmatrix} 0 & -I \\ I & 0 \end{pmatrix} \begin{pmatrix} Y^{1/2} & XY^{-1/2} \\ 0 & Y^{-1/2} \end{pmatrix} \begin{pmatrix} 0 & I \\ -I & 0 \end{pmatrix} \\ &\qquad = \begin{pmatrix} 0 & -I \\ I & 0 \end{pmatrix} \begin{pmatrix} -XY^{-1/2} & Y^{1/2} \\ -Y^{-1/2} & 0 \end{pmatrix} = \begin{pmatrix} Y^{-1/2} & 0 \\ -XY^{-1/2} & Y^{1/2} \end{pmatrix}. \end{aligned}$$

And the last three factors become

$$\begin{aligned} &\begin{pmatrix} 0 & -I \\ I & 0 \end{pmatrix} \begin{pmatrix} \operatorname{Re}(u) & \operatorname{Im}(u) \\ -\operatorname{Im}(u) & \operatorname{Re}(u) \end{pmatrix} \begin{pmatrix} 0 & I \\ -I & 0 \end{pmatrix} \\ &\qquad = \begin{pmatrix} 0 & -I \\ I & 0 \end{pmatrix} \begin{pmatrix} -\operatorname{Im}(u) & \operatorname{Re}(u) \\ -\operatorname{Re}(u) & -\operatorname{Im}(u) \end{pmatrix} = \begin{pmatrix} \operatorname{Re}(u) & \operatorname{Im}(u) \\ -\operatorname{Im}(u) & \operatorname{Re}(u) \end{pmatrix} = M(u). \end{aligned}$$

We may therefore express any matrix $M \in Sp(2n, \mathbb{R})$ in the form

$$M = \begin{pmatrix} F & 0 \\ G & F^{-1} \end{pmatrix} M(u), \tag{F.3}$$

with u unitary, $G = -XY^{-1/2}$, and $F = Y^{-1/2}$ a real, symmetric, positive definite matrix. We have already noted in §13.2 that $M(u)$ represents a symplectic matrix. Because the matrix M is symplectic—by assumption—the group property of $Sp(2n, \mathbb{R})$ implies that the first factor in (F.3) must also be symplectic. It then follows that (F.3) represents a factorization of the real symplectic matrix M into a product of two symplectic matrices. We call this form (F.3) a *modified Iwasawa factorization* of M.

Appendix G. The Coset Space $U(3)/SO(3)$

Theorem G.1. *Every unitary matrix $u \in U(3)$ has a representation of the form*

$$u = re^{iS}, \tag{G.1}$$

where $r \in SO(3,\mathbb{R})$, and S is real symmetric.

Proof. Given any matrix $u \in U(3)$, define the new matrix

$$w = \tilde{u}u,$$

and note that w is both symmetric and unitary. Then, as Gantmacher shows [43, Vol. II,p. 5], there exists a real symmetric (but not necessarily unique) matrix S' such that

$$w = e^{i2S'}.$$

To see the lack of uniqueness, consider the real symmetric matrix

$$S = S' + k\pi I,$$

where I denotes the 3×3 identity matrix, and $k \in \{0, 1\}$. Observe that S works as well as S':

$$e^{i2S} = e^{i2S' + i2k\pi I} = e^{i2S'} e^{i2k\pi I} = e^{i2S'} e^{i2k\pi} = e^{i2S'} = w.$$

Now examine the determinants of w and u. Note first that

$$\det w = \det(\tilde{u}u) = (\det u)^2,$$

and hence

$$\det u = \pm e^{i \operatorname{Tr} S'}.$$

But since

$$\operatorname{Tr} S = \operatorname{Tr} S' + 3k\pi,$$

it follows that one may choose $k \in \{0, 1\}$ so as to ensure that

$$e^{i \operatorname{Tr} S} = e^{i \operatorname{Tr} S'} e^{i3k\pi} = \det u.$$

Upon making this choice for k, define the matrix r by the relation (G.1):

$$r = ue^{-iS}.$$

To complete the proof, we need to show only that $r \in SO(3,\mathbb{R})$. Since

$$\tilde{r}r = e^{-i\tilde{S}} \tilde{u} u e^{-iS} = e^{-i\tilde{S}} w e^{-iS} = e^{-iS} e^{i2S} e^{-iS} = I,$$

and

$$\det r = \det(u) \det\bigl(e^{-iS}\bigr) = e^{i \operatorname{Tr} S} e^{-i \operatorname{Tr} S} = 1,$$

we conclude that $r \in SO(3)$. The fact that r is both unitary and orthogonal then shows that indeed $r \in SO(3,\mathbb{R})$. ∎

The alert reader will note that Theorem G.1 generalizes, in a reasonably obvious manner, so as to cover all odd-dimensional unitary matrices.

Appendix H. *Mathematica* Packages

This appendix contains all of the *Mathematica* packages referred to in the main text or used by the *Mathematica* notebooks listed in Appendix I. They are arranged as follows, in alphabetical order:

`AnhOsc.m`
`AnhOscTrack.m`
`AngMomD.m`
`ColonOps.m`
`CRconvert.m`
`ListManipulation.m`
`PBgrad.m`
`Polynomial.m`
`sp4.m`
`sp6.m`
`sp6tools.m`
`SU2phi.m`
`SU3.m`
`SU3wts.m`
`USp.m`

AnhOsc.m

```
(* AnhOsc.m
   This package contains functions for evaluating the analytic
solution to the anharmonic oscillator in a complex phase space.
Written by D. T. Abell.  Last modified 22 May 1992 *)

BeginPackage["AnhOsc`"]

AnhOsc::usage = "AnhOsc.m is a package of functions for
evaluating the complex anharmonic oscillator as a function of
time.  The Hamiltonian is p^2/2 + q^2/2 - q^4/4, and all
calculations use the Jacobian elliptic functions."

Ham::usage = "Ham[q,p] evaluates the Hamiltonian
p^2/2 + q^2/2 - q^4/4 for the anharmonic oscillator."

qf::usage = "qf[qin,pin,t] evaluates qf(t) for the anharmonic
oscillator, using the initial conditions (qin,pin).
qf[qin,pin,ti,tf,dt] evaluates qf(t) at times from ti to tf with
spacing dt."

pf::usage = "pf[qin,pin,t] evaluates pf(t) for the anharmonic
oscillator, using the initial conditions (qin,pin).
pf[qin,pin,ti,tf,dt] evaluates pf(t) at times from ti to tf with
spacing dt."

qfpf::usage = "qfpf[qin,pin,t] evaluates {qf(t),pf(t)} for the
anharmonic oscillator, using the initial conditions (qin,pin).
qfpf[qin,pin,ti,tf,dt] evaluates {qf(t),pf(t)} at times from ti
to tf with spacing dt."

qfpfLIN::usage = "qfpfLIN[qin,pin,t] evaluates the linear part of
{qf(t),pf(t)} for the anharmonic oscillator, using the initial
conditions (qin,pin).  This results in a simple rotation in
phase space."

qfpfNL::usage = "qfpfNL[qin,pin,t] evaluates the non-linear part
of {qf(t),pf(t)} for the anharmonic oscillator, using the initial
conditions (qin,pin)."

Begin["`Private`"]

EPS = 10.^-15

RT2 = Sqrt[2.]

Ham[q_,p_] = p^2/2 + q^2/2 - q^4/4

qf[qo_,po_,t_] :=
  Module[{nrgy,sgn,tanh,qmxSQ,wm,kovqmxSQ,kSQ,arg,sn,cn,dn},
         nrgy = N[Ham[qo,po]];
```

```
        Which[Abs[nrgy]<=EPS,
                Which[qo==0, 0.,
                      po==0, N[qo Sec[t]],
                      True, N[qo^2/(qo Cos[t] - po Sin[t])]],
              Abs[nrgy-0.25]<=EPS,
                Which[qo==0, N[RT2 po Tanh[t/RT2]],
                      po==0, N[qo],
                      True, sgn = (1-qo^2)/(RT2 po);
                            tanh = Tanh[t/RT2];
                            N[(qo+sgn tanh)/(1+sgn qo tanh)]],
              True,
                qmxSQ = 1-Sqrt[1-4 nrgy];
                wm = Sqrt[2. nrgy/qmxSQ];
                kovqmxSQ = qmxSQ/(4 nrgy);
                kSQ = kovqmxSQ qmxSQ;
                arg = N[wm t];
                sn = JacobiSN[arg,kSQ];
                cn = JacobiCN[arg,kSQ];
                dn = JacobiDN[arg,kSQ];
                N[(qo cn dn+(po/wm) sn)/(1-kovqmxSQ(qo sn)^2)]]]

qf[qo_,po_,ti_,tf_,dt_] :=
  Module[{nrgy,sgn,tanh,qmxSQ,wm,kovqmxSQ,kSQ,arg,sn,cn,dn},
        nrgy = N[Ham[qo,po]];
        Which[Abs[nrgy]<=EPS,
                Which[qo==0, Table[0.,{t,ti,tf,dt}],
                      po==0, N[Table[qo Sec[t],{t,ti,tf,dt}]],
                      True, N[Table[qo^2/(qo Cos[t]-po Sin[t]),
                                    {t,ti,tf,dt}]]],
              Abs[nrgy-0.25]<=EPS,
                Which[qo==0, N[RT2 po Table[Tanh[t/RT2],
                                            {t,ti,tf,dt}]],
                      po==0, N[Table[qo,{t,ti,tf,dt}]],
                      True, sgn = (1-qo^2)/(RT2 po);
                            tanh = Table[Tanh[t/RT2],
                                         {t,ti,tf,dt}];
                            N[(qo+sgn tanh)/(1+sgn qo tanh)]],
              True,
                qmxSQ = 1-Sqrt[1-4 nrgy];
                wm = Sqrt[2. nrgy/qmxSQ];
                kovqmxSQ = qmxSQ/(4 nrgy);
                kSQ = kovqmxSQ qmxSQ;
                arg = N[Table[wm t,{t,ti,tf,dt}]];
                sn = JacobiSN[#,kSQ]& /@ arg;
                cn = JacobiCN[#,kSQ]& /@ arg;
                dn = JacobiDN[#,kSQ]& /@ arg;
                N[(qo cn dn+(po/wm)sn)/(1-kovqmxSQ(qo sn)^2)]]]

pf[qo_,po_,t_] :=
  Module[{nrgy,cos,sin,sgn,tanh,qmxSQ,wm,kovqmxSQ,kSQ,arg,
          sn,cn,dn,snSQ,dneoscSQ,pnum},
        nrgy = N[Ham[qo,po]];
```

```
          Which[Abs[nrgy]<=EPS,
                  Which[qo==0, 0.,
                        po==0, N[qo Sec[t] Tan[t]],
                        True, cos = Cos[t];
                              sin = Sin[t];
                              N[qo^2 (po cos+qo sin)/
                                     (qo cos-po sin)^2]],
                Abs[nrgy-0.25]<=EPS,
                  Which[qo==0, N[po Sech[t/RT2]^2],
                        po==0, 0.,
                        True, sgn = (1-qo^2)/(RT2 po);
                              tanh = Tanh[t/RT2];
                              N[po(1-tanh^2)/(1+sgn qo tanh)^2])],
                True,
                  qmxSQ = 1-Sqrt[1-4 nrgy];
                  wm = Sqrt[2. nrgy/qmxSQ];
                  kovqmxSQ = qmxSQ/(4 nrgy);
                  kSQ = kovqmxSQ qmxSQ;
                  arg = N[wm t];
                  sn = JacobiSN[arg,kSQ];
                  cn = JacobiCN[arg,kSQ];
                  dn = JacobiDN[arg,kSQ];
                  snSQ = sn^2;
                  denoscSQ = kovqmxSQ qo^2 snSQ;
                  pnum = (po cn dn-(1+kSQ)wm qo sn)(1+dneoscSQ);
                  pnum += 2(kSQ snSQ+kovqmxSQ qo^2)wm qo sn;
                  N[pnum/(1-dneoscSQ)^2]]]

pf[qo_,po_,ti_,tf_,dt_] :=
  Module[{nrgy,cos,sin,sgn,tanh,qmxSQ,wm,kovqmxSQ,kSQ,arg,
          sn,cn,dn,snSQ,kqoqmSQ,dneoscSQ,wmqosn,pnum},
         nrgy = N[Ham[qo,po]];
         Which[Abs[nrgy]<=EPS,
                  Which[qo==0, Table[0.,{t,ti,tf,dt}],
                        po==0, N[Table[qo Sec[t] Tan[t],
                                       {t,ti,tf,dt}]],
                        True, cos = Table[Cos[t],{t,ti,tf,dt}];
                              sin = Table[Sin[t],{t,ti,tf,dt}];
                              N[qo^2 (po cos+qo sin)/
                                     (qo cos-po sin)^2]],
                Abs[nrgy-0.25]<=EPS,
                  Which[qo==0, N[po Table[Sech[t/RT2]^2,
                                          {t,ti,tf,dt}]],
                        po==0, Table[0.,{t,ti,tf,dt}],
                        True, sgn = (1-qo^2)/(RT2 po);
                              tanh = Table[Tanh[t/RT2],
                                           {t,ti,tf,dt}];
                              N[po(1-tanh^2)/(1+sgn qo tanh)^2]],
                True,
                  qmxSQ = 1-Sqrt[1-4 nrgy];
                  wm = Sqrt[2. nrgy/qmxSQ];
                  kovqmxSQ = qmxSQ/(4 nrgy);
```

```
                kSQ = kovqmxSQ qmxSQ;
                arg = N[Table[wm t,{t,ti,tf,dt}]];
                sn = JacobiSN[#,kSQ]& /@ arg;
                cn = JacobiCN[#,kSQ]& /@ arg;
                dn = JacobiDN[#,kSQ]& /@ arg;
                snSQ = sn^2;
                kqoqmSQ = kovqmxSQ qo^2;
                denoscSQ = kqoqmSQ snSQ;
                wmqosn = wm qo sn;
                pnum = (po cn dn-(1+kSQ)wmqosn)(1+denoscSQ);
                pnum += 2(kSQ snSQ+kqoqmSQ)wmqosn;
                N[pnum/(1-denoscSQ)^2]]]

qfpf[qo_,po_,t_] :=
  Module[{nrgy,cos,sin,den,tanh,sgn,qmxSQ,wm,kovqmxSQ,kSQ,arg,
          sn,cn,dn,cndn,kqoqmSQ,dneoscSQ,wmqosn,pnum},
         nrgy = N[Ham[qo,po]];
         Which[Abs[nrgy]<=EPS,
                 Which[qo==0, {0.,0.},
                       po==0, N[qo Sec[t] {1,Tan[t]}],
                       True, cos = Cos[t];
                             sin = Sin[t];
                             den = qo cos-po sin;
                          N[qo^2{1/den,(po cos+qo sin)/den^2}]],
               Abs[nrgy-0.25]<=EPS,
                 Which[qo==0, tanh = Tanh[t/RT2];
                              N[po{RT2 tanh,(1-tanh^2)}],
                       po==0, N[{qo,0.}],
                       True, sgn = (1-qo^2)/(RT2 po);
                             tanh = Tanh[t/RT2];
                             den = (1+sgn qo tanh);
                             N[{(qo+sgn tanh)/den,
                                po(1-tanh^2)/den^2}]],
               True,
                 qmxSQ = 1-Sqrt[1-4 nrgy];
                 wm = Sqrt[2. nrgy/qmxSQ];
                 kovqmxSQ = qmxSQ/(4 nrgy);
                 kSQ = kovqmxSQ qmxSQ;
                 arg = N[wm t];
                 sn = JacobiSN[arg,kSQ];
                 cn = JacobiCN[arg,kSQ];
                 dn = JacobiDN[arg,kSQ];
                 cndn = cn dn;
                 snSQ = sn^2;
                 kqoqmSQ = kovqmxSQ qo^2;
                 denoscSQ = kqoqmSQ snSQ;
                 wmqosn = wm qo sn;
                 pnum = (po cndn-(1+kSQ)wmqosn)(1+denoscSQ);
                 pnum += 2(kSQ snSQ+kqoqmSQ)wmqosn;
                 den = 1-denoscSQ;
                 N[{(qo cndn+(po/wm)sn)/den,pnum/den^2}]]]
```

```
qfpf[qo_,po_,ti_,tf_,dt_] :=
  Module[{nrgy,cos,sin,den,tanh,sgn,qmxSQ,wm,kovqmxSQ,kSQ,arg,
          sn,cn,dn,cndn,kqoqmSQ,dneoscSQ,wmqosn,pnum},
         nrgy = N[Ham[qo,po]];
         Which[Abs[nrgy]<=EPS,
                 Which[qo==0, Table[{0.,0.},{t,ti,tf,dt}],
                       po==0, N[Table[qo Sec[t] {1,Tan[t]},
                                      {t,ti,tf,dt}]],
                       True, cos = Table[Cos[t],{t,ti,tf,dt}];
                             sin = Table[Sin[t],{t,ti,tf,dt}];
                             den = qo cos-po sin;
                          N[qo^2{1/den,(po cos+qo sin)/den^2}]],
               Abs[nrgy-0.25]<=EPS,
                 Which[qo==0, tanh = Table[Tanh[t/RT2],
                                           {t,ti,tf,dt}];
                               N[po{RT2 tanh,(1-tanh^2)}],
                       po==0, N[Table[{qo,0.},{t,ti,tf,dt}]],
                       True, sgn = (1-qo^2)/(RT2 po);
                             tanh = Table[Tanh[t/RT2],
                                          {t,ti,tf,dt}];
                             den = (1+sgn qo tanh);
                             N[{(qo+sgn tanh)/den,
                                po(1-tanh^2)/den^2}])],
               True,
                 qmxSQ = 1-Sqrt[1-4 nrgy];
                 wm = Sqrt[2. nrgy/qmxSQ];
                 kovqmxSQ = qmxSQ/(4 nrgy);
                 kSQ = kovqmxSQ qmxSQ;
                 arg = N[Table[wm t,{t,ti,tf,dt}]];
                 sn = JacobiSN[#,kSQ]& /@ arg;
                 cn = JacobiCN[#,kSQ]& /@ arg;
                 dn = JacobiDN[#,kSQ]& /@ arg;
                 cndn = cn dn;
                 snSQ = sn^2;
                 kqoqmSQ = kovqmxSQ qo^2;
                 denoscSQ = kqoqmSQ snSQ;
                 wmqosn = wm qo sn;
                 pnum = (po cndn-(1+kSQ)wmqosn)(1+denoscSQ);
                 pnum += 2(kSQ snSQ+kqoqmSQ)wmqosn;
                 den = 1-denoscSQ;
                 Transpose[N[{(qo cndn+(po/wm)sn)/den,
                              pnum/den^2}]]]]


qfpfLIN[qo_,po_,t_] :=
  Module[{cos,sin},
         cos = Cos[t];
         sin = Sin[t];
         {cos qo + sin po, -sin qo + cos po}]
```

```
qfpfNL[qo_,po_,t_] :=
  Module[{qint,pint},
         {qint,pint} = qfpfLIN[qo,po,-t];
         qfpf[qint,pint,t]]

End[]

Protect[Ham,qf,pf,qfpf,qfpfLIN,qfpfNL]

EndPackage[]
```

AnhOscTrack.m

```
(* AnhOscTrack.m
   This package contains a set of functions for tracking the
poles of the anharmonic oscillator in the complex phase space.
Written by D. T. Abell.  Last modified 15 July 1992 *)

BeginPackage["AnhOscTrack`", "AnhOsc`", "CRconvert`"]

AnhOscTrack::usage =
  "AnhOscTrack.m is a package for tracking the complex
singularities of the anharmonic oscillator governed by the
Hamiltonian H = (p^2+q^2)/2 - q^4/4."

qfDenom::usage =
  "qfDenom[q,p,t] evaluates the denominator of the expression
q(t) for the anharmonic oscillator."

qContraction::usage =
  "qContraction[q,p,t] contracts the point (q,p) towards a zero
of the denominator of q(t).  The variable q is contracted while
p is held fixed."

pContraction::usage =
  "pContraction[q,p,t] contracts the point (q,p) towards a zero
of the denominator of q(t).  The variable p is contracted while
q is held fixed."

contractQ::usage =
  "contractQ[q,p,t,maxreps] repeatedly applies the qContraction
map to find a zero of the denominator of q(t), but does so no
more than maxreps times."

contractP::usage =
  "contractP[q,p,t,maxreps] repeatedly applies the pContraction
map to find a zero of the denominator of q(t), but does so no
more than maxreps times."

TrackZeroQArcP::usage =
  "TrackZeroArcP[qstart,absP,thetastart,dtheta,len,t] tracks a
q-zero of the denominator of q(t) as p.init varies along the arc
|p.init| = constant."

TrackZeroPArcQ::usage =
  "TrackZeroArcQ[pstart,absQ,thetastart,dtheta,len,t] tracks a
p-zero of the denominator of q(t) as q.init varies along the arc
|q.init| = constant."

TrackZeroQRadP::usage =
  "TrackZeroQRadP[qstart,theta,rpstart,drp,len,t] tracks a
q-zero of the denominator of q(t) along the line Arg(p.init) =
constant."
```

```
TrackZeroPRadQ::usage =
  "TrackZeroPRadQ[pstart,theta,rqstart,drq,len,t] tracks a
p-zero of the denominator of q(t) along the line Arg(q.init) =
constant."

TrackNearestQZero::usage =
  "TrackNearestQZero[qstart,pstart,drp,len,t] tracks a particular
zero (both q and p) of the denominator of q(t) as q.init and
p.init vary along a path chosen to keep |q.init| a min for each
value of |p.init|."

TrackNearestPZero::usage =
  "TrackNearestPZero[qstart,pstart,drq,len,t] tracks a particular
zero (both q and p) of the denominator of q(t) as q.init and
p.init vary along a path chosen to keep |p.init| a min for each
value of |q.init|."

DeltaEmax::usage =
  "DeltaEmax is an option for all of the functions in the
  AnhOscTrack.m package except for qfDenom.  It determines the
range of energies used to compute the energy derivative in the
contraction map.  The default value is DeltaEmax -> 10.^-4."

Options[AnhOscTrack] = {DeltaEmax -> 10.^-4}

Begin["`Private`"]

EPS = 10.^-15

RT2 = Sqrt[2.]

TINY = 10.^-9

(* Der::usage =
  "Der[func,xo,h] finds numerically the first-order
central-difference derivative of func at xo." *)

Der[f_Function,x_,h_] := (f[x+h]-f[x-h])/(2 h)

(* denomF::usage =
  "denomF[energy, time] evaluates the function (k/qmax)^2 sn^2
that appears in the denominator of the expression q(t) for the
anharmonic oscillator." *)

denomF[e_,t_] :=
  Module[{nrg,qmxSQ,kovqmxSQ,kSQ,arg,sn},
         nrg = N[e];
         Which[Abs[nrg]<=EPS, N[Sin[t]^2/2],
               Abs[nrg-0.25]<=EPS, N[Tanh[t/RT2]^2],
               True,
                 qmxSQ = 1.-Sqrt[1.-4. nrg];
```

```
                kovqmxSQ = qmxSQ/(4. nrg);
                kSQ = kovqmxSQ qmxSQ;
                arg = N[t] Sqrt[2. nrg/qmxSQ];
                sn = JacobiSN[arg,kSQ];
                kovqmxSQ sn^2]]

qfDenom[qo_,po_,t_] := N[1 - (qo^2) denomF[Ham[qo,po],t]]

qContraction[q_,p_,t_,opts___Rule] :=
  Module[{deltaE,nrg,eps,fprime,fE,qSQ},
         deltaE = DeltaEmax /. {opts} /. Options[AnhOscTrack];
         nrg = N[Ham[q,p]];
         eps = deltaE Max[1.,Abs[nrg]];
         fprime = Der[denomF[#,t]&,nrg,eps];
         fE = denomF[nrg,t];
         qSQ = q^2;
         q+(1-qSQ fE)/(q qSQ(1-qSQ)fprime + 2 q fE)]

pContraction[q_,p_,t_,opts___Rule] :=
  Module[{deltaE,nrg,eps,fprime,fE,qSQ},
         deltaE = DeltaEmax /. {opts} /. Options[AnhOscTrack];
         nrg = N[Ham[q,p]];
         eps = deltaE Max[1.,Abs[nrg]];
         fprime = Der[denomF[#,t]&,nrg,eps];
         fE = denomF[nrg,t];
         qSQ = q^2;
         p+(1-qSQ fE)/(qSQ p fprime)]

contractQ[q_,p_,t_,maxreps_,opts___Rule] :=
  FixedPoint[qContraction[#,p,t,opts]&,q,maxreps,
             SameTest->(Abs[#1-#2]<TINY&)]

contractP[q_,p_,t_,maxreps_,opts___Rule] :=
  FixedPoint[pContraction[q,#,t,opts]&,p,maxreps,
             SameTest->(Abs[#1-#2]<TINY&)]

TrackZeroQArcP[qstart_,absP_,thetastart_,dtheta_,len_,t_,
               opts___Rule] :=
  Module[{deltaE,ang=thetastart,mom,qroot,rtlist,nrg,del,df,
          qSQ,deltaQ,qtry},
         deltaE = DeltaEmax /. {opts} /. Options[AnhOscTrack];
         mom = N[P2C[{absP,ang}]];
         qroot = contractQ[qstart,mom,t,50];
         rtlist = {qroot};
         Do[nrg = Ham[qroot,mom];
            del = deltaE Max[1.,Abs[nrg]];
            df = Der[denomF[#,t]&,nrg,del];
            qSQ = qroot^2;
            deltaQ = -I dtheta qroot mom^2 df/
                     (qSQ(1.-qSQ)df + 2. denomF[nrg,t]);
            qtry = qroot + deltaQ;
            ang += dtheta;
```

```
            mom = N[P2C[{absP,ang}]];
            qroot = contractQ[qtry,mom,t,50];
            AppendTo[rtlist,qroot], {len}];
          rtlist]

TrackZeroPArcQ[pstart_,absQ_,thetastart_,dtheta_,len_,t_,
               opts___Rule] :=
  Module[{deltaE,ang=thetastart,pos,proot,rtlist,nrg,del,df,
          qSQ,deltaP,ptry},
         deltaE = DeltaEmax /. {opts} /. Options[AnhOscTrack];
         pos = N[P2C[{absQ,ang}]];
         proot = contractP[pos,pstart,t,50];
         rtlist = {proot};
         Do[nrg = Ham[pos,proot];
            del = deltaE Max[1.,Abs[nrg]];
            df = Der[denomF[#,t]&,nrg,del];
            qSQ = pos^2;
            deltaP = -I dtheta(qSQ(1.-qSQ)df + 2. denomF[nrg,t])/
                     (proot df);
            ptry = proot+deltaP;
            ang += dtheta;
            pos = N[P2C[{absQ,ang}]];
            proot = contractP[pos,ptry,t,50];
            AppendTo[rtlist,proot], {len}];
         rtlist]

TrackZeroQRadP[qstart_,theta_,rpstart_,drp_,len_,t_,
  opts___Rule] := Module[{deltaE,rp=rpstart,mom,qroot,rtlist,
                          nrg,del,df,qSQ,deltaQ,qtry},
         deltaE = DeltaEmax /. {opts} /. Options[AnhOscTrack];
         mom = N[P2C[{rp,theta}]];
         qroot = contractQ[qstart,mom,t,50];
         rtlist = {qroot};
         Do[nrg = Ham[qroot,mom];
            del = deltaE Max[1.,Abs[nrg]];
            df = Der[denomF[#,t]&,nrg,del];
            qSQ = qroot^2;
            deltaQ = -(drp/rp)qroot mom^2 df/
                     (qSQ(1.-qSQ)df + 2. denomF[nrg,t]);
            qtry = qroot+deltaQ;
            rp += drp;
            mom = N[P2C[{rp,theta}]];
            qroot = contractQ[qtry,mom,t,50];
            AppendTo[rtlist,qroot], {len}];
         rtlist]

TrackZeroPRadQ[pstart_,theta_,rqstart_,drq_,len_,t_,
  opts___Rule] := Module[{deltaE,rq=rqstart,pos,proot,rtlist,
                          nrg,del,df,qSQ,deltaQ,qtry},
         deltaE = DeltaEmax /. {opts} /. Options[AnhOscTrack];
         pos = N[P2C[{rq,theta}]];
         proot = contractP[pos,pstart,t,50];
```

```
          rtlist = {proot};
          Do[nrg = Ham[pos,proot];
             del = deltaE Max[1.,Abs[nrg]];
             df = Der[denomF[#,t]&,nrg,del];
             qSQ = pos^2;
             deltaP = -(drq/rq)(qSQ(1.-qSQ)df + 2. denomF[nrg,t])/
                      (proot df);
             ptry = proot+deltaP;
             rq += drq;
             pos = N[P2C[{rq,theta}]];
             proot = contractP[pos,ptry,t,50];
             AppendTo[rtlist,proot], {len}];
          rtlist]

TrackNearestQZero[qstart_,pstart_,drp_,len_,t_,opts___Rule] :=
  Module[{deltaE,qroot,proot,rtlist,nrg,del,df,qSQ,xsi,
          zee,drovr,eta,ang,phi,dp,qtry},
          deltaE = DeltaEmax /. {opts} /. Options[AnhOscTrack];
          qroot = contractQ[qstart,pstart,t,50];
          proot = N[pstart];
          rtlist = {{qroot,proot}};
          Do[nrg = Ham[qroot,proot];
             del = deltaE Max[1.,Abs[nrg]];
             df = Der[denomF[#,t]&,nrg,del];
             qSQ = qroot^2;
             xsi = proot df/(qSQ(1.-qSQ) df + 2. denomF[nrg,t]);
             zee = xsi proot;
             drovr = drp/Abs[proot];
             eta = (2.+drovr)drovr;
             phi = ang /. Last[
             FindMinimum[Abs[1-zee(Sqrt[eta+Cos[ang]^2]-Cos[ang])E^(ang I)],
                 {ang,{-0.1,0.1}}] ];
             dp = proot(Sqrt[eta+Cos[phi]^2]-Cos[phi])E^(phi I);
             proot += dp;
             qtry = qroot(1.-xsi dp);
             qroot = contractQ[qtry,proot,t,50];
             AppendTo[rtlist,{qroot,proot}], {len}];
          rtlist]

TrackNearestPZero[qstart_,pstart_,drq_,len_,t_,opts___Rule] :=
  Module[{deltaE,qroot,proot,rtlist,nrg,del,df,qSQ,zeta,
          zee,drovr,eta,ang,phi,dq,ptry},
          deltaE = DeltaEmax /. {opts} /. Options[AnhOscTrack];
          qroot = N[qstart];
          proot = contractP[qstart,pstart,t,50];
          rtlist = {{qroot,proot}};
          Do[nrg = Ham[qroot,proot];
             del = deltaE Max[1.,Abs[nrg]];
             df = Der[denomF[#,t]&,nrg,del];
             qSQ = qroot^2;
             zeta = (qSQ(1.-qSQ)df + 2. denomF[nrg,t])/
                    (qroot proot^2 df);
```

```
            zee = N[zeta qroot];
            drovr = N[drq/Abs[qroot]];
            eta = N[(2.+drovr)drovr];
            phi = ang /. Last[
            FindMinimum[Abs[1-zee(Sqrt[eta+Cos[ang]^2]-Cos[ang])E^(ang I)],
                {ang,{-0.1,0.1}}]];
            dq = qroot(Sqrt[eta+Cos[phi]^2]-Cos[phi])E^(phi I);
            qroot += dq;
            ptry = proot(1.-zeta dq);
            proot = contractP[qroot,ptry,t,50];
            AppendTo[rtlist,{qroot,proot}], {len}];
         rtlist]

End[]

Protect[contractP,contractQ,pContraction,qContraction,qfDenom,
        TrackZeroPArcQ,TrackZeroPRadQ,TrackZeroQArcP,
        TrackZeroQRadP,TrackNearestPZero,TrackNearestQZero]

EndPackage[]
```

AngMomD.m

```
(* AngMomD.m
   This package contains functions for evaluating the Wigner D
functions and their relatives.  Written by D. T. Abell, 27 May
1994. *)

BeginPackage["AngMomD`"]

AngMomD::usage = "The package AngMomD.m contains the Wigner D
functions and their relatives."

djm::usage = "djm[j,mp,m,b] returns the matrix element
<j,mp|D(R_y(b))|j,m>."

djmp::usage = "djmp[j,mp,m,b] returns the matrix element
<j,mp|D(R_y(b))|j,m> in the +J_y convention."

djmx::usage = "djmx[j,mp,m,b] is a faster version of djm.  It
uses the Jacobi polynomials."

WignerD::usage = "WignerD[j,mp,m,a,b,c] returns the matrix
element <j,mp|D(R_z(a)R_y(b)R_z(c))|j,m>."

WignerDx::usage = "WignerDx[j,mp,m,a,b,c] is a faster version of
WignerD.  It uses the Jacobi polynomials."

Begin["`Private`"]

djm[j_,mp_,m_,b_] :=
  Module[{c,s,np1,nm1,np2,nm2,kmn,kmx,sm},
         c=Cos[b/2]; s=Sin[b/2];
         {np1,nm1,np2,nm2}=j+{m,-m,mp,-mp};
         kmn=Max[0,-(m+mp)];
         kmx=Min[nm1,nm2];
         sm=Sum[(-1)^(nm1-k) c^(m+mp+2k) s^(nm1+nm2-2k)/
                   ((m+mp+k)!(nm1-k)!(nm2-k)!(k)!),
                {k,kmn,kmx}];
         Sqrt[np1! nm1! np2! nm2!]*sm
        ]

djmp[j_,mp_,m_,b_] :=
  Module[{c,s,np1,nm1,np2,nm2,kmn,kmx,sm},
         c=Cos[b/2]; s=Sin[b/2];
         {np1,nm1,np2,nm2}=j+{m,-m,mp,-mp};
         kmn=Max[0,m-mp];
         kmx=Min[np1,nm2];
         sm=Sum[(-1)^k c^(np1+nm2-2k) s^(mp-m+2k)/
                   ((mp-m+k)!(np1-k)!(nm2-k)!(k)!),
                {k,kmn,kmx}];
         Sqrt[np1! nm1! np2! nm2!]*sm
        ]
```

```
djmx[j_,mp_,m_,b_] := Sqrt[(j+m)!(j-m)!/((j+mp)!(j-mp)!)]*
   Cos[b/2]^(m+mp) Sin[b/2]^(m-mp) JacobiP[j-m,m-mp,m+mp,Cos[b]]

WignerD[j_,mp_,m_,a_,b_,c_] := E^(-I(mp*a+m*c)) djm[j,mp,m,b]

WignerDx[j_,mp_,m_,a_,b_,c_] := E^(-I(mp*a+m*c)) djmx[j,mp,m,b]

End[]

Protect[djm,djmp,djmx,WignerD,WignerDx]

EndPackage[]
```

ColonOps.m

```
(* ColonOps.m
   This package defines Lie operators for Hamiltonian dynamics.
Written by D. T. Abell, 29 October 1994. *)

BeginPackage["ColonOps`", "PBgrad`"]

ColonOps::usage = "The package ColonOps.m defines Lie operators
for Hamiltonian dynamics."

Colon::usage = "Colon[qs,ps][f] represents the Lie operator :f:,
where the canonical variables are given in the variable lists
'qs' and 'ps'.  Colon[qs,ps][f][g] returns :f:g == [f,g]."

ColonPower::usage = "ColonPower[qs,ps][f,n] represents the Lie
operator :f:^n."

ColonSqr::usage = "ColonSqr[qs,ps][f] represents the Lie operator
:f:^2."

Begin["`Private`"]

Colon[qs_List,ps_List][f_] := PB[qs,ps][f,#]&

ColonPower[qs_List,ps_List][f_,n_] := Nest[Colon[qs,ps][f],#,n]&

ColonSqr[qs_List,ps_List][f_] := ColonPower[qs,ps][f,2]

End[]

Protect[Colon,ColonPower,ColonSqr]

EndPackage[]
```

CRconvert.m

```
(* CRconvert.m
   This package contains functions for converting from a complex
number to a list of two real numbers and vice versa.  Written by
D. T. Abell.  Last modified 19 August 1994. *)

BeginPackage["CRconvert`"]

CRconvert::usage = "CRconvert.m is a package for converting
between real and complex numbers in rectangular or polar
notation."

C2R::usage = "C2R[z] converts a complex number z to the
rectagular pair {x,y}."

R2C::usage = "R2C[{x,y}] converts the rectagular pair {x,y} to a
complex number z."

C2P::usage = "C2P[z] converts a complex number z to the polar
pair {r,th}."

P2C::usage = "P2C[{r,th}] converts the polar pair {r,th} to a
complex number z."

R2P::usage = "R2P[{x,y}] converts the rectagular pair {x,y} to
the polar pair {r,th}."

P2R::usage = "P2R[{r,th}] converts the polar pair {r,th} to the
rectagular pair {x,y}."

R2S::usage = "R2S[{x,y,z}] converts the rectagular triplet
{x,y,z} to the spherical triplet {r,th,phi}."

S2R::usage = "S2R[{r,th,phi}] converts the spherical triplet
{r,th,phi} to the rectagular triplet {x,y,z}."

Begin["`Private`"]

SetAttributes[{C2R,C2P}, Listable]

C2R[z_] := {Re[z],Im[z]}

R2C[{x_,y_}] := (x) + (y) I

C2P[z_] := {Abs[z],Arg[z]}

P2C[{r_,th_}] := r E^(I th)

R2P[{x_,y_}] := C2P[ R2C[{x,y}] ]

P2R[{r_,th_}] := C2R[ P2C[{r,th}] ]
```

```
R2S[pt:{x_,y_,z_}] :=
  Module[{r}, r=Sqrt[Plus@@(pt^2)];
         Which[N[z==r],{r,0,0},
               N[z==-r],{r,Pi,0},
               True,{r,ArcCos[z/r],ArcTan[x,y]}]]

S2R[{r_,th_,ph_}] :=
  r Flatten[{Sin[th]{Cos[ph],Sin[ph]},Cos[th]}]

End[]

Protect[C2R,R2C,C2P,P2C,R2P,P2R,R2S,S2R]

EndPackage[]
```

ListManipulation.m

```
(* ListManipulation.m
   This package contains functions for doing simple manipulations
on Lists.  Written by D. T. Abell.  Fixed a bug in CompressList,
24 June 1994.  Added SortCount, 12 April 1995. *)

BeginPackage["ListManipulation`"]

ListManipulation::usage = "ListManipulation.m is a package of
functions for doing simple manipulations on Lists."

CompressList::usage = "CompressList[list, crit_List] selects from
list those elements for which the corresponding elements in crit
are 'True'."

SortCount::usage = "SortCount[list] returns a list of pairs.  The
first elements in each pair constitute a sorted list of the
elements in list.  The second element in each pair gives the
number of occurrences of the corresponding element in the
argument of SortCount[]."

Begin["`Private`"]

toTF = {1->True, 0->False}

CompressList::badarglen = "The arguments of CompressList have
different lengths."

CompressList[list_,tf_List] :=
  Module[{rlst},
         rlst=Select[Transpose[{tf/.toTF,list}], (#[[1]])&];
         If[Length[Dimensions[rlst]]==2,
            Transpose[rlst][[-1]], {}]] /;
    Length[list]==Length[tf] || Message[CompressList::badarglen]

SortCount[l_List] :=
  Module[{elements},
         elements = Union[l];
         clist = Count[l,#]& /@ elements;
         Transpose[{elements,clist}]] /; Length[Dimensions[l]]==1

End[]

Protect[CompressList,SortCount]

EndPackage[]
```

PBgrad.m

```
(* PBgrad.m
   This package defines the Poisson Bracket, PB[f,g], using the
definition based on derivatives.  Written by D. T. Abell,
26 January 1994. *)

BeginPackage["PBgrad`"]

PB::usage = "PB[qs_List,ps_List][f,g] computes the Poisson
bracket of f with g.  The qs and ps are respectively the
coordinates and conjugate momenta."

Grad::usage = "Grad[f,vars] computes the gradient of f with
respect to the variables in the list vars."

Begin["`Private`"]

Grad[f_,vars_List] := D[f,#]& /@ vars

PB[qs_List,ps_List][0,f_] = 0

PB[qs_List,ps_List][f_,0] = 0

PB[qs_List,ps_List][f_,f_] = 0

PB[qs_List,ps_List][f_,g_] :=
  Grad[f,qs].Grad[g,ps] - Grad[f,ps].Grad[g,qs]

End[]

Protect[Grad,PB]

EndPackage[]
```

Polynomial.m

```
(* Polynomial.m
   This package contains functions having to do with polynomials.
Written by D. T. Abell, 23 October 1994. Updated 31 January 1995
by DTA.  *)

BeginPackage["Polynomial`"]

Polynomial::usage = "Polynomial.m is a package of functions
having to do with polynomials."

DegreeList::usage = "DegreeList[f,x] returns a list containing
the degree in x for each term of the function f.  Note that x may
be either a single variable or a list of variables."

ExponentList::usage = "ExponentList[f,x] returns a list
containing the exponents of x for each term of the function f.
Note that x may be either a single variable or a list of
variables."

HomogeneousPolynomialQ::usage = "HomogeneousPolynomialQ[f,x]
returns True only if f is a homogeneous polynomial in the
variable(s) x.  HomogeneousPolynomialQ[f,x,n] returns True only
if f is a homogeneous polynomial of degree n in the variable(s)
x."

LinearPolynomialQ::usage = "LinearPolynomialQ[f,x] returns True
only if f is a homogeneous linear polynomial in the variable(s)
x."

NumberMonomials::usage = "NumberMonomials[d,n] returns the number
of monomials of degree d in n variables."

NumberTrigMonomials::usage = "NumberTrigMonomials[d,n] returns
the number of trigonometric monomials of degree d in n
variables."

NumberTrigMonomialsTotal::usage = "NumberTrigMonomialsTotal[d,n]
returns the number of trigonometric monomials of degree d and
smaller in n variables."

PolynomialDegree::usage = "PolynomialDegree[f,x] returns the
degree of f as a function of the variable(s) x."

Begin["`Private`"]

PolynomialDegree::badarg = "The first argument, `1`, is not a
polynomial in `2`."

DegreeList[f_,x_] := Apply[Plus,#]& /@ ExponentList[f,x]
```

```
ExponentList[f_,x_] := Module[{xf,terms},
    xf = Expand[f];
    terms = If[Head[xf]===Plus, List @@ xf, {xf}];
    Exponent[#,x]& /@ terms]

HomogeneousPolynomialQ[f_,x_] :=
  If[!PolynomialQ[f,qp], False,
     Equal @@ DegreeList[f,x]]

HomogeneousPolynomialQ[f_,x_,n_] :=
  If[!PolynomialQ[f,qp], False,
     And @@ Thread[n==DegreeList[f,x]]]

LinearPolynomialQ[f_,x_] := HomogeneousPolynomialQ[f,x,1]

NumberMonomials[deg_,nvar_] := Binomial[deg+nvar-1,deg]

NumberTrigMonomials[0,nvar_] = 1

NumberTrigMonomials[deg_,nvar_] :=
  Sum[Binomial[nvar,j] Binomial[deg-1,j-1] (2^j), {j,nvar}]

NumberTrigMonomialsTotal[deg_,nvar_] :=
  Sum[Binomial[nvar,j] Binomial[deg,j] (2^j), {j,0,nvar}]

PolynomialDegree[f_,x_] := Max[DegreeList[f,x]] /;
  PolynomialQ[f,x] || Message[PolynomialDegree::badarg,f,x]

End[]

Protect[DegreeList,ExponentList,HomogeneousPolynomialQ,
        LinearPolynomialQ,NumberMonomials,NumberTrigMonomials,
        NumberTrigMonomialsTotal,PolynomialDegree]

EndPackage[]
```

sp4.m

```
(* sp4.m
   This package contains a set of basis polynomials for the Lie
algebra of sp(4).  Written by D. T. Abell, 29 October 1994. *)

sp4::usage = "The package sp4.m defines a set of basis
polynomials for the Lie algebra of sp(4).  These are {b[0],...,
b[3],f[1],...,f[3], g[1],...,g[3]}."

Unprotect[b,f,g,qs,ps,zz,bs,fs,gs,fg,bfg];

Clear[b,f,g]

b[0] = (1/2) (q1^2 + p1^2 + q2^2 + p2^2)
b[1] =  q1 q2 + p1 p2
b[2] = -q1 p2 + q2 p1
b[3] = (1/2) (q1^2 + p1^2 - q2^2 - p2^2)

f[1] = (-1/2) (q1^2 - p1^2 - q2^2 + p2^2)
f[2] = -q1 p1 - q2 p2
f[3] =  q1 q2 - p1 p2

g[1] = -q1 p1 + q2 p2
g[2] = (1/2) (q1^2 - p1^2 + q2^2 - p2^2)
g[3] =  q1 p2 + q2 p1

qs = {q1,q2}
ps = {p1,p2}
zz = Flatten[{qs,ps}]

bs = b /@ Range[0,3]
fs = f /@ Range[3]
gs = g /@ Range[3]
fg = Flatten[{fs,gs}]
bfg = Flatten[{bs,fs,gs}]

Protect[b,f,g,qs,ps,zz,bs,fs,gs,fg,bfg];
```

sp6.m

```
(* sp6.m
   This package contains a set of basis polynomials for the Lie
algebra of sp(6).  Written by D. T. Abell, 29 October 1994. *)

sp6::usage = "The package sp6.m defines a set of basis
polynomials for the Lie algebra of sp(6).  These are
{b[0],...,b[8],f[1],...,f[6],g[1],...,g[6]}."

Unprotect[b,f,g,qs,ps,zz,bs,fs,gs,fg,bfg];

Clear[b,f,g]

b[0] = (q1^2 + p1^2 + q2^2 + p2^2 + q3^2 + p3^2)/2
b[1] = q1*q2 + p1*p2
b[2] = -q1*p2 + q2*p1
b[3] = (q1^2 + p1^2 - q2^2 - p2^2)/2
b[4] = q1*q3 + p1*p3
b[5] = -q1*p3 + q3*p1
b[6] = q2*q3 + p2*p3
b[7] = -q2*p3 + q3*p2
b[8] = (q1^2 + p1^2 + q2^2 + p2^2 - 2*q3^2 - 2*p3^2)/Sqrt[12]

f[1] = (q1^2 - p1^2)/2
f[2] = q1*q2 - p1*p2
f[3] = (q2^2 - p2^2)/2
f[4] = q2*q3 - p2*p3
f[5] = (q3^2 - p3^2)/2
f[6] = q3*q1 - p3*p1

g[1] = q1*p1
g[2] = q1*p2 + q2*p1
g[3] = q2*p2
g[4] = q2*p3 + q3*p2
g[5] = q3*p3
g[6] = q3*p1 + q1*p3

qs = {q1,q2,q3}
ps = {p1,p2,p3}
zz = Flatten[{qs,ps}]
bs = b /@ Range[0,8]
fs = f /@ Range[6]
gs = g /@ Range[6]
fg = Flatten[{fs,gs}]
bfg = Flatten[{bs,fs,gs}]

Protect[b,f,g,qs,ps,zz,bs,fs,gs,fg,bfg];
```

sp6tools.m

```
(* sp6tools.m
   This package defines Lie operators for sp(6,R) together with a
number of other tools useful for studying sp(6,R) and---in
particular---its compact sub-algebras u(3) and su(3).  Written by
D. T. Abell, 9 March 1995. *)

Needs["ColonOps`"]
Needs["SU3`"]
Needs["USp`"]
Get["sp6`"]

sp6tools::usage = "The package sp6tools.m defines a set of tools
for doing calculations in the Lie algebra sp(6).  It includes
the Lie operators for sp(6,R) and the USp(6)-invariant scalar
product.  It also includes a definition for Lie operators with
respect to the z's, the associated Lie operators defined in Beg
and Ruegg (1965) for the su(3) sub-algebra, and the orthonormal
basis polynomials that carry the irreducible representations of
SU(3)."

(* Lie operators generated by sp(6,R) basis polynomials in AJD's
lecture notes.  B0--B8 generate U(3) part; B1--B8 generate SU(3)
part; F1--F6, G1--G6 generate the non-compact part. *)
B0 = Colon[qs,ps][b[0]]
B1 = Colon[qs,ps][b[1]]
B2 = Colon[qs,ps][b[2]]
B3 = Colon[qs,ps][b[3]]
B4 = Colon[qs,ps][b[4]]
B5 = Colon[qs,ps][b[5]]
B6 = Colon[qs,ps][b[6]]
B7 = Colon[qs,ps][b[7]]
B8 = Colon[qs,ps][b[8]]
F1 = Colon[qs,ps][f[1]]
F2 = Colon[qs,ps][f[2]]
F3 = Colon[qs,ps][f[3]]
F4 = Colon[qs,ps][f[4]]
F5 = Colon[qs,ps][f[5]]
F6 = Colon[qs,ps][f[6]]
G1 = Colon[qs,ps][g[1]]
G2 = Colon[qs,ps][g[2]]
G3 = Colon[qs,ps][g[3]]
G4 = Colon[qs,ps][g[4]]
G5 = Colon[qs,ps][g[5]]
G6 = Colon[qs,ps][g[6]]

(* norm and inner product w/r.t. {q,p}'s *)
ip = USpInner[zz]
nrm = USpNorm[zz]

(* complex co-ordinates for the five-sphere *)
```

```
z5 = z /@ Range[3];
z5s = zs /@ Range[3];
zvec = Join[z5,z5s];
rsq = z5 . z5s;
Zmon[r_List] := Times @@ (zvec^r) /; Dimensions[r]=={6}

(* norm and inner product w/r.t. z's *)
zip = USpInner[zvec]
znrm = USpNorm[zvec]

(* Lie operators in terms of the z's *)
Zcolon[f_] := -I Colon[z5,z5s][f][#]&
ZcolonSqr[f_] := - ColonSqr[z5,z5s][f][#]&
ZcolonPower[f_,n_] := (-I)^n ColonPower[z5,z5s][f,n][#]&

(* routines for converting between the {q,p}'s and the z's *)
toQP[xpr_] := Expand[xpr /.
  {z[1]->(q1+I*p1)/Sqrt[2], zs[1]->(q1-I*p1)/Sqrt[2],
   z[2]->(q2+I*p2)/Sqrt[2], zs[2]->(q2-I*p2)/Sqrt[2],
   z[3]->(q3+I*p3)/Sqrt[2], zs[3]->(q3-I*p3)/Sqrt[2]}]
toZ[xpr_] := Expand[xpr /.
  {q1-> (z[1]+zs[1])/Sqrt[2], p1-> (z[1]-zs[1])/(I*Sqrt[2]),
   q2-> (z[2]+zs[2])/Sqrt[2], p2-> (z[2]-zs[2])/(I*Sqrt[2]),
   q3-> (z[3]+zs[3])/Sqrt[2], p3-> (z[3]-zs[3])/(I*Sqrt[2])}]

(* an alternative basis for the Lie sub-algebra of su(3) *)
h[1] = -I/(2 Sqrt[3]) (z[2] zs[2] - z[3] zs[3]);
h[2] = -I/6 (-2 z[1] zs[1] + z[2] zs[2] + z[3] zs[3]);
e[1] = -I/Sqrt[6] z[2] zs[3];
e[2] = -I/Sqrt[6] z[2] zs[1];
e[3] = -I/Sqrt[6] z[3] zs[1];
em[1] = -I/Sqrt[6] z[3] zs[2];
em[2] = -I/Sqrt[6] z[1] zs[2];
em[3] = -I/Sqrt[6] z[1] zs[3];

(* operators in the alternative su(3) basis *)
H1 = Zcolon[h[1]];
H2 = Zcolon[h[2]];
E1 = Zcolon[e[1]];
E2 = Zcolon[e[2]];
E3 = Zcolon[e[3]];
Em1 = Zcolon[em[1]];
Em2 = Zcolon[em[2]];
Em3 = Zcolon[em[3]];

(* operators for isotopic spin and hypercharge *)
I3 = Zcolon[Sqrt[3] h[1]];
Y  = Zcolon[2 h[2]];

(* ladder operators and their coefficients
   for su(2) sub-algebra *)
Iup = Zcolon[Sqrt[6] e[1]];
```

```
Idn = Zcolon[Sqrt[6] em[1]];
cu[j_,m_] := -Sqrt[(j-m)(j+m+1)]
cd[j_,m_] := -Sqrt[(j+m)(j-m+1)]

(* total isotopic spin and its coefficient *)
Isq = I3[I3[#]] + (1/2)(Iup[Idn[#]] + Idn[Iup[#]])&;
a2[j_] := j(j+1)

(* operators for checking the eigenvalues I3 and Y *)
I3Y = {I3[#],Y[#]}/#&;
II3Y = {Isq[#],I3[#],Y[#]}/#&;

(* su(3) basis polynomials for space of f(l)'s,
normalized using the USp(6) scalar product *)
psi[j1_,j2_,i_,i3_,y_,l_] :=
  Module[{xp,ket},
         xr=(l-j1-j2)/2;
         ket=rsq^xr SU3psiZ[j1,j2,i,i3,y];
         ket/znrm[ket]]

Protect[B0,B1,B2,B3,B4,B5,B6,B7,B8,F1,F2,F3,F4,F5,F6,G1,G2,G3,
        G4,G5,G6,ip,nrm,z5,z5s,zvec,zip,znrm,Zcolon,ZcolonSqr,
        ZcolonPower,toQP,toZ,h,e,em,H1,H2,E1,E2,E3,Em1,Em2,Em3,
        I3,Y,Iup,Idn,cu,cd,Isq,a2,I3Y,II3Y,psi];
```

SU2phi.m

```
(* SU2phi.m
   This package contains basis functions for the space of f_1's
through f_5's that transform as irreducible representations of
SU(2).  Written by D. T. Abell, 14 February 1995. *)

BeginPackage["SU2phi`"]

Phi::usage = "Phi[j,l,mu] returns the collection of SU2 functions
phi[j,m,l,mu] for m = {j,...,-j}."

phi::usage = "phi[j,m,l,mu] returns the SU2 function |j,m;l,mu>
written in terms of the y's."

(* f_1's *)

Phi[1/2,1,1] =
{phi[1/2, 1/2,1,1] = y1 (* =  (q1+iq2)/Sqrt[2] *),
 phi[1/2,-1/2,1,1] = y2 (* =  (p2+ip1)/Sqrt[2] *)}

Phi[1/2,1,0] =
{phi[1/2, 1/2,1,0] = y3 (* =  (p1+ip2)/Sqrt[2] *),
 phi[1/2,-1/2,1,0] = y4 (* = -(q2+iq1)/Sqrt[2] *)}


(* f_2's *)

Phi[1,2,2] =
{phi[1, 1, 2,2] = y1^2/Sqrt[2],
 phi[1, 0, 2,2] = y1 y2,
 phi[1,-1, 2,2] = y2^2/Sqrt[2]}

Phi[1,2,1] =
{phi[1, 1, 2,1] = y1 y3,
 phi[1, 0, 2,1] = (y1 y4 + y2 y3)/Sqrt[2],
 phi[1,-1, 2,1] = y2 y4}

Phi[1,2,0] =
{phi[1, 1, 2,0] = y3^2/Sqrt[2],
 phi[1, 0, 2,0] = y3 y4,
 phi[1,-1, 2,0] = y4^2/Sqrt[2]}

Phi[0,2,1] =
{phi[0, 0, 2,1] = (y1 y4 - y2 y3)/Sqrt[2]}


(* f_3's *)

Phi[3/2,3,3] =
{phi[3/2, 3/2, 3,3] = y1^3/Sqrt[3!],
 phi[3/2, 1/2, 3,3] = y1^2 y2/Sqrt[2],
```

```
 phi[3/2,-1/2, 3,3] = y1 y2^2/Sqrt[2],
 phi[3/2,-3/2, 3,3] = y2^3/Sqrt[3!]}

Phi[3/2,3,2] =
{phi[3/2, 3/2, 3,2] = y1^2 y3/Sqrt[2],
 phi[3/2, 1/2, 3,2] = (2 y1 y2 y3 + y1^2 y4)/Sqrt[3!],
 phi[3/2,-1/2, 3,2] = (2 y1 y2 y4 + y2^2 y3)/Sqrt[3!],
 phi[3/2,-3/2, 3,2] = y2^2 y4/Sqrt[2]}

Phi[3/2,3,1] =
{phi[3/2, 3/2, 3,1] = y1 y3^2/Sqrt[2],
 phi[3/2, 1/2, 3,1] = (2 y1 y3 y4 + y2 y3^2)/Sqrt[3!],
 phi[3/2,-1/2, 3,1] = (2 y2 y3 y4 + y1 y4^2)/Sqrt[3!],
 phi[3/2,-3/2, 3,1] = y2 y4^2/Sqrt[2]}

Phi[3/2,3,0] =
{phi[3/2, 3/2, 3,0] = y3^3/Sqrt[3!],
 phi[3/2, 1/2, 3,0] = y3^2 y4/Sqrt[2],
 phi[3/2,-1/2, 3,0] = y3 y4^2/Sqrt[2],
 phi[3/2,-3/2, 3,0] = y4^3/Sqrt[3!]}

Phi[1/2,3,2] =
{phi[1/2, 1/2, 3,2] = (y1^2 y4 - y1 y2 y3)/Sqrt[3],
 phi[1/2,-1/2, 3,2] = (y1 y2 y4 - y2^2 y3)/Sqrt[3]}

Phi[1/2,3,1] =
{phi[1/2, 1/2, 3,1] = (y2 y3^2 - y1 y3 y4)/Sqrt[3],
 phi[1/2,-1/2, 3,1] = (y2 y3 y4 - y1 y4^2)/Sqrt[3]}


(* f_4's *)

Phi[2,4,4] =
{phi[2, 2, 4,4] = y1^4/Sqrt[4!],
 phi[2, 1, 4,4] = y1^3 y2/Sqrt[3!],
 phi[2, 0, 4,4] = y1^2 y2^2/2,
 phi[2,-1, 4,4] = y1 y2^3/Sqrt[3!],
 phi[2,-2, 4,4] = y2^4/Sqrt[4!]}

Phi[2,4,3] =
{phi[2, 2, 4,3] = y1^3 y3/Sqrt[3!],
 phi[2, 1, 4,3] = (3 y1^2 y2 y3 + y1^3 y4)/Sqrt[4!],
 phi[2, 0, 4,3] = (y1 y2^2 y3 + y1^2 y2 y4)/2,
 phi[2,-1, 4,3] = (3 y1 y2^2 y4 + y2^3 y3)/Sqrt[4!],
 phi[2,-2, 4,3] = y2^3 y4/Sqrt[3!]}

Phi[2,4,2] =
{phi[2, 2, 4,2] = y1^2 y3^2/2,
 phi[2, 1, 4,2] = (y1 y2 y3^2 + y1^2 y3 y4)/2,
 phi[2, 0, 4,2] = (y1^2 y4^2 + 4 y1 y2 y3 y4 + y2^2 y3^2)/
                  Sqrt[4!],
 phi[2,-1, 4,2] = (y1 y2 y4^2 + y2^2 y3 y4)/2,
```

```
 phi[2,-2, 4,2] = y2^2 y4^2/2}

Phi[2,4,1] =
{phi[2, 2, 4,1] = y1 y3^3/Sqrt[3!],
 phi[2, 1, 4,1] = (3 y1 y3^2 y4 + y2 y3^3)/Sqrt[4!],
 phi[2, 0, 4,1] = (y1 y3 y4^2 + y2 y3^2 y4)/2,
 phi[2,-1, 4,1] = (3 y2 y3 y4^2 + y1 y4^3)/Sqrt[4!],
 phi[2,-2, 4,1] = y2 y4^3/Sqrt[3!]}

Phi[2,4,0] =
{phi[2, 2, 4,0] = y3^4/Sqrt[4!],
 phi[2, 1, 4,0] = y3^3 y4/Sqrt[3!],
 phi[2, 0, 4,0] = y3^2 y4^2/2,
 phi[2,-1, 4,0] = y3 y4^3/Sqrt[3!],
 phi[2,-2, 4,0] = y4^4/Sqrt[4!]}

Phi[1,4,3] =
{phi[1, 1, 4,3] = (y1^3 y4 - y1^2 y2 y3)/Sqrt[8],
 phi[1, 0, 4,3] = (y1^2 y2 y4 - y1 y2^2 y3)/2,
 phi[1,-1, 4,3] = (y1 y2^2 y4 - y2^3 y3)/Sqrt[8]}

Phi[1,4,2] =
{phi[1, 1, 4,2] = (y1^2 y3 y4 - y1 y2 y3^2)/2,
 phi[1, 0, 4,2] = (y1^2 y4^2 - y2^2 y3^2)/Sqrt[8],
 phi[1,-1, 4,2] = (y1 y2 y4^2 - y2^2 y3 y4)/2}

Phi[1,4,1] =
{phi[1, 1, 4,1] = (y2 y3^3 - y1 y3^2 y4)/Sqrt[8],
 phi[1, 0, 4,1] = (y2 y3^2 y4 - y1 y3 y4^2)/2,
 phi[1,-1, 4,1] = (y2 y3 y4^2 - y1 y4^3)/Sqrt[8]}

Phi[0,4,2] =
{phi[0, 0, 4,2] = (y1^2 y4^2 - 2 y1 y2 y3 y4 + y2^2 y3^2)/
                  Sqrt[12]}


(* f_5's *)

Phi[5/2,5,5] =
{phi[5/2, 5/2, 5,5] = y1^5/Sqrt[5!],
 phi[5/2, 3/2, 5,5] = y1^4 y2/Sqrt[4!],
 phi[5/2, 1/2, 5,5] = y1^3 y2^2/Sqrt[12],
 phi[5/2,-1/2, 5,5] = y1^2 y2^3/Sqrt[12],
 phi[5/2,-3/2, 5,5] = y1 y2^4/Sqrt[4!],
 phi[5/2,-5/2, 5,5] = y2^5/Sqrt[5!]}

Phi[5/2,5,4] =
{phi[5/2, 5/2, 5,4] = y1^4 y3/Sqrt[4!],
 phi[5/2, 3/2, 5,4] = (4 y1^3 y2 y3 + y1^4 y4)/Sqrt[5!],
 phi[5/2, 1/2, 5,4] = (3 y1^2 y2^2 y3 + 2 y1^3 y2 y4)/Sqrt[60],
 phi[5/2,-1/2, 5,4] = (3 y1^2 y2^2 y4 + 2 y1 y2^3 y3)/Sqrt[60],
 phi[5/2,-3/2, 5,4] = (4 y1 y2^3 y4 + y2^4 y3)/Sqrt[5!],
```

```
 phi[5/2,-5/2, 5,4] = y2^4 y4/Sqrt[4!]}

Phi[5/2,5,3] =
{phi[5/2, 5/2, 5,3] = y1^3 y3^2/Sqrt[12],
 phi[5/2, 3/2, 5,3] = (2 y1^3 y3 y4 + 3 y1^2 y2 y3^2)/Sqrt[60],
 phi[5/2, 1/2, 5,3] = (y1^3 y4^2 + 6 y1^2 y2 y3 y4
                                  + 3 y1 y2^2 y3^2)/Sqrt[5!],
 phi[5/2,-5/2, 5,3] = (y2^3 y3^2 + 6 y1 y2^2 y3 y4
                                  + 3 y1^2 y2 y4^2)/Sqrt[5!],
 phi[5/2,-3/2, 5,3] = (2 y2^3 y3 y4 + 3 y1 y2^2 y4^2)/Sqrt[60],
 phi[5/2,-1/2, 5,3] = y2^3 y4^2/Sqrt[12]}

Phi[5/2,5,2] =
{phi[5/2, 5/2, 5,2] = y1^2 y3^3/Sqrt[12],
 phi[5/2, 3/2, 5,2] = (2 y1 y2 y3^3 + 3 y1^2 y3^2 y4)/Sqrt[60],
 phi[5/2, 1/2, 5,2] = (y2^2 y3^3 + 6 y1 y2 y3^2 y4
                                  + 3 y1^2 y3 y4^2)/Sqrt[5!],
 phi[5/2,-1/2, 5,2] = (y1^2 y4^3 + 6 y1 y2 y3 y4^2
                                  + 3 y2^2 y3^2 y4)/Sqrt[5!],
 phi[5/2,-3/2, 5,2] = (2 y1 y2 y4^3 + 3 y2^2 y3 y4^2)/Sqrt[60],
 phi[5/2,-5/2, 5,2] = y2^2 y4^3/Sqrt[12]}

Phi[5/2,5,1] =
{phi[5/2, 5/2, 5,1] = y1 y3^4/Sqrt[4!],
 phi[5/2, 3/2, 5,1] = (4 y1 y3^3 y4 + y2 y3^4)/Sqrt[5!],
 phi[5/2, 1/2, 5,1] = (3 y1 y3^2 y4^2 + 2 y2 y3^3 y4)/Sqrt[60],
 phi[5/2,-1/2, 5,1] = (3 y2 y3^2 y4^2 + 2 y1 y3 y4^3)/Sqrt[60],
 phi[5/2,-3/2, 5,1] = (4 y2 y3 y4^3 + y1 y4^4)/Sqrt[5!],
 phi[5/2,-5/2, 5,1] = y2 y4^4/Sqrt[4!]}

Phi[5/2,5,0] =
{phi[5/2, 5/2, 5,0] = y3^5/Sqrt[5!],
 phi[5/2, 3/2, 5,0] = y3^4 y4/Sqrt[4!],
 phi[5/2, 1/2, 5,0] = y3^3 y4^2/Sqrt[12],
 phi[5/2,-1/2, 5,0] = y3^2 y4^3/Sqrt[12],
 phi[5/2,-3/2, 5,0] = y3 y4^4/Sqrt[4!],
 phi[5/2,-5/2, 5,0] = y4^5/Sqrt[5!]}

Phi[3/2,5,4] =
{phi[3/2, 3/2, 5,4] = (y1^4 y4 - y1^3 y2 y3)/Sqrt[30],
 phi[3/2, 1/2, 5,4] = (y1^3 y2 y4 - y1^2 y2^2 y3)/Sqrt[10],
 phi[3/2,-1/2, 5,4] = (y1^2 y2^2 y4 - y1 y2^3 y3)/Sqrt[10],
 phi[3/2,-3/2, 5,4] = (y1 y2^3 y4 - y2^4 y3)/Sqrt[30]}

Phi[3/2,5,3] =
{phi[3/2, 3/2, 5,3] = (y1^3 y3 y4 - y1^2 y2 y3^2)/Sqrt[10],
 phi[3/2, 1/2, 5,3] = (y1^3 y4^2 + y1^2 y2 y3 y4 -
                                   2 y1 y2^2 y3^2)/Sqrt[30],
 phi[3/2,-1/2, 5,3] = (2 y1^2 y2 y4^2 - y1 y2^2 y3 y4 -
                                      y2^3 y3^2)/Sqrt[30],
 phi[3/2,-3/2, 5,3] = (y1 y2^2 y4^2 - y2^3 y3 y4)/Sqrt[10]}
```

```
Phi[3/2,5,2] =
{phi[3/2, 3/2, 5,2] = (y1 y2 y3^3 - y1^2 y3^2 y4)/Sqrt[10],
 phi[3/2, 1/2, 5,2] = (y2^2 y3^3 + y1 y2 y3^2 y4 -
                                  2 y1^2 y3 y4^2)/Sqrt[30],
 phi[3/2,-1/2, 5,2] = (2 y2^2 y3^2 y4 - y1 y2 y3 y4^2 -
                                        y1^2 y4^3)/Sqrt[30],
 phi[3/2,-3/2, 5,2] = (y2^2 y3 y4^2 - y1 y2 y4^3)/Sqrt[10]}

Phi[3/2,5,1] =
{phi[3/2, 3/2, 5,1] = (y2 y3^4 - y1 y3^3 y4)/Sqrt[30],
 phi[3/2, 1/2, 5,1] = (y2 y3^3 y4 - y1 y3^2 y4^2)/Sqrt[10],
 phi[3/2,-1/2, 5,1] = (y2 y3^2 y4^2 - y1 y3 y4^3)/Sqrt[10],
 phi[3/2,-3/2, 5,1] = (y2 y3 y4^3 - y1 y4^4)/Sqrt[30]}

Phi[1/2,5,3] =
{phi[1/2, 1/2, 5,3] = (-y1 y2^2 y3^2 + 2 y1^2 y2 y3 y4 -
                                         y1^3 y4^2)/Sqrt[4!],
 phi[1/2,-1/2, 5,3] = (-y1^2 y2 y4^2 + 2 y1 y2^2 y3 y4 -
                                         y2^3 y3^2)/Sqrt[4!]}

Phi[1/2,5,2] =
{phi[1/2, 1/2, 5,2] = (-y1^2 y3 y4^2 + 2 y1 y2 y3^2 y4 -
                                          y2^2 y3^3)/Sqrt[4!],
 phi[1/2,-1/2, 5,2] = (-y2^2 y3^2 y4 + 2 y1 y2 y3 y4^2 -
                                         y1^2 y4^3)/Sqrt[4!]}

Protect[Phi,phi,y1,y2,y3,y4]

EndPackage[]
```

SU3.m

```
(* SU3.m
   This package contains functions that compute the harmonic
functions on the five-sphere as given in Beg and Ruegg,
J. Math. Phys., 6, 677--682 (1965).  Written by D. T. Abell. *)

BeginPackage["SU3`", "AngMomD`"]

SU3::usage = "SU3.m is a package that computes basis functions
for representations of SU(3)---in particular, the harmonic
functions on the five-sphere.  (See Beg and Ruegg, J. Math.
Phys., 6, 677--682 (1965).)"

SU3DirectProduct::usage = "SU3DirectProduct[j1,j2,j1p,j2p] uses
the Clebsch-Gordan series for SU(3) to return a list of the SU(3)
representations that occur in the direct product of (j1,j2) with
(j1p,j2p)."

SU3dim::usage = "SU3dim[p,q] returns the dimension of the SU(3)
representation (p,q)."

SU3psi::usage = "SU3psi[p,q,I,I3,Y] returns the SU(3) harmonic
function |p,q;I,I3,Y> written in terms of the angles on the
five-sphere: {th, xi, ph[1], ph[2], ph[3]}."

SU3psiZ::usage = "SU3psiZ[p,q,I,I3,Y] returns the SU(3) harmonic
function |p,q;I,I3,Y> written in terms of six complex variables:
{z[1], z*[1], z[2], z*[2], z[3], z*[3]}."

SU3reps::usage = "SU3reps[d] returns a list containing all of
the SU(3) representations carried by polynomials of degree d in
six variables."

th::usage =
  "One of the angles on the five-sphere; range [0,Pi/2]."

xi::usage =
  "One of the angles on the five-sphere; range [0,Pi/2]."

ph::usage = "The ph[j], j={1,2,3}, comprise three of the angles
on the five-sphere; each has a range [0,2Pi]."

z::usage = "The z[j], j={1,2,3}, comprise the three (complex)
variables that define the five-sphere.  In terms of angles on the
five-sphere z[1]=E^(I ph[1])*Cos[th],
z[2]=E^(I ph[2])*Sin[th]*Cos[xi], and
z[3]=E^(I ph[3])*Sin[th]*Sin[xi]."

zs::usage = "The zs[j], j={1,2,3}, denote the complex conjugates
of z[j].  The z[j] and z*[j] satisfy
z[1] z*[1] + z[2] z*[2] + z[3] z*[3] == 1."
```

```
Format[ph[j_]] := SequenceForm[ph,Subscript[j]]
Format[z[j_]] := SequenceForm[z,Subscript[j]]
Format[zs[j_]] := SequenceForm[z,"*",Subscript[j]]

Begin["`Private`"]

f[1]= Cos[th]
f[2]= Sin[th] Cos[xi]
f[3]= Sin[th] Sin[xi]

toza = {E^( I ph[j_]) :> z[j]/f[j],
  E^(-I ph[j_]) :> zs[j]/f[j],
  E^( I ph[j_]+x_) :> E^x z[j]/f[j],
  E^(-I ph[j_]+x_) :> E^x zs[j]/f[j],
  E^(Complex[0,n_?Positive] ph[j_]) :> (z[j]/f[j])^n,
  E^(Complex[0,n_?Negative] ph[j_]) :> (zs[j]/f[j])^(-n),
  E^(Complex[0,n_?Positive] ph[j_] + x_) :> E^x (z[j]/f[j])^n,
  E^(Complex[0,n_?Negative] ph[j_] + x_) :> E^x (zs[j]/f[j])^(-n)}

tozb = {
  Cos[xi]^(n_.) :> z[2]^(n/2) zs[2]^(n/2)/(Sin[th])^n /; EvenQ[n],
  Sin[xi]^(n_.) :> z[3]^(n/2) zs[3]^(n/2)/(Sin[th])^n /; EvenQ[n]}

tozc = {
  Cos[th]^(n_.) :> z[1]^(n/2) zs[1]^(n/2) /; EvenQ[n],
  Sin[th]^(n_.) :> (z[2] zs[2] + z[3] zs[3])^(n/2) /; EvenQ[n]}

su3sum[n_,np_,m_,mp_] :=
  Join[{{n+np,m+mp}},
       Table[{n+np-2i,m+mp+i},{i,Min[n,np]}],
       Table[{n+np+k,m+mp-2k},{k,Min[m,mp]}]]

(* NB: Cannot use djmx[]!! *)
SU3psi[j1_,j2_,j_,jz_,y_] := 1/Sin[th]*
  djm[(j1+j2+1)/2,(j1-j2-3y+6j+3)/6,(j1-j2-3y-6j-3)/6,2th]*
  djm[j,(j1-j2)/3+y/2,jz,2xi]*
  E^(I (j1-j2)(ph[1]+ph[2]+ph[3])/3)*
  E^(I jz(ph[2]-ph[3]))*
  E^(I y(-2ph[1]+ph[2]+ph[3])/2)

SU3psiZ[j1_,j2_,j_,jz_,y_] :=
  Expand[SU3psi[j1,j2,j,jz,y]] //. toza //. tozb //. tozc

SU3dim[j1_,j2_] := (j1+1)(j2+1)(j1+j2+2)/2

SU3dim[{j1_,j2_}] := SU3dim[j1,j2]

SU3reps[d_] :=
  Flatten[Table[{j1,j2},{j1,0,d},{j2,Mod[d-j1,2],d-j1,2}],1]
```

```
SU3DirectProduct[j1_,j2_,j1p_,j2p_] :=
  Reverse[Flatten[
  Table[su3sum[j1-i,j1p-k,j2-k,j2p-i],
        {i,0,Min[j1,j2p]},{k,0,Min[j2,j1p]}], 2]]

SU3DirectProduct[{j1_,j2_},{j1p_,j2p_}] :=
  SU3DirectProduct[j1,j2,j1p,j2p]

End[]

Protect[SU3dim,SU3DirectProduct,SU3psi,SU3psiZ,SU3reps,
        th,xi,ph,z,zs]

EndPackage[]
```

SU3wts.m

```
(* SU3wts.m
   This package contains functions that generate the weights for
any irreducible representation (j1,j2) of SU(3).  See
S. Gasiorowicz, Elementary Particle Physics (John Wiley & Sons,
1966) or S. Gasiorowicz, A Simple Graphical Method in the
Analysis of SU_3, ANL-6729 (Argonne National Laboratory, 1963).
Written by D. T. Abell, 3 July 1995. *)

BeginPackage["SU3wts`"]

SU3wts::usage = "The package SU3wts.m contains functions that
generate the weights for any irreducible representation (j1,j2)
of SU(3)."

HighestWeightSU3::usage = "HighestWeightSU3[j1,j2] returns the
highest weight for the irreducible SU(3) representation (j1,j2)."

SU3ii3y::usage = "SU3ii3y[j1,j2] returns the values of I, I3,
and Y for the irreducible representation (j1,j2) of SU(3).  In
the language of strongly interacting particles, these values
represent isotopic spin, z-component of isotopic spin, and
hypercharge."

SU3i3y::usage = "SU3i3y[j1,j2] returns the values of I3 and Y
for the irreducible representation (j1,j2) of SU(3).  In the
language of strongly interacting particles, these values
represent the z-component of isotopic spin and hypercharge."

SU3weights::usage = "SU3weights[j1,j2] returns the weights for
the irreducible representation (j1,j2) of SU(3)."

Begin["`Private`"]

IY[j1_,j2_] := Module[{wh,da,db,iyt,iy},
  wh={Sqrt[3],2}*HighestWeightSU3[j1,j2];
  da=Max[0,j2-j1];
  db=Max[0,j1-j2];
  iyt=If[j1>=j2,Table[{i-y/2,-y},{y,0,j1-j2},{i,0,-j2,-1}],
                Table[{i-y/2,y},{y,j2-j1,0,-1},{i,0,-j1,-1}]];
  iy=Table[{i-y/2,y},{y,j2,1+da,-1},{i,0,y-j2,-1}];
  iy=Join[iy,iyt];
  iy=Join[iy,Table[{i-y/2,-y},{y,1+db,j1},{i,0,y-j1,-1}]];
  wh+#& /@ Flatten[iy,1]]

toii3y[{i_,y_}] := Table[{i,i3,y},{i3,i,-i,-1}]

HighestWeightSU3[j1_,j2_] := {(j1+j2)/(2Sqrt[3]),(j1-j2)/6}

SU3ii3y[j1_,j2_] := Flatten[toii3y /@ IY[j1,j2], 1]
```

```
SU3i3y[j1_,j2_] := Drop[#,1]& /@ SU3ii3y[j1,j2]

SU3weights[j1_,j2_] := {1/Sqrt[3],1/2}*#& /@ SU3i3y[j1,j2]

HighestWeightSU3[{j1_,j2_}] := HighestWeightSU3[j1,j2]

SU3ii3y[{j1_,j2_}] := SU3ii3y[j1,j2]

SU3i3y[{j1_,j2_}] := SU3i3y[j1,j2]

SU3weights[{j1_,j2_}] := SU3weights[j1,j2]

End[]

Protect[HighestWeightSU3,SU3ii3y,SU3i3y,SU3weights]

EndPackage[]
```

USp.m

```
(* USp.m
   This package contains a function for evaluating the USp inner
product between polynomials.  Written by D. T. Abell,
21 March 1994. Added complex arguments 17 May 1994.  Added
USpNorm 22 June 1994. *)

BeginPackage["USp`"]

USp::usage = "The USp.m package defines for polynomials an inner
product, and its consequent norm, that is invariant under unitary
symplectic transformations."

USpInner::usage = "USpInner[qpvars][f,g] returns the USp(2n)
inner product between f and g.  Here f and g denote polynomials
in the 2n variables listed in qpvars."

USpNorm::usage = "USpNorm[qpvars][f] returns the USp(2n) norm
of f (i.e., Sqrt[<f,f>]).  Here f denotes a polynomial in the 2n
variables listed in qpvars."

Begin["`Private`"]

uspin[qps_][0,g_] := 0
uspin[qps_][f_,0] := 0

uspin[qps_][f_Plus,g_] := (uspin[qps][#,g]& /@ f)
uspin[qps_][f_,g_Plus] := (uspin[qps][f,#]& /@ g)

uspin[qps_][f_,g_] :=
  Module[{xf,xg,mon,cf,cg,usp},
         {xf,xg}=Exponent[#,qps]& /@ {f,g};
         If[xf=!=xg,0,
            mon=Times@@(qps^xf);
            {cf,cg}=Coefficient[#,mon]& /@ {f,g};
            usp=Times@@Factorial[xf];
            Conjugate[cf]*cg*usp] ]

USpInner[qps_][f_,g_] := uspin[qps][Expand[f],Expand[g]]

USpNorm[qps_][f_] := Sqrt[USpInner[qps][f,f]]

End[]

Protect[USpInner,USpNorm]

EndPackage[]
```

Appendix I. *Mathematica* Notebooks

This appendix contains all of the *Mathematica* "notebooks" referred to in the main text, most of which make use of the packages listed in Appendix H. These notebooks are arranged as follows, in order of appearance:

`SU2phiCG.ma` ..... §15.2.3
`GramXct_SU2.ma` ..... §15.2.4
`GramXct_U2.ma` ..... §15.2.5
`GramXct_SU3.ma` ..... §15.3.2
`GramXct_U1n.ma` ..... §15.4

SU2phiCG.ma

Using Clebsch-Gordan Coefficients and Ladder Operators to Compute the Higher-Order Basis Functions

This *Mathematica* notebook shows how to compute for four-dimensional phase space a set of basis functions that carry irreducible representations of $SU(2)$. The method used here employs the Clebsch-Gordan coefficients, supplied by *Mathematica*, and a lowering operator defined below.

■ Definitions and Functions

First let's import the packages that define Lie operators, the inner product <,>, and the basis elements of the $sp(4,\mathrm{R})$ Lie algebra.

```
<<ColonOps.m
<<USp.m
<<sp4.m
```

Now define the Hermitian basis elements `a[i]` for the $su(2)$ Lie subalgebra in $sp(4,\mathrm{R})$, and then go on to define the analogues of the various angular momentum operators usually defined in quantum mechanics.

```
{a[1],a[2],a[3]} = -I/2 {b[3],b[1],b[2]};

 (* Jx, Jy, Jz *)
Ax = Colon[qs,ps][a[1]];
Ay = Colon[qs,ps][a[2]];
Az = Colon[qs,ps][a[3]];

 (* J^2 *)
Asq = (ColonSqr[qs,ps][a[1]][#] +
       ColonSqr[qs,ps][a[2]][#] +
       ColonSqr[qs,ps][a[3]][#])&;

 (* ladder operators J+, J- *)
Aup = (Ax[#] + I Ay[#])&;
Adn = (Ax[#] - I Ay[#])&;

 (* coefficients for J^2, J+, J- *)
a2[j_] := j(j+1)
cu[j_,m_] := Sqrt[(j-m)(j+m+1)]
cd[j_,m_] := Sqrt[(j+m)(j-m+1)]
```

Here we define two abbreviations:

```
XA = ExpandAll;
rt2 = Sqrt[2];
```

All of the angular momentum-like operators defined above act with respect to the variables `{q1,q2,p1,p2}`, but we will want to express the basis functions we seek, the $\varphi(j,m;l,\mu)$, using the variables `{y1,y2,y3,y4}`. The following two functions convert back and forth between these two sets of variables.

```
toY[xpr_] := Expand[xpr /.
  {q1-> (y1+I*y4)/rt2,     q2-> (y1-I*y4)/(I rt2),
   p1-> (y2+I*y3)/(I rt2), p2-> (y2-I*y3)/rt2} ]
```

```
toQP[xpr_] := Expand[xpr /.
  {y1->(q1+I*q2)/rt2, y2->( p2+I*p1)/rt2,
   y3->(p1+I*p2)/rt2, y4->(-q2-I*q1)/rt2} ]
```

Also define the inner product $<,>$ and its corresponding norm specifically with respect to the y's.

```
yip = USpInner[{y1,y2,y3,y4}];
ynrm = USpNorm[{y1,y2,y3,y4}];
```

To determine the higher-order basis functions, we define the function `phisum[`$j1$`,`$j2$`,`$l2$`,`$\mu 2$`][`j`,`m`,`l`,`μ`]`, which forms a higher-order basis function φ in terms of a direct product of lower-order basis functions. We turn off the Clebsch-Gordan warning messages because non-physical Clebsch-Gordan coefficients are already defined to be zero and hence do no harm when they arise in the sum over `m2` in `phisum`.

```
phisum[j1_,j2_,l2_,mu2_][j_,m_,l_,mu_] :=
  Sum[ClebschGordan[{j1,m-m2},{j2,m2},{j,m}]*
       phi[j1,m-m2,l-l2,mu-mu2] * phi[j2,m2,l2,mu2],
      {m2,-j2,j2,1}]

Off[ClebschGordan::phy,ClebschGordan::tri]
```

We can use `phisum[]` to obtain the highest-spin basis polynomial that carries a given representation, and then use the lowering operator to obtain the remaining basis elements. Here we define the functions `lower[]` and `LowerAll[]` to perform these chores.

```
lower[j_,m_,f_] := toY[1/cd[j,m] Adn[toQP[f]]]

LowerAll[j_,l_,mu_] :=
  (phi[j,#-1,l,mu] = lower[j,#, phi[j,#,l,mu]])& /@
     Range[j,-j+1,-1]
```

The last function we define, `phirep[`j`,`l`,`μ`]`, simply returns all of the l-th degree basis functions that carry the representation labeled by spin j and index μ.

```
phirep[j_,l_,mu_] := phi[j,#,l,mu]& /@ Range[j,-j,-1]
```

■ Order 1

Begin by defining the basis functions of degree one.

□ Phi[1/2,1,1] ($j = 1/2$, $l = 1$, $\mu = 1$)

```
phi[1/2, 1/2,1,1] = y1;
phi[1/2,-1/2,1,1] = y2;
```

□ Phi[1/2,1,0]

```
phi[1/2, 1/2,1,0] = y3;
phi[1/2,-1/2,1,0] = y4;
```

■ Order 2

Now build the basis functions of degree two.

□ Phi[1,2,2]

Define `phi[1,1,2,2]` using `phi[1/2,1/2,1,1]` $\otimes$ `phi[1/2,1/2,1,1]`, and divide by `Sqrt[2]` to normalize the result.

```
phi[1,1,2,2] = phisum[1/2,1/2,1,1][1,1,2,2]/Sqrt[2]
```

```
    2
  y1
-------
Sqrt[2]
```

Now use the lowering operator to determine the other basis functions in this copy of spin-1,

```
LowerAll[1,2,2];
phirep[1,2,2] // Together
```

```
     2              2
   y1             y2
{-------, y1 y2, -------}
 Sqrt[2]        Sqrt[2]
```

and make sure they are properly normalized.

```
ynrm /@ %
```

```
{1, 1, 1}
```

□ Phi[1,2,1]

```
phi[1,1,2,1] = phisum[1/2,1/2,1,0][1,1,2,1]
```

```
y1 y3
```

```
LowerAll[1,2,1];
phirep[1,2,1] // Together
```

```
        Sqrt[2] y2 y3 + Sqrt[2] y1 y4
{y1 y3, -----------------------------, y2 y4}
                      2
```

```
ynrm /@ %
```

```
{1, 1, 1}
```

□ Phi[1,2,0]

```
phi[1,1,2,0] = phisum[1/2,1/2,1,0][1,1,2,0]/Sqrt[2]
```

```
    2
  y3
-------
Sqrt[2]
```

```
LowerAll[1,2,0];
phirep[1,2,0] // Together
```

```
     2              2
   y3             y4
{-------, y3 y4, -------}
 Sqrt[2]        Sqrt[2]
```

```
ynrm /@ %
```

```
{1, 1, 1}
```

□ Phi[0,2,1]

```
phi[0,0,2,1] = phisum[1/2,1/2,1,0][0,0,2,1] // Together
```

```
-(Sqrt[2] y2 y3) + Sqrt[2] y1 y4
--------------------------------
               2
```

```
ynrm[%]
```

```
1
```

■ Order 3

□ Phi[3/2,3,3]

```
phi[3/2,3/2,3,3] =
  phisum[1,1/2,1,1][3/2,3/2,3,3]/Sqrt[3]
```

```
    3
  y1
-------
Sqrt[6]
```

```
LowerAll[3/2,3,3];
phirep[3/2,3,3] // Together
```

```
     3      2           2       3
   y1     y1  y2   y1 y2      y2
{-------, -------, -------, -------}
 Sqrt[6]  Sqrt[2]  Sqrt[2]  Sqrt[6]
```

```
ynrm /@ %
```

```
{1, 1, 1, 1}
```

□ Phi[3/2,3,2]

```
phi[3/2,3/2,3,2] =
  phisum[1,1/2,1,0][3/2,3/2,3,2]
```

```
  2
y1  y3
-------
Sqrt[2]
```

```
LowerAll[3/2,3,2];
phirep[3/2,3,2] // Together
```

```
   2                                      2
 y1  y3   2 Sqrt[6] y1 y2 y3 + Sqrt[6] y1  y4
{-------, ----------------------------------,
 Sqrt[2]                  6

            2                             2
  Sqrt[6] y2  y3 + 2 Sqrt[6] y1 y2 y4  y2  y4
  ----------------------------------, -------}
                  6                   Sqrt[2]
```

```
ynrm /@ %
```

```
{1, 1, 1, 1}
```

□ Phi[3/2,3,1]

```
phi[3/2,3/2,3,1] =
  phisum[1,1/2,1,1][3/2,3/2,3,1]
```

```
     2
y1 y3
-------
Sqrt[2]
```

```
LowerAll[3/2,3,1];
phirep[3/2,3,1] // Together
```

```
      2                2
 y1 y3    Sqrt[6] y2 y3  + 2 Sqrt[6] y1 y3 y4
{-------, ----------------------------------,
 Sqrt[2]                   6

                                      2       2
  2 Sqrt[6] y2 y3 y4 + Sqrt[6] y1 y4   y2 y4
  ----------------------------------, -------}
                   6                  Sqrt[2]
```

```
ynrm /@ %
```

```
{1, 1, 1, 1}
```

□ Phi[3/2,3,0]

```
phi[3/2,3/2,3,0] =
  phisum[1,1/2,1,0][3/2,3/2,3,0]/Sqrt[3]
```

```
    3
  y3
-------
Sqrt[6]
```

```
LowerAll[3/2,3,0];
phirep[3/2,3,0] // Together
```

```
     3      2           2       3
   y3     y3  y4   y3 y4      y4
{-------, -------, -------, -------}
 Sqrt[6]  Sqrt[2]  Sqrt[2]  Sqrt[6]
```

```
ynrm /@ %
```

```
{1, 1, 1, 1}
```

□ Phi[1/2,3,2]

```
phi[1/2,1/2,3,2] =
  phisum[1,1/2,1,0][1/2,1/2,3,2]
```

```
                2
  y1 y2 y3    y1  y4
-(--------) + -------
  Sqrt[3]     Sqrt[3]
```

```
LowerAll[1/2,3,2];
phirep[1/2,3,2] // Together
```

```
                                      2
 -(Sqrt[3] y1 y2 y3) + Sqrt[3] y1  y4
{-----------------------------------,
                 3

              2
  -(Sqrt[3] y2  y3) + Sqrt[3] y1 y2 y4
  ------------------------------------}
                  3
```

```
ynrm /@ %
```

```
{1, 1}
```

□ Phi[1/2,3,1]

```
phi[1/2,1/2,3,1] =
  phisum[1,1/2,1,1][1/2,1/2,3,1]
```

```
     2
y2 y3     y1 y3 y4
------- - --------
Sqrt[3]   Sqrt[3]
```

```
LowerAll[1/2,3,1];
phirep[1/2,3,1] // Together
```

```
              2
 Sqrt[3] y2 y3  - Sqrt[3] y1 y3 y4
{---------------------------------,
                 3

                                    2
  Sqrt[3] y2 y3 y4 - Sqrt[3] y1 y4
  --------------------------------}
                  3
```

```
ynrm /@ %
```

```
{1, 1}
```

■ Order 4

□ Phi[2,4,4]

```
phi[2,2,4,4] = phisum[3/2,1/2,1,1][2,2,4,4]/2
```

```
     4
   y1
---------
2 Sqrt[6]
```

```
LowerAll[2,4,4];
phirep[2,4,4] // Together
```

```
      4       3        2   2       3        4
    y1      y1  y2   y1  y2   y1 y2       y2
{---------, -------, -------, -------, ---------}
 2 Sqrt[6]  Sqrt[6]     2     Sqrt[6]  2 Sqrt[6]
```

```
ynrm /@ %
```

```
{1, 1, 1, 1, 1}
```

□ Phi[2,4,3]

```
phi[2,2,4,3] = phisum[3/2,1/2,1,0][2,2,4,3]
```

```
  3
y1  y3
-------
Sqrt[6]
```

```
LowerAll[2,4,3];
phirep[2,4,3] // Together
```

```
   3                  2                    3
 y1  y3   3 Sqrt[6] y1  y2 y3 + Sqrt[6] y1  y4
{-------, ------------------------------------,
 Sqrt[6]                   12

      2        2
  y1 y2  y3 + y1  y2 y4
  ---------------------,
           2

           3                      2       3
  Sqrt[6] y2  y3 + 3 Sqrt[6] y1 y2  y4  y2  y4
  ------------------------------------, -------}
                  12                   Sqrt[6]
```

```
ynrm /@ %
```

```
{1, 1, 1, 1, 1}
```

□ Phi[2,4,2]

```
phi[2,2,4,2] = phisum[3/2,1/2,1,0][2,2,4,2]/Sqrt[2]
```

```
  2   2
y1  y3
-------
   2
```

```
LowerAll[2,4,2];
phirep[2,4,2] // Together
```

```
   2   2          2     2
 y1  y3   y1 y2 y3  + y1  y3 y4
{-------, --------------------,
    2               2

            2   2
  (Sqrt[6] y2  y3  + 4 Sqrt[6] y1 y2 y3 y4 +

                              2                 2
              2   2          y2  y3 y4 + y1 y2 y4
    Sqrt[6] y1  y4 ) / 12, ---------------------,
                                    2

    2   2
  y2  y4
  -------}
     2
```

```
ynrm /@ %
```

```
{1, 1, 1, 1, 1}
```

□ Phi[2,4,1]

```
phi[2,2,4,1] = phisum[3/2,1/2,1,1][2,2,4,1]
```

```
     3
y1 y3
-------
Sqrt[6]
```

```
LowerAll[2,4,1];
phirep[2,4,1] // Together
```

```
      3                3                   2
 y1 y3    Sqrt[6] y2 y3  + 3 Sqrt[6] y1 y3  y4
{-------, ----------------------------------,
 Sqrt[6]                   12

       2             2
  y2 y3  y4 + y1 y3 y4
  --------------------,
            2

                    2                3       3
  3 Sqrt[6] y2 y3 y4  + Sqrt[6] y1 y4   y2 y4
  ------------------------------------, -------}
                   12                   Sqrt[6]
```

```
ynrm /@ %
```

```
{1, 1, 1, 1, 1}
```

□ Phi[2,4,0]

```
phi[2,2,4,0] = phisum[3/2,1/2,1,0][2,2,4,0]/2
```

```
     4
   y3
---------
2 Sqrt[6]
```

```
LowerAll[2,4,0];
phirep[2,4,0] // Together
```

```
      4       3        2   2       3        4
    y3      y3  y4   y3  y4   y3 y4       y4
{---------, -------, -------, -------, ---------}
 2 Sqrt[6]  Sqrt[6]     2     Sqrt[6]  2 Sqrt[6]
```

```
ynrm /@ %
```

```
{1, 1, 1, 1, 1}
```

□ Phi[1,4,3]

```
phi[1,1,4,3] = phisum[3/2,1/2,1,0][1,1,4,3]
```

```
    2             3
-(y1  y2 y3)    y1  y4
------------ + ---------
 2 Sqrt[2]     2 Sqrt[2]
```

```
LowerAll[1,4,3];
phirep[1,4,3] // Together
```

```
             2                    3
 -(Sqrt[2] y1  y2 y3) + Sqrt[2] y1  y4
{-----------------------------------,
                   4

         2         2
  -(y1 y2  y3) + y1  y2 y4
  ------------------------,
            2

             3                    2
  -(Sqrt[2] y2  y3) + Sqrt[2] y1 y2  y4
  -----------------------------------}
                   4
```

```
ynrm /@ %
```

```
{1, 1, 1}
```

□ Phi[1,4,2]

```
phi[1,1,4,2] = phisum[3/2,1/2,1,0][1,1,4,2] Sqrt[3/2] // XA
```

```
          2      2
-(y1 y2 y3 )   y1  y3 y4
------------ + ---------
     2             2
```

```
LowerAll[1,4,2];
phirep[1,4,2] // Together
```

```
           2      2
 -(y1 y2 y3 ) + y1  y3 y4
{------------------------,
            2

              2   2              2   2
  -(Sqrt[2] y2  y3 ) + Sqrt[2] y1  y4
  -----------------------------------,
                   4

      2                  2
  -(y2  y3 y4) + y1 y2 y4
  -----------------------}
            2
```

```
ynrm /@ %
```

```
{1, 1, 1}
```

□ Phi[1,4,1]

```
phi[1,1,4,1] = phisum[3/2,1/2,1,1][1,1,4,1]
```

```
      3          2
 y2 y3      y1 y3  y4
--------- - ---------
2 Sqrt[2]   2 Sqrt[2]
```

```
LowerAll[1,4,1];
phirep[1,4,1] // Together
```

```
              3                2
 Sqrt[2] y2 y3  - Sqrt[2] y1 y3  y4
{---------------------------------,
                4

       2             2
  y2 y3  y4 - y1 y3 y4
  --------------------,
           2

                  2                3
  Sqrt[2] y2 y3 y4  - Sqrt[2] y1 y4
  ---------------------------------}
                  4
```

```
ynrm /@ %
```

```
{1, 1, 1}
```

□ Phi[0,4,2]

```
phi[0,0,4,2] = phisum[1,1,2,0][0,0,4,2]
```

```
   2   2                    2   2
 y2  y3     y1 y2 y3 y4    y1  y4
--------- - ----------- + ---------
2 Sqrt[3]     Sqrt[3]     2 Sqrt[3]
```

```
Together[%]
```

```
           2   2
(Sqrt[3] y2  y3  - 2 Sqrt[3] y1 y2 y3 y4 +

              2   2
    Sqrt[3] y1  y4 ) / 6
```

```
ynrm[%]
```

```
1
```

■ Order 5

□ Phi[5/2,5,5]

```
phi[5/2,5/2,5,5] = phisum[3/2,1,2,2][5/2,5/2,5,5]/Sqrt[10]
```

```
     5
   y1
----------
2 Sqrt[30]
```

```
LowerAll[5/2,5,5];
phirep[5/2,5,5] // Together
```

```
      5         4          3   2      2   3
     y1        y1  y2     y1  y2     y1  y2
{----------, ---------, ---------, ---------,
 2 Sqrt[30]  2 Sqrt[6]  2 Sqrt[3]  2 Sqrt[3]

       4         5
    y1 y2        y2
   ---------, ----------}
   2 Sqrt[6]  2 Sqrt[30]
```

```
ynrm /@ %
```

```
{1, 1, 1, 1, 1, 1}
```

□ Phi[5/2,5,4]

```
phi[5/2,5/2,5,4] = phisum[3/2,1,2,1][5/2,5/2,5,4]/2
```

```
   4
 y1  y3
---------
2 Sqrt[6]
```

```
LowerAll[5/2,5,4];
phirep[5/2,5,4] // Together
```

```
    4                    3                     4
  y1  y3    4 Sqrt[30] y1  y2 y3 + Sqrt[30] y1  y4
{---------, ------------------------------------,
 2 Sqrt[6]                   60

              2   2                   3
  3 Sqrt[15] y1  y2  y3 + 2 Sqrt[15] y1  y2 y4
  ------------------------------------------,
                      30

                3                   2   2
  2 Sqrt[15] y1 y2  y3 + 3 Sqrt[15] y1  y2  y4
  ------------------------------------------,
                      30

            4                      3        4
  Sqrt[30] y2  y3 + 4 Sqrt[30] y1 y2  y4   y2  y4
  ----------------------------------, ---------}
                  60                  2 Sqrt[6]
```

```
ynrm /@ %
```

```
{1, 1, 1, 1, 1, 1}
```

□ Phi[5/2,5,3]

```
phi[5/2,5/2,5,3] = phisum[3/2,1,2,1][5/2,5/2,5,3]/Sqrt[6]
```

```
   3   2
 y1  y3
---------
2 Sqrt[3]
```

```
LowerAll[5/2,5,3];
phirep[5/2,5,3] // Together
```

```
    3   2
  y1  y3
{---------,
 2 Sqrt[3]

                2      2                3
   3 Sqrt[15] y1  y2 y3  + 2 Sqrt[15] y1  y3 y4
   ------------------------------------------,
                      30

                  2   2                2
  (3 Sqrt[30] y1 y2  y3  + 6 Sqrt[30] y1  y2 y3 y4 +

                3   2
     Sqrt[30] y1  y4 ) / 60,

              3   2                   2
  (Sqrt[30] y2  y3  + 6 Sqrt[30] y1 y2  y3 y4 +


                  2      2
     3 Sqrt[30] y1  y2 y4 ) / 60,

              3                         2   2
  2 Sqrt[15] y2  y3 y4 + 3 Sqrt[15] y1 y2  y4
  ------------------------------------------,
                      30

     3   2
   y2  y4
  ---------}
  2 Sqrt[3]
```

```
ynrm /@ %
```

```
{1, 1, 1, 1, 1, 1}
```

□ Phi[5/2,5,2]

```
phi[5/2,5/2,5,2] = phisum[3/2,1,2,1][5/2,5/2,5,2]/Sqrt[6]
```

```
   2   3
 y1  y3
---------
2 Sqrt[3]
```

```
LowerAll[5/2,5,2];
phirep[5/2,5,2] // Together
```

```
    2   3
  y1  y3
{---------,
 2 Sqrt[3]
```

```
                    3               2   2
 2 Sqrt[15] y1 y2 y3  + 3 Sqrt[15] y1  y3  y4
 ----------------------------------------,
                   30

           2   3                     2
(Sqrt[30] y2  y3  + 6 Sqrt[30] y1 y2 y3  y4 +

               2      2
  3 Sqrt[30] y1  y3 y4 ) / 60,

             2   2                            2
(3 Sqrt[30] y2  y3  y4 + 6 Sqrt[30] y1 y2 y3 y4  +

             2   3
  Sqrt[30] y1  y4 ) / 60,

            2      2                     3
3 Sqrt[15] y2  y3 y4  + 2 Sqrt[15] y1 y2 y4
----------------------------------------,
                   30

   2   3
 y2  y4
---------}
2 Sqrt[3]
```

```
ynrm /@ %
```

```
{1, 1, 1, 1, 1, 1}
```

□ Phi[5/2,5,1]

```
phi[5/2,5/2,5,1] = phisum[3/2,1,2,1][5/2,5/2,5,1]/2
```

```
      4
 y1 y3
---------
2 Sqrt[6]
```

```
LowerAll[5/2,5,1];
phirep[5/2,5,1] // Together
```

```
       4                 4                   3
  y1 y3     Sqrt[30] y2 y3  + 4 Sqrt[30] y1 y3  y4
{---------, ------------------------------------,
 2 Sqrt[6]                  60

                3                     2   2
  2 Sqrt[15] y2 y3  y4 + 3 Sqrt[15] y1 y3  y4
  ----------------------------------------,
                   30

                2   2                     3
  3 Sqrt[15] y2 y3  y4  + 2 Sqrt[15] y1 y3 y4
  ----------------------------------------,
                   30
```

```
                    3                 4        4
  4 Sqrt[30] y2 y3 y4  + Sqrt[30] y1 y4    y2 y4
  ------------------------------------, ---------}
                   60                   2 Sqrt[6]
```

```
ynrm /@ %
```

```
{1, 1, 1, 1, 1, 1}
```

□ Phi[5/2,5,0]

```
phi[5/2,5/2,5,0] = phisum[3/2,1,2,0][5/2,5/2,5,0]/Sqrt[10]
```

```
     5
   y3
----------
2 Sqrt[30]
```

```
LowerAll[5/2,5,0];
phirep[5/2,5,0] // Together
```

```
      5         4          3   2      2   3
    y3        y3  y4     y3  y4     y3  y4
{----------, ---------, ---------, ---------,
 2 Sqrt[30]  2 Sqrt[6]  2 Sqrt[3]  2 Sqrt[3]

        4         5
   y3 y4        y4
  ---------, ----------}
  2 Sqrt[6]  2 Sqrt[30]
```

```
ynrm /@ %
```

```
{1, 1, 1, 1, 1, 1}
```

□ Phi[3/2,5,4]

```
phi[3/2,3/2,5,4] =
  phisum[3/2,1,2,1][3/2,3/2,5,4] Sqrt[2/3] // XA
```

```
    3            4
  y1  y2 y3     y1  y4
-(---------) + --------
  Sqrt[30]     Sqrt[30]
```

```
LowerAll[3/2,5,4];
phirep[3/2,5,4] // Together
```

```
              3                    4
 -(Sqrt[30] y1  y2 y3) + Sqrt[30] y1  y4
{-------------------------------------,
                   30

              2   2                  3
  -(Sqrt[10] y1  y2  y3) + Sqrt[10] y1  y2 y4
  ------------------------------------------,
                     10

                3                   2   2
  -(Sqrt[10] y1 y2  y3) + Sqrt[10] y1  y2  y4
  ------------------------------------------,
                     10
```

```
                4                      3
  -(Sqrt[30] y2  y3) + Sqrt[30] y1 y2  y4
  ----------------------------------------}
                   30
```

```
ynrm /@ %
```

```
{1, 1, 1, 1}
```

□ Phi[3/2,5,3]

```
phi[3/2,3/2,5,3] =
  phisum[3/2,1,2,1][3/2,3/2,5,3] Sqrt[6] // XA
```

```
    2      2      3
  y1  y2 y3     y1  y3 y4
-(----------) + ---------
   Sqrt[10]     Sqrt[10]
```

```
LowerAll[3/2,5,3];
phirep[3/2,5,3] // Together
```

```
              2      2               3
 -(Sqrt[10] y1  y2 y3 ) + Sqrt[10] y1  y3 y4
{----------------------------------------,
                     10

                    2   2              2
  (-2 Sqrt[30] y1 y2  y3  + Sqrt[30] y1  y2 y3 y4 +

                3   2
     Sqrt[30] y1  y4 ) / 30,

                3   2                  2
  (-(Sqrt[30] y2  y3 ) - Sqrt[30] y1 y2  y3 y4 +

                  2      2
     2 Sqrt[30] y1  y2 y4 ) / 30,

              3                        2   2
  -(Sqrt[10] y2  y3 y4) + Sqrt[10] y1 y2  y4
  ------------------------------------------}
                     10
```

```
ynrm /@ %
```

```
{1, 1, 1, 1}
```

□ Phi[3/2,5,2]

```
phi[3/2,3/2,5,2] =
  phisum[3/2,1,2,1][3/2,3/2,5,2] Sqrt[6] // XA
```

```
       3     2   2
y1 y2 y3    y1  y3  y4
--------- - ----------
Sqrt[10]     Sqrt[10]
```

```
LowerAll[3/2,5,2];
phirep[3/2,5,2] // Together
```

```
                  3             2   2
 Sqrt[10] y1 y2 y3  - Sqrt[10] y1  y3  y4
{--------------------------------------,
                   10

             2   3                    2
  (Sqrt[30] y2  y3  + Sqrt[30] y1 y2 y3  y4 -


                  2      2
     2 Sqrt[30] y1  y3 y4 ) / 30,

               2   2                          2
  (2 Sqrt[30] y2  y3  y4 - Sqrt[30] y1 y2 y3 y4  -

               2   3
     Sqrt[30] y1  y4 ) / 30,

            2      2                    3
  Sqrt[10] y2  y3 y4  - Sqrt[10] y1 y2 y4
  ---------------------------------------}
                   10
```

```
ynrm /@ %
```

```
{1, 1, 1, 1}
```

□ Phi[3/2,5,1]

```
phi[3/2,3/2,5,1] =
  phisum[3/2,1,2,1][3/2,3/2,5,1] Sqrt[2/3] // XA
```

```
      4         3
 y2 y3     y1 y3  y4
-------- - ---------
Sqrt[30]   Sqrt[30]
```

```
LowerAll[3/2,5,1];
phirep[3/2,5,1] // Together
```

```
               4                3
 Sqrt[30] y2 y3  - Sqrt[30] y1 y3  y4
{-----------------------------------,
                  30

               3                   2   2
  Sqrt[10] y2 y3  y4 - Sqrt[10] y1 y3  y4
  ---------------------------------------,
                   10

               2   2                    3
  Sqrt[10] y2 y3  y4  - Sqrt[10] y1 y3 y4
  ---------------------------------------,
                   10

                  3                4
  Sqrt[30] y2 y3 y4  - Sqrt[30] y1 y4
  -----------------------------------}
                  30
```

```
ynrm /@ %
```

```
{1, 1, 1, 1}
```

□ Phi[1/2,5,3]

```
phi[1/2,1/2,5,3] =
  phisum[3/2,1,2,1][1/2,1/2,5,3] Sqrt[3/2] // XA
```

```
       2   2      2               3   2
-(y1 y2  y3 )   y1  y2 y3 y4    y1  y4
------------- + ------------ - ---------
  2 Sqrt[6]       Sqrt[6]      2 Sqrt[6]
```

```
LowerAll[1/2,5,3];
phirep[1/2,5,3] // Together
```

```
                  2   2                2
{(-(Sqrt[6] y1 y2  y3 ) + 2 Sqrt[6] y1  y2 y3 y4 -

                3   2
     Sqrt[6] y1  y4 ) / 12,

                3   2                   2
  (-(Sqrt[6] y2  y3 ) + 2 Sqrt[6] y1 y2  y3 y4 -

                2      2
     Sqrt[6] y1  y2 y4 ) / 12}
```

```
ynrm /@ %
```

```
{1, 1}
```

□ Phi[1/2,5,2]

```
phi[1/2,1/2,5,2] =
  phisum[3/2,1,2,1][1/2,1/2,5,2] Sqrt[3/2] // XA
```

```
    2   3            2        2      2
-(y2  y3 )   y1 y2 y3  y4   y1  y3 y4
---------- + ------------ - ----------
2 Sqrt[6]      Sqrt[6]      2 Sqrt[6]
```

```
LowerAll[1/2,5,2];
phirep[1/2,5,2] // Together
```

```
               2   3                      2
{(-(Sqrt[6] y2  y3 ) + 2 Sqrt[6] y1 y2 y3  y4 -

                2      2
     Sqrt[6] y1  y3 y4 ) / 12,

                2   2                            2
  (-(Sqrt[6] y2  y3  y4) + 2 Sqrt[6] y1 y2 y3 y4  -

                2   3
     Sqrt[6] y1  y4 ) / 12}
```

```
ynrm /@ %
```

```
{1, 1}
```

GramXct_SU2.ma

Continuum-Limit Gram Eigenvalues for Two Degrees of Freedom using $SU(2)$

This *Mathematica* notebook shows how to compute the continuum-limit Gram eigenvalues for the case $n = 2$ when we include all linear symplectic transformations in $SU(2)$.

■ Definitions and Functions

First import the packages that define the inner product <,> and the basis functions $\varphi(j, m; l, \mu)$. Then define the inner product <,> specifically with respect to the y's, and define the q's in terms of the y's.

```
<<USp.m
<<SU2phi.m

yip = USpInner[{y1,y2,y3,y4}];

q1 = (y1 + I y4)/Sqrt[2];
q2 = (y1 - I y4)/(I Sqrt[2]);
```

Now define the function `Nc` and the q-monomials `Qlk`:

```
Nc[l_,c_] := If[c==l/2, 1, 2]
Qlk[l_,k_] := q1^(l-k) q2^k/Sqrt[(l-k)! k!]
```

The following function returns the continuum-limit Gram eigenvalues:

```
GramEV4[l_,j_,mu_] := 1/((l+1)*(2j+1)) *
  Sum[Nc[l,c] Abs[ yip[ phi[j,mu-l/2,l,mu], Qlk[l,c] ] ]^2,
      {c,0,Floor[l/2]}]
```

■ Gram Eigenvalues

☐ Eigenvalues for order 1

```
GramEV4[1, 1/2, 0]
```

```
1
-
4
```

☐ Eigenvalues for order 2

```
GramEV4[2, 1, 1]
```

```
1
--
18
```

```
GramEV4[2, 1, 0]
```

```
1
-
9
```

```
GramEV4[2, 0, 1]
```

```
1
-
6
```

☐ Eigenvalues for order 3

```
GramEV4[3, 3/2, 1]
```

```
1
--
48
```

```
GramEV4[3, 3/2, 0]
```

```
1
--
16
```

```
GramEV4[3, 1/2, 1]
```

```
1
--
12
```

☐ Eigenvalues for order 4

```
GramEV4[4, 2, 2]
```

```
 1
---
150
```

```
GramEV4[4, 2, 1]
```

```
 1
---
100
```

```
GramEV4[4, 2, 0]
```

```
1
--
25
```

```
GramEV4[4, 1, 2]
```

```
1
--
30
```

```
GramEV4[4, 1, 1]
```

```
1
--
20
```

```
GramEV4[4, 0, 2]
```

```
1
--
15
```

☐ Eigenvalues for order 5

```
GramEV4[5, 5/2, 2]
```

```
 1
---
360
```

```
GramEV4[5, 5/2, 1]

 1
---
180

GramEV4[5, 5/2, 0]

1
--
36

GramEV4[5, 3/2, 2]

1
--
60

GramEV4[5, 3/2, 1]

1
--
30

GramEV4[5, 1/2, 2]

1
--
24
```

GramXct_U2.ma

Continuum-Limit Gram Eigenvalues for Two Degrees of Freedom using $U(2)$

This *Mathematica* notebook shows how to compute the continuum-limit Gram eigenvalues for the case $n = 2$ when we include all linear symplectic transformations in $U(2)$.

■ Definitions and Functions

First import the packages that define the inner product <,> and the basis functions $\varphi(j, m; l, \mu)$. Then define the y's, what $:b[0]:$ does to the y's, and the inner product <,> specifically with respect to the y's.

```
<<USp.m
<<SU2phi.m

ys = {y1,y2,y3,y4};
bys = {-y3,-y4,y1,y2};
ip = USpInner[ys];
```

Also define the operator `Rop` $= \exp(-\theta/2\,:b[0]:)$ according to its action on the y's, and define its matrix elements `R`.

```
Rop[th_,f_] := f /.
 Thread[ys -> ys Cos[th/2] - bys Sin[th/2]]

R[th_,l_,j_,mu_,nu_] :=
  ip[ phi[j,j,l,mu], Rop[th, phi[j,j,l,nu]] ]
```

Now define a function `Rmat` that returns the matrix representation for the operator `Rop`. The obvious way to do this defines `Rmat` using `Table` in a straightforward manner. To take advantage of the symmetry, however, we define `Rsym`; it looks messier, but computes more quickly.

```
Rmat[th_,l_,j_] :=
  Table[R[th,l,j,mu,nu],
        {mu,l/2-j,l/2+j,1},{nu,l/2-j,l/2+j,1}]

Rsym[th_,l_Integer,j_] :=
  Module[{rj,l2,os,mu,nu,re,ret},
    rj=Table[0,{2j+1},{2j+1}];
    l2=l/2;
    os=1-(l2-j);
    For[mu=l2-j, mu<=l2+j, mu++,
        rj[[mu+os,mu+os]] = R[th,l,j,mu,mu];
        For[nu=mu+1, nu<=l2+j, nu++,
            re = R[th,l,j,mu,nu];
            rj[[mu+os,nu+os]] = re;
            rj[[nu+os,mu+os]] = re /. th->(-th);
           ]
       ];
    rj] /; IntegerQ[l/2-j]
```

We need two more tools: a diagonal matrix containing the $SU(2)$ Gram eigenvalues, and an integral over the $U(1)$ part of $U(2)$.

```
 (* see below for the gramev4[l,j,mu] *)
Lambda[l_,j_] := DiagonalMatrix[
  Table[gramev4[l,j,mu], {mu,l/2-j,l/2+j,1}] ]

int[f_] := 1/(2 Pi) * Integrate[f,{th,0,2 Pi}]
```

We can now define functions that return the Gram matrix and its eigenvalues. Here we actually define these functions just for the block labeled j.

```
Gram4u[l_,j_] :=
  Module[{rj,rjm},
         rj = Rmat[th,l,j];
         rjm = rj /. th->(-th);
         int[rj.Lambda[l,j].rjm] ]

GramEV4u[l_,j_] := Eigenvalues[Gram4u[l,j]]
```

As with `Rmat`, we can use the known symmetry of the Gram matrix to speed up the calculation:

```
GramSym4u[l_Integer,j_] :=
  Module[{rj,rjm,kj,gm,l2,os,mu,nu,ge},
    rj = Rsym[th,l,j];
    rjm = rj /. th->(-th);
    kj = rj.Lambda[l,j].rjm;
    gm=Table[0,{2j+1},{2j+1}];
    l2=l/2;
    os=1-(l2-j);
    For[mu=l2-j, mu<=l2+j, mu++,
        gm[[mu+os,mu+os]] = int[kj[[mu+os,mu+os]]];
        For[nu=mu+1, nu<=l2+j, nu++,
            ge = int[kj[[mu+os,nu+os]]];
            gm[[mu+os,nu+os]] = ge;
            gm[[nu+os,mu+os]] = ge;
           ]
       ];
    gm] /; IntegerQ[l/2-j]

GramSymEV4u[l_,j_] := Eigenvalues[GramSym4u[l,j]]
```

□ Gram eigenvalues from the SU(2) calculation

Here we list all of the $SU(2)$ Gram eigenvalues, `gramev4[`j`,`l`,`μ`]`, for $l \leq 5$:

```
gramev4[1, 1/2, 1] = 1/4;
gramev4[1, 1/2, 0] = 1/4;

gramev4[2,  1,  2] = 1/9;
gramev4[2,  1,  1] = 1/18;
gramev4[2,  1,  0] = 1/9;
gramev4[2,  0,  1] = 1/6;

gramev4[3, 3/2, 3] = 1/16;
gramev4[3, 3/2, 2] = 1/48;
gramev4[3, 3/2, 1] = 1/48;
gramev4[3, 3/2, 0] = 1/16;
gramev4[3, 1/2, 2] = 1/12;
```

```
gramev4[3, 1/2, 1] = 1/12;

gramev4[4,  2,  4] = 1/25;
gramev4[4,  2,  3] = 1/100;
gramev4[4,  2,  2] = 1/150;
gramev4[4,  2,  1] = 1/100;
gramev4[4,  2,  0] = 1/25;
gramev4[4,  1,  3] = 1/20;
gramev4[4,  1,  2] = 1/30;
gramev4[4,  1,  1] = 1/20;
gramev4[4,  0,  2] = 1/15;

gramev4[5, 5/2, 5] = 1/36;
gramev4[5, 5/2, 4] = 1/180;
gramev4[5, 5/2, 3] = 1/360;
gramev4[5, 5/2, 2] = 1/360;
gramev4[5, 5/2, 1] = 1/180;
gramev4[5, 5/2, 0] = 1/36;
gramev4[5, 3/2, 4] = 1/30;
gramev4[5, 3/2, 3] = 1/60;
gramev4[5, 3/2, 2] = 1/60;
gramev4[5, 3/2, 1] = 1/30;
gramev4[5, 1/2, 3] = 1/24;
gramev4[5, 1/2, 2] = 1/24;
```

■ Gram Eigenvalues for U(2)

□ Order 1

```
GramSymEV4u[1,1/2]

 1  1
{-, -}
 4  4
```

□ Order 2

```
GramSymEV4u[2,1]

 1   1   1
{--, --, -}
 12  12  9

GramSymEV4u[2,0]

 1
{-}
 6
```

□ Order 3

```
GramSymEV4u[3,3/2]

 1   1   5   5
{--, --, --, --}
 32  32  96  96
```

```
GramSymEV4u[3,1/2]
```

```
 1   1
{--, --}
 12  12
```

□ Order 4

```
GramSymEV4u[4,2]
```

```
 1   1   1   1   19
{--, --, --, --, ---}
 80  80  40  40  600
```

```
GramSymEV4u[4,1]
```

```
 1   1   1
{--, --, --}
 24  24  20
```

```
GramSymEV4u[4,0]
```

```
 1
{--}
 15
```

□ Order 5

```
GramSymEV4u[5,5/2]
```

```
  1    1    7    7    3    3
{---, ---, ---, ---, ---, ---}
 192  192  576  576  160  160
```

```
GramSymEV4u[5,3/2]
```

```
 1   1    7    7
{--, --, ---, ---}
 48  48  240  240
```

```
GramSymEV4u[5,1/2]
```

```
 1   1
{--, --}
 24  24
```

GramXct_SU3.ma

Continuum-Limit Gram Eigenvalues for Three Degrees of Freedom using $SU(3)$

This *Mathematica* notebook shows how to compute the continuum-limit Gram eigenvalues for the case $n = 3$ when we include all linear symplectic transformations in $SU(3)$.

■ Definitions

First import the packages that define the $SU(3)$ basis functions `psi[]` and the weights for the irreducible representations of $SU(3)$.

```
<<sp6tools.m
<<SU3wts.m
```

Now list representative elements for each of the equivalence classes of Q's under permutation of q-indices. Also list the order of each equivalence class.

```
Qc[1] = {q1};
Qc[2] = {q1^2/Sqrt[2], q1 q2};
Qc[3] = {q1^3/Sqrt[3!], q1^2 q2/Sqrt[2], q1 q2 q3};
Qc[4] = {q1^4/Sqrt[4!], q1^3 q2/Sqrt[3!], q1^2 q2^2/2,
         q1^2 q2 q3/Sqrt[2]};
Qc[5] = {q1^5/Sqrt[5!], q1^4 q2/Sqrt[4!],
         q1^3 q2^2/Sqrt[3! 2], q1^3 q2 q3/Sqrt[3!],
         q1^2 q2^2 q3/2};
Qc[6] = {q1^6/Sqrt[6!], q1^5 q2/Sqrt[5!],
         q1^4 q2^2/Sqrt[4! 2], q1^4 q2 q3/Sqrt[4!],
         q1^3 q2^3/(3!), q1^3 q2^2 q3/Sqrt[3! 2!],
         q1^2 q2^2 q3^2/Sqrt[2 2 2]};
Qc[7] = {q1^7/Sqrt[7!], q1^6 q2/Sqrt[6!],
         q1^5 q2^2/Sqrt[5! 2], q1^5 q2 q3/Sqrt[5!],
         q1^4 q2^3/Sqrt[4! 3!], q1^4 q2^2 q3/Sqrt[4! 2!],
         q1^3 q2^3 q3/(3!), q1^3 q2^2 q3^2/Sqrt[3! 2 2]};

Nc[1] = {3};
Nc[2] = {3,3};
Nc[3] = {3,6,1};
Nc[4] = {3,6,3,3};
Nc[5] = {3,6,6,3,3};
Nc[6] = {3,6,6,3,3,6,1};
Nc[7] = {3,6,6,3,6,6,3,3};
```

The following function returns the values of `k2` and `k3`—the exponents of `q2` and `q3` for a given Q:

```
K23[Q_] := Exponent[Q,#]& /@ {q2,q3}
```

The following two functions return the ranges of the eigenvalues `I3` and `Y` for a Q defined by the values `k2` and `k3`:

```
I3range[k2_,k3_] := Range[-(k2+k3)/2,(k2+k3)/2,1]
Yrange[l_,k2_,k3_] :=
  Range[-(2l-k2-k3)/3,(2l-k2-k3)/3,If[k2==0==k3,4/3,2/3]]
```

The following two functions together compute the continuum-limit Gram eigenvalues:

```
nusum[l_,j1_,j2_,Q_] :=
  Module[k2,k3,i3s,ys,ii3ys,imax},
   k2,k3}=K23[Q];
   i3s = I3range[k2,k3];
   ys = Yrange[l,k2,k3];
   ii3ys = Select[SU3ii3y[j1,j2],MemberQ[i3s,#[[2]]]&];
   ii3ys = Select[ii3ys,MemberQ[ys,#[[3]]]&];
   (* imax = Max[i3s];
      ii3ys = Select[ii3ys,#[[1]]<=imax&]; *)
   Plus @@
     (zip[psi[j1,j2,(Sequence @@ #),l],toZ[Q]]^2& /@ ii3ys)]

GramEV6[l_,j1_,j2_] := 2/((l+1)(l+2)SU3dim[j1,j2]) *
  Plus @@ (Nc[l]*(nusum[l,j1,j2,#]& /@ Qc[l]))
```

■ Gram Eigenvalues

□ Eigenvalues for order 1

```
GramEV6[1,1,0]
```

```
1
-
6
```

□ Eigenvalues for order 2

```
GramEV6[2,2,0]
```

```
1
--
24
```

```
GramEV6[2,1,1]
```

```
5
--
96
```

```
GramEV6[2,0,0]
```

```
1
--
12
```

□ Eigenvalues for order 3

```
GramEV6[3,3,0]
```

```
1
--
80
```

```
GramEV6[3,2,1]
```

```
 3
---
160
```

```
GramEV6[3,1,0]
```

```
1
--
32
```

□ Eigenvalues for order 4

```
GramEV6[4,4,0]
```

```
 1
---
240
```

```
GramEV6[4,3,1]
```

```
 7
---
960
```

```
GramEV6[4,2,2]
```

```
 19
----
2160
```

```
GramEV6[4,2,0]
```

```
1
--
80
```

```
GramEV6[4,1,1]
```

```
 7
---
480
```

```
GramEV6[4,0,0]
```

```
1
--
48
```

□ Eigenvalues for order 5

```
GramEV6[5,5,0]
```

```
 1
---
672
```

```
GramEV6[5,4,1]
```

```
 1
---
336
```

```
GramEV6[5,3,2]
```

```
 17
----
4032
```

```
GramEV6[5,3,0]

 1
---
192

GramEV6[5,2,1]

 1
---
144

GramEV6[5,1,0]

1
--
96
```

□ Eigenvalues for order 6

```
GramEV6[6,6,0]

 1
----
1792

GramEV6[6,5,1]

 9
----
7168

GramEV6[6,4,2]

 11
----
5376

GramEV6[6,3,3]

 69
-----
28672

GramEV6[6,4,0]

 1
---
448

GramEV6[6,3,1]

 3
---
896

GramEV6[6,2,2]

 31
----
8064
```

```
GramEV6[6,2,0]

 1
---
192

GramEV6[6,1,1]

 3
---
512

GramEV6[6,0,0]

 1
---
128
```

□ Eigenvalues for order 7

```
GramEV6[7,7,0]

 1
----
4608

GramEV6[7,6,1]

 5
----
9216

GramEV6[7,5,2]

 83
-----
82944

GramEV6[7,4,3]

 25
-----
18432

GramEV6[7,5,0]

 1
----
1024

GramEV6[7,4,1]

 5
----
3072

GramEV6[7,3,2]

 13
----
6144
```

```
GramEV6[7,3,0]

 1
---
384

GramEV6[7,2,1]

 5
----
1536

GramEV6[7,1,0]

 7
----
1536
```

GramXct_U1n

Continuum-Limit Gram Eigenvalues for n Degrees of Freedom using $[U(1)]^n$

This *Mathematica* notebook shows how to compute the continuum-limit Gram eigenvalues for the n-degree-of-freedom case when we include all linear symplectic transformations in the space $[U(1)]^n$.

■ Definitions and Functions

First import a couple of useful packages. Here the package `Polynomial.m` defines the function `NumberMonomials[]`, while the package `ListManipulation.m` defines the function `SortCount[]`.

```
<<Polynomial.m
<<ListManipulation.m
```

Now define a function to compute the Gram eigenvalues for the general case.

```
gt1Q = #>1&;

GramEvU1n[1,l_?NumberQ,r_?NumberQ] :=
  Binomial[l,r]/2^l

GramEvU1n[n_?gt1Q,l_List,r_List] :=
  Module[deg},
         deg = (Plus @@ l);
         Product[Binomial[l[[j]],r[[j]]],j,n}]/
          (NumberMonomials[deg,n] 2^deg)] /;
  Dimensions[l]==Dimensions[r]==n}
```

■ n=2

Here define `gevs2[]` to return the Gram eigenvalues specifically for the case $n = 2$, and evaluate it for polynomials of degrees 1 through 5.

```
gevs2[l_] := Flatten[
  Table[GramEvU1n[2,{l-j,j},{r,s}],
        {j,0,l},{r,0,l-j},{s,0,j}]]

gevs2[1] // SortCount // TableForm
```

```
1
-
4   4
```

```
gevs2[2] // SortCount // TableForm
```

```
1
--
12   8
```

```
1
-
6    2
```

```
gevs2[3] // SortCount // TableForm
```

```
1
--
32   12

1
--
16   4

3
--
32   4
```

```
gevs2[4] // SortCount // TableForm
```

```
1
--
80   16

1
--
40   4
3
--
80   8

1
--
20   5

3
--
40   2
```

```
gevs2[5] // SortCount // TableForm
```

```
 1
---
192   20

1
--
96    4

1
--
64    8

1
--
48    8

 5
---
192   4
```

```
1
--
32    8

5
--
96    4
```

```
gevs2[6] // SortCount // TableForm
```

```
 1
---
448   24

 1
---
224   4

 3
---
448   8

 1
---
112   8

 5
---
448   8

 3
---
224   8

1
--
56    4

 9
---
448   4

 5
---
224   8

 3
---
112   2

15
---
448   4

 5
---
112   2
```

```
gevs2[7] // SortCount // TableForm

 1
----
1024   28

 1
---
512    4

 3
----
1024   8

 1
---
256    8

 5
----
1024   8

 3
---
512    12

 7
----
1024   4

 5
---
512    12

 3
---
256    8

 15
----
1024   8

 9
---
512    4

 5
---
256    8

 21
----
1024   4

 35
----
1024   4
```

■ n=3

Here define `gevs3[]` to return the Gram eigenvalues specifically for the case $n = 3$, and evaluate it for polynomials of degrees 1 through 5.

```
gevs3[l_] := Flatten[
  Table[GramEvU1n[3,{l-j-k,j,k},{r,s,t}],
        {j,0,l},{k,0,l-j},{r,0,l-j-k},{s,0,j},{t,0,k}]]

gevs3[1] // SortCount // TableForm

1
-
6   6

gevs3[2] // SortCount // TableForm

1
--
24   18

1
--
12   3

gevs3[3] // SortCount // TableForm

1
--
80   38

1
--
40   12

3
--
80   6

gevs3[4] // SortCount // TableForm

 1
---
240   66

 1
---
120   24

1
--
80    24

1
--
60    9

1
--
40    3
```

```
gevs3[5] // SortCount // TableForm
```

```
 1
---
672   102

 1
---
336   36

 1
---
224   48

 1
---
168   30

 5
---
672   6

 1
---
112   24

 5
---
336   6
```

```
gevs3[6] // SortCount // TableForm
```

```
 1
----
1792   146

 1
---
896    48

 3
----
1792   72

 1
---
448    54

 5
----
1792   24

 3
---
896    54
```

```
 1
---
224    13

 9
----
1792   12

 5
---
896    24

 3
---
448    6

 15
----
1792   6

 5
---
448    3
```

```
gevs3[7] // SortCount // TableForm
```

```
 1
----
4608   198

 1
----
2304   60

 1
----
1536   96

 1
----
1152   78

 5
----
4608   48

 1
---
768    84

 7
----
4608   6

 1
---
576    24
```

```
 1
---
512    24

 5
----
2304   60

 1
---
384    42

 5
----
1536   24

 1
---
256    12

 5
----
1152   24

 7
----
1536   6

 35
----
4608   6
```

References

1. Edwin A. Abbott, *Flatland: A Romance of Many Dimensions*, Sixth ed., Dover, New York, NY, 1953.
2. Milton Abramowitz and Irene A. Stegun (eds.), *Handbook of Mathematical Functions*, Dover, New York, NY, 1972.
3. Naum I. Akhiezer, *Elements of the Theory of Elliptic Functions*, Translations of Mathematical Monographs, vol. 79, American Mathematical Society, Providence, RI, 1990.
4. Joseph Bak and Donald J. Newman, *Complex Analysis*, Undergraduate Texts in Mathematics, Springer-Verlag, New York, NY, 1982.
5. Eiichi Bannai, *Spherical t-designs which are orbits of finite groups*, J. Math. Soc. Japan **36** (1984), no. 2, 341–354.
6. Stephen Barnett, *Matrices: Methods and Applications*, Oxford Applied Mathematics and Computing Science Series, Oxford University Press, New York, NY, 1990.
7. Gordon Baym, *Lectures on Quantum Mechanics*, Lecture Notes and Supplements in Physics, Benjamin/Cummings, Reading, MA, 1973.
8. Brian L. Beers and Alex J. Dragt, *New theorems about spherical harmonic expansions and $SU(2)$*, J. Math. Phys. **11** (1970), no. 8, 2313–2328.
9. Mirza A. B. Bég and Henri Ruegg, *A set of harmonic functions for the group $SU(3)$*, J. Math. Phys. **6** (1965), no. 5, 677–682.
10. R. E. Behrends, J. Dreitlein, C. Fronsdal, and W. Lee, *Simple groups and strong interaction symmetries*, Rev. Modern Phys. **34** (1962), no. 1, 1–40.
11. Martin Berz, *Differential algebraic description of beam dynamics to very high orders*, Part. Accel. **24** (1989), no. 2, 109–124.
12. Martin Berz and H. Wollnik, *The program HAMILTON for the solution of the equations of motion through fifth order*, Nucl. Instr. and Meth. **A258** (1987), 364–373.
13. Fred Brauer and John A. Nohel, *The Qualitative Theory of Ordinary Differential Equations*, W. A. Benjamin, New York, NY, 1969.
14. Paul F. Byrd and Morris D. Friedman, *Handbook of Elliptic Functions for Engineers and Physicists*, Springer-Verlag, Berlin, 1954.
15. Ruel V. Churchill and James Ward Brown, *Complex Variables and Applications*, Fourth ed., McGraw-Hill, New York, NY, 1984.
16. Lothar Collatz, *Functional Analysis and Numerical Mathematics*, Academic Press, New York, NY, 1966, translated from the German edition by Hansjörg Oser.
17. Ronald Cools, private communication.
18. ———, *A survey of methods for constructing cubature formulae*, Numerical Integration: Recent Developments, Software, and Applications, Bergen, Norway, June 17–21, 1991 (Dordrecht) (Terje O. Espelid and Alan Genz, eds.), NATO ASI Series C, vol. 357, Kluwer Academic Pub., 1992, pp. 1–24.
19. Ronald Cools and Ian H. Sloan, *Minimal cubature formulae of trigonometric degree*, to appear in Math. Comp., 1995.
20. J. F. Cornwell, *Group Theory in Physics*, Techniques in Physics 7, Academic Press, London, 1984, two volumes.
21. Luigi Cremona, *Opere Mathematiche di Luigi Cremona*, Ulrico Hoepli, Milano, Italy, 1914, published under the auspices of R. Accademia dei Lincei, three volumes.
22. Lawrence Davis (ed.), *Genetic Algorithms and Simulated Annealing*, Morgan Kaufmann Pub., Los Altos, CA, 1987.
23. Kenneth De Jong (ed.), *Evolutionary Computation*, The MIT Press, Cambridge, MA, published quarterly.
24. P. Delsarte, J. M. Goethals, and J. J. Seidel, *Spherical codes and designs*, Geom. Dedicata **6** (1977), 363–388.
25. David R. Douglas, *Lie Algebraic Methods for Particle Accelerator Theory*, Ph.D. thesis, University of Maryland, College Park, MD, 1982.
26. Alex J. Dragt, *Classification of three-particle states according to SU_3*, J. Math. Phys. **6** (1965), no. 4, 533–553.
27. ———, *Relativistic three-particle SU_3 states*, J. Math. Phys. **6** (1965), no. 11, 1621–1625.
28. ———, *Lectures on Non-linear Orbit Dynamics*, Physics of High-Energy Particle Accelerators, AIP Conference Proceedings No. 87 (New York, NY) (M. Month. R. A. Carrigan, F. R. Huson, ed.), AIP, 1982, pp. 147–313.
29. ———, *Computation of maps for particle and light optics by scaling, splitting, and squaring*, to appear in Phys. Rev. Lett., 1995.
30. ———, *Lectures on Nonlinear Dynamics and Lie Methods with Applications to Accelerator Physics*, Center for Theoretical Physics, University of Maryland at College Park, 1995.
31. Alex J. Dragt and Dan T. Abell, *Symplectic maps and computation of orbits in particle accelerators*, to appear in Fields Inst. Comm., 1995.

32. Alex J. Dragt, David R. Douglas, et al., MaryLie *3.0 User's Manual*, Center for Theoretical Physics, University of Maryland at College Park, 1992.
33. Alex J. Dragt and John M. Finn, *Lie series and invariant functions for analytic symplectic maps*, J. Math. Phys. **17** (1976), no. 12, 2215–2227.
34. Alex J. Dragt, Ivan M. Gjaja, and Govindan Rangarajan, *Kick factorization of symplectic maps*, Conference Record of the 1991 IEEE Particle Accelerator Conference (Piscataway, NJ), vol. 3, IEEE, 1991, pp. 1621–23.
35. A. R. Edmonds, *Angular Momentum in Quantum Mechanics*, Second ed., Princeton University Press, Princeton, NJ, 1960.
36. W. Engel, *Ein satz über ganze Cremona-transformationen der ebene*, Math. Ann. **130** (1955), 11–19.
37. ———, *Ganze Cremona-transformationen von primzahlgrad in der ebene*, Math. Ann. **136** (1958), 319–325.
38. W. M. Fairbairn, T. Fulton, and W. H. Klink, *Finite and disconnected subgroups of SU_3 and their application to the elementary-particle spectrum*, J. Math. Phys. **5** (1964), no. 8, 1038–1051.
39. Étienne Forest, private communication.
40. Stephanie Forrest, *Genetic algorithms: Principles of natural selection applied to computation*, Science **261** (1993), 872–878.
41. Jr. Frederick W. Byron and Robert W. Fuller, *Mathematics of Classical and Quantum Physics*, Dover, New York, NY, 1992, unabridged and corrected republication (in one volume) of the two volume work published by Addison-Wesley in 1969 (Vol. One) and 1970 (Vol. Two).
42. Avner Friedman, *Partial Differential Equations*, Holt, Rinehart and Winston, New York, NY, 1969.
43. Feliks R. Gantmacher, *The Theory of Matrices*, Chelsea Pub. Co., New York, NY, 1959, two volumes.
44. James W. L. Glaisher, *On elliptic functions*, Messenger of Mathematics **11** (1882), 81–98.
45. David E. Goldberg, *Genetic Algorithms in Search, Optimization, and Machine Learning*, Addison-Wesley, Reading, MA, 1989.
46. Peter J. Grabner and Robert F. Tichy, *Spherical designs, discrepancy and numerical integration*, Math. Comp. **60** (1993), no. 201, 327–336.
47. I. S. Gradshteyn and I. M. Ryzhik, *Table of Integrals, Series, and Products*, Corrected and Enlarged ed., Academic Press, New York, NY, 1980, Alan Jeffrey, ed., incorporates the fourth Russian edition prepared by Yu. V. Geronimus and M. Yu. Tseytlin.
48. Johannes Hagel and B. Zotter, *Comparison of tracking results with exact solutions of non-linear equations*, Part. Accel. **34** (1990), 67–87.
49. Liam M. Healy, *Lie Algebraic Methods for Treating Lattice Parameter Errors in Particle Accelerators*, Ph.D. thesis, University of Maryland, College Park, MD, 1986.
50. Francis B. Hildebrand, *Introduction to Numerical Analysis*, Second ed., Dover, New York, NY, 1987, slightly corrected republication of the Second edition published by McGraw-Hill in 1974.
51. John Irwin, *A multi-kick factorization algorithm for non-linear maps*, Accelerator Physics at the Superconducting Super Collider, AIP Conference Proceedings No. 326 (New York, NY) (Yiton T. Yan, James P. Naples, and Michael J. Syphers, eds.), AIP Press, 1995, originally written in 1989 as report SSC-228, pp. 662–669.
52. Wilfred Kaplan, *Functions of Several Complex Variables*, Ann-Arbor Publishers, Ann-Arbor, MI, 1964.
53. ———, *Introduction to Analytic Functions*, Addison-Wesley, Reading, MA, 1966.
54. O.-H. Keller, *Ganze Cremona-transformationen*, Monatshefte Math. Phys. **47** (1939), 299–306.
55. Konrad Knopp, *Theory of Functions, Part II*, Dover Publications, New York, NY, 1947.
56. S. I. Konjaev, *Quadratures of Gaussian type for a sphere invariant under the icosahedral group with inversion*, Soviet Math. Dokl. **18** (1976), no. 2, 497–501.
57. ———, *Ninth-order quadrature formulas invariant with respect to the icosahedral group*, Math. Notes **25** (1979), no. 4, 326–329.
58. V. I. Lebedev, *Values of the nodes and weights of ninth to seventeenth order Gauss-Markov quadrature formulae invariant under the octahedron group with inversion*, USSR Comp. Math. Math. Phys. **15** (1975), no. 1, 44–51.
59. ———, *On a type of quadrature formula of increased algebraic accuracy for a sphere*, Soviet Math. Dokl. **17** (1976), no. 6, 1515–1517.
60. ———, *Quadratures on a sphere*, USSR Comp. Math. Math. Phys. **16** (1976), no. 2, 10–24.
61. ———, *Spherical quadrature formulas exact to orders* 25–29, Siberian Math. J. **18** (1977), no. 1, 99–107.
62. A. J. Lichtenberg and M. A. Lieberman, *Regular and Chaotic Dynamics*, Second ed., Applied Mathematical Sciences 38, Springer-Verlag, New York, NY, 1992.
63. A. D. McLaren, *Optimal numerical integration on a sphere*, Math. Comp. **17** (1963), no. 84, 361–383.
64. Eugen Merzbacher, *Quantum Mechanics*, Second ed., John Wiley & Sons, New York, NY, 1970.
65. George A. Miller, Hans F. Blichfeldt, and Leonard E. Dickson, *Theory and Applications of Finite Groups*, G. E. Stechert & Co., New York, NY, 1938, reprint of 1916 edition with corrections.

66. Cleve Moler and Charles Van Loan, *Nineteen dubious ways to compute the exponential of a matrix*, SIAM Rev. **20** (1978), no. 4, 801–836.
67. Phillip M. Morse and Herman Feshbach, *Methods of Theoretical Physics*, International Series in Pure and Applied Physics, McGraw-Hill, New York, NY, 1953, two volumes.
68. Jürgen Moser, *On the integrability of area-preserving Cremona mappings near an elliptic fixed-point*, Boletin de la Soc. Mat. Mexicana (1960), 176–180.
69. Eric H. Neville, *Jacobian Elliptic Functions*, Oxford University Press, London, 1944.
70. ———, *Elliptic Functions: A Primer*, Pergamon Press, Oxford, 1971, prepared for publication by W. J. Langford.
71. Ivan Georgievich Petrovski, *Ordinary Differential Equations*, Prentice-Hall, Englewood Cliffs, NJ, 1966.
72. L. B. Rall, *The arithmetic of differentiation*, Math. Mag. **59** (1986), no. 5, 275–282.
73. Govindan Rangarajan, *Invariants for Symplectic Maps and Symplectic Completion of Symplectic Jets*, Ph.D. thesis, University of Maryland, College Park, MD, 1990.
74. Harry E. Rauch and Aaron Lebowitz, *Elliptic Functions, Theta Functions, and Riemann Surfaces*, Williams & Wilkins Co., Baltimore, MD, 1973.
75. M. E. Rose, *Elementary Theory of Angular Momentum*, John Wiley & Sons, New York, NY, 1957.
76. Walter Rudin, *Principles of Mathematical Analysis*, Third ed., International Series in Pure and Applied Mathematics, McGraw-Hill, New York, NY, 1976.
77. Jun John Sakurai, *Modern Quantum and Mechanics*, Benjamin/Cummings, Menlo Park, CA, 1985, San Fu Tuan (ed.).
78. J. J. Seidel, *Integration over spheres*, Congr. Numer. **56** (1987), 53–61, originally published in *Discrete Geometry*, Salzburg (1985).
79. Boris Vladimirovich Shabat, *Introduction to Complex Analysis, Part II: Functions of Several Variables*, Translations of Mathematical Monographs, vol. 110, American Mathematical Society, Providence, RI, 1992.
80. Igor B. Shafarevich, *Basic Algebraic Geometry*, Second ed., Springer-Verlag, Berlin, 1994, two volumes.
81. Ian H. Sloan and Stephen Joe, *Lattice Methods for Multiple Integration*, Oxford Science Publications, Oxford University Press, New York, NY, 1994.
82. Virgil Snyder, Amos H. Black, Arthur B. Cole, et al., *Selected Topics in Algebraic Geometry*, Second ed., Chelsea Pub. Co., New York, NY, 1970.
83. Jerome Spanier and Keith B. Oldham, *An Atlas of Functions*, Hemisphere Publishing, New York, NY, 1987.
84. George Springer, *Introduction to Riemann Surfaces*, Second ed., Chelsea Pub. Co., New York, NY, 1981.
85. A. H. Stroud, *Approximate Calculation of Multiple Integrals*, Prentice-Hall Series in Automatic Computation, Prentice-Hall, Englewood Cliffs, NJ, 1971.
86. Richard Talman, *Differential maps, difference maps, interpolated maps, and long-term prediction*, Part. Accel. **34** (1990), 1–11.
87. Johannes van Zeijts, TLIE, private communication.
88. Edmund Taylor Whittaker and George Neville Watson, *A Course of Modern Analysis*, The University Press, Cambridge, 1944, reprint published by AMS in 1979.